Phys. Lett. B 849 (2024) 138469

Contents lists available at ScienceDirect

Physics Letters B

journal homepage: www.elsevier.com/locate/physletb

Letter

Probing the CP nature of the top–Higgs Yukawa coupling in $t\bar{t}H$ and tH events with $H \to b\bar{b}$ decays using the ATLAS detector at the LHC

The ATLAS Collaboration *

ARTICLE INFO

Editor: M. Doser

ABSTRACT

The CP properties of the coupling between the Higgs boson and the top quark are investigated using 139 fb^{-1} of proton–proton collision data recorded by the ATLAS experiment at the LHC at a centre-of-mass energy of $\sqrt{s} = 13$ TeV. The CP structure of the top quark–Higgs boson Yukawa coupling is probed in events with a Higgs boson decaying into a pair of b-quarks and produced in association with either a pair of top quarks, $t\bar{t}H$, or a single top quark, tH. Events containing one or two electrons or muons are used for the measurement. Multivariate techniques are used to select regions enriched in $t\bar{t}H$ and tH events, where dedicated CP-sensitive observables are exploited. In an extension of the Standard Model (SM) with a CP-odd admixture in the top–Higgs Yukawa coupling, the mixing angle between CP-even and CP-odd couplings is measured to be $\alpha = 11\,^{\circ}{}^{+52^{\circ}}_{-73^{\circ}}$, compatible with the SM prediction corresponding to $\alpha = 0$.

1. Introduction

Since the observation of the Higgs boson at the LHC [1,2], its properties have been studied in great detail. In particular, the observation of the Higgs boson production in association with a top-quark pair, $t\bar{t}H$ [3,4], provides direct experimental access to the top-quark Yukawa coupling at the tree-level. The increasing datasets at the LHC have recently allowed the ATLAS and CMS Collaborations to probe the charge-conjugation and parity (CP) properties of this coupling using $t\bar{t}H$ events in different decay channels [5–7]. This letter reports on a study of the CP properties of the top-quark Yukawa coupling using $t\bar{t}H$ and tH production, in the $H \to b\bar{b}$ decay channel. The analysis targets final states where at least one top quark decays semi-leptonically to electrons or muons. It uses $\sqrt{s} = 13$ TeV pp collision data recorded by the ATLAS experiment during Run 2, corresponding to an integrated luminosity of 139 fb^{-1}.

The Standard Model (SM) predicts the Higgs boson to be a scalar particle with quantum numbers $J^{CP} = 0^{++}$. Considering the possibility of beyond the Standard Model (BSM) couplings, a CP-odd component of the vector-boson couplings to the Higgs boson is naturally suppressed by the scale at which new physics would become relevant [8,9]. This suppression does not happen for Yukawa couplings, where CP-odd Higgs–fermion couplings may be significant already at tree level [10]. One of the first ATLAS and CMS measurements have excluded the pure $J^P = 0^-$ hypothesis by more than 95% CL using $H \to \gamma\gamma$, $H \to ZZ^*$ and $H \to WW^*$ decays [11,12]. Dedicated searches for CP-mixed couplings between the Higgs boson and vector bosons set stringent limits on the CP-odd components [13–21]. Analyses of $t\bar{t}H$ events with $H \to \gamma\gamma$ decays [5,6] and in the multilepton final state [7] have also excluded pure CP-odd top–Higgs couplings at more than a 3 σ significance. But mixing of CP-odd and CP-even states has not been ruled out and is worth investigating. The observation of a non-zero CP-odd coupling component would in fact signal the existence of BSM physics, and open up the possibility of CP-violation in the Higgs sector [22–25]. Such a new source of CP violation could play a fundamental role in explaining the matter–antimatter asymmetry of the universe. This analysis targets $t\bar{t}H$ and tH events, which are sensitive to the top–Higgs coupling including any potential CP-mixing at the tree-level. This avoids the need for assumptions about the influence of BSM effects which may be present in other, more indirect measurements [26–28]. In particular, current limits on electron and neutron electrical dipole moments place indirect model-dependent constraints on a possible pseudoscalar component of the top-quark Yukawa coupling [29–31].

The top–Higgs interaction can be extended beyond the SM as [26]:

$$\mathcal{L}_{t\bar{t}H} = -\kappa_t' y_t \phi \bar{\psi}_t (\cos\alpha + i\gamma_5 \sin\alpha)\psi_t\,, \tag{1}$$

where y_t is the SM Yukawa coupling strength, modified by a coupling modifier κ_t'; α is the CP-mixing angle; ϕ is the Higgs field; ψ_t and $\bar{\psi}_t$ are top-quark spinor fields and γ_5 is a Dirac matrix. The term containing γ_5 corresponds to a pseudoscalar component. The above expression reduces to the SM case for $\kappa_t' = 1$ and $\alpha = 0$. An anomalous value of α would produce an admixture with a pseudoscalar coupling ($J^{CP} = 0^{+-}$) and change the differential cross-section relative to the SM

* E-mail address: atlas.publications@cern.ch.

https://doi.org/10.1016/j.physletb.2024.138469
Received 13 March 2023; Received in revised form 15 January 2024; Accepted 15 January 2024
Available online 18 January 2024

expectation, while a variation of κ_t' would induce a change in the total cross-section [22,32–35].

This study measures simultaneously the values of κ_t' and α with a binned profile likelihood fit to data, exploiting dedicated CP-sensitive observables. It closely follows a recent analysis optimised for the measurement of the $t\bar{t}H(\rightarrow b\bar{b})$ production cross-section [36]. This analysis studies an identical phase space using the same physics object definitions and a similar methodology for event selection and evaluation of systematic uncertainties. A notable exception is that this analysis considers both the $t\bar{t}H$ and tH production modes as signals. No attempt was made to optimise the analysis strategy for the tH signal, as its small yield makes this channel relevant only in one analysis region. Other noteworthy differences with respect to the analysis documented in Ref. [36] are detailed in the text. These include the definition of signal regions, the signal-background discrimination strategy and a few details in the definition of systematic uncertainties in signal and background modelling. In the case of tH production, the destructive interference between the diagrams with t–H and W–H couplings leads to the negligible tH production cross-section in the SM. Any change in the relative t–H and W–H coupling strengths would result in a rapid increase in the cross-section. Considering the Lagrangian density in Eqn. 1, the tH production cross-section is expected to grow for values of the mixing angle α different from zero [23]. An opposite and less pronounced dependence exists for the $t\bar{t}H$ cross-section. The ratio of tH to $t\bar{t}H$ cross-sections varies from 0.06 in the SM scenario to more than 1.2 in the pure CP-odd scenario [23]. For the present measurement, the $H \rightarrow b\bar{b}$ branching ratio is assumed to be equal to its SM value of 58.2% ± 0.5% [37].

2. The ATLAS experiment

The ATLAS experiment [38–40] at the LHC is a multipurpose particle detector with a forward–backward symmetric cylindrical geometry and a near 4π coverage in solid angle.[1] It consists of an inner tracking detector surrounded by a thin superconducting solenoid providing a 2 T axial magnetic field, electromagnetic and hadron calorimeters and a muon spectrometer. A two-level trigger system is used to reduce the total event rate to 1 kHz on average, depending on the data-taking conditions [41]. An extensive software suite [42] is used in the reconstruction and analysis of real and simulated data, in detector operations, and in the trigger and data acquisition systems of the experiment. The events used in this analysis are selected using single-lepton triggers [43,44], with either low thresholds for the lepton transverse momentum (p_{T}) and a lepton isolation requirement, or higher thresholds, looser identification criteria and without any isolation requirement. The lowest p_{T} threshold for muons is 20 (26) GeV, while for electrons the threshold is 24 (26) GeV for the data taken in 2015 (2016–2018).

3. Event preselection

Events are required to have at least one primary vertex, formed by two or more associated tracks with transverse momenta greater than 0.5 GeV. The vertex with the highest sum of p_{T}^2 of associated tracks is selected as the hard-scattering primary vertex. Events with exactly one lepton (electrons or muons, denoted as ℓ) or two oppositely charged leptons are considered in this analysis, referred to as the ℓ + jets channel and dilepton channel, respectively. Electrons are identified using the 'Tight' likelihood criterion [45] and are required to have $p_{\mathrm{T}} > 10$ GeV and $|\eta| < 2.47$, excluding those in the calorimeter barrel–endcap transition region ($1.37 < |\eta| < 1.52$). Muons are selected with the 'Medium' identification criterion [46] and are required to have $p_{\mathrm{T}} > 10$ GeV and $|\eta| < 2.5$. Electrons (muons) are required to pass the 'Gradient' ('Fixed-Cut-Tight-Track-Only') isolation requirements [45,46]. All leptons are required to originate from the primary vertex. At least one of the leptons must have $p_{\mathrm{T}} > 27$ GeV and match the corresponding lepton used in the trigger decision. In events with an ee or $\mu\mu$ pair, the dilepton invariant mass is required to be above 15 GeV and outside the Z boson mass window of 83–99 GeV.

This analysis targets events with high jet multiplicities, including b-quark jets expected in the final state of $t\bar{t}H$ and tH events with a subsequent $H \rightarrow b\bar{b}$ decay. Following the same procedure as Ref. [36], jets are reconstructed from topological clusters of energy depositions in the calorimeter [47,48] using the anti-k_t algorithm [49,50] with a radius parameter of $R = 0.4$. The MV2c10 algorithm [51] is used to identify (or 'b-tag') jets containing b-hadrons. By placing different selections on the MV2c10 discriminant, four working points are defined with average b-jet tagging efficiencies of 60%, 70%, 77% and 85% and different c- and light-jet rejection rates. The corresponding efficiencies and rejection rates are calibrated to data [51–53]. A pseudo-continuous b-tagging score is assigned to each jet. A score of two, three, four and five is assigned if a jet passes the 85%, 77%, 70% and 60% working point, but fails the adjacent tighter one. If a jet fails all working points, a score of one is assigned. In the ℓ + jets (dilepton) channel, events are required to have at least five (three) jets with $p_{\mathrm{T}} > 25$ GeV and $|\eta| < 2.5$, and at least four (three) of the jets are required to be b-tagged at the 70% efficiency working point.

The missing transverse momentum is reconstructed as the negative vector sum of the p_{T} of all selected objects in the event, with an extra 'soft term' built from additional tracks associated with the primary vertex [54].

The analysis also exploits the collimated decay topology from high-p_{T} Higgs bosons. Jets with a radius parameter of $R = 0.4$ are reclustered [55] using the anti-k_t algorithm with a radius parameter of $R = 1.0$. The resulting jets are referred to as *large-R* jets. The large-R jets are required to have a mass larger than 50 GeV, $p_{\mathrm{T}} > 200$ GeV and at least two constituent jets with $R = 0.4$.

4. Signal and background modelling

After applying the above selection criteria, background events are dominated by $t\bar{t}$ production with additional jets ($t\bar{t}$ + jets), that contain heavy-flavour hadrons (b- and c-hadrons). Other processes contribute less than 10% of the total expected background. All background processes are estimated using Monte Carlo (MC) simulations, closely following Ref. [36].

The simulated events were produced using the ATLAS detector simulation [56] based on GEANT4 [57]. To simulate the effects of multiple interactions in the same and neighbouring bunch crossings (pile-up), additional interactions were generated using PYTHIA 8.186 [58] with a set of tuned parameters called the A3 tune [59] and overlaid on the simulated hard-scatter event. Simulated events are reweighted to match the pile-up conditions observed in the full Run 2 dataset. All simulated event samples are processed through the same reconstruction algorithms and analysis chain as the data [42].

Events in the simulated $t\bar{t}$ + jets background sample are categorised according to the flavour of the additional jets which do not originate from the top-quark decay. The simulation of each set of backgrounds is treated independently as this allows for a more accurate modelling of $t\bar{t}$ + jets events. The categorisation is based on 'MC-truth jets' that are clustered with stable generated particles (with mean lifetime $\tau > 3 \times 10^{-11}$ s) in the final state using the anti-k_t algorithm with $R = 0.4$. MC-truth jets with $p_{\mathrm{T}} > 15$ GeV and $|\eta| < 2.5$ in the simulated events are used for the categorisation. Their MC-truth flavour is

[1] ATLAS uses a right-handed coordinate system with its origin at the nominal interaction point (IP) in the centre of the detector and the z-axis along the beam pipe. The x-axis points from the IP to the centre of the LHC ring, and the y-axis points upwards. Cylindrical coordinates (r, ϕ) are used in the transverse plane, ϕ being the azimuthal angle around the z-axis. The momentum component in the transverse plane is referred to as the transverse momentum (p_{T}). The pseudorapidity is defined in terms of the polar angle θ as $\eta = -\ln\tan(\theta/2)$. Angular distance is measured in units of $\Delta R \equiv \sqrt{(\Delta\eta)^2 + (\Delta\phi)^2}$.

determined by counting the number of b/c-hadrons contained within $\Delta R = 0.4$ of the jet axis. Events with at least one MC-truth jet containing b-hadrons not originating from a top-quark decay are labelled as $t\bar{t}+\geq 1b$. This can be further separated into subcomponents corresponding to $t\bar{t}+1b$ and $t\bar{t}+\geq 2b$. Events failing to satisfy that criterion but with at least one MC-truth jet containing c-hadrons not originating from top-quark decay are labelled $t\bar{t}+\geq 1c$. The rest of the events are labelled as $t\bar{t}+$light. The dominant $t\bar{t}+\geq 1b$ background is modelled using a sample of $t\bar{t}+b\bar{b}$ events generated at next-to-leading order (NLO) in QCD in the four-flavour scheme, with two additional massive b-quarks produced at the matrix element (ME) level. The ME simulation was performed using the Powheg Box Res generator and OpenLoops [60–63], with the NNPDF3.0nlo nf4 [64] parton distribution function (PDF) set and Pythia 8.230 [58] with the A14 set of tuned parameters [65] for the simulation of the parton shower (PS) and hadronisation. Given that the production rate of $t\bar{t}$ with additional b-jets is observed to be underestimated by the current predictions [66,67], the normalisation of the $t\bar{t}+\geq 1b$ background is determined from the analysed data without prior constraints. The $t\bar{t}+\geq 1c$ and $t\bar{t}+$light backgrounds are modelled from a subset of an inclusive $t\bar{t}+$jets sample generated at NLO in QCD using Powheg Box v2 [68–71] as the ME generator interfaced with Pythia 8.230 for the PS and hadronisation. This inclusive $t\bar{t}+$jets sample is generated with the five-flavour scheme, where c- and b-quarks not originating from a top-quark decay are assumed to be massless. Due to limited knowledge regarding $t\bar{t}+\geq 1c$ production, an additional 100% uncertainty is included in its normalisation. Additionally, a prior uncertainty of 6% is assigned to the inclusive $t\bar{t}+$jets production cross-sections according to the predicted inclusive $t\bar{t}$ production cross-section at NNLO+NNLL [72–78]. Other background processes include the production of $W+$ jets, $Z+$ jets, $t\bar{t}W$, $t\bar{t}Z$, tZq, tWZ, $t\bar{t}t\bar{t}$ and $WW/WZ/ZZ$ events. These are all subdominant and modelled from simulation as detailed in Ref. [36]. A small fraction of events contains misidentified leptons or leptons originating from the decay of heavy-flavour hadrons. The contribution from these events is found to be negligible in the $\ell+$jets channel. In the dilepton channel, this small contribution is modelled using a simulation.

The signal processes, $t\bar{t}H$ and tH, are simulated with different values of α and κ_t'. All other parameters were fixed to their SM values, including the $H\to b\bar{b}$ branching ratio. The alternative scenarios were simulated using the NLO Higgs Characterisation [37,79] model implemented in MadGraph5_aMC@NLO with FeynRules [80,81]. With a few exceptions, all signal samples were generated using the MadGraph5_aMC@NLO 2.6.2 [82] generator at NLO in QCD using the five-flavour scheme with the NNPDF3.0nnlo PDF set, interfaced with Pythia 8.230 with the A14 set of tune parameters for PS and hadronisation. The SM $t\bar{t}H$ events were simulated using MadGraph5_aMC@NLO 2.6.0. The renormalisation and factorisation scales were set to $\sqrt[3]{m_{\mathrm{T}}(t)\cdot m_{\mathrm{T}}(\bar{t})\cdot m_{\mathrm{T}}(H)}$, where $m_{\mathrm{T}}=\sqrt{m^2+p_{\mathrm{T}}^2}$ is the transverse mass of a particle. The cross-section is normalised to 507 fb from the fixed-order calculation including NLO QCD and electroweak corrections, with an uncertainty of 3.6% from variations in PDF and α_{s} and 9.2% due to variations of the renormalisation and factorisation scales [37,83–87]. A K-factor of 1.1 is derived by taking the ratio of the cross-section from the above fixed-order calculation to that from MadGraph5_aMC@NLO, and is applied to all $t\bar{t}H$ samples with different values of α and κ_t'. For the tH signal, two subprocesses, $tHjb$ and tWH, are considered. The $tHjb$ (tWH) events were generated in the four(five)-flavour scheme using the NNPDF3.0nnlo nf4 (NNPDF3.0nnlo) PDF set [64], with the renormalisation and factorisation scales set to the generator's default. The cross-sections for the $tHjb$ and tWH samples are obtained directly from MadGraph5_aMC@NLO. In the SM scenario, the cross-section for $tHjb$ and tWH are 60.1 fb and 16.7 fb, respectively. Variations of the renormalisation and factorisation scales, including the consideration of the flavour scheme choice for the $tHjb$ process, contribute 15% and 6.7% to the uncertainty of the cross-sections of $tHjb$ and tWH respectively. Similarly, variations of the PDFs and α_{s} result in a 3.7% and 6.3% uncertainty in the $tHjb$ and tWH cross-sections, respectively. A diagram removal scheme [88] is applied in the simulation of the tWH events in order to remove diagrams already included in the $t\bar{t}H$ simulation.

The yields of $t\bar{t}H$ and tH signals are parameterised as a function of the model parameters by smoothly interpolating between generated MC samples with varying α and κ_t'. The parameterisation is performed in each analysis bin. Two $t\bar{t}H$ samples with alternative values of α were generated, corresponding to a pure CP-odd interaction ($\alpha=90°$) and maximal CP-odd/CP-even mixing ($\alpha=45°$). The $t\bar{t}H$ yields, $N_{t\bar{t}H}(\kappa_t',\alpha)$, are parameterised using the SM sample and the pure CP-odd sample as $\kappa_t'^2 c_\alpha^2 N_{CP\text{-even}} + \kappa_t'^2 s_\alpha^2 N_{CP\text{-odd}}$, where $c_\alpha=\cos\alpha$, $s_\alpha=\sin\alpha$, and $N_{CP\text{-even}}$ and $N_{CP\text{-odd}}$ are the expected yields predicted by the SM and the CP-odd $t\bar{t}H$ simulations, respectively. This was verified to be a good approximation using the maximal mixing sample ($\alpha=45°$), with the difference in any analysis bin smaller than the uncertainties due to the limited number of simulated events. In the case of tH, the interference between diagrams with CP-even and CP-odd $t-H$ and SM $W-H$ couplings are considered in the parameterisation, assuming contributions from lowest order diagrams of $tHjb$ and tWH processes. The signal yield in each analysis bin is parameterised as $N_{tH}(\kappa_t',\alpha)=A\kappa_t'^2 c_\alpha^2 + B\kappa_t'^2 s_\alpha^2 + C\kappa_t' c_\alpha + D\kappa_t' s_\alpha + E\kappa_t'^2 c_\alpha s_\alpha + F$. Coefficients A-F are derived separately for each analysis bin, by fitting to the yields predicted by multiple simulated samples with varying κ_t' and α. The terms with c_α^2 and s_α^2 correspond to the contribution from CP-even and CP-odd t-H coupling, respectively. The terms at the first order of c_α and s_α account for potential interference effects between CP-even and CP-odd t-H coupling and SM W-H coupling contributions. The term F represents the contribution from only the SM W-H coupling. Ten samples generated with different values of α and κ_t' in addition to the SM tH sample are used for the parameterisation. These samples include: samples where $\kappa_t'=1$ and α is set between 15° to 90° in steps of 15°, samples with $\kappa_t'=$ -1, 0.5, and 2 where $\alpha=0°$ and an additional sample with $\alpha=45°$ and $\kappa_t'=2$. Uncertainties due to limited number of MC events in these simulated samples are considered when performing the parameterisation fit in each bin. Good closure was observed: the largest χ^2 per degree of freedom was 0.19 in any given bin. Uncertainties pertaining to the parameterisation of either signal were found to have a negligible impact on the measured values of α and κ_t'.

5. Analysis strategy

In order to optimise the analysis sensitivity, events satisfying the preselection criteria are categorised into orthogonal regions in two steps. In the first step, control regions (CR) and training regions (TR) are defined using requirements on jet multiplicity, b-tagging and large-R jets. The TRs are defined according to the expected numbers of objects from the decay of the signal events, whilst the CRs with lower object multiplicities are signal depleted. The TRs broadly contain the signals and are used to train various multivariate algorithms (MVA). Dedicated observables are constructed in the TRs to enhance sensitivity to the top-Higgs Yukawa CP coupling. In the second step, MVAs are used to divide the TRs into signal regions (SR) and additional CRs with relatively high and low signal purity, respectively. Given the small contribution expected from tH events, the categorisation, MVAs and CP-sensitive observables are optimised for the $t\bar{t}H$ signal. All regions labelled CR and SR are simultaneously fit to the data using either specific observables or simple yields as specified below. Both steps are described in detail below.

The first step of categorisation adopts a strategy similar to that described in Ref. [36], devised to separate the SM signal from the various backgrounds. A 'boosted' region, labelled as $\mathrm{TR}_{\mathrm{boosted}}$, is firstly defined in the $\ell+$jets channel by requiring the presence of a high-p_{T} Higgs boson candidate which is identified using a deep neural network (DNN). The DNN is trained to identify the boosted Higgs boson candidates from among large-R jets with $p_{\mathrm{T}}>300$ GeV [36]. A mixture of constituent

Table 1
Definition of the CRs and TRs according to the number of jets and b-tagged jets using different b-tagging selection criteria, and the number of boosted Higgs boson candidates. For CRs, the bottom row indicates the observables used in the fit to data in the corresponding regions. For the $\mathrm{TR}_{\mathrm{boosted}}$region, the b-tagged jets flagged with † are not constituents of the boosted Higgs boson candidate. Events must pass $N_{b\text{-tag}}$ requirements for each b-tagging selection criteria.

Region		Dilepton				ℓ + jets			
		$\mathrm{TR}^{\geq 4j,\geq 4b}$	$\mathrm{CR}^{\geq 4j,3b}_{\mathrm{hi}}$	$\mathrm{CR}^{\geq 4j,3b}_{\mathrm{lo}}$	$\mathrm{CR}^{3j,3b}_{\mathrm{hi}}$	$\mathrm{TR}^{\geq 6j,\geq 4b}$	$\mathrm{CR}^{5j,\geq 4b}_{\mathrm{hi}}$	$\mathrm{CR}^{5j,\geq 4b}_{\mathrm{lo}}$	$\mathrm{TR}_{\mathrm{boosted}}$
N_{jets}		≥ 4			$=3$	≥ 6	$=5$		≥ 4
$N_{b\text{-tag}}$	@85%	–				≥ 4			
	@77%	–				–			$\geq 2^{\dagger}$
	@70%	≥ 4	$=3$			≥ 4			–
	@60%	–	$=3$	<3	$=3$	–	≥ 4	<4	–
$N_{\mathrm{boosted\ cand.}}$		–				0			≥ 1
Fit observable		–	Yield			–	$\Delta R^{\mathrm{avg}}_{bb}$		–

Table 2
Summary of the selections used to define SRs and CRs from the TRs, based on the classification BDT score. In the boosted region, the selection requirement is applied and rejected events are removed entirely from further analysis. In the dilepton channel, events with failed reconstruction due to absence of a real solution from the neutrino weighting are categorised into an additional region known as $\mathrm{CR}^{\geq 4j,\geq 4b}_{\text{no-reco}}$. The fitted discriminating variable in each region is indicated in the last column.

Channel (TR)	Final SRs and CRs	Classification BDT selection	Fitted observable
Dilepton ($\mathrm{TR}^{\geq 4j,\geq 4b}$)	$\mathrm{CR}^{\geq 4j,\geq 4b}_{\text{no-reco}}$	–	$\Delta\eta_{\ell\ell}$
	$\mathrm{CR}^{\geq 4j,\geq 4b}$	$\mathrm{BDT}^{\geq 4j,\geq 4b} \in [-1,-0.086)$	b_4
	$\mathrm{SR}^{\geq 4j,\geq 4b}_{1}$	$\mathrm{BDT}^{\geq 4j,\geq 4b} \in [-0.086,0.186)$	b_4
	$\mathrm{SR}^{\geq 4j,\geq 4b}_{2}$	$\mathrm{BDT}^{\geq 4j,\geq 4b} \in [0.186,1]$	b_4
ℓ + jets ($\mathrm{TR}^{\geq 6j,\geq 4b}$)	$\mathrm{CR}^{\geq 6j,\geq 4b}_{1}$	$\mathrm{BDT}^{\geq 6j,\geq 4b} \in [-1,-0.128)$	b_2
	$\mathrm{CR}^{\geq 6j,\geq 4b}_{2}$	$\mathrm{BDT}^{\geq 6j,\geq 4b} \in [-0.128,0.249)$	b_2
	$\mathrm{SR}^{\geq 6j,\geq 4b}$	$\mathrm{BDT}^{\geq 6j,\geq 4b} \in [0.249,1]$	b_2
ℓ + jets ($\mathrm{TR}_{\mathrm{boosted}}$)	$\mathrm{SR}_{\mathrm{boosted}}$	$\mathrm{BDT}^{\mathrm{boosted}} \in [-0.05,1]$	$\mathrm{BDT}^{\mathrm{boosted}}$

jet masses, pseudo-continuous b-tagging scores and jet substructure observables [89] are used as input features for the training. Events failing this DNN selection defining the $\mathrm{TR}_{\mathrm{boosted}}$ region are categorised into CRs and TRs according to the number of jets (j) and various b-tagging (b) requirements. Events in the TRs are required to have at least the number of jets and b-tagged jets expected from the final state of the $t\bar{t}H$ signal. This results in four statistically independent regions in the dilepton channel, named $\mathrm{CR}^{3j,3b}_{\mathrm{hi}}$, $\mathrm{CR}^{\geq 4j,3b}_{\mathrm{lo}}$, $\mathrm{CR}^{\geq 4j,3b}_{\mathrm{hi}}$ and $\mathrm{TR}^{\geq 4j,\geq 4b}$, and three regions in the ℓ + jets channel, named $\mathrm{CR}^{5j,\geq 4b}_{\mathrm{lo}}$, $\mathrm{CR}^{5j,\geq 4b}_{\mathrm{hi}}$ and $\mathrm{TR}^{\geq 6j,\geq 4b}$. The yields of these regions enter the fit. The requirements used to define all CRs and TRs are summarised in Table 1. Regions labelled with 'hi' ('lo') have relatively higher (lower) fractions of events with true b-jets not from top-quark decays, and are selected with tight (loose) b-tagging requirements. The average ΔR separation between b-jets ($\Delta R^{\mathrm{avg}}_{bb}$) is used as the observable which enters the fit for $\mathrm{CR}^{5j,\geq 4b}_{\mathrm{lo}}$ and $\mathrm{CR}^{5j,\geq 4b}_{\mathrm{hi}}$ regions as it better constrains the shape of the backgrounds. All mentioned CRs have different fractions of $t\bar{t}$ + light, $t\bar{t}+\geq 1c$ and $t\bar{t}+\geq 1b$ events and this helps to constrain the systematic uncertainties in each of these components.

In the TRs, two sets of boosted decision trees (BDT) are trained: reconstruction BDTs and classification BDTs. The former is trained to assign jets as coming from the decay of the Higgs boson or top quarks in $t\bar{t}H$ events, while the latter is trained to discriminate the $t\bar{t}H$ signal against the backgrounds. Both the reconstruction and classification BDTs are trained using simulated SM $t\bar{t}H$ events. It was tested that their performance is equally good for a pure CP-odd signal. For both the reconstruction and classification BDTs, the training procedures are performed independently for each TR and are identical to those used in Ref. [36]. The reconstruction BDTs are trained to classify the correct combinations of jet assignments from random ones. The training explores the relative positional information between pairs of objects, and the invariant masses of object pairs and triplets that form W-boson and top-quark candidates. In order to reconstruct the top-quark and Higgs boson candidates, for each event, all possible permutations of jet assignments are evaluated and the permutation with the highest BDT score is selected. The reconstruction BDTs provide important information that improves the performance of the classification BDTs, whilst allowing for the calculation of observables sensitive to the CP nature of the Yukawa coupling. Classification BDT inputs include reconstruction BDT (DNN in the boosted channel) outputs, pseudo-continuous b-tagging discriminant scores of jets, and kinematic features, such as angular separations and invariant masses of pairs of b-tagged jets. The classification BDTs are used to further refine the TRs to define the final CRs and SRs, as detailed later. The classification BDTs used in $\mathrm{TR}^{\geq 4j,\geq 4b}$, $\mathrm{TR}^{\geq 6j,\geq 4b}$ and $\mathrm{TR}_{\mathrm{boosted}}$ are henceforth denoted by $\mathrm{BDT}^{\geq 4j,\geq 4b}$, $\mathrm{BDT}^{\geq 6j,\geq 4b}$ and $\mathrm{BDT}^{\mathrm{boosted}}$, respectively.

Dedicated CP-sensitive observables are computed in $\mathrm{TR}^{\geq 4j,\geq 4b}$ and $\mathrm{TR}^{\geq 6j,\geq 4b}$ and are used in the fit to determine the CP properties of the top-quark Yukawa coupling. Two CP observables, b_2 and b_4 [22,35], were found to provide the best discrimination in $\mathrm{TR}^{\geq 6j,\geq 4b}$ of the ℓ + jets channel and $\mathrm{TR}^{\geq 4j,\geq 4b}$ of the dilepton channel, respectively. They are defined as:

$$b_2 = \frac{(\vec{p}_1 \times \hat{z}) \cdot (\vec{p}_2 \times \hat{z})}{|\vec{p}_1||\vec{p}_2|}, \text{ and } b_4 = \frac{(\vec{p}_1 \cdot \hat{z})(\vec{p}_2 \cdot \hat{z})}{|\vec{p}_1||\vec{p}_2|},$$

where $\vec{p}_i$ with $i = 1,2$ are the momentum three-vectors of the two top quarks in the events and $\hat{z}$ is a unit vector in the direction of the beamline and defines the z-axis. The b_4 observable exploits the enhanced production of top quarks travelling in opposite longitudinal directions and closer to the beamline in CP-odd $t\bar{t}H$ production. The observ-

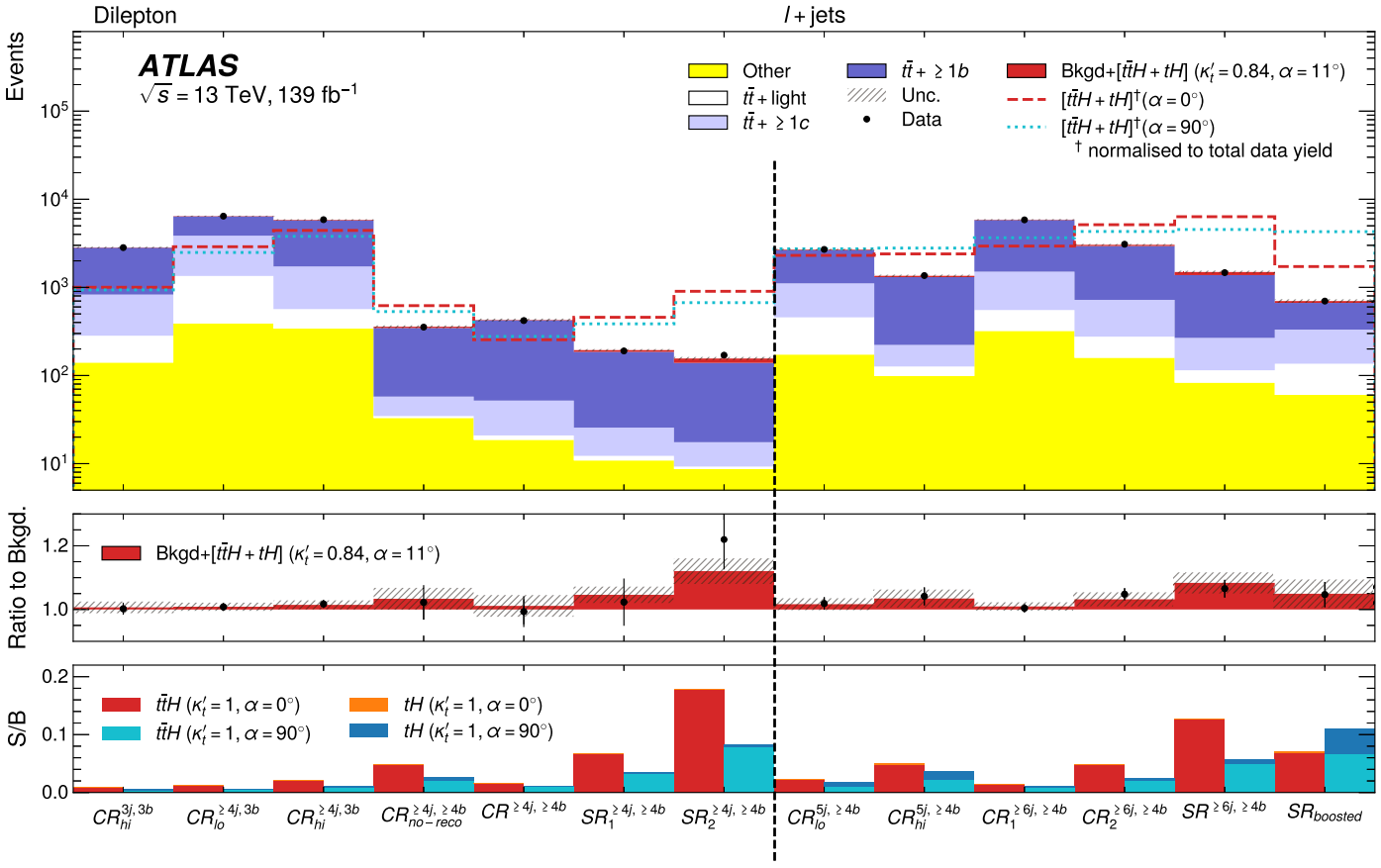

Fig. 1. Yields calculated following a fit with κ_t' and α as free parameters, compared to the observed data in all analysis regions. The different backgrounds and the signal are shown in coloured stack. The background component labelled "other" corresponds to the production of $W+$ jets, $Z+$ jets, $t\bar{t}W$, $t\bar{t}Z$, tZq, tWZ, $t\bar{t}t\bar{t}$ and $WW/WZ/ZZ$ events, as in Ref. [36]. The dashed and dotted lines show the sum of $t\bar{t}H + tH$ signals for pure CP-even and CP-odd hypotheses normalised to the total data yields including all regions. The hashed area around the prediction illustrates the total post-fit uncertainties. In the middle panel, the best-fit model is compared with the data by showing ratios of its value to the post-fit background prediction. The histogram represents the total post-fit model including the best-fit signals. The hashed band represents the total post-fit uncertainty as a ratio to the background. In the bottom panel, the S/B is shown for pure CP-even and CP-odd signals, separately. The histograms are shown as a stack of $t\bar{t}H$ and tH.

able b_2 relies simultaneously on the smaller azimuthal separation of top quarks and on their larger longitudinal fraction of momentum in CP-odd $t\bar{t}H$ production. The calculation of b_2 is performed in the $t\bar{t}H$ rest frame [35], which enhances the discrimination power.

Computation of b_2 and b_4 requires the full reconstruction of both top quarks and the Higgs boson. However, the reconstruction BDTs only resolve the hadronic part of the $t\bar{t}H$ system. In the ℓ + jets channel, the missing transverse momentum is used as a proxy for the p_{T} of the undetected neutrino from the semileptonically decaying top quark. The z component of the neutrino four-momentum is obtained from a quadratic equation constructed from the lepton four-momentum and the missing transverse momentum, using as a constraint the leptonic W boson's mass, assumed to be its on-shell value. Both solutions of the quadratic equation are used to reconstruct the top-quark mass, and the one yielding a mass closer to 172.5 GeV is chosen. In the case of a negative determinant, a solution is obtained by setting the determinant to zero. In the dilepton channel, the neutrino weighting technique is used to determine the four momenta of the two neutrinos [90,91]. Neutrino weighting provides a solution for reconstructing the $t\bar{t}$ pair for 68% of the events in $\mathrm{TR}^{\geq 4j,\geq 4b}$.

In contrast to the $\mathrm{TR}^{\geq 4j,\geq 4b}$ and $\mathrm{TR}^{\geq 6j,\geq 4b}$ regions, the CP-odd signals are strongly enhanced in comparison with the CP-even signals in the $\mathrm{TR}_{\mathrm{boosted}}$ region. The yields of $t\bar{t}H$ with pure CP-even and CP-odd couplings are approximately equal in the $\mathrm{TR}_{\mathrm{boosted}}$ region. Additionally, the yield of the tH signal with a pure CP-odd coupling is comparable to the $t\bar{t}H$ signal yield. The total CP-odd signal is therefore expected to be 50% larger than a CP-even signal in this region. Given the substantial sensitivity provided by the yield in this region, the distribution of the classification BDT ($\mathrm{BDT}^{\mathrm{boosted}}$) is used instead of a dedicated CP-sensitive observable.

In the second step of the categorisation, TRs are further refined to CRs and SRs according to the output of the reconstruction and classification BDTs. A summary of the selections used to define the regions is detailed in Table 2. In $\mathrm{TR}_{\mathrm{boosted}}$, events below a classification BDT score of –0.05 are discarded to reduce contamination of $t\bar{t}+$light events. $\mathrm{TR}^{\geq 4j,\geq 4b}$ and $\mathrm{TR}^{\geq 6j,\geq 4b}$ are further categorised, each into three regions, according to the classification BDT score. The resulting regions have similar background compositions but different expected signal-to-background ratios (S/B). The BDT thresholds are determined by optimising the sensitivity to the SM $t\bar{t}H$ signal. The three regions (one in ℓ + jets and two in dilepton) with an $S/B > 7\%$ are referred to as SRs. The remaining three regions (two in ℓ + jets and one in dilepton) are used as additional CRs to constrain the modelling of the CP observables in the backgrounds events. The highest S/B in the resulting SRs is 22% (10%) for a pure CP-even (CP-odd) signal. For $\mathrm{SR}^{\geq 4j,\geq 4b}$ in the dilepton channel, b_4 cannot be calculated for events where the neutrino weighting fails to provide a solution. These events are categorised as an additional region, $\mathrm{CR}^{\geq 4j,\geq 4b}_{\text{no-reco}}$, where the difference in η between the two leptons, $\Delta\eta_{\ell\ell}$, is used as a CP-sensitive observable instead [26].

Table 3
The observed data yields and the expected signal and background yields in the ℓ + jets channel. The expected yields of pure CP-even and CP-odd $t\bar{t}H$ and tH signals, with $\kappa_t' = 1$, are shown at the top of the table. The uncertainties in the pure CP-even and CP-odd $t\bar{t}H$ and tH signals are the total uncertainties before fitting to data. Below that are shown the post-fit $t\bar{t}H$ and tH yields, corresponding to $\kappa_t' = 0.84$ and $\alpha = 11°$. The following seven rows show the yields and uncertainties of individual background sources, where "other" corresponds to W+ jets, Z+ jets, $t\bar{t}W$, $t\bar{t}Z$, tZq, tWZ, $t\bar{t}t\bar{t}$ and $WW/WZ/ZZ$ events, as in Ref. [36]. The row labelled 'Total' represents the total signal plus background post-fit yields. The uncertainties in the post-fit yields are evaluated from the post-fit nuisance parameters as well as the post-fit uncertainties in the fitted free parameters (α and κ_t' for the signals and $k_{t\bar{t}+b}$ for the $t\bar{t}+\geq 1b$ background) that affect the corresponding processes. The correlations amongst all fitted parameters are taken into account. Due to these correlations the uncertainties on the total yields do not correspond to the quadrature sum of uncertainties of individual signals and backgrounds.

	$CR_{lo}^{5j,\geq 4b}$	$CR_{hi}^{5j,\geq 4b}$	$CR_{1}^{\geq 6j,\geq 4b}$	$CR_{2}^{\geq 6j,\geq 4b}$	$SR^{\geq 6j,\geq 4b}$	$SR_{boosted}$
$t\bar{t}H$ $(1,0°)$	60±9	63±10	78±11	139±18	173±26	46±6
$tH(1,0°)$	3.5±0.5	3.8±0.6	3.3±0.6	2.3±0.6	1.3±0.4	1.9±0.4
$t\bar{t}H$ $(1,90°)$	28±6	28±6	45±11	61±12	68±16	45±6
$tH(1,90°)$	19.0±2.8	19.4±3.1	17.4±3.1	13.1±3.5	10±4	29±6
$t\bar{t}H$ $(0.84,11°)$	40±30	41±31	50±40	90±70	110±80	30±22
tH $(0.84,11°)$	3±4	3.9±1.9	3.1±1.9	1.9±0.8	1.3±1.7	3±5
$t\bar{t}+\geq 1b$	1530±80	1090±60	4300±120	2220±120	1110±110	335±30
$t\bar{t}+\geq 1c$	650±50	96±11	950±80	450±40	153±15	196±22
$t\bar{t}$+ light	280±40	28±8	230±60	117±26	32±11	76±15
Other	173±30	99±20	320±50	159±21	83±11	60±11
Total	2690±50	1350±40	5870±80	3040±70	1500±50	701±31
Data	2696	1363	5837	3090	1470	699

Table 4
The observed data yields and the expected signal and background yields in the dilepton channel. The expected yields of pure CP-even and CP-odd $t\bar{t}H$ and tH signals, with $\kappa_t' = 1$, are shown at the top of the table. The uncertainties in the pure CP-even and CP-odd $t\bar{t}H$ and tH signals are the total uncertainties before fitting to data. Below that are shown the post-fit $t\bar{t}H$ and tH yields, corresponding to $\kappa_t' = 0.84$ and $\alpha = 11°$. The following seven rows show the yields and uncertainties of individual background sources, where "other" corresponds to W+ jets, Z+ jets, $t\bar{t}W$, $t\bar{t}Z$, tZq, tWZ, $t\bar{t}t\bar{t}$ and $WW/WZ/ZZ$ events, as in Ref. [36]. The row labelled 'Total' represents the total signal plus background post-fit yields. The uncertainties in the post-fit yields are evaluated from the post-fit nuisance parameters as well as the post-fit uncertainties in the fitted free parameters (α and κ_t' for the signals and $k_{t\bar{t}+b}$ for the $t\bar{t}+\geq 1b$ background) that affect the corresponding processes. The correlations amongst all fitted parameters are taken into account. Due to these correlations the uncertainties in the total yields do not correspond to the quadrature sum of uncertainties of individual signals and backgrounds.

	$CR_{hi}^{3j,3b}$	$CR_{lo}^{\geq 4j,3b}$	$CR_{hi}^{\geq 4j,3b}$	$CR_{no\text{-}reco}^{\geq 4j,\geq 4b}$	$CR^{\geq 4j,\geq 4b}$	$SR_{1}^{\geq 4j,\geq 4b}$	$SR_{2}^{\geq 4j,\geq 4b}$
$t\bar{t}H$ $(1,0°)$	26±4	79±8	120±12	16.9±2.1	6.9±1.1	12.5±1.5	24.8±2.9
$tH(1,0°)$	1.12±0.13	0.90±0.13	1.74±0.20	0.19±0.08	0.087±0.035	0.100±0.033	0.09±0.06
$t\bar{t}H$ $(1,90°)$	10.6±1.6	35.6±3.5	54±5	7.2±0.9	4.3±0.6	6.1±0.7	10.9±1.3
$tH(1,90°)$	5.4±0.6	7.0±1.0	10.7±1.2	1.8±0.8	0.48±0.19	0.48±0.16	0.5±0.4
$t\bar{t}H$ $(0.84,11°)$	18±14	50±40	80±60	11±9	4.7±3.4	8±6	17±12
tH $(0.84,11°)$	0.9±0.5	1.0±1.9	1.5±1.3	0.17±0.16	0.068±0.016	0.08±0.14	0.07±0.09
$t\bar{t}+\geq 1b$	1990±80	2520±110	4040±130	288±15	371±16	160±8	122±11
$t\bar{t}+\geq 1c$	550±50	2510±150	1160±90	23±4	31.1±2.5	13.4±1.6	8.2±1.0
$t\bar{t}$+ light	143±27	960±130	230±40	1.7±0.4	2.3±0.8	1.4±0.8	0.57±0.25
Other	140±11	390±19	340±40	33±8	18.6±2.5	10.9±1.3	8.7±1.0
Total	2840±50	6430±80	5850±80	358±12	428±15	194±5	156±6
Data	2827	6429	5865	354	420	190	170

6. Systematic uncertainties

Systematic uncertainties are assessed for three main sources: theoretical modelling of the signal processes, background modelling which is dominated by the uncertainties in the $t\bar{t}+\geq 1b$ background and experimental sources involving the (mis)identification rates and energy calibration of leptons, jets, b-jets and missing transverse momentum. Uncertainties accounting for the limited number of events in all simulated samples are also considered. Systematic variations can affect the overall yields, relative yields between analysis regions and shapes of observables.

Uncertainties associated with the modelling of the $t\bar{t}H$ signals include variations due to initial and final state radiation (ISR and FSR), choice of the NLO matching procedure as well as the PS and hadronisation model. These uncertainties are evaluated using events generated with POWHEG BOX + PYTHIA 8, which are produced with the same PDF set and renormalisation and factorisation scales as the nominal MADGRAPH5_AMC@NLO + PYTHIA 8 sample, unless otherwise specified.

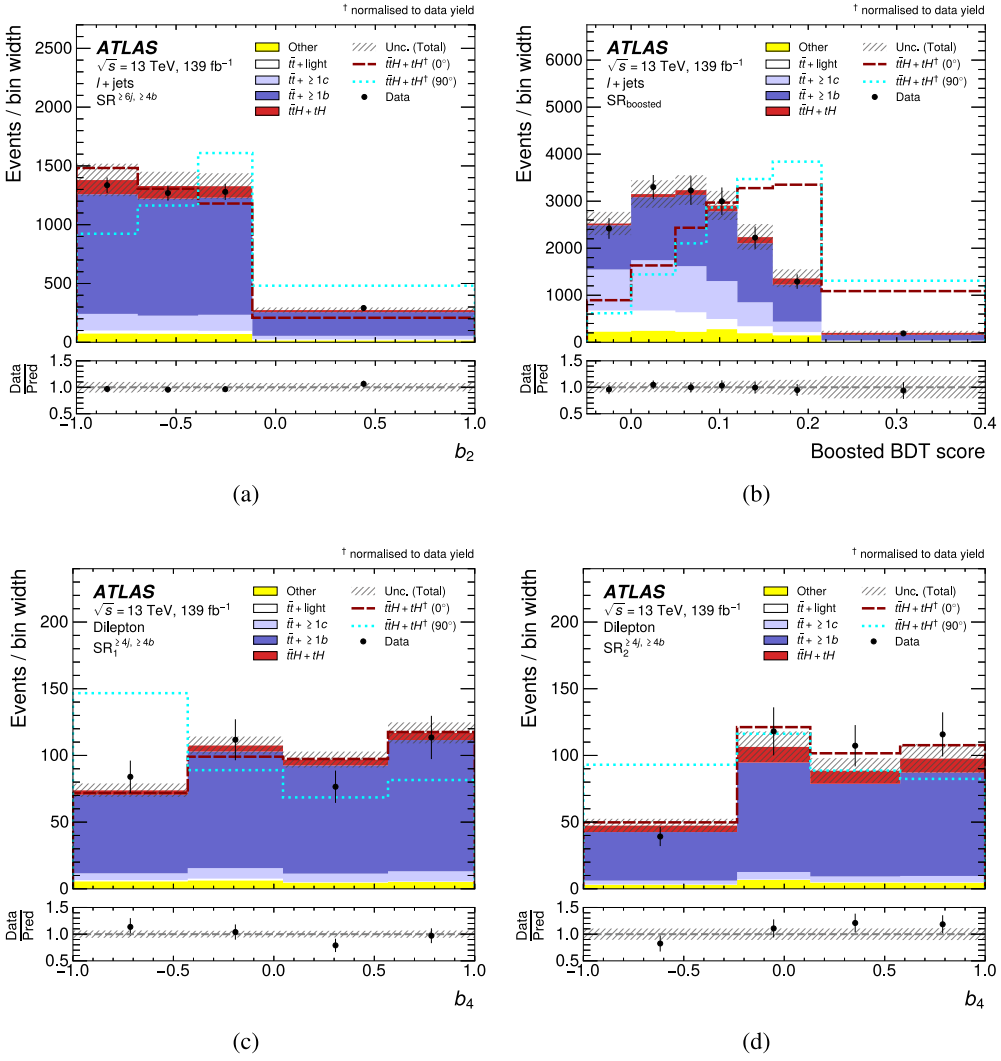

Fig. 2. The distributions of the fitted variables in all signal regions. The stacked histograms represent the predictions from a fit of signal and background to data with both κ_t' and α as free parameters. This is compared with data shown with black dots. The solid red histogram shows the best-fit signal with $\alpha = 11°$ and $\kappa_t' = 0.84$. The dashed and dotted lines show $t\bar{t}H + tH$ signal predictions for pure CP-even and CP-odd hypotheses, respectively, normalised to the total data yield per region in order to illustrate the shapes of the signal distribution. The hashed area around the prediction illustrates the total post-fit uncertainties. The lower panel shows the ratio of data to the predicted yields from a fit of signal and background in which κ_t' and α are free parameters.

Variations relative to the SM hypothesis are propagated to scenarios with alternative values of α and κ_t'. To estimate the uncertainty related to the amount of partonic ISR, the renormalisation and factorisation scales in the ME and α_S^{ISR} in the PS are varied simultaneously [92]. The impact of the FSR is evaluated by varying α_S^{FSR} in the PS. The impact of varying the PS and hadronisation models is estimated by comparing $t\bar{t}H$ samples generated using POWHEG BOX + PYTHIA 8.230 with those generated from POWHEG BOX + HERWIG 7.04 [93]. The uncertainty due to the choice of NLO matching procedure is derived by directly comparing the POWHEG BOX + PYTHIA 8 sample with the nominal MADGRAPH5_AMC@NLO + PYTHIA 8 sample. The uncertainties in the modelling of tH are estimated using the nominal sample generated using MADGRAPH5_AMC@NLO + PYTHIA 8. For each tH subprocess ($tHjb$ and tWH), two sources of modelling uncertainty are considered: that associated with the description of PDFs, and the uncertainty due to missing higher-order QCD contributions. The former is estimated from the standard deviation of the expected yields using 100 NNPDF3.0NLO eigenvector PDF sets, in each analysis bin used to build the likelihood function. The latter is estimated by coherently varying μ_r and μ_f by factors of 0.5 and 2.

The most important uncertainties in the background estimation come from the modelling of the $t\bar{t} + \geq 1b$ background. These uncertainties are designed to account for the choice of NLO matching procedure, PS and hadronisation model as well as the flavour scheme utilised in the $t\bar{t} + \geq 1b$ event generation. An uncertainty in the ME-to-PS matching procedure is assessed by comparing the POWHEG BOX + PYTHIA 8 sample with a sample generated using MADGRAPH5_AMC@NLO + PYTHIA 8, both in the five-flavour scheme. The variation by comparing these two samples is propagated to the nominal $t\bar{t} + \geq 1b$ sample generated with POWHEG BOX RES + PYTHIA 8 in the four-flavour scheme. This uncertainty is separated into three components that are treated independently: one for the dilepton channel, another for the non-boosted regions in the ℓ + jets channel, and a third for the ℓ + jets boosted region. This treatment is found to be important because it provides the fit with enough flexibility to cover the potential background mismodelling. Uncertainties in the choice of the PS model are evaluated by comparing the nominal sample with the one produced with POWHEG BOX + HERWIG 7. These uncertainties are treated in the same way as the uncertainty in the NLO matching procedure. An additional source of systematic uncertainty is introduced to address the choice of flavour scheme used for the generation of the $t\bar{t} + \geq 1b$ events. It is evaluated by

comparing the nominal sample, generated in the four-flavour scheme using POWHEG + PYTHIA 8, with that produced in the five-flavour scheme reweighted to remove differences in scale settings. Uncertainties in ISR and FSR are estimated using the same procedure as used for the $t\bar{t}H$ signals. An uncertainty due to differences in relative fraction of $t\bar{t}+1b$ and $t\bar{t}+\geq 2b$ subcomponents from different MC predictions is also considered. Other uncertainties in $t\bar{t}+\geq 1b$ and uncertainties in other background components are treated identically to the procedure described in Ref. [36].

Aside from the modelling uncertainties described above, experimental uncertainties are also considered. These arise from the modelling of trigger, reconstruction, identification and isolation efficiencies, as well as the calibration of energy and momentum scales for all physics objects, including electrons, muons, jets, b-tagged jets and $E_{\mathrm{T}}^{\mathrm{miss}}$. Uncertainties in the measured integrated luminosity and in the modelling of additional pp collisions are included.

7. Results

A binned profile likelihood fit is performed including all analysis regions simultaneously in order to determine the α and κ_t' parameters. The likelihood function, $\mathcal{L}(\alpha, \kappa_t', \boldsymbol{\theta})$, is constructed as the product of Poisson terms, with each term corresponding to an analysis bin. The value of the likelihood varies according to the expected signal yields, as a function of α and κ_t', and background yields of the analysis bins, as well as $\boldsymbol{\theta}$, representing the nuisance parameters encoding the effects of the systematic uncertainties and a single parameter controlling the normalisation of the $t\bar{t}+\geq 1b$ background. The nuisance parameters are constrained with Gaussian or log-normal functions. The normalisation of the $t\bar{t}+\geq 1b$ background is controlled by an unconstrained parameter $k_{t\bar{t}+b}$. A profile likelihood ratio is used as the test statistic, following Ref. [94]. By scanning the value of the test statistic in grid points in κ_t' and α, two-dimensional exclusion contours in the (κ_t', α) plane are obtained.

Fig. 1 compares the observed yield of data in each analysis region with that expected after the fit to data (post-fit). The expected yields for pure CP-even and CP-odd signals, normalised to the total data yields, are overlaid and shown with dashed lines in the top panels. These illustrate the signal-to-background separation provided by the classification BDTs. In the middle panel, the best-fit model is compared with the data by showing ratios of its value to the post-fit background prediction. The post-fit model agrees well with the observed data. In addition, the expected S/B for pure CP-even and CP-odd signals are shown for both $t\bar{t}H$ and tH. The post-fit yields for all backgrounds and the signals are summarised in Tables 3 and 4 for the $\ell+$ jets and dilepton channels, respectively. The expected yields of pure CP-even and CP-odd signals are compared with the post-fit yields. In all fitted regions, the best-fit signal yields are lower than their SM predictions. The fitted value of $k_{t\bar{t}+b}$ is $1.30^{+0.09}_{-0.08}$, consistent with the value measured in Ref. [36]. Fig. 2 shows the distributions of the fitted observables in the four SRs. The post-fit predictions are in agreement with data. Goodness-of-fit was evaluated using a likelihood ratio test, comparing the likelihood value from the nominal fit with the one obtained from a saturated model built with one free-floating normalisation factor for each fitted bin [95]. The probability that the post-fit prediction is compatible with the observed data is 80%. The pure CP-even and CP-odd signals are shown overlaid and normalised to the data yield to indicate the kinematic discrimination of the b_2 and b_4 observables.

The best-fit values and the exclusion contours in α and κ_t' are displayed in Fig. 3 in the $(\kappa_t' \cos\alpha, \kappa_t' \sin\alpha)$ plane. The best-fit value for the CP mixing angle α is $11^{\circ}{}^{+52^{\circ}}_{-73^{\circ}}$ and overall coupling strength κ_t' is $0.84^{+0.30}_{-0.46}$, which are in agreement with the SM expectations of $\alpha = 0^{\circ}$ and $\kappa_t' = 1$. The data disfavour the pure CP-odd hypothesis with a 1.2 σ significance. The significance of the observed $t\bar{t}H$ and tH signals over the background prediction is 1.3 σ. The compatibility of this analysis with the $t\bar{t}H$ cross-section measurement [36] was tested with the same

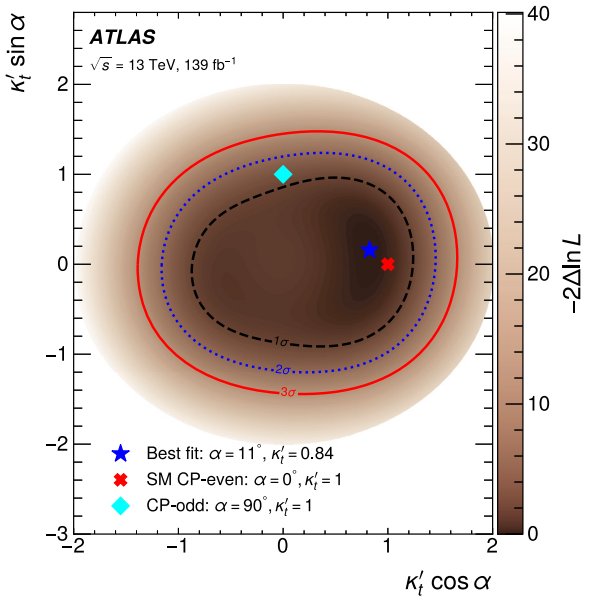

Fig. 3. The observed exclusion contours in the $(\kappa_t' \cos\alpha, \kappa_t' \sin\alpha)$ plane. Regions contained in the dashed, dotted and solid lines are compatible with the best-fit results at 1, 2 and 3 σ standard deviations. The cross (diamond) represents the CP-even (CP-odd) with $\kappa_t' = 1$ and the best-fit result is represented with a pentagram.

parameter of interest: a single free-floating signal strength, $\mu_{t\bar{t}H}$, controlling the normalisation of $t\bar{t}H$ production in the SM scenario. The tH process was fixed to its SM prediction with an identical systematic model. The compatibility is tested using the bootstrap technique [96]. The difference in the measured $\mu_{t\bar{t}H}$ is sampled by fitting to toy datasets generated by varying the event weights entering the Asimov dataset according to the Poisson fluctuations expected in data. The measured values of $\mu_{t\bar{t}H}$ were found to be compatible within one standard deviation, when accounting for the statistical correlations between the two measurements.

The impact of a group of systematic uncertainties on α (κ_t') is assessed by fixing the nuisance parameters to their best fit values and subtracting the subsequent α (κ_t') uncertainty in quadrature from the total α (κ_t') uncertainty. The uncertainty in the measured value of α is dominated by $t\bar{t}+\geq 1b$ modelling uncertainties which contribute $^{+37^{\circ}}_{-51^{\circ}}$ to the overall uncertainty. This is driven by: the NLO matching procedure between the ME and PS; PS and hadronisation; and the choice of flavour scheme. These uncertainties contribute $^{+22^{\circ}}_{-33^{\circ}}$, $^{+16^{\circ}}_{-24^{\circ}}$ and $^{+23^{\circ}}_{-37^{\circ}}$, respectively. Smaller effects from the $t\bar{t}+\geq 1b$ modelling originate from the ISR uncertainty and the relative fractions of $t\bar{t}+\geq 2b$ and $t\bar{t}+1b$, contributing $^{+14^{\circ}}_{-24^{\circ}}$ and $^{+14^{\circ}}_{-21^{\circ}}$. The $t\bar{t}+\geq 1c$ modelling uncertainties contribute only $^{+6.6^{\circ}}_{-11^{\circ}}$ to the uncertainty in α. The 100% $t\bar{t}+\geq 1c$ normalisation uncertainty is constrained to 50% with a pull of 0.6 σ, and has negligible impact on the fitted α and κ_t'. Through a correlation with α, the measured κ_t' contributes $^{+17^{\circ}}_{-33^{\circ}}$ to the α uncertainty. Experimental uncertainties are smaller than the $t\bar{t}+\geq 1b$ modelling uncertainties. The statistical uncertainty is $^{+32^{\circ}}_{-49^{\circ}}$.

8. Summary

In conclusion, the CP properties of the top-quark's Yukawa coupling to the Higgs boson are probed in $t\bar{t}H$ and tH production with $H \to b\bar{b}$ decays, which had not been studied before. Dedicated CP-sensitive variables relying on angular separations between reconstructed top quarks or lepton candidates were used directly. Assuming the SM branching ratio for the Higgs boson decay, the best-fit values of the CP-mixing angle and the overall coupling strength are $\alpha = 11^{\circ}{}^{+52^{\circ}}_{-73^{\circ}}$

and $\kappa_t' = 0.84^{+0.30}_{-0.46}$. These values can be compared with the expected allowed 1 σ ranges of α and κ_t', obtained using Asimov datasets constructed with either a pure CP-even or -odd signal. For a CP-even scenario $\alpha \in [-180°, -173°] \cup [-50°, 52°] \cup [171°, 180°]$ and $\kappa_t' = 1.00^{+0.29}_{-0.27}$, whilst for a pure CP-odd scenario $\alpha \in [-157°, -41°] \cup [43°, 157°]$ and $\kappa_t' = 1.00^{+0.22}_{-0.33}$. The sensitivity of this measurement is driven by the systematic uncertainties.

These results complement previous ATLAS measurements in the $H \to \gamma\gamma$ decay channel and will allow for a future combined measurement of the CP properties of the top-quark Yukawa coupling. Due to the tree-level sensitivity and the high $H \to b\bar{b}$ branching ratio, it can be expected that future measurements in the $t\bar{t}H$ and tH channels will become quite sensitive to the CP properties of the top-quark Yukawa coupling. Additional LHC data and a better theoretical understanding of the $t\bar{t} + \geq 1b$ process will be essential ingredients in order to achieve this sensitivity.

Declaration of competing interest

The authors declare that they have no known competing financial interests or personal relationships that could have appeared to influence the work reported in this paper.

Data availability

Data will be made available on request.

Acknowledgements

We thank CERN for the very successful operation of the LHC, as well as the support staff from our institutions without whom ATLAS could not be operated efficiently.

We acknowledge the support of ANPCyT, Argentina; YerPhI, Armenia; ARC, Australia; BMWFW and FWF, Austria; ANAS, Azerbaijan; CNPq and FAPESP, Brazil; NSERC, NRC and CFI, Canada; CERN; ANID, Chile; CAS, MOST and NSFC, China; Minciencias, Colombia; MEYS CR, Czech Republic; DNRF and DNSRC, Denmark; IN2P3-CNRS and CEA-DRF/IRFU, France; SRNSFG, Georgia; BMBF, HGF and MPG, Germany; GSRI, Greece; RGC and Hong Kong SAR, China; ISF and Benoziyo Center, Israel; INFN, Italy; MEXT and JSPS, Japan; CNRST, Morocco; NWO, Netherlands; RCN, Norway; MEiN, Poland; FCT, Portugal; MNE/IFA, Romania; MESTD, Serbia; MSSR, Slovakia; ARRS and MIZŠ, Slovenia; DSI/NRF, South Africa; MICINN, Spain; SRC and Wallenberg Foundation, Sweden; SERI, SNSF and Cantons of Bern and Geneva, Switzerland; MOST, Taiwan; TENMAK, Türkiye; STFC, United Kingdom; DOE and NSF, United States of America. In addition, individual groups and members have received support from BCKDF, Canarie, Compute Canada and CRC, Canada; PRIMUS 21/SCI/017 and UNCE SCI/013, Czech Republic; COST, ERC, ERDF, Horizon 2020, ICSC-NextGenerationEU and Marie Skłodowska-Curie Actions, European Union; Investissements d'Avenir Labex, Investissements d'Avenir Idex and ANR, France; DFG and AvH Foundation, Germany; Herakleitos, Thales and Aristeia programmes co-financed by EU-ESF and the Greek NSRF, Greece; BSF-NSF and MINERVA, Israel; Norwegian Financial Mechanism 2014-2021, Norway; NCN and NAWA, Poland; La Caixa Banking Foundation, CERCA Programme Generalitat de Catalunya and PROMETEO and GenT Programmes Generalitat Valenciana, Spain; Göran Gustafssons Stiftelse, Sweden; The Royal Society and Leverhulme Trust, United Kingdom.

The crucial computing support from all WLCG partners is acknowledged gratefully, in particular from CRN, the ATLAS Tier-1 facilities at TRIUMF (Canada), NDGF (Denmark, Norway, Sweden), CC-IN2P3 (France), KIT/GridKA (Germany), INFN-CNAF (Italy), NL-T1 (Netherlands), PIC (Spain), ASGC (Taiwan), RAL (UK) and BNL (USA), the Tier-2 facilities worldwide and large non-WLCG resource providers. Major contributors of computing resources are listed in Ref. [97].

References

[1] ATLAS Collaboration, Observation of a new particle in the search for the Standard Model Higgs boson with the ATLAS detector at the LHC, Phys. Lett. B 716 (2012) 1, arXiv:1207.7214 [hep-ex].

[2] CMS Collaboration, Observation of a new boson with mass near 125 GeV in pp collisions at $\sqrt{s} = 7$ and 8 TeV, J. High Energy Phys. 06 (2013) 081, arXiv:1303.4571 [hep-ex].

[3] ATLAS Collaboration, Observation of Higgs boson production in association with a top quark pair at the LHC with the ATLAS detector, Phys. Lett. B 784 (2018) 173, arXiv:1806.00425 [hep-ex].

[4] CMS Collaboration, Observation of $t\bar{t}H$ production, Phys. Rev. Lett. 120 (2018) 231801, arXiv:1804.02610 [hep-ex].

[5] ATLAS Collaboration, CP properties of Higgs boson interactions with top quarks in the $t\bar{t}H$ and tH processes using $H \to \gamma\gamma$ with the ATLAS detector, Phys. Rev. Lett. 125 (2020) 061802, arXiv:2004.04545 [hep-ex].

[6] CMS Collaboration, Measurements of $t\bar{t}H$ production and the CP structure of the Yukawa interaction between the Higgs boson and top quark in the diphoton decay channel, Phys. Rev. Lett. 125 (2020) 061801, arXiv:2003.10866 [hep-ex].

[7] CMS Collaboration, Search for CP violation in ttH and tH production in multilepton channels in proton–proton collisions at $\sqrt{s} = 13\,TeV$, J. High Energy Phys. 07 (2022) 092, arXiv:2208.02686 [hep-ex].

[8] W. Buchmüller, D. Wyler, Effective Lagrangian analysis of new interactions and flavour conservation, Nucl. Phys. B (ISSN 0550-3213) 268 (1986) 621.

[9] V. Hankele, G. Klämke, D. Zeppenfeld, T. Figy, Anomalous Higgs boson couplings in vector boson fusion at the CERN LHC, Phys. Rev. D 74 (2006).

[10] D. Fontes, J.C. Romão, R. Santos, J.P. Silva, Large pseudoscalar Yukawa couplings in the complex 2HDM, J. High Energy Phys. 2015 (2015) 60, arXiv:1502.01720v2 [hep-ph].

[11] ATLAS Collaboration, Evidence for the spin-0 nature of the Higgs boson using ATLAS data, Phys. Lett. B 726 (2013) 120, arXiv:1307.1432 [hep-ex].

[12] CMS Collaboration, Study of the mass and spin-parity of the Higgs boson candidate via its decays to Z boson pairs, Phys. Rev. Lett. 110 (2013) 081803, arXiv:1212.6639 [hep-ex].

[13] ATLAS Collaboration, Search for a CP-odd Higgs boson decaying to Zh in pp collisions at $\sqrt{s} = 8\,TeV$ with the ATLAS detector, Phys. Lett. B 744 (2015) 163, arXiv:1502.04478 [hep-ex].

[14] ATLAS Collaboration, Test of CP invariance in vector-boson fusion production of the Higgs boson in the $H \to \tau\tau$ channel in proton–proton collisions at $\sqrt{s} = 13\,TeV$ with the ATLAS detector, Phys. Lett. B 805 (2020) 135426, arXiv:2002.05315 [hep-ex].

[15] ATLAS Collaboration, Measurements of Higgs boson properties in the diphoton decay channel with 36 fb^{-1} of pp collision data at $\sqrt{s} = 13\,TeV$ with the ATLAS detector, Phys. Rev. D 98 (2018) 052005, arXiv:1802.04146 [hep-ex].

[16] ATLAS Collaboration, Measurement of the Higgs boson coupling properties in the $H \to ZZ^* \to 4\ell$ decay channel at $\sqrt{s} = 13\,TeV$ with the ATLAS detector, J. High Energy Phys. 03 (2018) 095, arXiv:1712.02304 [hep-ex].

[17] CMS Collaboration, Combined search for anomalous pseudoscalar HVV couplings in $VH(H \to b\bar{b})$ production and $H \to VV$ decay, Phys. Lett. B 759 (2016) 672, arXiv:1602.04305 [hep-ex].

[18] CMS Collaboration, Constraints on anomalous Higgs boson couplings using production and decay information in the four-lepton final state, Phys. Lett. B 775 (2017) 1, arXiv:1707.00541 [hep-ex].

[19] CMS Collaboration, Measurements of the Higgs boson width and anomalous HVV couplings from on-shell and off-shell production in the four-lepton final state, Phys. Rev. D 99 (2019) 112003, arXiv:1901.00174 [hep-ex].

[20] CMS Collaboration, Constraints on anomalous Higgs boson couplings to vector bosons and fermions from the production of Higgs bosons using the $\tau\tau$ final state, arXiv:2205.05120 [hep-ex], 2022.

[21] ATLAS Collaboration, Test of CP-invariance of the Higgs boson in vector-boson fusion production and its decay into four leptons, arXiv:2304.09612 [hep-ex], 2023.

[22] J.F. Gunion, X.-G. He, Determining the CP nature of a neutral Higgs boson at the CERN large hadron collider, Phys. Rev. Lett. 76 (1996) 4468, arXiv:hep-ph/9602226.

[23] J. Ellis, D.S. Hwang, K. Sakurai, M. Takeuchi, Disentangling Higgs-top couplings in associated production, J. High Energy Phys. 04 (2014) 004, arXiv:1312.5736 [hep-ph].

[24] X.-G. He, G.-N. Li, Y.-J. Zheng, Probing Higgs boson CP properties with $t\bar{t}H$ at the LHC and the 100 TeV pp collider, Int. J. Mod. Phys. A 30 (2014) 1550156, arXiv:1501.00012 [hep-ph].

[25] F. Boudjema, D. Guadagnoli, R.M. Godbole, K.A. Mohan, Laboratory-frame observables for probing the top-Higgs boson interaction, Phys. Rev. D 92 (2015) 015019, arXiv:1501.03157 [hep-ph].

[26] F. Demartin, F. Maltoni, K. Mawatari, B. Page, M. Zaro, Higgs characterisation at NLO in QCD: CP properties of the top-quark Yukawa interaction, Eur. Phys. J. C 74 (2014) 3065, arXiv:1407.5089 [hep-ph].

[27] H. Bahl, et al., Indirect CP probes of the Higgs-top-quark interaction: current LHC constraints and future opportunities, J. High Energy Phys. 2020 (2020) 127, arXiv:2007.08542 [hep-ph].

[28] D. Gonçalves, J.H. Kim, K. Kong, Y. Wu, Direct Higgs-top CP-phase measurement with $t\bar{t}h$ at the 14 TeV LHC and 100 TeV FCC, J. High Energy Phys. 2022 (2022) 158, arXiv:2108.01083 [hep-ph].

[29] J. Brod, U. Haisch, J. Zupan, Constraints on CP-violating Higgs couplings to the third generation, J. High Energy Phys. 11 (2013) 180, arXiv:1310.1385 [hep-ph].

[30] V. Andreev, et al., Improved limit on the electric dipole moment of the electron, Nature 562 (2018) 355.

[31] C. Abel, et al., Measurement of the permanent electric dipole moment of the neutron, Phys. Rev. Lett. 124 (2020) 081803, arXiv:2001.11966 [hep-ex].

[32] M.R. Buckley, D. Goncalves, Boosting the direct CP measurement of the Higgs-top coupling, Phys. Rev. Lett. 116 (2016) 091801, arXiv:1507.07926 [hep-ph].

[33] D. Gonçalves, J.H. Kim, K. Kong, Probing the top-Higgs Yukawa CP structure in dileptonic $t\bar{t}h$ with M $_2$-assisted reconstruction, J. High Energy Phys. 06 (2018) 079, arXiv:1804.05874 [hep-ph].

[34] D. Azevedo, A. Onofre, F. Filthaut, R. Gonçalo, CP tests of Higgs couplings in $t\bar{t}h$ semileptonic events at the LHC, Phys. Rev. D 98 (2018) 033004, arXiv:1711.05292 [hep-ph].

[35] A. Ferroglia, M.C.N. Fiolhais, E. Gouveia, A. Onofre, Role of the $t\bar{t}h$ rest frame in direct top-quark Yukawa coupling measurements, Phys. Rev. D 100 (2019) 075034, arXiv:1909.00490 [hep-ph].

[36] ATLAS Collaboration, Measurement of Higgs boson decay into b-quarks in associated production with a top-quark pair in pp collisions at $\sqrt{s} = 13\,TeV$ with the ATLAS detector, J. High Energy Phys. 06 (2022) 097, arXiv:2111.06712 [hep-ex].

[37] D. de Florian, et al., Handbook of LHC Higgs cross sections: 4. deciphering the nature of the Higgs sector, arXiv:1610.07922 [hep-ph], 2016.

[38] ATLAS Collaboration, The ATLAS experiment at the CERN large hadron collider, J. Instrum. 3 (2008) S08003.

[39] ATLAS Collaboration, ATLAS insertable B-layer: technical design report, ATLAS-TDR-19; CERN-LHCC-2010-013, https://cds.cern.ch/record/1291633, 2010; Addendum: ATLAS-TDR-19-ADD-1; CERN-LHCC-2012-009, https://cds.cern.ch/record/1451888, 2012.

[40] B. Abbott, et al., Production and integration of the ATLAS insertable B-layer, J. Instrum. 13 (2018) T05008, arXiv:1803.00844 [physics.ins-det].

[41] ATLAS Collaboration, Performance of the ATLAS trigger system in 2015, Eur. Phys. J. C 77 (2017) 317, arXiv:1611.09661 [hep-ex].

[42] ATLAS Collaboration, The ATLAS Collaboration software and firmware, ATL-SOFT-PUB-2021-001, https://cds.cern.ch/record/2767187, 2021.

[43] ATLAS Collaboration, Performance of the ATLAS muon triggers in Run 2, J. Instrum. 15 (2020) P09015, arXiv:2004.13447 [physics.ins-det].

[44] ATLAS Collaboration, Performance of electron and photon triggers in ATLAS during LHC Run 2, Eur. Phys. J. C 80 (2020) 47, arXiv:1909.00761 [hep-ex].

[45] ATLAS Collaboration, Electron and photon performance measurements with the ATLAS detector using the 2015–2017 LHC proton–proton collision data, J. Instrum. 14 (2019) P12006, arXiv:1908.00005 [hep-ex].

[46] ATLAS Collaboration, Muon reconstruction and identification efficiency in ATLAS using the full Run 2 pp collision data set at $\sqrt{s} = 13\,TeV$, Eur. Phys. J. C 81 (2021) 578, arXiv:2012.00578 [hep-ex].

[47] ATLAS Collaboration, Topological cell clustering in the ATLAS calorimeters and its performance in LHC Run 1, Eur. Phys. J. C 77 (2017) 490, arXiv:1603.02934 [hep-ex].

[48] ATLAS Collaboration, Jet energy scale and resolution measured in proton–proton collisions at $\sqrt{s} = 13\,TeV$ with the ATLAS detector, Eur. Phys. J. C 81 (2020) 689, arXiv:2007.02645 [hep-ex].

[49] M. Cacciari, G.P. Salam, G. Soyez, The anti-k_t jet clustering algorithm, J. High Energy Phys. 04 (2008) 063, arXiv:0802.1189 [hep-ph].

[50] M. Cacciari, G.P. Salam, G. Soyez, FastJet user manual, Eur. Phys. J. C 72 (2012) 1896, arXiv:1111.6097 [hep-ph].

[51] ATLAS Collaboration, ATLAS b-jet identification performance and efficiency measurement with $t\bar{t}$ events in pp collisions at $\sqrt{s} = 13\,TeV$, Eur. Phys. J. C 79 (2019) 970, arXiv:1907.05120 [hep-ex].

[52] ATLAS Collaboration, Measurement of b-tagging efficiency of c-jets in $t\bar{t}$ events using a likelihood approach with the ATLAS detector, ATLAS-CONF-2018-001, https://cds.cern.ch/record/2306649, 2018.

[53] ATLAS Collaboration, Calibration of light-flavour b-jet mistagging rates using ATLAS proton–proton collision data at $\sqrt{s} = 13\,TeV$, ATLAS-CONF-2018-006, https://cds.cern.ch/record/2314418, 2018.

[54] ATLAS Collaboration, Performance of missing transverse momentum reconstruction with the ATLAS detector using proton–proton collisions at $\sqrt{s} = 13\,TeV$, Eur. Phys. J. C 78 (2018) 903, arXiv:1802.08168 [hep-ex].

[55] B. Nachman, P. Nef, A. Schwartzman, M. Swiatlowski, C. Wanotayaroj, Jets from jets: re-clustering as a tool for large radius jet reconstruction and grooming at the LHC, J. High Energy Phys. 02 (2015) 075, arXiv:1407.2922 [hep-ph].

[56] ATLAS Collaboration, The ATLAS simulation infrastructure, Eur. Phys. J. C 70 (2010) 823, arXiv:1005.4568 [physics.ins-det].

[57] S. Agostinelli, et al., Geant4 – a simulation toolkit, Nucl. Instrum. Methods A 506 (2003) 250.

[58] T. Sjöstrand, et al., An introduction to PYTHIA 8.2, Comput. Phys. Commun. 191 (2015) 159, arXiv:1410.3012 [hep-ph].

[59] ATLAS Collaboration, The Pythia 8 A3 tune description of ATLAS minimum bias and inelastic measurements incorporating the Donnachie–Landshoff diffractive model, ATL-PHYS-PUB-2016-017, https://cds.cern.ch/record/2206965, 2016.

[60] T. Ježo, J.M. Lindert, N. Moretti, S. Pozzorini, New NLOPS predictions for $t\bar{t}$ + b-jet production at the LHC, Eur. Phys. J. C 78 (2018) 502, arXiv:1802.00426 [hep-ph].

[61] F. Cascioli, P. Maierhöfer, S. Pozzorini, Scattering amplitudes with open loops, Phys. Rev. Lett. 108 (2012) 111601, arXiv:1111.5206 [hep-ph].

[62] A. Denner, S. Dittmaier, L. Hofer, Collier: a fortran-based complex one-loop library in extended regularizations, Comput. Phys. Commun. 212 (2017) 220, arXiv:1604.06792 [hep-ph].

[63] T. Ježo, Powheg-Box-Res ttbb source code, https://gitlab.cern.ch/tjezo/powheg-box-res_ttbb/, 2019.

[64] The NNPDF Collaboration, R.D. Ball, et al., Parton distributions for the LHC run II, J. High Energy Phys. 04 (2015) 040, arXiv:1410.8849 [hep-ph].

[65] ATLAS Collaboration, ATLAS Pythia 8 tunes to 7 TeV data, ATL-PHYS-PUB-2014-021, https://cds.cern.ch/record/1966419, 2014.

[66] ATLAS Collaboration, Measurements of inclusive and differential fiducial cross-sections of $t\bar{t}$ production with additional heavy-flavour jets in proton–proton collisions at $\sqrt{s} = 13\,TeV$ with the ATLAS detector, J. High Energy Phys. 04 (2019) 046, arXiv:1811.12113 [hep-ex].

[67] CMS Collaboration, Measurement of the $t\bar{t}b\bar{b}$ production cross section in the all-jet final state in pp collisions at $\sqrt{s} = 13\,TeV$, Phys. Lett. B 803 (2020) 135285, arXiv:1909.05306 [hep-ex].

[68] P. Nason, A new method for combining NLO QCD with shower Monte Carlo algorithms, J. High Energy Phys. 11 (2004) 040, arXiv:hep-ph/0409146.

[69] S. Frixione, P. Nason, C. Oleari, Matching NLO QCD computations with parton shower simulations: the POWHEG method, J. High Energy Phys. 11 (2007) 070, arXiv:0709.2092 [hep-ph].

[70] S. Alioli, P. Nason, C. Oleari, E. Re, A general framework for implementing NLO calculations in shower Monte Carlo programs: the POWHEG BOX, J. High Energy Phys. 06 (2010) 043, arXiv:1002.2581 [hep-ph].

[71] H.B. Hartanto, B. Jäger, L. Reina, D. Wackeroth, Higgs boson production in association with top quarks in the POWHEG BOX, Phys. Rev. D 91 (2015) 094003, arXiv:1501.04498 [hep-ph].

[72] M. Beneke, P. Falgari, S. Klein, C. Schwinn, Hadronic top-quark pair production with NNLL threshold resummation, Nucl. Phys. B 855 (2012) 695, arXiv:1109.1536 [hep-ph].

[73] M. Cacciari, M. Czakon, M. Mangano, A. Mitov, P. Nason, Top-pair production at hadron colliders with next-to-next-to-leading logarithmic soft-gluon resummation, Phys. Lett. B 710 (2012) 612, arXiv:1111.5869 [hep-ph].

[74] P. Bärnreuther, M. Czakon, A. Mitov, Percent-level-precision physics at the tevatron: next-to-next-to-leading order QCD corrections to $q\bar{q} \to t\bar{t} + X$, Phys. Rev. Lett. 109 (2012) 132001, arXiv:1204.5201 [hep-ph].

[75] M. Czakon, A. Mitov, NNLO corrections to top-pair production at hadron colliders: the all-fermionic scattering channels, J. High Energy Phys. 12 (2012) 054, arXiv:1207.0236 [hep-ph].

[76] M. Czakon, A. Mitov, NNLO corrections to top pair production at hadron colliders: the quark-gluon reaction, J. High Energy Phys. 01 (2013) 080, arXiv:1210.6832 [hep-ph].

[77] M. Czakon, P. Fiedler, A. Mitov, Total top-quark pair-production cross section at hadron colliders through $O(\alpha_S^4)$, Phys. Rev. Lett. 110 (2013) 252004, arXiv:1303.6254 [hep-ph].

[78] M. Czakon, A. Mitov, Top++: a program for the calculation of the top-pair cross-section at hadron colliders, Comput. Phys. Commun. 185 (2014) 2930, arXiv:1112.5675 [hep-ph].

[79] P. Artoisenet, et al., A framework for Higgs characterisation, J. High Energy Phys. 11 (2013) 043, arXiv:1306.6464 [hep-ph].

[80] A. Alloul, N.D. Christensen, C. Degrande, C. Duhr, B. Fuks, FeynRules 2.0 - a complete toolbox for tree-level phenomenology, Comput. Phys. Commun. 185 (2014) 2250, arXiv:1310.1921 [hep-ph].

[81] C. Degrande, et al., UFO - the universal FeynRules output, Comput. Phys. Commun. 183 (2012) 1201, arXiv:1108.2040 [hep-ph].

[82] J. Alwall, et al., The automated computation of tree-level and next-to-leading order differential cross sections, and their matching to parton shower simulations, J. High Energy Phys. 07 (2014) 079, arXiv:1405.0301 [hep-ph].

[83] R. Raitio, W.W. Wada, Higgs-boson production at large transverse momentum in quantum chromodynamics, Phys. Rev. D 19 (1979) 941.

[84] W. Beenakker, et al., NLO QCD corrections to $t\bar{t}H$ production in hadron collisions, Nucl. Phys. B 653 (2003) 151, arXiv:hep-ph/0211352 [hep-ph].

[85] S. Dawson, C. Jackson, L.H. Orr, L. Reina, D. Wackeroth, Associated Higgs boson production with top quarks at the CERN Large Hadron Collider: NLO QCD corrections, Phys. Rev. D 68 (2003) 034022, arXiv:hep-ph/0305087v2 [hep-ph].

[86] Y. Zhang, W.-G. Ma, R.-Y. Zhang, C. Chen, L. Guo, QCD NLO and EW NLO corrections to $t\bar{t}H$ production with top quark decays at hadron collider, Phys. Lett. B 738 (2014) 1, arXiv:1407.1110 [hep-ph].

[87] S. Frixione, V. Hirschi, D. Pagani, H.-S. Shao, M. Zaro, Electroweak and QCD corrections to top-pair hadroproduction in association with heavy bosons, J. High Energy Phys. 06 (2015) 184, arXiv:1504.03446 [hep-ph].

[88] S. Frixione, E. Laenen, P. Motylinski, B.R. Webber, Angular correlations of lepton pairs from vector boson and top quark decays in Monte Carlo simulations, J. High Energy Phys. 04 (2007) 081, arXiv:hep-ph/0702198.

[89] ATLAS Collaboration, Performance of jet substructure techniques for large-R jets in proton–proton collisions at $\sqrt{s} = 7\,TeV$ using the ATLAS detector, J. High Energy Phys. 09 (2013) 076, arXiv:1306.4945 [hep-ex].

[90] DØ Collaboration, Measurement of the top quark mass using dilepton events, Phys. Rev. Lett. 80 (1998) 2063, arXiv:hep-ex/9706014.
[91] ATLAS Collaboration, Measurements of top-quark pair differential cross-sections in the $e\mu$ channel in pp collisions at $\sqrt{s} = 13$ TeV using the ATLAS detector, Eur. Phys. J. C 77 (2017) 292, arXiv:1612.05220 [hep-ex].
[92] ATLAS Collaboration, Study of top-quark pair modelling and uncertainties using ATLAS measurements at $\sqrt{s} = 13$ TeV, ATL-PHYS-PUB-2020-023, https://cds.cern.ch/record/2730443, 2020.
[93] J. Bellm, et al., Herwig 7.0/Herwig++ 3.0 release note, Eur. Phys. J. C 76 (2016) 196, arXiv:1512.01178 [hep-ph].
[94] G. Cowan, K. Cranmer, E. Gross, O. Vitells, Asymptotic formulae for likelihood-based tests of new physics, Eur. Phys. J. C 71 (2011) 1554, arXiv:1007.1727 [physics.data-an]; Erratum: Eur. Phys. J. C 73 (2013) 2501.
[95] R. Cousins, Generalization of chisquare goodness-of-fit test for binned data using saturated models, with application to histograms, http://www.physics.ucla.edu/~cousins/stats/cousins_saturated.pdf, 2013.
[96] ATLAS Collaboration, Evaluating statistical uncertainties and correlations using the bootstrap method, ATL-PHYS-PUB-2021-011, https://cds.cern.ch/record/2759945, 2021.
[97] ATLAS Collaboration, ATLAS computing acknowledgements, ATL-SOFT-PUB-2023-001, https://cds.cern.ch/record/2869272, 2023.

The ATLAS Collaboration

G. Aad [101], B. Abbott [119], D.C. Abbott [102], K. Abeling [55], S.H. Abidi [29], A. Aboulhorma [35e], H. Abramowicz [150], H. Abreu [149], Y. Abulaiti [116], A.C. Abusleme Hoffman [136a], B.S. Acharya [68a,68b,p], B. Achkar [55], L. Adam [99], C. Adam Bourdarios [4], L. Adamczyk [84a], L. Adamek [154], S.V. Addepalli [26], J. Adelman [114], A. Adiguzel [21c], S. Adorni [56], T. Adye [133], A.A. Affolder [135], Y. Afik [36], M.N. Agaras [13], J. Agarwala [72a,72b], A. Aggarwal [99], C. Agheorghiesei [27c], J.A. Aguilar-Saavedra [129f], A. Ahmad [36], F. Ahmadov [38,z], W.S. Ahmed [103], S. Ahuja [94], X. Ai [48], G. Aielli [75a,75b], I. Aizenberg [168], M. Akbiyik [99], T.P.A. Åkesson [97], A.V. Akimov [37], K. Al Khoury [41], G.L. Alberghi [23b], J. Albert [164], P. Albicocco [53], M.J. Alconada Verzini [89], S. Alderweireldt [52], M. Aleksa [36], I.N. Aleksandrov [38], C. Alexa [27b], T. Alexopoulos [10], A. Alfonsi [113], F. Alfonsi [23b], M. Alhroob [119], B. Ali [131], S. Ali [147], M. Aliev [37], G. Alimonti [70a], C. Allaire [36], B.M.M. Allbrooke [145], P.P. Allport [20], A. Aloisio [71a,71b], F. Alonso [89], C. Alpigiani [137], E. Alunno Camelia [75a,75b], M. Alvarez Estevez [98], M.G. Alviggi [71a,71b], Y. Amaral Coutinho [81b], A. Ambler [103], C. Amelung [36], C.G. Ames [108], D. Amidei [105], S.P. Amor Dos Santos [129a], S. Amoroso [48], K.R. Amos [162], C.S. Amrouche [56], V. Ananiev [124], C. Anastopoulos [138], N. Andari [134], T. Andeen [11], J.K. Anders [19], S.Y. Andrean [47a,47b], A. Andreazza [70a,70b], S. Angelidakis [9], A. Angerami [41,ac], A.V. Anisenkov [37], A. Annovi [73a], C. Antel [56], M.T. Anthony [138], E. Antipov [120], M. Antonelli [53], D.J.A. Antrim [17a], F. Anulli [74a], M. Aoki [82], J.A. Aparisi Pozo [162], M.A. Aparo [145], L. Aperio Bella [48], C. Appelt [18], N. Aranzabal [36], V. Araujo Ferraz [81a], C. Arcangeletti [53], A.T.H. Arce [51], E. Arena [91], J-F. Arguin [107], S. Argyropoulos [54], J.-H. Arling [48], A.J. Armbruster [36], O. Arnaez [154], H. Arnold [113], Z.P. Arrubarrena Tame [108], G. Artoni [74a,74b], H. Asada [110], K. Asai [117], S. Asai [152], N.A. Asbah [61], E.M. Asimakopoulou [160], K. Assamagan [29], R. Astalos [28a], R.J. Atkin [33a], M. Atkinson [161], N.B. Atlay [18], H. Atmani [62b], P.A. Atmasiddha [105], K. Augsten [131], S. Auricchio [71a,71b], A.D. Auriol [20], V.A. Austrup [170], G. Avner [149], G. Avolio [36], K. Axiotis [56], M.K. Ayoub [14c], G. Azuelos [107,ag], D. Babal [28a], H. Bachacou [134], K. Bachas [151,s], A. Bachiu [34], F. Backman [47a,47b], A. Badea [61], P. Bagnaia [74a,74b], M. Bahmani [18], A.J. Bailey [162], V.R. Bailey [161], J.T. Baines [133], C. Bakalis [10], O.K. Baker [171], P.J. Bakker [113], E. Bakos [15], D. Bakshi Gupta [8], S. Balaji [146], R. Balasubramanian [113], E.M. Baldin [37], P. Balek [132], E. Ballabene [70a,70b], F. Balli [134], L.M. Baltes [63a], W.K. Balunas [32], J. Balz [99], E. Banas [85], M. Bandieramonte [128], A. Bandyopadhyay [24], S. Bansal [24], L. Barak [150], E.L. Barberio [104], D. Barberis [57b,57a], M. Barbero [101], G. Barbour [95], K.N. Barends [33a], T. Barillari [109], M-S. Barisits [36], J. Barkeloo [122], T. Barklow [142], R.M. Barnett [17a], P. Baron [121], D.A. Baron Moreno [100], A. Baroncelli [62a], G. Barone [29], A.J. Barr [125], L. Barranco Navarro [47a,47b], F. Barreiro [98], J. Barreiro Guimarães da Costa [14a], U. Barron [150], M.G. Barros Teixeira [129a], S. Barsov [37], F. Bartels [63a], R. Bartoldus [142], A.E. Barton [90], P. Bartos [28a], A. Basalaev [48],

A. Basan [99], M. Baselga [49], I. Bashta [76a,76b], A. Bassalat [66,b], M.J. Basso [154], C.R. Basson [100], R.L. Bates [59], S. Batlamous [35e], J.R. Batley [32], B. Batool [140], M. Battaglia [135], M. Bauce [74a,74b], P. Bauer [24], A. Bayirli [21a], J.B. Beacham [51], T. Beau [126], P.H. Beauchemin [157], F. Becherer [54], P. Bechtle [24], H.P. Beck [19,r], K. Becker [166], C. Becot [48], A.J. Beddall [21d], V.A. Bednyakov [38], C.P. Bee [144], L.J. Beemster [15], T.A. Beermann [36], M. Begalli [81b,81d], M. Begel [29], A. Behera [144], J.K. Behr [48], C. Beirao Da Cruz E Silva [36], J.F. Beirer [55,36], F. Beisiegel [24], M. Belfkir [158], G. Bella [150], L. Bellagamba [23b], A. Bellerive [34], P. Bellos [20], K. Beloborodov [37], K. Belotskiy [37], N.L. Belyaev [37], D. Benchekroun [35a], F. Bendebba [35a], Y. Benhammou [150], D.P. Benjamin [29], M. Benoit [29], J.R. Bensinger [26], S. Bentvelsen [113], L. Beresford [36], M. Beretta [53], D. Berge [18], E. Bergeaas Kuutmann [160], N. Berger [4], B. Bergmann [131], J. Beringer [17a], S. Berlendis [7], G. Bernardi [5], C. Bernius [142], F.U. Bernlochner [24], T. Berry [94], P. Berta [132], A. Berthold [50], I.A. Bertram [90], O. Bessidskaia Bylund [170], S. Bethke [109], A. Betti [74a,74b], A.J. Bevan [93], M. Bhamjee [33c], S. Bhatta [144], D.S. Bhattacharya [165], P. Bhattarai [26], V.S. Bhopatkar [6], R. Bi [128], R. Bi [29,aj], R.M. Bianchi [128], O. Biebel [108], R. Bielski [122], N.V. Biesuz [73a,73b], M. Biglietti [76a], T.R.V. Billoud [131], M. Bindi [55], A. Bingul [21b], C. Bini [74a,74b], S. Biondi [23b,23a], A. Biondini [91], C.J. Birch-sykes [100], G.A. Bird [20,133], M. Birman [168], T. Bisanz [36], D. Biswas [169,l], A. Bitadze [100], K. Bjørke [124], I. Bloch [48], C. Blocker [26], A. Blue [59], U. Blumenschein [93], J. Blumenthal [99], G.J. Bobbink [113], V.S. Bobrovnikov [37], M. Boehler [54], D. Bogavac [36], A.G. Bogdanchikov [37], C. Bohm [47a], V. Boisvert [94], P. Bokan [48], T. Bold [84a], M. Bomben [5], M. Bona [93], M. Boonekamp [134], C.D. Booth [94], A.G. Borbély [59], H.M. Borecka-Bielska [107], L.S. Borgna [95], G. Borissov [90], D. Bortoletto [125], D. Boscherini [23b], M. Bosman [13], J.D. Bossio Sola [36], K. Bouaouda [35a], J. Boudreau [128], E.V. Bouhova-Thacker [90], D. Boumediene [40], R. Bouquet [5], A. Boveia [118], J. Boyd [36], D. Boye [29], I.R. Boyko [38], J. Bracinik [20], N. Brahimi [62d,62c], G. Brandt [170], O. Brandt [32], F. Braren [48], B. Brau [102], J.E. Brau [122], W.D. Breaden Madden [59], K. Brendlinger [48], R. Brener [168], L. Brenner [36], R. Brenner [160], S. Bressler [168], B. Brickwedde [99], D. Britton [59], D. Britzger [109], I. Brock [24], G. Brooijmans [41], W.K. Brooks [136f], E. Brost [29], P.A. Bruckman de Renstrom [85], B. Brüers [48], D. Bruncko [28b,*], A. Bruni [23b], G. Bruni [23b], M. Bruschi [23b], N. Bruscino [74a,74b], L. Bryngemark [142], T. Buanes [16], Q. Buat [137], P. Buchholz [140], A.G. Buckley [59], I.A. Budagov [38,*], M.K. Bugge [124], O. Bulekov [37], B.A. Bullard [61], S. Burdin [91], C.D. Burgard [48], A.M. Burger [40], B. Burghgrave [8], J.T.P. Burr [32], C.D. Burton [11], J.C. Burzynski [141], E.L. Busch [41], V. Büscher [99], P.J. Bussey [59], J.M. Butler [25], C.M. Buttar [59], J.M. Butterworth [95], W. Buttinger [133], C.J. Buxo Vazquez [106], A.R. Buzykaev [37], G. Cabras [23b], S. Cabrera Urbán [162], D. Caforio [58], H. Cai [128], Y. Cai [14a,14d], V.M.M. Cairo [36], O. Cakir [3a], N. Calace [36], P. Calafiura [17a], G. Calderini [126], P. Calfayan [67], G. Callea [59], L.P. Caloba [81b], D. Calvet [40], S. Calvet [40], T.P. Calvet [101], M. Calvetti [73a,73b], R. Camacho Toro [126], S. Camarda [36], D. Camarero Munoz [98], P. Camarri [75a,75b], M.T. Camerlingo [76a,76b], D. Cameron [124], C. Camincher [164], M. Campanelli [95], A. Camplani [42], V. Canale [71a,71b], A. Canesse [103], M. Cano Bret [79], J. Cantero [162], Y. Cao [161], F. Capocasa [26], M. Capua [43b,43a], A. Carbone [70a,70b], R. Cardarelli [75a], J.C.J. Cardenas [8], F. Cardillo [162], T. Carli [36], G. Carlino [71a], B.T. Carlson [128,t], E.M. Carlson [164,155a], L. Carminati [70a,70b], M. Carnesale [74a,74b], S. Caron [112], E. Carquin [136f], S. Carrá [70a], G. Carratta [23b,23a], F. Carrio Argos [33g], J.W.S. Carter [154], T.M. Carter [52], M.P. Casado [13,i], A.F. Casha [154], E.G. Castiglia [171], F.L. Castillo [63a], L. Castillo Garcia [13], V. Castillo Gimenez [162], N.F. Castro [129a,129e], A. Catinaccio [36], J.R. Catmore [124],

V. Cavaliere [29], N. Cavalli [23b,23a], V. Cavasinni [73a,73b], E. Celebi [21a], F. Celli [125], M.S. Centonze [69a,69b], K. Cerny [121], A.S. Cerqueira [81a], A. Cerri [145], L. Cerrito [75a,75b], F. Cerutti [17a], A. Cervelli [23b], S.A. Cetin [21d], Z. Chadi [35a], D. Chakraborty [114], M. Chala [129f], J. Chan [169], W.S. Chan [113], W.Y. Chan [152], J.D. Chapman [32], B. Chargeishvili [148b], D.G. Charlton [20], T.P. Charman [93], M. Chatterjee [19], S. Chekanov [6], S.V. Chekulaev [155a], G.A. Chelkov [38,a], A. Chen [105], B. Chen [150], B. Chen [164], C. Chen [62a], H. Chen [14c], H. Chen [29], J. Chen [62c], J. Chen [26], S. Chen [152], S.J. Chen [14c], X. Chen [62c], X. Chen [14b,af], Y. Chen [62a], C.L. Cheng [169], H.C. Cheng [64a], A. Cheplakov [38], E. Cheremushkina [48], E. Cherepanova [113], R. Cherkaoui El Moursli [35e], E. Cheu [7], K. Cheung [65], L. Chevalier [134], V. Chiarella [53], G. Chiarelli [73a], G. Chiodini [69a], A.S. Chisholm [20], A. Chitan [27b], Y.H. Chiu [164], M.V. Chizhov [38], K. Choi [11], A.R. Chomont [74a,74b], Y. Chou [102], E.Y.S. Chow [113], T. Chowdhury [33g], L.D. Christopher [33g], K.L. Chu [64a], M.C. Chu [64a], X. Chu [14a,14d], J. Chudoba [130], J.J. Chwastowski [85], D. Cieri [109], K.M. Ciesla [84a], V. Cindro [92], A. Ciocio [17a], F. Cirotto [71a,71b], Z.H. Citron [168,m], M. Citterio [70a], D.A. Ciubotaru [27b], B.M. Ciungu [154], A. Clark [56], P.J. Clark [52], J.M. Clavijo Columbie [48], S.E. Clawson [100], C. Clement [47a,47b], J. Clercx [48], L. Clissa [23b,23a], Y. Coadou [101], M. Cobal [68a,68c], A. Coccaro [57b], R.F. Coelho Barrue [129a], R. Coelho Lopes De Sa [102], S. Coelli [70a], H. Cohen [150], A.E.C. Coimbra [70a,70b], B. Cole [41], J. Collot [60], P. Conde Muiño [129a,129g], S.H. Connell [33c], I.A. Connelly [59], E.I. Conroy [125], F. Conventi [71a,ah], H.G. Cooke [20], A.M. Cooper-Sarkar [125], F. Cormier [163], L.D. Corpe [36], M. Corradi [74a,74b], E.E. Corrigan [97], F. Corriveau [103,y], A. Cortes-Gonzalez [18], M.J. Costa [162], F. Costanza [4], D. Costanzo [138], B.M. Cote [118], G. Cowan [94], J.W. Cowley [32], K. Cranmer [116], S. Crépé-Renaudin [60], F. Crescioli [126], M. Cristinziani [140], M. Cristoforetti [77a,77b,d], V. Croft [157], G. Crosetti [43b,43a], A. Cueto [36], T. Cuhadar Donszelmann [159], H. Cui [14a,14d], Z. Cui [7], A.R. Cukierman [142], W.R. Cunningham [59], F. Curcio [43b,43a], P. Czodrowski [36], M.M. Czurylo [63b], M.J. Da Cunha Sargedas De Sousa [62a], J.V. Da Fonseca Pinto [81b], C. Da Via [100], W. Dabrowski [84a], T. Dado [49], S. Dahbi [33g], T. Dai [105], C. Dallapiccola [102], M. Dam [42], G. D'amen [29], V. D'Amico [76a,76b], J. Damp [99], J.R. Dandoy [127], M.F. Daneri [30], M. Danninger [141], V. Dao [36], G. Darbo [57b], S. Darmora [6], S.J. Das [29,aj], A. Dattagupta [122], S. D'Auria [70a,70b], C. David [155b], T. Davidek [132], D.R. Davis [51], B. Davis-Purcell [34], I. Dawson [93], K. De [8], R. De Asmundis [71a], M. De Beurs [113], S. De Castro [23b,23a], N. De Groot [112], P. de Jong [113], H. De la Torre [106], A. De Maria [14c], A. De Salvo [74a], U. De Sanctis [75a,75b], M. De Santis [75a,75b], A. De Santo [145], J.B. De Vivie De Regie [60], D.V. Dedovich [38], J. Degens [113], A.M. Deiana [44], F. Del Corso [23b,23a], J. Del Peso [98], F. Del Rio [63a], F. Deliot [134], C.M. Delitzsch [49], M. Della Pietra [71a,71b], D. Della Volpe [56], A. Dell'Acqua [36], L. Dell'Asta [70a,70b], M. Delmastro [4], P.A. Delsart [60], S. Demers [171], M. Demichev [38], S.P. Denisov [37], L. D'Eramo [114], D. Derendarz [85], F. Derue [126], P. Dervan [91], K. Desch [24], K. Dette [154], C. Deutsch [24], P.O. Deviveiros [36], F.A. Di Bello [74a,74b], A. Di Ciaccio [75a,75b], L. Di Ciaccio [4], A. Di Domenico [74a,74b], C. Di Donato [71a,71b], A. Di Girolamo [36], G. Di Gregorio [73a,73b], A. Di Luca [77a,77b], B. Di Micco [76a,76b], R. Di Nardo [76a,76b], C. Diaconu [101], F.A. Dias [113], T. Dias Do Vale [141], M.A. Diaz [136a,136b], F.G. Diaz Capriles [24], M. Didenko [162], E.B. Diehl [105], L. Diehl [54], S. Díez Cornell [48], C. Diez Pardos [140], C. Dimitriadi [24,160], A. Dimitrievska [17a], W. Ding [14b], J. Dingfelder [24], I-M. Dinu [27b], S.J. Dittmeier [63b], F. Dittus [36], F. Djama [101], T. Djobava [148b], J.I. Djuvsland [16], D. Dodsworth [26], C. Doglioni [100,97], J. Dolejsi [132], Z. Dolezal [132], M. Donadelli [81c], B. Dong [62c], J. Donini [40], A. D'Onofrio [14c], M. D'Onofrio [91], J. Dopke [133], A. Doria [71a], M.T. Dova [89], A.T. Doyle [59], M.A. Draguet [125], E. Drechsler [141], E. Dreyer [168], I. Drivas-koulouris [10], A.S. Drobac [157], D. Du [62a], T.A. du Pree [113], F. Dubinin [37],

M. Dubovsky [28a], E. Duchovni [168], G. Duckeck [108], O.A. Ducu [36], D. Duda [109], A. Dudarev [36], M. D'uffizi [100], L. Duflot [66], M. Dührssen [36], C. Dülsen [170], A.E. Dumitriu [27b], M. Dunford [63a], S. Dungs [49], K. Dunne [47a,47b], A. Duperrin [101], H. Duran Yildiz [3a], M. Düren [58], A. Durglishvili [148b], B.L. Dwyer [114], G.I. Dyckes [17a], M. Dyndal [84a], S. Dysch [100], B.S. Dziedzic [85], Z.O. Earnshaw [145], B. Eckerova [28a], M.G. Eggleston [51], E. Egidio Purcino De Souza [81b], L.F. Ehrke [56], G. Eigen [16], K. Einsweiler [17a], T. Ekelof [160], P.A. Ekman [97], Y. El Ghazali [35b], H. El Jarrari [35e,147], A. El Moussaouy [35a], V. Ellajosyula [160], M. Ellert [160], F. Ellinghaus [170], A.A. Elliot [93], N. Ellis [36], J. Elmsheuser [29], M. Elsing [36], D. Emeliyanov [133], A. Emerman [41], Y. Enari [152], I. Ene [17a], S. Epari [13], J. Erdmann [49], A. Ereditato [19], P.A. Erland [85], M. Errenst [170], M. Escalier [66], C. Escobar [162], E. Etzion [150], G. Evans [129a], H. Evans [67], M.O. Evans [145], A. Ezhilov [37], S. Ezzarqtouni [35a], F. Fabbri [59], L. Fabbri [23b,23a], G. Facini [95], V. Fadeyev [135], R.M. Fakhrutdinov [37], S. Falciano [74a], L.F. Falda Ulhoa Coelho [36], P.J. Falke [24], S. Falke [36], J. Faltova [132], Y. Fan [14a], Y. Fang [14a,14d], G. Fanourakis [46], M. Fanti [70a,70b], M. Faraj [68a,68b], A. Farbin [8], A. Farilla [76a], T. Farooque [106], S.M. Farrington [52], F. Fassi [35e], D. Fassouliotis [9], M. Faucci Giannelli [75a,75b], W.J. Fawcett [32], L. Fayard [66], O.L. Fedin [37,a], G. Fedotov [37], M. Feickert [161], L. Feligioni [101], A. Fell [138], D.E. Fellers [122], C. Feng [62b], M. Feng [14b], M.J. Fenton [159], A.B. Fenyuk [37], L. Ferencz [48], S.W. Ferguson [45], J. Ferrando [48], A. Ferrari [160], P. Ferrari [113], R. Ferrari [72a], D. Ferrere [56], C. Ferretti [105], F. Fiedler [99], A. Filipčič [92], E.K. Filmer [1], F. Filthaut [112], M.C.N. Fiolhais [129a,129c,c], L. Fiorini [162], F. Fischer [140], W.C. Fisher [106], T. Fitschen [20,66], I. Fleck [140], P. Fleischmann [105], T. Flick [170], L. Flores [127], M. Flores [33d,ad], L.R. Flores Castillo [64a], F.M. Follega [77a,77b], N. Fomin [16], J.H. Foo [154], B.C. Forland [67], A. Formica [134], A.C. Forti [100], E. Fortin [101], A.W. Fortman [61], M.G. Foti [17a], L. Fountas [9,j], D. Fournier [66], H. Fox [90], P. Francavilla [73a,73b], S. Francescato [61], M. Franchini [23b,23a], S. Franchino [63a], D. Francis [36], L. Franco [112], L. Franconi [19], M. Franklin [61], G. Frattari [26], A.C. Freegard [93], P.M. Freeman [20], W.S. Freund [81b], N. Fritzsche [50], A. Froch [54], D. Froidevaux [36], J.A. Frost [125], Y. Fu [62a], M. Fujimoto [117], E. Fullana Torregrosa [162,*], J. Fuster [162], A. Gabrielli [23b,23a], A. Gabrielli [36], P. Gadow [48], G. Gagliardi [57b,57a], L.G. Gagnon [17a], G.E. Gallardo [125], E.J. Gallas [125], B.J. Gallop [133], R. Gamboa Goni [93], K.K. Gan [118], S. Ganguly [152], J. Gao [62a], Y. Gao [52], F.M. Garay Walls [136a,136b], B. Garcia [29], C. García [162], J.E. García Navarro [162], J.A. García Pascual [14a], M. Garcia-Sciveres [17a], R.W. Gardner [39], D. Garg [79], R.B. Garg [142,q], S. Gargiulo [54], C.A. Garner [154], V. Garonne [29], S.J. Gasiorowski [137], P. Gaspar [81b], G. Gaudio [72a], V. Gautam [13], P. Gauzzi [74a,74b], I.L. Gavrilenko [37], A. Gavrilyuk [37], C. Gay [163], G. Gaycken [48], E.N. Gazis [10], A.A. Geanta [27b], C.M. Gee [135], J. Geisen [97], M. Geisen [99], C. Gemme [57b], M.H. Genest [60], S. Gentile [74a,74b], S. George [94], W.F. George [20], T. Geralis [46], L.O. Gerlach [55], P. Gessinger-Befurt [36], M. Ghasemi Bostanabad [164], M. Ghneimat [140], A. Ghosal [140], A. Ghosh [159], A. Ghosh [7], B. Giacobbe [23b], S. Giagu [74a,74b], N. Giangiacomi [154], P. Giannetti [73a], A. Giannini [62a], S.M. Gibson [94], M. Gignac [135], D.T. Gil [84b], A.K. Gilbert [84a], B.J. Gilbert [41], D. Gillberg [34], G. Gilles [113], N.E.K. Gillwald [48], L. Ginabat [126], D.M. Gingrich [2,ag], M.P. Giordani [68a,68c], P.F. Giraud [134], G. Giugliarelli [68a,68c], D. Giugni [70a], F. Giuli [36], I. Gkialas [9,j], L.K. Gladilin [37], C. Glasman [98], G.R. Gledhill [122], M. Glisic [122], I. Gnesi [43b,f], Y. Go [29,aj], M. Goblirsch-Kolb [26], D. Godin [107], S. Goldfarb [104], T. Golling [56], M.G.D. Gololo [33g], D. Golubkov [37], J.P. Gombas [106], A. Gomes [129a,129b], G. Gomes Da Silva [140], A.J. Gomez Delegido [162], R. Goncalves Gama [55], R. Gonçalo [129a,129c], G. Gonella [122], L. Gonella [20], A. Gongadze [38], F. Gonnella [20], J.L. Gonski [41],

R.Y. González Andana [52], S. González de la Hoz [162], S. Gonzalez Fernandez [13], R. Gonzalez Lopez [91], C. Gonzalez Renteria [17a], R. Gonzalez Suarez [160], S. Gonzalez-Sevilla [56], G.R. Gonzalvo Rodriguez [162], L. Goossens [36], N.A. Gorasia [20], P.A. Gorbounov [37], B. Gorini [36], E. Gorini [69a,69b], A. Gorišek [92], A.T. Goshaw [51], M.I. Gostkin [38], C.A. Gottardo [112], M. Gouighri [35b], V. Goumarre [48], A.G. Goussiou [137], N. Govender [33c], C. Goy [4], I. Grabowska-Bold [84a], K. Graham [34], E. Gramstad [124], S. Grancagnolo [18], M. Grandi [145], V. Gratchev [37,*], P.M. Gravila [27f], F.G. Gravili [69a,69b], H.M. Gray [17a], M. Greco [69a,69b], C. Grefe [24], I.M. Gregor [48], P. Grenier [142], C. Grieco [13], A.A. Grillo [135], K. Grimm [31,n], S. Grinstein [13,v], J.-F. Grivaz [66], E. Gross [168], J. Grosse-Knetter [55], C. Grud [105], A. Grummer [111], J.C. Grundy [125], L. Guan [105], W. Guan [169], C. Gubbels [163], J.G.R. Guerrero Rojas [162], G. Guerrieri [68a,68c], F. Guescini [109], R. Gugel [99], J.A.M. Guhit [105], A. Guida [48], T. Guillemin [4], E. Guilloton [166,133], S. Guindon [36], F. Guo [14a,14d], J. Guo [62c], L. Guo [66], Y. Guo [105], R. Gupta [48], S. Gurbuz [24], S.S. Gurdasani [54], G. Gustavino [36], M. Guth [56], P. Gutierrez [119], L.F. Gutierrez Zagazeta [127], C. Gutschow [95], C. Guyot [134], C. Gwenlan [125], C.B. Gwilliam [91], E.S. Haaland [124], A. Haas [116], M. Habedank [48], C. Haber [17a], H.K. Hadavand [8], A. Hadef [99], S. Hadzic [109], M. Haleem [165], J. Haley [120], J.J. Hall [138], G.D. Hallewell [101], L. Halser [19], K. Hamano [164], H. Hamdaoui [35e], M. Hamer [24], G.N. Hamity [52], J. Han [62b], K. Han [62a], L. Han [14c], L. Han [62a], S. Han [17a], Y.F. Han [154], K. Hanagaki [82], M. Hance [135], D.A. Hangal [41,ac], M.D. Hank [39], R. Hankache [100], J.B. Hansen [42], J.D. Hansen [42], P.H. Hansen [42], K. Hara [156], D. Harada [56], T. Harenberg [170], S. Harkusha [37], Y.T. Harris [125], N.M. Harrison [118], P.F. Harrison [166], N.M. Hartman [142], N.M. Hartmann [108], Y. Hasegawa [139], A. Hasib [52], S. Haug [19], R. Hauser [106], M. Havranek [131], C.M. Hawkes [20], R.J. Hawkings [36], S. Hayashida [110], D. Hayden [106], C. Hayes [105], R.L. Hayes [163], C.P. Hays [125], J.M. Hays [93], H.S. Hayward [91], F. He [62a], Y. He [153], Y. He [126], M.P. Heath [52], V. Hedberg [97], A.L. Heggelund [124], N.D. Hehir [93,*], C. Heidegger [54], K.K. Heidegger [54], W.D. Heidorn [80], J. Heilman [34], S. Heim [48], T. Heim [17a], J.G. Heinlein [127], J.J. Heinrich [122], L. Heinrich [36], J. Hejbal [130], L. Helary [48], A. Held [116], S. Hellesund [124], C.M. Helling [163], S. Hellman [47a,47b], C. Helsens [36], R.C.W. Henderson [90], L. Henkelmann [32], A.M. Henriques Correia [36], H. Herde [142], Y. Hernández Jiménez [144], H. Herr [99], M.G. Herrmann [108], T. Herrmann [50], G. Herten [54], R. Hertenberger [108], L. Hervas [36], N.P. Hessey [155a], H. Hibi [83], E. Higón-Rodriguez [162], S.J. Hillier [20], I. Hinchliffe [17a], F. Hinterkeuser [24], M. Hirose [123], S. Hirose [156], D. Hirschbuehl [170], T.G. Hitchings [100], B. Hiti [92], J. Hobbs [144], R. Hobincu [27e], N. Hod [168], M.C. Hodgkinson [138], B.H. Hodkinson [32], A. Hoecker [36], J. Hofer [48], D. Hohn [54], T. Holm [24], M. Holzbock [109], L.B.A.H. Hommels [32], B.P. Honan [100], J. Hong [62c], T.M. Hong [128], Y. Hong [55], J.C. Honig [54], A. Hönle [109], B.H. Hooberman [161], W.H. Hopkins [6], Y. Horii [110], S. Hou [147], A.S. Howard [92], J. Howarth [59], J. Hoya [89], M. Hrabovsky [121], A. Hrynevich [37], T. Hryn'ova [4], P.J. Hsu [65], S.-C. Hsu [137], Q. Hu [41,ac], Y.F. Hu [14a,14d,ai], D.P. Huang [95], S. Huang [64b], X. Huang [14c], Y. Huang [62a], Y. Huang [14a], Z. Huang [100], Z. Hubacek [131], M. Huebner [24], F. Huegging [24], T.B. Huffman [125], M. Huhtinen [36], S.K. Huiberts [16], R. Hulsken [103], N. Huseynov [12,a], J. Huston [106], J. Huth [61], R. Hyneman [142], S. Hyrych [28a], G. Iacobucci [56], G. Iakovidis [29], I. Ibragimov [140], L. Iconomidou-Fayard [66], P. Iengo [71a,71b], R. Iguchi [152], T. Iizawa [56], Y. Ikegami [82], A. Ilg [19], N. Ilic [154], H. Imam [35a], T. Ingebretsen Carlson [47a,47b], G. Introzzi [72a,72b], M. Iodice [76a], V. Ippolito [74a,74b], M. Ishino [152], W. Islam [169], C. Issever [18,48], S. Istin [21a,ak], H. Ito [167], J.M. Iturbe Ponce [64a], R. Iuppa [77a,77b], A. Ivina [168], J.M. Izen [45],

V. Izzo [71a], P. Jacka [130,131], P. Jackson [1], R.M. Jacobs [48], B.P. Jaeger [141], C.S. Jagfeld [108], G. Jäkel [170], K. Jakobs [54], T. Jakoubek [168], J. Jamieson [59], K.W. Janas [84a], G. Jarlskog [97], A.E. Jaspan [91], T. Javůrek [36], M. Javurkova [102], F. Jeanneau [134], L. Jeanty [122], J. Jejelava [148a,aa], P. Jenni [54,g], C.E. Jessiman [34], S. Jézéquel [4], J. Jia [144], X. Jia [61], X. Jia [14a,14d], Z. Jia [14c], Y. Jiang [62a], S. Jiggins [52], J. Jimenez Pena [109], S. Jin [14c], A. Jinaru [27b], O. Jinnouchi [153], H. Jivan [33g], P. Johansson [138], K.A. Johns [7], C.A. Johnson [67], D.M. Jones [32], E. Jones [166], P. Jones [32], R.W.L. Jones [90], T.J. Jones [91], J. Jovicevic [15], X. Ju [17a], J.J. Junggeburth [36], A. Juste Rozas [13,v], S. Kabana [136e], A. Kaczmarska [85], M. Kado [74a,74b], H. Kagan [118], M. Kagan [142], A. Kahn [41], A. Kahn [127], C. Kahra [99], T. Kaji [167], E. Kajomovitz [149], N. Kakati [168], C.W. Kalderon [29], A. Kamenshchikov [154], N.J. Kang [135], Y. Kano [110], D. Kar [33g], K. Karava [125], M.J. Kareem [155b], E. Karentzos [54], I. Karkanias [151], S.N. Karpov [38], Z.M. Karpova [38], V. Kartvelishvili [90], A.N. Karyukhin [37], E. Kasimi [151], C. Kato [62d], J. Katzy [48], S. Kaur [34], K. Kawade [139], K. Kawagoe [88], T. Kawaguchi [110], T. Kawamoto [134], G. Kawamura [55], E.F. Kay [164], F.I. Kaya [157], S. Kazakos [13], V.F. Kazanin [37], Y. Ke [144], J.M. Keaveney [33a], R. Keeler [164], G.V. Kehris [61], J.S. Keller [34], A.S. Kelly [95], D. Kelsey [145], J.J. Kempster [20], J. Kendrick [20], K.E. Kennedy [41], O. Kepka [130], B.P. Kerridge [166], S. Kersten [170], B.P. Kerševan [92], L. Keszeghova [28a], S. Ketabchi Haghighat [154], M. Khandoga [126], A. Khanov [120], A.G. Kharlamov [37], T. Kharlamova [37], E.E. Khoda [137], T.J. Khoo [18], G. Khoriauli [165], J. Khubua [148b], Y.A.R. Khwaira [66], M. Kiehn [36], A. Kilgallon [122], D.W. Kim [47a,47b], E. Kim [153], Y.K. Kim [39], N. Kimura [95], A. Kirchhoff [55], D. Kirchmeier [50], C. Kirfel [24], J. Kirk [133], A.E. Kiryunin [109], T. Kishimoto [152], D.P. Kisliuk [154], C. Kitsaki [10], O. Kivernyk [24], M. Klassen [63a], C. Klein [34], L. Klein [165], M.H. Klein [105], M. Klein [91], U. Klein [91], P. Klimek [36], A. Klimentov [29], F. Klimpel [109], T. Klingl [24], T. Klioutchnikova [36], F.F. Klitzner [108], P. Kluit [113], S. Kluth [109], E. Kneringer [78], T.M. Knight [154], A. Knue [54], D. Kobayashi [88], R. Kobayashi [86], M. Kocian [142], T. Kodama [152], P. Kodyš [132], D.M. Koeck [145], P.T. Koenig [24], T. Koffas [34], N.M. Köhler [36], M. Kolb [134], I. Koletsou [4], T. Komarek [121], K. Köneke [54], A.X.Y. Kong [1], T. Kono [117], N. Konstantinidis [95], B. Konya [97], R. Kopeliansky [67], S. Koperny [84a], K. Korcyl [85], K. Kordas [151], G. Koren [150], A. Korn [95], S. Korn [55], I. Korolkov [13], N. Korotkova [37], B. Kortman [113], O. Kortner [109], S. Kortner [109], W.H. Kostecka [114], V.V. Kostyukhin [140], A. Kotsokechagia [66], A. Kotwal [51], A. Koulouris [36], A. Kourkoumeli-Charalampidi [72a,72b], C. Kourkoumelis [9], E. Kourlitis [6], O. Kovanda [145], R. Kowalewski [164], W. Kozanecki [134], A.S. Kozhin [37], V.A. Kramarenko [37], G. Kramberger [92], P. Kramer [99], M.W. Krasny [126], A. Krasznahorkay [36], J.A. Kremer [99], T. Kresse [50], J. Kretzschmar [91], K. Kreul [18], P. Krieger [154], F. Krieter [108], S. Krishnamurthy [102], A. Krishnan [63b], M. Krivos [132], K. Krizka [17a], K. Kroeninger [49], H. Kroha [109], J. Kroll [130], J. Kroll [127], K.S. Krowpman [106], U. Kruchonak [38], H. Krüger [24], N. Krumnack [80], M.C. Kruse [51], J.A. Krzysiak [85], A. Kubota [153], O. Kuchinskaia [37], S. Kuday [3a], D. Kuechler [48], J.T. Kuechler [48], S. Kuehn [36], T. Kuhl [48], V. Kukhtin [38], Y. Kulchitsky [37,a], S. Kuleshov [136d,136b], M. Kumar [33g], N. Kumari [101], M. Kuna [60], A. Kupco [130], T. Kupfer [49], A. Kupich [37], O. Kuprash [54], H. Kurashige [83], L.L. Kurchaninov [155a], Y.A. Kurochkin [37], A. Kurova [37], E.S. Kuwertz [36], M. Kuze [153], A.K. Kvam [102], J. Kvita [121], T. Kwan [103], K.W. Kwok [64a], C. Lacasta [162], F. Lacava [74a,74b], H. Lacker [18], D. Lacour [126], N.N. Lad [95], E. Ladygin [38], B. Laforge [126], T. Lagouri [136e], S. Lai [55], I.K. Lakomiec [84a], N. Lalloue [60], J.E. Lambert [119], S. Lammers [67], W. Lampl [7], C. Lampoudis [151], A.N. Lancaster [114],

E. Lançon [29], U. Landgraf [54], M.P.J. Landon [93], V.S. Lang [54], R.J. Langenberg [102], A.J. Lankford [159], F. Lanni [29], K. Lantzsch [24], A. Lanza [72a], A. Lapertosa [57b,57a], J.F. Laporte [134], T. Lari [70a], F. Lasagni Manghi [23b], M. Lassnig [36], V. Latonova [130], T.S. Lau [64a], A. Laudrain [99], A. Laurier [34], S.D. Lawlor [94], Z. Lawrence [100], M. Lazzaroni [70a,70b], B. Le [100], B. Leban [92], A. Lebedev [80], M. LeBlanc [36], T. LeCompte [6], F. Ledroit-Guillon [60], A.C.A. Lee [95], G.R. Lee [16], L. Lee [61], S.C. Lee [147], S. Lee [47a,47b], L.L. Leeuw [33c], H.P. Lefebvre [94], M. Lefebvre [164], C. Leggett [17a], K. Lehmann [141], G. Lehmann Miotto [36], W.A. Leight [102], A. Leisos [151,u], M.A.L. Leite [81c], C.E. Leitgeb [48], R. Leitner [132], K.J.C. Leney [44], T. Lenz [24], S. Leone [73a], C. Leonidopoulos [52], A. Leopold [143], C. Leroy [107], R. Les [106], C.G. Lester [32], M. Levchenko [37], J. Levêque [4], D. Levin [105], L.J. Levinson [168], D.J. Lewis [20], B. Li [14b], B. Li [62b], C. Li [62a], C-Q. Li [62c,62d], H. Li [62a], H. Li [62b], H. Li [14c], H. Li [62b], J. Li [62c], K. Li [137], L. Li [62c], M. Li [14a,14d], Q.Y. Li [62a], S. Li [62d,62c,e], T. Li [62b], X. Li [103], Z. Li [62b], Z. Li [125], Z. Li [103], Z. Li [91], Z. Liang [14a], M. Liberatore [48], B. Liberti [75a], K. Lie [64c], J. Lieber Marin [81b], K. Lin [106], R.A. Linck [67], R.E. Lindley [7], J.H. Lindon [2], A. Linss [48], E. Lipeles [127], A. Lipniacka [16], T.M. Liss [161,ae], A. Lister [163], J.D. Little [4], B. Liu [14a], B.X. Liu [141], D. Liu [62d,62c], J.B. Liu [62a], J.K.K. Liu [32], K. Liu [62d,62c], M. Liu [62a], M.Y. Liu [62a], P. Liu [14a], Q. Liu [62d,137,62c], X. Liu [62a], Y. Liu [48], Y. Liu [14c,14d], Y.L. Liu [105], Y.W. Liu [62a], M. Livan [72a,72b], J. Llorente Merino [141], S.L. Lloyd [93], E.M. Lobodzinska [48], P. Loch [7], S. Loffredo [75a,75b], T. Lohse [18], K. Lohwasser [138], M. Lokajicek [130,*], J.D. Long [161], I. Longarini [74a,74b], L. Longo [69a,69b], R. Longo [161], I. Lopez Paz [36], A. Lopez Solis [48], J. Lorenz [108], N. Lorenzo Martinez [4], A.M. Lory [108], A. Lösle [54], X. Lou [47a,47b], X. Lou [14a,14d], A. Lounis [66], J. Love [6], P.A. Love [90], J.J. Lozano Bahilo [162], G. Lu [14a,14d], M. Lu [79], S. Lu [127], Y.J. Lu [65], H.J. Lubatti [137], C. Luci [74a,74b], F.L. Lucio Alves [14c], A. Lucotte [60], F. Luehring [67], I. Luise [144], O. Lukianchuk [66], O. Lundberg [143], B. Lund-Jensen [143], N.A. Luongo [122], M.S. Lutz [150], D. Lynn [29], H. Lyons [91], R. Lysak [130], E. Lytken [97], F. Lyu [14a], V. Lyubushkin [38], T. Lyubushkina [38], H. Ma [29], L.L. Ma [62b], Y. Ma [95], D.M. Mac Donell [164], G. Maccarrone [53], J.C. MacDonald [138], R. Madar [40], W.F. Mader [50], J. Maeda [83], T. Maeno [29], M. Maerker [50], V. Magerl [54], J. Magro [68a,68c], H. Maguire [138], D.J. Mahon [41], C. Maidantchik [81b], A. Maio [129a,129b,129d], K. Maj [84a], O. Majersky [28a], S. Majewski [122], N. Makovec [66], V. Maksimovic [15], B. Malaescu [126], Pa. Malecki [85], V.P. Maleev [37], F. Malek [60], D. Malito [43b,43a], U. Mallik [79], C. Malone [32], S. Maltezos [10], S. Malyukov [38], J. Mamuzic [13], G. Mancini [53], G. Manco [72a,72b], J.P. Mandalia [93], I. Mandić [92], L. Manhaes de Andrade Filho [81a], I.M. Maniatis [151], M. Manisha [134], J. Manjarres Ramos [50], D.C. Mankad [168], K.H. Mankinen [97], A. Mann [108], A. Manousos [78], B. Mansoulie [134], S. Manzoni [36], A. Marantis [151,u], G. Marchiori [5], M. Marcisovsky [130], L. Marcoccia [75a,75b], C. Marcon [97], M. Marinescu [20], M. Marjanovic [119], Z. Marshall [17a], S. Marti-Garcia [162], T.A. Martin [166], V.J. Martin [52], B. Martin dit Latour [16], L. Martinelli [74a,74b], M. Martinez [13,v], P. Martinez Agullo [162], V.I. Martinez Outschoorn [102], P. Martinez Suarez [13], S. Martin-Haugh [133], V.S. Martoiu [27b], A.C. Martyniuk [95], A. Marzin [36], S.R. Maschek [109], L. Masetti [99], T. Mashimo [152], J. Masik [100], A.L. Maslennikov [37], L. Massa [23b], P. Massarotti [71a,71b], P. Mastrandrea [73a,73b], A. Mastroberardino [43b,43a], T. Masubuchi [152], T. Mathisen [160], A. Matic [108], N. Matsuzawa [152], J. Maurer [27b], B. Maček [92], D.A. Maximov [37], R. Mazini [147], I. Maznas [151], M. Mazza [106], S.M. Mazza [135], C. Mc Ginn [29], J.P. Mc Gowan [103], S.P. Mc Kee [105], T.G. McCarthy [109], W.P. McCormack [17a], E.F. McDonald [104], A.E. McDougall [113], J.A. Mcfayden [145], G. Mchedlidze [148b], R.P. Mckenzie [33g], T.C. Mclachlan [48], D.J. Mclaughlin [95], K.D. McLean [164], S.J. McMahon [133], P.C. McNamara [104], R.A. McPherson [164,y], J.E. Mdhluli [33g], S. Meehan [36],

T. Megy [40], S. Mehlhase [108], A. Mehta [91], B. Meirose [45], D. Melini [149], B.R. Mellado Garcia [33g], A.H. Melo [55], F. Meloni [48], E.D. Mendes Gouveia [129a], A.M. Mendes Jacques Da Costa [20], H.Y. Meng [154], L. Meng [90], S. Menke [109], M. Mentink [36], E. Meoni [43b,43a], C. Merlassino [125], L. Merola [71a,71b], C. Meroni [70a,70b], G. Merz [105], O. Meshkov [37], J.K.R. Meshreki [140], J. Metcalfe [6], A.S. Mete [6], C. Meyer [67], J-P. Meyer [134], M. Michetti [18], R.P. Middleton [133], L. Mijović [52], G. Mikenberg [168], M. Mikestikova [130], M. Mikuž [92], H. Mildner [138], A. Milic [154], C.D. Milke [44], D.W. Miller [39], L.S. Miller [34], A. Milov [168], D.A. Milstead [47a,47b], T. Min [14c], A.A. Minaenko [37], I.A. Minashvili [148b], L. Mince [59], A.I. Mincer [116], B. Mindur [84a], M. Mineev [38], Y. Minegishi [152], Y. Mino [86], L.M. Mir [13], M. Miralles Lopez [162], M. Mironova [125], T. Mitani [167], A. Mitra [166], V.A. Mitsou [162], O. Miu [154], P.S. Miyagawa [93], Y. Miyazaki [88], A. Mizukami [82], J.U. Mjörnmark [97], T. Mkrtchyan [63a], M. Mlynarikova [114], T. Moa [47a,47b], S. Mobius [55], K. Mochizuki [107], P. Moder [48], P. Mogg [108], A.F. Mohammed [14a,14d], S. Mohapatra [41], G. Mokgatitswane [33g], B. Mondal [140], S. Mondal [131], K. Mönig [48], E. Monnier [101], L. Monsonis Romero [162], J. Montejo Berlingen [36], M. Montella [118], F. Monticelli [89], N. Morange [66], A.L. Moreira De Carvalho [129a], M. Moreno Llácer [162], C. Moreno Martinez [13], P. Morettini [57b], S. Morgenstern [166], M. Morii [61], M. Morinaga [152], V. Morisbak [124], A.K. Morley [36], F. Morodei [74a,74b], L. Morvaj [36], P. Moschovakos [36], B. Moser [36], M. Mosidze [148b], T. Moskalets [54], P. Moskvitina [112], J. Moss [31,o], E.J.W. Moyse [102], S. Muanza [101], J. Mueller [128], D. Muenstermann [90], R. Müller [19], G.A. Mullier [97], J.J. Mullin [127], D.P. Mungo [70a,70b], J.L. Munoz Martinez [13], D. Munoz Perez [162], F.J. Munoz Sanchez [100], M. Murin [100], W.J. Murray [166,133], A. Murrone [70a,70b], J.M. Muse [119], M. Muškinja [17a], C. Mwewa [29], A.G. Myagkov [37,a], A.J. Myers [8], A.A. Myers [128], G. Myers [67], M. Myska [131], B.P. Nachman [17a], O. Nackenhorst [49], A. Nag [50], K. Nagai [125], K. Nagano [82], J.L. Nagle [29,aj], E. Nagy [101], A.M. Nairz [36], Y. Nakahama [82], K. Nakamura [82], H. Nanjo [123], R. Narayan [44], E.A. Narayanan [111], I. Naryshkin [37], M. Naseri [34], C. Nass [24], G. Navarro [22a], J. Navarro-Gonzalez [162], R. Nayak [150], P.Y. Nechaeva [37], F. Nechansky [48], T.J. Neep [20], A. Negri [72a,72b], M. Negrini [23b], C. Nellist [112], C. Nelson [103], K. Nelson [105], S. Nemecek [130], M. Nessi [36,h], M.S. Neubauer [161], F. Neuhaus [99], J. Neundorf [48], R. Newhouse [163], P.R. Newman [20], C.W. Ng [128], Y.S. Ng [18], Y.W.Y. Ng [159], B. Ngair [35e], H.D.N. Nguyen [107], R.B. Nickerson [125], R. Nicolaidou [134], J. Nielsen [135], M. Niemeyer [55], N. Nikiforou [36], V. Nikolaenko [37,a], I. Nikolic-Audit [126], K. Nikolopoulos [20], P. Nilsson [29], H.R. Nindhito [56], A. Nisati [74a], N. Nishu [2], R. Nisius [109], J-E. Nitschke [50], E.K. Nkadimeng [33g], S.J. Noacco Rosende [89], T. Nobe [152], D.L. Noel [32], Y. Noguchi [86], T. Nommensen [146], M.A. Nomura [29], M.B. Norfolk [138], R.R.B. Norisam [95], B.J. Norman [34], J. Novak [92], T. Novak [48], O. Novgorodova [50], L. Novotny [131], R. Novotny [111], L. Nozka [121], K. Ntekas [159], E. Nurse [95], F.G. Oakham [34,ag], J. Ocariz [126], A. Ochi [83], I. Ochoa [129a], S. Oda [88], S. Oerdek [160], A. Ogrodnik [84a], A. Oh [100], C.C. Ohm [143], H. Oide [153], R. Oishi [152], M.L. Ojeda [48], Y. Okazaki [86], M.W. O'Keefe [91], Y. Okumura [152], A. Olariu [27b], L.F. Oleiro Seabra [129a], S.A. Olivares Pino [136e], D. Oliveira Damazio [29], D. Oliveira Goncalves [81a], J.L. Oliver [159], M.J.R. Olsson [159], A. Olszewski [85], J. Olszowska [85,*], Ö.O. Öncel [54], D.C. O'Neil [141], A.P. O'Neill [19], A. Onofre [129a,129e], P.U.E. Onyisi [11], M.J. Oreglia [39], G.E. Orellana [89], D. Orestano [76a,76b], N. Orlando [13], R.S. Orr [154], V. O'Shea [59], R. Ospanov [62a], G. Otero y Garzon [30], H. Otono [88], P.S. Ott [63a], G.J. Ottino [17a], M. Ouchrif [35d], J. Ouellette [29,aj], F. Ould-Saada [124], M. Owen [59], R.E. Owen [133], K.Y. Oyulmaz [21a], V.E. Ozcan [21a], N. Ozturk [8], S. Ozturk [21d], J. Pacalt [121], H.A. Pacey [32], A. Pacheco Pages [13], C. Padilla Aranda [13],

G. Padovano [74a,74b], S. Pagan Griso [17a], G. Palacino [67], A. Palazzo [69a,69b], S. Palazzo [52], S. Palestini [36], M. Palka [84b], J. Pan [171], T. Pan [64a], D.K. Panchal [11], C.E. Pandini [113], J.G. Panduro Vazquez [94], H. Pang [14b], P. Pani [48], G. Panizzo [68a,68c], L. Paolozzi [56], C. Papadatos [107], S. Parajuli [44], A. Paramonov [6], C. Paraskevopoulos [10], D. Paredes Hernandez [64b], T.H. Park [154], M.A. Parker [32], F. Parodi [57b,57a], E.W. Parrish [114], V.A. Parrish [52], J.A. Parsons [41], U. Parzefall [54], B. Pascual Dias [107], L. Pascual Dominguez [150], V.R. Pascuzzi [17a], F. Pasquali [113], E. Pasqualucci [74a], S. Passaggio [57b], F. Pastore [94], P. Pasuwan [47a,47b], J.R. Pater [100], J. Patton [91], T. Pauly [36], J. Pearkes [142], M. Pedersen [124], R. Pedro [129a], S.V. Peleganchuk [37], O. Penc [130], C. Peng [64b], H. Peng [62a], M. Penzin [37], B.S. Peralva [81a,81d], A.P. Pereira Peixoto [60], L. Pereira Sanchez [47a,47b], D.V. Perepelitsa [29,aj], E. Perez Codina [155a], M. Perganti [10], L. Perini [70a,70b,*], H. Pernegger [36], A. Perrevoort [112], O. Perrin [40], K. Peters [48], R.F.Y. Peters [100], B.A. Petersen [36], T.C. Petersen [42], E. Petit [101], V. Petousis [131], C. Petridou [151], A. Petrukhin [140], M. Pettee [17a], N.E. Pettersson [36], A. Petukhov [37], K. Petukhova [132], A. Peyaud [134], R. Pezoa [136f], L. Pezzotti [36], G. Pezzullo [171], T. Pham [104], P.W. Phillips [133], M.W. Phipps [161], G. Piacquadio [144], E. Pianori [17a], F. Piazza [70a,70b], R. Piegaia [30], D. Pietreanu [27b], A.D. Pilkington [100], M. Pinamonti [68a,68c], J.L. Pinfold [2], B.C. Pinheiro Pereira [129a], C. Pitman Donaldson [95], D.A. Pizzi [34], L. Pizzimento [75a,75b], A. Pizzini [113], M.-A. Pleier [29], V. Plesanovs [54], V. Pleskot [132], E. Plotnikova [38], G. Poddar [4], R. Poettgen [97], R. Poggi [56], L. Poggioli [126], I. Pogrebnyak [106], D. Pohl [24], I. Pokharel [55], S. Polacek [132], G. Polesello [72a], A. Poley [141,155a], R. Polifka [131], A. Polini [23b], C.S. Pollard [125], Z.B. Pollock [118], V. Polychronakos [29], D. Ponomarenko [37], L. Pontecorvo [36], S. Popa [27a], G.A. Popeneciu [27d], D.M. Portillo Quintero [155a], S. Pospisil [131], P. Postolache [27c], K. Potamianos [125], I.N. Potrap [38], C.J. Potter [32], H. Potti [1], T. Poulsen [48], J. Poveda [162], G. Pownall [48], M.E. Pozo Astigarraga [36], A. Prades Ibanez [162], M.M. Prapa [46], J. Pretel [54], D. Price [100], M. Primavera [69a], M.A. Principe Martin [98], M.L. Proffitt [137], N. Proklova [37], K. Prokofiev [64c], G. Proto [75a,75b], S. Protopopescu [29], J. Proudfoot [6], M. Przybycien [84a], J.E. Puddefoot [138], D. Pudzha [37], P. Puzo [66], D. Pyatiizbyantseva [37], J. Qian [105], Y. Qin [100], T. Qiu [93], A. Quadt [55], M. Queitsch-Maitland [24], G. Rabanal Bolanos [61], D. Rafanoharana [54], F. Ragusa [70a,70b], J.L. Rainbolt [39], J.A. Raine [56], S. Rajagopalan [29], E. Ramakoti [37], K. Ran [14a,14d], V. Raskina [126], D.F. Rassloff [63a], S. Rave [99], B. Ravina [59], I. Ravinovich [168], M. Raymond [36], A.L. Read [124], N.P. Readioff [138], D.M. Rebuzzi [72a,72b], G. Redlinger [29], K. Reeves [45], J.A. Reidelsturz [170], D. Reikher [150], A. Reiss [99], A. Rej [140], C. Rembser [36], A. Renardi [48], M. Renda [27b], M.B. Rendel [109], A.G. Rennie [59], S. Resconi [70a], M. Ressegotti [57b,57a], E.D. Resseguie [17a], S. Rettie [95], B. Reynolds [118], E. Reynolds [17a], M. Rezaei Estabragh [170], O.L. Rezanova [37], P. Reznicek [132], E. Ricci [77a,77b], R. Richter [109], S. Richter [47a,47b], E. Richter-Was [84b], M. Ridel [126], P. Rieck [116], P. Riedler [36], M. Rijssenbeek [144], A. Rimoldi [72a,72b], M. Rimoldi [48], L. Rinaldi [23b,23a], T.T. Rinn [29], M.P. Rinnagel [108], G. Ripellino [143], I. Riu [13], P. Rivadeneira [48], J.C. Rivera Vergara [164], F. Rizatdinova [120], E. Rizvi [93], C. Rizzi [56], B.A. Roberts [166], B.R. Roberts [17a], S.H. Robertson [103,y], M. Robin [48], D. Robinson [32], C.M. Robles Gajardo [136f], M. Robles Manzano [99], A. Robson [59], A. Rocchi [75a,75b], C. Roda [73a,73b], S. Rodriguez Bosca [63a], Y. Rodriguez Garcia [22a], A. Rodriguez Rodriguez [54], A.M. Rodríguez Vera [155b], S. Roe [36], J.T. Roemer [159], A.R. Roepe-Gier [119], J. Roggel [170], O. Røhne [124], R.A. Rojas [164], B. Roland [54], C.P.A. Roland [67], J. Roloff [29], A. Romaniouk [37], E. Romano [72a,72b], M. Romano [23b], A.C. Romero Hernandez [161], N. Rompotis [91], L. Roos [126], S. Rosati [74a], B.J. Rosser [39], E. Rossi [4],

E. Rossi [71a,71b], L.P. Rossi [57b], L. Rossini [48], R. Rosten [118], M. Rotaru [27b], B. Rottler [54], D. Rousseau [66], D. Rousso [32], G. Rovelli [72a,72b], A. Roy [161], A. Rozanov [101], Y. Rozen [149], X. Ruan [33g], A. Rubio Jimenez [162], A.J. Ruby [91], T.A. Ruggeri [1], F. Rühr [54], A. Ruiz-Martinez [162], A. Rummler [36], Z. Rurikova [54], N.A. Rusakovich [38], H.L. Russell [164], J.P. Rutherfoord [7], E.M. Rüttinger [138], K. Rybacki [90], M. Rybar [132], E.B. Rye [124], A. Ryzhov [37], J.A. Sabater Iglesias [56], P. Sabatini [162], L. Sabetta [74a,74b], H.F-W. Sadrozinski [135], F. Safai Tehrani [74a], B. Safarzadeh Samani [145], M. Safdari [142], S. Saha [103], M. Sahinsoy [109], M. Saimpert [134], M. Saito [152], T. Saito [152], D. Salamani [36], G. Salamanna [76a,76b], A. Salnikov [142], J. Salt [162], A. Salvador Salas [13], D. Salvatore [43b,43a], F. Salvatore [145], A. Salzburger [36], D. Sammel [54], D. Sampsonidis [151], D. Sampsonidou [62d,62c], J. Sánchez [162], A. Sanchez Pineda [4], V. Sanchez Sebastian [162], H. Sandaker [124], C.O. Sander [48], J.A. Sandesara [102], M. Sandhoff [170], C. Sandoval [22b], D.P.C. Sankey [133], A. Sansoni [53], L. Santi [74a,74b], C. Santoni [40], H. Santos [129a,129b], S.N. Santpur [17a], A. Santra [168], K.A. Saoucha [138], J.G. Saraiva [129a,129d], J. Sardain [101], O. Sasaki [82], K. Sato [156], C. Sauer [63b], F. Sauerburger [54], E. Sauvan [4], P. Savard [154,ag], R. Sawada [152], C. Sawyer [133], L. Sawyer [96], I. Sayago Galvan [162], C. Sbarra [23b], A. Sbrizzi [23b,23a], T. Scanlon [95], J. Schaarschmidt [137], P. Schacht [109], D. Schaefer [39], U. Schäfer [99], A.C. Schaffer [66], D. Schaile [108], R.D. Schamberger [144], E. Schanet [108], C. Scharf [18], V.A. Schegelsky [37], D. Scheirich [132], F. Schenck [18], M. Schernau [159], C. Scheulen [55], C. Schiavi [57b,57a], Z.M. Schillaci [26], E.J. Schioppa [69a,69b], M. Schioppa [43b,43a], B. Schlag [99], K.E. Schleicher [54], S. Schlenker [36], K. Schmieden [99], C. Schmitt [99], S. Schmitt [48], L. Schoeffel [134], A. Schoening [63b], P.G. Scholer [54], E. Schopf [125], M. Schott [99], J. Schovancova [36], S. Schramm [56], F. Schroeder [170], H-C. Schultz-Coulon [63a], M. Schumacher [54], B.A. Schumm [135], Ph. Schune [134], A. Schwartzman [142], T.A. Schwarz [105], Ph. Schwemling [134], R. Schwienhorst [106], A. Sciandra [135], G. Sciolla [26], F. Scuri [73a], F. Scutti [104], C.D. Sebastiani [91], K. Sedlaczek [49], P. Seema [18], S.C. Seidel [111], A. Seiden [135], B.D. Seidlitz [41], T. Seiss [39], C. Seitz [48], J.M. Seixas [81b], G. Sekhniaidze [71a], S.J. Sekula [44], L. Selem [4], N. Semprini-Cesari [23b,23a], S. Sen [51], D. Sengupta [56], V. Senthilkumar [162], L. Serin [66], L. Serkin [68a,68b], M. Sessa [76a,76b], H. Severini [119], S. Sevova [142], F. Sforza [57b,57a], A. Sfyrla [56], E. Shabalina [55], R. Shaheen [143], J.D. Shahinian [127], N.W. Shaikh [47a,47b], D. Shaked Renous [168], L.Y. Shan [14a], M. Shapiro [17a], A. Sharma [36], A.S. Sharma [163], P. Sharma [79], S. Sharma [48], P.B. Shatalov [37], K. Shaw [145], S.M. Shaw [100], Q. Shen [62c], P. Sherwood [95], L. Shi [95], C.O. Shimmin [171], Y. Shimogama [167], J.D. Shinner [94], I.P.J. Shipsey [125], S. Shirabe [60], M. Shiyakova [38,x], J. Shlomi [168], M.J. Shochet [39], J. Shojaii [104], D.R. Shope [143], S. Shrestha [118], E.M. Shrif [33g], M.J. Shroff [164], P. Sicho [130], A.M. Sickles [161], E. Sideras Haddad [33g], O. Sidiropoulou [36], A. Sidoti [23b], F. Siegert [50], Dj. Sijacki [15], R. Sikora [84a], F. Sili [89], J.M. Silva [20], M.V. Silva Oliveira [36], S.B. Silverstein [47a], S. Simion [66], R. Simoniello [36], E.L. Simpson [59], N.D. Simpson [97], S. Simsek [21d], S. Sindhu [55], P. Sinervo [154], V. Sinetckii [37], S. Singh [141], S. Singh [154], S. Sinha [48], S. Sinha [33g], M. Sioli [23b,23a], I. Siral [122], S.Yu. Sivoklokov [37,*], J. Sjölin [47a,47b], A. Skaf [55], E. Skorda [97], P. Skubic [119], M. Slawinska [85], V. Smakhtin [168], B.H. Smart [133], J. Smiesko [132], S.Yu. Smirnov [37], Y. Smirnov [37], L.N. Smirnova [37,a], O. Smirnova [97], E.A. Smith [39], H.A. Smith [125], J.L. Smith [91], R. Smith [142], M. Smizanska [90], K. Smolek [131], A. Smykiewicz [85], A.A. Snesarev [37], H.L. Snoek [113], S. Snyder [29], R. Sobie [164,y], A. Soffer [150], C.A. Solans Sanchez [36], E.Yu. Soldatov [37], U. Soldevila [162], A.A. Solodkov [37], S. Solomon [54], A. Soloshenko [38], K. Solovieva [54], O.V. Solovyanov [37], V. Solovyev [37], P. Sommer [36], A. Sonay [13], W.Y. Song [155b], A. Sopczak [131], A.L. Sopio [95], F. Sopkova [28b], V. Sothilingam [63a], S. Sottocornola [72a,72b],

R. Soualah [115b], Z. Soumaimi [35e], D. South [48], S. Spagnolo [69a,69b], M. Spalla [109], F. Spanò [94], D. Sperlich [54], G. Spigo [36], M. Spina [145], S. Spinali [90], D.P. Spiteri [59], M. Spousta [132], E.J. Staats [34], A. Stabile [70a,70b], R. Stamen [63a], M. Stamenkovic [113], A. Stampekis [20], M. Standke [24], E. Stanecka [85], B. Stanislaus [17a], M.M. Stanitzki [48], M. Stankaityte [125], B. Stapf [48], E.A. Starchenko [37], G.H. Stark [135], J. Stark [101,ab], D.M. Starko [155b], P. Staroba [130], P. Starovoitov [63a], S. Stärz [103], R. Staszewski [85], G. Stavropoulos [46], J. Steentoft [160], P. Steinberg [29], A.L. Steinhebel [122], B. Stelzer [141,155a], H.J. Stelzer [128], O. Stelzer-Chilton [155a], H. Stenzel [58], T.J. Stevenson [145], G.A. Stewart [36], M.C. Stockton [36], G. Stoicea [27b], M. Stolarski [129a], S. Stonjek [109], A. Straessner [50], J. Strandberg [143], S. Strandberg [47a,47b], M. Strauss [119], T. Strebler [101], P. Strizenec [28b], R. Ströhmer [165], D.M. Strom [122], L.R. Strom [48], R. Stroynowski [44], A. Strubig [47a,47b], S.A. Stucci [29], B. Stugu [16], J. Stupak [119], N.A. Styles [48], D. Su [142], S. Su [62a], W. Su [62d,137,62c], X. Su [62a,66], K. Sugizaki [152], V.V. Sulin [37], M.J. Sullivan [91], D.M.S. Sultan [77a,77b], L. Sultanaliyeva [37], S. Sultansoy [3b], T. Sumida [86], S. Sun [105], S. Sun [169], O. Sunneborn Gudnadottir [160], M.R. Sutton [145], M. Svatos [130], M. Swiatlowski [155a], T. Swirski [165], I. Sykora [28a], M. Sykora [132], T. Sykora [132], D. Ta [99], K. Tackmann [48,w], A. Taffard [159], R. Tafirout [155a], J.S. Tafoya Vargas [66], R.H.M. Taibah [126], R. Takashima [87], K. Takeda [83], E.P. Takeva [52], Y. Takubo [82], M. Talby [101], A.A. Talyshev [37], K.C. Tam [64b], N.M. Tamir [150], A. Tanaka [152], J. Tanaka [152], R. Tanaka [66], M. Tanasini [57b,57a], J. Tang [62c], Z. Tao [163], S. Tapia Araya [80], S. Tapprogge [99], A. Tarek Abouelfadl Mohamed [106], S. Tarem [149], K. Tariq [62b], G. Tarna [27b], G.F. Tartarelli [70a], P. Tas [132], M. Tasevsky [130], E. Tassi [43b,43a], A.C. Tate [161], G. Tateno [152], Y. Tayalati [35e], G.N. Taylor [104], W. Taylor [155b], H. Teagle [91], A.S. Tee [169], R. Teixeira De Lima [142], P. Teixeira-Dias [94], J.J. Teoh [154], K. Terashi [152], J. Terron [98], S. Terzo [13], M. Testa [53], R.J. Teuscher [154,y], A. Thaler [78], N. Themistokleous [52], T. Theveneaux-Pelzer [18], O. Thielmann [170], D.W. Thomas [94], J.P. Thomas [20], E.A. Thompson [48], P.D. Thompson [20], E. Thomson [127], E.J. Thorpe [93], Y. Tian [55], V. Tikhomirov [37,a], Yu.A. Tikhonov [37], S. Timoshenko [37], E.X.L. Ting [1], P. Tipton [171], S. Tisserant [101], S.H. Tlou [33g], A. Tnourji [40], K. Todome [23b,23a], S. Todorova-Nova [132], S. Todt [50], M. Togawa [82], J. Tojo [88], S. Tokár [28a], K. Tokushuku [82], R. Tombs [32], M. Tomoto [82,110], L. Tompkins [142,q], P. Tornambe [102], E. Torrence [122], H. Torres [50], E. Torró Pastor [162], M. Toscani [30], C. Tosciri [39], D.R. Tovey [138], A. Traeet [16], I.S. Trandafir [27b], T. Trefzger [165], A. Tricoli [29], I.M. Trigger [155a], S. Trincaz-Duvoid [126], D.A. Trischuk [163], B. Trocmé [60], A. Trofymov [66], C. Troncon [70a], L. Truong [33c], M. Trzebinski [85], A. Trzupek [85], F. Tsai [144], M. Tsai [105], A. Tsiamis [151], P.V. Tsiareshka [37], S. Tsigaridas [155a], A. Tsirigotis [151,u], V. Tsiskaridze [144], E.G. Tskhadadze [148a], M. Tsopoulou [151], Y. Tsujikawa [86], I.I. Tsukerman [37], V. Tsulaia [17a], S. Tsuno [82], O. Tsur [149], D. Tsybychev [144], Y. Tu [64b], A. Tudorache [27b], V. Tudorache [27b], A.N. Tuna [36], S. Turchikhin [38], I. Turk Cakir [3a], R. Turra [70a], T. Turtuvshin [38], P.M. Tuts [41], S. Tzamarias [151], P. Tzanis [10], E. Tzovara [99], K. Uchida [152], F. Ukegawa [156], P.A. Ulloa Poblete [136c], G. Unal [36], M. Unal [11], A. Undrus [29], G. Unel [159], K. Uno [152], J. Urban [28b], P. Urquijo [104], G. Usai [8], R. Ushioda [153], M. Usman [107], Z. Uysal [21b], V. Vacek [131], B. Vachon [103], K.O.H. Vadla [124], T. Vafeiadis [36], C. Valderanis [108], E. Valdes Santurio [47a,47b], M. Valente [155a], S. Valentinetti [23b,23a], A. Valero [162], A. Vallier [101,ab], J.A. Valls Ferrer [162], T.R. Van Daalen [137], P. Van Gemmeren [6], S. Van Stroud [95], I. Van Vulpen [113], M. Vanadia [75a,75b], W. Vandelli [36], M. Vandenbroucke [134], E.R. Vandewall [120], D. Vannicola [150], L. Vannoli [57b,57a], R. Vari [74a], E.W. Varnes [7], C. Varni [17a], T. Varol [147], D. Varouchas [66],

L. Varriale [162], K.E. Varvell [146], M.E. Vasile [27b], L. Vaslin [40], G.A. Vasquez [164], F. Vazeille [40], T. Vazquez Schroeder [36], J. Veatch [31], V. Vecchio [100], M.J. Veen [113], I. Veliscek [125], L.M. Veloce [154], F. Veloso [129a,129c], S. Veneziano [74a], A. Ventura [69a,69b], A. Verbytskyi [109], M. Verducci [73a,73b], C. Vergis [24], M. Verissimo De Araujo [81b], W. Verkerke [113], J.C. Vermeulen [113], C. Vernieri [142], P.J. Verschuuren [94], M. Vessella [102], M.L. Vesterbacka [116], M.C. Vetterli [141,ag], A. Vgenopoulos [151], N. Viaux Maira [136f], T. Vickey [138], O.E. Vickey Boeriu [138], G.H.A. Viehhauser [125], L. Vigani [63b], M. Villa [23b,23a], M. Villaplana Perez [162], E.M. Villhauer [52], E. Vilucchi [53], M.G. Vincter [34], G.S. Virdee [20], A. Vishwakarma [52], C. Vittori [23b,23a], I. Vivarelli [145], V. Vladimirov [166], E. Voevodina [109], F. Vogel [108], P. Vokac [131], J. Von Ahnen [48], E. Von Toerne [24], B. Vormwald [36], V. Vorobel [132], K. Vorobev [37], M. Vos [162], J.H. Vossebeld [91], M. Vozak [113], L. Vozdecky [93], N. Vranjes [15], M. Vranjes Milosavljevic [15], M. Vreeswijk [113], R. Vuillermet [36], O. Vujinovic [99], I. Vukotic [39], S. Wada [156], C. Wagner [102], W. Wagner [170], S. Wahdan [170], H. Wahlberg [89], R. Wakasa [156], M. Wakida [110], V.M. Walbrecht [109], J. Walder [133], R. Walker [108], W. Walkowiak [140], A.M. Wang [61], A.Z. Wang [169], C. Wang [62a], C. Wang [62c], H. Wang [17a], J. Wang [64a], P. Wang [44], R.-J. Wang [99], R. Wang [61], R. Wang [6], S.M. Wang [147], S. Wang [62b], T. Wang [62a], W.T. Wang [79], W.X. Wang [62a], X. Wang [14c], X. Wang [161], X. Wang [62c], Y. Wang [62d], Y. Wang [14c], Z. Wang [105], Z. Wang [62d,51,62c], Z. Wang [105], A. Warburton [103], R.J. Ward [20], N. Warrack [59], A.T. Watson [20], M.F. Watson [20], G. Watts [137], B.M. Waugh [95], A.F. Webb [11], C. Weber [29], M.S. Weber [19], S.A. Weber [34], S.M. Weber [63a], C. Wei [62a], Y. Wei [125], A.R. Weidberg [125], J. Weingarten [49], M. Weirich [99], C. Weiser [54], C.J. Wells [48], T. Wenaus [29], B. Wendland [49], T. Wengler [36], N.S. Wenke [109], N. Wermes [24], M. Wessels [63a], K. Whalen [122], A.M. Wharton [90], A.S. White [61], A. White [8], M.J. White [1], D. Whiteson [159], L. Wickremasinghe [123], W. Wiedenmann [169], C. Wiel [50], M. Wielers [133], N. Wieseotte [99], C. Wiglesworth [42], L.A.M. Wiik-Fuchs [54], D.J. Wilbern [119], H.G. Wilkens [36], D.M. Williams [41], H.H. Williams [127], S. Williams [32], S. Willocq [102], P.J. Windischhofer [125], F. Winklmeier [122], B.T. Winter [54], M. Wittgen [142], M. Wobisch [96], A. Wolf [99], R. Wölker [125], J. Wollrath [159], M.W. Wolter [85], H. Wolters [129a,129c], V.W.S. Wong [163], A.F. Wongel [48], S.D. Worm [48], B.K. Wosiek [85], K.W. Woźniak [85], K. Wraight [59], J. Wu [14a,14d], M. Wu [64a], S.L. Wu [169], X. Wu [56], Y. Wu [62a], Z. Wu [134,62a], J. Wuerzinger [125], T.R. Wyatt [100], B.M. Wynne [52], S. Xella [42], L. Xia [14c], M. Xia [14b], J. Xiang [64c], X. Xiao [105], M. Xie [62a], X. Xie [62a], J. Xiong [17a], I. Xiotidis [145], D. Xu [14a], H. Xu [62a], H. Xu [62a], L. Xu [62a], R. Xu [127], T. Xu [105], W. Xu [105], Y. Xu [14b], Z. Xu [62b], Z. Xu [142], B. Yabsley [146], S. Yacoob [33a], N. Yamaguchi [88], Y. Yamaguchi [153], H. Yamauchi [156], T. Yamazaki [17a], Y. Yamazaki [83], J. Yan [62c], S. Yan [125], Z. Yan [25], H.J. Yang [62c,62d], H.T. Yang [17a], S. Yang [62a], T. Yang [64c], X. Yang [62a], X. Yang [14a], Y. Yang [44], Z. Yang [62a,105], W-M. Yao [17a], Y.C. Yap [48], H. Ye [14c], J. Ye [44], S. Ye [29], X. Ye [62a], Y. Yeh [95], I. Yeletskikh [38], M.R. Yexley [90], P. Yin [41], K. Yorita [167], C.J.S. Young [54], C. Young [142], M. Yuan [105], R. Yuan [62b,k], L. Yue [95], X. Yue [63a], M. Zaazoua [35e], B. Zabinski [85], E. Zaid [52], T. Zakareishvili [148b], N. Zakharchuk [34], S. Zambito [56], J. Zang [152], D. Zanzi [54], O. Zaplatilek [131], S.V. Zeißner [49], C. Zeitnitz [170], J.C. Zeng [161], D.T. Zenger Jr [26], O. Zenin [37], T. Ženiš [28a], S. Zenz [93], S. Zerradi [35a], D. Zerwas [66], B. Zhang [14c], D.F. Zhang [138], G. Zhang [14b], J. Zhang [6], K. Zhang [14a,14d], L. Zhang [14c], R. Zhang [169], S. Zhang [105], T. Zhang [152], X. Zhang [62c], X. Zhang [62b], Z. Zhang [17a], Z. Zhang [66], H. Zhao [137], P. Zhao [51], T. Zhao [62b], Y. Zhao [135], Z. Zhao [62a], A. Zhemchugov [38], Z. Zheng [142], D. Zhong [161], B. Zhou [105], C. Zhou [169], H. Zhou [7], N. Zhou [62c], Y. Zhou [7], C.G. Zhu [62b],

C. Zhu [14a,14d], H.L. Zhu [62a], H. Zhu [14a], J. Zhu [105], Y. Zhu [62a], X. Zhuang [14a], K. Zhukov [37], V. Zhulanov [37], N.I. Zimine [38], J. Zinsser [63b], M. Ziolkowski [140], L. Živković [15], A. Zoccoli [23b,23a], K. Zoch [56], T.G. Zorbas [138], O. Zormpa [46], W. Zou [41], L. Zwalinski [36]

[1] Department of Physics, University of Adelaide, Adelaide; Australia
[2] Department of Physics, University of Alberta, Edmonton AB; Canada
[3] [(a)] Department of Physics, Ankara University, Ankara; [(b)] Division of Physics, TOBB University of Economics and Technology, Ankara; Türkiye
[4] LAPP, Université Savoie Mont Blanc, CNRS/IN2P3, Annecy; France
[5] APC, Université Paris Cité, CNRS/IN2P3, Paris; France
[6] High Energy Physics Division, Argonne National Laboratory, Argonne IL; United States of America
[7] Department of Physics, University of Arizona, Tucson AZ; United States of America
[8] Department of Physics, University of Texas at Arlington, Arlington TX; United States of America
[9] Physics Department, National and Kapodistrian University of Athens, Athens; Greece
[10] Physics Department, National Technical University of Athens, Zografou; Greece
[11] Department of Physics, University of Texas at Austin, Austin TX; United States of America
[12] Institute of Physics, Azerbaijan Academy of Sciences, Baku; Azerbaijan
[13] Institut de Física d'Altes Energies (IFAE), Barcelona Institute of Science and Technology, Barcelona; Spain
[14] [(a)] Institute of High Energy Physics, Chinese Academy of Sciences, Beijing; [(b)] Physics Department, Tsinghua University, Beijing; [(c)] Department of Physics, Nanjing University, Nanjing; [(d)] University of Chinese Academy of Science (UCAS), Beijing; China
[15] Institute of Physics, University of Belgrade, Belgrade; Serbia
[16] Department for Physics and Technology, University of Bergen, Bergen; Norway
[17] [(a)] Physics Division, Lawrence Berkeley National Laboratory, Berkeley CA; [(b)] University of California, Berkeley CA; United States of America
[18] Institut für Physik, Humboldt Universität zu Berlin, Berlin; Germany
[19] Albert Einstein Center for Fundamental Physics and Laboratory for High Energy Physics, University of Bern, Bern; Switzerland
[20] School of Physics and Astronomy, University of Birmingham, Birmingham; United Kingdom
[21] [(a)] Department of Physics, Bogazici University, Istanbul; [(b)] Department of Physics Engineering, Gaziantep University, Gaziantep; [(c)] Department of Physics, Istanbul University, Istanbul; [(d)] Istinye University, Sariyer, Istanbul; Türkiye
[22] [(a)] Facultad de Ciencias y Centro de Investigaciónes, Universidad Antonio Nariño, Bogotá; [(b)] Departamento de Física, Universidad Nacional de Colombia, Bogotá; Colombia
[23] [(a)] Dipartimento di Fisica e Astronomia A. Righi, Università di Bologna, Bologna; [(b)] INFN Sezione di Bologna; Italy
[24] Physikalisches Institut, Universität Bonn, Bonn; Germany
[25] Department of Physics, Boston University, Boston MA; United States of America
[26] Department of Physics, Brandeis University, Waltham MA; United States of America
[27] [(a)] Transilvania University of Brasov, Brasov; [(b)] Horia Hulubei National Institute of Physics and Nuclear Engineering, Bucharest; [(c)] Department of Physics, Alexandru Ioan Cuza University of Iasi, Iasi; [(d)] National Institute for Research and Development of Isotopic and Molecular Technologies, Physics Department, Cluj-Napoca; [(e)] University Politehnica Bucharest, Bucharest; [(f)] West University in Timisoara, Timisoara; [(g)] Faculty of Physics, University of Bucharest, Bucharest; Romania
[28] [(a)] Faculty of Mathematics, Physics and Informatics, Comenius University, Bratislava; [(b)] Department of Subnuclear Physics, Institute of Experimental Physics of the Slovak Academy of Sciences, Kosice; Slovak Republic
[29] Physics Department, Brookhaven National Laboratory, Upton NY; United States of America
[30] Universidad de Buenos Aires, Facultad de Ciencias Exactas y Naturales, Departamento de Física, y CONICET, Instituto de Física de Buenos Aires (IFIBA), Buenos Aires; Argentina
[31] California State University, CA; United States of America
[32] Cavendish Laboratory, University of Cambridge, Cambridge; United Kingdom
[33] [(a)] Department of Physics, University of Cape Town, Cape Town; [(b)] iThemba Labs, Western Cape; [(c)] Department of Mechanical Engineering Science, University of Johannesburg, Johannesburg; [(d)] National Institute of Physics, University of the Philippines Diliman (Philippines); [(e)] University of South Africa, Department of Physics, Pretoria; [(f)] University of Zululand, KwaDlangezwa; [(g)] School of Physics, University of the Witwatersrand, Johannesburg; South Africa
[34] Department of Physics, Carleton University, Ottawa ON; Canada
[35] [(a)] Faculté des Sciences Ain Chock, Réseau Universitaire de Physique des Hautes Energies – Université Hassan II, Casablanca; [(b)] Faculté des Sciences, Université Ibn-Tofail, Kénitra; [(c)] Faculté des Sciences Semlalia, Université Cadi Ayyad, LPHEA, Marrakech; [(d)] LPMR, Faculté des Sciences, Université Mohamed Premier, Oujda; [(e)] Faculté des sciences, Université Mohammed V, Rabat; [(f)] Institute of Applied Physics, Mohammed VI Polytechnic University, Ben Guerir; Morocco
[36] CERN, Geneva; Switzerland
[37] Affiliated with an institute covered by a cooperation agreement with CERN
[38] Affiliated with an international laboratory covered by a cooperation agreement with CERN
[39] Enrico Fermi Institute, University of Chicago, Chicago IL; United States of America
[40] LPC, Université Clermont Auvergne, CNRS/IN2P3, Clermont-Ferrand; France
[41] Nevis Laboratory, Columbia University, Irvington NY; United States of America
[42] Niels Bohr Institute, University of Copenhagen, Copenhagen; Denmark
[43] [(a)] Dipartimento di Fisica, Università della Calabria, Rende; [(b)] INFN Gruppo Collegato di Cosenza, Laboratori Nazionali di Frascati; Italy
[44] Physics Department, Southern Methodist University, Dallas TX; United States of America
[45] Physics Department, University of Texas at Dallas, Richardson TX; United States of America
[46] National Centre for Scientific Research "Demokritos", Agia Paraskevi; Greece
[47] [(a)] Department of Physics, Stockholm University; [(b)] Oskar Klein Centre, Stockholm; Sweden
[48] Deutsches Elektronen-Synchrotron DESY, Hamburg and Zeuthen; Germany
[49] Fakultät Physik , Technische Universität Dortmund, Dortmund; Germany
[50] Institut für Kern- und Teilchenphysik, Technische Universität Dresden, Dresden; Germany
[51] Department of Physics, Duke University, Durham NC; United States of America
[52] SUPA – School of Physics and Astronomy, University of Edinburgh, Edinburgh; United Kingdom
[53] INFN e Laboratori Nazionali di Frascati, Frascati; Italy
[54] Physikalisches Institut, Albert-Ludwigs-Universität Freiburg, Freiburg; Germany
[55] II. Physikalisches Institut, Georg-August-Universität Göttingen, Göttingen; Germany
[56] Département de Physique Nucléaire et Corpusculaire, Université de Genève, Genève; Switzerland
[57] [(a)] Dipartimento di Fisica, Università di Genova, Genova; [(b)] INFN Sezione di Genova; Italy
[58] II. Physikalisches Institut, Justus-Liebig-Universität Giessen, Giessen; Germany
[59] SUPA – School of Physics and Astronomy, University of Glasgow, Glasgow; United Kingdom
[60] LPSC, Université Grenoble Alpes, CNRS/IN2P3, Grenoble INP, Grenoble; France
[61] Laboratory for Particle Physics and Cosmology, Harvard University, Cambridge MA; United States of America
[62] [(a)] Department of Modern Physics and State Key Laboratory of Particle Detection and Electronics, University of Science and Technology of China, Hefei; [(b)] Institute of Frontier and Interdisciplinary Science and Key Laboratory of Particle Physics and Particle Irradiation (MOE), Shandong University, Qingdao; [(c)] School of Physics and Astronomy, Shanghai Jiao Tong University, Key Laboratory for Particle Astrophysics and Cosmology (MOE), SKLPPC, Shanghai; [(d)] Tsung-Dao Lee Institute, Shanghai; China
[63] [(a)] Kirchhoff-Institut für Physik, Ruprecht-Karls-Universität Heidelberg, Heidelberg; [(b)] Physikalisches Institut, Ruprecht-Karls-Universität Heidelberg, Heidelberg; Germany

[64] [(a)] Department of Physics, Chinese University of Hong Kong, Shatin, N.T., Hong Kong; [(b)] Department of Physics, University of Hong Kong, Hong Kong; [(c)] Department of Physics and Institute for Advanced Study, Hong Kong University of Science and Technology, Clear Water Bay, Kowloon, Hong Kong; China
[65] Department of Physics, National Tsing Hua University, Hsinchu; Taiwan
[66] IJCLab, Université Paris-Saclay, CNRS/IN2P3, 91405, Orsay; France
[67] Department of Physics, Indiana University, Bloomington IN; United States of America
[68] [(a)] INFN Gruppo Collegato di Udine, Sezione di Trieste, Udine; [(b)] ICTP, Trieste; [(c)] Dipartimento Politecnico di Ingegneria e Architettura, Università di Udine, Udine; Italy
[69] [(a)] INFN Sezione di Lecce; [(b)] Dipartimento di Matematica e Fisica, Università del Salento, Lecce; Italy
[70] [(a)] INFN Sezione di Milano; [(b)] Dipartimento di Fisica, Università di Milano, Milano; Italy
[71] [(a)] INFN Sezione di Napoli; [(b)] Dipartimento di Fisica, Università di Napoli, Napoli; Italy
[72] [(a)] INFN Sezione di Pavia; [(b)] Dipartimento di Fisica, Università di Pavia, Pavia; Italy
[73] [(a)] INFN Sezione di Pisa; [(b)] Dipartimento di Fisica E. Fermi, Università di Pisa, Pisa; Italy
[74] [(a)] INFN Sezione di Roma; [(b)] Dipartimento di Fisica, Sapienza Università di Roma, Roma; Italy
[75] [(a)] INFN Sezione di Roma Tor Vergata; [(b)] Dipartimento di Fisica, Università di Roma Tor Vergata, Roma; Italy
[76] [(a)] INFN Sezione di Roma Tre; [(b)] Dipartimento di Matematica e Fisica, Università Roma Tre, Roma; Italy
[77] [(a)] INFN-TIFPA; [(b)] Università degli Studi di Trento, Trento; Italy
[78] Universität Innsbruck, Department of Astro and Particle Physics, Innsbruck; Austria
[79] University of Iowa, Iowa City IA; United States of America
[80] Department of Physics and Astronomy, Iowa State University, Ames IA; United States of America
[81] [(a)] Departamento de Engenharia Elétrica, Universidade Federal de Juiz de Fora (UFJF), Juiz de Fora; [(b)] Universidade Federal do Rio De Janeiro COPPE/EE/IF, Rio de Janeiro; [(c)] Instituto de Física, Universidade de São Paulo, São Paulo; [(d)] Rio de Janeiro State University, Rio de Janeiro; Brazil
[82] KEK, High Energy Accelerator Research Organization, Tsukuba; Japan
[83] Graduate School of Science, Kobe University, Kobe; Japan
[84] [(a)] AGH University of Krakow, Faculty of Physics and Applied Computer Science, Krakow; [(b)] Marian Smoluchowski Institute of Physics, Jagiellonian University, Krakow; Poland
[85] Institute of Nuclear Physics Polish Academy of Sciences, Krakow; Poland
[86] Faculty of Science, Kyoto University, Kyoto; Japan
[87] Kyoto University of Education, Kyoto; Japan
[88] Research Center for Advanced Particle Physics and Department of Physics, Kyushu University, Fukuoka; Japan
[89] Instituto de Física La Plata, Universidad Nacional de La Plata and CONICET, La Plata; Argentina
[90] Physics Department, Lancaster University, Lancaster; United Kingdom
[91] Oliver Lodge Laboratory, University of Liverpool, Liverpool; United Kingdom
[92] Department of Experimental Particle Physics, Jožef Stefan Institute and Department of Physics, University of Ljubljana, Ljubljana; Slovenia
[93] School of Physics and Astronomy, Queen Mary University of London, London; United Kingdom
[94] Department of Physics, Royal Holloway University of London, Egham; United Kingdom
[95] Department of Physics and Astronomy, University College London, London; United Kingdom
[96] Louisiana Tech University, Ruston LA; United States of America
[97] Fysiska institutionen, Lunds universitet, Lund; Sweden
[98] Departamento de Física Teorica C-15 and CIAFF, Universidad Autónoma de Madrid, Madrid; Spain
[99] Institut für Physik, Universität Mainz, Mainz; Germany
[100] School of Physics and Astronomy, University of Manchester, Manchester; United Kingdom
[101] CPPM, Aix-Marseille Université, CNRS/IN2P3, Marseille; France
[102] Department of Physics, University of Massachusetts, Amherst MA; United States of America
[103] Department of Physics, McGill University, Montreal QC; Canada
[104] School of Physics, University of Melbourne, Victoria; Australia
[105] Department of Physics, University of Michigan, Ann Arbor MI; United States of America
[106] Department of Physics and Astronomy, Michigan State University, East Lansing MI; United States of America
[107] Group of Particle Physics, University of Montreal, Montreal QC; Canada
[108] Fakultät für Physik, Ludwig-Maximilians-Universität München, München; Germany
[109] Max-Planck-Institut für Physik (Werner-Heisenberg-Institut), München; Germany
[110] Graduate School of Science and Kobayashi-Maskawa Institute, Nagoya University, Nagoya; Japan
[111] Department of Physics and Astronomy, University of New Mexico, Albuquerque NM; United States of America
[112] Institute for Mathematics, Astrophysics and Particle Physics, Radboud University/Nikhef, Nijmegen; Netherlands
[113] Nikhef National Institute for Subatomic Physics and University of Amsterdam, Amsterdam; Netherlands
[114] Department of Physics, Northern Illinois University, DeKalb IL; United States of America
[115] [(a)] New York University Abu Dhabi, Abu Dhabi; [(b)] University of Sharjah, Sharjah; United Arab Emirates
[116] Department of Physics, New York University, New York NY; United States of America
[117] Ochanomizu University, Otsuka, Bunkyo-ku, Tokyo; Japan
[118] Ohio State University, Columbus OH; United States of America
[119] Homer L. Dodge Department of Physics and Astronomy, University of Oklahoma, Norman OK; United States of America
[120] Department of Physics, Oklahoma State University, Stillwater OK; United States of America
[121] Palacký University, Joint Laboratory of Optics, Olomouc; Czech Republic
[122] Institute for Fundamental Science, University of Oregon, Eugene, OR; United States of America
[123] Graduate School of Science, Osaka University, Osaka; Japan
[124] Department of Physics, University of Oslo, Oslo; Norway
[125] Department of Physics, Oxford University, Oxford; United Kingdom
[126] LPNHE, Sorbonne Université, Université Paris Cité, CNRS/IN2P3, Paris; France
[127] Department of Physics, University of Pennsylvania, Philadelphia PA; United States of America
[128] Department of Physics and Astronomy, University of Pittsburgh, Pittsburgh PA; United States of America
[129] [(a)] Laboratório de Instrumentação e Física Experimental de Partículas – LIP, Lisboa; [(b)] Departamento de Física, Faculdade de Ciências, Universidade de Lisboa, Lisboa; [(c)] Departamento de Física, Universidade de Coimbra, Coimbra; [(d)] Centro de Física Nuclear da Universidade de Lisboa, Lisboa; [(e)] Departamento de Física, Universidade do Minho, Braga; [(f)] Departamento de Física Teórica y del Cosmos, Universidad de Granada, Granada (Spain); [(g)] Departamento de Física, Instituto Superior Técnico, Universidade de Lisboa, Lisboa; Portugal
[130] Institute of Physics of the Czech Academy of Sciences, Prague; Czech Republic
[131] Czech Technical University in Prague, Prague; Czech Republic
[132] Charles University, Faculty of Mathematics and Physics, Prague; Czech Republic
[133] Particle Physics Department, Rutherford Appleton Laboratory, Didcot; United Kingdom
[134] IRFU, CEA, Université Paris-Saclay, Gif-sur-Yvette; France
[135] Santa Cruz Institute for Particle Physics, University of California Santa Cruz, Santa Cruz CA; United States of America
[136] [(a)] Departamento de Física, Pontificia Universidad Católica de Chile, Santiago; [(b)] Millennium Institute for Subatomic physics at high energy frontier (SAPHIR), Santiago; [(c)] Instituto de Investigación Multidisciplinario en Ciencia y Tecnología, y Departamento de Física, Universidad de La Serena; [(d)] Universidad Andres Bello, Department of Physics, Santiago; [(e)] Instituto de Alta Investigación, Universidad de Tarapacá, Arica; [(f)] Departamento de Física, Universidad Técnica Federico Santa María, Valparaíso; Chile
[137] Department of Physics, University of Washington, Seattle WA; United States of America

Eur. Phys. J. C (2025) 85:210
https://doi.org/10.1140/epjc/s10052-025-13740-x

THE EUROPEAN PHYSICAL JOURNAL C

Regular Article - Experimental Physics

Measurement of the associated production of a top-antitop-quark pair and a Higgs boson decaying into a $b\bar{b}$ pair in pp collisions at $\sqrt{s} = 13$ TeV using the ATLAS detector at the LHC

ATLAS Collaboration[*]

CERN,1211 Geneva 23, Switzerland

Received: 16 July 2024 / Accepted: 2 January 2025

Abstract This paper reports the measurement of Higgs boson production in association with a $t\bar{t}$ pair in the $H \to b\bar{b}$ decay channel. The analysis uses 140 fb^{-1} of 13 TeV proton–proton collision data collected with the ATLAS detector at the Large Hadron Collider. The final states with one or two electrons or muons are employed. An excess of events over the expected background is found with an observed (expected) significance of 4.6 (5.4) standard deviations. The $t\bar{t}H$ cross-section is $\sigma_{t\bar{t}H} = 411\,^{+101}_{-92}$ fb $= 411 \pm 54$(stat.) $^{+85}_{-75}$(syst.) fb for a Higgs boson mass of 125.09 GeV, consistent with the prediction of the Standard Model of 507^{+35}_{-50} fb. The cross-section is also measured differentially in bins of the Higgs boson transverse momentum within the simplified template cross-section framework.

Contents

1 Introduction

After the discovery of the Higgs boson [1–3] in 2012 by the ATLAS [4] and CMS [5] collaborations, attention has turned to detailed measurements of its properties and couplings as a means of testing the predictions of the Standard Model (SM) [6–8]. The Higgs boson coupling to the top quark, the heaviest particle in the SM, is of special interest as it could be very sensitive to effects of physics beyond the SM (BSM) [9]. It is indirectly constrained assuming no BSM contributions to loop-induced processes from measurements of gluon–gluon fusion Higgs boson production and decay into $\gamma\gamma$ [10,11]. The Higgs boson production in association with a pair of top quarks ($t\bar{t}H$), where the top quark couples to the Higgs boson at tree level, provides a possibility for a direct measurement of the top-quark's Yukawa coupling without assumptions about the potential presence of BSM physics [12–15]. It was observed by the ATLAS and CMS collaborations using several Higgs boson decay modes [16,17].

The decay into two b-quarks is predicted to have the largest branching fraction of about 58% [18] and has the advantage of allowing for the reconstruction of the Higgs boson four-momentum from the kinematics of its decay products. Furthermore, the $t\bar{t}H(b\bar{b})$ channel involves only fermionic Higgs boson couplings in the production and decay, leading to an enhanced sensitivity for probing them. However, this final state is affected by a large irreducible background arising from the $t\bar{t}$ production in associations with jets ($t\bar{t}$+jets), in particular when the jets originate from b- or c-quarks, which is challenging to predict theoretically.

The ATLAS Collaboration has measured the $t\bar{t}H(b\bar{b})$ production at $\sqrt{s} = 13$ TeV in the final state with at least one lepton using the full Run 2 dataset collected in proton–proton (pp) collisions at the Large Hadron Collider (LHC) [19] between 2015 and 2018, corresponding to an integrated luminosity of 139 fb^{-1} [20]. The measured signal strength, defined as the ratio of the measured cross-section to that predicted by the SM, was found to be $0.35^{+0.36}_{-0.34}$, and corresponds to an observed (expected) significance of 1.0 (2.7) standard deviations. The signal strength was also measured differen-

[*] e-mail: atlas.publications@cern.ch

Published online: 24 February 2025

tially in five intervals of the Higgs boson transverse momentum (p_{T}^{H}) in the simplified template cross-section framework (STXS) [18], probing potential p_{T}^{H}-dependent deviations from the SM expectation.

The CMS Collaboration also recently released a measurement of the $t\bar{t}H(b\bar{b})$ production using 138 fb^{-1} of data collected at $\sqrt{s} = 13$ TeV in 2016–2018 [21]. The analysis achieved an observed (expected) significance of 1.3 (4.1) standard deviation and measured a signal strength of 0.33 ± 0.26. Additionally, the $t\bar{t}H$ production rate was determined in intervals of p_{T}^{H}.

This paper presents a re-analysis of the full Run 2 dataset collected at $\sqrt{s} = 13$ TeV with the ATLAS detector in final states with one or two leptons, referred to in the following as single-lepton and dilepton channels, and supersedes the result of Ref. [20]. Compared with the previous result, this analysis has an increased acceptance by selecting events with less restrictive requirements on the number of jets identified as originating from b-hadrons (b-jets), resulting in an increased efficiency to select $t\bar{t}H$ signal. It utilises a revised treatment of the different flavour components of the $t\bar{t}$ + jets background, and in particular, of the $t\bar{t}$ production in association with b-jets, the main background and the dominant source of the systematic uncertainty in the previous $t\bar{t}H(b\bar{b})$ measurement. For the modelling of this background, a new sample of Monte Carlo (MC) simulated events with improved settings was produced, and a corresponding set of systematic uncertainties was developed [22,23]. This measurement also uses improved analysis techniques: an advanced b-jet identification and an improved event categorisation. In particular, unlike the previous result, where the event categorisation into the background-dominated and signal-rich categories was made based on the number of jets and the number of b-jets, this analysis uses a multiclass neural network to define regions enriched in different components of the main background, the $t\bar{t}$ + jets production processes, and the signal. A more powerful multivariate discriminant is also employed to separate the signal from background and to reconstruct p_{T}^{H}. These improvements lead to better overall sensitivity and allow for a measurement of the $t\bar{t}H(b\bar{b})$ production cross-section in six bins of p_{T}^{H}, 0–60 GeV, 60–120 GeV, 120–200 GeV, 200–300 GeV, 300–450 GeV, and ≥ 450 GeV, as obtained from the MC event record before the Higgs boson decays, in the STXS formalism.

2 ATLAS detector

The ATLAS experiment [24] at the LHC is a multipurpose particle detector with a forward–backward symmetric cylindrical geometry and a near 4π coverage in solid angle.[1] It consists of an inner tracking detector (ID) surrounded by a thin superconducting solenoid providing a 2 T axial magnetic field, electromagnetic and hadronic calorimeters, and a muon spectrometer. The inner tracking detector covers the pseudorapidity range $|\eta| < 2.5$. It consists of silicon pixel, silicon microstrip, and transition radiation tracking detectors. Lead/liquid-argon (LAr) sampling calorimeters provide electromagnetic (EM) energy measurements with high granularity within the region $|\eta| < 3.2$. A steel/scintillator-tile hadronic calorimeter covers the central pseudorapidity range ($|\eta| < 1.7$). The endcap and forward regions are instrumented with LAr calorimeters for EM and hadronic energy measurements up to $|\eta| = 4.9$. The muon spectrometer (MS) surrounds the calorimeters and is based on three large superconducting air-core toroidal magnets with eight coils each. The field integral of the toroids ranges between 2.0 and 6.0 Tm across most of the detector. The muon spectrometer includes a system of precision tracking chambers up to $|\eta| = 2.7$ and fast detectors for triggering up to $|\eta| = 2.4$. The luminosity is measured mainly by the LUCID-2 [25] detector, which is located close to the beampipe. A two-level trigger system is used to select events [26]. The first-level trigger is implemented in hardware and uses a subset of the detector information to accept events at a rate below 100 kHz. This is followed by a software-based trigger that reduces the accepted event rate to 1 kHz on average depending on the data-taking conditions. A software suite [27] is used in data simulation, in the reconstruction and analysis of real and simulated data, in detector operations, and in the trigger and data acquisition systems of the experiment.

3 Data and Monte Carlo simulation samples

This analysis was performed using the pp collision data collected by the ATLAS detector between 2015 and 2018 at $\sqrt{s} = 13$ TeV. After the application of data-quality requirements [28], the dataset corresponds to an integrated luminosity of 140 fb^{-1}. Samples of simulated events were produced to model the different signal and background processes. Additional samples were produced to estimate the modelling uncertainties for each process. The effects of the additional pp collisions in the same or a nearby bunch crossing (pile-up) were modelled by overlaying minimum bias events generated with Pythia8 [29] using the A3 set of tunable parameters [30] onto the simulated hard-scatter

[1] ATLAS uses a right-handed coordinate system with its origin at the nominal interaction point (IP) in the centre of the detector and the z-axis along the beam pipe. The x-axis points from the IP to the centre of the LHC ring, and the y-axis points upwards. Cylindrical coordinates (r, ϕ) are used in the transverse plane, ϕ being the azimuthal angle around the z-axis. The pseudorapidity is defined in terms of the polar angle θ as $\eta = -\ln\tan(\theta/2)$. Angular distance is measured in units of $\Delta R \equiv \sqrt{(\Delta\eta)^2 + (\Delta\phi)^2}$.

event. The MC events were weighted to reproduce the distribution of the average number of interactions per bunch crossing observed in the data. The MC samples were processed using the full ATLAS detector simulation [31] based on GEANT4 [32]. Some alternative samples used to evaluate the modelling uncertainties were produced using fast simulation, where the full GEANT4 simulation of the calorimeter response is replaced by a detailed parameterisation of the shower shapes. For the observables used in this analysis, both simulations were found to give similar modelling. All MC samples were reconstructed using the same software as for collider data. Corrections were applied to the simulated events so that the selection efficiencies, energy scales and energy resolutions of the physics objects closely match those determined from data control samples.

All samples generated with POWHEGBOX [33–36] and MADGRAPH5_AMC@NLO [37] were interfaced to PYTHIA8 [38] to simulate the parton shower (PS), fragmentation, and underlying event with the A14 tune [39] and the NNPDF2.3LO [40] parton distribution function (PDF) set. Some alternative samples use the HERWIG7 [41,42] PS model with the H7UE set of tuned parameters [42] and the MMHT2014LO PDF set [43]. Samples using PYTHIA8 and HERWIG7 have heavy-flavour hadron decays modelled by EvtGen [44]. The masses of the top quark, m_{top}, and of the Higgs boson, m_{H}, are set to 172.5 GeV and 125 GeV, respectively.

The nominal $t\bar{t}H$ signal sample was generated at next-to-leading order (NLO) in the five flavour scheme (5FS) using the POWHEGBOX [45] generator with the NNPDF3.0NLO [40] PDF set. The h_{damp} parameter[2] was set to $3/4 \cdot (m_t + m_{\bar{t}} + m_H) = 352.5$ GeV, and the functional form of the renormalisation and factorisation scales was set to $\sqrt[3]{m_{\text{T}}(t) \cdot m_{\text{T}}(\bar{t}) \cdot m_{\text{T}}(H)}$, where $m_{\text{T}} = \sqrt{m^2 + p_{\text{T}}^2}$ is the transverse mass of a generated particle, m is its mass, and p_{T} is its transverse momentum. It is normalised to the theoretical prediction of Ref. [18] computed at NLO in QCD.[3]

An alternative $t\bar{t}H$ sample generated with the same POWHEGBOX set-up, but interfaced to HERWIG7 is used to evaluate uncertainties due to the choice of parton shower, hadronisation and underlying event model. The uncertainty related to the matching between the matrix element (ME) generator and the PS is accessed by changing the definition of the hardness of the POWHEG emission calculated by PYTHIA8 via the parameter $p_{\text{T}}^{\text{hard}}$ from the value provided by POWHEG to the p_{T} of the POWHEG emission following Refs. [47,48].

Several MC samples with different accuracy in ME generator and with different PS models are used in this analysis to model the main $t\bar{t}$ + jets background. This background is categorised according to the flavour of the additional jets in the event, excluding jets from top-quark or W boson decays, using the same procedure as described in Ref. [49]. Generator-level particle jets are reconstructed from stable particles (mean lifetime $\tau > 3 \times 10^{-11}$ s, excluding muons and neutrinos) using the anti-k_t algorithm [50] with a radius parameter $R = 0.4$, and are required to have transverse momentum $p_{\text{T}} > 15$ GeV and $|\eta| < 2.5$. The flavour of a jet is determined by counting b- or c-hadrons within $\Delta R < 0.4$ of the jet axis. Jets matched to exactly one b-hadron, with p_{T} above 5 GeV, are labelled single-b-jets, while those matched to two or more b-hadrons are labelled B-jets (with no p_{T} requirement on the second b-hadron); single-c- and C-jets are defined analogously, only considering jets not already defined as single-b- or B-jets. Events that have a single-b- or B-jet, are labelled as $t\bar{t}+1b$ and $t\bar{t}+1B$ respectively, events with two or more b-jets are labelled as $t\bar{t}+\geq 2b$. These three categories together are collectively referred to as $t\bar{t}+\geq 1b$. Events with no single-b- or B-jet but at least one single-c- or C-jet are labelled as $t\bar{t}+\geq 1c$. Finally, events not containing any heavy-flavour jets aside from those from top-quark or W boson decays are labelled as $t\bar{t}$ + light.

The $t\bar{t}$ + light and $t\bar{t}+\geq 1c$ contributions are modelled by a MC sample produced with the HVQ programme [34] in the POWHEGBOX generator at NLO in QCD in the five flavour scheme (5FS) with the NNPDF3.0NLO PDF set. The h_{damp} parameter was set to 1.5 m_{top} [39,51]. An additional sample was generated with the h_{damp} parameter increased by a factor of two to evaluate the uncertainty in the modelling of $t\bar{t}$ + light and $t\bar{t}+\geq 1c$ stemming from the choice of the h_{damp} value.

To predict the $t\bar{t}+\geq 1b$ background with the highest available precision, the $t\bar{t}b\bar{b}$ MC sample is generated at NLO, where the additional b-quarks are included in the ME. The four flavour scheme (4FS) was used for this sample. It was produced with the POWHEGBOXRES [52] generator and OPENLOOPS [53–55], using the implementation of this process in POWHEGBOXRES [56], with the NNPDF3.1NNLONF4 [69] PDF set interfaced to PYTHIA8. Based on the studies of Ref. [22], the factorisation scale is set to $\frac{1}{2}\sum_{i=t,\bar{t},b,\bar{b},j} m_{\text{T},i}$, the renormalisation scale is set to $\frac{1}{2} \cdot \sqrt[4]{m_{\text{T}}(t) \cdot m_{\text{T}}(\bar{t}) \cdot m_{\text{T}}(b) \cdot m_{\text{T}}(\bar{b})}$, and the h_{damp} parameter is set to $H_{\text{T}}/2$. The POWHEG internal parameter h_{bzd} that regulates the damping function together with the parameter h_{damp}, was set to 5. The choice of model used for the recoil in the initial state parton shower was found to impact significantly the $t\bar{t}+\geq 1b$ background predictions [23]. The corresponding uncertainty is evaluated by changing the PYTHIA8 parameter from a global recoil to a dipole recoil while keep-

[2] The h_{damp} parameter controls the transverse momentum p_{T} of the first additional emission beyond the leading-order Feynman diagram in the PS and therefore regulates the high-p_{T} emission against which the $t\bar{t}$ system recoils.

[3] A new theoretical computation of the $t\bar{t}H$ production at next-to-next-to-leading order in QCD was published recently in Ref. [46].

ing the rest of the settings identical to the nominal $t\bar{t}b\bar{b}$ sample.

Similar to the $t\bar{t}H$ signal sample, alternative samples were generated to assess the PS and matching uncertainties in the modelling of $t\bar{t}+$light, $t\bar{t}+\geq 1c$ and $t\bar{t}+\geq 1b$ by replacing in the corresponding nominal set-ups the PYTHIA8 shower model by HERWIG and producing samples with a varied $p_{\mathrm{T}}^{\mathrm{hard}}$ parameter.

For an independent pseudo-data test, additional samples of $t\bar{t}$ events were produced to model $t\bar{t}+$light and $t\bar{t}+\geq 1c$ events with the SHERPA [57] generator. The NLO-accurate matrix elements for up to one additional parton, and LO-accurate matrix elements for up to four additional partons were calculated with the COMIX [58] and OPENLOOPS libraries. They were matched with the SHERPA PS [59] with the default set of tuned parameters using the MEPS@NLO prescription [60–63] with a matching scale of 30 GeV. Furthermore, $t\bar{t}+\geq 1b$ events were simulated using SHERPA and OPENLOOPSwith $t\bar{t}b\bar{b}$ ME calculated at NLO accuracy using COMIX in the 4FS using the same functional form of the factorisation and renormalisation scales as in the nominal $t\bar{t}b\bar{b}$ set-up.

Single-top-quark production processes, i.e. tW associated production, t-channel and s-channel production, were modelled using the POWHEGBOX [64–66] generator at NLO in QCD. The t-channel process was generated in the 4FS with the NNPDF3.0NLONF4 PDF set, while for tW and s-channel processes the 5FS NNPDF3.0NLO PDF was used. The tW MC sample was generated using the factorisation and renormalisation scales set to $H_{\mathrm{T}}/2$ with H_{T} defined as a sum of the transverse mass of the W boson, the top quark and the transverse momentum of an additional parton. The overlap between tW and $t\bar{t}$ production [66] was removed using the diagram-removal scheme [67]. An alternative tW MC sample implementing the diagram subtraction scheme [66] was produced to evaluate the systematic uncertainty due to the tW and $t\bar{t}$ interference treatment.

The events in the nominal $t\bar{t}W$ sample were simulated using the SHERPA [68] generator with the NNPDF3.0NNLO PDF set. The ME was calculated for up to one additional parton at NLO and up to two partons at LO using COMIX and OPENLOOPS, and merged with the SHERPA PS using the MEPS@NLO prescription with a merging scale of 30 GeV. The alternative sample was generated with MADGRAPH5_AMC@NLO with up to one additional parton in the final state at NLO accuracy in the strong coupling, using the NNPDF3.1NNLO [69] PDF set. The different jet multiplicities were merged using the FxFx NLO ME and PS merging prescription [70] with a merging scale of 30 GeV. Background events from $t\bar{t}Z/\gamma^*$ and the rare processes $tZq, tWZ, tHjb$, tWH and $t\bar{t}t\bar{t}$ were simulated at NLO in QCD using the MADGRAPH5_AMC@NLO generator. The alternative sample used to evaluate the PS uncertainty in the $t\bar{t}Z$ background was generated with the same set-up as the nominal but interfaced to HERWIG7.

The production of $V+$jets events (where $V = W$ or Z) was simulated with the SHERPA generator using NLO-accurate matrix elements for up to two partons and LO-accurate matrix elements for up to four partons. Samples of diboson final states (VV) were also simulated with the SHERPA generator.

All MC samples corresponding to small backgrounds were normalised to the most precise available theoretical predictions closely following Ref. [20]. The normalisation of the $t\bar{t}W$ background was updated to the most recent prediction of Ref. [71]. The $t\bar{t}+$ light and $t\bar{t}+\geq 1c$ components were normalised to the $t\bar{t}$ cross-section computed at next-to-next-to-leading order (NNLO) in QCD including the resummation of next-to-next-to-leading-logarithmic (NNLL) soft-gluon terms [72] while the $t\bar{t}+\geq 1b$ normalisation is taken from the $t\bar{t}b\bar{b}$ MC simulation.

4 Objects and event selection

Events are selected using single-lepton triggers with variable electron and muon transverse momentum thresholds, and various identification and isolation criteria depending on the lepton flavour and the data-taking period [73,74]. The lowest p_{T} threshold at trigger level used for muons is 20 GeV (26 GeV), while for electrons the threshold is 24 GeV (26 GeV) in 2015 (2016–2018). Events are required to have at least one vertex with at least two associated ID tracks with $p_{\mathrm{T}} > 0.5$ GeV. In each event, the primary vertex is defined as the reconstructed vertex having the highest scalar sum of squared p_{T} of associated tracks [75] among the vertices consistent with the average beam-spot position.

Electron candidates are reconstructed from energy deposits in the electromagnetic calorimeter matched to tracks reconstructed in the ID system and are required to satisfy the *MediumLH* identification criterion [76]. They are required to have $p_{\mathrm{T}} > 10$ GeV and $|\eta| < 2.47$, excluding the calorimeter barrel-endcap transition region ($1.37 < |\eta| < 1.52$). Muon candidates are reconstructed from tracks in the MS that are associated with tracks from the ID and are required to satisfy the *Loose* identification criterion [77] and to have $p_{\mathrm{T}} > 10$ GeV, $|\eta| < 2.5$. Electron (muon) candidates must be associated with the primary vertex of the event: the transverse impact parameter divided by its estimated uncertainty, $|d_0|/\sigma(d_0)$, is required to be less than five (three) for electron (muon) candidates. The longitudinal impact parameter must satisfy $|z_0 \sin(\theta)| < 0.5$ mm for both lepton flavours.

Jets are reconstructed from particle flow objects [78] using the anti-k_t jet clustering algorithm in the FASTJET implementation [79] with a radius parameter $R = 0.4$. Jets are required to satisfy the *Tight* criterion of the *jet vertex tagger* (JVT)

algorithm [80] to mitigate the contribution from pile-up jets, and to have $p_{\mathrm{T}} > 25$ GeV and $|\eta| < 2.5$. The jet energy scale (JES) and resolution are calibrated using simulations with in situ corrections obtained from data [81]. Events containing jets originating from non-collision sources or detector noise are removed.

Jets containing b-hadrons, referred to as b-jets, are identified using the DL1r b-tagging algorithm [82] that uses a neural network based on the distinctive features of b-hadron decays, primarily the impact parameters of tracks and the displaced vertices reconstructed in the ID. Additional input to this network is provided by discriminating variables constructed by a recurrent neural network that exploits the spatial and kinematic correlations between tracks originating from the same b-hadron. A multivariate b-tagging discriminant value is calculated for each jet. The b-tagged jets are required to satisfy the working point (WP) corresponding to an efficiency of 70% or 85% for identifying b-quark initiated jets in $t\bar{t}$ simulated events for the single-lepton and dilepton channels, respectively. For the 70% (85%) WP the rejection factors against light-quark/gluon jets and c-quark jets are 625 and 12 (40 and 3), respectively. To fully exploit the b-tagging information of an event, each jet is assigned a b-tagging score that defines if a jet satisfies a given WP but fails to satisfy the adjacent tighter one. In addition to the standard JES calibration, b-tagged jets satisfying the 85% WP receive additional flavour-specific corrections to their four-vectors to improve their energy measurement (scale and resolution) following the *muon-in-jet* procedure described in Ref. [83].

Hadronically decaying τ-leptons (τ_{had}) are distinguished from jets using their track multiplicity and a multivariate discriminant based on their shower shapes in calorimeter and on tracking information [84]. They are required to have $p_{\mathrm{T}} > 25$ GeV and $|\eta| < 2.5$, and to pass the *Medium* τ-lepton identification working point.

The missing transverse momentum vector, with magnitude $E_{\mathrm{T}}^{\mathrm{miss}}$, is defined as the negative sum of the transverse momenta of the reconstructed and calibrated physical objects, plus a 'soft term' built from all other tracks associated with the primary vertex [85] and not matched to a reconstructed object.

Targeting event topologies with a Higgs boson decaying into collimated hadronic final states, reclustered (RC) jets [86] are reconstructed from the selected jets, using the anti-k_t jet clustering algorithm with a radius parameter $R = 1.0$. RC jets are required to have an invariant mass $M > 50$ GeV, $p_{\mathrm{T}} > 200$ GeV, $|\eta| < 2.0$, have at least two constituent small-R jets (subjets) and have an angular distance $\Delta R > 1.0$ from all electrons.

An overlap removal procedure is applied to avoid the double counting of detector signatures. Electron candidates sharing a track with a muon candidate are first removed. Jets found within a $\Delta R = 0.2$ cone of an electron are removed and electrons within a $\Delta R = 0.4$ cone of a remaining jet are rejected. Jets with less than three associated tracks and within $\Delta R = 0.2$ of a muon and muons within $\Delta R = 0.4$ of a jet with more than two associated tracks are rejected. A τ_{had} candidate is rejected if it is separated by $\Delta R < 0.2$ from any selected electron or muon. No overlap removal is performed between jets and τ_{had} candidates.

Events are selected if they contain exactly one lepton candidate in the single-lepton channel and exactly two lepton candidates with opposite electric charges in the dilepton channel. At least one lepton should have $p_{\mathrm{T}} > 27$ GeV and be matched to the corresponding object at the trigger level. In the events with two electrons, the second lepton is required to have $p_{\mathrm{T}} > 15$ GeV while in the other two dilepton channels, $e\mu$ and $\mu\mu$, it must have $p_{\mathrm{T}} > 10$ GeV. In events with two electrons or two muons, the dilepton invariant mass is required to be above 15 GeV, to suppress contribution from the decays of heavy-flavour resonances and low-mass Drell–Yan processes, and be outside a window of $\pm$ 8 GeV centred at the Z boson mass. To maintain orthogonality with other $t\bar{t}H$ decay channels, events are vetoed if they contain one or more (two or more) τ_{had} candidates in the dilepton (single-lepton) channel.

To reduce the non-prompt and mis-identified lepton background contribution, additional lepton identification and isolation requirements are applied. Electrons (muons) are required to satisfy the *TightLH* (*Medium*) identification criteria and the tight isolation criteria based on the calorimeter and tracking information for electrons [76] and on tracking information only for muons [77]. Events for which the leptons fail to meet these requirements are removed.

In the single-lepton channel two event categories are defined, referred in the following as resolved and boosted categories. The latter is designed to select events in which the Higgs boson is produced with high transverse momentum as a collimated large-R jet. Events that do not satisfy the boosted category selection are assigned to the resolved one. In the single-lepton resolved channel, events are selected if they contain at least five jets, at least three of which satisfy the 70% b-tagging WP. In the single-lepton boosted channel, events are required to have at least one large-R jet and at least four small-R jets, including those contained within the large-R jet, at least three of which must satisfy the 85% b-tagging WP. In the dilepton channel, events are selected if they contain at least three jets satisfying the 85% b-tagging WP, and among these at least two jets that satisfy the 70% b-tagging WP. These requirements are henceforth referred to as "preselection" and have an acceptance of 6.3% for selecting $t\bar{t}H$ events with $H \to b\bar{b}$ decay, an acceptance that is more than a factor of three larger than in the previous analysis [20]. The corresponding acceptance in the signal regions is 2.1%.

5 Background modelling

The largest background from $t\bar{t}$+jets production is modelled by MC simulation with the data-driven corrections described in Sect. 5.1. Small backgrounds include single top production, $t\bar{t}W$, $t\bar{t}Z$, $t\bar{t}t\bar{t}$, rare top-quark processes and non-top-quark processes such as V+jets and diboson production. All of them are estimated from simulations. The contribution from the background arising from non-prompt or mis-identified leptons is determined from data in the single-lepton channel (see Sect. 5.2), and from MC simulation in the dilepton channel, where this background arises primarily from $t\bar{t}$ events with one prompt lepton and is very small.

5.1 Modelling of $t\bar{t}$ + jets background

The $t\bar{t}$ sample used to model the $t\bar{t}$ + light and $t\bar{t} + \geq 1c$ contributions is generated at NLO as described in Sect. 3, with up to one additional parton from the ME calculation. All jets not originating from the decay chain of one of the top quarks, i.e. additional jets, are produced by the parton shower. The dedicated measurement [87] demonstrated deficiencies in modelling the number of additional jets in the $t\bar{t}$ events and the scalar sum of the transverse momenta of the top quarks. Moreover, the rate of $t\bar{t}$ production in association with c- and b-jets was observed to be underestimated in the previous analysis [20]. The new $t\bar{t}b\bar{b}$ MC sample produced for this analysis with lower value of the renormalisation scale than the one used in Ref. [20] predicts larger inclusive $t\bar{t} + \geq 1b$ cross-section, which is expected to match data well. Nevertheless, the rate of the components of the $t\bar{t} + \geq 1b$ background defined in Sect. 3, $t\bar{t} + 1B$, $t\bar{t} + 1b$ and $t\bar{t} + \geq 2b$, could still be mismodelled. Thus, to obtain a reliable estimate of the $t\bar{t}$ + jets background, the $t\bar{t}$ MC events are reweighted using data. The corrections applied include a rescaling of the $t\bar{t}$ + jets flavour components followed by a kinematic reweighting and are described in the next paragraph. Any possible residual mismodelling is accounted for by the systematic uncertainties in the profile-likelihood fit used for the extraction of the signal strength which is described in Sect. 6.

Initial scaling factors for the five $t\bar{t}$ + jets flavour components, $t\bar{t}$ + light, $t\bar{t} + \geq 1c$, $t\bar{t} + 1B$, $t\bar{t} + 1b$ and $t\bar{t} + \geq 2b$, are obtained separately for the single-lepton and dilepton channels from the profile-likelihood fit to data. The fit is performed in background-dominated control regions including all systematic uncertainties (see Sect. 7) prior to the signal extraction fit described in Sect. 6. These scaling factors have similar values to those shown in Table 5. Following the flavour components rescaling, a reweighting is used to mitigate the kinematic mismodelling of the scalar sum of the p_{T}'s of the reconstructed leptons and jets, H_{T}, observed for the $t\bar{t}$ + light and $t\bar{t} + \geq 1c$ components of the inclusive $t\bar{t}$ + jets POWHEG + PYTHIA8 sample. The $t\bar{t} + \geq 1b$ component is excluded from the reweighting since it is simulated by a dedicated $t\bar{t}b\bar{b}$ MC sample. Thus the reweighting derived in the regions dominated by $t\bar{t}$ + light and $t\bar{t} + \geq 1c$ might not be applicable to $t\bar{t} + \geq 1b$. A dedicated reweighting was investigated for the $t\bar{t} + \geq 1b$ component but found to have a negligible effect and is not used in the analysis.

The reweighting corrects the distributions of H_{T} in exclusive jet multiplicity bins from $N_{\mathrm{jets}} = 5$ to $N_{\mathrm{jets}} \geq 8$ in the single-lepton channel and from $N_{\mathrm{jets}} = 3$ to $N_{\mathrm{jets}} \geq 6$ in the dilepton channel. It is derived in $t\bar{t}$ enriched regions selected by using looser b-tagging requirements after subtracting from data all contributions except for $t\bar{t}$ + light and $t\bar{t} + \geq 1c$ and taking the ratio of data to the sum of $t\bar{t}$ + light and $t\bar{t} + \geq 1c$ yields predicted by MC in each H_{T} bin. These regions are orthogonal to the signal and control regions of the analysis and contain less that 0.2% of signal.

The reweighting factors are also derived in the same way for each systematic variation affecting the $t\bar{t}$ + light and $t\bar{t} + \geq 1c$ predictions, such that all systematic variations match the H_{T} distribution in data.

5.2 Non-prompt or mis-identified lepton background

A data-driven method, referred to as "fake factor" method [88], based on the measurement of lepton selection efficiencies using different identification and isolation criteria, is used to estimate the non-prompt or mis-identified (fake) lepton background in the single-lepton channel.

The fake rate is measured in a fake-dominated region selected by requiring exactly one lepton with loose identification and isolation criteria, at least two jets, at least two b-tagged jets satisfying the 70% WP, and a scalar sum of missing transverse energy and the leptonically-decaying W boson mass below 60 GeV. It is parameterised as a function of the leading jet p_{T} and the lepton $|\eta|$. The expected number of events arising from the fake lepton background is determined by applying the measured lepton fake rate to data events satisfying the selection requirements of each analysis region except that the lepton is required to pass loose identification and isolation criteria and to fail the tighter requirements.

6 Signal extraction

After the preselection, events are classified into non-overlapping background-dominated or control regions (CR) and signal-enriched regions (SR) with higher signal-to-background ratios. The CRs provide stringent constraints on the normalisation of the backgrounds and the systematic uncertainties in a combined fit with the signal regions.

To define the regions in the single-lepton and dilepton channels, a multiclass classification neural network based

on the permutation-invariant transformer architecture with attention mechanism [89] is trained to predict the probability of an event to be from the $t\bar{t}H$ signal or from one of the five $t\bar{t}$+jets background categories introduced in Sect. 3: $t\bar{t}+1b$, $t\bar{t}+1B$, $t\bar{t}+\geq 2b$, $t\bar{t}+\geq 1c$, $t\bar{t}+$light jets. The probability p_i of a network class i is converted into a discriminant d_i in order to maximise the separation between the class and all the other classes ($i \neq j$), to yield a similar number of events in the $t\bar{t}+1b$, $t\bar{t}+1B$, and inclusive $t\bar{t}+\geq 2b$ control regions, and to maximise sensitivity. They are defined as

$$d_i = \frac{p_i}{\sum_{j\neq i} p_j \cdot \hat{N}_{ij}}. \quad (1)$$

Here, the denominator of each discriminant is a weighted average of all the remaining class probabilities $p_{j\neq i}$. The weights $\hat{N}_{ij} = N_j/\sum_{k\neq i} N_k$ are the respective fractions of event yields N_j relative to the total yield of all the remaining classes $k \neq i$. These yields are determined from MC simulation after the preselection and incorporate the $t\bar{t}+$ jets scaling factors described in Sect. 5.1.

In the single-lepton (dilepton) channel, events fulfilling $d_{t\bar{t}H} > 4.072$ ($d_{t\bar{t}H} > 9.031$) are assigned to the signal region. The thresholds are defined to maximize the ratio of signal to the square root of the background in the inclusive signal regions. All other events are assigned to the $t\bar{t}+$ jets background category with the highest value of the discriminant. By far the dominant Higgs boson decay mode in the signal region is $H \to b\bar{b}$ with a fraction of more than 97% (94%) of the $t\bar{t}H$ events in the single-lepton (dilepton) channel followed by the $H \to WW$ decay. This motivates the training of a second neural network, based on the same architecture, to identify the two jets most likely originating from the Higgs boson decay, to reconstruct p_{T}^H that is used to further classify the signal region events into the six reconstructed STXS regions. The performance of this reconstruction network to correctly identify both Higgs boson decay products decreases with increasing jet multiplicity and generally increases with increasing true p_{T}^H. Both Higgs boson decay products are correctly identified for 51% (58%) of $t\bar{t}H(b\bar{b})$ events in the single-lepton resolved (dilepton) channel. The boundaries of the regions are optimised to maximise fraction of the events with the corresponding truth p_{T}^H, listed in Fig. 1, separately per $t\bar{t}$ decay channel to capture potential differences due to the final states and separate neural networks. This optimisation leads, in particular, to improved purity in the highest truth p_{T}^H bins, the region of the phase space where this analysis provides a particularly valuable contribution to the global Higgs boson combination. The optimal reconstructed p_{T}^H boundaries are found to be [0, 60, 114, 186, 270, 402, ∞] GeV in the dilepton channel and [0, 60, 114, 192, 282, 408, ∞] GeV in the single-lepton resolved channel. They are referred to in the following as STXS 1–6 regions.

The inclusive control region dominated by the $t\bar{t}+\geq 2b$ background in the single-lepton channel is further split into three categories encompassing STXS regions 1–2, 3–4, and 5–6, to ensure a good control of the $t\bar{t}+\geq 2b$ background modelling over the bins of reconstructed Higgs boson p_{T}. These regions are henceforth referred to as $t\bar{t}+\geq 2b$ CR 1, CR 2, and CR 3. The split is not applied in the dilepton channel due to limited statistics.

Events fulfilling the boosted selection criteria are assigned to dedicated boosted signal and control regions. RC jets are used as input to a multiclass deep neural network (DNN), trained to distinguish high-p_{T} Higgs boson candidates decaying into collimated final states from top quarks and multijet backgrounds following the same strategy as in the previous analysis [20]. An event is flagged as containing a boosted Higgs boson candidate if one of the RC jets has a high probability of originating from a Higgs boson, as estimated by the DNN. Boosted Higgs boson candidates are required to have $p_{\mathrm{T}} \geq 300$ GeV, a mass consistent with the Higgs boson mass window of 100–140 GeV, contain at least two subjets, of which exactly two are required to satisfy the b-tagging 85% WP, and have a DNN score above 0.4. At least two small-R jets that do not form the Higgs boson candidate are required to satisfy the b-tagging 77% WP. The flowchart in Fig. 1 summarises the event classification strategy.

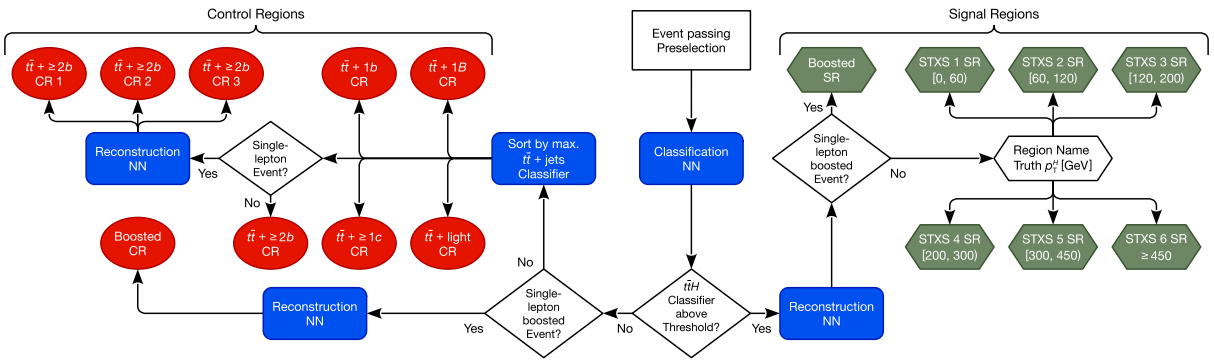

Fig. 1 Flowchart depicting the event classification and Higgs boson p_{T} reconstruction strategy used in the analysis

The transformer networks are trained using low-level features of the reconstructed jets, electrons, muons, and the missing transverse momentum of the event. For each reconstructed object, the kinematic features used are the x-, y- and z-component of the momentum (p_x, p_y, p_z), the energy, the p_{T}, the mass, the pseudorapidity, the azimuthal angle and its sine and cosine. Supplying redundant four-vector information is observed to improve network performance. Additionally, the DL1r pseudo-continuous b-tagging score is included for jets, and the electric charge and a variable indicating if it is an electron or a muon is included for leptons.

The multiclass event-classification network is trained using events sampled from the nominal and alternative $t\bar{t}H$ and $t\bar{t}+$jets background samples to profit from an increased number of events in training. The classification network yields an area under the receiver-operator characteristic curve (AUC) of 0.753 (0.774) for discriminating between $t\bar{t}H$ and the $t\bar{t}+\geq 1b$ background for events satisfying the preselection in the single-lepton resolved (dilepton) channel. The Higgs boson p_{T} reconstruction network is trained using only the $t\bar{t}H$ samples. Figure 2 shows for each bin of truth p_{T}^{H} the fraction of $t\bar{t}H$ events assigned to each of the STXS signal regions.

In the single-lepton channel, a total of 15 analysis regions are defined, including six STXS signal regions, two boosted regions (signal and control) and seven control regions targeting the different components of the $t\bar{t}+$jets background. In the dilepton channel, a total of 11 analysis regions are defined, including the six STXS signal regions and five $t\bar{t}+$jets control regions. The expected yields in the single-lepton (dilepton) signal and control regions are summarised in Tables 1 and 2 (3 and 4) after applying the data-driven corrections to the $t\bar{t}+$jets background discussed in Sect. 5.1.

The $t\bar{t}H$ inclusive signal strength, $\mu_{t\bar{t}H}$, defined as the ratio of the measured $t\bar{t}H$ cross-section including all Higgs boson decay modes to the corresponding SM prediction, or the signal strengths in each of the six STXS bins, μ_i, and the normalisation factors of the components of the $t\bar{t}+$jets background are determined via a binned likelihood fit to the distributions in all signal and control regions defined above. The $t\bar{t}H$ signal sample is split up according to the true p_{T}^{H} in each event, and the μ_i act on the respective component. In the resolved signal and control regions, the corresponding discriminant distribution is used in the likelihood fit, while in the boosted regions, event yields in two bins of the reconstructed p_{T}^{H} distribution, 300–450 GeV and ≥ 450 GeV, are used in the fit.

The $t\bar{t}+1b$, $t\bar{t}+\geq 1c$ and $t\bar{t}+$light normalisation factors are chosen to float independently in the single-lepton and dilepton channels, while the normalisations of the $t\bar{t}+\geq 2b$ and $t\bar{t}+1B$ backgrounds are scaled in a correlated way between the two channels. This choice is made based on studies of the different correlation assumptions between the normalisation factors in the combined fit. The chosen configuration provides enough freedom for the fit model and minimises pulls and constraints of the nuisance parameters in the fit to data.

The inclusive measurement of the signal strength and cross-section is performed in the full phase space. The measurement of these parameters in STXS bins is carried out for $t\bar{t}H$ events with a Higgs boson produced centrally within $|y|\leq 2.5$ at truth level, while the remaining forward events are considered as background.

The statistical model is based on a likelihood function built with HistFactory [90] as the product over every bin of the Poisson probability for the observed data, given the SM prediction. The value of each nuisance parameter, describing the systematic uncertainties for both signal and background processes (see Sect. 7), is constrained by a Gaussian penalty term present in the likelihood function, while all normalisation factors are unconstrained. The statistical uncertainty arising from the limited number of simulated events is included in the likelihood in the form of additional nuisance parameters with Poisson constraint terms. The maximum-likelihood fit is performed with the RooFit package [91]. A test statistic based on the profile-likelihood ratio is used to assess the compatibility of the observed data with the background-only hypothesis ($\mu=0$) [92].

Tests of the statistical model fitted to pseudo-data constructed with the SHERPA $t\bar{t}+$jets samples were performed to help inform the choice of fit variables and uncertainty model, with the goal of minimising bias, maximising robustness and optimising sensitivity.

7 Systematic uncertainties

Multiple sources of systematic uncertainty, arising from detector effects, theoretical assumptions and the limited number of events in the MC simulations, are considered in the analysis. They affect the categorisation of events as well as the normalisation and shape of the distributions used in the signal extraction fit.

All the sources of experimental uncertainty, except the uncertainty in the integrated luminosity, affect both the normalisations and the shapes of the distributions in all simulated samples. The uncertainty in the integrated luminosity is 0.83% [93], obtained using the LUCID-2 detector [25] for the primary luminosity measurements, complemented by measurements using the inner detector and calorimeters. The uncertainty in the pile-up modelling is obtained by varying the pile-up reweighting in the simulation within its uncertainties.

The correction factors applied to the simulated samples to improve the description of the lepton reconstruction, identification and isolation efficiencies, momentum scale and res-

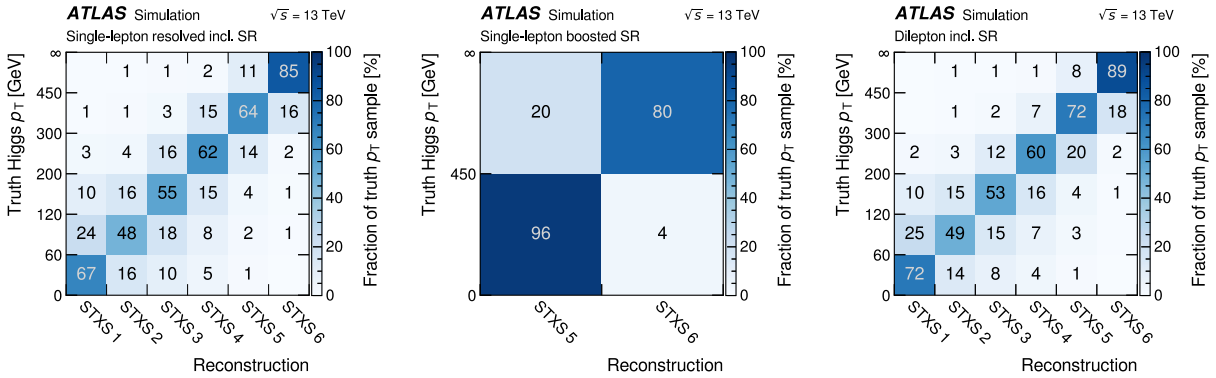

(a) (b) (c)

Fig. 2 STXS migration matrices for the $t\bar{t}H$ signal regions in (**a**) the single-lepton resolved, (**b**) the single-lepton boosted, and (**c**) the dilepton channel. The yield fractions of the predicted STXS bins are normalised per truth STXS sample

Table 1 Expected yields in the single-lepton signal regions before the fit to data. The data-driven corrections to the $t\bar{t}$ + jets background are applied and all uncertainties are included, except the ones associated with the $t\bar{t}$ + jets background normalisation factors, which are not defined pre-fit. The "Other" category includes the s- and t-channel single-top, tZq and tWZ processes. The $t\bar{t}H$ signal is normalised to the SM $t\bar{t}H$ cross-section. For presentation purposes, uncertainties are symmetrised

	STXS 1 SR	STXS 2 SR	STXS 3 SR	STXS 4 SR	STXS 5 SR	STXS 6 SR	Boosted SR
$t\bar{t}H$ truth p_T^H 0–60 GeV	77 ± 12	18.7 ± 3.2	11.1 ± 2.3	5.7 ± 1.0	1.66 ± 0.2	0.42 ± 0.09	0.58 ± 0.13
$t\bar{t}H$ truth p_T^H 60–120 GeV	49 ± 5	99 ± 13	37 ± 6	15.5 ± 2.2	4.4 ± 0.5	1.25 ± 0.19	1.54 ± 0.25
$t\bar{t}H$ truth p_T^H 120–200 GeV	22.7 ± 2.2	37 ± 4	125 ± 16	34 ± 5	8.1 ± 1.3	2.0 ± 0.4	2.31 ± 0.28
$t\bar{t}H$ truth p_T^H 200–300 GeV	4.0 ± 0.5	5.5 ± 0.7	22.5 ± 2.9	88 ± 12	19.4 ± 3.0	2.7 ± 0.4	3.3 ± 0.6
$t\bar{t}H$ truth p_T^H 300–450 GeV	0.39 ± 0.11	0.64 ± 0.16	1.4 ± 0.4	7.6 ± 1.3	32 ± 5	8.0 ± 1.3	20 ± 3
$t\bar{t}H$ truth p_T^H ≥450 GeV	<0.1	<0.1	0.14 ± 0.06	0.21 ± 0.09	1.30 ± 0.31	9.8 ± 1.8	6.9 ± 1.3
$t\bar{t}H$ $\|y\| > 2.5$	0.16 ± 0.06	0.10 ± 0.04	<0.1	<0.1	<0.1	<0.1	<0.1
$t\bar{t}$ + ≥ 2b	870 ± 80	870 ± 90	980 ± 100	640 ± 60	270 ± 40	92 ± 21	103 ± 8
$t\bar{t}$ + 1b	210 ± 60	210 ± 50	250 ± 80	180 ± 60	78 ± 28	25 ± 9	17 ± 5
$t\bar{t}$ + 1B	64 ± 19	73 ± 24	100 ± 40	87 ± 30	46 ± 19	22 ± 11	11 ± 4
$t\bar{t}$ + ≥ 1c	210 ± 50	210 ± 50	250 ± 50	190 ± 50	88 ± 24	27 ± 13	22 ± 8
$t\bar{t}$ + light	42 ± 16	45 ± 12	68 ± 22	64 ± 19	31 ± 11	12 ± 11	3.2 ± 3
$t\bar{t}Z$	36 ± 6	38 ± 6	53 ± 8	43 ± 8	24 ± 5	7.2 ± 1.1	5.8 ± 1.2
tW	20 ± 8	35 ± 12	60 ± 33	55 ± 32	33 ± 25	17 ± 15	5 ± 4
W+jets	10 ± 6	12 ± 8	30 ± 15	29 ± 14	23 ± 12	12 ± 6	3.7 ± 1.9
$t\bar{t}W$	4.2 ± 0.5	5.9 ± 0.8	9.8 ± 1.6	8.9 ± 1.9	5.6 ± 0.7	3.2 ± 0.5	1.06 ± 0.26
Z+jets	2.5 ± 1.1	5.1 ± 2	6.5 ± 2.6	7.4 ± 2.7	3.1 ± 1.1	1.7 ± 0.6	0.5 ± 0.2
Diboson	1.3 ± 0.8	2.5 ± 1.40	4.4 ± 2.3	4.7 ± 2.7	3.1 ± 1.6	1.4 ± 0.7	0.7 ± 0.4
$t\bar{t}t\bar{t}$	5.1 ± 2.2	6.7 ± 3	11 ± 5	9 ± 4	4.8 ± 2.1	2.5 ± 1.1	1.1 ± 0.5
$tHjb$	0.77 ± 0.22	1.06 ± 0.21	1.61 ± 0.32	1.58 ± 0.28	1.11 ± 0.30	0.26 ± 0.12	0.72 ± 0.14
tWH	1.68 ± 0.23	2.16 ± 0.27	3.8 ± 0.4	4.1 ± 0.5	2.22 ± 0.25	1.03 ± 0.12	1.01 ± 0.11
Other	11.3 ± 1.2	11 ± 1.5	14.4 ± 2	11.9 ± 1.5	7.3 ± 1.1	2.43 ± 0.35	2.2 ± 0.6
Fakes	29 ± 12	29 ± 15	27 ± 12	31 ± 19	22 ± 13	3.8 ± 2.5	8 ± 5
Total	1670 ± 160	1710 ± 170	2060 ± 210	1520 ± 150	710 ± 80	250 ± 40	221 ± 19
Data	1672	1657	2016	1441	676	241	216

Table 2 Expected yields in the single-lepton control regions before the fit to data. The data-driven corrections to the $t\bar{t}+$ jets background are applied and all uncertainties are included, except the ones associated with the $t\bar{t}+$ jets background normalisation factors, which are not defined pre-fit. The "Other" category includes the s- and t-channel single-top, tZq and tWZ processes. The $t\bar{t}H$ signal is normalised to the SM $t\bar{t}H$ cross-section. For presentation purposes, uncertainties are symmetrised

	$t\bar{t}+$ light CR	$t\bar{t}+\geq 1c$ CR	$t\bar{t}+1b$ CR	$t\bar{t}+1B$ CR	$t\bar{t}+\geq 2b$ CR 1	$t\bar{t}+\geq 2b$ CR 2	$t\bar{t}+\geq 2b$ CR 3	Boosted CR
$t\bar{t}H$ truth p_{T}^{H} 0–60 GeV	56 ± 6	59 ± 7	89 ± 11	46 ± 6	80 ± 10	12.5 ± 1.7	2.09 ± 0.26	0.54 ± 0.14
$t\bar{t}H$ truth p_{T}^{H} 60–120 GeV	86 ± 5	98 ± 8	133 ± 12	92 ± 13	112 ± 11	33 ± 5	4.5 ± 0.9	1.15 ± 0.23
$t\bar{t}H$ truth p_{T}^{H} 120–200 GeV	59 ± 4	76 ± 7	76 ± 8	88 ± 11	41 ± 4	68 ± 8	5.4 ± 1.1	1.36 ± 0.28
$t\bar{t}H$ truth p_{T}^{H} 200–300 GeV	23 ± 2.5	31.9 ± 3.5	21.2 ± 3.1	41 ± 5	7.3 ± 1.1	34 ± 4	6.7 ± 1.1	1.42 ± 0.32
$t\bar{t}H$ truth p_{T}^{H} 300–450 GeV	7.7 ± 1.0	10 ± 1.5	4.7 ± 0.8	14.3 ± 2	1.12 ± 0.27	4.4 ± 0.8	9.8 ± 1.5	4.8 ± 0.7
$t\bar{t}H$ truth $p_{\mathrm{T}}^{H} \geq 450$ GeV	1.67 ± 0.27	2.4 ± 0.5	0.78 ± 0.19	4.1 ± 0.7	0.18 ± 0.05	0.35 ± 0.12	3 ± 0.7	1.75 ± 0.32
$t\bar{t}H$ $\lvert y\rvert > 2.5$	0.98 ± 0.08	0.72 ± 0.17	1.38 ± 0.22	0.57 ± 0.15	0.37 ± 0.05	0.188 ± 0.029	<0.1	<0.1
$t\bar{t}+\geq 2b$	2320 ± 280	3800 ± 400	5400 ± 600	3500 ± 400	7200 ± 600	4900 ± 500	1140 ± 170	141 ± 10
$t\bar{t}+1b$	3900 ± 400	4600 ± 700	10600 ± 1700	5100 ± 600	2100 ± 500	1120 ± 320	230 ± 100	54 ± 19
$t\bar{t}+1B$	890 ± 80	1390 ± 270	1780 ± 270	5100 ± 400	530 ± 190	380 ± 140	100 ± 50	32 ± 7
$t\bar{t}+\geq 1c$	17000 ± 3300	17900 ± 2600	7800 ± 1000	5400 ± 1300	2500 ± 500	1220 ± 270	240 ± 70	133 ± 35
$t\bar{t}+$ light	31800 ± 3500	5900 ± 1100	4000 ± 600	2000 ± 500	700 ± 180	320 ± 110	49 ± 26	34 ± 8
$t\bar{t}Z$	152 ± 20	171 ± 25	151 ± 21	146 ± 22	122 ± 18	117 ± 15	36 ± 5	5.7 ± 0.9
tW	1040 ± 200	750 ± 220	820 ± 240	560 ± 190	350 ± 140	360 ± 150	130 ± 90	10 ± 6
W+jets	370 ± 180	370 ± 180	230 ± 120	170 ± 80	370 ± 190	250 ± 130	90 ± 40	5.6 ± 2.9
$t\bar{t}W$	100 ± 12	114 ± 17	43 ± 7	44 ± 5	25.6 ± 3.5	26 ± 5	10.5 ± 1.6	1.97 ± 0.33
Z+jets	110 ± 40	110 ± 40	110 ± 40	64 ± 23	100 ± 40	55 ± 20	16 ± 6	0.9 ± 0.4
Diboson	37 ± 19	39 ± 20	23 ± 12	21 ± 11	24 ± 13	23 ± 12	10 ± 5	1.1 ± 0.7
$t\bar{t}t\bar{t}$	2.9 ± 1.2	24 ± 10	7.1 ± 3	19 ± 8	21 ± 9	33 ± 14	17 ± 7	1.4 ± 0.6
$tHjb$	8.2 ± 1.4	5.4 ± 0.9	8.1 ± 1.6	3.5 ± 0.6	5.4 ± 1.1	3.6 ± 0.7	0.53 ± 0.15	0.65 ± 0.20
tWH	7.1 ± 0.7	6.7 ± 0.7	9.6 ± 1	5.7 ± 0.6	5.4 ± 0.6	5.8 ± 0.7	1.78 ± 0.2	0.44 ± 0.07
Other	370 ± 40	370 ± 40	303 ± 35	228 ± 22	179 ± 22	111 ± 12	27.4 ± 2.8	3.9 ± 0.9
Fakes	810 ± 300	800 ± 400	880 ± 350	340 ± 140	660 ± 300	280 ± 130	57 ± 32	6.3 ± 3.3
Total	59000 ± 6000	37000 ± 4000	32500 ± 2900	22900 ± 2200	15200 ± 1700	9400 ± 1000	2190 ± 270	440 ± 50
Data	61954	36528	32887	23245	15595	9397	2097	426

Table 3 Expected yields in the dilepton signal regions before the fit to data. The data-driven corrections to the $t\bar{t}$+jets background are applied and all uncertainties are included, except the ones associated with the $t\bar{t}$+jets background normalisation factors, which are not defined pre-fit. The "Other" category includes the tZq, tWZ and diboson processes. The $t\bar{t}H$ signal is normalised to the SM $t\bar{t}H$ cross-section. For presentation purposes, uncertainties are symmetrised

	STXS 1 SR	STXS 2 SR	STXS 3 SR	STXS 4 SR	STXS 5 SR	STXS 6 SR
$t\bar{t}H$ truth p_{T}^{H} 0–60 GeV	10.6 ± 1.5	2.03 ± 0.31	1.14 ± 0.17	0.63 ± 0.11	0.19 ± 0.07	0.046 ± 0.023
$t\bar{t}H$ truth p_{T}^{H} 60–120 GeV	6.5 ± 0.7	13.0 ± 1.8	4.1 ± 0.7	1.9 ± 0.4	0.7 ± 0.11	0.13 ± 0.07
$t\bar{t}H$ truth p_{T}^{H} 120–200 GeV	3.06 ± 0.34	4.7 ± 0.5	16.3 ± 2.0	5.0 ± 0.7	1.36 ± 0.19	0.24 ± 0.07
$t\bar{t}H$ truth p_{T}^{H} 200–300 GeV	0.5 ± 0.07	0.72 ± 0.08	2.5 ± 0.29	13.0 ± 1.7	4.4 ± 0.6	0.41 ± 0.06
$t\bar{t}H$ truth p_{T}^{H} 300–450 GeV	<0.1	<0.1	0.197 ± 0.033	0.82 ± 0.18	8.0 ± 1.1	1.98 ± 0.32
$t\bar{t}H$ truth $p_{\mathrm{T}}^{H} \geq 450$ GeV	<0.1	<0.1	<0.1	<0.1	0.26 ± 0.08	2.8 ± 0.5
$t\bar{t}H$ $\lvert y\rvert > 2.5$	<0.1	<0.1	<0.1	<0.1	<0.1	<0.1
$t\bar{t} + \geq 2b$	81 ± 8	76 ± 7	81 ± 13	59 ± 4	36.2 ± 3.0	11.7 ± 2.1
$t\bar{t} + 1b$	14 ± 5	15 ± 6	20 ± 9	17 ± 5	11 ± 6	2.9 ± 1.9
$t\bar{t} + 1B$	4.4 ± 2.6	4.8 ± 3.2	5.7 ± 2.3	6.2 ± 1.9	6.6 ± 2.9	3.5 ± 2.3
$t\bar{t} + \geq 1c$	11.3 ± 2.4	11.7 ± 2.6	15.4 ± 3.4	12.5 ± 2.6	7.1 ± 2.6	3.0 ± 1.7
$t\bar{t}$ + light	1.1 ± 0.7	0.9 ± 0.5	1.4 ± 0.8	1.0 ± 0.5	1.0 ± 0.4	0.37 ± 0.30
$t\bar{t}Z$	4.6 ± 0.7	4.6 ± 1.1	7.2 ± 1.1	6.2 ± 1.3	5.3 ± 1.1	2 ± 0.6
tW	1.7 ± 0.8	3 ± 1.8	6 ± 4	8 ± 5	7 ± 5	3.1 ± 2.9
$t\bar{t}W$	0.65 ± 0.11	1.18 ± 0.15	2.1 ± 0.23	2.64 ± 0.3	2.7 ± 0.4	1.2 ± 0.5
Z+jets	1.8 ± 0.9	1.9 ± 0.9	3.4 ± 1.3	3.8 ± 1.4	3.3 ± 1.2	1.8 ± 0.7
$t\bar{t}t\bar{t}$	0.9 ± 0.4	1.1 ± 0.5	1.8 ± 0.7	1.7 ± 0.7	1.3 ± 0.6	0.65 ± 0.28
tWH	0.23 ± 0.04	0.31 ± 0.04	0.57 ± 0.07	0.7 ± 0.08	0.66 ± 0.07	0.24 ± 0.03
Other	<0.1	<0.1	0.28 ± 0.14	0.42 ± 0.19	0.23 ± 0.08	0.29 ± 0.13
Fakes	1.7 ± 0.9	2.2 ± 1.1	3.2 ± 1.6	2.9 ± 1.5	2.6 ± 1.3	1.1 ± 0.6
Total	144 ± 13	144 ± 13	173 ± 20	143 ± 12	100 ± 11	38 ± 6
Data	150	149	161	149	76	35

olution, and lepton trigger efficiencies are varied within their uncertainties [76,77] to estimate the corresponding systematic uncertainty.

The JES uncertainty [81] accounts for contributions from jet-flavour composition, η-intercalibration, punch-through, single-particle response, calorimeter response to different jet flavours, and pile-up, resulting in 31 uncorrelated JES uncertainty components. The jet energy resolution was measured separately for data and MC using two in situ techniques [81]. The systematic uncertainty is defined as the quadratic difference between the jet energy resolutions for data and simulation and split into 13 uncorrelated uncertainty components. The uncertainty associated with the JVT discriminant is obtained by varying the efficiency correction factors [80].

The uncertainties associated with the b-tagging algorithm calibration are derived separately for b-jets, c-jets and light-flavour jets, as a function of the jet p_{T}, and decomposed into several uncorrelated components for each category, corresponding to the number of p_{T} bins multiplied by the number of DL1r pseudo-continuous scores [94–96]. This yields a total of 45 components for b-jets and 20 each for c- and light jets. For jets with a p_{T} above the p_{T} threshold where the b-tagging algorithm is calibrated, high-p_{T} extrapolation uncertainties derived using MC simulation are included.

The uncertainty in $E_{\mathrm{T}}^{\mathrm{miss}}$ results from the propagation of the uncertainties in the energy scales and resolutions of photons, leptons and jets, and from the modelling of its soft term [85].

For the $t\bar{t}H$ signal, two cross-section uncertainties are applied accounting for the effect of varying the PDF and α_S and for missing higher order terms in the fixed order perturbative QCD calculations. They amount to $\pm 3.6\%$ and $\pm 9.2\%$, respectively [18]. The systematic uncertainty in the $t\bar{t}H$ cross-section includes theory uncertainties due to migrations of events between the truth Higgs boson p_{T} bins [97]. An uncertainty of 2.2% is assigned to the $H \to b\bar{b}$ branching fraction [18]. Two uncertainties due to missing higher order terms in the MC simulation are estimated by varying independently the renormalisation and factorisation scales in the ME of the nominal MC sample by a factor of two up and down. The uncertainties in the amount of initial- and final-state QCD radiation (ISR and FSR) predicted by the PS are estimated by varying the scale in α_S^{ISR} according to the values given by *var3c* in the PYTHIA8 A14 tune and by varying

Table 4 Expected yields in the dilepton control regions before the fit to data. The data-driven corrections to the $t\bar{t}$+jets background are applied and all uncertainties are included, except the ones associated with the $t\bar{t}$+jets background normalisation factors, which are not defined pre-fit. The "Other" category includes the tZq, tWZ and diboson processes. The $t\bar{t}H$ signal is normalised to the SM $t\bar{t}H$ cross-section. For presentation purposes, uncertainties are symmetrised

	$t\bar{t}$ + light CR	$t\bar{t} + \geq 1c$ CR	$t\bar{t} + 1b$ CR	$t\bar{t} + 1B$ CR	$t\bar{t} + \geq 2b$ CR
$t\bar{t}H$ truth p_{T}^{H} 0–60 GeV	11.9 ± 1.4	19.7 ± 2.3	19.8 ± 2.3	9.9 ± 1.4	26.0 ± 3.0
$t\bar{t}H$ truth p_{T}^{H} 60–120 GeV	17.0 ± 1.3	34.5 ± 2.9	29.5 ± 3.0	20.4 ± 2.5	42.0 ± 4.0
$t\bar{t}H$ truth p_{T}^{H} 120–200 GeV	10.0 ± 0.9	27.1 ± 2.7	17.0 ± 2.1	19.2 ± 2.4	34.0 ± 3.5
$t\bar{t}H$ truth p_{T}^{H} 200–300 GeV	3.1 ± 0.35	11.1 ± 1.3	4.6 ± 0.7	9.2 ± 1.2	14.9 ± 1.9
$t\bar{t}H$ truth p_{T}^{H} 300–450 GeV	0.94 ± 0.15	3.5 ± 0.5	0.94 ± 0.19	3.3 ± 0.5	5.4 ± 0.8
$t\bar{t}H$ truth $p_{\mathrm{T}}^{H} \geq 450$ GeV	0.33 ± 0.07	0.65 ± 0.12	0.116 ± 0.033	0.97 ± 0.15	1.33 ± 0.26
$t\bar{t}H$ $\lvert y\rvert > 2.5$	0.31 ± 0.05	0.25 ± 0.04	0.4 ± 0.05	0.127 ± 0.028	0.166 ± 0.018
$t\bar{t} + \geq 2b$	495 ± 35	860 ± 60	1080 ± 200	650 ± 100	2700 ± 200
$t\bar{t} + 1b$	1410 ± 130	1790 ± 230	3600 ± 700	1540± 180	1200 ± 400
$t\bar{t} + 1B$	310 ± 40	460 ± 40	540± 210	1560 ± 230	310 ± 110
$t\bar{t} + \geq 1c$	5600 ± 500	7700 ± 600	2210 ± 280	1590 ± 330	1070 ± 170
$t\bar{t}$ + light	9200 ± 1500	2800 ± 400	590 ± 130	410 ± 90	190 ± 70
$t\bar{t}Z$	43 ± 6	81 ± 12	35 ± 6	36 ± 5	92 ± 12
tW	300 ± 60	210 ± 50	220 ± 70	150 ± 50	300 ± 140
$t\bar{t}W$	37 ± 5	72 ± 7	12.1 ± 1.3	14.3 ± 3.3	29.8 ± 3.5
Z+jets	340 ± 130	260 ± 100	250 ± 90	93 ± 34	320 ± 120
$t\bar{t}t\bar{t}$	1.6 ± 0.7	10± 4	1± 0.4	4.8 ± 2	28 ± 12
tWH	0.98 ± 0.11	2.24 ± 0.22	2.69 ± 0.29	1.42 ± 0.14	4.0 ± 0.4
Other	5.6 ± 2.4	8.1 ± 3.1	4.4 ± 2.0	2.1 ± 0.7	12 ± 5
Fakes	110 ± 50	120 ± 60	40 ± 20	40 ± 20	80 ± 40
Total	18000 ± 2000	14400 ± 1100	8700 ± 900	6200 ± 500	6400 ± 700
Data	18557	14361	8624	5830	6448

the scale in α_S^{FSR} by a factor two up and down. To assess the uncertainties associated with the PS, hadronisation and underlying event, the nominal $t\bar{t}H$ sample is compared with the alternative POWHEG+HERWIG7 sample, while the uncertainty due to the NLO matching procedure is estimated with POWHEG+PYTHIA8 with a varied $p_{\mathrm{T}}^{\mathrm{hard}}$ parameter value.

All the modelling uncertainties in the $t\bar{t}$+jets background have independent nuisance parameters for the $t\bar{t}+1b$, $t\bar{t}+1B$, $t\bar{t}+\geq 2b$, $t\bar{t}+\geq 1c$ and $t\bar{t}$+light processes. These systematic variations are normalised to conserve the total nominal event count after the preselection for each process. Uncertainties due to missing higher order terms in the perturbative QCD calculations, in the amount of ISR and FSR as well as the uncertainties associated with the PS and hadronisation, and with the NLO matching procedure are estimated in the same way as for the $t\bar{t}H$ signal.

For $t\bar{t} + \geq 1b$, the choice of recoil scheme in the ISR PS has a sizeable effect in the normalisations and shapes of the distributions used in the analysis within the detector acceptance [22]. The uncertainty associated with the choice of the global recoil scheme is assessed by comparing the nominal sample with an alternative sample produced with the dipole recoil scheme. For $t\bar{t}$ + light and $t\bar{t} + \geq 1c$, the uncertainty in the choice of the h_{damp} parameter is estimated by using the alternative POWHEGBOX+PYTHIA8 sample with $h_{\mathrm{damp}} = 3\ m_{\mathrm{top}}$.

Uncertainties related to the H_{T} reweighting procedure described in Sect. 5.1 are assigned independently in the single-lepton and dilepton channels. The $t\bar{t}$ + light and $t\bar{t} + \geq 1c$ normalisation factors are varied within their uncertainties to estimate the corresponding systematic uncertainty. An additional uncertainty is estimated by comparing the distributions with and without the weights derived in the H_{T} reweighting procedure, in bins of jet multiplicity.

A ±5% normalisation uncertainty is considered for the cross-sections of the t- and s- single-top production modes [98,99]. The normalisation uncertainty of the tW background is 3.7% [100]. Modelling uncertainties in the tW production due to the choice of the PS and hadronisation model, the NLO matching and the h_{damp} parameter choice are evaluated in the same way as for the $t\bar{t}$ + light and $t\bar{t} + \geq 1c$ backgrounds. The uncertainty associated with the interference between tW and $t\bar{t}$ production at NLO is assessed by comparing the nominal POWHEGBOX+PYTHIA8 sample pro-

duced using the diagram removal scheme to an alternative sample produced with the same generator but using the diagram subtraction scheme.

The total uncertainty in the theoretical $t\bar{t}W$ cross-section computed at NNLO in the QCD and at NLO in the electroweak interactions is 7.4% [71]. The modelling uncertainty in the $t\bar{t}W$ background is evaluated by comparing the nominal SHERPA simulation with the sample produced using MADGRAPH5_AMC@NLO. For the $t\bar{t}Z$ production, the uncertainty in the predicted cross-section at NLO in QCD is 12% [18]. The modelling uncertainty in the $t\bar{t}Z$ background is evaluated by comparing the nominal MADGRAPH5_AMC@NLO+PYTHIA8 sample with the sample where PYTHIA8 is replaced by HERWIG7 to simulate the PS and hadronisation.

A normalisation uncertainty of $^{+70\%}_{-15\%}$ is assigned for the $t\bar{t}t\bar{t}$ background. The down variation corresponds to the theory uncertainty covering effects from varying the factorisation and renormalisation scales, the PDFs and α_S [101] while the up variation covers the measured $t\bar{t}t\bar{t}$ cross-section [102]. For tZq, the total normalisation uncertainty is 7.9% [37]. A normalisation uncertainty of 15.4% (9.2%) calculated using MADGRAPH5_AMC@NLO at NLO is applied to the $tHjb$ (tWH) background normalisation [103]. For tWZ, an uncertainty of ±50% is used [37].

The treatment of V+jets uncertainties follows the previous analysis [104]. An uncertainty of 40% is assumed for the W+jets cross-section, with an additional 30% normalisation uncertainty used for W boson production in association with heavy-flavour jets, taken as uncorrelated between events with two and events with more than two truth-level heavy-flavour jets. These uncertainties are based on variations of the factorisation and renormalisation scales and of the matching parameters in the SHERPA samples. An uncertainty of 35% is applied to the Z+jets normalisation to account for both the variations of the scales and matching parameters in the SHERPA samples and the uncertainty in the correction factor for the Z boson production accompanied by two b-jets extracted from data. A 50% normalisation uncertainty is used for the diboson background, which includes uncertainties in the inclusive cross-section and additional jet production [105–107].

A 50% normalisation uncertainty is assigned to the fake-lepton background estimate in the single-lepton and dilepton channels separately. An additional uncertainty obtained by using an alternative parameterisation of the fake rate (Sect. 5.2) is considered in the single-lepton channel.

8 Results

An excess of events over the expected background is found with an observed (expected) significance of 4.6 (5.4) standard deviations, in a combined profile-likelihood fit to data in all signal and control regions. The measured $t\bar{t}H$ signal strength for $m_H = 125.09$ GeV [108] is

$$\mu_{t\bar{t}H} = 0.81^{+0.22}_{-0.19} = 0.81 \pm 0.11(\text{stat.})\,^{+0.20}_{-0.16}(\text{syst.}). \quad (2)$$

The total statistical uncertainty is defined as the uncertainty in $\mu_{t\bar{t}H}$ when all nuisance parameters associated with the systematic uncertainties are fixed to their best-fit values. The total systematic uncertainty is then defined as the difference in quadrature between the total and statistical uncertainties. The systematic uncertainty in the signal strength $\mu_{t\bar{t}H}$ includes the theoretical uncertainties in the SM $t\bar{t}H$ cross-section described in Sect. 7. The measured $t\bar{t}H$ signal strength in the single-lepton channel is

$$\mu_{t\bar{t}H} = 0.72 \pm 0.12(\text{stat.})\,^{+0.21}_{-0.17}(\text{syst.}) \quad (3)$$

and in the dilepton channel is

$$\mu_{t\bar{t}H} = 1.03 \pm 0.26(\text{stat.})\,^{+0.28}_{-0.22}(\text{syst.}). \quad (4)$$

The combined $\mu_{t\bar{t}H}$ is converted into an inclusive cross-section using the SM theoretical cross-section of 507^{+35}_{-50} fb for $m_H = 125.09$ GeV and excluding its uncertainty [18]. The resulting cross-section is

$$\sigma_{t\bar{t}H} = 411\,^{+101}_{-92}\ \text{fb} = 411 \pm 54(\text{stat.})\,^{+85}_{-75}(\text{syst.})\ \text{fb}, \quad (5)$$

with a relative uncertainty of $^{+25\%}_{-22\%}$, consistent with the SM prediction. The sensitivity is driven by the single-lepton channel, where the systematic component of the uncertainty dominates. The sensitivity of the dilepton channel is limited by the size of the dataset.

The measured values of the $t\bar{t}$ + jets background normalisation factors, which are free parameters of the fit, are listed in Table 5. They are compatible between the single-lepton and the dilepton channels within two standard deviations. For $t\bar{t}+1b$, the measured value of the normalisation factor is slightly larger in the dilepton channel than in the single-lepton channel.

Compared with the previous analysis using the same dataset, the current analysis selects 64% (29%) new events in the single-lepton (dilepton) SR that did not enter the selection of the previous analysis. This is consistent with the increase of the overall acceptance by a factor of three. The statistical correlation between the two analyses is estimated using a booststrap method to be 19%, assuming that the systematic uncertainties are independent. This assumption is justified by the fact that the systematic model of the most important $t\bar{t}+\geq 1b$ background is different between the two analyses and the experimental uncertainties are updated. Based on

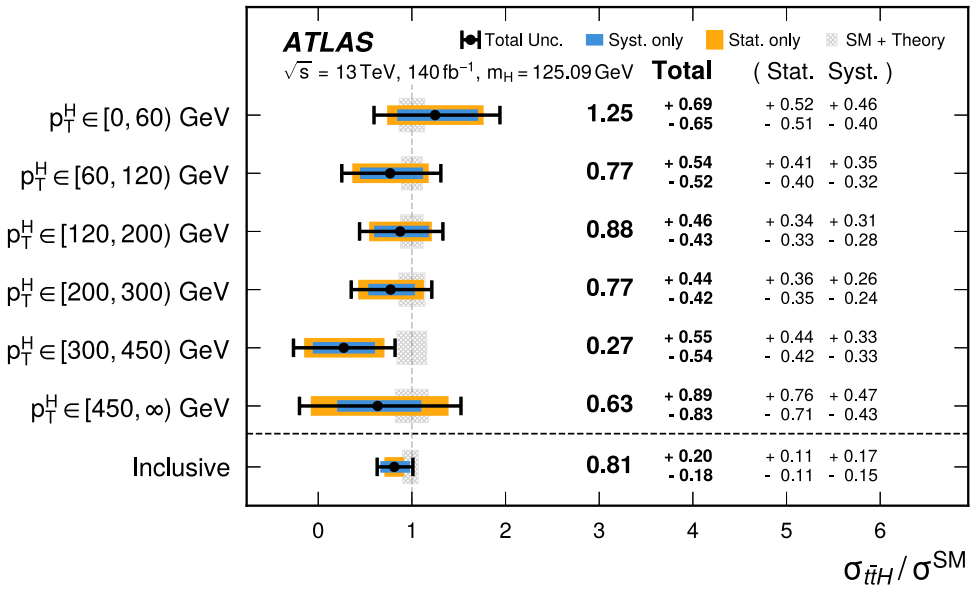

Fig. 3 The $t\bar{t}H$ cross-sections measured in bins of truth Higgs boson p_{T} for a Higgs boson rapidity $|y| \leq 2.5$, and measured inclusively in the full phase space, normalised to their SM predictions, as obtained from a combined profile-likelihood fit to data in all signal and control regions. The uncertainties are shown separately for the measurement and the prediction

Table 5 Best-fit values of the $t\bar{t}+$ jets normalisation factors obtained from the fit to data with a single inclusive $t\bar{t}H$ signal strength parameter. Independent normalisation factors for $t\bar{t}+1b$, $t\bar{t}+\geq 1c$ and $t\bar{t}+$ light components are used in the dilepton and single-lepton channels. Before the fit, the $t\bar{t}+$ light and $t\bar{t}+\geq 1c$ components are normalised to the $t\bar{t}$ cross-section computed at NNLO in QCD including the resummation of NNLL soft-gluon terms [72] while the $t\bar{t}+\geq 1b$ normalisation is taken from the $t\bar{t}b\bar{b}$ MC simulation

Normalisation factor	$t\bar{t}+$ light	$t\bar{t}+\geq 1c$	$t\bar{t}+1b$	$t\bar{t}+1B$	$t\bar{t}+\geq 2b$
Single-lepton	$0.78^{+0.08}_{-0.08}$	$1.51^{+0.19}_{-0.18}$	$1.06^{+0.10}_{-0.10}$	$1.15^{+0.15}_{-0.14}$	$0.94^{+0.08}_{-0.08}$
Dilepton	$0.88^{+0.11}_{-0.10}$	$1.36^{+0.10}_{-0.10}$	$1.24^{+0.09}_{-0.09}$		

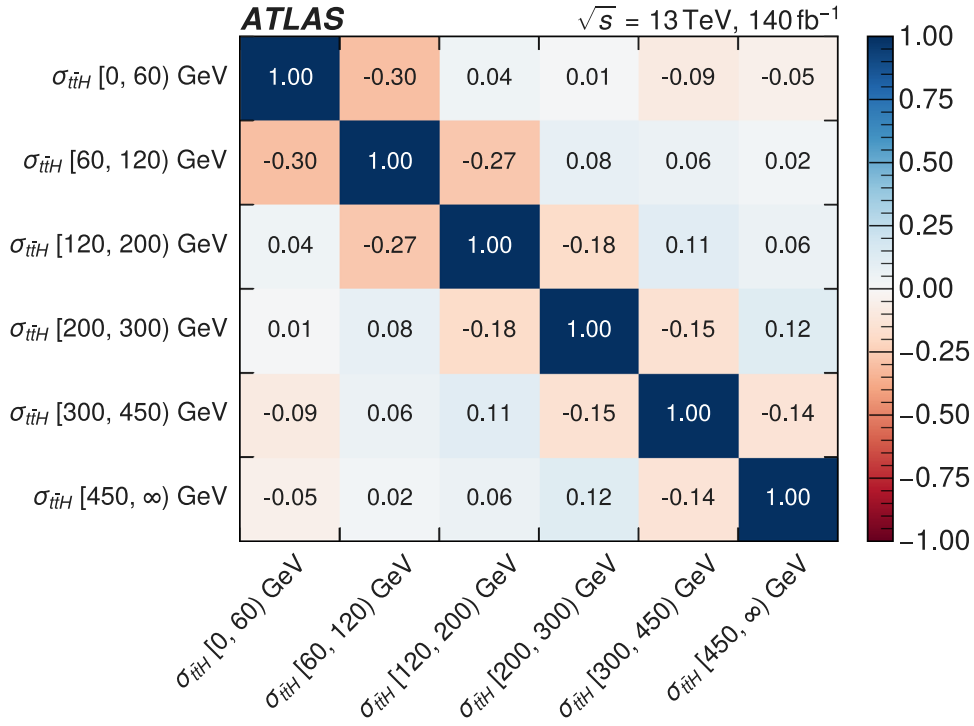

Fig. 4 Post-fit correlations between the measured values of the $t\bar{t}H$ cross-section, $\sigma_{t\bar{t}H}$, in bins of truth p_{T}^{H}

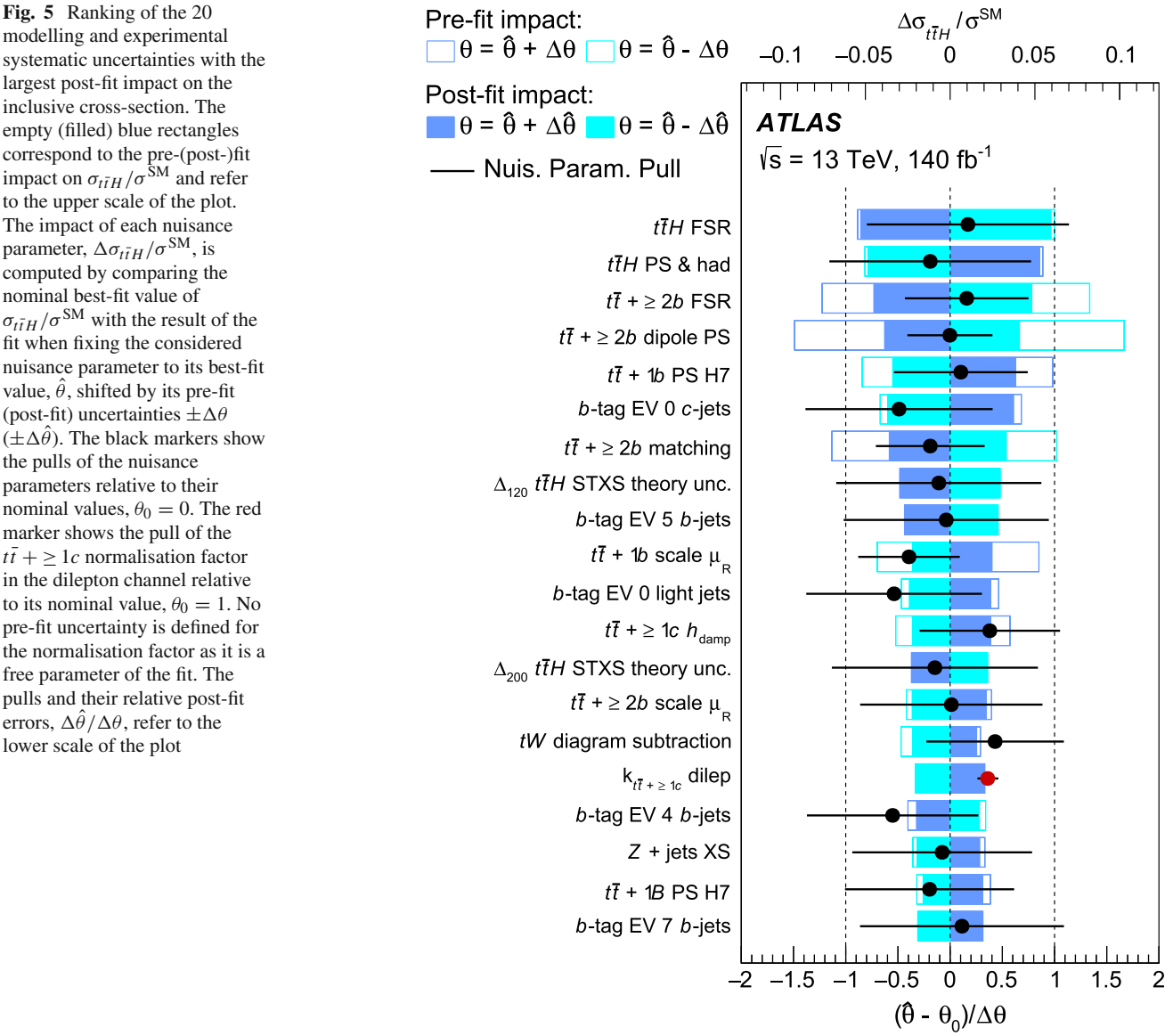

Fig. 5 Ranking of the 20 modelling and experimental systematic uncertainties with the largest post-fit impact on the inclusive cross-section. The empty (filled) blue rectangles correspond to the pre-(post-)fit impact on $\sigma_{t\bar{t}H}/\sigma^{\mathrm{SM}}$ and refer to the upper scale of the plot. The impact of each nuisance parameter, $\Delta\sigma_{t\bar{t}H}/\sigma^{\mathrm{SM}}$, is computed by comparing the nominal best-fit value of $\sigma_{t\bar{t}H}/\sigma^{\mathrm{SM}}$ with the result of the fit when fixing the considered nuisance parameter to its best-fit value, $\hat{\theta}$, shifted by its pre-fit (post-fit) uncertainties $\pm\Delta\theta$ ($\pm\Delta\hat{\theta}$). The black markers show the pulls of the nuisance parameters relative to their nominal values, $\theta_0 = 0$. The red marker shows the pull of the $t\bar{t} + \geq 1c$ normalisation factor in the dilepton channel relative to its nominal value, $\theta_0 = 1$. No pre-fit uncertainty is defined for the normalisation factor as it is a free parameter of the fit. The pulls and their relative post-fit errors, $\Delta\hat{\theta}/\Delta\theta$, refer to the lower scale of the plot

Fig. 6 Post-fit summary of the yields in the (**a**) dilepton and (**b**) single-lepton signal regions, with all regions aggregated into a single bin each. The uncertainty band includes all uncertainties and their correlations

Table 6 A list of the absolute and relative uncertainties in the measured $\sigma_{t\bar{t}H}$ grouped in categories. The contributions from different sources of uncertainty are evaluated after the fit. The quoted values are obtained by repeating the fit, while fixing the set of nuisance parameters of the sources corresponding to each category to their best-fit values, and subtracting in quadrature the resulting uncertainty from the total uncertainty of the nominal fit presented in the last row. The total uncertainty is different from the sum in quadrature of the different components due to correlations between nuisance parameters in the fit. The $t\bar{t}H$ and $t\bar{t}+\geq 1b$ radiation uncertainty categories include the renormalisation and factorisation scales, ISR and FSR uncertainties. The "$t\bar{t}H$ theory" category includes STXS-related theoretical uncertainties and uncertainty in the $H \to b\bar{b}$ branching fraction. The "Minor background modelling" category includes uncertainties in the fake-lepton background and in minor backgrounds as defined in the text. The total statistical uncertainty includes uncertainties in the normalisation factors

Uncertainty source	$\Delta\sigma_{t\bar{t}H}$ (fb)		$\Delta\sigma_{t\bar{t}H}/\sigma_{t\bar{t}H}$ (%)	
Process modelling				
$t\bar{t}H$ modelling				
$t\bar{t}H$ radiation	+35	−21	+9	−5
$t\bar{t}H$ parton shower	+32	−19	+8	−5
$t\bar{t}H$ matching	<0.1	−0.3	<0.1	−0.1
$t\bar{t}H$ theory	+25	−17	+6	−4
$t\bar{t}+\geq 1b$ modelling				
$t\bar{t}+\geq 1b$ radiation	±31		±8	
$t\bar{t}+\geq 1b$ parton shower	±29		±7	
$t\bar{t}+\geq 1b$ matching	±19		±5	
$t\bar{t}+\geq 1c$ modelling	±18		±4	
$t\bar{t}+$ light modelling	±5		±1	
tW modelling	±16		±4	
Minor background modelling	±19		±5	
Flavour tagging	±36		±9	
Jet modelling	±22		±5	
Monte-Carlo statistics	±17		±4	
Other instrumental	±10		±2	
Total systematic uncertainty	+85	−75	+21	−18
Normalisation factors	±21		±5	
Total statistical uncertainty	±54		±13	
Total uncertainty	+101	− 92	+25	− 22

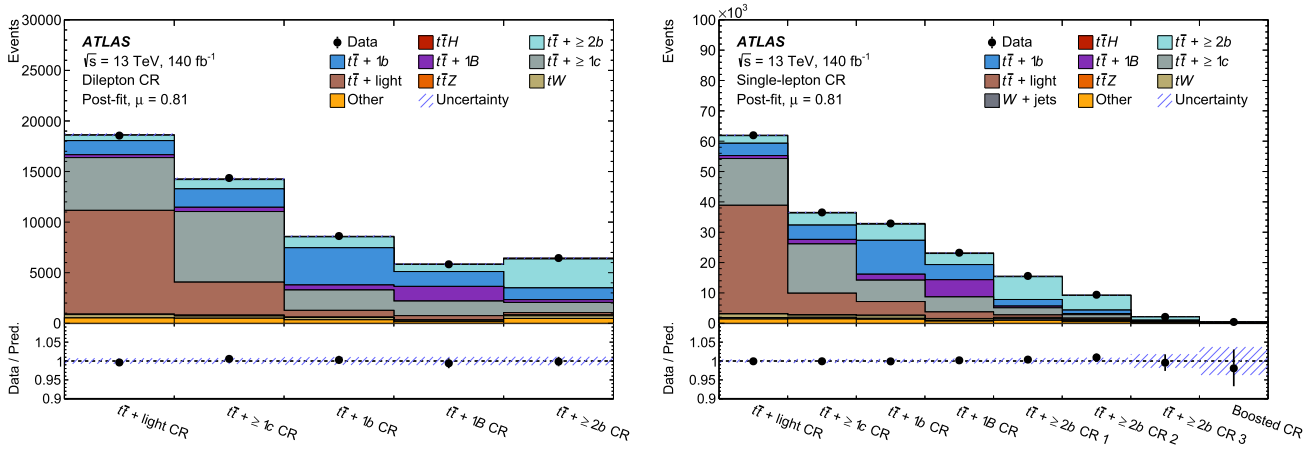

(a) (b)

Fig. 7 Post-fit summary of the yields in the (**a**) dilepton and (**b**) single-lepton control regions, with all regions aggregated into a single bin each. The uncertainty band includes all uncertainties and their correlations

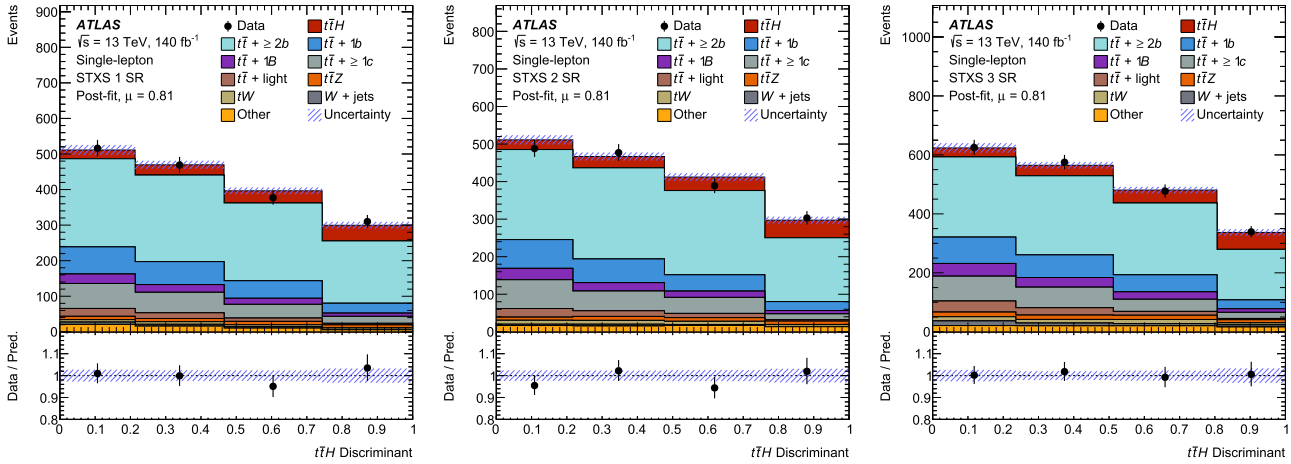

(a)

(b)

(c)

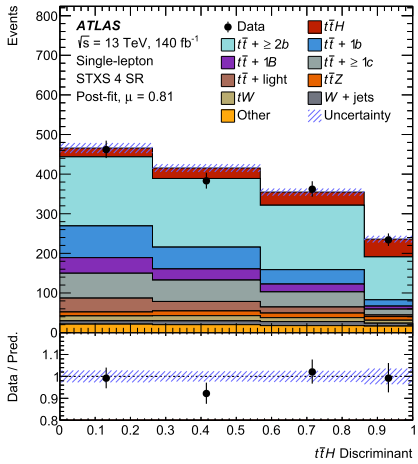

(d)

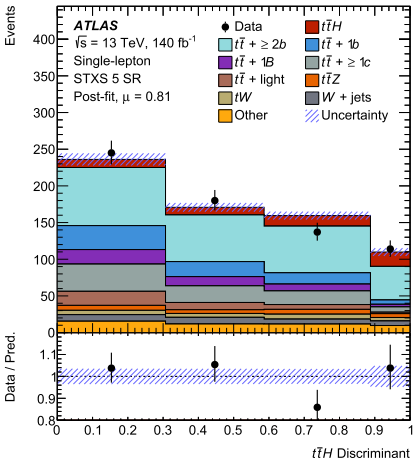

(e)

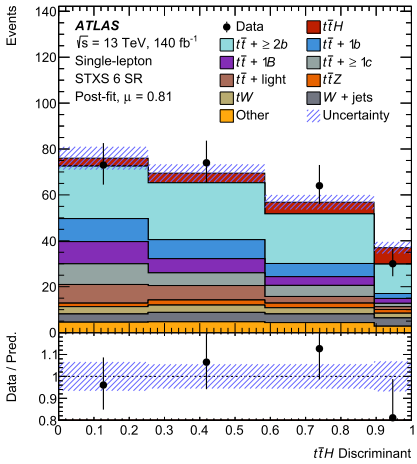

(f)

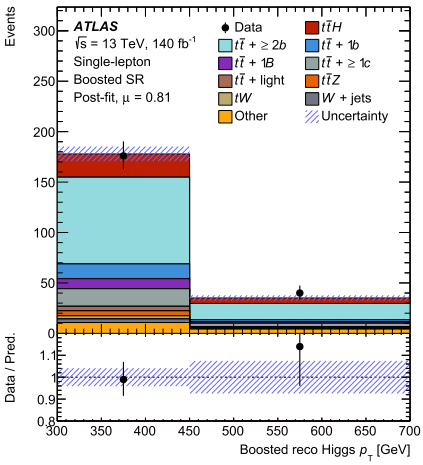

(g)

Fig. 8 Post-fit data/prediction comparisons of the signal region distributions entering the fit in the single-lepton channel. The discriminants are rescaled to lie between zero and one using a logistic function. The signal and background normalisation parameters and the nuisance parameters are set to their best-fit values. The uncertainty band includes all uncertainties and their correlations. For the reconstructed Higgs boson p_T in the boosted signal region, the first (last) bin includes the underflow (overflow) contributions

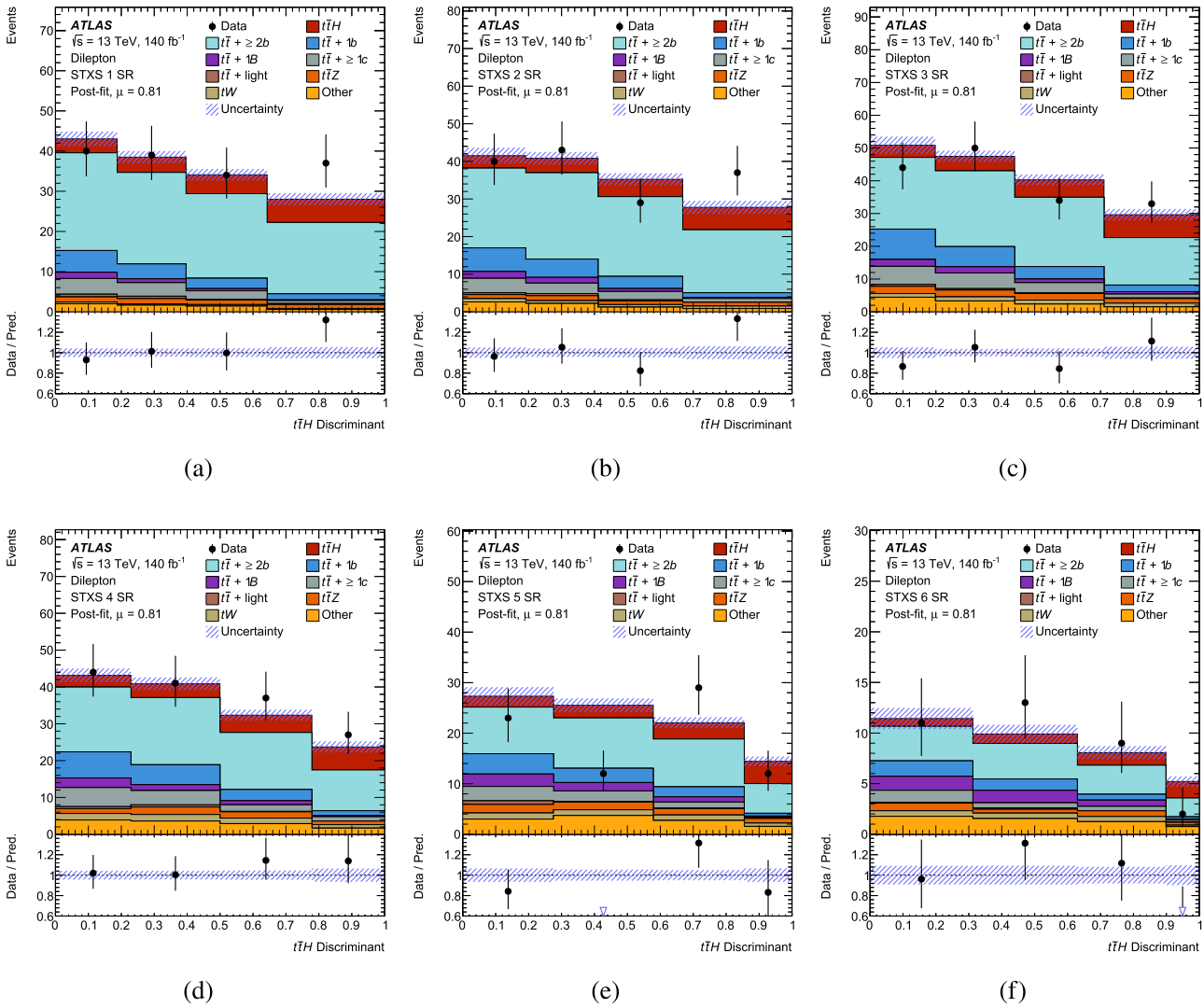

Fig. 9 Post-fit data/prediction comparisons of the signal region distributions entering the fit in the dilepton channel. The discriminants are rescaled to lie between zero and one using a logistic function. The signal and background normalisation parameters and the nuisance parameters are set to their best-fit values. The uncertainty band includes all uncertainties and their correlations

this, the probability that the current result is compatible with the result of Ref. [20] is estimated as 21%.

Figure 3 shows the measured values of $\sigma_{t\bar{t}H}/\sigma^{\mathrm{SM}}$ in bins of the Higgs boson p_{T}, obtained from a combined profile-likelihood fit to data with a free $t\bar{t}H$ signal strength parameter for each bin. The result of this measurement is compatible with the SM prediction with a p-value of 89%, taking into account theoretical uncertainties in the SM $t\bar{t}H$ cross-section. The measured value of the inclusive signal strength is also shown. The measurement of $\sigma_{t\bar{t}H}/\sigma^{\mathrm{SM}}$ in the [300, 450) GeV and [450, ∞) GeV p_{T}^{H} bins is limited by statistical uncertainties. In the remaining bins, there is a similar contribution from statistical and systematic uncertainties. Defining boosted regions improves sensitivity in the [450, ∞) GeV p_{T}^{H} bin by about 15%, compared with the scenario where only the resolved event selection is applied to these events. The correlations between the parameters of interest are shown in Fig. 4. They do not exceed 30% and are larger in the lower Higgs boson transverse momentum region.

The fitted values of $t\bar{t}$ + jets background normalisation factors are consistent with those obtained in the fit with a single $\mu_{t\bar{t}H}$ parameter shown in Table 5.

The absolute and relative systematic uncertainties in the measurement of $\sigma_{t\bar{t}H}$, grouped in categories, are shown in Table 6, and the effect of individual nuisance parameters ranked according to their impact on the inclusive $\sigma_{t\bar{t}H}/\sigma^{\mathrm{SM}}$ is shown in Fig. 5. The largest impact originates from the signal

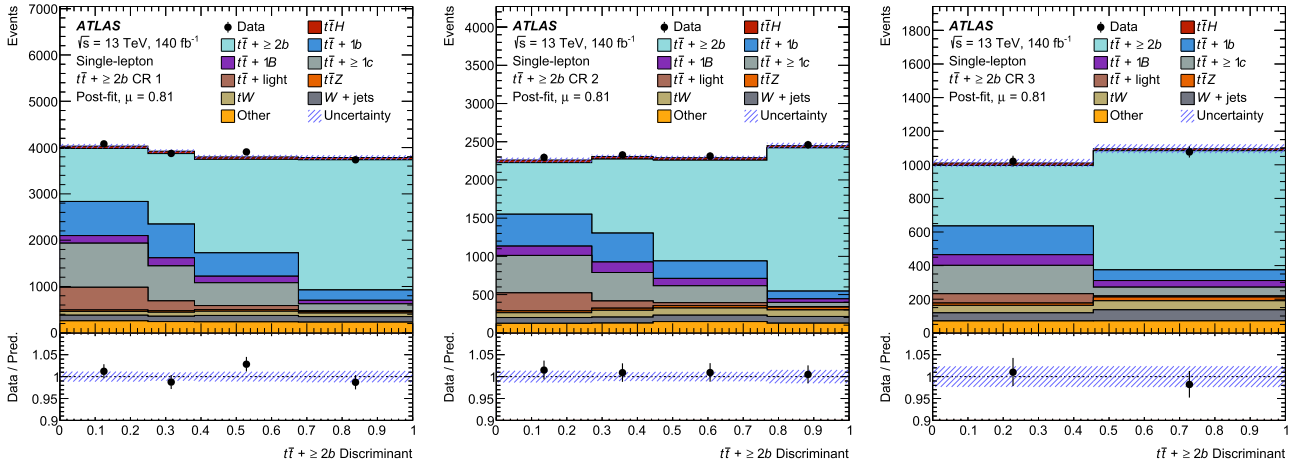

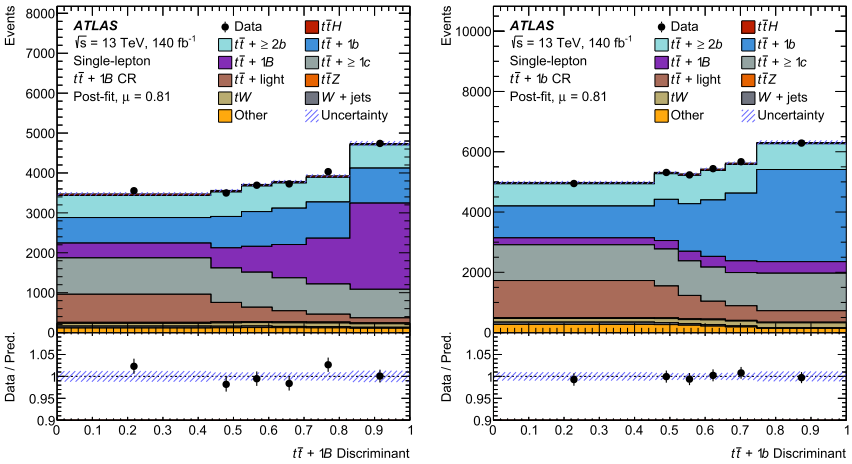

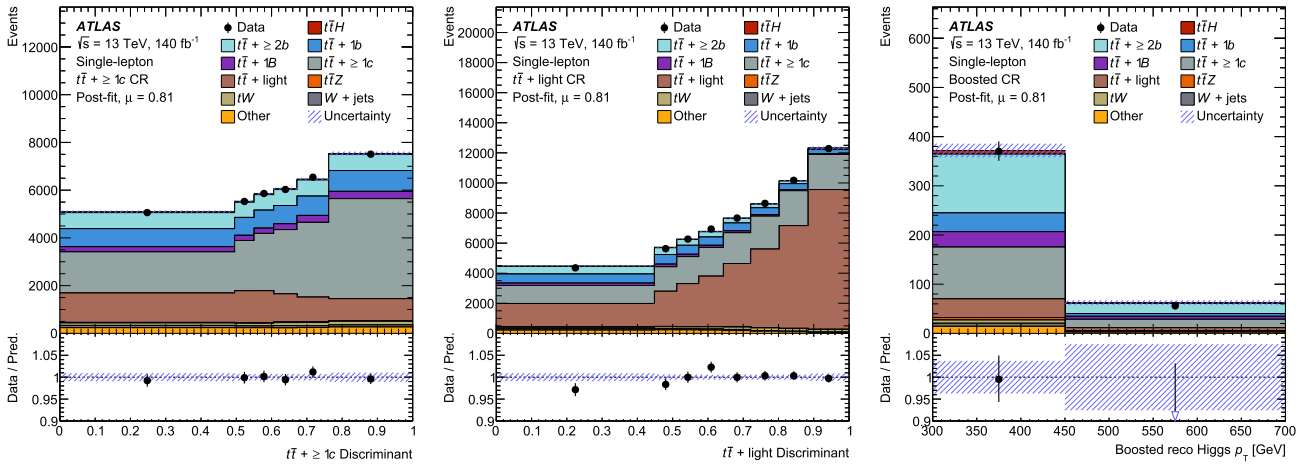

Fig. 10 Post-fit data/prediction comparisons of the control region distributions entering the fit in the single-lepton channel. The discriminants are rescaled to lie between zero and one using a logistic function. The signal and background normalisation parameters and the nuisance parameters are set to their best-fit values. The uncertainty band includes all uncertainties and their correlations. For the reconstructed Higgs boson p_T in the boosted control region, the first (last) bin includes the underflow (overflow) contributions

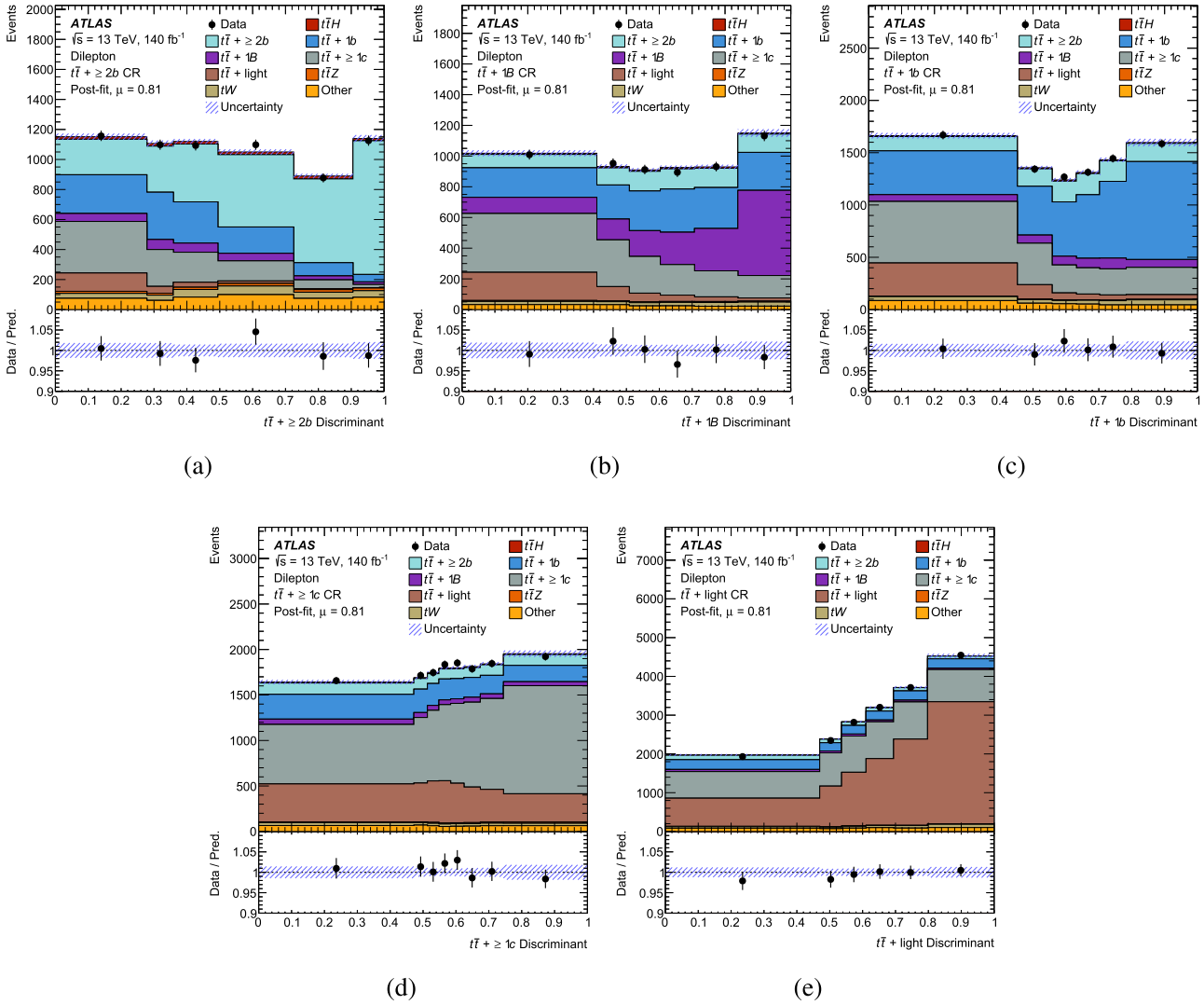

Fig. 11 Post-fit data/prediction comparisons of the control region distributions entering the fit in the dilepton channel. The discriminants are rescaled to lie between zero and one using a logistic function. The signal and background normalisation parameters and the nuisance parameters are set to their best-fit values. The uncertainty band includes all uncertainties and their correlations

modelling, followed by the $t\bar{t}+\geq 2b$ background modelling. In both cases, the dominant effects arise from the modelling of the FSR and the choice of the PS model. Among the experimental uncertainties, the largest effects come from the b-jet tagging and the jet energy scale.

Among the eight highest ranked nuisance parameters in Fig. 5, the largest constraints are observed for the $t\bar{t}+\geq 2b$ uncertainties arising from the dipole shower model and the choice of matching algorithm. These constraints predominantly originate from the single-lepton channel, and more specifically the SRs and the $t\bar{t}+\geq 2b$ CR where the $t\bar{t}+\geq 2b$ background contribution is large. The constraints are more pronounced when the $t\bar{t}+\geq 2b$ CR is split into three in the single-lepton channel to better control the $t\bar{t}+\geq 2b$ background modelling in bins of the reconstructed Higgs boson p_{T}.

The observed yields in all signal and control regions are compared to the post-fit predictions in Figs. 6 and 7. In each region, all bins are aggregated into a single bin. Figures 89 and 10 11 show a more detailed comparison in the single-lepton (dilepton) signal and control regions. The signal and background predictions in all post-fit distributions are obtained by setting the free parameters and the nuisance parameters to their best-fit values. In all post-fit plots, the uncertainty band includes all uncertainties and their correlations. The discriminant output in the plots is rescaled to be between zero and one using a logistic function.

The global goodness of fit [109,110] is 87% for the $\sigma_{t\bar{t}H}/\sigma^{\mathrm{SM}}$ measurement in p_{T}^{H} bins, highlighting that good post-fit modelling is achieved.

Figure 12 shows the event yield in data compared with the post-fit signal (S) and total background (B) predictions. It is ordered by the signal-to-background ratio of the bins from all the fitted regions. The predictions are shown for the best-fit signal strength and for the SM prediction. The observed data shows an excess over the background compatible with the best-fit signal strength $\mu_{t\bar{t}H}=0.81$ in the high $\log_{10}(S/B)$ region.

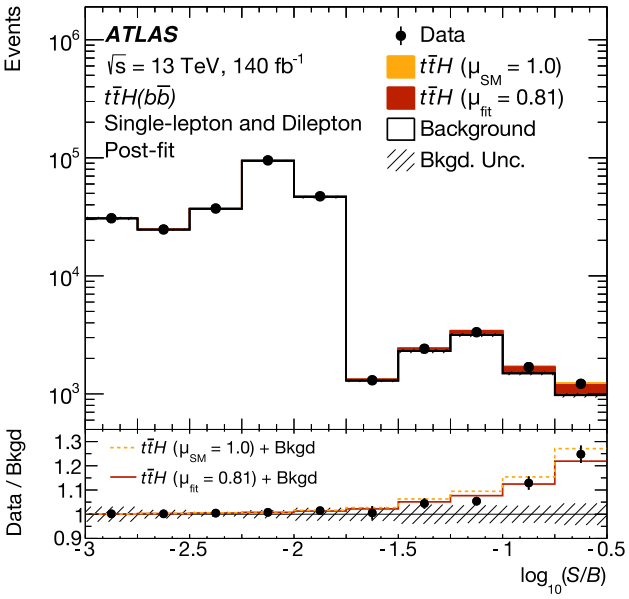

Fig. 12 Observed and expected event yields as a function of $\log_{10}(S/B)$, where S and B are the post-fit signal and total background yields, respectively. The bins in all fitted regions are ordered and grouped in bins of $\log_{10}(S/B)$. The signal is shown for the best-fit signal strength, $\mu=0.81$, or the SM prediction, $\mu=1.0$. The lower panel shows the ratio of the data to the post-fit background prediction, compared with the signal-plus-background prediction with the best-fit signal strength and the SM prediction. The shaded band represents the total uncertainty in the background prediction. The first (last) bin includes the underflow (overflow) contributions

9 Conclusion

The associated production of a Higgs boson with a pair of top quarks was measured in the $H\to b\bar{b}$ decay channel, using the full Run 2 proton–proton collision dataset collected at $\sqrt{s}=13$ TeV by the ATLAS detector at the LHC, corresponding to 140 fb^{-1}. The measurement uses final states containing one or two leptons. The measured inclusive cross-section assuming a Higgs boson mass of 125.09 GeV is $411\pm 54(\mathrm{stat.})\,^{+85}_{-75}(\mathrm{syst.})$ fb with a relative uncertainty of 24%, consistent with the SM prediction. The measurement is dominated by the systematic uncertainties arising from the $t\bar{t}H$ signal modelling followed by the $t\bar{t}+$ jets background modelling. The observed (expected) significance of the $t\bar{t}H$ signal relative to the SM background-only hypothesis is 4.6 (5.4) standard deviations. The cross-section measurement is also performed in six bins of p_{T}^{H} in the STXS framework with the highest bin probing Higgs bosons with p_{T}^{H} above 450 GeV. The uncertainty in the measurement for p_{T}^{H} above 300 GeV is dominated by the limited number of data events.

With respect to the previous iteration of the analysis, this measurement profits from looser selection requirements and improved b-jet identification that increase the $t\bar{t}H$ signal acceptance. Control regions enriched in each of the $t\bar{t}+$ jets components are defined based on a more powerful multi-class neural network. Together with data-driven modelling corrections for the $t\bar{t}+\geq 1c$ and $t\bar{t}+$ light components, and a dedicated MC simulation and systematic model for the $t\bar{t}+\geq 1b$ component, they provide improved signal sensitivity and better control over the background, such that the modelling uncertainty in $t\bar{t}+\geq 1b$ is no longer the dominant contribution to the total systematic uncertainty.

This analysis is the most precise $t\bar{t}H$ cross-section measurement in a single decay channel, inclusively and in each p_{T}^{H} bin.

Acknowledgements We thank CERN for the very successful operation of the LHC and its injectors, as well as the support staff at CERN and at our institutions worldwide without whom ATLAS could not be operated efficiently. The crucial computing support from all WLCG partners is acknowledged gratefully, in particular from CERN, the ATLAS Tier-1 facilities at TRIUMF/SFU (Canada), NDGF (Denmark, Norway, Sweden), CC-IN2P3 (France), KIT/GridKA (Germany), INFN-CNAF (Italy), NL-T1 (Netherlands), PIC (Spain), RAL (UK) and BNL (USA), the Tier-2 facilities worldwide and large non-WLCG resource providers. Major contributors of computing resources are listed in Ref. [111]. We gratefully acknowledge the support of ANPCyT, Argentina; YerPhI, Armenia; ARC, Australia; BMWFW and FWF, Austria; ANAS, Azerbaijan; CNPq and FAPESP, Brazil; NSERC, NRC and CFI, Canada; CERN; ANID, Chile; CAS, MOST and NSFC, China; Minciencias, Colombia; MEYS CR, Czech Republic; DNRF and DNSRC, Denmark; IN2P3-CNRS and CEA-DRF/IRFU, France; SRNSFG, Georgia; BMBF, HGF and MPG, Germany; GSRI, Greece; RGC and Hong Kong SAR, China; ISF and Benoziyo Center, Israel; INFN, Italy; MEXT and JSPS, Japan; CNRST, Morocco; NWO, Netherlands; RCN, Norway; MNiSW, Poland; FCT, Portugal; MNE/IFA, Romania; MSTDI, Serbia; MSSR, Slovakia; ARIS and MVZI, Slovenia; DSI/NRF, South Africa; MICIU/AEI, Spain; SRC and Wallenberg Foundation, Sweden; SERI, SNSF and Cantons of Bern and Geneva, Switzerland; NSTC, Taipei; TENMAK, Türkiye; STFC/UKRI, United Kingdom; DOE and NSF, United States of America. Individual groups and members have received support from BCKDF, CANARIE, CRC and DRAC, Canada; CERN-CZ, FORTE and PRIMUS, Czech Republic; COST, ERC, ERDF, Horizon 2020, ICSC-NextGenerationEU and Marie Skłodowska-Curie Actions, European Union; Investissements d'Avenir Labex, Investissements d'Avenir Idex and ANR, France; DFG and AvH Foundation, Germany; Herakleitos, Thales and Aristeia programmes co-financed by EU-ESF and the Greek NSRF, Greece; BSF-NSF and MINERVA, Israel; NCN and NAWA, Poland; La Caixa Banking Foundation, CERCA Programme Generalitat de Catalunya and PROMETEO and GenT Programmes Generalitat Valenciana, Spain; Göran Gustafssons Stiftelse, Sweden; The Royal Society and Leverhulme Trust, United Kingdom. In addition, individual members wish to acknowledge support from Armenia: Yerevan Physics Institute (FAPERJ); CERN: European Organization for Nuclear Research (CERN PJAS); Chile: Agencia Nacional de Investigación y Desarrollo (FONDECYT 1230812, FONDECYT 1230987, FONDECYT 1240864); China: Chinese Ministry of Science and Technology (MOST-2023YFA1605700), National Natural Science Foundation of China (NSFC - 12175119, NSFC 12275265, NSFC-12075060); Czech Republic: Czech Science Foundation (GACR - 24-11373S), Ministry of Education Youth and Sports (FORTE CZ.02.01.01/00/22_008/0004632), PRIMUS Research Programme (PRIMUS/21/SCI/017); EU: H2020 European Research Council (ERC - 101002463); European Union: European Research Council (ERC - 948254, ERC 101089007), Horizon 2020 Framework Programme (MUCCA - CHIST-ERA-19-XAI-00), European Union, Future Artificial Intelligence Research (FAIR-NextGenerationEU PE00000013), Italian Center for High Performance Computing, Big Data and Quantum Computing (ICSC, NextGenerationEU); France: Agence Nationale de la Recherche (ANR-20-CE31-0013, ANR-21-CE31-0013, ANR-21-CE31-0022, ANR-22-EDIR-0002), Investissements d'Avenir Labex (ANR-11-LABX-0012); Germany: Baden-Württemberg Stiftung (BW Stiftung-Postdoc Eliteprogramme), Deutsche Forschungsgemeinschaft (DFG - 469666862, DFG - CR 312/5-2); Italy: Istituto Nazionale di Fisica Nucleare (ICSC, NextGenerationEU), Ministero dell'Università e della Ricerca (PRIN - 20223N7F8K - PNRR M4.C2.1.1); Japan: Japan Society for the Promotion of Science (JSPS KAKENHI JP22H01227, JSPS KAKENHI JP22H04944, JSPS KAKENHI JP22KK0227, JSPS KAKENHI JP23KK0245); Netherlands: Netherlands Organisation for Scientific Research (NWO Veni 2020 - VI.Veni.202.179); Norway: Research Council of Norway (RCN-314472); Poland: Ministry of Science and Higher Education (IDUB AGH, POB8, D4 no 9722), Polish National Agency for Academic Exchange (PPN/PPO/2020/1/00002/U/00001), Polish National Science Centre (NCN 2021/42/E/ST2/00350, NCN OPUS nr 2022/47/B/ST2/03059, NCN UMO-2019/34/E/ST2/00393, NCN & H2020 MSCA 945339, UMO-2020/37/B/ST2/01043, UMO-2021/40/C/ST2/00187, UMO-2022/47/O/ST2/00148, UMO-2023/49/B/ST2/04085, UMO-2023/51/B/ST2/00920); Slovenia: Slovenian Research Agency (ARIS grant J1-3010); Spain: Generalitat Valenciana (Artemisa, FEDER, IDIFEDER/2018/048), Ministry of Science and Innovation (MCIN & NextGenEU PCI2022-135018-2, MICIN & FEDER PID2021-125273NB, RYC2019-028510-I, RYC2020-030254-I, RYC2021-031273-I, RYC2022-038164-I), PROMETEO and GenT Programmes Generalitat Valenciana (CIDEGENT/2019/027); Sweden: Carl Trygger Foundation (Carl Trygger Foundation CTS 22:2312), Swedish Research Council (Swedish Research Council 2023-04654, VR 2018-00482, VR 2022-03845, VR 2022-04683, VR 2023-03403, VR grant 2021-03651), Knut and Alice Wallenberg Foundation (KAW 2018.0157, KAW 2018.0458, KAW 2019.0447, KAW 2022.0358); Switzerland: Swiss National Science Foundation (SNSF - PCEFP2_194658); United Kingdom: Leverhulme Trust (Leverhulme Trust RPG-2020-004), Royal Society (NIF-R1-231091); United States of America: U.S. Department of Energy (ECA DE-AC02-76SF00515), Neubauer Family Foundation.

Data Availability Statement My manuscript has no associated data. [Authors' comment: All ATLAS scientific output is published in journals, and preliminary results are made available in Conference Notes. All are openly available, without restriction on use by external parties beyond copyright law and the standard conditions agreed by CERN. Data associated with journal publications are also made available: tables and data from plots (e.g. cross section values, likelihood profiles, selection efficiencies, cross section limits, ...) are stored in appropriate repositories such as HEPDATA (http://hepdata.cedar.ac.uk/). ATLAS also strives to make additional material related to the paper available that allows a reinterpretation of the data in the context of new theoretical models. For example, an extended encapsulation of the analysis is often provided for measurements in the framework of RIVET (http://rivet.hepforge.org/). This information is taken from the ATLAS Data Access Policy, which is a public document that can be downloaded from http://opendata.cern.ch/record/413 [opendata.cern.ch].]

Code Availability Statement My manuscript has no associated code/software. [Authors' comment: ATLAS collaboration software is open source, and all code necessary to recreate an analysis is publicly available. The Athena (http://gitlab.cern.ch/atlas/athena) software repository provides all code needed for calibration and uncertainty application, with configuration files that are also publicly available via Docker containers and cvmfs. The specific code and configurations written in support of this analysis are not public; however, these are internally preserved.]

Funded by SCOAP[3].

References

1. F. Englert, R. Brout, Broken symmetry and the mass of gauge vector mesons. Phys. Rev. Lett. **13**, 321 (1964). https://doi.org/10.1103/PhysRevLett.13.321
2. P.W. Higgs, Broken symmetries and the masses of gauge bosons. Phys. Rev. Lett. **13**, 508 (1964). https://doi.org/10.1103/PhysRevLett.13.508
3. G.S. Guralnik, C.R. Hagen, T.W.B. Kibble, Global conservation laws and massless particles. Phys. Rev. Lett. **13**, 585 (1964). https://doi.org/10.1103/PhysRevLett.13.585
4. ATLAS Collaboration, Observation of a new particle in the search for the Standard Model Higgs boson with the ATLAS detector at the LHC. Phys. Lett. B **716**, 1 (2012). https://doi.org/10.1016/j.physletb.2012.08.020. arXiv:1207.7214 [hep-ex]
5. C.M.S. Collaboration, Observation of a new boson at a mass of 125 GeV with the CMS experiment at the LHC. Phys. Lett. B **716**, 30 (2012). https://doi.org/10.1016/j.physletb.2012.08.021. arXiv:1207.7235 [hep-ex]
6. S.L. Glashow, Partial-symmetries of weak interactions. Nucl. Phys. **22**, 579 (1961). https://doi.org/10.1016/0029-5582(61)90469-2
7. S. Weinberg, A model of leptons. Phys. Rev. Lett. **19**, 1264 (1967). https://doi.org/10.1103/PhysRevLett.19.1264
8. A. Salam, Weak and electromagnetic interactions. Conf. Proc. **C680519**, 367 (1968)
9. C. Englert et al., Precision measurements of Higgs couplings: implications for new physics scales. J. Phys. G **41**, 113001 (2014). https://doi.org/10.1088/0954-3899/41/11/113001. arXiv:1403.7191 [hep-ph]
10. ATLAS Collaboration, A detailed map of Higgs boson interactions by the ATLAS experiment ten years after the discovery. Nature **607**, 52 (2022). https://doi.org/10.1038/s41586-022-04893-w. arXiv:2207.00092 [hep-ex]. [Erratum: Nature **612**, E24 (2022)]. https://doi.org/10.1038/s41586-022-05581-5
11. CMS Collaboration, A portrait of the Higgs boson by the CMS experiment ten years after the discovery. Nature **607**, 60 (2022). https://doi.org/10.1038/s41586-022-04892-x. arXiv:2207.00043 [hep-ex]. [Erratum: Nature **623**, E4 (2023)]. https://doi.org/10.1038/s41586-023-06164-8
12. J.N. Ng, P. Zakarauskas, QCD-parton calculation of conjoined production of Higgs bosons and heavy flavors in $p\bar{p}$ collision. Phys. Rev. D **29**, 876 (1984). https://doi.org/10.1103/PhysRevD.29.876
13. Z. Kunszt, Associated production of heavy Higgs boson with top quarks. Nucl. Phys. B **247**, 339 (1984). https://doi.org/10.1016/0550-3213(84)90553-4
14. S. Dawson, L.H. Orr, L. Reina, D. Wackeroth, Next-to-leading order QCD corrections to $pp \to t\bar{t}h$ at the CERN Large Hadron Collider. Phys. Rev. D **67**, 071503 (2003). https://doi.org/10.1103/PhysRevD.67.071503. arXiv:hep-ph/0211438
15. W. Beenakker et al., Higgs radiation off top quarks at the tevatron and the LHC. Phys. Rev. Lett. **87**, 201805 (2001). https://doi.org/10.1103/PhysRevLett.87.201805. arXiv:hep-ph/0107081
16. ATLAS Collaboration, Observation of Higgs boson production in association with a top quark pair at the LHC with the ATLAS detector. Phys. Lett. B **784**, 173 (2018). https://doi.org/10.1016/j.physletb.2018.07.035. arXiv:1806.00425 [hep-ex]
17. CMS Collaboration, Observation of $t\bar{t}H$ production. Phys. Rev. Lett. **120**, 231801 (2018). https://doi.org/10.1103/PhysRevLett.120.231801. arXiv:1804.02610 [hep-ex]
18. D. de Florian et al., Handbook of LHC Higgs Cross Sections: 4. Deciphering the Nature of the Higgs Sector (2017). https://doi.org/10.23731/CYRM-2017-002. arXiv:1610.07922 [hep-ph]
19. L. Evans, P. Bryant, LHC machine. JINST **3**, S08001 (2008). https://doi.org/10.1088/1748-0221/3/08/S08001
20. ATLAS Collaboration, Measurement of Higgs boson decay into b-quarks in associated production with a top-quark pair in pp collisions at $\sqrt{s} = 13$ TeV with the ATLAS detector. JHEP. **06**, 097 (2022). https://doi.org/10.1007/JHEP06(2022)097. arXiv:2111.06712 [hep-ex]
21. CMS Collaboration, Measurement of the $\mathrm{t\bar{t}}H$ and tH production rates in the $H \to \mathrm{b\bar{b}}$ decay channel using proton-proton collision data at $\sqrt{s} = 13$ TeV (2024). arXiv:2407.10896 [hep-ex]
22. ATLAS Collaboration, Studies of Monte Carlo predictions for the $t\bar{t}b\bar{b}$ process. ATL-PHYS-PUB-2022-006 (2022). https://cds.cern.ch/record/2802806
23. ATLAS Collaboration, Study of $ttbb$ and ttW background modelling for ttH analyses, ATL-PHYS-PUB-2022-026 (2022). https://cds.cern.ch/record/2810864
24. ATLAS Collaboration, The ATLAS experiment at the CERN Large Hadron Collider. JINST. **3**, S08003 (2008). https://doi.org/10.1088/1748-0221/3/08/S08003
25. G. Avoni et al., The new LUCID-2 detector for luminosity measurement and monitoring in ATLAS. JINST **13**, P07017 (2018). https://doi.org/10.1088/1748-0221/13/07/P07017
26. ATLAS Collaboration, Performance of the ATLAS trigger system in 2015. Eur. Phys. J. C **77**, 317 (2017). https://doi.org/10.1140/epjc/s10052-017-4852-3. arXiv:1611.09661 [hep-ex]
27. ATLAS Collaboration, Software and computing for Run 3 of the ATLAS experiment at the LHC (2024). arXiv:2404.06335 [hep-ex]
28. ATLAS Collaboration, ATLAS data quality operations and performance for 2015–2018 data-taking. JINST **15**, P04003 (2020). https://doi.org/10.1088/1748-0221/15/04/P04003. arXiv:1911.04632 [physics.ins-det]
29. T. Sjöstrand, S. Mrenna, P. Skands, A brief introduction to PYTHIA 8.1. Comput. Phys. Commun. **178**, 852 (2008). https://doi.org/10.1016/j.cpc.2008.01.036. arXiv:0710.3820 [hep-ph]
30. ATLAS Collaboration, The Pythia 8 A3 tune description of ATLAS minimum bias and inelastic measurements incorporating the Donnachie–Landshoff diffractive model, ATL-PHYS-PUB-2016-017 (2016). https://cds.cern.ch/record/2206965
31. ATLAS Collaboration, The ATLAS simulation infrastructure. Eur. Phys. J. C **70**, 823 (2010). https://doi.org/10.1140/epjc/s10052-010-1429-9. arXiv:1005.4568 [physics.ins-det]
32. S. Agostinelli et al., GEANT4—a simulation toolkit. Nucl. Instrum. Methods A **506**, 250 (2003). https://doi.org/10.1016/S0168-9002(03)01368-8
33. P. Nason, A new method for combining NLO QCD with shower Monte Carlo algorithms. JHEP **11**, 040 (2004). https://doi.org/10.1088/1126-6708/2004/11/040. arXiv:hep-ph/0409146
34. S. Frixione, G. Ridolfi, P. Nason, A positive-weight next-to-leading-order Monte Carlo for heavy flavour hadroproduction. JHEP **09**, 126 (2007). https://doi.org/10.1088/1126-6708/2007/09/126. arXiv:0707.3088 [hep-ph]
35. S. Frixione, P. Nason, C. Oleari, Matching NLO QCD computations with parton shower simulations: the POWHEG method. JHEP **11**, 070 (2007). https://doi.org/10.1088/1126-6708/2007/11/070. arXiv:0709.2092 [hep-ph]
36. S. Alioli, P. Nason, C. Oleari, E. Re, A general framework for implementing NLO calculations in shower Monte Carlo programs: the POWHEG BOX. JHEP **06**, 043 (2010). https://doi.org/10.1007/JHEP06(2010)043. arXiv:1002.2581 [hep-ph]
37. J. Alwall et al., The automated computation of tree-level and next-to-leading order differential cross sections, and their matching to parton shower simulations. JHEP **07**, 079 (2014). https://doi.org/10.1007/JHEP07(2014)079. arXiv:1405.0301 [hep-ph]

38. T. Sjöstrand et al., An introduction to PYTHIA 8.2. Comput. Phys. Commun. **191**, 159 (2015). https://doi.org/10.1016/j.cpc.2015.01.024. arXiv:1410.3012 [hep-ph]
39. ATLAS Collaboration, ATLAS Pythia 8 tunes to 7 TeV data, ATL-PHYS-PUB-2014-021 (2014). https://cds.cern.ch/record/1966419
40. NNPDF Collaboration, R.D. Ball et al., Parton distributions for the LHC run II. JHEP **04**, 040 (2015). https://doi.org/10.1007/JHEP04(2015)040. arXiv:1410.8849 [hep-ph]
41. M. Bähr et al., Herwig++ physics and manual. Eur. Phys. J. C **58**, 639 (2008). https://doi.org/10.1140/epjc/s10052-008-0798-9. arXiv:0803.0883 [hep-ph]
42. J. Bellm et al., Herwig 7.0/Herwig++ 3.0 release note. Eur. Phys. J. C **76**, 196 (2016). https://doi.org/10.1140/epjc/s10052-016-4018-8. arXiv:1512.01178 [hep-ph]
43. L.A. Harland-Lang, A.D. Martin, P. Motylinski, R.S. Thorne, Parton distributions in the LHC era: MMHT 2014 PDFs. Eur. Phys. J. C **75**, 204 (2015). https://doi.org/10.1140/epjc/s10052-015-3397-6. arXiv:1412.3989 [hep-ph]
44. D.J. Lange, The EvtGen particle decay simulation package. Nucl. Instrum. Methods A **462**, 152 (2001). https://doi.org/10.1016/S0168-9002(01)00089-4
45. H.B. Hartanto, B. Jäger, L. Reina, D. Wackeroth, Higgs boson production in association with top quarks in the POWHEG BOX. Phys. Rev. D **91**, 094003 (2015). https://doi.org/10.1103/PhysRevD.91.094003. arXiv:1501.04498 [hep-ph]
46. S. Catani et al., Higgs boson production in association with a top-antitop quark pair in next-to-next-to-leading order QCD. Phys. Rev. Lett. **130**, 111902 (2023). https://doi.org/10.1103/physrevlett.130.111902. arXiv:2210.07846 [hep-ph]
47. ATLAS Collaboration, Studies on the improvement of the matching uncertainty definition in top-quark processes simulated with POWHEG+PYTHIA8, ATL-PHYS-PUB-2023-029 (2013). https://cds.cern.ch/record/2872787
48. S. Höche, S. Mrenna, S. Payne, C.T. Preuss, P. Skands, A study of QCD radiation in VBF Higgs production with Vincia and Pythia. SciPost Phys. **12**, 010 (2022). https://doi.org/10.21468/SciPostPhys.12.1.010. arXiv:2106.10987 [hep-ph]
49. ATLAS Collaboration, Search for the Standard Model Higgs boson produced in association with top quarks and decaying into $b\bar{b}$ in pp collisions at $\sqrt{s} = 8$ TeV with the ATLAS detector. Eur. Phys. J. C **75**, 349 (2015). https://doi.org/10.1140/epjc/s10052-015-3543-1. arXiv:1503.05066 [hep-ex]
50. M. Cacciari, G.P. Salam, G. Soyez, The anti-k_t jet clustering algorithm. JHEP **04**, 063 (2008). https://doi.org/10.1088/1126-6708/2008/04/063. arXiv:0802.1189 [hep-ph]
51. ATLAS Collaboration, Studies on top-quark Monte Carlo modelling for Top2016, ATL-PHYS-PUB-2016-020 (2016). https://cds.cern.ch/record/2216168
52. T. Ježo, J.M. Lindert, N. Moretti, S. Pozzorini, New NLOPS predictions for $t\bar{t} + b$-jet production at the LHC. Eur. Phys. J. C **78**, 502 (2018). https://doi.org/10.1140/epjc/s10052-018-5956-0. arXiv:1802.00426 [hep-ph]
53. F. Buccioni et al., OpenLoops 2. Eur. Phys. J. C **79**, 866 (2019). https://doi.org/10.1140/epjc/s10052-019-7306-2. arXiv:1907.13071 [hep-ph]
54. F. Cascioli, P. Maierhöfer, S. Pozzorini, Scattering amplitudes with open loops. Phys. Rev. Lett. **108**, 111601 (2012). https://doi.org/10.1103/PhysRevLett.108.111601. arXiv:1111.5206 [hep-ph]
55. A. Denner, S. Dittmaier, L. Hofer, COLLIER: a fortran-based complex one-loop library in extended regularizations. Comput. Phys. Commun. **212**, 220 (2017). https://doi.org/10.1016/j.cpc.2016.10.013. arXiv:1604.06792 [hep-ph]
56. T. Ježo, Powheg-Box-Res $ttbb$ source code (2019). https://gitlab.cern.ch/tjezo/powheg-box-res_ttbb/
57. E. Bothmann et al., Event generation with Sherpa 2.2. SciPost Phys. **7**, 034 (2019). https://doi.org/10.21468/SciPostPhys.7.3.034. arXiv:1905.09127 [hep-ph]
58. T. Gleisberg, S. Höche, Comix, a new matrix element generator. JHEP **12**, 039 (2008). https://doi.org/10.1088/1126-6708/2008/12/039. arXiv:0808.3674 [hep-ph]
59. S. Schumann, F. Krauss, A parton shower algorithm based on Catani–Seymour dipole factorisation. JHEP **03**, 038 (2008). https://doi.org/10.1088/1126-6708/2008/03/038. arXiv:0709.1027 [hep-ph]
60. S. Höche, F. Krauss, M. Schönherr, F. Siegert, A critical appraisal of NLO+PS matching methods. JHEP **09**, 049 (2012). https://doi.org/10.1007/JHEP09(2012)049. arXiv:1111.1220 [hep-ph]
61. S. Höche, F. Krauss, M. Schönherr, F. Siegert, QCD matrix elements + parton showers. The NLO case. JHEP **04**, 027 (2013). https://doi.org/10.1007/JHEP04(2013)027. arXiv:1207.5030 [hep-ph]
62. S. Catani, F. Krauss, B.R. Webber, R. Kuhn, QCD matrix elements + parton showers. JHEP **11**, 063 (2001). https://doi.org/10.1088/1126-6708/2001/11/063. arXiv:hep-ph/0109231
63. S. Höche, F. Krauss, S. Schumann, F. Siegert, QCD matrix elements and truncated showers. JHEP **05**, 053 (2009). https://doi.org/10.1088/1126-6708/2009/05/053. arXiv:0903.1219 [hep-ph]
64. E. Re, Single-top Wt-channel production matched with parton showers using the POWHEG method. Eur. Phys. J. C **71**, 1547 (2011). https://doi.org/10.1140/epjc/s10052-011-1547-z. arXiv:1009.2450 [hep-ph]
65. S. Alioli, P. Nason, C. Oleari, E. Re, NLO single-top production matched with shower in POWHEG: s- and t-channel contributions, JHEP **09**, 111 (2009). https://doi.org/10.1088/1126-6708/2009/09/111. arXiv:0907.4076 [hep-ph], Erratum: **02**, 011 (2010). https://doi.org/10.1007/JHEP02(2010)011JHEP
66. S. Frixione, E. Laenen, P. Motylinski, C. White, B.R. Webber, Single-top hadroproduction in association with a W boson. JHEP **07**, 029 (2008). https://doi.org/10.1088/1126-6708/2008/07/029. arXiv:0805.3067 [hep-ph]
67. ATLAS Collaboration, Studies of $t\bar{t}/tW$ interference effects in $b\bar{b}\ell^+\ell^-\nu\bar{\nu}'$ final states with POWHEG and MADGRAPH5_AMC@NLO setups, ATL-PHYS-PUB-2021-042 (2021). https://cds.cern.ch/record/2792254
68. T. Gleisberg et al., Event generation with SHERPA 1.1. JHEP **02**, 007 (2009). https://doi.org/10.1088/1126-6708/2009/02/007. arXiv:0811.4622 [hep-ph]
69. NNPDF Collaboration, R.D. Ball et al., Parton distributions from high-precision collider data. Eur. Phys. J. C 77, 663 (2017). https://doi.org/10.1140/epjc/s10052-017-5199-5. arXiv:1706.00428 [hep-ph]
70. R. Frederix, S. Frixione, Merging meets matching in MC@NLO. JHEP **12**, 061 (2012). https://doi.org/10.1007/JHEP12(2012)061. arXiv:1209.6215 [hep-ph]
71. L. Buonocore et al., Precise predictions for the associated production of a W boson with a top-antitop quark pair at the LHC. Phys. Rev. Lett. 131 (2023). https://doi.org/10.1103/physrevlett.131.231901. arXiv:2306.16311 [hep-ph]
72. M. Czakon, A. Mitov, Top++: a program for the calculation of the top-pair cross-section at hadron colliders. Comput. Phys. Commun. **185**, 2930 (2014). https://doi.org/10.1016/j.cpc.2014.06.021. arXiv:1112.5675 [hep-ph]
73. ATLAS Collaboration, Performance of the ATLAS muon triggers in Run 2. JINST **15**, P09015 (2020). https://doi.org/10.1088/1748-0221/15/09/p09015. arXiv:2004.13447 [physics.ins-det]
74. ATLAS Collaboration, Performance of electron and photon triggers in ATLAS during LHC Run 2. Eur. Phys. J. C **80**, 47 (2020). https://doi.org/10.1140/epjc/s10052-019-7500-2. arXiv:1909.00761 [hep-ex]

75. ATLAS Collaboration, Vertex Reconstruction Performance of the ATLAS Detector at $\sqrt{s} = 13$ TeV, ATL-PHYS-PUB-2015-026 (2015). https://cds.cern.ch/record/2037717
76. ATLAS Collaboration, Electron and photon performance measurements with the ATLAS detector using the 2015–2017 LHC proton–proton collision data. JINST **14**, P12006 (2019). https://doi.org/10.1088/1748-0221/14/12/P12006. arXiv:1908.00005 [hep-ex]
77. ATLAS Collaboration, Muon reconstruction and identification efficiency in ATLAS using the full Run 2 pp collision data set at $\sqrt{s} = 13$ TeV. Eur. Phys. J. C **81**, 578 (2021). https://doi.org/10.1140/epjc/s10052-021-09233-2. arXiv:2012.00578 [hep-ex]
78. ATLAS Collaboration, Jet reconstruction and performance using particle flow with the ATLAS detector. Eur. Phys. J. C **77**, 466 (2017). https://doi.org/10.1140/epjc/s10052-017-5031-2. arXiv:1703.10485 [hep-ex]
79. M. Cacciari, G.P. Salam, G. Soyez, FastJet user manual. Eur. Phys. J. C **72**, 1896 (2012). https://doi.org/10.1140/epjc/s10052-012-1896-2. arXiv:1111.6097 [hep-ph]
80. ATLAS Collaboration, Performance of pile-up mitigation techniques for jets in pp collisions at $\sqrt{s} = 8$ TeV using the ATLAS detector. Eur. Phys. J. C **76**, 581 (2016). https://doi.org/10.1140/epjc/s10052-016-4395-z. arXiv:1510.03823 [hep-ex]
81. ATLAS Collaboration, Jet energy scale and resolution measured in proton–proton collisions at $\sqrt{s} = 13$ TeV with the ATLAS detector. Eur. Phys. J. C **81**, 689 (2021). https://doi.org/10.1140/epjc/s10052-021-09402-3. arXiv:2007.02645 [hep-ex]
82. ATLAS Collaboration, ATLAS flavour-tagging algorithms for the LHC Run 2 pp collision dataset. Eur. Phys. J. C **83**, 681 (2023). https://doi.org/10.1140/epjc/s10052-023-11699-1. arXiv:2211.16345 [physics.data-an]
83. ATLAS Collaboration, Evidence for the $H \to b\bar{b}$ decay with the ATLAS detector. JHEP **12**, 024 (2017). https://doi.org/10.1007/JHEP12(2017)024. arXiv:1708.03299 [hep-ex]
84. ATLAS Collaboration, Identification of hadronic tau lepton decays using neural networks in the ATLAS experiment, ATL-PHYS-PUB-2019-033 (2019). https://cds.cern.ch/record/2688062
85. ATLAS Collaboration, The performance of missing transverse momentum reconstruction and its significance with the ATLAS detector using 140 fb^{-1} of $\sqrt{s} = 13$ TeV pp collisions (2024). arXiv:2402.05858 [hep-ex]
86. B. Nachman, P. Nef, A. Schwartzman, M. Swiatlowski, C. Wanotayaroj, Jets from jets: re-clustering as a tool for large radius jet reconstruction and grooming at the LHC. JHEP **02**, 075 (2015). https://doi.org/10.1007/JHEP02(2015)075. arXiv:1407.2922 [hep-ph]
87. ATLAS Collaboration, Measurements of top-quark pair differential and double-differential cross-sections in the ℓ+jets channel with pp collisions at $\sqrt{s} = 13$ TeV using the ATLAS detector. Eur. Phys. J. C **79**, 1028 (2019). https://doi.org/10.1140/epjc/s10052-019-7525-6. arXiv:1908.07305 [hep-ex]. [Erratum: Eur. Phys. J. C **80**, 1092 (2020)]. https://doi.org/10.1140/epjc/s10052-020-08541-3
88. ATLAS Collaboration, Tools for estimating fake/non-prompt lepton backgrounds with the ATLAS detector at the LHC. JINST **18**, T11004 (2023). https://doi.org/10.1088/1748-0221/18/11/T11004. arXiv:2211.16178 [hep-ex]
89. A. Vaswani et al., Attention Is All You Need (2023). arXiv:1706.03762 [cs.CL]
90. K. Cranmer, G. Lewis, L. Moneta, A. Shibata, W. Verkerke, HistFactory: a tool for creating statistical models for use with RooFit and RooStats, CERN-OPEN-2012-016 (2012). https://cds.cern.ch/record/1456844
91. W. Verkerke, D. Kirkby, The RooFit toolkit for data modeling (2003). arXiv:physics/0306116 [physics.data-an]
92. G. Cowan, K. Cranmer, E. Gross, O. Vitells, Asymptotic formulae for likelihood-based tests of new physics. Eur. Phys. J. C **71**, 1554 (2011). https://doi.org/10.1140/epjc/s10052-013-2501-z. arXiv:1007.1727 [physics.data-an]. [Erratum: Eur. Phys. J. C **73**, 2501 (2013)]. https://doi.org/10.1140/epjc/s10052-011-1554-0
93. ATLAS Collaboration, Luminosity determination in pp collisions at $\sqrt{s} = 13$ TeV using the ATLAS detector at the LHC. Eur. Phys. J. C **83**, 982 (2023). https://doi.org/10.1140/epjc/s10052-023-11747-w. arXiv:2212.09379 [hep-ex]
94. ATLAS Collaboration, ATLAS b-jet identification performance and efficiency measurement with $t\bar{t}$ events in pp collisions at $\sqrt{s} = 13$ TeV. Eur. Phys. J. C **79**, 970 (2019). https://doi.org/10.1140/epjc/s10052-019-7450-8. arXiv:1907.05120 [hep-ex]
95. ATLAS Collaboration, Measurement of the c-jet mistagging efficiency in $t\bar{t}$ events using pp collision data at $\sqrt{s} = 13$ TeV collected with the ATLAS detector. Eur. Phys. J. C **82**, 95 (2022). https://doi.org/10.1140/epjc/s10052-021-09843-w. arXiv:2109.10627 [hep-ex]
96. ATLAS Collaboration, Calibration of the light-flavour jet mistagging efficiency of the b-tagging algorithms with Z+jets events using 139 fb^{-1} of ATLAS proton–proton collision data at $\sqrt{s} = 13$ TeV. Eur. Phys. J. C **83**, 728 (2023). https://doi.org/10.1140/epjc/s10052-023-11736-z. arXiv:2301.06319 [hep-ex]
97. ATLAS Collaboration, Evaluation of QCD uncertainties for Higgs boson production through gluon fusion and in association with two top quarks for simplified template cross-section measurements, ATL-PHYS-PUB-2023-031 (2023). https://cds.cern.ch/record/2878797
98. N. Kidonakis, Next-to-next-to-leading-order collinear and soft gluon corrections for t-channel single top quark production. Phys. Rev. D **83**, 091503 (2011). https://doi.org/10.1103/PhysRevD.83.091503. arXiv:1103.2792 [hep-ph]
99. N. Kidonakis, Next-to-next-to-leading logarithm resummation for s-channel single top quark production. Phys. Rev. D **81**, 054028 (2010). https://doi.org/10.1103/PhysRevD.81.054028. arXiv:1001.5034 [hep-ph]
100. N. Kidonakis, N. Yamanaka, Higher-order corrections for tW production at high-energy hadron colliders. JHEP **05**, 278 (2021). https://doi.org/10.1007/JHEP05(2021)278. arXiv:2102.11300 [hep-ph]
101. M. van Beekveld, A. Kulesza, L.M. Valero, Threshold resummation for the production of four top quarks at the LHC (2022). arXiv:2212.03259 [hep-ph]
102. ATLAS Collaboration, Observation of four-top-quark production in the multilepton final state with the ATLAS detector. Eur. Phys. J. C **83**, 496 (2023). https://doi.org/10.1140/epjc/s10052-023-11573-0. arXiv:2303.15061 [hep-ex]

103. ATLAS Collaboration, Probing the CP nature of the top-Higgs Yukawa coupling in $t\bar{t}H$ and tH events with $H \to b\bar{b}$ decays using the ATLAS detector at the LHC. Phys. Lett. B **849**, 138469 (2023). https://doi.org/10.1016/j.physletb.2024.138469. arXiv:2303.05974 [hep-ex]
104. ATLAS Collaboration, Probing the CP nature of the top-Higgs Yukawa coupling in $t\bar{t}H$ and tH events with $H \to b\bar{b}$ decays using the ATLAS detector at the LHC. Phys. Lett. B **849**, 138469 (2024). https://doi.org/10.1016/j.physletb.2024.138469. arXiv:2303.05974 [hep-ex]
105. M. Grazzini, S. Kallweit, D. Rathlev, M. Wiesemann, $W^{\pm}Z$ production at hadron colliders in NNLO QCD. Phys. Lett. B **761**, 179 (2016). https://doi.org/10.1016/j.physletb.2016.08.017. arXiv:1604.08576 [hep-ph]
106. ATLAS Collaboration, Multi-boson simulation for 13 TeV ATLAS analyses, ATL-PHYS-PUB-2016-002 (2016). https://cds.cern.ch/record/2119986
107. ATLAS Collaboration, Measurement of $W^{\pm}Z$ production cross sections and gauge boson polarisation in pp collisions at $\sqrt{s} =$ 13 TeV with the ATLAS detector. Eur. Phys. J. C **79**, 535 (2019). https://doi.org/10.1140/epjc/s10052-019-7027-6. arXiv:1902.05759 [hep-ex]
108. ATLAS and CMS Collaborations, Combined measurement of the Higgs boson mass in pp collisions at $\sqrt{s} = 7$ and 8 TeV with the ATLAS and CMS experiments. Phys. Rev. Lett. **114**, 191803 (2015). https://doi.org/10.1103/PhysRevLett.114.191803. arXiv:1503.07589 [hep-ex]
109. S. Baker, R.D. Cousins, Clarification of the use of CHI-square and likelihood functions in fits to histograms. Nucl. Instrum. Methods **221**, 437 (1984). https://doi.org/10.1016/0167-5087(84)90016-4
110. R.D. Cousins, Lectures on Statistics in Theory: Prelude to Statistics in Practice (2024). arXiv:1807.05996 [physics.data-an]
111. ATLAS Collaboration, ATLAS Computing Acknowledgements, ATL-SOFT-PUB-2023-001 (2023). https://cds.cern.ch/record/2869272

ATLAS Collaboration*

G. Aad[104], E. Aakvaag[17], B. Abbott[123], S. Abdelhameed[119a], K. Abeling[56], N. J. Abicht[50], S. H. Abidi[30], M. Aboelela[45], A. Aboulhorma[36e], H. Abramowicz[155], H. Abreu[154], Y. Abulaiti[120], B. S. Acharya[70a,70b,k], A. Ackermann[64a], C. Adam Bourdarios[4], L. Adamczyk[87a], S. V. Addepalli[27], M. J. Addison[103], J. Adelman[118], A. Adiguzel[22c], T. Adye[137], A. A. Affolder[139], Y. Afik[40], M. N. Agaras[13], J. Agarwala[74a,74b], A. Aggarwal[102], C. Agheorghiesei[28c], F. Ahmadov[39,y], W. S. Ahmed[106], S. Ahuja[97], X. Ai[63e], G. Aielli[77a,77b], A. Aikot[166], M. Ait Tamlihat[36e], B. Aitbenchikh[36a], M. Akbiyik[102], T. P. A. Åkesson[100], A. V. Akimov[38], D. Akiyama[171], N. N. Akolkar[25], S. Aktas[22a], K. Al Khoury[42], G. L. Alberghi[24b], J. Albert[168], P. Albicocco[54], G. L. Albouy[61], S. Alderweireldt[53], Z. L. Alegria[124], M. Aleksa[37], I. N. Aleksandrov[39], C. Alexa[28b], T. Alexopoulos[10], F. Alfonsi[24b], M. Algren[57], M. Alhroob[170], B. Ali[135], H. M. J. Ali[93,s], S. Ali[32], S. W. Alibocus[94], M. Aliev[34c], G. Alimonti[72a], W. Alkakhi[56], C. Allaire[67], B. M. M. Allbrooke[150], J. S. Allen[103], J. F. Allen[53], C. A. Allendes Flores[140f], P. P. Allport[21], A. Aloisio[73a,73b], F. Alonso[92], C. Alpigiani[142], Z. M. K. Alsolami[93], M. Alvarez Estevez[101], A. Alvarez Fernandez[102], M. Alves Cardoso[57], M. G. Alviggi[73a,73b], M. Aly[103], Y. Amaral Coutinho[84b], A. Ambler[106], C. Amelung[37], M. Amerl[103], C. G. Ames[111], D. Amidei[108], B. Amini[55], K. J. Amirie[158], S. P. Amor Dos Santos[133a], K. R. Amos[166], D. Amperiadou[156], S. An[85], V. Ananiev[128], C. Anastopoulos[143], T. Andeen[11], J. K. Anders[37], A. C. Anderson[60], S. Y. Andrean[48a,48b], A. Andreazza[72a,72b], S. Angelidakis[9], A. Angerami[42], A. V. Anisenkov[38], A. Annovi[75a], C. Antel[57], E. Antipov[149], M. Antonelli[54], F. Anulli[76a], M. Aoki[85], T. Aoki[157], M. A. Aparo[150], L. Aperio Bella[49], C. Appelt[19], A. Apyan[27], S. J. Arbiol Val[88], C. Arcangeletti[54], A. T. H. Arce[52], J.-F. Arguin[110], S. Argyropoulos[156], J.-H. Arling[49], O. Arnaez[4], H. Arnold[149], G. Artoni[76a,76b], H. Asada[113], K. Asai[121], S. Asai[157], N. A. Asbah[37], R. A. Ashby Pickering[170], K. Assamagan[30], R. Astalos[29a], K. S. V. Astrand[100], S. Atashi[162], R. J. Atkin[34a], M. Atkinson[165], H. Atmani[36f], P. A. Atmasiddha[131], K. Augsten[135], S. Auricchio[73a,73b], A. D. Auriol[21], V. A. Austrup[103], G. Avolio[37], K. Axiotis[57], G. Azuelos[110,ad], D. Babal[29b], H. Bachacou[138], K. Bachas[156,o], A. Bachiu[35], E. Bachmann[51], F. Backman[48a,48b], A. Badea[40], T. M. Baer[108], P. Bagnaia[76a,76b], M. Bahmani[19], D. Bahner[55], K. Bai[126], J. T. Baines[137], L. Baines[96], O. K. Baker[175], E. Bakos[16], D. Bakshi Gupta[8], L. E. Balabram Filho[84b], V. Balakrishnan[123], R. Balasubramanian[4], E. M. Baldin[38], P. Balek[87a], E. Ballabene[24a,24b], F. Balli[138], L. M. Baltes[64a], W. K. Balunas[33], J. Balz[102], I. Bamwidhi[119b], E. Banas[88], M. Bandieramonte[132], A. Bandyopadhyay[25], S. Bansal[25], L. Barak[155], M. Barakat[49], E. L. Barberio[107], D. Barberis[58a,58b], M. Barbero[104], M. Z. Barel[117], T. Barillari[112], M.-S. Barisits[37], T. Barklow[147], P. Baron[125], D. A. Baron Moreno[103], A. Baroncelli[63a], A. J. Barr[129], J. D. Barr[98], F. Barreiro[101], J. Barreiro Guimarães da Costa[14], U. Barron[155], M. G. Barros Teixeira[133a], S. Barsov[38], F. Bartels[64a], R. Bartoldus[147], A. E. Barton[93], P. Bartos[29a], A. Basan[102], M. Baselga[50], A. Bassalat[67,b], M. J. Basso[159a], S. Bataju[45], R. Bate[167], R. L. Bates[60], S. Batlamous[101], B. Batool[145], M. Battaglia[139], D. Battulga[19], M. Bauce[76a,76b], M. Bauer[80], P. Bauer[25], L. T. Bazzano Hurrell[31], J. B. Beacham[52],

T. Beau[130], J. Y. Beaucamp[92], P. H. Beauchemin[161], P. Bechtle[25], H. P. Beck[20,n], K. Becker[170], A. J. Beddall[83], V. A. Bednyakov[39], C. P. Bee[149], L. J. Beemster[16], T. A. Beermann[37], M. Begalli[84d], M. Begel[30], A. Behera[149], J. K. Behr[49], J. F. Beirer[37], F. Beisiegel[25], M. Belfkir[119b], G. Bella[155], L. Bellagamba[24b], A. Bellerive[35], P. Bellos[21], K. Beloborodov[38], D. Benchekroun[36a], F. Bendebba[36a], Y. Benhammou[155], K. C. Benkendorfer[62], L. Beresford[49], M. Beretta[54], E. Bergeaas Kuutmann[164], N. Berger[4], B. Bergmann[135], J. Beringer[18a], G. Bernardi[5], C. Bernius[147], F. U. Bernlochner[25], F. Bernon[37], A. Berrocal Guardia[13], T. Berry[97], P. Berta[136], A. Berthold[51], S. Bethke[112], A. Betti[76a,76b], A. J. Bevan[96], N. K. Bhalla[55], S. Bhatta[149], D. S. Bhattacharya[169], P. Bhattarai[147], K. D. Bhide[55], V. S. Bhopatkar[124], R. M. Bianchi[132], G. Bianco[24a,24b], O. Biebel[111], R. Bielski[126], M. Biglietti[78a], C. S. Billingsley[45], Y. Bimgdi[36f], M. Bindi[56], A. Bingul[22b], C. Bini[76a,76b], G. A. Bird[33], M. Birman[172], M. Biros[136], S. Biryukov[150], T. Bisanz[50], E. Bisceglie[44a,44b], J. P. Biswal[137], D. Biswas[145], I. Bloch[49], A. Blue[60], U. Blumenschein[96], J. Blumenthal[102], V. S. Bobrovnikov[38], M. Boehler[55], B. Boehm[169], D. Bogavac[37], A. G. Bogdanchikov[38], L. S. Boggia[130], C. Bohm[48a], V. Boisvert[97], P. Bokan[37], T. Bold[87a], M. Bomben[5], M. Bona[96], M. Boonekamp[138], C. D. Booth[97], A. G. Borbély[60], I. S. Bordulev[38], G. Borissov[93], D. Bortoletto[129], D. Boscherini[24b], M. Bosman[13], J. D. Bossio Sola[37], K. Bouaouda[36a], N. Bouchhar[166], L. Boudet[4], J. Boudreau[132], E. V. Bouhova-Thacker[93], D. Boumediene[41], R. Bouquet[58a,58b], A. Boveia[122], J. Boyd[37], D. Boye[30], I. R. Boyko[39], L. Bozianu[57], J. Bracinik[21], N. Brahimi[4], G. Brandt[174], O. Brandt[33], F. Braren[49], B. Brau[105], J. E. Brau[126], R. Brener[172], L. Brenner[117], R. Brenner[164], S. Bressler[172], G. Brianti[79a,79b], D. Britton[60], D. Britzger[112], I. Brock[25], R. Brock[109], G. Brooijmans[42], E. M. Brooks[159b], E. Brost[30], L. M. Brown[168], L. E. Bruce[62], T. L. Bruckler[129], P. A. Bruckman de Renstrom[88], B. Brüers[49], A. Bruni[24b], G. Bruni[24b], M. Bruschi[24b], N. Bruscino[76a,76b], T. Buanes[17], Q. Buat[142], D. Buchin[112], A. G. Buckley[60], O. Bulekov[38], B. A. Bullard[147], S. Burdin[94], C. D. Burgard[50], A. M. Burger[37], B. Burghgrave[8], O. Burlayenko[55], J. Burleson[165], J. T. P. Burr[33], J. C. Burzynski[146], E. L. Busch[42], V. Büscher[102], P. J. Bussey[60], J. M. Butler[26], C. M. Buttar[60], J. M. Butterworth[98], W. Buttinger[137], C. J. Buxo Vazquez[109], A. R. Buzykaev[38], S. Cabrera Urbán[166], L. Cadamuro[67], D. Caforio[59], H. Cai[132], Y. Cai[14,114c], Y. Cai[114a], V. M. M. Cairo[37], O. Cakir[3a], N. Calace[37], P. Calafiura[18a], G. Calderini[130], P. Calfayan[69], G. Callea[60], L. P. Caloba[84b], D. Calvet[41], S. Calvet[41], M. Calvetti[75a,75b], R. Camacho Toro[130], S. Camarda[37], D. Camarero Munoz[27], P. Camarri[77a,77b], M. T. Camerlingo[73a,73b], D. Cameron[37], C. Camincher[168], M. Campanelli[98], A. Camplani[43], V. Canale[73a,73b], A. C. Canbay[3a], E. Canonero[97], J. Cantero[166], Y. Cao[165], F. Capocasa[27], M. Capua[44a,44b], A. Carbone[72a,72b], R. Cardarelli[77a], J. C. J. Cardenas[8], G. Carducci[44a,44b], T. Carli[37], G. Carlino[73a], J. I. Carlotto[13], B. T. Carlson[132,p], E. M. Carlson[159a,168], J. Carmignani[94], L. Carminati[72a,72b], A. Carnelli[138], M. Carnesale[37], S. Caron[116], E. Carquin[140f], I. B. Carr[107], S. Carrá[72a], G. Carratta[24a,24b], A. M. Carroll[126], M. P. Casado[13,h], M. Caspar[49], F. L. Castillo[4], L. Castillo Garcia[13], V. Castillo Gimenez[166], N. F. Castro[133a,133e], A. Catinaccio[37], J. R. Catmore[128], T. Cavaliere[4], V. Cavaliere[30], N. Cavalli[24a,24b], L. J. Caviedes Betancourt[23b], Y. C. Cekmecelioglu[49], E. Celebi[83], S. Cella[37], M. S. Centonze[71a,71b], V. Cepaitis[57], K. Cerny[125], A. S. Cerqueira[84a], A. Cerri[150], L. Cerrito[77a,77b], F. Cerutti[18a], B. Cervato[145], A. Cervelli[24b], G. Cesarini[54], S. A. Cetin[83], D. Chakraborty[118], J. Chan[18a], W. Y. Chan[157], J. D. Chapman[33], E. Chapon[138], B. Chargeishvili[153b], D. G. Charlton[21], M. Chatterjee[20], C. Chauhan[136], Y. Che[114a], S. Chekanov[6], S. V. Chekulaev[159a], G. A. Chelkov[39,a], A. Chen[108], B. Chen[155], B. Chen[168], H. Chen[114a], H. Chen[30], J. Chen[63c], J. Chen[146], M. Chen[129], S. Chen[89], S. J. Chen[114a], X. Chen[63c], X. Chen[15,ac], Y. Chen[63a], C. L. Cheng[173], H. C. Cheng[65a], S. Cheong[147], A. Cheplakov[39], E. Cheremushkina[49], E. Cherepanova[117], R. Cherkaoui El Moursli[36e], E. Cheu[7], K. Cheung[66], L. Chevalier[138], V. Chiarella[54], G. Chiarelli[75a], N. Chiedde[104], G. Chiodini[71a], A. S. Chisholm[21], A. Chitan[28b], M. Chitishvili[166], M. V. Chizhov[39,q], K. Choi[11], Y. Chou[142], E. Y. S. Chow[116], K. L. Chu[172], M. C. Chu[65a], X. Chu[14,114c], Z. Chubinidze[54], J. Chudoba[134], J. J. Chwastowski[88], D. Cieri[112], K. M. Ciesla[87a], V. Cindro[95], A. Ciocio[18a], F. Cirotto[73a,73b], Z. H. Citron[172], M. Citterio[72a], D. A. Ciubotaru[28b], A. Clark[57], P. J. Clark[53], N. Clarke Hall[98], C. Clarry[158], J. M. Clavijo Columbie[49], S. E. Clawson[49], C. Clement[48a,48b], Y. Coadou[104], M. Cobal[70a,70c], A. Coccaro[58b], R. F. Coelho Barrue[133a], R. Coelho Lopes De Sa[105], S. Coelli[72a], L. S. Colangeli[158], B. Cole[42], J. Collot[61], P. Conde Muiño[133a,133g], M. P. Connell[34c], S. H. Connell[34c], E. I. Conroy[129], F. Conventi[73a,ae], H. G. Cooke[21], A. M. Cooper-Sarkar[129], F. A. Corchia[24a,24b], A. Cordeiro Oudot Choi[130], L. D. Corpe[41], M. Corradi[76a,76b], F. Corriveau[106,x], A. Cortes-Gonzalez[19], M. J. Costa[166], F. Costanza[4], D. Costanzo[143], B. M. Cote[122], J. Couthures[4], G. Cowan[97], K. Cranmer[173], L. Cremer[50], D. Cremonini[24a,24b], S. Crépé-Renaudin[61],

F. Crescioli[130], M. Cristinziani[145], M. Cristoforetti[79a,79b], V. Croft[117], J. E. Crosby[124], G. Crosetti[44a,44b], A. Cueto[101], H. Cui[98], Z. Cui[7], W. R. Cunningham[60], F. Curcio[166], J. R. Curran[53], P. Czodrowski[37], M. J. Da Cunha Sargedas De Sousa[58a,58b], J. V. Da Fonseca Pinto[84b], C. Da Via[103], W. Dabrowski[87a], T. Dado[37], S. Dahbi[152], T. Dai[108], D. Dal Santo[20], C. Dallapiccola[105], M. Dam[43], G. D'amen[30], V. D'Amico[111], J. Damp[102], J. R. Dandoy[35], D. Dannheim[37], M. Danninger[146], V. Dao[149], G. Darbo[58b], S. J. Das[30], F. Dattola[49], S. D'Auria[72a,72b], A. D'Avanzo[73a,73b], C. David[34a], T. Davidek[136], I. Dawson[96], H. A. Day-hall[135], K. De[8], R. De Asmundis[73a], N. De Biase[49], S. De Castro[24a,24b], N. De Groot[116], P. de Jong[117], H. De la Torre[118], A. De Maria[114a], A. De Salvo[76a], U. De Sanctis[77a,77b], F. De Santis[71a,71b], A. De Santo[150], J. B. De Vivie De Regie[61], J. Debevc[95], D. V. Dedovich[39], J. Degens[94], A. M. Deiana[45], F. Del Corso[24a,24b], J. Del Peso[101], L. Delagrange[130], F. Deliot[138], C. M. Delitzsch[50], M. Della Pietra[73a,73b], D. Della Volpe[57], A. Dell'Acqua[37], L. Dell'Asta[72a,72b], M. Delmastro[4], P. A. Delsart[61], S. Demers[175], M. Demichev[39], S. P. Denisov[38], L. D'Eramo[41], D. Derendarz[88], F. Derue[130], P. Dervan[94], K. Desch[25], C. Deutsch[25], F. A. Di Bello[58a,58b], A. Di Ciaccio[77a,77b], L. Di Ciaccio[4], A. Di Domenico[76a,76b], C. Di Donato[73a,73b], A. Di Girolamo[37], G. Di Gregorio[37], A. Di Luca[79a,79b], B. Di Micco[78a,78b], R. Di Nardo[78a,78b], K. F. Di Petrillo[40], M. Diamantopoulou[35], F. A. Dias[117], T. Dias Do Vale[146], M. A. Diaz[140a,140b], F. G. Diaz Capriles[25], A. R. Didenko[39], M. Didenko[166], E. B. Diehl[108], S. Díez Cornell[49], C. Diez Pardos[145], C. Dimitriadi[164], A. Dimitrievska[21], J. Dingfelder[25], T. Dingley[129], I.-M. Dinu[28b], S. J. Dittmeier[64b], F. Dittus[37], M. Divisek[136], B. Dixit[94], F. Djama[104], T. Djobava[153b], C. Doglioni[100,103], A. Dohnalova[29a], J. Dolejsi[136], Z. Dolezal[136], K. Domijan[87a], K. M. Dona[40], M. Donadelli[84d], B. Dong[109], J. Donini[41], A. D'Onofrio[73a,73b], M. D'Onofrio[94], J. Dopke[137], A. Doria[73a], N. Dos Santos Fernandes[133a], P. Dougan[103], M. T. Dova[92], A. T. Doyle[60], M. A. Draguet[129], M. P. Drescher[56], E. Dreyer[172], I. Drivas-koulouris[10], M. Drnevich[120], M. Drozdova[57], D. Du[63a], T. A. du Pree[117], F. Dubinin[38], M. Dubovsky[29a], E. Duchovni[172], G. Duckeck[111], O. A. Ducu[28b], D. Duda[53], A. Dudarev[37], E. R. Duden[27], M. D'uffizi[103], L. Duflot[67], M. Dührssen[37], I. Duminica[28g], A. E. Dumitriu[28b], M. Dunford[64a], S. Dungs[50], K. Dunne[48a,48b], A. Duperrin[104], H. Duran Yildiz[3a], M. Düren[59], A. Durglishvili[153b], B. L. Dwyer[118], G. I. Dyckes[18a], M. Dyndal[87a], B. S. Dziedzic[37], Z. O. Earnshaw[150], G. H. Eberwein[129], B. Eckerova[29a], S. Eggebrecht[56], E. Egidio Purcino De Souza[84e], L. F. Ehrke[57], G. Eigen[17], K. Einsweiler[18a], T. Ekelof[164], P. A. Ekman[100], S. El Farkh[36b], Y. El Ghazali[63a], H. El Jarrari[37], A. El Moussaouy[36a], V. Ellajosyula[164], M. Ellert[164], F. Ellinghaus[174], N. Ellis[37], J. Elmsheuser[30], M. Elsawy[119a], M. Elsing[37], D. Emeliyanov[137], Y. Enari[85], I. Ene[18a], S. Epari[13], P. A. Erland[88], D. Ernani Martins Neto[88], M. Errenst[174], M. Escalier[67], C. Escobar[166], E. Etzion[155], G. Evans[133a], H. Evans[69], L. S. Evans[97], A. Ezhilov[38], S. Ezzarqtouni[36a], F. Fabbri[24a,24b], L. Fabbri[24a,24b], G. Facini[98], V. Fadeyev[139], R. M. Fakhrutdinov[38], D. Fakoudis[102], S. Falciano[76a], L. F. Falda Ulhoa Coelho[37], F. Fallavollita[112], G. Falsetti[44a,44b], J. Faltova[136], C. Fan[165], K. Y. Fan[65b], Y. Fan[14], Y. Fang[14,114c], M. Fanti[72a,72b], M. Faraj[70a,70b], Z. Farazpay[99], A. Farbin[8], A. Farilla[78a], T. Farooque[109], S. M. Farrington[53], F. Fassi[36e], D. Fassouliotis[9], M. Faucci Giannelli[77a,77b], W. J. Fawcett[33], L. Fayard[67], P. Federic[136], P. Federicova[134], O. L. Fedin[38,a], M. Feickert[173], L. Feligioni[104], D. E. Fellers[126], C. Feng[63b], Z. Feng[117], M. J. Fenton[162], L. Ferencz[49], R. A. M. Ferguson[93], S. I. Fernandez Luengo[140f], P. Fernandez Martinez[68], M. J. V. Fernoux[104], J. Ferrando[93], A. Ferrari[164], P. Ferrari[116,117], R. Ferrari[74a], D. Ferrere[57], C. Ferretti[108], D. Fiacco[76a,76b], F. Fiedler[102], P. Fiedler[135], S. Filimonov[38], A. Filipčič[95], E. K. Filmer[159a], F. Filthaut[116], M. C. N. Fiolhais[133a,133c,c], L. Fiorini[166], W. C. Fisher[109], T. Fitschen[103], P. M. Fitzhugh[138], I. Fleck[145], P. Fleischmann[108], T. Flick[174], M. Flores[34d,aa], L. R. Flores Castillo[65a], L. Flores Sanz De Acedo[37], F. M. Follega[79a,79b], N. Fomin[33], J. H. Foo[158], A. Formica[138], A. C. Forti[103], E. Fortin[37], A. W. Fortman[18a], M. G. Foti[18a], L. Fountas[9,i], D. Fournier[67], H. Fox[93], P. Francavilla[75a,75b], S. Francescato[62], S. Franchellucci[57], M. Franchini[24a,24b], S. Franchino[64a], D. Francis[37], L. Franco[116], V. Franco Lima[37], L. Franconi[49], M. Franklin[62], G. Frattari[27], Y. Y. Frid[155], J. Friend[60], N. Fritzsche[37], A. Froch[55], D. Froidevaux[37], J. A. Frost[129], Y. Fu[63a], S. Fuenzalida Garrido[140f], M. Fujimoto[104], K. Y. Fung[65a], E. Furtado De Simas Filho[84e], M. Furukawa[157], J. Fuster[166], A. Gaa[56], A. Gabrielli[24a,24b], A. Gabrielli[158], P. Gadow[37], G. Gagliardi[58a,58b], L. G. Gagnon[18a], S. Gaid[163], S. Galantzan[155], J. Gallagher[1], E. J. Gallas[129], B. J. Gallop[137], K. K. Gan[122], S. Ganguly[157], Y. Gao[53], F. M. Garay Walls[140a,140b], B. Garcia[30], C. García[166], A. Garcia Alonso[117], A. G. Garcia Caffaro[175], J. E. García Navarro[166], M. Garcia-Sciveres[18a], G. L. Gardner[131], R. W. Gardner[40], N. Garelli[161], D. Garg[81], R. B. Garg[147], J. M. Gargan[53], C. A. Garner[158], C. M. Garvey[34a], V. K. Gassmann[161], G. Gaudio[74a], V. Gautam[13], P. Gauzzi[76a,76b], J. Gavranovic[95], I. L. Gavrilenko[38], A. Gavrilyuk[38], C. Gay[167], G. Gaycken[126],

E. N. Gazis[10], A. A. Geanta[28b], C. M. Gee[139], A. Gekow[122], C. Gemme[58b], M. H. Genest[61], A. D. Gentry[115], S. George[97], W. F. George[21], T. Geralis[47], P. Gessinger-Befurt[37], M. E. Geyik[174], M. Ghani[170], K. Ghorbanian[96], A. Ghosal[145], A. Ghosh[162], A. Ghosh[7], B. Giacobbe[24b], S. Giagu[76a,76b], T. Giani[117], A. Giannini[63a], S. M. Gibson[97], M. Gignac[139], D. T. Gil[87b], A. K. Gilbert[87a], B. J. Gilbert[42], D. Gillberg[35], G. Gilles[117], L. Ginabat[130], D. M. Gingrich[2,ad], M. P. Giordani[70a,70c], P. F. Giraud[138], G. Giugliarelli[70a,70c], D. Giugni[72a], F. Giuli[77a,77b], I. Gkialas[9,i], L. K. Gladilin[38], C. Glasman[101], G. R. Gledhill[126], G. Glemža[49], M. Glisic[126], I. Gnesi[44b], Y. Go[30], M. Goblirsch-Kolb[37], B. Gocke[50], D. Godin[110], B. Gokturk[22a], S. Goldfarb[107], T. Golling[57], M. G. D. Gololo[34g], D. Golubkov[38], J. P. Gombas[109], A. Gomes[133a,133b], G. Gomes Da Silva[145], A. J. Gomez Delegido[166], R. Gonçalo[133a], L. Gonella[21], A. Gongadze[153c], F. Gonnella[21], J. L. Gonski[147], R. Y. González Andana[53], S. González de la Hoz[166], R. Gonzalez Lopez[94], C. Gonzalez Renteria[18a], M. V. Gonzalez Rodrigues[49], R. Gonzalez Suarez[164], S. Gonzalez-Sevilla[57], L. Goossens[37], B. Gorini[37], E. Gorini[71a,71b], A. Gorišek[95], T. C. Gosart[131], A. T. Goshaw[52], M. I. Gostkin[39], S. Goswami[124], C. A. Gottardo[37], S. A. Gotz[111], M. Gouighri[36b], V. Goumarre[49], A. G. Goussiou[142], N. Govender[34c], R. P. Grabarczyk[129], I. Grabowska-Bold[87a], K. Graham[35], E. Gramstad[128], S. Grancagnolo[71a,71b], C. M. Grant[1,138], P. M. Gravila[28f], F. G. Gravili[71a,71b], H. M. Gray[18a], M. Greco[71a,71b], M. J. Green[1], C. Grefe[25], A. S. Grefsrud[17], I. M. Gregor[49], K. T. Greif[162], P. Grenier[147], S. G. Grewe[112], A. A. Grillo[139], K. Grimm[32], S. Grinstein[13,t], J.-F. Grivaz[67], E. Gross[172], J. Grosse-Knetter[56], L. Guan[108], J. G. R. Guerrero Rojas[166], G. Guerrieri[37], R. Gugel[102], J. A. M. Guhit[108], A. Guida[19], E. Guilloton[170], S. Guindon[37], F. Guo[14,114c], J. Guo[63c], L. Guo[49], L. Guo[14], Y. Guo[108], A. Gupta[50], R. Gupta[132], S. Gurbuz[25], S. S. Gurdasani[55], G. Gustavino[76a,76b], P. Gutierrez[123], L. F. Gutierrez Zagazeta[131], M. Gutsche[51], C. Gutschow[98], C. Gwenlan[129], C. B. Gwilliam[94], E. S. Haaland[128], A. Haas[120], M. Habedank[60], C. Haber[18a], H. K. Hadavand[8], A. Hadef[51], S. Hadzic[112], A. I. Hagan[93], J. J. Hahn[145], E. H. Haines[98], M. Haleem[169], J. Haley[124], G. D. Hallewell[104], L. Halser[20], K. Hamano[168], M. Hamer[25], E. J. Hampshire[97], J. Han[63b], L. Han[114a], L. Han[63a], S. Han[18a], Y. F. Han[158], K. Hanagaki[85], M. Hance[139], D. A. Hangal[42], H. Hanif[146], M. D. Hank[131], J. B. Hansen[43], P. H. Hansen[43], D. Harada[57], T. Harenberg[174], S. Harkusha[176], M. L. Harris[105], Y. T. Harris[25], J. Harrison[13], N. M. Harrison[122], P. F. Harrison[170], N. M. Hartman[112], N. M. Hartmann[111], R. Z. Hasan[97,137], Y. Hasegawa[144], F. Haslbeck[129], S. Hassan[17], R. Hauser[109], C. M. Hawkes[21], R. J. Hawkings[37], Y. Hayashi[157], D. Hayden[109], C. Hayes[108], R. L. Hayes[117], C. P. Hays[129], J. M. Hays[96], H. S. Hayward[94], F. He[63a], M. He[14,114c], Y. He[49], Y. He[98], N. B. Heatley[96], V. Hedberg[100], A. L. Heggelund[128], N. D. Hehir[96,*], C. Heidegger[55], K. K. Heidegger[55], J. Heilman[35], S. Heim[49], T. Heim[18a], J. G. Heinlein[131], J. J. Heinrich[126], L. Heinrich[112,ab], J. Hejbal[134], A. Held[173], S. Hellesund[17], C. M. Helling[167], S. Hellman[48a,48b], R. C. W. Henderson[93], L. Henkelmann[33], A. M. Henriques Correia[37], H. Herde[100], Y. Hernández Jiménez[149], L. M. Herrmann[25], T. Herrmann[51], G. Herten[55], R. Hertenberger[111], L. Hervas[37], M. E. Hesping[102], N. P. Hessey[159a], J. Hessler[112], M. Hidaoui[36b], N. Hidic[136], E. Hill[158], S. J. Hillier[21], J. R. Hinds[109], F. Hinterkeuser[25], M. Hirose[127], S. Hirose[160], D. Hirschbuehl[174], T. G. Hitchings[103], B. Hiti[95], J. Hobbs[149], R. Hobincu[28e], N. Hod[172], M. C. Hodgkinson[143], B. H. Hodkinson[129], A. Hoecker[37], D. D. Hofer[108], J. Hofer[166], T. Holm[25], M. Holzbock[37], L. B. A. H. Hommels[33], B. P. Honan[103], J. J. Hong[69], J. Hong[63c], T. M. Hong[132], B. H. Hooberman[165], W. H. Hopkins[6], M. C. Hoppesch[165], Y. Horii[113], M. E. Horstmann[112], S. Hou[152], A. S. Howard[95], J. Howarth[60], J. Hoya[6], M. Hrabovsky[125], A. Hrynevich[49], T. Hryn'ova[4], P. J. Hsu[66], S.-C. Hsu[142], T. Hsu[67], M. Hu[18a], Q. Hu[63a], S. Huang[33], X. Huang[14,114c], Y. Huang[143], Y. Huang[102], Y. Huang[14], Z. Huang[103], Z. Hubacek[135], M. Huebner[25], F. Huegging[25], T. B. Huffman[129], M. Hufnagel Maranha De Faria[84a], C. A. Hugli[49], M. Huhtinen[37], S. K. Huiberts[17], R. Hulsken[106], N. Huseynov[12,f], J. Huston[109], J. Huth[62], R. Hyneman[147], G. Iacobucci[57], G. Iakovidis[30], L. Iconomidou-Fayard[67], J. P. Iddon[37], P. Iengo[73a,73b], R. Iguchi[157], Y. Iiyama[157], T. Iizawa[129], Y. Ikegami[85], N. Ilic[158], H. Imam[84c], G. Inacio Goncalves[84d], T. Ingebretsen Carlson[48a,48b], J. M. Inglis[96], G. Introzzi[74a,74b], M. Iodice[78a], V. Ippolito[76a,76b], R. K. Irwin[94], M. Ishino[157], W. Islam[173], C. Issever[19], S. Istin[22a,ah], H. Ito[171], R. Iuppa[79a,79b], A. Ivina[172], J. M. Izen[46], V. Izzo[73a], P. Jacka[134], P. Jackson[1], C. S. Jagfeld[111], G. Jain[159a], P. Jain[49], K. Jakobs[55], T. Jakoubek[172], J. Jamieson[60], W. Jang[157], M. Javurkova[105], P. Jawahar[103], L. Jeanty[126], J. Jejelava[153a,z], P. Jenni[55,e], C. E. Jessiman[35], C. Jia[63b], H. Jia[167], J. Jia[149], X. Jia[14,114c], Z. Jia[114a], C. Jiang[53], S. Jiggins[49], J. Jimenez Pena[13], S. Jin[114a], A. Jinaru[28b], O. Jinnouchi[141], P. Johansson[143], K. A. Johns[7], J. W. Johnson[139], F. A. Jolly[49], D. M. Jones[150], E. Jones[49], K. S. Jones[8], P. Jones[33], R. W. L. Jones[93], T. J. Jones[94], H. L. Joos[37,56], R. Joshi[122],

J. Jovicevic[16], X. Ju[18a], J. J. Junggeburth[105], T. Junkermann[64a], A. Juste Rozas[13,t], M. K. Juzek[88], S. Kabana[140e], A. Kaczmarska[88], M. Kado[112], H. Kagan[122], M. Kagan[147], A. Kahn[131], C. Kahra[102], T. Kaji[157], E. Kajomovitz[154], N. Kakati[172], I. Kalaitzidou[55], C. W. Kalderon[30], N. J. Kang[139], D. Kar[34g], K. Karava[129], M. J. Kareem[159b], E. Karentzos[55], O. Karkout[117], S. N. Karpov[39], Z. M. Karpova[39], V. Kartvelishvili[93], A. N. Karyukhin[38], E. Kasimi[156], J. Katzy[49], S. Kaur[35], K. Kawade[144], M. P. Kawale[123], C. Kawamoto[89], T. Kawamoto[63a], E. F. Kay[37], F. I. Kaya[161], S. Kazakos[109], V. F. Kazanin[38], Y. Ke[149], J. M. Keaveney[34a], R. Keeler[168], G. V. Kehris[62], J. S. Keller[35], J. J. Kempster[150], O. Kepka[134], B. P. Kerridge[137], S. Kersten[174], B. P. Kerševan[95], L. Keszeghova[29a], S. Ketabchi Haghighat[158], R. A. Khan[132], A. Khanov[124], A. G. Kharlamov[38], T. Kharlamova[38], E. E. Khoda[142], M. Kholodenko[133a], T. J. Khoo[19], G. Khoriauli[169], J. Khubua[153b,*], Y. A. R. Khwaira[130], B. Kibirige[34g], D. Kim[6], D. W. Kim[48a,48b], Y. K. Kim[40], N. Kimura[98], M. K. Kingston[56], A. Kirchhoff[56], C. Kirfel[25], F. Kirfel[25], J. Kirk[137], A. E. Kiryunin[112], S. Kita[160], C. Kitsaki[10], O. Kivernyk[25], M. Klassen[161], C. Klein[35], L. Klein[169], M. H. Klein[45], S. B. Klein[57], U. Klein[94], A. Klimentov[30], T. Klioutchnikova[37], P. Kluit[117], S. Kluth[112], E. Kneringer[80], T. M. Knight[158], A. Knue[50], D. Kobylianskii[172], S. F. Koch[129], M. Kocian[147], P. Kodyš[136], D. M. Koeck[126], P. T. Koenig[25], T. Koffas[35], O. Kolay[51], I. Koletsou[4], T. Komarek[88], K. Köneke[55], A. X. Y. Kong[1], T. Kono[121], N. Konstantinidis[98], P. Kontaxakis[57], B. Konya[100], R. Kopeliansky[42], S. Koperny[87a], K. Korcyl[88], K. Kordas[156,d], A. Korn[98], S. Korn[56], I. Korolkov[13], N. Korotkova[38], B. Kortman[117], O. Kortner[112], S. Kortner[112], W. H. Kostecka[118], V. V. Kostyukhin[145], A. Kotsokechagia[37], A. Kotwal[52], A. Koulouris[37], A. Kourkoumeli-Charalampidi[74a,74b], C. Kourkoumelis[9], E. Kourlitis[112,ab], O. Kovanda[126], R. Kowalewski[168], W. Kozanecki[126], A. S. Kozhin[38], V. A. Kramarenko[38], G. Kramberger[95], P. Kramer[102], M. W. Krasny[130], A. Krasznahorkay[37], A. C. Kraus[118], J. W. Kraus[174], J. A. Kremer[49], T. Kresse[51], L. Kretschmann[174], J. Kretzschmar[94], K. Kreul[19], P. Krieger[158], M. Krivos[136], K. Krizka[21], K. Kroeninger[50], H. Kroha[112], J. Kroll[134], J. Kroll[131], K. S. Krowpman[109], U. Kruchonak[39], H. Krüger[25], N. Krumnack[82], M. C. Kruse[52], O. Kuchinskaia[38], S. Kuday[3a], S. Kuehn[37], R. Kuesters[55], T. Kuhl[49], V. Kukhtin[39], Y. Kulchitsky[38,a], S. Kuleshov[140b,140d], M. Kumar[34g], N. Kumari[49], P. Kumari[159b], A. Kupco[134], T. Kupfer[50], A. Kupich[38], O. Kuprash[55], H. Kurashige[86], L. L. Kurchaninov[159a], O. Kurdysh[67], Y. A. Kurochkin[38], A. Kurova[38], M. Kuze[141], A. K. Kvam[105], J. Kvita[125], T. Kwan[106], N. G. Kyriacou[108], L. A. O. Laatu[104], C. Lacasta[166], F. Lacava[76a,76b], H. Lacker[19], D. Lacour[130], N. N. Lad[98], E. Ladygin[39], A. Lafarge[41], B. Laforge[130], T. Lagouri[175], F. Z. Lahbabi[36a], S. Lai[56], J. E. Lambert[168], S. Lammers[69], W. Lampl[7], C. Lampoudis[156,d], G. Lamprinoudis[102], A. N. Lancaster[118], E. Lançon[30], U. Landgraf[55], M. P. J. Landon[96], V. S. Lang[55], O. K. B. Langrekken[128], A. J. Lankford[162], F. Lanni[37], K. Lantzsch[25], A. Lanza[74a], M. Lanzac Berrocal[166], J. F. Laporte[138], T. Lari[72a], F. Lasagni Manghi[24b], M. Lassnig[37], V. Latonova[134], A. Laurier[154], S. D. Lawlor[143], Z. Lawrence[103], R. Lazaridou[170], M. Lazzaroni[72a,72b], B. Le[103], H. D. M. Le[109], E. M. Le Boulicaut[175], L. T. Le Pottier[18a], B. Leban[24a,24b], A. Lebedev[82], M. LeBlanc[103], F. Ledroit-Guillon[61], S. C. Lee[152], S. Lee[48a,48b], T. F. Lee[94], L. L. Leeuw[34c], H. P. Lefebvre[97], M. Lefebvre[168], C. Leggett[18a], G. Lehmann Miotto[37], M. Leigh[57], W. A. Leight[105], W. Leinonen[116], A. Leisos[156,r], M. A. L. Leite[84c], C. E. Leitgeb[19], R. Leitner[136], K. J. C. Leney[45], T. Lenz[25], S. Leone[75a], C. Leonidopoulos[53], A. Leopold[148], R. Les[109], C. G. Lester[33], M. Levchenko[38], J. Levêque[4], L. J. Levinson[172], G. Levrini[24a,24b], M. P. Lewicki[88], C. Lewis[142], D. J. Lewis[4], L. Lewitt[143], A. Li[30], B. Li[63b], C. Li[63a], C.-Q. Li[112], H. Li[63a], H. Li[63b], H. Li[114a], H. Li[15], H. Li[63b], J. Li[63c], K. Li[14], L. Li[63c], M. Li[14,114c], S. Li[14,114c], S. Li[63c,63d], T. Li[5], X. Li[106], Z. Li[157], Z. Li[14,114c], Z. Li[63a], S. Liang[14,114c], Z. Liang[14], M. Liberatore[138], B. Liberti[77a], K. Lie[65c], J. Lieber Marin[84e], H. Lien[69], H. Lin[108], K. Lin[109], R. E. Lindley[7], J. H. Lindon[2], J. Ling[62], E. Lipeles[131], A. Lipniacka[17], A. Lister[167], J. D. Little[69], B. Liu[14], B. X. Liu[114b], D. Liu[63c,63d], E. H. L. Liu[21], J. B. Liu[63a], J. K. K. Liu[33], K. Liu[63d], K. Liu[63c,63d], M. Liu[63a], M. Y. Liu[63a], P. Liu[14], Q. Liu[63c,63d,142], X. Liu[63a], X. Liu[63b], Y. Liu[114b,114c], Y. L. Liu[63b], Y. W. Liu[63a], S. L. Lloyd[96], E. M. Lobodzinska[49], P. Loch[7], E. Lodhi[158], T. Lohse[19], K. Lohwasser[143], E. Loiacono[49], J. D. Lomas[21], J. D. Long[42], I. Longarini[162], R. Longo[165], I. Lopez Paz[68], A. Lopez Solis[49], N. A. Lopez-canelas[7], N. Lorenzo Martinez[4], A. M. Lory[111], M. Losada[119a], G. Löschcke Centeno[150], O. Loseva[38], X. Lou[48a,48b], X. Lou[14,114c], A. Lounis[67], P. A. Love[93], G. Lu[14,114c], M. Lu[67], S. Lu[131], Y. J. Lu[66], H. J. Lubatti[142], C. Luci[76a,76b], F. L. Lucio Alves[114a], F. Luehring[69], O. Lukianchuk[67], B. S. Lunday[131], O. Lundberg[148], B. Lund-Jensen[148,*], N. A. Luongo[6], M. S. Lutz[37], A. B. Lux[26], D. Lynn[30], R. Lysak[134], E. Lytken[100], V. Lyubushkin[39], T. Lyubushkina[39], M. M. Lyukova[149], M. Firdaus M. Soberi[53], H. Ma[30], K. Ma[63a], L. L. Ma[63b],

W. Ma[63a], Y. Ma[124], J. C. MacDonald[102], P. C. Machado De Abreu Farias[84e], R. Madar[41], T. Madula[98], J. Maeda[86], T. Maeno[30], H. Maguire[143], V. Maiboroda[138], A. Maio[133a,133b,133d], K. Maj[87a], O. Majersky[49], S. Majewski[126], N. Makovec[67], V. Maksimovic[16], B. Malaescu[130], Pa. Malecki[88], V. P. Maleev[38], F. Malek[61,m], M. Mali[95], D. Malito[97], U. Mallik[81,*], S. Maltezos[10], S. Malyukov[39], J. Mamuzic[13], G. Mancini[54], M. N. Mancini[27], G. Manco[74a,74b], J. P. Mandalia[96], S. S. Mandarry[150], I. Mandić[95], L. Manhaes de Andrade Filho[84a], I. M. Maniatis[172], J. Manjarres Ramos[91], D. C. Mankad[172], A. Mann[111], S. Manzoni[37], L. Mao[63c], X. Mapekula[34c], A. Marantis[156,r], G. Marchiori[5], M. Marcisovsky[134], C. Marcon[72a], E. Maricic[16], M. Marinescu[21], S. Marium[49], M. Marjanovic[123], A. Markhoos[55], M. Markovitch[67], E. J. Marshall[93], Z. Marshall[18a], S. Marti-Garcia[166], J. Martin[98], T. A. Martin[137], V. J. Martin[53], B. Martin dit Latour[17], L. Martinelli[76a,76b], M. Martinez[13,t], P. Martinez Agullo[166], V. I. Martinez Outschoorn[105], P. Martinez Suarez[13], S. Martin-Haugh[137], G. Martinovicova[136], V. S. Martoiu[28b], A. C. Martyniuk[98], A. Marzin[37], D. Mascione[79a,79b], L. Masetti[102], J. Masik[103], A. L. Maslennikov[38], S. L. Mason[42], P. Massarotti[73a,73b], P. Mastrandrea[75a,75b], A. Mastroberardino[44a,44b], T. Masubuchi[127], T. T. Mathew[126], T. Mathisen[164], J. Matousek[136], D. M. Mattern[50], J. Maurer[28b], T. Maurin[60], A. J. Maury[67], B. Maček[95], D. A. Maximov[38], A. E. May[103], R. Mazini[152], I. Maznas[118], M. Mazza[109], S. M. Mazza[139], E. Mazzeo[72a,72b], C. Mc Ginn[30], J. P. Mc Gowan[168], S. P. Mc Kee[108], C. A. Mc Lean[6], C. C. McCracken[167], E. F. McDonald[107], A. E. McDougall[117], J. A. Mcfayden[150], R. P. McGovern[131], R. P. Mckenzie[34g], T. C. Mclachlan[49], D. J. Mclaughlin[98], S. J. McMahon[137], C. M. Mcpartland[94], R. A. McPherson[168,x], S. Mehlhase[111], A. Mehta[94], D. Melini[166], B. R. Mellado Garcia[34g], A. H. Melo[56], F. Meloni[49], A. M. Mendes Jacques Da Costa[103], H. Y. Meng[158], L. Meng[93], S. Menke[112], M. Mentink[37], E. Meoni[44a,44b], G. Mercado[118], S. Merianos[156], C. Merlassino[70a,70c], L. Merola[73a,73b], C. Meroni[72a,72b], J. Metcalfe[6], A. S. Mete[6], E. Meuser[102], C. Meyer[69], J.-P. Meyer[138], R. P. Middleton[137], L. Mijović[53], G. Mikenberg[172], M. Mikestikova[134], M. Mikuž[95], H. Mildner[102], A. Milic[37], D. W. Miller[40], E. H. Miller[147], L. S. Miller[35], A. Milov[172], D. A. Milstead[48a,48b], T. Min[114a], A. A. Minaenko[38], I. A. Minashvili[153b], L. Mince[60], A. I. Mincer[120], B. Mindur[87a], M. Mineev[39], Y. Mino[89], L. M. Mir[13], M. Miralles Lopez[60], M. Mironova[18a], M. C. Missio[116], A. Mitra[170], V. A. Mitsou[166], Y. Mitsumori[113], O. Miu[158], P. S. Miyagawa[96], T. Mkrtchyan[64a], M. Mlinarevic[98], T. Mlinarevic[98], M. Mlynarikova[37], S. Mobius[20], P. Mogg[111], M. H. Mohamed Farook[115], A. F. Mohammed[14,114c], S. Mohapatra[42], G. Mokgatitswane[34g], L. Moleri[172], B. Mondal[145], S. Mondal[135], K. Mönig[49], E. Monnier[104], L. Monsonis Romero[166], J. Montejo Berlingen[13], A. Montella[48a,48b], M. Montella[122], F. Montereali[78a,78b], F. Monticelli[92], S. Monzani[70a,70c], A. Morancho Tarda[43], N. Morange[67], A. L. Moreira De Carvalho[49], M. Moreno Llácer[166], C. Moreno Martinez[57], J. M. Moreno Perez[23b], P. Morettini[58b], S. Morgenstern[37], M. Morii[62], M. Morinaga[157], M. Moritsu[90], F. Morodei[76a,76b], P. Moschovakos[37], B. Moser[129], M. Mosidze[153b], T. Moskalets[45], P. Moskvitina[116], J. Moss[32,j], P. Moszkowicz[87a], A. Moussa[36d], E. J. W. Moyse[105], O. Mtintsilana[34g], S. Muanza[104], J. Mueller[132], D. Muenstermann[93], R. Müller[37], G. A. Mullier[164], A. J. Mullin[33], J. J. Mullin[131], A. E. Mulski[62], D. P. Mungo[158], D. Munoz Perez[166], F. J. Munoz Sanchez[103], M. Murin[103], W. J. Murray[137,170], M. Muškinja[95], C. Mwewa[30], A. G. Myagkov[38,a], A. J. Myers[8], G. Myers[108], M. Myska[135], B. P. Nachman[18a], O. Nackenhorst[50], K. Nagai[129], K. Nagano[85], R. Nagasaka[157], J. L. Nagle[30,af], E. Nagy[104], A. M. Nairz[37], Y. Nakahama[85], K. Nakamura[85], K. Nakkalil[5], H. Nanjo[127], E. A. Narayanan[45], I. Naryshkin[38], L. Nasella[72a,72b], M. Naseri[35], S. Nasri[119b], C. Nass[25], G. Navarro[23a], J. Navarro-Gonzalez[166], R. Nayak[155], A. Nayaz[19], P. Y. Nechaeva[38], S. Nechaeva[24a,24b], F. Nechansky[134], L. Nedic[129], T. J. Neep[21], A. Negri[74a,74b], M. Negrini[24b], C. Nellist[117], C. Nelson[106], K. Nelson[108], S. Nemecek[134], M. Nessi[37,g], M. S. Neubauer[165], F. Neuhaus[102], J. Neundorf[49], J. Newell[94], P. R. Newman[21], C. W. Ng[132], Y. W. Y. Ng[49], B. Ngair[119a], H. D. N. Nguyen[110], R. B. Nickerson[129], R. Nicolaidou[138], J. Nielsen[139], M. Niemeyer[56], J. Niermann[56], N. Nikiforou[37], V. Nikolaenko[38,a], I. Nikolic-Audit[130], K. Nikolopoulos[21], P. Nilsson[30], I. Ninca[49], G. Ninio[155], A. Nisati[76a], N. Nishu[2], R. Nisius[112], N. Nitika[70a,70c], J.-E. Nitschke[51], E. K. Nkadimeng[34g], T. Nobe[157], T. Nommensen[151], M. B. Norfolk[143], B. J. Norman[35], M. Noury[36a], J. Novak[95], T. Novak[95], L. Novotny[135], R. Novotny[115], L. Nozka[125], K. Ntekas[162], N. M. J. Nunes De Moura Junior[84b], J. Ocariz[130], A. Ochi[86], I. Ochoa[133a], S. Oerdek[49,u], J. T. Offermann[40], A. Ogrodnik[136], A. Oh[103], C. C. Ohm[148], H. Oide[85], R. Oishi[157], M. L. Ojeda[37], Y. Okumura[157], L. F. Oleiro Seabra[133a], I. Oleksiyuk[57], S. A. Olivares Pino[140d], G. Oliveira Correa[13], D. Oliveira Damazio[30], J. L. Oliver[162], Ö. O. Öncel[55], A. P. O'Neill[20], A. Onofre[133a,133e], P. U. E. Onyisi[11], M. J. Oreglia[40], G. E. Orellana[92], D. Orestano[78a,78b],

N. Orlando[13], R. S. Orr[158], L. M. Osojnak[131], R. Ospanov[63a], Y. Osumi[113], G. Otero y Garzon[31], H. Otono[90], P. S. Ott[64a], G. J. Ottino[18a], M. Ouchrif[36d], F. Ould-Saada[128], T. Ovsiannikova[142], M. Owen[60], R. E. Owen[137], V. E. Ozcan[22a], F. Ozturk[88], N. Ozturk[8], S. Ozturk[83], H. A. Pacey[129], A. Pacheco Pages[13], C. Padilla Aranda[13], G. Padovano[76a,76b], S. Pagan Griso[18a], G. Palacino[69], A. Palazzo[71a,71b], J. Pampel[25], J. Pan[175], T. Pan[65a], D. K. Panchal[11], C. E. Pandini[117], J. G. Panduro Vazquez[137], H. D. Pandya[1], H. Pang[15], P. Pani[49], G. Panizzo[70a,70c], L. Panwar[130], L. Paolozzi[57], S. Parajuli[165], A. Paramonov[6], C. Paraskevopoulos[54], D. Paredes Hernandez[65b], A. Pareti[74a,74b], K. R. Park[42], T. H. Park[158], M. A. Parker[33], F. Parodi[58a,58b], E. W. Parrish[118], V. A. Parrish[53], J. A. Parsons[42], U. Parzefall[55], B. Pascual Dias[110], L. Pascual Dominguez[101], E. Pasqualucci[76a], S. Passaggio[58b], F. Pastore[97], P. Patel[88], U. M. Patel[52], J. R. Pater[103], T. Pauly[37], F. Pauwels[136], C. I. Pazos[161], M. Pedersen[128], R. Pedro[133a], S. V. Peleganchuk[38], O. Penc[37], E. A. Pender[53], S. Peng[15], G. D. Penn[175], K. E. Penski[111], M. Penzin[38], B. S. Peralva[84d], A. P. Pereira Peixoto[142], L. Pereira Sanchez[147], D. V. Perepelitsa[30,af], G. Perera[105], E. Perez Codina[159a], M. Perganti[10], H. Pernegger[37], S. Perrella[76a,76b], O. Perrin[41], K. Peters[49], R. F. Y. Peters[103], B. A. Petersen[37], T. C. Petersen[43], E. Petit[104], V. Petousis[135], C. Petridou[156,d], T. Petru[136], A. Petrukhin[145], M. Pettee[18a], A. Petukhov[38], K. Petukhova[37], R. Pezoa[140f], L. Pezzotti[37], G. Pezzullo[175], A. J. Pfleger[37], T. M. Pham[173], T. Pham[107], P. W. Phillips[137], G. Piacquadio[149], E. Pianori[18a], F. Piazza[126], R. Piegaia[31], D. Pietreanu[28b], A. D. Pilkington[103], M. Pinamonti[70a,70c], J. L. Pinfold[2], B. C. Pinheiro Pereira[133a], J. Pinol Bel[13], A. E. Pinto Pinoargote[138], L. Pintucci[70a,70c], K. M. Piper[150], A. Pirttikoski[57], D. A. Pizzi[35], L. Pizzimento[65b], A. Pizzini[117], M.-A. Pleier[30], V. Pleskot[136], E. Plotnikova[39], G. Poddar[96], R. Poettgen[100], L. Poggioli[130], I. Pokharel[56], S. Polacek[136], G. Polesello[74a], A. Poley[146,159a], A. Polini[24b], C. S. Pollard[170], Z. B. Pollock[122], E. Pompa Pacchi[76a,76b], N. I. Pond[98], D. Ponomarenko[69], L. Pontecorvo[37], S. Popa[28a], G. A. Popeneciu[28d], A. Poreba[37], D. M. Portillo Quintero[159a], S. Pospisil[135], M. A. Postill[143], P. Postolache[28c], K. Potamianos[170], P. A. Potepa[87a], I. N. Potrap[39], C. J. Potter[33], H. Potti[151], J. Poveda[166], M. E. Pozo Astigarraga[37], A. Prades Ibanez[77a,77b], J. Pretel[168], D. Price[103], M. Primavera[71a], L. Primomo[70a,70c], M. A. Principe Martin[101], R. Privara[125], T. Procter[60], M. L. Proffitt[142], N. Proklova[131], K. Prokofiev[65c], G. Proto[112], J. Proudfoot[6], M. Przybycien[87a], W. W. Przygoda[87b], A. Psallidas[47], J. E. Puddefoot[143], D. Pudzha[55], D. Pyatiizbyantseva[38], J. Qian[108], R. Qian[109], D. Qichen[103], Y. Qin[13], T. Qiu[53], A. Quadt[56], M. Queitsch-Maitland[103], G. Quetant[57], R. P. Quinn[167], G. Rabanal Bolanos[62], D. Rafanoharana[55], F. Raffaeli[77a,77b], F. Ragusa[72a,72b], J. L. Rainbolt[40], J. A. Raine[57], S. Rajagopalan[30], E. Ramakoti[38], L. Rambelli[58a,58b], I. A. Ramirez-Berend[35], K. Ran[49,114c], D. S. Rankin[131], N. P. Rapheeha[34g], H. Rasheed[28b], V. Raskina[130], D. F. Rassloff[64a], A. Rastogi[18a], S. Rave[102], S. Ravera[58a,58b], B. Ravina[56], I. Ravinovich[172], M. Raymond[37], A. L. Read[128], N. P. Readioff[143], D. M. Rebuzzi[74a,74b], G. Redlinger[30], A. S. Reed[112], K. Reeves[27], J. A. Reidelsturz[174], D. Reikher[126], A. Rej[50], C. Rembser[37], M. Renda[28b], F. Renner[49], A. G. Rennie[162], A. L. Rescia[49], S. Resconi[72a], M. Ressegotti[58a,58b], S. Rettie[37], J. G. Reyes Rivera[109], E. Reynolds[18a], O. L. Rezanova[38], P. Reznicek[136], H. Riani[36d], N. Ribaric[52], E. Ricci[79a,79b], R. Richter[112], S. Richter[48a,48b], E. Richter-Was[87b], M. Ridel[130], S. Ridouani[36d], P. Rieck[120], P. Riedler[37], E. M. Riefel[48a,48b], J. O. Rieger[117], M. Rijssenbeek[149], M. Rimoldi[37], L. Rinaldi[24a,24b], P. Rincke[56,164], T. T. Rinn[30], M. P. Rinnagel[111], G. Ripellino[164], I. Riu[13], J. C. Rivera Vergara[168], F. Rizatdinova[124], E. Rizvi[96], B. R. Roberts[18a], S. S. Roberts[139], S. H. Robertson[106,x], D. Robinson[33], M. Robles Manzano[102], A. Robson[60], A. Rocchi[77a,77b], C. Roda[75a,75b], S. Rodriguez Bosca[37], Y. Rodriguez Garcia[23a], A. Rodriguez Rodriguez[55], A. M. Rodríguez Vera[118], S. Roe[37], J. T. Roemer[37], A. R. Roepe-Gier[139], O. Røhne[128], R. A. Rojas[105], C. P. A. Roland[130], J. Roloff[30], A. Romaniouk[80], E. Romano[74a,74b], M. Romano[24b], A. C. Romero Hernandez[165], N. Rompotis[94], L. Roos[130], S. Rosati[76a], B. J. Rosser[40], E. Rossi[129], E. Rossi[73a,73b], L. P. Rossi[62], L. Rossini[55], R. Rosten[122], M. Rotaru[28b], B. Rottler[55], C. Rougier[91], D. Rousseau[67], D. Rousso[49], A. Roy[165], S. Roy-Garand[158], A. Rozanov[104], Z. M. A. Rozario[60], Y. Rozen[154], A. Rubio Jimenez[166], A. J. Ruby[94], V. H. Ruelas Rivera[19], T. A. Ruggeri[1], A. Ruggiero[129], A. Ruiz-Martinez[166], A. Rummler[37], Z. Rurikova[55], N. A. Rusakovich[39], H. L. Russell[168], G. Russo[76a,76b], J. P. Rutherfoord[7], S. Rutherford Colmenares[33], M. Rybar[136], E. B. Rye[128], A. Ryzhov[45], J. A. Sabater Iglesias[57], H. F.-W. Sadrozinski[139], F. Safai Tehrani[76a], B. Safarzadeh Samani[137], S. Saha[1], M. Sahinsoy[83], A. Saibel[166], M. Saimpert[138], M. Saito[157], T. Saito[157], A. Sala[72a,72b], D. Salamani[37], A. Salnikov[147], J. Salt[166], A. Salvador Salas[155], D. Salvatore[44a,44b], F. Salvatore[150], A. Salzburger[37], D. Sammel[55], E. Sampson[93], D. Sampsonidis[156,d], D. Sampsonidou[126], J. Sánchez[166], V. Sanchez Sebastian[166], H. Sandaker[128], C. O. Sander[49], J. A. Sandesara[105], M. Sandhoff[174], C. Sandoval[23b],

L. Sanfilippo[64a], D. P. C. Sankey[137], T. Sano[89], A. Sansoni[54], L. Santi[37,76b], C. Santoni[41], H. Santos[133a,133b], A. Santra[172], E. Sanzani[24a,24b], K. A. Saoucha[163], J. G. Saraiva[133a,133d], J. Sardain[7], O. Sasaki[85], K. Sato[160], C. Sauer[64b], E. Sauvan[4], P. Savard[158,ad], R. Sawada[157], C. Sawyer[137], L. Sawyer[99], C. Sbarra[24b], A. Sbrizzi[24a,24b], T. Scanlon[98], J. Schaarschmidt[142], U. Schäfer[102], A. C. Schaffer[45,67], D. Schaile[111], R. D. Schamberger[149], C. Scharf[19], M. M. Schefer[20], V. A. Schegelsky[38], D. Scheirich[136], M. Schernau[162], C. Scheulen[56], C. Schiavi[58a,58b], M. Schioppa[44a,44b], B. Schlag[147], S. Schlenker[37], J. Schmeing[174], M. A. Schmidt[174], K. Schmieden[102], C. Schmitt[102], N. Schmitt[102], S. Schmitt[49], L. Schoeffel[138], A. Schoening[64b], P. G. Scholer[35], E. Schopf[129], M. Schott[25], J. Schovancova[37], S. Schramm[57], T. Schroer[57], H.-C. Schultz-Coulon[64a], M. Schumacher[55], B. A. Schumm[139], Ph. Schune[138], A. J. Schuy[142], H. R. Schwartz[139], A. Schwartzman[147], T. A. Schwarz[108], Ph. Schwemling[138], R. Schwienhorst[109], F. G. Sciacca[20], A. Sciandra[30], G. Sciolla[27], F. Scuri[75a], C. D. Sebastiani[94], K. Sedlaczek[118], S. C. Seidel[115], A. Seiden[139], B. D. Seidlitz[42], C. Seitz[49], J. M. Seixas[84b], G. Sekhniaidze[73a], L. Selem[61], N. Semprini-Cesari[24a,24b], D. Sengupta[57], V. Senthilkumar[166], L. Serin[67], M. Sessa[77a,77b], H. Severini[123], F. Sforza[58a,58b], A. Sfyrla[57], Q. Sha[14], E. Shabalina[56], A. H. Shah[33], R. Shaheen[148], J. D. Shahinian[131], D. Shaked Renous[172], L. Y. Shan[14], M. Shapiro[18a], A. Sharma[37], A. S. Sharma[167], P. Sharma[81], P. B. Shatalov[38], K. Shaw[150], S. M. Shaw[103], Q. Shen[63c], D. J. Sheppard[146], P. Sherwood[98], L. Shi[98], X. Shi[14], S. Shimizu[85], C. O. Shimmin[175], J. D. Shinner[97], I. P. J. Shipsey[129,*], S. Shirabe[90], M. Shiyakova[39,v], M. J. Shochet[40], D. R. Shope[128], B. Shrestha[123], S. Shrestha[122,ag], I. Shreyber[38], M. J. Shroff[168], P. Sicho[134], A. M. Sickles[165], E. Sideras Haddad[34g], A. C. Sidley[117], A. Sidoti[24b], F. Siegert[51], Dj. Sijacki[16], F. Sili[92], J. M. Silva[53], I. Silva Ferreira[84b], M. V. Silva Oliveira[30], S. B. Silverstein[48a], S. Simion[67], R. Simoniello[37], E. L. Simpson[103], H. Simpson[150], L. R. Simpson[108], S. Simsek[83], S. Sindhu[56], P. Sinervo[158], S. Singh[30], S. Sinha[49], S. Sinha[103], M. Sioli[24a,24b], I. Siral[37], E. Sitnikova[49], J. Sjölin[48a,48b], A. Skaf[56], E. Skorda[21], P. Skubic[123], M. Slawinska[88], V. Smakhtin[172], B. H. Smart[137], S.Yu. Smirnov[38], Y. Smirnov[38], L. N. Smirnova[38,a], O. Smirnova[100], A. C. Smith[42], D. R. Smith[162], E. A. Smith[40], J. L. Smith[103], R. Smith[147], M. Smizanska[93], K. Smolek[135], A. A. Snesarev[38], H. L. Snoek[117], S. Snyder[30], R. Sobie[168,x], A. Soffer[155], C. A. Solans Sanchez[37], E.Yu. Soldatov[38], U. Soldevila[166], A. A. Solodkov[38], S. Solomon[27], A. Soloshenko[39], K. Solovieva[55], O. V. Solovyanov[41], P. Sommer[51], A. Sonay[13], W. Y. Song[159b], A. Sopczak[135], A. L. Sopio[53], F. Sopkova[29b], J. D. Sorenson[115], I. R. Sotarriva Alvarez[141], V. Sothilingam[64a], O. J. Soto Sandoval[140b,140c], S. Sottocornola[69], R. Soualah[163], Z. Soumaimi[36e], D. South[49], N. Soybelman[172], S. Spagnolo[71a,71b], M. Spalla[112], D. Sperlich[55], G. Spigo[37], B. Spisso[73a,73b], D. P. Spiteri[60], M. Spousta[136], E. J. Staats[35], R. Stamen[64a], A. Stampekis[21], E. Stanecka[88], W. Stanek-Maslouska[49], M. V. Stange[51], B. Stanislaus[18a], M. M. Stanitzki[49], B. Stapf[49], E. A. Starchenko[38], G. H. Stark[139], J. Stark[91], P. Staroba[134], P. Starovoitov[64a], S. Stärz[106], R. Staszewski[88], G. Stavropoulos[47], A. Stefl[37], P. Steinberg[30], B. Stelzer[146,159a], H. J. Stelzer[132], O. Stelzer-Chilton[159a], H. Stenzel[59], T. J. Stevenson[150], G. A. Stewart[37], J. R. Stewart[124], M. C. Stockton[37], G. Stoicea[28b], M. Stolarski[133a], S. Stonjek[112], A. Straessner[51], J. Strandberg[148], S. Strandberg[48a,48b], M. Stratmann[174], M. Strauss[123], T. Strebler[104], P. Strizenec[29b], R. Ströhmer[169], D. M. Strom[126], R. Stroynowski[45], A. Strubig[48a,48b], S. A. Stucci[30], B. Stugu[17], J. Stupak[123], N. A. Styles[49], D. Su[147], S. Su[63a], W. Su[63d], X. Su[63a], D. Suchy[29a], K. Sugizaki[157], V. V. Sulin[38], M. J. Sullivan[94], D. M. S. Sultan[129], L. Sultanaliyeva[38], S. Sultansoy[3b], T. Sumida[89], S. Sun[173], O. Sunneborn Gudnadottir[164], N. Sur[104], M. R. Sutton[150], H. Suzuki[160], M. Svatos[134], M. Swiatlowski[159a], T. Swirski[169], I. Sykora[29a], M. Sykora[136], T. Sykora[136], D. Ta[102], K. Tackmann[49,u], A. Taffard[162], R. Tafirout[159a], J. S. Tafoya Vargas[67], Y. Takubo[85], M. Talby[104], A. A. Talyshev[38], K. C. Tam[65b], N. M. Tamir[155], A. Tanaka[157], J. Tanaka[157], R. Tanaka[67], M. Tanasini[149], Z. Tao[167], S. Tapia Araya[140f], S. Tapprogge[102], A. Tarek Abouelfadl Mohamed[109], S. Tarem[154], K. Tariq[14], G. Tarna[28b], G. F. Tartarelli[72a], M. J. Tartarin[91], P. Tas[136], M. Tasevsky[134], E. Tassi[44a,44b], A. C. Tate[165], G. Tateno[157], Y. Tayalati[36e,w], G. N. Taylor[107], W. Taylor[159b], R. Teixeira De Lima[147], P. Teixeira-Dias[97], J. J. Teoh[158], K. Terashi[157], J. Terron[101], S. Terzo[13], M. Testa[54], R. J. Teuscher[158,x], A. Thaler[80], O. Theiner[57], T. Theveneaux-Pelzer[104], O. Thielmann[174], D. W. Thomas[97], J. P. Thomas[21], E. A. Thompson[18a], P. D. Thompson[21], E. Thomson[131], R. E. Thornberry[45], C. Tian[63a], Y. Tian[57], V. Tikhomirov[38,a], Yu.A. Tikhonov[38], S. Timoshenko[38], D. Timoshyn[136], E. X. L. Ting[1], P. Tipton[175], A. Tishelman-Charny[30], S. H. Tlou[34g], K. Todome[141], S. Todorova-Nova[136], S. Todt[51], L. Toffolin[70a,70c], M. Togawa[85], J. Tojo[90], S. Tokár[29a], K. Tokushuku[85], O. Toldaiev[69], M. Tomoto[85,113], L. Tompkins[147,l], K. W. Topolnicki[87b], E. Torrence[126], H. Torres[91], E. Torró Pastor[166], M. Toscani[31],

C. Tosciri[40], M. Tost[11], D. R. Tovey[143], I. S. Trandafir[28b], T. Trefzger[169], A. Tricoli[30], I. M. Trigger[159a], S. Trincaz-Duvoid[130], D. A. Trischuk[27], B. Trocmé[61], A. Tropina[39], L. Truong[34c], M. Trzebinski[88], A. Trzupek[88], F. Tsai[149], M. Tsai[108], A. Tsiamis[156], P. V. Tsiareshka[38], S. Tsigaridas[159a], A. Tsirigotis[156,r], V. Tsiskaridze[158], E. G. Tskhadadze[153a], M. Tsopoulou[156], Y. Tsujikawa[89], I. I. Tsukerman[38], V. Tsulaia[18a], S. Tsuno[85], K. Tsuri[121], D. Tsybychev[149], Y. Tu[65b], A. Tudorache[28b], V. Tudorache[28b], A. N. Tuna[62], S. Turchikhin[58a,58b], I. Turk Cakir[3a], R. Turra[72a], T. Turtuvshin[39], P. M. Tuts[42], S. Tzamarias[156,d], E. Tzovara[102], F. Ukegawa[160], P. A. Ulloa Poblete[140b,140c], E. N. Umaka[30], G. Unal[37], A. Undrus[30], G. Unel[162], J. Urban[29b], P. Urrejola[140a], G. Usai[8], R. Ushioda[141], M. Usman[110], F. Ustuner[53], Z. Uysal[83], V. Vacek[135], B. Vachon[106], T. Vafeiadis[37], A. Vaitkus[98], C. Valderanis[111], E. Valdes Santurio[48a,48b], M. Valente[159a], S. Valentinetti[24a,24b], A. Valero[166], E. Valiente Moreno[166], A. Vallier[91], J. A. Valls Ferrer[166], D. R. Van Arneman[117], T. R. Van Daalen[142], A. Van Der Graaf[50], P. Van Gemmeren[6], M. Van Rijnbach[37], S. Van Stroud[98], I. Van Vulpen[117], P. Vana[136], M. Vanadia[77a,77b], U. M. Vande Voorde[148], W. Vandelli[37], E. R. Vandewall[124], D. Vannicola[155], L. Vannoli[54], R. Vari[76a], E. W. Varnes[7], C. Varni[18b], T. Varol[152], D. Varouchas[67], L. Varriale[166], K. E. Varvell[151], M. E. Vasile[28b], L. Vaslin[85], G. A. Vasquez[168], A. Vasyukov[39], L. M. Vaughan[124], R. Vavricka[102], T. Vazquez Schroeder[37], J. Veatch[32], V. Vecchio[103], M. J. Veen[105], I. Veliscek[30], L. M. Veloce[158], F. Veloso[133a,133c], S. Veneziano[76a], A. Ventura[71a,71b], S. Ventura Gonzalez[138], A. Verbytskyi[112], M. Verducci[75a,75b], C. Vergis[96], M. Verissimo De Araujo[84b], W. Verkerke[117], J. C. Vermeulen[117], C. Vernieri[147], M. Vessella[105], M. C. Vetterli[146,ad], A. Vgenopoulos[102], N. Viaux Maira[140f], T. Vickey[143], O. E. Vickey Boeriu[143], G. H. A. Viehhauser[129], L. Vigani[64b], M. Vigl[112], M. Villa[24a,24b], M. Villaplana Perez[166], E. M. Villhauer[53], E. Vilucchi[54], M. G. Vincter[35], A. Visibile[117], C. Vittori[37], I. Vivarelli[24a,24b], E. Voevodina[112], F. Vogel[111], J. C. Voigt[51], P. Vokac[135], Yu. Volkotrub[87b], E. Von Toerne[25], B. Vormwald[37], V. Vorobel[136], K. Vorobev[38], M. Vos[166], K. Voss[145], M. Vozak[117], L. Vozdecky[123], N. Vranjes[16], M. Vranjes Milosavljevic[16], M. Vreeswijk[117], N. K. Vu[63c,63d], R. Vuillermet[37], O. Vujinovic[102], I. Vukotic[40], I. K. Vyas[35], S. Wada[160], C. Wagner[147], J. M. Wagner[18a], W. Wagner[174], S. Wahdan[174], H. Wahlberg[92], C. H. Waits[123], J. Walder[137], R. Walker[111], W. Walkowiak[145], A. Wall[131], E. J. Wallin[100], T. Wamorkar[6], A. Z. Wang[139], C. Wang[102], C. Wang[11], H. Wang[18a], J. Wang[65c], P. Wang[98], R. Wang[62], R. Wang[6], S. M. Wang[152], S. Wang[63b], S. Wang[14], T. Wang[63a], W. T. Wang[81], W. Wang[14], X. Wang[114a], X. Wang[165], X. Wang[63c], Y. Wang[63d], Y. Wang[114a], Y. Wang[63a], Z. Wang[108], Z. Wang[52,63c,63d], Z. Wang[108], A. Warburton[106], R. J. Ward[21], N. Warrack[60], S. Waterhouse[97], A. T. Watson[21], H. Watson[53], M. F. Watson[21], E. Watton[60,137], G. Watts[142], B. M. Waugh[98], J. M. Webb[55], C. Weber[30], H. A. Weber[19], M. S. Weber[20], S. M. Weber[64a], C. Wei[63a], Y. Wei[55], A. R. Weidberg[129], E. J. Weik[120], J. Weingarten[50], C. Weiser[55], C. J. Wells[49], T. Wenaus[30], B. Wendland[50], T. Wengler[37], N. S. Wenke[112], N. Wermes[25], M. Wessels[64a], A. M. Wharton[93], A. S. White[62], A. White[8], M. J. White[1], D. Whiteson[162], L. Wickremasinghe[127], W. Wiedenmann[173], M. Wielers[137], C. Wiglesworth[43], D. J. Wilbern[123], H. G. Wilkens[37], J. J. H. Wilkinson[33], D. M. Williams[42], H. H. Williams[131], S. Williams[33], S. Willocq[105], B. J. Wilson[103], P. J. Windischhofer[40], F. I. Winkel[31], F. Winklmeier[126], B. T. Winter[55], J. K. Winter[103], M. Wittgen[147], M. Wobisch[99], T. Wojtkowski[61], Z. Wolffs[117], J. Wollrath[162], M. W. Wolter[88], H. Wolters[133a,133c], M. C. Wong[139], E. L. Woodward[42], S. D. Worm[49], B. K. Wosiek[88], K. W. Woźniak[88], S. Wozniewski[56], K. Wraight[60], C. Wu[21], M. Wu[114b], M. Wu[116], S. L. Wu[173], X. Wu[57], Y. Wu[63a], Z. Wu[4], J. Wuerzinger[112,ab], T. R. Wyatt[103], B. M. Wynne[53], S. Xella[43], L. Xia[114a], M. Xia[15], M. Xie[63a], S. Xin[14,114c], A. Xiong[126], J. Xiong[18a], D. Xu[14], H. Xu[63a], L. Xu[63a], R. Xu[131], T. Xu[108], Y. Xu[15], Z. Xu[53], Z. Xu[114a], B. Yabsley[151], S. Yacoob[34a], Y. Yamaguchi[85], E. Yamashita[157], H. Yamauchi[160], T. Yamazaki[18a], Y. Yamazaki[86], S. Yan[60], Z. Yan[105], H. J. Yang[63c,63d], H. T. Yang[63a], S. Yang[63a], T. Yang[65c], X. Yang[37], X. Yang[14], Y. Yang[45], Y. Yang[63a], Z. Yang[63a], W.-M. Yao[18a], H. Ye[114a], H. Ye[56], J. Ye[14], S. Ye[30], X. Ye[63a], Y. Yeh[98], I. Yeletskikh[39], B. Yeo[18b], M. R. Yexley[98], T. P. Yildirim[129], P. Yin[42], K. Yorita[171], S. Younas[28b], C. J. S. Young[37], C. Young[147], C. Yu[14,114c], Y. Yu[63a], J. Yuan[14,114c], M. Yuan[108], R. Yuan[63c,63d], L. Yue[98], M. Zaazoua[63a], B. Zabinski[88], E. Zaid[53], Z. K. Zak[88], T. Zakareishvili[166], S. Zambito[57], J. A. Zamora Saa[140b,140d], J. Zang[157], D. Zanzi[55], O. Zaplatilek[135], C. Zeitnitz[174], H. Zeng[14], J. C. Zeng[165], D. T. Zenger Jr[27], O. Zenin[38], T. Ženiš[29a], S. Zenz[96], S. Zerradi[36a], D. Zerwas[67], M. Zhai[14,114c], D. F. Zhang[143], J. Zhang[63b], J. Zhang[6], K. Zhang[14,114c], L. Zhang[63a], L. Zhang[114a], P. Zhang[14,114c], R. Zhang[173], S. Zhang[108], S. Zhang[91], T. Zhang[157], X. Zhang[63c], X. Zhang[63b], Y. Zhang[142], Y. Zhang[98], Y. Zhang[114a], Z. Zhang[18a], Z. Zhang[63b], Z. Zhang[67], H. Zhao[142], T. Zhao[63b], Y. Zhao[139], Z. Zhao[63a], Z. Zhao[63a], A. Zhemchugov[39], J. Zheng[114a],

K. Zheng[165], X. Zheng[63a], Z. Zheng[147], D. Zhong[165], B. Zhou[108], H. Zhou[7], N. Zhou[63c], Y. Zhou[15], Y. Zhou[114a], Y. Zhou[7], C. G. Zhu[63b], J. Zhu[108], X. Zhu[63d], Y. Zhu[63c], Y. Zhu[63a], X. Zhuang[14], K. Zhukov[69], N. I. Zimine[39], J. Zinsser[64b], M. Ziolkowski[145], L. Živković[16], A. Zoccoli[24a,24b], K. Zoch[62], T. G. Zorbas[143], O. Zormpa[47], W. Zou[42], L. Zwalinski[37]

[1] Department of Physics, University of Adelaide, Adelaide, Australia
[2] Department of Physics, University of Alberta, Edmonton, AB, Canada
[3] [(a)]Department of Physics, Ankara University, Ankara, Türkiye; [(b)]Division of Physics, TOBB University of Economics and Technology, Ankara, Türkiye
[4] LAPP, CNRS/IN2P3, Université Savoie Mont Blanc, Annecy, France
[5] APC, CNRS/IN2P3, Université Paris Cité, Paris, France
[6] High Energy Physics Division, Argonne National Laboratory, Argonne, IL, USA
[7] Department of Physics, University of Arizona, Tucson, AZ, USA
[8] Department of Physics, University of Texas at Arlington, Arlington, TX, USA
[9] Physics Department, National and Kapodistrian University of Athens, Athens, Greece
[10] Physics Department, National Technical University of Athens, Zografou, Greece
[11] Department of Physics, University of Texas at Austin, Austin, TX, USA
[12] Institute of Physics, Azerbaijan Academy of Sciences, Baku, Azerbaijan
[13] Institut de Física d'Altes Energies (IFAE), Barcelona Institute of Science and Technology, Barcelona, Spain
[14] Institute of High Energy Physics, Chinese Academy of Sciences, Beijing, China
[15] Physics Department, Tsinghua University, Beijing, China
[16] Institute of Physics, University of Belgrade, Belgrade, Serbia
[17] Department for Physics and Technology, University of Bergen, Bergen, Norway
[18] [(a)]Physics Division, Lawrence Berkeley National Laboratory, Berkeley, CA, USA; [(b)]University of California, Berkeley, CA, USA
[19] Institut für Physik, Humboldt Universität zu Berlin, Berlin, Germany
[20] Albert Einstein Center for Fundamental Physics and Laboratory for High Energy Physics, University of Bern, Bern, Switzerland
[21] School of Physics and Astronomy, University of Birmingham, Birmingham, UK
[22] [(a)]Department of Physics, Bogazici University, Istanbul, Türkiye; [(b)]Department of Physics Engineering, Gaziantep University, Gaziantep, Türkiye; [(c)]Department of Physics, Istanbul University, Istanbul, Türkiye
[23] [(a)]Facultad de Ciencias y Centro de Investigaciónes, Universidad Antonio Nariño, Bogotá, Colombia; [(b)]Departamento de Física, Universidad Nacional de Colombia, Bogotá, Colombia
[24] [(a)]Dipartimento di Fisica e Astronomia A. Righi, Università di Bologna, Bologna, Italy; [(b)]INFN Sezione di Bologna, Bologna, Italy
[25] Physikalisches Institut, Universität Bonn, Bonn, Germany
[26] Department of Physics, Boston University, Boston, MA, USA
[27] Department of Physics, Brandeis University, Waltham, MA, USA
[28] [(a)]Transilvania University of Brasov, Brasov, Romania; [(b)]Horia Hulubei National Institute of Physics and Nuclear Engineering, Bucharest, Romania; [(c)]Department of Physics, Alexandru Ioan Cuza University of Iasi, Iasi, Romania; [(d)]National Institute for Research and Development of Isotopic and Molecular Technologies, Physics Department, Cluj-Napoca, Romania; [(e)]National University of Science and Technology Politechnica, Bucharest, Romania; [(f)]West University in Timisoara, Timisoara, Romania; [(g)]Faculty of Physics, University of Bucharest, Bucharest, Romania
[29] [(a)]Faculty of Mathematics, Physics and Informatics, Comenius University, Bratislava, Slovakia; [(b)]Department of Subnuclear Physics, Institute of Experimental Physics of the Slovak Academy of Sciences, Kosice, Slovak Republic
[30] Physics Department, Brookhaven National Laboratory, Upton, NY, USA
[31] Universidad de Buenos Aires, Facultad de Ciencias Exactas y Naturales, Departamento de Física, y CONICET, Instituto de Física de Buenos Aires (IFIBA), Buenos Aires, Argentina
[32] California State University, Los Angeles, CA, USA
[33] Cavendish Laboratory, University of Cambridge, Cambridge, UK
[34] [(a)]Department of Physics, University of Cape Town, Cape Town, South Africa; [(b)]iThemba Labs, Western Cape, South Africa; [(c)]Department of Mechanical Engineering Science, University of Johannesburg, Johannesburg,

South Africa; [d]National Institute of Physics, University of the Philippines Diliman (Philippines), Quezon City, Philippines; [e]University of South Africa, Department of Physics, Pretoria, South Africa; [f]University of Zululand, KwaDlangezwa, South Africa; [g]School of Physics, University of the Witwatersrand, Johannesburg, South Africa
[35] Department of Physics, Carleton University, Ottawa, ON, Canada
[36] [a]Faculté des Sciences Ain Chock, Université Hassan II de Casablanca, Casablanca, Morocco; [b]Faculté des Sciences, Université Ibn-Tofail, Kenitra, Morocco; [c]Faculté des Sciences Semlalia, LPHEA-Marrakech, Université Cadi Ayyad, Marrakech, Morocco; [d]LPMR, Faculté des Sciences, Université Mohamed Premier, Oujda, Morocco; [e]Faculté des sciences, Université Mohammed V, Rabat, Morocco; [f]Institute of Applied Physics, Mohammed VI Polytechnic University, Ben Guerir, Morocco
[37] CERN, Geneva, Switzerland
[38] Affiliated with an Institute Covered by a Cooperation Agreement with CERN, Geneva, Switzerland
[39] Affiliated with an International Laboratory Covered by a Cooperation Agreement with CERN, Geneva, Switzerland
[40] Enrico Fermi Institute, University of Chicago, Chicago, IL, USA
[41] LPC, CNRS/IN2P3, Université Clermont Auvergne, Clermont-Ferrand, France
[42] Nevis Laboratory, Columbia University, Irvington, NY, USA
[43] Niels Bohr Institute, University of Copenhagen, Copenhagen, Denmark
[44] [a]Dipartimento di Fisica, Università della Calabria, Rende, Italy; [b]INFN Gruppo Collegato di Cosenza, Laboratori Nazionali di Frascati, Cosenza, Italy
[45] Physics Department, Southern Methodist University, Dallas, TX, USA
[46] Physics Department, University of Texas at Dallas, Richardson, TX, USA
[47] National Centre for Scientific Research "Demokritos", Agia Paraskevi, Greece
[48] [a]Department of Physics, Stockholm University, Stockholm, Sweden; [b]Oskar Klein Centre, Stockholm, Sweden
[49] Deutsches Elektronen-Synchrotron DESY, Hamburg and Zeuthen, Germany
[50] Fakultät Physik , Technische Universität Dortmund, Dortmund, Germany
[51] Institut für Kern- und Teilchenphysik, Technische Universität Dresden, Dresden, Germany
[52] Department of Physics, Duke University, Durham, NC, USA
[53] SUPA-School of Physics and Astronomy, University of Edinburgh, Edinburgh, UK
[54] INFN e Laboratori Nazionali di Frascati, Frascati, Italy
[55] Physikalisches Institut, Albert-Ludwigs-Universität Freiburg, Freiburg, Germany
[56] II. Physikalisches Institut, Georg-August-Universität Göttingen, Göttingen, Germany
[57] Département de Physique Nucléaire et Corpusculaire, Université de Genève, Geneva, Switzerland
[58] [a]Dipartimento di Fisica, Università di Genova, Genoa, Italy; [b]INFN Sezione di Genova, Genoa, Italy
[59] II. Physikalisches Institut, Justus-Liebig-Universität Giessen, Giessen, Germany
[60] SUPA-School of Physics and Astronomy, University of Glasgow, Glasgow, UK
[61] LPSC, Université Grenoble Alpes, CNRS/IN2P3, Grenoble INP, Grenoble, France
[62] Laboratory for Particle Physics and Cosmology, Harvard University, Cambridge, MA, USA
[63] [a]Department of Modern Physics and State Key Laboratory of Particle Detection and Electronics, University of Science and Technology of China, Hefei, China; [b]Institute of Frontier and Interdisciplinary Science and Key Laboratory of Particle Physics and Particle Irradiation (MOE), Shandong University, Qingdao, China; [c]School of Physics and Astronomy, Key Laboratory for Particle Astrophysics and Cosmology (MOE), Shanghai Jiao Tong University, SKLPPC, Shanghai, China; [d]Tsung-Dao Lee Institute, Shanghai, China; [e]School of Physics, Zhengzhou University, Zhengzhou, China
[64] [a]Kirchhoff-Institut für Physik, Ruprecht-Karls-Universität Heidelberg, Heidelberg, Germany; [b]Physikalisches Institut, Ruprecht-Karls-Universität Heidelberg, Heidelberg, Germany
[65] [a]Department of Physics, Chinese University of Hong Kong, Shatin, N.T., Hong Kong, China; [b]Department of Physics, University of Hong Kong, Pok Fu Lam, Hong Kong, China; [c]Department of Physics and Institute for Advanced Study, Hong Kong University of Science and Technology, Clear Water Bay, Kowloon, Hong Kong, China
[66] Department of Physics, National Tsing Hua University, Hsinchu, Taiwan
[67] IJCLab, CNRS/IN2P3, Université Paris-Saclay, 91405 Orsay, France
[68] Centro Nacional de Microelectrónica (IMB-CNM-CSIC), Barcelona, Spain
[69] Department of Physics, Indiana University, Bloomington, IN, USA
[70] [a]INFN Gruppo Collegato di Udine, Sezione di Trieste, Udine, Italy; [b]ICTP, Trieste, Italy; [c]Dipartimento Politecnico di Ingegneria e Architettura, Università di Udine, Udine, Italy

[71] [(a)]INFN Sezione di Lecce, Lecce, Italy; [(b)]Dipartimento di Matematica e Fisica, Università del Salento, Lecce, Italy
[72] [(a)]INFN Sezione di Milano, Milan, Italy; [(b)]Dipartimento di Fisica, Università di Milano, Milan, Italy
[73] [(a)]INFN Sezione di Napoli, Naples, Italy; [(b)]Dipartimento di Fisica, Università di Napoli, Naples, Italy
[74] [(a)]INFN Sezione di Pavia, Pavia, Italy; [(b)]Dipartimento di Fisica, Università di Pavia, Pavia, Italy
[75] [(a)]INFN Sezione di Pisa, Pisa, Italy; [(b)]Dipartimento di Fisica E. Fermi, Università di Pisa, Pisa, Italy
[76] [(a)]INFN Sezione di Roma, Rome, Italy; [(b)]Dipartimento di Fisica, Sapienza Università di Roma, Rome, Italy
[77] [(a)]INFN Sezione di Roma Tor Vergata, Rome, Italy; [(b)]Dipartimento di Fisica, Università di Roma Tor Vergata, Rome, Italy
[78] [(a)]INFN Sezione di Roma Tre, Rome, Italy; [(b)]Dipartimento di Matematica e Fisica, Università Roma Tre, Rome, Italy
[79] [(a)]INFN-TIFPA, Povo, Italy; [(b)]Università degli Studi di Trento, Trento, Italy
[80] Universität Innsbruck, Department of Astro and Particle Physics, Innsbruck, Austria
[81] University of Iowa, Iowa City, IA, USA
[82] Department of Physics and Astronomy, Iowa State University, Ames, IA, USA
[83] Istinye University, Sariyer, Istanbul, Türkiye
[84] [(a)]Departamento de Engenharia Elétrica, Universidade Federal de Juiz de Fora (UFJF), Juiz de Fora, Brazil; [(b)]Universidade Federal do Rio De Janeiro COPPE/EE/IF, Rio de Janeiro, Brazil; [(c)]Instituto de Física, Universidade de São Paulo, São Paulo, Brazil; [(d)]Rio de Janeiro State University, Rio de Janeiro, Brazil; [(e)]Federal University of Bahia, Bahia, Brazil
[85] KEK, High Energy Accelerator Research Organization, Tsukuba, Japan
[86] Graduate School of Science, Kobe University, Kobe, Japan
[87] [(a)]AGH University of Krakow, Faculty of Physics and Applied Computer Science, Kraków, Poland; [(b)]Marian Smoluchowski Institute of Physics, Jagiellonian University, Kraków, Poland
[88] Institute of Nuclear Physics Polish Academy of Sciences, Kraków, Poland
[89] Faculty of Science, Kyoto University, Kyoto, Japan
[90] Research Center for Advanced Particle Physics and Department of Physics, Kyushu University, Fukuoka , Japan
[91] L2IT, CNRS/IN2P3, UPS, Université de Toulouse, Toulouse, France
[92] Instituto de Física La Plata, Universidad Nacional de La Plata and CONICET, La Plata, Argentina
[93] Physics Department, Lancaster University, Lancaster, UK
[94] Oliver Lodge Laboratory, University of Liverpool, Liverpool, UK
[95] Department of Experimental Particle Physics, Jožef Stefan Institute and Department of Physics, University of Ljubljana, Ljubljana, Slovenia
[96] School of Physics and Astronomy, Queen Mary University of London, London, UK
[97] Department of Physics, Royal Holloway University of London, Egham, UK
[98] Department of Physics and Astronomy, University College London, London, UK
[99] Louisiana Tech University, Ruston, LA, USA
[100] Fysiska institutionen, Lunds universitet, Lund, Sweden
[101] Departamento de Física Teorica C-15 and CIAFF, Universidad Autónoma de Madrid, Madrid, Spain
[102] Institut für Physik, Universität Mainz, Mainz, Germany
[103] School of Physics and Astronomy, University of Manchester, Manchester, UK
[104] CPPM, CNRS/IN2P3, Aix-Marseille Université, Marseille, France
[105] Department of Physics, University of Massachusetts, Amherst, MA, USA
[106] Department of Physics, McGill University, Montreal, QC, Canada
[107] School of Physics, University of Melbourne, Victoria, Australia
[108] Department of Physics, University of Michigan, Ann Arbor, MI, USA
[109] Department of Physics and Astronomy, Michigan State University, East Lansing, MI, USA
[110] Group of Particle Physics, University of Montreal, Montreal, QC, Canada
[111] Fakultät für Physik, Ludwig-Maximilians-Universität München, Munich, Germany
[112] Max-Planck-Institut für Physik (Werner-Heisenberg-Institut), Munich, Germany
[113] Graduate School of Science and Kobayashi-Maskawa Institute, Nagoya University, Nagoya, Japan
[114] [(a)]Department of Physics, Nanjing University, Nanjing, China; [(b)]School of Science, Shenzhen Campus of Sun Yat-sen University, Guangzhou, China; [(c)]University of Chinese Academy of Science (UCAS), Beijing, China
[115] Department of Physics and Astronomy, University of New Mexico, Albuquerque, NM, USA
[116] Institute for Mathematics, Astrophysics and Particle Physics, Radboud University/Nikhef, Nijmegen, Netherlands

[117] Nikhef National Institute for Subatomic Physics and University of Amsterdam, Amsterdam, Netherlands
[118] Department of Physics, Northern Illinois University, DeKalb, IL, USA
[119] [(a)]New York University Abu Dhabi, Abu Dhabi, United Arab Emirates; [(b)]United Arab Emirates University, Al Ain, United Arab Emirates
[120] Department of Physics, New York University, New York, NY, USA
[121] Ochanomizu University, Otsuka, Bunkyo-ku, Tokyo, Japan
[122] Ohio State University, Columbus, OH, USA
[123] Homer L. Dodge Department of Physics and Astronomy, University of Oklahoma, Norman, OK, USA
[124] Department of Physics, Oklahoma State University, Stillwater, OK, USA
[125] Joint Laboratory of Optics, Palacký University, Olomouc, Czech Republic
[126] Institute for Fundamental Science, University of Oregon, Eugene, OR, USA
[127] Graduate School of Science, Osaka University, Osaka, Japan
[128] Department of Physics, University of Oslo, Oslo, Norway
[129] Department of Physics, Oxford University, Oxford, UK
[130] LPNHE, CNRS/IN2P3, Sorbonne Université, Université Paris Cité, Paris, France
[131] Department of Physics, University of Pennsylvania, Philadelphia, PA, USA
[132] Department of Physics and Astronomy, University of Pittsburgh, Pittsburgh, PA, USA
[133] [(a)]Laboratório de Instrumentação e Física Experimental de Partículas-LIP, Lisbon, Portugal; [(b)]Departamento de Física, Faculdade de Ciências, Universidade de Lisboa, Lisbon, Portugal; [(c)]Departamento de Física, Universidade de Coimbra, Coimbra, Portugal; [(d)]Centro de Física Nuclear da Universidade de Lisboa, Lisbon, Portugal; [(e)]Departamento de Física, Universidade do Minho, Braga, Portugal; [(f)]Departamento de Física Teórica y del Cosmos, Universidad de Granada, Granada, Spain; [(g)]Departamento de Física, Instituto Superior Técnico, Universidade de Lisboa, Lisbon, Portugal
[134] Institute of Physics of the Czech Academy of Sciences, Prague, Czech Republic
[135] Czech Technical University in Prague, Prague, Czech Republic
[136] Charles University, Faculty of Mathematics and Physics, Prague, Czech Republic
[137] Particle Physics Department, Rutherford Appleton Laboratory, Didcot, UK
[138] IRFU, CEA, Université Paris-Saclay, Gif-sur-Yvette, France
[139] Santa Cruz Institute for Particle Physics, University of California Santa Cruz, Santa Cruz, CA, USA
[140] [(a)]Departamento de Física, Pontificia Universidad Católica de Chile, Santiago, Chile; [(b)]Millennium Institute for Subatomic physics at high energy frontier (SAPHIR), Santiago, Chile; [(c)]Instituto de Investigación Multidisciplinario en Ciencia y Tecnología y Departamento de Física, Universidad de La Serena, La Serena, Chile; [(d)]Department of Physics, Universidad Andres Bello, Santiago, Chile; [(e)]Instituto de Alta Investigación, Universidad de Tarapacá, Arica, Chile; [(f)]Departamento de Física, Universidad Técnica Federico Santa María, Valparaiso, Chile
[141] Department of Physics, Institute of Science, Tokyo, Japan
[142] Department of Physics, University of Washington, Seattle, WA, USA
[143] Department of Physics and Astronomy, University of Sheffield, Sheffield, UK
[144] Department of Physics, Shinshu University, Nagano, Japan
[145] Department Physik, Universität Siegen, Siegen, Germany
[146] Department of Physics, Simon Fraser University, Burnaby, BC, Canada
[147] SLAC National Accelerator Laboratory, Stanford, CA, USA
[148] Department of Physics, Royal Institute of Technology, Stockholm, Sweden
[149] Departments of Physics and Astronomy, Stony Brook University, Stony Brook, NY, USA
[150] Department of Physics and Astronomy, University of Sussex, Brighton, UK
[151] School of Physics, University of Sydney, Sydney, Australia
[152] Institute of Physics, Academia Sinica, Taipei, Taiwan
[153] [(a)]E. Andronikashvili Institute of Physics, Iv. Javakhishvili Tbilisi State University, Tbilisi, Georgia; [(b)]High Energy Physics Institute, Tbilisi State University, Tbilisi, Georgia; [(c)]University of Georgia, Tbilisi, Georgia
[154] Department of Physics, Technion, Israel Institute of Technology, Haifa, Israel
[155] Raymond and Beverly Sackler School of Physics and Astronomy, Tel Aviv University, Tel Aviv, Israel
[156] Department of Physics, Aristotle University of Thessaloniki, Thessaloníki, Greece
[157] International Center for Elementary Particle Physics and Department of Physics, University of Tokyo, Tokyo, Japan
[158] Department of Physics, University of Toronto, Toronto, ON, Canada
[159] [(a)]TRIUMF, Vancouver, BC, Canada; [(b)]Department of Physics and Astronomy, York University, Toronto, ON, Canada

[160] Division of Physics and Tomonaga Center for the History of the Universe, Faculty of Pure and Applied Sciences, University of Tsukuba, Tsukuba, Japan
[161] Department of Physics and Astronomy, Tufts University, Medford, MA, USA
[162] Department of Physics and Astronomy, University of California Irvine, Irvine, CA, USA
[163] University of Sharjah, Sharjah, United Arab Emirates
[164] Department of Physics and Astronomy, University of Uppsala, Uppsala, Sweden
[165] Department of Physics, University of Illinois, Urbana, IL, USA
[166] Instituto de Física Corpuscular (IFIC), Centro Mixto Universidad de Valencia-CSIC, Valencia, Spain
[167] Department of Physics, University of British Columbia, Vancouver, BC, Canada
[168] Department of Physics and Astronomy, University of Victoria, Victoria, BC, Canada
[169] Fakultät für Physik und Astronomie, Julius-Maximilians-Universität Würzburg, Würzburg, Germany
[170] Department of Physics, University of Warwick, Coventry, UK
[171] Waseda University, Tokyo, Japan
[172] Department of Particle Physics and Astrophysics, Weizmann Institute of Science, Rehovot, Israel
[173] Department of Physics, University of Wisconsin, Madison, WI, USA
[174] Fakultät für Mathematik und Naturwissenschaften, Fachgruppe Physik, Bergische Universität Wuppertal, Wuppertal, Germany
[175] Department of Physics, Yale University, New Haven, CT, USA
[176] Yerevan Physics Institute, Yerevan, Armenia

[a] Also Affiliated with an Institute Covered by a Cooperation Agreement with CERN, Geneva, Switzerland
[b] Also at An-Najah National University, Nablus, Palestine
[c] Also at Borough of Manhattan Community College, City University of New York, New York, NY, USA
[d] Also at Center for Interdisciplinary Research and Innovation (CIRI-AUTH), Thessaloníki, Greece
[e] Also at CERN, Geneva, Switzerland
[f] Also at CMD-AC UNEC Research Center, Azerbaijan State University of Economics (UNEC), Baku, Azerbaijan
[g] Also at Département de Physique Nucléaire et Corpusculaire, Université de Genève, Geneva, Switzerland
[h] Also at Departament de Fisica de la Universitat Autonoma de Barcelona, Barcelona, Spain
[i] Also at Department of Financial and Management Engineering, University of the Aegean, Chios, Greece
[j] Also at Department of Physics, California State University, Sacramento, USA
[k] Also at Department of Physics, King's College London, London, UK
[l] Also at Department of Physics, Stanford University, Stanford, CA, USA
[m] Also at Department of Physics, Stellenbosch University, Stellenbosch, South Africa
[n] Also at Department of Physics, University of Fribourg, Fribourg, Switzerland
[o] Also at Department of Physics, University of Thessaly, Thessaly, Greece
[p] Also at Department of Physics, Westmont College, Santa Barbara, USA
[q] Also at Faculty of Physics, Sofia University, 'St. Kliment Ohridski', Sofia, Bulgaria
[r] Also at Hellenic Open University, Patras, Greece
[s] Also at Imam Mohammad Ibn Saud Islamic University, Riyadh, Saudi Arabia
[t] Also at Institucio Catalana de Recerca i Estudis Avancats, ICREA, Barcelona, Spain
[u] Also at Institut für Experimentalphysik, Universität Hamburg, Hamburg, Germany
[v] Also at Institute for Nuclear Research and Nuclear Energy (INRNE) of the Bulgarian Academy of Sciences, Sofia, Bulgaria
[w] Also at Institute of Applied Physics, Mohammed VI Polytechnic University, Ben Guerir, Morocco
[x] Also at Institute of Particle Physics (IPP), Ottawa, Canada
[y] Also at Institute of Physics, Azerbaijan Academy of Sciences, Baku, Azerbaijan
[z] Also at Institute of Theoretical Physics, Ilia State University, Tbilisi, Georgia
[aa] Also at National Institute of Physics, University of the Philippines Diliman (Philippines), Quezon City, Philippines
[ab] Also at Technical University of Munich, Munich, Germany
[ac] Also at The Collaborative Innovation Center of Quantum Matter (CICQM), Beijing, China
[ad] Also at TRIUMF, Vancouver, BC, Canada
[ae] Also at Università di Napoli Parthenope, Naples, Italy
[af] Also at Department of Physics, University of Colorado Boulder, Colorado, USA

[ag] Also at Washington College, Chestertown, MD, USA
[ah] Also at Physics Department, Yeditepe University, Istanbul, Türkiye
* Deceased

Published for SISSA by Springer

Received: *August 21, 2025*
Accepted: *September 15, 2025*
Published: *October 10, 2025*

Search for the production of a Higgs boson in association with a single top quark in pp collisions at $\sqrt{s} = 13$ TeV with the ATLAS detector

The ATLAS collaboration

E-mail: atlas.publications@cern.ch

Abstract: A search for the production of a Higgs boson in association with a single top quark, tH, is presented. The analysis uses proton-proton collision data corresponding to an integrated luminosity of 140 fb^{-1} at a centre-of-mass energy of 13 TeV, collected by the ATLAS detector at the LHC. The search targets Higgs-boson decays into $b\bar{b}$, WW^*, ZZ^*, and $\tau\tau$, accompanied by an isolated lepton (electron or muon) from the top-quark decay. Multivariate techniques are employed to enhance the separation between signal and background processes. The observed signal strength, μ_{tH}, defined as the ratio between the measured cross-section and the predicted Standard Model value, is $\mu_{tH} = 8.1 \pm 2.6\,(\text{stat.}) \pm 2.0\,(\text{syst.})$. The significance of the observed (expected) signal above the background-only expectation is 2.8 (0.4) standard deviations. The corresponding observed (expected) upper limit at the 95% confidence level on the tH cross-section is found to be 13.9 (6.1) times the value predicted by the Standard Model. An interpretation with an inverted sign of the top-quark Yukawa coupling is performed, and the signal strength and corresponding limit are reported.

Keywords: Hadron-Hadron Scattering

ArXiv ePrint: 2508.14695

https://doi.org/10.1007/JHEP10(2025)093

JHEP10(2025)093

Contents

1 Introduction

The discovery of a particle with properties consistent with the Higgs boson [1, 2] of the Standard Model (SM) in 2012 by the ATLAS and CMS experiments [3, 4] opened a new field of exploration in the realm of particle physics. Studying the Higgs-boson couplings is essential to test whether the observed particle corresponds to the Higgs boson predicted

JHEP10(2025)093

by the SM. In the SM, the strength of these interactions with other elementary particles is proportional to their masses (or masses squared).

Specifically, the Higgs boson interacts with fermions via Yukawa couplings [5]. Among these, the Yukawa coupling to the top quark, y_t, is of special interest as it is the largest with a value close to unity. Given its large value, y_t plays a crucial role in radiative corrections to the Higgs potential [6, 7], influencing the shape of the potential and, consequently, the stability of the electroweak (EW) vacuum [8]. In addition, it significantly affects the running of SM parameters, impacting the scale at which new physics might appear [7]. For all these reasons the Yukawa coupling of the Higgs boson to the top quark is considered a good probe for new physics. In particular, the study of its charge-conjugation and parity (CP) properties could provide insight into the observed baryon asymmetry of the universe [9–11].

The magnitude of y_t can be determined indirectly from Higgs-boson production via a top-quark loop or directly through cross-section measurements of top-quark pair production in association with a Higgs boson ($t\bar{t}H$). The $t\bar{t}H$ production process was observed [12, 13] in 2018. The production cross-section of the Higgs boson in association with a single top quark is sensitive to both the magnitude of y_t and its sign [14–18]. While the sign of y_t is not defined in an absolute sense, it is instead defined relative to the coupling strength of the W boson to the Higgs boson. In the following, this relative-sign convention is adopted throughout, and the sign of y_t is referred to accordingly, without explicitly restating its dependence on the W-boson coupling. Measurements of Higgs-boson processes conducted by the ATLAS and CMS Collaborations, such as the Higgs-boson decay into photon pairs ($H \to \gamma\gamma$) [19, 20], provide insight into the sign of the y_t coupling. Similar information comes from the combination of other Higgs-boson measurements. These include the simplified template cross-section (STXS) combination for gluon-gluon fusion (ggF), vector-boson fusion (VBF), and associated production with vector bosons (VH, where V refers to the W and Z bosons) or $t\bar{t}H$ in different decay channels [21, 22]. These measurements probe indirect effects in loop interactions and currently disfavour a negative value of the coupling [23], under the assumption that only SM particles contribute to the loops.

Higgs-boson production in association with a single top quark occurs via the EW interaction through three distinct production modes: t-channel (tHq), tWH and s-channel [24, 25]. The main production mode in proton-proton (pp) collisions at the Large Hadron Collider (LHC) [26] is the tHq process, followed by the associated tWH process and the s-channel. In this paper, the tHq and tWH processes are collectively referred to as tH production and are the ones used for the measurements presented, while s-channel production is neglected due to its extremely low production cross-section (3% of the total tH cross-section).

In the tHq process, an incoming light-flavour quark (i.e. up-type quark or down-type antiquark) from one of the colliding protons interacts with a b-quark by exchanging a space-like virtual W boson. The origin of the b-quark depends on the flavour scheme (FS) used in the calculation: in the five-flavour scheme (5FS), it is treated as a massless parton originating from the proton sea, while in the four-flavour scheme (4FS), where b-quarks are not included in the proton parton distribution functions (PDFs), it arises from gluon splitting into a $b\bar{b}$ pair [27–29]. In the tWH process, a gluon from one of the protons interacts with a b-quark from the other proton or from gluon splitting, via the exchange of a time-like virtual top

JHEP10(2025)093

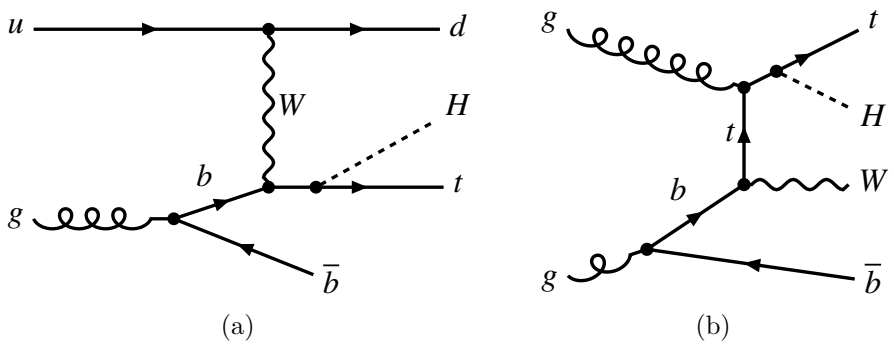

Figure 1. Representative dominant Feynman diagrams for (a) tHq and (b) tWH production at LO, in the 4FS. The tHq event topology (a) is characterised by two heavy objects, the top quark and the Higgs boson plus an energetic light-flavour quark (dominantly a u-quark), referred to as the spectator quark, and an extra soft b-quark from gluon splitting. The tWH event topology (b) is characterised by three heavy objects, the top quark, the Higgs boson and a W boson and an extra soft b-quark from gluon splitting.

quark t. Two examples of dominant leading-order (LO) Feynman diagrams for the tHq and tWH processes, both in the 4FS, are shown in figure 1.

Under the SM hypothesis ($\kappa_t = y_t/y_t^{\mathrm{SM}} = +1$), the interference between diagrams in which the Higgs boson couples to the top quark and those where it couples to the W boson is destructive, leading to a strongly suppressed cross-section. In contrast, in scenarios beyond the SM, such as those involving CP-even and CP-odd admixtures in the top-quark Yukawa coupling structure, the relative sign between the Higgs-boson couplings to the top quark and the W boson can be altered, enhancing the tH cross-section up to an order of magnitude [24, 25]. The maximum enhancement occurs when $\kappa_t = -1$, corresponding to fully constructive interference between the contributing diagrams.

The tHq event topology is characterised by two heavy objects, a top quark and a Higgs boson, which is radiated from the latter, plus an energetic light-flavour quark (dominantly a u- or $\bar{d}$-quark), known as the spectator quark, and an extra soft b-quark from gluon splitting. The top-quark and Higgs-boson systems are produced in the central part of the detector recoiling against each other. The production of tWH is characterised by three heavy objects, the top quark, a W boson, a Higgs boson that is radiated from one of these two particles and an extra soft b-quark from gluon splitting. This event topology closely resembles $t\bar{t}H$ production and has an identical final state.

The CMS Collaboration searched for $tHq + tWH$ production in pp collisions at a centre-of-mass energy of $\sqrt{s} = 13\,\mathrm{TeV}$ with an integrated luminosity of $35.9\,\mathrm{fb}^{-1}$ [30]. The observed cross-section limits are 1.94 pb for the SM and 0.74 pb for the inverted top-quark Yukawa coupling (ITC) (i.e. $\mathrm{sign}(y_t) = \kappa_t = -1$) hypothesis. More recently, using the full Run-2 dataset, the CMS Collaboration reported updated $t\bar{t}H$ and $tHq + tWH$ results in the multi-lepton and $b\bar{b}$ final states in ref. [31] and ref. [32], respectively. In the multi-lepton final state, the measured signal strength is $\mu_{tHq+tWH} = 5.7 \pm 2.7\,(\mathrm{stat.}) \pm 3.0\,(\mathrm{syst.})$. In the $b\bar{b}$ final state, the observed upper limit relative to the SM prediction is 14.6 at 95% confidence level.

JHEP10(2025)093

The analysis presented in this paper uses an integrated luminosity of 140 $\text{fb}^{-1}$of data collected with the ATLAS detector at $\sqrt{s} = 13\,\text{TeV}$ between 2015 and 2018 at the LHC. The search targets signatures that are primarily sensitive to $H \to b\bar{b}$, $H \to WW^*$, $H \to ZZ^*$ and $H \to \tau\tau$ decays. Backgrounds are estimated with a combination of simulation and data-driven techniques, and a global fit in all final states is used to extract the best estimate for the tH production rate under both the SM and ITC hypotheses.

2 Analysis strategy

The search described in this paper considers three mutually orthogonal final states, hereafter referred to as channels, distinguished by the number of light-flavour leptons (ℓ), i.e. electron (e) or muon (μ):

- one lepton ($H \to b\bar{b}$);
- two same-charge leptons ($2\ell\,\text{SS}$);
- three leptons (3ℓ).

Events with τ-leptons decaying into an electron or a muon are part of selection, while events containing hadronically decaying τ-leptons (τ_{had}) are vetoed in all three channels.

Each channel targets different Higgs-boson decay modes. The $H \to b\bar{b}$ channel is most sensitive to the $H \to b\bar{b}$ decay, while the $2\ell\,\text{SS}$ and 3ℓ channels mostly probe $H \to W\,W^*$. In the $2\ell\,\text{SS}$ and 3ℓ channels, subleading contributions arise from $H \to \tau\tau$ and from $H \to ZZ^*$ decays.

These three channels are characterised by different background compositions, therefore they are analysed and fitted separately and combined afterwards.Each channel defines multiple analysis regions: signal regions (SRs), which are enriched in signal events, and control regions (CRs), which are designed to constrain the dominant background contributions. In the $H \to b\bar{b}$ channel, two regions are defined: one SR targeting the signal, and a CR dedicated to top-quark pair ($t\bar{t}$) production in association with b-jets, denoted CR($t\bar{t}+ \geq 1b$). In both the $2\ell\,\text{SS}$ and 3ℓ channels, five regions are defined: one SR, three CRs to constrain backgrounds from non-prompt and fake leptons, and one CR targeting the associated production of a W boson with a top-quark pair ($t\bar{t}\,W$).

To enhance signal-to-background separation, all channels employ multivariate analysis techniques, specifically Boosted Decision Trees (BDTs). These methods are used both to discriminate signal from background and to separate different background components to better constrain them, as well as to define the analysis regions. Details are provided in section 6.

A profile likelihood fit, implemented using the TRExFitter framework [33], is used to simultaneously extract the signal strength, μ_{tH}, and the normalisations of the dominant backgrounds in each channel. The signal strength is first fitted separately in each channel, and then in a combined fit.

The manuscript is structured as follows: section 3 describes the ATLAS detector, while details of the data and MC simulated event samples used in the analysis are provided in

JHEP10(2025)093

section 4. Section 5 outlines the object definitions. The event selection, multivariate analysis techniques, and analysis region definitions for each channel are presented in section 6, while section 7 describes the background estimates and its results. All uncertainties considered in this measurement are discussed in section 8. The resulting constraints on the signal process in both the SM and ITC scenarios are shown in section 9, for each channel and their combination. Finally, the conclusions are presented in section 10.

3 ATLAS detector

The ATLAS detector [34] at the LHC covers nearly the entire solid angle around the collision point.[1] It consists of an inner tracking detector surrounded by a thin superconducting solenoid, electromagnetic and hadronic calorimeters, and a muon spectrometer incorporating three large superconducting air-core toroidal magnets.

The inner-detector system (ID) is immersed in a 2 T axial magnetic field and provides charged-particle tracking in the range of $|\eta| < 2.5$. The high-granularity silicon pixel detector covers the vertex region and typically provides four measurements per track, the first hit generally being in the insertable B-layer (IBL) installed before the LHC Run 2 [35, 36]. It is followed by the SemiConductor Tracker (SCT), which usually provides eight measurements per track. These silicon detectors are complemented by the Transition Radiation Tracker (TRT), which enables radially extended track reconstruction up to $|\eta| = 2.0$. The TRT also provides electron identification information based on the fraction of hits (typically 30 in total) above a higher energy-deposit threshold corresponding to transition radiation.

The calorimeter system covers the pseudorapidity range $|\eta| < 4.9$. Within the region $|\eta| < 3.2$, electromagnetic calorimetry is provided by barrel and endcap high-granularity lead/liquid-argon (LAr) calorimeters, with an additional thin LAr presampler covering $|\eta| < 1.8$ to correct for energy loss in material upstream of the calorimeters. Hadronic calorimetry is provided by the steel/scintillator-tile calorimeter, segmented into three barrel structures within $|\eta| < 1.7$, and two copper/LAr hadronic endcap calorimeters. The solid angle coverage is completed with forward copper/LAr and tungsten/LAr calorimeter modules optimised for electromagnetic and hadronic energy measurements, respectively.

The muon spectrometer (MS) comprises separate trigger and high-precision tracking chambers measuring the deflection of muons in a magnetic field generated by the superconducting air-core toroidal magnets. The field integral of the toroids ranges between 2.0 and 6.0 T m across most of the detector. Three layers of precision chambers, each consisting of layers of monitored drift tubes, cover the region $|\eta| < 2.7$, complemented by cathode-strip chambers in the forward region, where the background is highest. The muon trigger system covers the range $|\eta| < 2.4$ with resistive-plate chambers in the barrel, and thin-gap chambers in the endcap regions.

[1] ATLAS uses a right-handed coordinate system with its origin at the nominal interaction point (IP) in the centre of the detector and the z-axis along the beam pipe. The x-axis points from the IP to the centre of the LHC ring, and the y-axis points upwards. Cylindrical coordinates (r, ϕ) are used in the transverse plane, ϕ being the azimuthal angle around the z-axis. The pseudorapidity is defined in terms of the polar angle θ as $\eta = -\ln\tan(\theta/2)$. Angular distance is measured in units of $\Delta R \equiv \sqrt{(\Delta\eta)^2 + (\Delta\phi)^2}$.

JHEP10(2025)093

The luminosity is measured mainly by the LUCID-2 [37] detector that records Cherenkov light produced in the quartz windows of photomultipliers located close to the beampipe.

Events were selected by the first-level trigger system implemented in custom hardware, followed by selections made by algorithms implemented in software in the high-level trigger [38]. The first-level trigger accepted events from the 40 MHz bunch crossings at a rate close to 100 kHz, which the high-level trigger further reduced in order to record complete events to disk at about 1.25 kHz.

A software suite [39] is used in data simulation, in the reconstruction and analysis of real and simulated data, in detector operations, and in the trigger and data acquisition systems of the experiment.

4 Data and simulated event samples

4.1 Data event samples

This analysis uses data from pp collisions at $\sqrt{s} = 13$ TeV collected with the ATLAS detector at the LHC during 2015–2018. Stringent detector and data-quality requirements were applied [40], resulting in a data sample corresponding to a total integrated luminosity of 140 fb^{-1}. The events were selected by single-lepton triggers with variable electron and muon transverse momentum (p_{T}) thresholds, and various identification and isolation criteria depending on the lepton flavour and the data-taking period [41, 42]. The lowest p_{T} threshold at trigger level used for electrons was 24 GeV (26 GeV), while for muons the threshold was 20 GeV (26 GeV) in 2015 (2016–2018).

4.2 Simulated event samples

Samples of simulated events were produced using different Monte Carlo (MC) event generators including parton shower (PS) and hadronisation models for both signal and background processes. The effect of multiple interactions in the same and neighbouring bunch crossings (pile-up) was modelled by overlaying the hard-scattering event with simulated minimum-bias events generated with Pythia 8.186 [43, 44] using the NNPDF2.3LO set of PDFs [45] and the A3 set of tuned parameters (A3 tune) [46]. Events were reweighted such that the distribution of the average number of interactions per bunch crossing matches that observed in data.

Table 1 presents a summary of all configurations used to generate events for signal (tHq and tWH) and background processes, for both nominal and alternative simulated samples. In all simulated signal and background samples, the top-quark mass was set to $m_{\mathrm{top}} = 172.5$ GeV and the Higgs-boson mass to $m_H = 125.0$ GeV. Moreover, the strong coupling constant was set to $\alpha_{\mathrm{s}} = 0.118$ [47] at the reference scale of the Z-boson mass. These values are also used in the computation of production cross-sections for processes involving these particles. The bottom and charm hadron decays were simulated with EvtGen [48] for all event samples, except those generated with Sherpa.

Systematic uncertainties from different modelling choices are evaluated by comparing alternative simulated samples to the nominal ones. These alternative samples are generated either through reweighting or with dedicated event generators. Each variation is applied

JHEP10(2025)093

Process	Generator	ME order	Parton shower	PDF set	Tune
tHq	MG5_aMC	NLO	Pythia 8	NNPDF3.0nlo	A14
	(MG5_aMC)	(NLO)	(Herwig 7)	(NNPDF3.0nlo)	(Herwig 7.1)
tWH	MG5_aMC	NLO	Pythia 8	NNPDF3.0nlo	A14
	(MG5_aMC)	(NLO)	(Herwig 7)	(NNPDF3.0nlo)	(Herwig 7.1)
$t\bar{t}$	Powheg Box	NLO	Pythia 8	NNPDF3.0nlo	A14
	(Powheg Box)	(NLO)	(Herwig 7)	(NNPDF3.0nlo)	(Herwig 7.1)
	(Powheg Box)	(NLO)	(Pythia 8)	(NNPDF3.0nlo)	(A14 $p_{\mathrm{T}}^{\mathrm{hard}}$)
	(MG5_aMC)	(NLO)	(Pythia 8)	(NNPDF3.0nlo)	(A14)
$t\bar{t}+b\bar{b}$	(Powheg Box Res)	(NLO)	(Pythia 8)	(NNPDF3.0nlo)	(A14)
$t\bar{t}H$	Powheg Box	NLO	Pythia 8	NNPDF3.0nlo	A14
	(Powheg Box)	(NLO)	(Herwig 7)	(NNPDF3.0nlo)	(Herwig 7.1)
	(MG5_aMC)	(NLO)	(Pythia 8)	(NNPDF3.0nlo)	(A14)
$t\bar{t}W$	Sherpa 2.2.10	NLO QCD+EW	Sherpa	NNPDF3.0nnlo	default
	(MG5_aMC)	(NLO QCD+EW)	(Pythia 8)	NNPDF3.0nnlo	(A14)
$t\bar{t}W$ (EW)	Sherpa 2.2.10	LO	Sherpa	NNPDF3.0nnlo	default
	(MG5_aMC)	(LO)	(Pythia 8)	(NNPDF3.0nlo)	(A14)
$t\bar{t}Z$	MG5_aMC	NLO	Pythia 8	NNPDF3.0nlo	A14
	(Sherpa 2.2.10)	(LO)	(Sherpa)	(NNPDF3.0nnlo)	(default)
	(MG5_aMC)	(NLO)	(Herwig 7)	(NNPDF3.0nlo)	(Herwig 7.1)
Single top quark (t-ch., tW, s-ch.)	Powheg Box	NLO	Pythia 8	NNPDF3.0nlo	A14
	(Powheg Box)	(NLO)	(Herwig 7)	(NNPDF3.0nlo)	(Herwig 7.1)
	(MG5_aMC)	(NLO)	(Herwig 7)	(NNPDF3.0nlo)	(Herwig 7.1)
V + jets	Sherpa 2.2.1	MEPS@NLO	Sherpa	NNPDF3.0nlo	default
VV, $qqVV$	Sherpa 2.2.2	MEPS@NLO	Sherpa	NNPDF3.0nnlo	default
	(Powheg Box)	(NLO)	(Pythia 8)	(NNPDF3.0nlo)	(A14)
VVV	Sherpa 2.2.2	MEPS@NLO	Sherpa	NNPDF3.0nnlo	default
tZ	MG5_aMC	NLO	Pythia 8	NNPDF3.1nlo	A14
tWZ	MG5_aMC	NLO DR1	Pythia 8	NNPDF2.3lo	A14
	(MG5_aMC)	(NLO DR2)	(Pythia 8)	NNPDF2.3lo	(A14)
$t\bar{t}t$, $t\bar{t}t\bar{t}$	MG5_aMC	QCD NLO	Pythia 8	NNPDF3.1nlo	A14
ggH, qqH	Powheg Box	QCD NLO	Pythia 8	CTEQ6L1	AZNLO
WH, ZH	Pythia 8	QCD NLO	Pythia 8	NNPDF2.3lo	A14

Table 1. The configurations used to generate events for signal (tHq and tWH) and background processes. The simulation samples used to estimate the systematic uncertainties are shown in parentheses and in grey.

independently, unless explicitly stated otherwise, to ensure a consistent evaluation of its individual impact on the analysis.

4.2.1 Simulated signal event samples

The production of a Higgs boson with a single top quark in the t-channel, tHq, was modelled using MadGraph5_aMC@NLO 2.6.2 [49] with matrix elements (MEs) at next-to-leading-order (NLO) accuracy in QCD in the 4FS using the NNPDF3.0nlo nf4 [50] PDF set. The renormalisation (μ_{r}) and factorisation (μ_{f}) scales were set to $0.5 \times \sum_i \sqrt{m_i^2 + p_{\mathrm{T},i}^2}$, summing over all ME-generated particles with mass m and transverse momentum p_{T}. Events were interfaced with Pythia 8.230 using the A14 set of tuned parameters (A14

JHEP10(2025)093

tune) [51] and the NNPDF2.3LO PDF set. The simulated tHq signal samples were normalised to the NLO QCD theory prediction without NLO EW corrections at $\sqrt{s} = 13\,\text{TeV}$ and in the 5FS of $74.3^{+6.5\%}_{-14.9\%}$ (QCD) $\pm$ 3.7% (PDF+α_s) fb [52, 53]. The PDF and α_s uncertainties are calculated using the PDF4LHC15_nlo_30_pdfas PDF sets [54] and added in quadrature. The QCD uncertainty is computed from a combination of QCD scale variations and the difference of predictions in the 4FS and 5FS schemes, using the PDF4LHC15_nlo_nf4_100 PDF (central) set.

The associated production of a Higgs boson with a single top quark, tWH, was modelled using MadGraph5_aMC@NLO 2.8.1 with MEs at NLO accuracy in QCD in the 5FS using the NNPDF3.0NLO PDF set. The functional forms of the μ_r and μ_f scales were set the same as for the tHq simulation sample. The diagram-removal (DR) scheme (DR1) [55] was employed to remove the overlap between tWH and $t\bar{t}H$ simulation samples [56]. The events were interfaced with Pythia 8.245 using the A14 tune and the NNPDF2.3lo PDF set. The simulated tWH signal samples were normalised to the NLO QCD theory prediction in the 5FS [52, 53] and using the DR2 scheme [25] to handle the overlap between the tWH and $t\bar{t}H$ processes. At $\sqrt{s} = 13\,\text{TeV}$ the predicted cross-section is $\sigma(tWH)_{\text{NLO}} = 15.2^{+4.9\%}_{-6.7\%}$ (QCD scale) $\pm$ 6.3% (PDF+α_s) fb [52, 53].

To assess the modelling uncertainty due to the choice of the PS and hadronisation model, alternative event samples were produced for signal processes. Both tHq and tWH processes were produced using MadGraph5_aMC@NLO with the nominal set-up but interfaced with Herwig 7.1.6 [57, 58] using the MMHT2014nnlo [59] PDF set, with the Herwig 7.1 default set of tuned parameters (Herwig 7.1 tune) [58]. Moreover, simulated signal samples for both tHq and tWH with the ITC hypothesis were produced using similar set-ups as the ones used to produce SM simulated samples. In this case, the samples were normalised to the cross-section, for pp collisions at $\sqrt{s} = 13\,\text{TeV}$, of $\sigma(tHq)^{\kappa_t=-1}_{\text{NLO}} = 873\,\text{fb}$ and $\sigma(tWH)^{\kappa_t=-1}_{\text{NLO}} = 114\,\text{fb}$, respectively. For both nominal and ITC simulated signal samples, alternative variations of μ_r and μ_f scales and initial-/final-state radiation (ISR/FSR) were produced within the nominal set-up (i.e. MadGraph5_aMC@NLO +Pythia 8) as reweighted events.

4.2.2 Simulated background event samples

The production of $t\bar{t}$ events were modelled using Powheg Box v2 [60–63] at NLO QCD in 5FS with the NNPDF3.0NLO PDF set. In this case, the h_{damp} parameter[2] was set to $1.5 \times m_{\text{top}}$ [56]. Events were interfaced with Pythia 8.230 using the A14 tune and the NNPDF2.3LO PDF set. The simulated samples are normalised to the theory prediction at next-to-next-to-leading-order (NNLO) in QCD including the resummation of next-to-next-to-leading logarithmic (NNLL) soft-gluon terms calculated using Top++2.0 [64–70], equals to 834^{+29}_{-37} pb, where the uncertainty is the sum in quadrature of scale, PDF and α_s uncertainties.

A series of alternative $t\bar{t}$ simulated event samples were produced to evaluate the impact of modelling uncertainties. The effect of the choice of the PS and hadronisation model is quantified by comparing the nominal simulation with one produced using the same ME generator but interfaced with Herwig 7.1.6. To evaluate the impact of the choice of the NLO

[2]The h_{damp} parameter controls the p_T of the first additional emission beyond the LO Feynman diagram in the PS and therefore regulates the high-p_T emission against which the $t\bar{t}$ system recoils.

JHEP10(2025)093

matching scheme two samples were produced: one where the parameter $p_{\mathrm{T}}^{\mathrm{hard}}$, which regulates the definition of the vetoed region of the Pythia 8 showering [71], was halved, and other event sample generated by MadGraph5_aMC@NLO and matched to Herwig 7. Moreover, to assess the choice of the value of the h_{damp} parameter, alternative simulated samples generated using the nominal set-up but with $h_{\mathrm{damp}} = 3.0 \times m_{\mathrm{top}}$ were considered. A 4FS $t\bar{t}+b\bar{b}$ simulated sample was produced using Powheg Box Res with the OpenLoops [72–74] library and the NNPDF3.1nnlo nf4 PDF set, interfaced with Pythia 8.244. The simulation used a b-quark mass of 4.95 GeV and dynamic scales μ_{f} set to $0.5 \times \sum_{i=t,\bar{t},b,\bar{b},j} m_{\mathrm{T},i}$ and μ_{r} set to $0.5 \times \sqrt[4]{m_{\mathrm{T},t} \cdot m_{\mathrm{T},\bar{t}} \cdot m_{\mathrm{T},b} \cdot m_{\mathrm{T},\bar{b}}}$, where $m_{\mathrm{T},i} = \sqrt{m_i^2 + p_{\mathrm{T},i}^2}$ denotes the transverse mass of particle i. The h_{damp} parameter was defined as $0.5 \times \sum_{i=t,\bar{t},b,\bar{b}} m_{\mathrm{T},i}$, and the parameter h_{bzd} was set to 5. Here, h_{bzd} controls the suppression of the Born-zero configurations in Powheg. This sample is considered to evaluate the impact of using the 4FS instead of the 5FS and also the effect of generating additional b-quarks explicitly at NLO in the ME in the 4FS, as opposed to their approximate treatment via the PS in the 5FS set-up.

The $t\bar{t}H$ events were simulated using Powheg Box v2 at NLO accuracy in QCD in 5FS with the NNPDF3.0NLO PDF set, and with μ_{r} and μ_{f} scales set to $\sqrt[3]{m_{\mathrm{T},t} \cdot m_{\mathrm{T},\bar{t}} \cdot m_{\mathrm{T},H}}$ [75]. Events were interfaced with Pythia 8.230 using the A14 tune and the NNPDF2.3LO PDF set. The NLO QCD+EW cross-section at $\sqrt{s} = 13$ TeV is 507^{+35}_{-50} fb [52], where the uncertainties were estimated from variations of α_{s} and the μ_{r} and μ_{f} scales. Additional variations use event weights for QCD scales and radiation, with an alternative PS simulated sample using Herwig 7.04.

The $t\bar{t}W$ events were produced using Sherpa 2.2.10 [76] at NLO (LO) accuracy in QCD for up to one (two) additional partons. The NNPDF3.0nnlo PDF set was used along with the dedicated set of tuned PS parameters developed by the Sherpa authors. In addition, EW corrections were also produced with Sherpa 2.2.10 at LO accuracy for up to one additional parton. The $t\bar{t}W$ cross-section is calculated at NLO QCD with up to two additional partons using an improved MadGraph5_aMC@NLO FxFx merging procedure [77, 78] and combines it with leading $\mathcal{O}(\alpha^2\alpha_s^2)$ and subleading $\mathcal{O}(\alpha^3\alpha_s)$ NLO EW corrections. This calculation also includes on-shell LO decays of the $t\bar{t}W$ including the tree-level spin correlations within the narrow-width approximation. At $\sqrt{s} = 13$ TeV, this yields 722^{+70}_{-78} (scale)$^{+7}_{-7}$ (PDF) fb [78]. The choice of the NLO matching scheme was evaluated using an alternative simulated sample produced with MadGraph5_aMC@NLO 2.3.3 with the FxFx [77] merging scheme simulated samples including EW corrections.

The associated production of the Z boson with a top-quark pair ($t\bar{t}Z$) was simulated using MadGraph5_aMC@NLO 2.3.3 at NLO QCD with the NNPDF3.0nlo PDF set, interfaced with Pythia 8.210 using the A14 tune and the NNPDF2.3lo PDF set. The $t\bar{t}Z$ cross-section, including off-shell effects and Z/γ^* interference, was calculated at NLO QCD+EW as $0.88^{+0.09}_{-0.10}$ pb [52, 79], where the uncertainties were estimated from variations of α_{s} and the μ_{r} and μ_{f} scales. The choice of the NLO matching scheme was evaluated using an alternative simulated sample produced with Sherpa 2.2.0 at LO accuracy along with the NNPDF3.0nnlo PDF set, using the MEPS@LO prescription [80], with up to one additional parton for the $t\bar{t}Z(\to \ell\ell)$ sample and two additional partons for the $t\bar{t}Z(\to qq)$ and $t\bar{t}Z(\to \nu\nu)$ samples.

JHEP10(2025)093

All single top-quark events were generated with Powheg Box v2 at NLO in QCD with either the NNPDF3.0nlo nf4 or NNPDF3.0nlo PDF sets, with μ_{f} and μ_{r} scales set to $\sqrt{m_b^2 + p_{\mathrm{T},b}^2}$ [81, 82]. The t-channel was produced considering the 4FS, while the s-channel and associated tW processes used the 5FS. The latter process also employed the DR1 scheme to remove the overlap between tW and $t\bar{t}$ [56]. Events were interfaced with Pythia 8.230 using the A14 tune and the NNPDF2.3lo PDF set. Systematic variations include QCD μ_{r} and μ_{f} scales and radiation uncertainties, alternative PS using Powheg Box v2 with Herwig 7.16, and matching scheme uncertainties using MadGraph5_aMC@NLO 2.6.2 with Herwig 7.16 and the MMHT2014nnlo PDF set. For associated tW, an additional simulated sample using the diagram subtraction (DS) scheme was produced to evaluate the $t\bar{t}$ interference uncertainties.

The production of single-boson (V + jets), diboson (VV), and triboson (VVV) processes were simulated using either Sherpa 2.2.1 or Sherpa 2.2.2, with varying levels of QCD accuracy depending on the process. The NNPDF3.0nnlo PDF set was used along with a dedicated set of Sherpa-tuned PS parameters. For the V + jets processes, MEs were generated at NLO (LO) accuracy in QCD for up to two (four) partons, using the Comix library [83]. Simulated samples were normalised to NNLO predictions [84]. For the VV processes, MEs accounted for off-shell effects and included Higgs-boson contributions where relevant. Fully leptonic and semileptonic final states, where one boson decays leptonically and the other hadronically, were simulated at NLO (LO) accuracy in QCD for up to one (three) additional partons. Loop-induced processes $gg \to VV$ were generated at LO accuracy in QCD with up to one additional parton, for both fully leptonic and semileptonic final states. The EW production of a VV pair in association with two jets ($VVjj$) was simulated at LO accuracy in QCD. For the VVV processes, MEs were generated with factorised gauge-boson decays at NLO accuracy in QCD for the inclusive process and at LO accuracy in QCD for up to two additional parton emissions. In all cases, NLO MEs were matched to PS using a colour-exact variant of the MC@NLO algorithm [85]. Different jet multiplicities were merged via the CKKW matching procedure [86, 87], extended to NLO QCD accuracy through the MEPS@NLO [80] prescription, with a merging threshold set to 20 GeV. Leading-order MEs were merged using the MEPS@LO prescription. These calculations were performed in the G_μ scheme, which uses the Fermi constant as input, ensuring an optimal description of pure EW interactions at the EW scale.

To assess modelling uncertainties, scale uncertainties were evaluated using seven μ_{r} and μ_{f} variations (by factors of 0.5 and 2) as event weights. Furthermore, in the particular case of the VV processes, alternative event simulated samples were produced to evaluate the impact of different ME, PS, and hadronisation models by comparing the nominal diboson Sherpa event samples with Powheg Box v2 simulations of WW, WZ, and ZZ [88] processes at NLO accuracy in QCD. The effects of singly resonant amplitudes and interference due to Z/γ^* exchange, as well as same-flavour lepton combinations in the final state, were included where relevant. However, WW/ZZ interference in same-flavour lepton and neutrino final states was neglected. Events were interfaced with Pythia 8.186 using the AZNLO set of tuned parameters (AZNLO tune) [89]. The CT10 PDF set [90] was used for hard-scattering calculations, while the CTEQ6L1 [91] PDF set was applied for PS. The μ_{f} and μ_{r} scales

JHEP10(2025)093

were set to the boson-pair invariant mass, with a requirement of $m_{\ell\ell} > 4\,\text{GeV}$ at the ME level for same-flavour lepton pairs.

The tZq event sample was simulated using MadGraph5_aMC@NLO 2.3.3 at NLO accuracy in QCD in the 4FS with the NNPDF3.0nlo PDF set. The events were interfaced with Pythia 8.230 using the A14 tune and the NNPDF2.3lo PDF set. Off-resonance events away from the Z-mass peak were included. The functional form of the μ_r and μ_f scales was set to $4\sqrt{m_b^2 + p_{\text{T},b}^2}$, where the b-quark was the one produced by a gluon splitting in the event. The uncertainty due to initial-state radiation and to higher/lower parton radiation were estimated following exactly the same prescription as with the t-channel process.

The tWZ event production was modelled using MadGraph5_aMC@NLO 2.3.3 at NLO QCD with the NNPDF3.0nlo PDF set in the 5FS. Events were interfaced with Pythia 8.212, using the A14 tune and the NNPDF2.3lo PDF set. The DR1 scheme was used to remove the overlap between the tWZ and $t\bar{t}Z$ processes. Parton radiation uncertainties follow the same prescription as the t-channel process. An alternative DR scheme [25] was simulated to assess systematic uncertainty.

The production of three top-quark process ($t\bar{t}t$) events was modelled using MadGraph5_aMC@NLO 2.2.2 with NLO accuracy in QCD interfaced with Pythia 8.186, using the NNPDF2.3lo PDF set and the A14 tune. The production of four top-quark process ($t\bar{t}t\bar{t}$) events was modelled using MadGraph5_aMC@NLO 2.3.3 with NLO accuracy in QCD with the NNPDF3.1nlo PDF set. The events were interfaced with Pythia 8.230 for the PS and hadronisation, using the A14 tune and the NNPDF2.3lo PDF set.

Four SM Higgs-boson processes are considered as minor backgrounds: gluon-gluon fusion (ggH), VBF (qqH), and associated production with W and Z bosons (WH and ZH). The ggH and VBF events were modelled with either Powheg Box v2 or v1 (r2856) [92, 93], providing NLO accuracy in QCD with the CT10 PDF set. The μ_r and μ_f scales were set to $\sqrt{m_H^2 + p_{\text{T},H}^2}$. These generated events were interfaced with either Pythia 8.210 or 8.186 for PS and hadronisation, using the AZNLO tune and the CTEQ6L1 PDF set. The WH and ZH production was modelled with Pythia 8.186, using the A14 tune and the NNPDF2.3lo PDF set.

Most of the MC simulated samples used for the nominal estimates were processed through a simulation [94] of the ATLAS detector based on Geant4 [95], while those used for evaluating systematic uncertainties were processed with a fast simulation [94] that relies on a parameterisation of the calorimeter response [96]. Furthermore, fast-simulated event samples were used for certain nominal samples, particularly for the tHq and tWH signal processes and the $t\bar{t}t\bar{t}$ background process with no loss of accuracy.

5 Object definitions

Interaction vertices from the pp collisions are reconstructed from at least two tracks in the ID system with p_T larger than 500 MeV that are consistent with originating from the beam collision region in the x–y plane. If more than one primary vertex candidate is found in the event, the candidate for which the associated tracks form the largest sum of squared p_T is selected as the hard-scatter primary vertex [97].

JHEP10(2025)093

Electron candidates are reconstructed from energy clusters in the electromagnetic calorimeter matched to a track in the ID [98]. They are required to satisfy $p_{\mathrm{T}} > 10\,\mathrm{GeV}$ and $|\eta| < 2.47$, excluding the transition region between the endcap and barrel calorimeters ($1.37 < |\eta| < 1.52$). `Loose` and `Tight` electron identification working points are used, based on a likelihood discriminant employing calorimeter, tracking and combined variables that provide separation between electrons and jets.

Muon candidates are reconstructed from tracks measured in the ID matched to tracks measured in the MS [99, 100]. The resulting muon candidates are re-fitted using the complete track information from both detector systems. They are required to satisfy $p_{\mathrm{T}} > 10\,\mathrm{GeV}$ and $|\eta| < 2.5$. `Loose` and `Medium` muon identification working points are used.

Electron (muon) candidates are matched to the primary vertex by requiring that the significance of their transverse impact parameter, d_0,[3] satisfies $|d_0/\sigma(d_0)| < 5.0\,(3.0)$, where $\sigma(d_0)$ is the measured uncertainty in d_0, and by requiring that their longitudinal impact parameter, $z_0 \sin\theta$,[4] satisfies $|z_0 \sin\theta| < 0.5\,\mathrm{mm}$ [98, 99].

To further suppress leptons from heavy-flavour hadron decays, misidentified jets, or photon conversions (collectively referred to as "non-prompt leptons"), a BDT discriminant, referred to as the non-prompt-lepton BDT [101], based on isolation and lifetime information associated with a track jet that matches the selected electron or muon, is employed. The `Tight` working point based on the non-prompt-lepton BDT is used, which allows prompt muons (barrel/endcap electrons) to be selected with an efficiency that is about 60% (60%/70%) for $p_{\mathrm{T}} \sim 20\,\mathrm{GeV}$ and reaches a plateau of 95% (95%/90%) for $p_{\mathrm{T}} \sim 40$ (40/65)GeV, while the rejection factor against leptons from the decay of b-hadrons is about 20.

For the $2\ell\,\mathrm{SS}$ channel, to further suppress electrons with incorrect charge assignment, a BDT discriminant based on calorimeter and tracking quantities [102] is used, reducing the signal by 1.9% and the total background by approximately 40%, both at preselection level (see section 6.2). The electron candidates are separated into three classes: "material conversion", "internal conversion", and "non-conversion" electron candidates. Most electrons originating from photon conversions, whether from material conversions in the detector or internal conversions, are rejected by the standard electron identification criteria. To further suppress remaining conversion electrons in the $2\ell\,\mathrm{SS}$ and 3ℓ channels, additional vetoes are applied, except in control regions specifically targeting conversion electrons (e^*). Material conversion candidates have a reconstructed displaced vertex with radius $r > 20$ mm that includes the track associated with the electron.[5] The invariant mass of the associated track and the closest (in $\Delta\eta$) opposite-charge track reconstructed in the silicon detector, calculated at the conversion vertex, is required to be $< 100\,\mathrm{MeV}$. Internal conversion candidates must fail to satisfy the requirements for material conversions, and the di-track invariant mass, calculated here at the primary vertex, is required to be $< 100\,\mathrm{MeV}$.

The various lepton working points used are summarised in table 2. Lepton candidates are initially selected using relatively "*Loose*" criteria (labelled as L), and a subset may later

[3]The transverse impact parameter, d_0, is defined in the x–y plane as the distance of closest approach of the track to the beamline.

[4]The longitudinal impact parameter, z_0, is defined as the distance in z between the primary vertex and the point on the track used to evaluate d_0.

[5]The beampipe and IBL inner radii are 23.5 mm and 33 mm, respectively.

JHEP10(2025)093

	Electron		Muon	
Lepton definition	L	T	L	T
Identification	`Loose`	`Tight`	`Loose`	`Medium`
Transverse impact parameter significance $\lvert d_0\rvert/\sigma_{d_0}$	< 5.0		< 3.0	
Longitudinal impact parameter z_0	$\lvert z_0 \sin\theta\rvert < 0.5$ mm			
Isolation (Non-prompt lepton BDT)	No	Yes	No	Yes
Electron charge-misassignment veto	No	Yes	–	
Electron conversion candidate veto	No	Yes (except e^*)	–	

Table 2. Description of the *Loose* (L) and *Tight* (T) lepton definitions. The electron e^* is required to fulfil, in addition to the corresponding lepton definition requirements, those corresponding to an internal or material conversion candidate.

be required to satisfy stricter "*Tight*" criteria (labelled as T) to further optimise the event selection. The choice of working point depends on the main background processes in each category. The specific selections adopted for the signal and control regions are described in section 6. The lepton working points used here (*Loose* and *Tight*) are not to be confused with the identification working points such as `Loose`, `Medium`, and `Tight`.

The constituents for jet reconstruction are identified by combining measurements from both the ID and the calorimeter using a particle flow (PFlow) algorithm [103]. Jet candidates are reconstructed from these PFlow objects using the anti-k_t algorithm [104, 105] with a radius parameter of $\Delta R = 0.4$. They are calibrated using simulation with corrections obtained by using in situ techniques in data [106]. Only jet candidates with $p_{\mathrm{T}} > 20\,\mathrm{GeV}$ and within $|\eta| < 4.5$ are selected. To reduce the effect of pile-up, each jet with $p_{\mathrm{T}} < 60\,\mathrm{GeV}$ and $|\eta| < 2.4$ must satisfy the `Tight` working point of the jet vertex tagger (JVT) [107] criteria used to identify jets that originate from the primary vertex. Moreover, jets within $2.5 < |\eta| < 4.5$ (hereafter called "forward jets") and $p_{\mathrm{T}} < 120\,\mathrm{GeV}$ must satisfy the `Tight` working point of the forward jet vertex tagger (fJVT) [108] criteria. A set of quality criteria is also applied to reject events containing at least one jet arising from non-collision sources or detector noise [109].

Jets containing b-hadrons are identified (b-tagged) via the `DL1r` [110] algorithm that uses a deep feed-forward neural network based on the distinctive features of b-hadron decays, primarily the impact parameters of tracks and the displaced vertices reconstructed in the ID. Additional input to this network is provided by discriminating variables constructed by a recurrent neutral network (RNN) [111], which exploits the spatial and kinematic correlations between tracks originating from the same b-hadron. A multivariate b-tagging discriminant value is calculated for each jet. In this measurement, a jet is considered b-tagged if it passes the working point corresponding to 85%, 77%, 70%, or 60% average expected efficiency to tag a b-quark jet, with a light-jet[6] rejection factor of about 40 to 2500, and a charm-jet (c-jet) rejection factor of about 3 to 40, as determined for jets with $p_{\mathrm{T}} > 20\,\mathrm{GeV}$ and

[6] 'Light jet' or 'Light-flavour jet' refers to a jet originating from the hadronisation of a light-flavour quark (u, d, s) or a gluon.

JHEP10(2025)093

$|\eta| < 2.5$ in simulated $t\bar{t}$ events. This discrete version of the b-tagging discriminant, named pseudo-continuous b-tagging score (PCBT), is also exploited as jet variable.

The reconstruction of the τ_{had} is seeded by jets reconstructed via the anti-k_t algorithm, using calibrated energy clusters as inputs, with a distance parameter of $\Delta R = 0.4$ [112–115]. Jets seeding τ_{had} candidates are additionally required to have $p_{\text{T}} > 10\,\text{GeV}$ and $|\eta| < 2.5$. To separate the τ_{had} candidates initiated by hadronic τ-lepton decays from jets initiated by quarks or gluons, a RNN [114] identification method was trained on information from reconstructed charged-particle tracks and clusters of energy in the calorimeter associated with τ_{had} candidates as well as high-level discriminating variables. A separate multivariate discriminant based on a BDT [113, 115] is also used to reject backgrounds arising from electrons mimicking a τ_{had}. This discriminant (eBDT) is built using information from the calorimeter and the tracking detector. Transition radiation information from the TRT system plays a key role in the performance of this discriminant. Baseline τ_{had} are required to have one or three associated tracks, electric charge of ± 1, $p_{\text{T}} > 20\,\text{GeV}$ and $|\eta| < 2.5$, excluding the barrel-endcap transition region. Each τ_{had} must satisfy the `Medium` RNN identification selection requirement, with efficiencies of 75% for 1-prong and 60% for 3-prong taus, and the `Loose` eBDT requirement, with an efficiency of 95% [113, 115].

Ambiguities between independently reconstructed electrons, muons, jets and τ_{had} can arise. A sequential "overlap removal" procedure is performed to resolve these ambiguities and thus avoid double counting of candidates. This procedure is applied to electrons and muons satisfying the L criteria. If two electrons are separated by $\Delta R < 0.1$, only the one with the higher p_{T} is kept. If an electron and a muon overlap within $\Delta R < 0.1$, the muon is removed if it is reconstructed only from an ID track and calorimeter energy deposits consistent with a minimum-ionising particle (i.e. if it is "calorimeter-tagged"), otherwise the electron is removed. If an electron and a selected jet are found within $\Delta R < 0.2$, the jet is removed. Any electron later found within ΔR of 0.4 of a jet is removed. Muons associated with a jet must satisfy a jet-muon separation of $\Delta R < 0.4$. If the overlapping jet contains less than three tracks with $p_{\text{T}} > 500\,\text{MeV}$, the jet is removed, otherwise the muon is rejected. Any τ_{had} found within a ΔR of 0.2 of an electron is removed. Any τ_{had} found within a ΔR of 0.2 of any type of muon with p_{T} greater than 2 GeV is removed, although if the τ_{had} p_{T} is greater than 50 GeV, it will only be removed if it is found to overlap with a reconstructed muon. Finally, if a jet is found within a ΔR of 0.2 of a τ_{had}, the jet is removed.

The missing transverse momentum $\vec{p}_{\text{T}}^{\,\text{miss}}$ (with magnitude $E_{\text{T}}^{\text{miss}}$) is defined as the negative vector sum of the transverse momenta of all identified and calibrated objects and remaining unclustered energy, the latter of which is estimated from low-p_{T} tracks associated with the primary vertex but not assigned to any lepton or jet candidate [116]. The $E_{\text{T}}^{\text{miss}}$ is taken as a measurement of the undetectable particles, and is affected by energy losses due to detector inefficiencies and acceptance, and by energy resolution.

6 Event selection and classification

Events must satisfy the single-electron or single-muon trigger requirements described in section 4.1. Selected events are required to contain one lepton matched to the corresponding lepton reconstructed by the trigger within $\Delta R < 0.15$ and with $p_{\text{T}} > 27\,\text{GeV}$. These criteria

JHEP10(2025)093

ensure operation on the trigger efficiency plateau, thereby minimising the corrections needed in simulation to reproduce the per-lepton trigger efficiencies measured in data [41, 42].

Events selected by the trigger are required to have at least one primary vertex with at least two associated ID tracks with $p_{\mathrm{T}} > 0.5\,\mathrm{GeV}$. In each event, the primary vertex is defined as the reconstructed vertex having the highest scalar sum of squared p_{T} of associated tracks [97] among the vertices consistent with the average beam-spot position. These events are also required to contain either one lepton and at least three b-tagged jets (70% working point), two leptons with the same electric charge or three leptons, based on the *Loose* lepton definition introduced in section 5. Events containing τ_{had} leptons are explicitly vetoed in all three channels.

The sensitivity of the analysis relies on the discrimination provided by the multivariate response that combines different event-based variables. In each channel, BDTs with gradient boosting (BDTGs) are trained on simulated events in a preselection region using the `XGBoost` Python package [117]. The model performance is evaluated using the hold-out method, in which the considered data sample is randomly divided into an independent training-data sample and a test-data sample that is used as a proxy to evaluate the performance of the model on unseen data. In all channels, only the tHq process is considered as a signal in the BDTG training. This decision is driven by the similarities observed between the tWH and $t\bar{t}H$ topologies, so that including the tWH process in the training weakens the separation between tHq and $t\bar{t}H$ and other background processes. While the tWH sample is not part of the BDTG training, its contribution is fully accounted for in the signal yield and in the limit setting later on. A strong separation of the signal from the $t\bar{t}H$ process leads to a reduced interplay between $t\bar{t}H$ and the tH signal in the results.

Details on the definition of the preselection regions and the background composition are given in the following while the yields are reported in table 3.

6.1 $H \to b\bar{b}$ channel

The $H \to b\bar{b}$ preselection region is defined by requiring the presence of exactly one *Tight* lepton (electron or muon) with $p_{\mathrm{T}} > 27\,\mathrm{GeV}$. The 70% working point of the `DL1r` tagger is used to select at least three b-tagged jets. All events with at least five jets and at least four b-tagged jets are vetoed. This requirement has a negligible impact on the signal acceptance and will help any future combination with other $t\bar{t}H$ analyses. Given the presence of one neutrino coming from the W-boson decay, the event is expected to have a non-zero $E_{\mathrm{T}}^{\mathrm{miss}}$. For this reason an $E_{\mathrm{T}}^{\mathrm{miss}} > 25\,\mathrm{GeV}$ requirement is applied.

As shown in Table 3, the main contribution to the background in the preselection region comes from $t\bar{t}+\mathrm{jets}$ events, constituting 90% of the expected total yield. The $t\bar{t}+\mathrm{jets}$ events are further classified depending on the flavour of the additional jets produced. Simulated events where at least one of the additional jets is matched to a b-hadron are classified as $t\bar{t}+\geq 1b$ (30% of the expected $t\bar{t}+\mathrm{jets}$ yield); if no matched b-jet is found but at least one jet is matched to a c-hadron the event is classified as $t\bar{t}+\geq 1c$ (17% of the expected $t\bar{t}+\mathrm{jets}$ yield) while all the other events are classified as $t\bar{t}+\geq 0$ light (53% of the expected $t\bar{t}+\mathrm{jets}$ yield). The latter contribution also includes $t\bar{t}$ events with no additional jets.

JHEP10(2025)093

Process	$H \to b\bar{b}$	2ℓ SS	3ℓ
tHq	91.1 ± 1.7	12.41 ± 0.17	3.15 ± 0.05
tWH	37.21 ± 0.26	3.97 ± 0.09	2.36 ± 0.07
$t\bar{t}$	–	1430 ± 14	324 ± 6
$t\bar{t}+ \geq 1b$	60170 ± 90	–	–
$t\bar{t}+ \geq 1c$	33585 ± 70	–	–
$t\bar{t}+ \geq 0$ light	106290 ± 120	–	–
e/μ_{Fakes}	8028 ± 80	–	–
$t\bar{t}H$	1676.9 ± 1.5	126.6 ± 1.2	74.62 ± 0.25
$t\bar{t}W$	362.0 ± 1.6	798.0 ± 2.1	205.7 ± 1.1
$t\bar{t}Z$	891.0 ± 6	165.3 ± 1.0	567.8 ± 1.7
tZq	170.5 ± 1.3	88.9 ± 0.5	273 ± 0.9
tWZ	2.22 ± 0.22	18.73 ± 0.08	80.47 ± 0.16
Z/W+jets	4681 ± 34	518 ± 30	131 ± 25
VV, VVV	292 ± 6	298.6 ± 3.3	579 ± 4
Single-top	9331 ± 31	164 ± 4	20.1 ± 1.5
$t\bar{t}t$, $t\bar{t}t\bar{t}$	8.9 ± 0.1	4.81 ± 0.06	4.88 ± 0.06
$VH, \text{VBF}H, ggH$	25.0 ± 0.1	19 ± 4	7.4 ± 2.8
Total	225640 ± 190	3650 ± 33	2274 ± 26

Table 3. Preselection region yields as predicted by the MC simulation. The uncertainty is statistical only and the PDG rounding is applied. The $t\bar{t}$ background is split into $t\bar{t}+ \geq 1b$, $t\bar{t}+ \geq 1c$ and $t\bar{t}+ \geq 0$ light categories for the $H \to b\bar{b}$ channel only; therefore the $t\bar{t}$ contribution for this channel is absent. Moreover, for the $H \to b\bar{b}$ channel only the data-driven estimate of the non-prompt and fake leptons background is given due to lack of a MC-based estimate.

In the $H \to b\bar{b}$ channel, the preselected events are used to train a five-dimensional BDTG including the categories tHq, $t\bar{t}+ \geq 1b$, $t\bar{t}+ \geq 1c$, $t\bar{t}+ \geq 0$ light and others. The "others" category includes all the remaining backgrounds. A Deep Neural Network (DNN) is also tested to validate the results obtained with the BDTG. Since the BDTG shows slightly better performance, it is chosen for the final results.

In total, 25 variables were used in the training, such as the number of jets, the lepton charge and flavour information, invariant mass and angular separation of various reconstructed jets, the minimum χ^2 values from reconstructing the W-bosons and top-quark masses from their decay products under the $t\bar{t}+ \geq 0$ light or $t\bar{t}+ \geq 1b$ hypotheses, as well as the pseudo-continuous b-tagging discriminant of selected jets (see table 6). These variables are motivated by the expected kinematic properties of the signal. The tHq topology features a forward spectator jet from the scattered incoming light-flavour quark, a hadronically decaying top quark, and a different multiplicity of b-jets compared to the dominant $t\bar{t}$ background. The most important variables entering the BDTG reflect these features: the number of jets associated with the reconstructed hadronic top quark from different $t\bar{t}$ reconstruction techniques provides strong separation from the $t\bar{t}$ background; the lepton charge helps distinguish tHq events, as the incoming light-flavour quark is dominantly a u-quark from one of the colliding protons, leading mostly to positively charged top quarks (and hence positive leptons), from charge-

JHEP10(2025)093

Channel	Region	BDT score	Conversion cut	Jets	Leptons flavour (p_{T} ordered)	Other
$H \to b\bar{b}$	SR	—	—	$N^{70}_{\text{not-}b} < 2$ $N^{\text{jet}}_{\text{forward}} \geq 1$	—	—
	CR($t\bar{t}+ \geq 1b$)	—	—	$N^{70}_{\text{not-}b} \geq 2$ $N^{\text{jet}}_{\text{forward}} = 0$	—	
2ℓ SS	SR	BDT(tHq) > 0.65 BDT($t\bar{t}$) < 0.5 BDT($t\bar{t}W$) < 0.6 and BDT(VV) < 0.8	yes	—	—	—
	CR(μ_{HF})	BDT(tHq) < 0.65 BDT($t\bar{t}$) > 0.3 BDT($t\bar{t}W$) < 0.6 and BDT(VV) < 0.9	yes	—	$\mu\ \mu$	—
	CR(e_{HF})	BDT(tHq) < 0.65 BDT($t\bar{t}$) > 0.3 BDT($t\bar{t}W$) < 0.6 and BDT(VV) < 0.9	yes	—	$\mu\ e$, $e\ e$	$H_{\mathrm{T}}(\ell) < 225$ GeV
	CR(e_{conv})	BDT($t\bar{t}$) > 0.3	inverted	—	$\mu\ e$, $e\ e$	m($\ell\ell$) < 150 GeV
	CR($t\bar{t}W$)	BDT($t\bar{t}W$) > 0.6 BDT($t\bar{t}$) < 0.3	yes	—	—	—
3ℓ	SR	BDT(tHq) > 0.7 BDT($t\bar{t}$) < 0.9 BDT($t\bar{t}W$) < 0.8	yes	—	—	—
	CR(μ_{HF})	BDT(tHq) < 0.7 BDT($t\bar{t}$) > 0.5 BDT($t\bar{t}W$) < 0.8	yes	—	$\mu\ \mu\ \mu$, $e\ \mu\ \mu$, $\mu\ e\ \mu$, $e\ e\ \mu$	—
	CR(e_{HF})	BDT(tHq) < 0.7 $BDT(t\bar{t}) > 0.5$ $BDT(t\bar{t}W) < 0.8$	yes	—	$\mu\ \mu\ e$, $e\ \mu\ e$ $\mu\ e\ e$, $e\ e\ e$	—
	CR(e_{conv})	—	inverted	—	$\mu\ \mu\ e$, $e\ \mu\ e$, $\mu\ e\ e$, $e\ e\ e$	—
	CR($t\bar{t}W$)	BDT($t\bar{t}W$) > 0.8	yes	—	—	—

Table 4. Regions selection requirements for $H \to b\bar{b}$, 2ℓ SS and 3ℓ channels. The regions are defined using a mixture of requirements on the BDTGs outputs, the flavour of the leptons, the number of jets and b-tagged jets, the sum of the transverse momentum of the leptons H_{T} (ℓ), the leptons invariant masses ($m(\ell\ell)$) and the conversion criteria.

symmetric backgrounds such as $t\bar{t}$, $t\bar{t}W$, $t\bar{t}Z$ or $t\bar{t}H$; the p_{T} of the highest-p_{T} forward jet is characteristic of the spectator jet in tHq production; and the event sphericity encodes the more isotropic topology of $t\bar{t}$ events compared to the typically more forward-backward structure of tHq events [118]. The complete lists of input variables can be found in section A. Variable importance is evaluated using the "gain" metric provided by the `XGBoost` algorithm, which reflects the relative improvement in model accuracy due to each variable.

The preselection phase-space is then split into two regions, defined by rectangular requirements on the number of forward jets ($N^{\text{jet}}_{\text{forward}}$) and the number of central jets failing to meet the `DL1r` tagger 70% working-point requirement ($N^{70}_{\text{not-}b}$). In the $H \to b\bar{b}$ channel, a jet is classified as forward if its pseudorapodity is $2.5 < |\eta| < 4.5$ or if its pseudorapodity is $2 < |\eta| < 2.5$ and it fails to meet the 70% b-tagging requirement. The two regions are enhanced in the tH contribution and $t\bar{t}+ \geq 1b$ and they are referred to as SR and CR($t\bar{t}+ \geq 1b$), respectively. The SR selection requires at least one forward jet and at most one central jet failing to meet the 70% b-tagging requirement, while for CR($t\bar{t}+ \geq 1b$) no forward jet should be present and at least two central jets must fail to meet the 70% b-tagging requirement. table 4 summarises the selections applied to define the SR and CR.

JHEP10(2025)093

6.2 2ℓ SS channel

The 2ℓ SS preselection region is defined by requiring exactly two *Tight* light leptons (electrons or muons) with the same electric charge. For the selected events, the leading lepton must have $p_{\mathrm{T}} > 27\,\mathrm{GeV}$ and the sub-leading lepton must have $p_{\mathrm{T}} > 20\,\mathrm{GeV}$.

The number of jets with $|\eta| < 4.5$ is required to be between one and six. The 70% working point of the `DL1r` tagger is used to select b-jets. The number of b-jets is required to be between one and three.

As shown in Table 3, the dominant source of background in the preselection region stems from $t\bar{t}$ followed by $t\bar{t}W$ and $Z+$jets production. Both $t\bar{t}$ and $Z+$jets enter the preselection region if a non-prompt or fake lepton is in the event or if the charge of one of the electrons is wrongly measured. The rest of the background processes consists of $t\bar{t}W$, $t\bar{t}Z$ or diboson production.

Four binary-classifier BDTGs are trained in the 2ℓ SS channel, each targeting the tHq signal or one of the main background processes ($t\bar{t}$, $t\bar{t}W$, and diboson) against the sum of the remaining three classes. These classifiers are used to define mutually exclusive enriched regions. In total, 52 variables were used in the training: 28, 19, 29 and 27 for the four BDTGs, respectively. These variables include kinematic and topological quantities that characterise the signal and its main backgrounds. The most important variables include the charge of the two leptons, H_{T},[7] the number of b-tagged jets, the invariant masses and angular separations of pairs of reconstructed jets and leptons (see table 6). The charge of the two leptons is highly discriminating, since the tHq process favours positively charged top quarks as explained before, while dominant backgrounds such as $t\bar{t}$, $t\bar{t}H$, and diboson production are charge-symmetric. Invariant masses of leptons and jets also provide discriminating power, as the decay kinematics and spatial correlations in the tHq topology produce characteristic patterns between leptons from top-quark decays and the forward spectator jet or b-jet. In contrast, in backgrounds such as $t\bar{t}$, $t\bar{t}H$, and dibosons, these correlations are absent or substantially altered due to additional heavy resonances or differing event topologies. The other variables further exploit differences in global event activity, jet and b-jet multiplicities, and the more isotropic topology of $t\bar{t}$, $t\bar{t}W$ and $t\bar{t}Z$ compared to the forward — backward structure of tHq events. The complete lists of input variables can be found in section A.

Five regions are defined in the 2ℓ SS channel: the SR is designed to maximise the tHq contribution, while the CRs target the main background processes. The regions are defined using a mixture of requirements on the BDTGs outputs, selecting a given flavour for the two leptons in the final state or cutting on event kinematic variables such as H_{T} or leptons invariant masses. The material- or internal-conversion cuts defined in section 5 are applied to all the electrons in all regions, except for the conversion control region, CR(e_{conv}), where this requirement is inverted. The regions described here are orthogonal to one another. table 4 summarises the selections applied to define the SR and CRs. Three CRs are defined to derive mis-identified leptons background: CR(μ_{HF}), CR(e_{HF}) and CR(e_{conv}). The CR(e_{conv}) is enriched in events with one electron stemming from γ-conversion (e_{conv}), while CR(μ_{HF})

[7] The H_{T} variable is defined performing the scalar sum of the transverse momentum of all the reconstructed objects in the final state, in this case jets and leptons. The $H_{\mathrm{T}}(\ell)$ variable instead is computed including only leptons.

JHEP10(2025)093

and CR(e_{HF}) are enriched in contributions from non-prompt electrons or muons stemming from heavy-flavoured (containing a b- or c-quark) hadron decay, e_{HF} and μ_{HF}, respectively. One CR is defined to target the irreducible $t\bar{t}W$ background.

6.3 3ℓ channel

The 3ℓ preselection region is defined by requiring the presence of exactly three *Tight* light leptons (electrons or muons). The sum of the leptons' charges is required to be ± 1. The light leptons are ordered based on their p_{T}, with the leading lepton having $p_{\text{T}} > 27\,\text{GeV}$, the sub-leading lepton required to have $p_{\text{T}} > 20\,\text{GeV}$ and the softest lepton to have $p_{\text{T}} > 10\,\text{GeV}$. The number of jets with $|\eta| < 4.5$ is required to be between one and six. The 70% working point of the `DL1r` tagger is used to select b-jets. The number of b-jets is required to be between one and three. As shown in Table 3, the dominant background contributions in the preselection region arise from diboson, $t\bar{t}Z$, and $t\bar{t}$ processes.

Three binary-classifier BDTGs are trained in the 3ℓ channel, each targeting the tHq signal or one of the main background processes ($t\bar{t}$ and $t\bar{t}W$) against the sum of the remaining two classes. These classifiers are used to define regions enriched in tHq and in each of the background processes included in the training. A total of 50 input variables are used in the training: 22, 19, and 30 for each of the three classifiers, respectively. These variables include kinematic and topological quantities that characterise the signal and its main backgrounds. The most important ones include the invariant masses of leptons, the p_{T} of leptons, the sum of leptons' charges, and the multiplicity of central and b-tagged jets. The dilepton invariant masses are powerful discriminants, since in backgrounds such as $t\bar{t}Z$ and diboson production leptons often originate from on-shell Z bosons, producing peaks around the Z-boson mass, while in tHq events they mainly arise from W-boson decays and do not show such resonant structures (see table 6). The sum of leptons' charges is also discriminant similarly to the other two channels. The lepton transverse momenta provide additional separation, as backgrounds with extra vector bosons typically yield harder leptons than those expected in tHq events. Finally, the number of b-tagged jets provides discrimination, as tHq process typically features fewer central and b-jets than backgrounds such as $t\bar{t}$, $t\bar{t}H$, $t\bar{t}W$, and $t\bar{t}Z$. The complete lists of input variables can be found in section A.

Five orthogonal regions are defined in the 3ℓ channel: one SR to maximise the tHq contribution, three CRs to estimate in data the mis-identified leptons background and one CR to estimate the $t\bar{t}W$ background. The regions are defined using a mixture of requirements on the BDTGs outputs, the number of jets and invariant masses. The material- and internal-conversion requirements defined in section 5 are applied to all the electrons in all regions, except for one region where this requirement is inverted to enhance the contribution of the process targeted by that region. Table 4 summarises the selection criteria applied to define the SR and CRs.

7 Background estimation

The background processes satisfying the SR and CR selections are categorised into irreducible and reducible backgrounds. Irreducible backgrounds arise from processes that have an identical number of prompt leptons from weak boson or leptonic τ-lepton decays, and a

JHEP10(2025)093

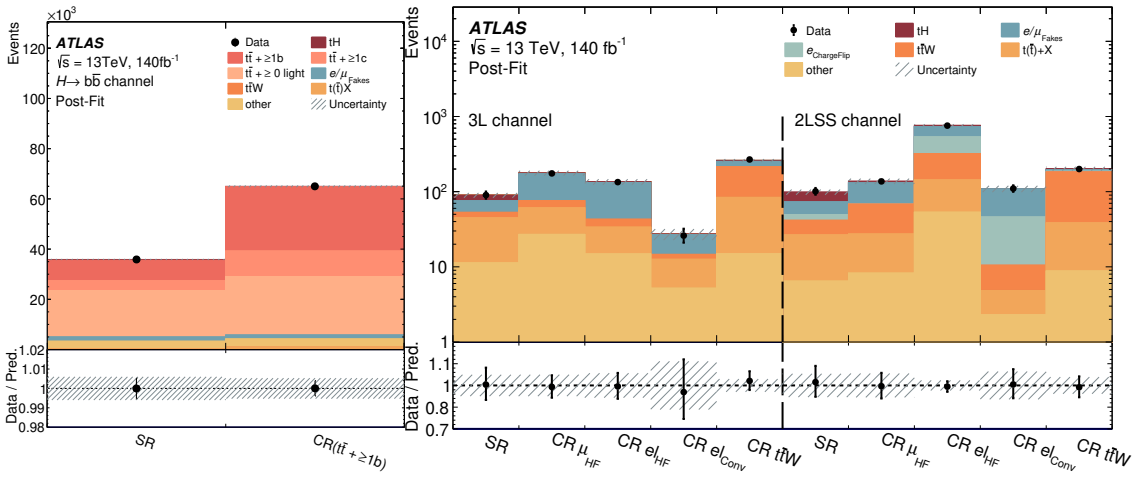

(a) (b)

Figure 2. The data and estimated signal-plus-background yields in the SR and CRs of the (a) $H \to b\bar{b}$ channel and (b) 3ℓ and 2ℓ SS channels. The term e/μ_{Fakes} refers to backgrounds from non-prompt or misidentified leptons, namely contributions from heavy-flavour decays and photon conversions. Both signal and background events are estimated with a likelihood fit to data ("Post-Fit"), as described in sections 7 and 9. The uncertainty band includes statistical and systematic contributions.

similar number of b-jets as the targeted signal. Reducible backgrounds arise instead from particle mis-identification in the detector, mis-assigning of the lepton charge or mis-tagging a charm or light-flavoured jet as a b-jet. Fake and non-prompt leptons can originate from different sources like decays of bottom or charm mesons, photon conversions or light jets creating accidentally a detector signature similar to a light lepton.

The contribution of irreducible backgrounds is generally derived through the respective simulated samples and constrained in CRs where needed. A data-driven estimate is provided for most of the reducible backgrounds and for background processes where the MC prediction is not in good agreement with the data. Figure 2 compares the total data yields in all SRs and CRs as defined in section 6 for the three analysis channels to the signal plus background predictions obtained by the likelihood fit to data described in section 7 and section 9.

7.1 Background estimation in the $H \to b\bar{b}$ channel

As already discussed in section 6.1, the main source of background in the $H \to b\bar{b}$ channel consists of $t\bar{t}$ +jets events. The production of the $t\bar{t}$ in association with heavy flavour jets is known to be not well modelled by the simulation. For this reason, simulated $t\bar{t}$ +jets events are split into $t\bar{t}+ \geq 1b$, $t\bar{t}+ \geq 1c$ and $t\bar{t}+ \geq 0$ light categories and the CR($t\bar{t}+ \geq 1b$) is included in the fit to constrain its contribution from data. The normalisation factor of the $t\bar{t}+ \geq 1b$ background found in the combined fit to data is $k(t\bar{t}+ \geq 1b) = 1.24^{+0.17}_{-0.15}$. The $t\bar{t}+ \geq 1c$ predicted yield has no dedicated correction factor due to the difficulty in building a pure CR. Instead, an overall uncertainty on the $t\bar{t}+ \geq 1c$ prediction is included in the fit as described in section 8.2. The remaining irreducible backgrounds are all estimated by using the MC predictions. The small contribution of reducible background from non-prompt and fake leptons is estimated using the matrix-method technique described in ref. [119].

JHEP10(2025)093

7.2 Background estimation in the 2ℓ SS and 3ℓ channels

In the 2ℓ SS channel, the main irreducible backgrounds originate from $t\bar{t}W$ production, having final states and kinematic properties inherently similar to the tHq signal. Smaller contributions originate from the following rare processes: tZq, $t\bar{t}H$ and tWZ production. Backgrounds with prompt leptons are directly estimated from simulation using the samples described in section 4, except for $t\bar{t}W$, for which the normalisation is fitted. In the 3ℓ channel instead, the main irreducible backgrounds originate from diboson production, $t\bar{t}Z$ and tZq. Other minor irreducible backgrounds are triboson, other Higgs-boson production modes such as ggH, VBF (qqH) and VH, and $t\bar{t}t$ and $t\bar{t}t\bar{t}$. A CR dedicated to the $t\bar{t}W$ background, CR($t\bar{t}W$), is defined in both the 2ℓ and 3ℓ channel to better constrain its contribution from data. The normalisation factor associated with the $t\bar{t}W$ background as estimated from the combined fit is found to be $k(t\bar{t}W) = 1.09 \pm 0.11$.

The most important sources of reducible background in both the 2ℓ SS and 3ℓ channels are the $t\bar{t}$, W/Z+jets and single-top-quark processes. These processes can satisfy the preselection requirement due to the presence of a fake or non-prompt lepton in the final state. These backgrounds are estimated from simulation, with the normalisation determined by the likelihood fit through the use of the dedicated CRs introduced earlier. The non-prompt leptons in the simulated event samples are labelled according to whether they originate from heavy-flavour or light-flavour hadron decays, or from a material/internal conversion. The light-flavour category is negligible. In the 2ℓ SS channel, normalisation factors are extracted to be $k(e_{\text{conv}})_{2\ell\,\text{SS}} = 1.20\pm0.47$, $k(e_{\text{HF}})_{2\ell\,\text{SS}} = 0.55\pm0.65$ and $k(\mu_{\text{HF}})_{2\ell\,\text{SS}} = 0.80\pm0.32$. In the 3ℓ channel, the normalisation factors extracted are $k(e_{\text{conv}})_{3\ell} = 0.82\pm0.59$, $k(e_{\text{HF}})_{3\ell} = 1.47\pm0.42$ and $k(\mu_{\text{HF}})_{3\ell} = 0.91 \pm 0.24$.

Electrons with mis-identified electric charge ("charge-flip"), with one electron either undergoing hard bremsstrahlung followed by an asymmetric conversion ($e^{\pm} \to e^{\pm}\gamma^* \to e^{\pm}e^{+}e^{-}$) or having mismeasured track curvature, represent another source of reducible background. This contribution is negligible in the 3ℓ channel and sizeable in the 2ℓ SS channel. The muon charge misassignment rate is negligible in the p_{T} range relevant to this analysis. The electron charge misassignment rate is measured in data by using samples of $Z \to e^{+}e^{-}$ events reconstructed as either same-charge pairs or opposite-charge pairs, with the non-Z background subtracted via a sideband method utilising events outside the Z-boson mass window. The charge misassignment rate is extracted from the ratio of the numbers of same-charge and opposite-charge events close to the Z-boson mass through a likelihood approach taking into account the possibility that both electron charges are misassigned. The rates are parameterised as a function of electron p_{T} and $|\eta|$, and vary from about 10^{-5} for low-p_{T} electrons ($17 \le p_{\text{T}} \le 50\,\text{GeV}$) with $|\eta| \le 1.37$, to about 4×10^{-3} for high-p_{T} electrons ($p_{\text{T}} \ge 100\,\text{GeV}$) with $2 \le |\eta| \le 2.47$. To estimate the charge-flip background in each 2ℓ SS region, the measured charge misassignment rate is applied to data events satisfying the requirements of the region, except that the two leptons must have opposite charges.

JHEP10(2025)093

8 Sources of systematic uncertainty

Different sources of systematic uncertainty are considered for this measurement. They are grouped into three categories: instrumental uncertainties that affect physics object reconstruction; modelling uncertainties relevant for MC simulation-based estimations; and uncertainties affecting the estimate of fake and non-prompt lepton backgrounds. All uncertainties include both shape and normalisation effect, unless otherwise stated in their description.

The description of the sources of systematic uncertainties is organised as follows: first, those common to all three channels are presented, followed by sections addressing uncertainties specific to the $H \to b\bar{b}$ channel and the 2ℓ SS and 3ℓ channels.

8.1 Common systematic uncertainties

Instrumental systematic uncertainties considered are related to: trigger efficiency; lepton reconstruction, identification and isolation efficiencies; lepton calibration; jet calibration; JVT and fJVT efficiencies; b-tagging efficiency; $E_{\mathrm{T}}^{\mathrm{miss}}$ calibration. The experimental systematic uncertainties are applied either as an event-reweighting correction factor or as a rescaling or smearing of the object energy and momentum for scale and resolution uncertainties.

Uncertainties associated with the lepton selection arise from the trigger, reconstruction, identification and isolation efficiencies, and the lepton momentum scale and resolution as described in refs. [98–100]. Uncertainties on the efficiency of the BDT designed to reject non-prompt leptons are estimated through a $Z \to \ell\ell$ tag-and-probe method and cover contributions related to the $Z(\to \ell\ell)$+jets MC modelling, the template cut/shape, the $m_{\ell\ell}$ window, the tag-and-probe lepton selections, the multijet background, the non-prompt lepton background, the luminosity, the cross-sections of the considered processes, and the limited number of events in simulation and data.

Uncertainties associated with jet reconstruction and calibration arise from the jet energy scale (JES), jet energy resolution (JER) and the JVT/fJVT requirements. The JES uncertainty accounts for contributions from composition of jet flavour, η-intercalibration, punch-through, single-particle response, calorimeter response and pile-up making up for a total of 31 independent variations [106]. The JER is measured separately for data and MC using an in-situ technique and the associated uncertainties are split into 13 components [106]. The JVT efficiency is measured in data and correction factors are applied to simulated events to correct the simulated performance. The uncertainty associated with the JVT performance is obtained by varying the correction factors [107].

The uncertainty in $E_{\mathrm{T}}^{\mathrm{miss}}$ results from the propagation of the uncertainties in the energy scales and resolutions of photons, leptons and jets, and from the modelling of its soft term [120].

The efficiency of the b-tagging algorithm is measured for each jet flavour using control samples in data and in simulation. From these measurements, correction factors are derived to correct the tagging rates in the simulation. For b-jets, the correction factors and their uncertainties are estimated from data using dileptonic $t\bar{t}$ events [110, 121]. For c-jets, they are derived from jets arising from W boson decays in $t\bar{t}$ events [122]. For light-flavour jets, the correction factors are derived from $Z+$jets events [123]. Uncertainties from sources

JHEP10(2025)093

affecting the b-tagging efficiencies of b-jets, c-jets and light-jets are evaluated as a function of jet p_{T}, including bin-to-bin correlations.

The uncertainty in the reweighting of the MC pile-up distribution to match the distribution in data is evaluated by varying the reweighting factors and has a very small impact on either the combined or individual results. The uncertainty in the combined 2015–2018 integrated luminosity is 0.83% [124], obtained using the LUCID-2 detector for the primary luminosity measurements, complemented by measurements using the inner detector and calorimeters.

Systematic uncertainties in the tHq and tWH MC predictions due to missing higher-order QCD corrections in the modelling are estimated by doubling and halving the μ_{r} and μ_{f} scales chosen for the nominal sample. A systematic uncertainty due to the choice of the PS model is estimated as the relative difference between the Powheg +Pythia 8 and Powheg +Herwig 7 predictions and applied to the nominal predictions. An uncertainty is considered on the cross-section summing in quadrature the contributions from QCD scale, flavour scheme, PDF and α_s from a NLO QCD prediction: the values obtained are equal to 15.4% and 9.2% for tHq and tWH, respectively [52, 53].

The uncertainty in the $t\bar{t}$ modelling due to the choice of the h_{damp} parameter, which controls the resummation of higher-order terms, is estimated by comparing the nominal prediction with a Powheg +Pythia 8 sample where the parameter is set to $3 \times m_{\mathrm{top}}$. Reweighted events are used to assess the impact of ISR simulation within the nominal Powheg +Pythia 8 simulation: μ_{f} and μ_{r} scales are varied by 0.5 (high radiation) or 2.0 (low radiation) together with the PS tune `Var3c` [51]. The μ_{r} and μ_{f} scales are varied in both the hard-scatter process and PS and they are modified independently. The hadronisation model uncertainty and other non-perturbative effects in the PS are evaluated by comparing the nominal sample with Powheg+Herwig 7.2.1. The PS scale uncertainty is evaluated using the `Var3c` eigentune variation of the A14 tune [125]. The impact of FSR is evaluated by varying the renormalisation scale for PS emissions by factors of 0.5 and 2.0, using reweighted events.

The uncertainty in $t\bar{t}H$ modelling due to the ISR is estimated by using weights in the ME calculation and the PS. The μ_{r} and μ_{f} scales are varied, and ISR α_{s} variations are evaluated similarly to the $t\bar{t}$ process. The impact of FSR is evaluated using PS weights that vary the renormalisation scale for QCD emission in the FSR by a factor of 0.5 and 2.0. Additionally, uncertainties in the ME (PS, hadronisation and underlying-event modelling) are estimated by comparing the nominal Powheg +Pythia 8 MC simulation with aMC@NLO +Pythia 8 (Powheg +Herwig 7). The predicted $t\bar{t}H$ cross-section uncertainty is $^{+5.8\%}_{-9.2\%}$(scale) + 3.6%(PDF+α_{s}) [52] and the two components are considered uncorrelated.

Systematic uncertainties in the $t\bar{t}W$ MC predictions due to missing higher-order QCD corrections in the modelling are considered. To estimate the uncertainty due to ambiguities in the ME and PS algorithm and parameter choices, the nominal Sherpa prediction is compared with the prediction of the MadGraph5_aMC@NLO +Pythia 8 FxFx sample described in section 4. In addition, a dedicated PS model uncertainty is estimated as the relative difference between the Powheg +Pythia 8 and Powheg +Herwig 7 predictions and applied to the nominal $t\bar{t}W$ prediction. Modelling uncertainties due to μ_{r} and μ_{f} scales [126], and the amounts of ISR/FSR are evaluated similarly to the $t\bar{t}$ and $t\bar{t}H$ processes. Uncertainties in the PDF modelling are included by varying the value of α_{s} and using different PDF sets.

JHEP10(2025)093

The predicted $t\bar{t}W$ cross-section uncertainty is $^{+9.7\%}_{-10.8\%}$(scale) + 7.2%(PDF+α_s) [78] and the two components are considered uncorrelated. The uncertainty on the theoretical prediction of the $t\bar{t}W$ cross-section is dropped in the 3ℓ and 2ℓ SS channels as the normalisation of this background is estimated from data.

Uncertainties due to missing higher orders in QCD are estimated for $t\bar{t}Z$ production by varying the nominal μ_r and μ_f scales are evaluated similarly to the $t\bar{t}$, $t\bar{t}H$ and $t\bar{t}W$ processes. Uncertainties in additional-jet modelling are estimated with ISR α_s variations taken from the A14 tune. To estimate the uncertainty due to ambiguities in the ME and PS algorithm and parameter choices, the nominal prediction is compared with Sherpa. PS, hadronisation and underlying-event modelling uncertainties are estimated by comparing the nominal aMC@NLO +Pythia 8 MC simulation with MadGraph5+Herwig 7. The predicted $t\bar{t}Z$ cross-section uncertainty is $^{+9.6\%}_{-11.3\%}$(scale) + 4%(PDF+α_s) [52].

Systematic uncertainties due to missing higher-order QCD corrections are also considered for the three single-top-quark processes: t-channel, tW and s-channel. The uncertainty due to the choice of the hadronisation model and the other non-perturbative aspects of the PS is evaluated comparing the nominal prediction with that provided by the Powheg+Herwig 7.1.6 simulation. An uncertainty is also attributed to the choice of the Powheg approach to perform the matching between the hard-scatter and the PS. This uncertainty is estimated comparing the nominal Powheg+Pythia 8 prediction with the aMC@NLO+Pythia 8 simulation for the tW process, and the Powheg+Herwig 7.1.6 with the aMC@NLO+Herwig 7.1.6 prediction for the t-channel and s-channel. An additional uncertainty is quoted for the tW process to estimate the difference between the DS and DR schemes. Finally, a conservative 5% uncertainty on the theoretical cross-section of single-top-quark processes (t-channel, tW and s-channel) is considered in the $H \to b\bar{b}$ channel. In the 3ℓ channel, a 5.4% uncertainty on the tW production cross-section [127] is considered. For the 2ℓ SS channel, where single-top-quark contributions are negligible, no uncertainty from these processes is included.

Uncertainties in diboson modelling due to missing higher orders in QCD are estimated by varying the nominal μ_r and μ_f scales by factors of 0.5 and 2.0. In addition, a normalisation uncertainty of 24.5% is considered, as a result of adding in quadrature the theory uncertainty (5%) and 24% per additional jet, accordingly to the Berends-Giele scaling [128].

For minor backgrounds such as Z + jets, W + jets, tZq, tWZ, rare top-quark ($t\bar{t}t$ and $t\bar{t}t\bar{t}$) and other Higgs-boson production modes (ggH, VBF and VH) only the theoretical uncertainty on the predicted cross-section is considered. A normalisation uncertainty of 35% and 40% is considered for the Z + jets and W + jets processes in the $H \to b\bar{b}$ channel only. This is the result of adding in quadrature the theory uncertainty (4% for W + jets and 5% for Z + jets) and 24% per additional jet. In the 2ℓ SS and 3ℓ channels, the normalisation of these processes is derived from data as part of the fake and non-prompt leptons estimate. The predicted tZq cross-section uncertainty is $^{+7.7\%}_{-7.9\%}$(scale) + 0.9%(PDF+α_s) [49] and the two components are considered uncorrelated. The contribution of the tWZ, rare top-quark and other Higgs-boson production processes is small in all the channels, for this reason a conservative 50% uncertainty on their cross-section is applied.

JHEP10(2025)093

8.2 Channel-specific uncertainties: $H \to b\bar{b}$ channel

In the $H \to b\bar{b}$ channel, the effect of every modelling uncertainty associated to the $t\bar{t}$ simulation are considered independently for the three categories, $t\bar{t}+ \geq 1b$, $t\bar{t}+ \geq 1c$ and $t\bar{t}+ \geq 0$ light. In the $t\bar{t}+ \geq 1b$ case, since its yield is estimated from data, the normalisation of alternative samples is rescaled to match the nominal prediction in the preselection region. In addition to the $t\bar{t}$ modelling uncertainties common to all the channels, one from the NLO matching scheme in the $t\bar{t}$ simulated sample is also included comparing the nominal sample to the $p_{\mathrm{T}}^{\mathrm{hard}}$ varied one. A modelling uncertainty due to the differences between the nominal $t\bar{t}+ \geq 1b$ simulation in the 5FS and an alternative $t\bar{t} + b\bar{b}$ simulation in the 4FS is considered [129]. The uncertainty is applied independently to three sub-components of the $t\bar{t}+ \geq 1b$ background, defined according to the number of hadrons matched to the additional jet produced in association with the top-quark pair. The three sub-components are:

- $t\bar{t}$ $+1b$, if one additional jet in the event is matched to a single b-hadron,
- $t\bar{t}$ $+1B$, if one additional jet in the event is matched to a gluon splitting $g \to b\bar{b}$,
- $t\bar{t}$ $+2b$, if two additional jets in the event are matched to a single b-hadron each.

A 50% uncertainty on the normalisation of the $t\bar{t}+ \geq 1c$ is also considered in the fit model [130]. Finally, a theoretical uncertainty of 6% is applied on the $t\bar{t}+ \geq 0$ light normalisation as estimated in a dedicated validation region.

A systematic uncertainty is included to account for the difference between lepton fake rates originating from heavy-flavour decays versus those from misidentified jets. This uncertainty is evaluated separately for muons and electrons and its normalisation component contributes approximately 10% for muons and 30% for electrons.

8.3 Channel-specific uncertainties: 2ℓ SS and 3ℓ channels

For both the 2ℓ SS and 3ℓ channels, all the common $t\bar{t}$ modelling uncertainties are considered, as the $t\bar{t}$ simulation is used to estimate non-prompt lepton backgrounds originating from heavy-flavour decays and conversions. The modelling uncertainties associated to $t\bar{t}$ simulation are considered correlated among the various non-prompt leptons categories and between the 2ℓ SS and 3ℓ channels. Their effect is shape only as the normalisation of these backgrounds is estimated from data. In addition to the $t\bar{t}$ modelling uncertainties common to all the channels, one from the NLO matching scheme in the $t\bar{t}$ simulated sample is also included comparing predictions from Powheg+Herwig 7.1.3 and MadGraph5_aMC@NLO+Herwig 7.1.3 simulations. A conservative uncertainty of 50% is assigned to a small fraction of events, roughly 3% in the preselection region, where the origin of the non-prompt lepton could not be identified.

In the 2ℓ SS channel a systematic uncertainty of 10%–60% is assigned to the estimation of background from electrons with misidentified charge as described in section 7.2.

9 Results

A maximum-likelihood fit to all bins in the three SRs and the nine CRs (see table 4) is performed to simultaneously determine the background and the tH signal yields in the data.

JHEP10(2025)093

The discriminant variable used in the SRs is defined as follows: for the $H \to b\bar{b}$ channel, it is the BDTG response for tHq signal-like events, P(tHq); for the 2ℓ SS and 3ℓ channels, it is given by the output of the BDTG trained to target tHq events, BDT(tHq). In the CR($t\bar{t}+ \geq 1b$), the discriminant is the BDTG response for $t\bar{t}+ \geq 1b$-like events, P($t\bar{t}+ \geq 1b$). The H_{T} variable is used in all the CRs of the 2ℓ SS channel and in the 3ℓ channel control region targeting the $t\bar{t}W$ process. Finally, the $\Delta R(\ell_C, \ell_A + \ell_B)$ variable[8] is used in the CR(μ_{HF}) and CR(e_{HF}) of the 3ℓ channel while the BDTG response of the binary classifier targetting $t\bar{t}$ is used in the CR(e_{conv}).

The likelihood function $\mathcal{L}(\mu, \vec{k}, \vec{\theta})$ is constructed as a product of Poisson probability terms over all bins considered in the measurement, and depends on the following: the signal-strength parameter, μ, defined as a multiplicative factor applied to the predicted yield for the tHq and tWH signal processes; $\vec{k}$, the normalisation factors for several backgrounds; and $\vec{\theta}$, a set of nuisance parameters (NPs) encoding systematic uncertainties in the signal and background expectations [131]. Systematic uncertainties can impact the estimated signal and background rates, the migration of events between categories, and the shape of the fitted distributions; they are summarised in section 8. Both μ and $\vec{k}$ are treated as free parameters in the likelihood fit. The NPs $\vec{\theta}$ allow variations of the expectations for signal and background according to the systematic uncertainties, subject to Gaussian constraints in the likelihood fit. Their fitted values represent the deviations from the nominal expectations that are needed to provide the best fit to the data. Statistical uncertainties in each bin due to the limited size of the simulated event samples are taken into account with dedicated parameters, using the Beeston-Barlow "lite" technique [132]. All systematic uncertainties are fully correlated across channels, except for those that are specific to a given channel.

The best-fit value of the tHq and tWH signal strength, μ_{tH}, is:

$$\mu_{tH} = 8.1 \pm 2.6 \text{ (stat.)} \pm 2.0 \text{ (syst.)}.$$

This value corresponds to a measured value of the cross-section of $\sigma(tH) = 720 \pm 270$ fb. Figure 3(a) shows the signal strength measured in the different channels together with their combined value.

The compatibility of the signal strength evaluated from the different channels and the combined value is assessed by performing a likelihood ratio test and a p-value of 91% is obtained. The significance of the observed (expected) signal above the background-only expectation is 2.8 (0.4) standard deviations. The significance of the observed signal compared with the signal-plus-background hypothesis is instead 2.4. In the absence of a significant deviation from the background-only hypothesis, a 95% CL upper limit on the signal strength is set at 13.9 (6.1) times the observed (expected) SM prediction, as shown in figure 3(b). To quantify how well the fit model describes the data, a goodness-of-fit test is performed. The test consists of comparing the nominal model to a so-called saturated model [133], one constructed with enough degrees of freedom to describe the data perfectly. The probability obtained for the goodness-of-fit test is 98%, confirming excellent fit quality.

[8] Among the three leptons in the event in the 3ℓ channel, the lepton with the highest p_{T} is called ℓ_A, the one with the second highest p_{T} is called ℓ_B while the lepton with the softest p_{T} is called ℓ_C. The variable $\Delta R(\ell_C, \ell_A + \ell_B)$ is defined computing the ΔR value of the ℓ_C lepton with the system composed by summing the four vectors of leptons ℓ_A and ℓ_B.

JHEP10(2025)093

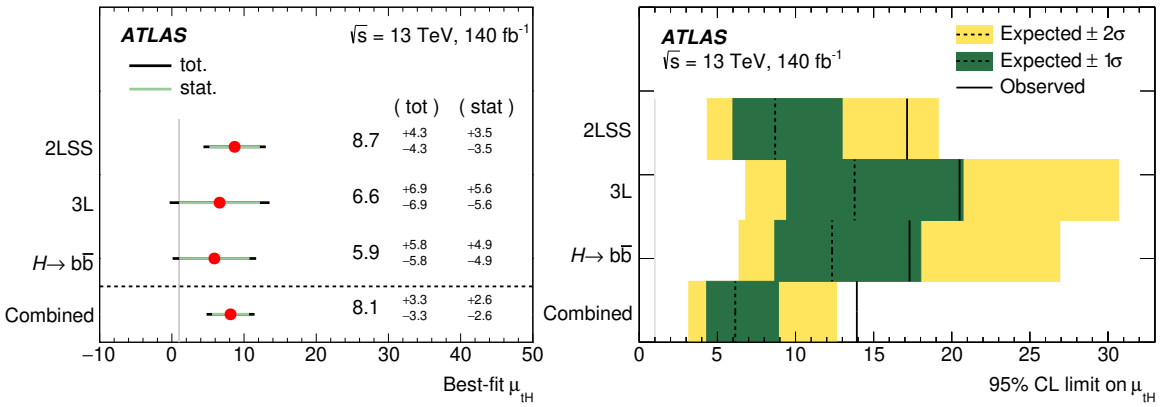

(a) (b)

Figure 3. The (a) fitted values of the μ_{tH} and (b) 95% CL upper limits in the individual channels and in the combined measurement. The values reported for the individual channels are obtained by fitting μ_{tH} separately for each channel, whereas the combined measurement is derived by simultaneously fitting all channels together. The observed limits are shown (solid black lines), together with the expected limits under the SM hypothesis (dotted black lines). A grey line is added in correspondence of the μ_{tH} equal to one. In the case of the expected limits, the one- and two-standard-deviation uncertainty bands are also shown.

The contributions from the different sources of uncertainty affecting the measured μ_{tH} are evaluated using the covariance-matrix decomposition method [134] and are shown, grouped by category, in table 5. The leading source of uncertainty is the statistical uncertainty. The largest source of systematic uncertainty is the theoretical uncertainty with the biggest contribution coming from the uncertainty on the signal prediction and $t\bar{t}$. Among the experimental uncertainties, the leading contribution stems from the JES and JER.

The impact of the top 20 NPs in the fit on μ_{tH} is shown in figure 4 for the SM scenario and it is assessed as follows: if the uncertainty on the parameter is σ_k, the uncertainty on μ_{tH} is σ_μ, and the correlation between the parameter and μ_{tH} is $\rho_{k,\mu}$, the impact is computed as $\sigma_k \rho_{k,\mu} \sigma_\mu$. The plot shows the measured NPs and their agreement with the expected values. The most constrained NP corresponds to the PS uncertainty in the $t\bar{t}+ \geq 0$ light category. All pulls are below one standard deviation with the strongest pull stemming from the PS uncertainty on the $t\bar{t}+ \geq 1b$ category, suggesting a mild mis-modelling of this contribution in the $H \to b\bar{b}$ channel. Overall, the lack of significant pulls or constraints in the NPs indicates a good agreement between data and the fit model, supporting the robustness of the fit and the reliability of the extracted signal strength.

The observed and expected yields in the three SRs and the nine CRs after the combined likelihood fit under the signal-plus-background hypothesis are compared with data in figures 5 and 6. Detailed tables showing pre-fit and post-fit yields for all regions are reported in section B. A good agreement between data and prediction is found in all the regions.

Additional measurements are performed using the ITC hypothesis ($\kappa_t = -1$) as signal model. The best-fit value of the tH signal strength under the ITC hypothesis is:

$$\mu_{tH}(\kappa_t = -1) \;=\; 1.2 \;\pm\; 0.4 \;\;(\text{stat.}) \;\pm\; 0.5 \;\;(\text{syst.})\,.$$

JHEP10(2025)093

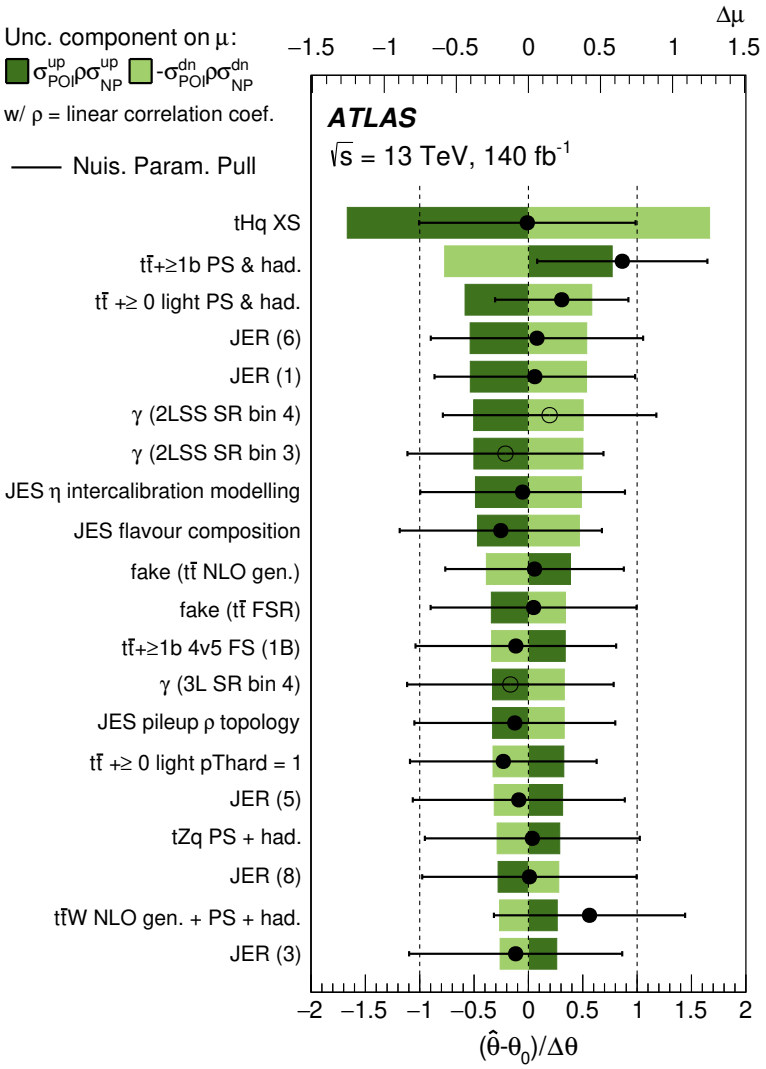

Figure 4. The impact of the top 20 most important systematic uncertainties on the fitted μ_{tH} in the SM scenario. The uncertainties are listed in decreasing order of their impact on μ_{tH}. The filled boxes show the relative impact on μ_{tH}, referring to the top x-axis. The points, referring to the bottom x-axis, show the deviations on the fitted NPs $\boldsymbol{\theta}_0$ from their nominal values, expressed in terms of standard deviations with respect to their nominal uncertainties. The associated black uncertainty bars show the fitted uncertainties of the NPs, relative to their nominal uncertainties. Filled markers refer to systematic uncertainties, while empty black markers refer to statistical uncertainties in the MC simulation in a given bin of an analysis region and they are labelled as γ. The results shown are extracted from the fit including all channels.

JHEP10(2025)093

Source	Impact on μ_{tH}			
	Combination	$H \to b\bar{b}$	2ℓ SS	3ℓ
Theory uncertainties (modelling)	1.69	2.97	1.64	2.63
Signal	1.26	0.88	1.33	1.22
$t\bar{t}+ \geq 1b$	0.70	2.57	—	—
$t\bar{t}+ \geq 0$ light and $t\bar{t}+ \geq 1c$	0.54	1.04	—	—
$t\bar{t}\,W$	0.23	<0.01	0.52	0.18
$t\bar{t}$	0.43	—	0.52	1.95
Rest of backgrounds	0.50	0.60	0.63	1.23
Experimental uncertainties	1.07	0.95	1.61	2.61
JES and JER	1.00	0.51	1.57	2.51
Non-prompt lepton bkg. modelling	0.25	0.59	0.22	0.07
Flavour tagging	0.17	0.52	0.13	0.17
Muons	0.12	< 0.01	0.12	0.40
$E_{\mathrm{T}}^{\mathrm{miss}}$	0.10	0.04	0.20	0.03
Pile-up	0.12	0.04	0.05	0.44
Electrons	0.10	0.07	0.11	0.32
Charge mis-identification	0.07	—	0.06	—
JVT and fJVT	0.04	0.10	0.11	0.06
Luminosity	0.09	0.09	0.10	0.14
Total systematic uncertainty	2.01	3.11	2.30	4.06
Statistical uncertainty	2.56	4.87	3.5	5.60
Normalisation factors	0.50	0.04	0.84	0.73
MC statistics	0.64	< 0.01	1.05	1.67
Total	3.3	5.8	4.3	6.9

Table 5. The absolute contribution of the main sources of uncertainty on the signal strength μ_{tH}. Some NPs with small impacts are grouped into categories, with the impact of the category being the quadrature sum of individual parameter impacts. Indentation is used to denote subcategories.

The observed and expected yields in the three SRs after the combined likelihood fit under the signal-plus-background hypothesis are compared with data in figure 7 for the ITC hypothesis.

The measured inverted-coupling signal strengths in the individual channels and the combined result are summarised in figure 8(a). The corresponding observed (expected) 95% CL exclusion limit is 2.4 (1.2), which is shown in figure 8(b) for both the individual channels and the combined measurement. The goodness-of-fit test probability for the $\kappa_t = -1$ scenario fit is 95%. In contrast to the SM case, under the ITC hypothesis the channel with the highest sensitivity is the $H \to b\bar{b}$ channel, overtaking the multi-lepton channels despite its modest signal-to-background ratio in the SM case (see section B). This inversion arises from the strong enhancement of the tHq cross-section together with the discriminating power of key variables in the $H \to b\bar{b}$ channel, such as the number of jets and number of jets associated with the reconstructed hadronic top quark from different $t\bar{t}$ reconstruction

JHEP10(2025)093

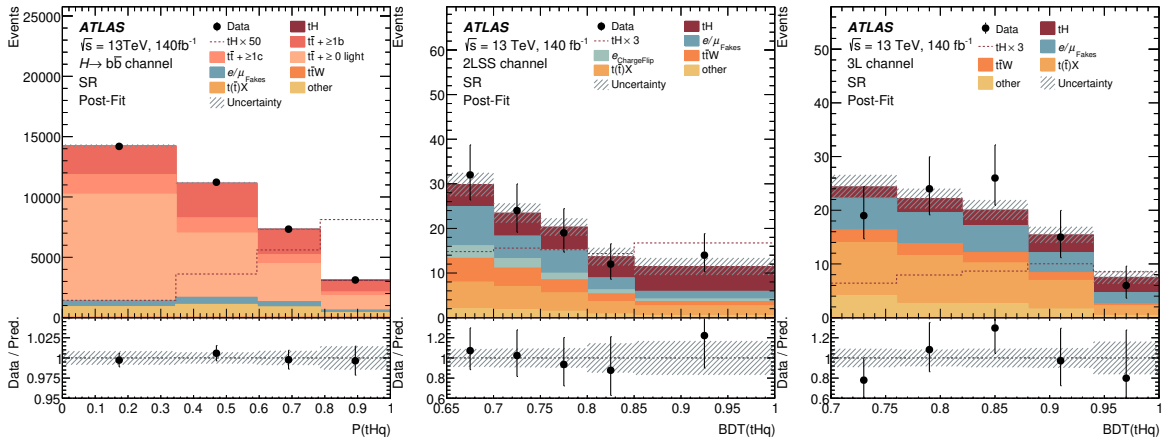

(a) (b) (c)

Figure 5. Comparison between data and the signal-plus-background prediction for the event yields in the (a) $H \to b\bar{b}$, (b) 2ℓ SS and (c) 3ℓ SRs. The term e/μ_{Fakes} refers to backgrounds from non-prompt or misidentified leptons, namely contributions from heavy-flavour decays and photon conversions. The SM signal and the background contributions after the likelihood fit to data ("Post-Fit") under the signal-plus-background hypothesis are shown as filled histograms. A dashed red line is added to the plot to show the signal contribution normalised to the measured value multiplied by 50 for the $H \to b\bar{b}$ channel and by 3 for the 2ℓ SS and 3ℓ channels. The ratio of the data to the total post-fit prediction ("Pred.") is shown in the lower panel. The combined statistical and systematic uncertainty in the prediction is indicated by the grey hatched band.

techniques. By contrast, variables used in training the BDT(tHq) classifiers in the 2ℓ SS and 3ℓ channels, such as invariant masses or angular distances of leptons, show a similar behaviour as the background under the $\kappa_t = -1$ hypothesis, leading to a loss of signal-to-background discrimination power. The uncertainty on the measured signal strength for the ITC hypothesis is dominated by systematic sources. In particular, the absolute uncertainty on $\mu_{tH}(\kappa_t = -1)$ from the theoretical uncertainty in the $t\bar{t}+ \geq 1b$ category is 0.25, the JES and JER together contribute 0.20, the uncertainty from the signal theoretical prediction is 0.18, and that from the modelling of $t\bar{t}$ in the 2ℓ SS and 3ℓ channels is 0.17.

JHEP10(2025)093

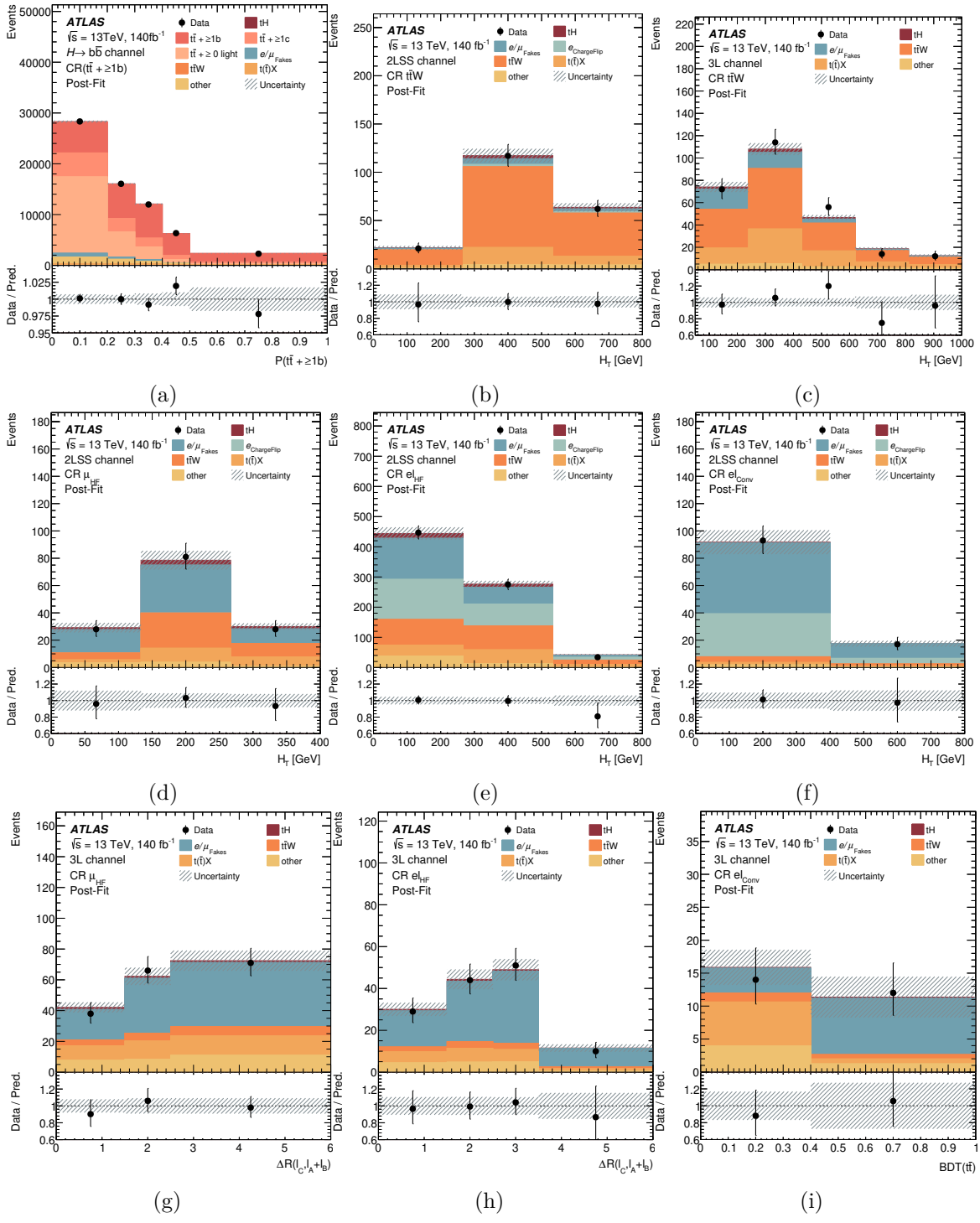

Figure 6. Comparison between data and the signal-plus-background prediction for the event yields in the nine CRs. The term e/μ_{Fakes} refers to backgrounds from non-prompt or misidentified leptons, namely contributions from heavy-flavour decays and photon conversions. The signal and background contributions after the likelihood fit to data ("Post-Fit") under the signal-plus-background hypothesis are shown as filled histograms. The ratio of the data to the total prediction ("Pred.") is shown in the lower panel. The combined statistical and systematic uncertainty in the prediction is indicated by the grey hatched band.

JHEP10(2025)093

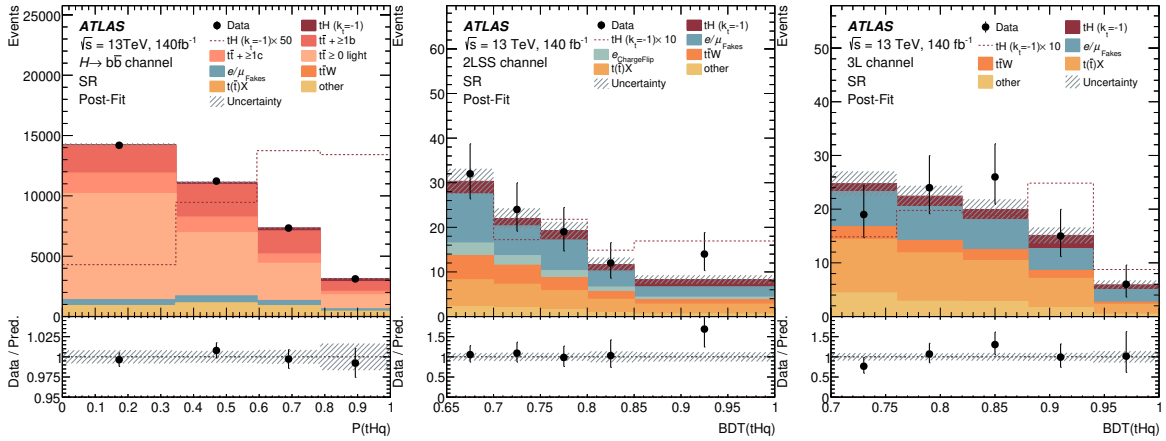

(a) (b) (c)

Figure 7. Comparison between data and the signal-plus-background prediction for the event yields in the (a) $H \to b\bar{b}$, (b) 2ℓSS and (c) 3ℓ SRs in the ITC hypothesis. The term e/μ_{Fakes} refers to backgrounds from non-prompt or misidentified leptons, namely contributions from heavy-flavour decays and photon conversions. The ITC signal and the background contributions after the likelihood fit to data ("Post-Fit") under the signal-plus-background hypothesis are shown as filled histograms. A dashed red line is added to the plot to show the signal contribution normalised to the measured value multiplied by 50 for the $H \to b\bar{b}$ channel and by 10 for the 2ℓSS and 3ℓ channels. The ratio of the data to the total post-fit prediction ("Pred.") is shown in the lower panel. The combined statistical and systematic uncertainty in the prediction is indicated by the grey hatched band.

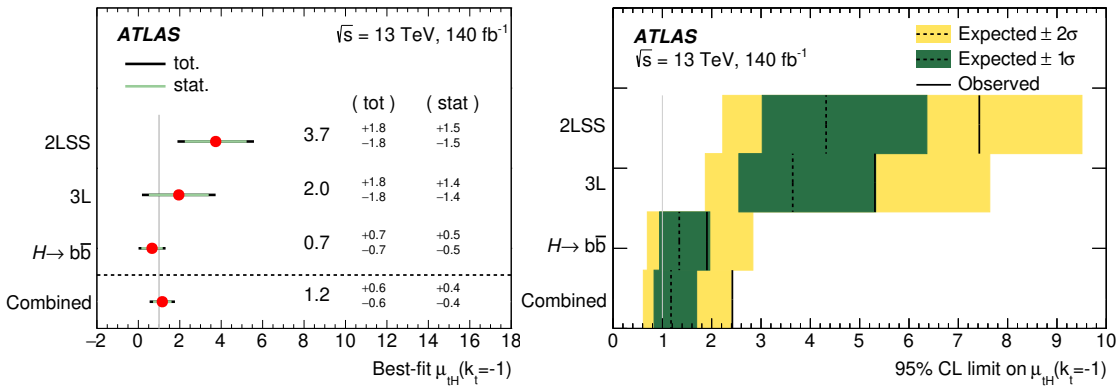

(a) (b)

Figure 8. Fitted values of (a) $\mu_{tH}(\kappa_t = -1)$ and (b) the 95% CL upper limits, shown for the individual channels and the combined measurement. The values reported for the individual channels are obtained by fitting $\mu_{tH}(\kappa_t = -1)$ separately for each channel, whereas the combined measurement is derived by simultaneously fitting all channels together. The observed limits are shown (solid black lines), together with the expected limits under the ITC hypothesis (dotted black lines). A grey line is added in correspondence of the $\mu_{tH}(\kappa_t = -1)$ equal to one. In the case of the expected limits, the one- and two-standard-deviation uncertainty bands are also shown.

JHEP10(2025)093

10 Conclusion

The search for the production of a Higgs boson in association with a single top quark (tH) is presented. The analysis is based on pp collision data at 13 TeV with an integrated luminosity of 140 fb^{-1}, recorded from 2015 to 2018 with the ATLAS detector at the LHC. The signal regions are split into final states with one, two same-sign or three isolated leptons (electrons or muons) probing the $H \to b\bar{b}$, $H \to WW^*$, $H \to ZZ^*$ and $H \to \tau\tau$ decays of the Higgs boson. Additional background-enriched regions are used in the fit to improve the modelling of several leading backgrounds, such as $t\bar{t}+ \geq 1b$, $t\bar{t}W$ and three different categories of the fake and non-prompt leptons background. The tH signal strength is found to be $\mu_{tH} = 8.1 \pm 2.6$ (stat.) $\pm$ 2.0 (syst.) in the SM hypothesis. The measured value of the SM cross-section is $\sigma(tH) = 720 \pm 270$ fb. The main source of uncertainty for this measurement is the one associated with the available experimental data, therefore a better constraint can be obtained analysing a larger event sample. Despite the analysis being optimised to set the best tH limit under the SM hypothesis, it is possible to also test the ITC hypothesis. The signal strength value in this case is found to be $\mu_{tH}(\kappa_t = -1) = 1.2 \pm 0.4$ (stat.) $\pm$ 0.5 (syst.). The excess in data favours the ITC hypothesis, but both hypotheses are compatible with the data.

Acknowledgments

We thank CERN for the very successful operation of the LHC and its injectors, as well as the support staff at CERN and at our institutions worldwide without whom ATLAS could not be operated efficiently.

The crucial computing support from all WLCG partners is acknowledged gratefully, in particular from CERN, the ATLAS Tier-1 facilities at TRIUMF/SFU (Canada), NDGF (Denmark, Norway, Sweden), CC-IN2P3 (France), KIT/GridKA (Germany), INFN-CNAF (Italy), NL-T1 (Netherlands), PIC (Spain), RAL (U.K.) and BNL (U.S.A.), the Tier-2 facilities worldwide and large non-WLCG resource providers. Major contributors of computing resources are listed in ref. [135].

We gratefully acknowledge the support of ANPCyT, Argentina; YerPhI, Armenia; ARC, Australia; BMWFW and FWF, Austria; ANAS, Azerbaijan; CNPq and FAPESP, Brazil; NSERC, NRC and CFI, Canada; CERN; ANID, Chile; CAS, MOST and NSFC, China; Minciencias, Colombia; MEYS CR, Czech Republic; DNRF and DNSRC, Denmark; IN2P3-CNRS and CEA-DRF/IRFU, France; SRNSFG, Georgia; BMFTR, HGF and MPG, Germany; GSRI, Greece; RGC and Hong Kong SAR, China; ICHEP and Academy of Sciences and Humanities, Israel; INFN, Italy; MEXT and JSPS, Japan; CNRST, Morocco; NWO, Netherlands; RCN, Norway; MNiSW, Poland; FCT, Portugal; MNE/IFA, Romania; MSTDI, Serbia; MSSR, Slovakia; ARIS and MVZI, Slovenia; DSI/NRF, South Africa; MICIU/AEI, Spain; SRC and Wallenberg Foundation, Sweden; SERI, SNSF and Cantons of Bern and Geneva, Switzerland; NSTC, Taipei; TENMAK, Türkiye; STFC/UKRI, United Kingdom; DOE and NSF, United States of America.

Individual groups and members have received support from BCKDF, CANARIE, CRC and DRAC, Canada; CERN-CZ, FORTE and PRIMUS, Czech Republic; COST, ERC, ERDF, Horizon 2020, ICSC-NextGenerationEU and Marie Skłodowska-Curie Actions, European

JHEP10(2025)093

Union; Investissements d'Avenir Labex, Investissements d'Avenir Idex and ANR, France; DFG and AvH Foundation, Germany; Herakleitos, Thales and Aristeia programmes co-financed by EU-ESF and the Greek NSRF, Greece; BSF-NSF and MINERVA, Israel; NCN and NAWA, Poland; La Caixa Banking Foundation, CERCA Programme Generalitat de Catalunya and PROMETEO and GenT Programmes Generalitat Valenciana, Spain; Göran Gustafssons Stiftelse, Sweden; The Royal Society and Leverhulme Trust, United Kingdom.

In addition, individual members wish to acknowledge support from CERN: European Organization for Nuclear Research (CERN DOCT); Chile: Agencia Nacional de Investigación y Desarrollo (FONDECYT 1230812, FONDECYT 1240864, Fondecyt 3240661); China: Chinese Ministry of Science and Technology (MOST-2023YFA1605700, MOST-2023YFA1609300), National Natural Science Foundation of China (NSFC — 12175119, NSFC 12275265); Czech Republic: Czech Science Foundation (GACR — 24-11373S), Ministry of Education Youth and Sports (ERC-CZ-LL2327, FORTE CZ.02.01.01/00/22_008/0004632), PRIMUS Research Programme (PRIMUS/21/SCI/017); EU: H2020 European Research Council (ERC — 101002463); European Union: European Research Council (BARD No. 101116429, ERC — 948254, ERC 101089007), European Regional Development Fund (SMASH COFUND 101081355, SLO ERDF), Horizon 2020 Framework Programme (MUCCA — CHIST-ERA-19-XAI-00), European Union, Future Artificial Intelligence Research (FAIR-NextGenerationEU PE00000013), Italian Center for High Performance Computing, Big Data and Quantum Computing (ICSC, NextGenerationEU); France: Agence Nationale de la Recherche (ANR-21-CE31-0022, ANR-22-EDIR-0002); Germany: Baden-Württemberg Stiftung (BW Stiftung-Postdoc Eliteprogramme), Deutsche Forschungsgemeinschaft (DFG — 469666862, DFG — CR 312/5-2); China: Research Grants Council (GRF); Italy: Istituto Nazionale di Fisica Nucleare (ICSC, NextGenerationEU), Ministero dell'Università e della Ricerca (NextGenEU 153D23001490006 M4C2.1.1, NextGenEU I53D23000820006 M4C2.1.1, NextGenEU I53D23001490006 M4C2.1.1, SOE2024_0000023); Japan: Japan Society for the Promotion of Science (JSPS KAKENHI JP22H01227, JSPS KAKENHI JP22H04944, JSPS KAKENHI JP22KK0227, JSPS KAKENHI JP24K23939, JSPS KAKENHI JP24KK0251, JSPS KAKENHI JP25H00650, JSPS KAKENHI JP25H01291, JSPS KAKENHI JP25K01023); Norway: Research Council of Norway (RCN-314472); Poland: Ministry of Science and Higher Education (IDUB AGH, POB8, D4 no 9722), Polish National Science Centre (NCN 2021/42/E/ST2/00350, NCN OPUS 2023/51/B/ST2/02507, NCN OPUS nr 2022/47/B/ST2/03059, NCN UMO-2019/34/E/ST2/00393, UMO-2022/47/O/ST2/00148, UMO-2023/49/B/ST2/04085, UMO-2023/51/B/ST2/00920, UMO-2024/53/N/ST2/00869); Portugal: Foundation for Science and Technology (FCT); Spain: Ministry of Science and Innovation (MCIN & NextGenEU PCI2022-135018-2, MICIN & FEDER PID2021-125273NB, RYC2019-028510-I, RYC2020-030254-I, RYC2021-031273-I, RYC2022-038164-I); Sweden: Carl Trygger Foundation (Carl Trygger Foundation CTS 22:2312), Swedish Research Council (Swedish Research Council 2023-04654, VR 2021-03651, VR 2022-03845, VR 2022-04683, VR 2023-03403, VR 2024-05451), Knut and Alice Wallenberg Foundation (KAW 2018.0458, KAW 2022.0358, KAW 2023.0366); Switzerland: Swiss National Science Foundation (SNSF — PCEFP2_194658); United Kingdom: Royal Society (NIF-R1-231091); United States of America: U.S. Department of Energy (ECA DE-AC02-76SF00515), Neubauer Family Foundation.

JHEP10(2025)093

A List of input variables used to train the different BDTGs

For the 2ℓ SS and 3ℓ channels, leptons are ordered in three different ways:

- *Transverse momentum* ordering: the lepton with the highest p_{T} is called ℓ_A, the one with the second highest p_{T} is called ℓ_B while the lepton with the softest p_{T} is called ℓ_C;
- *Charge and ΔR between leptons* ordering: the lepton with the charge opposite to the sum of the three lepton charges is called ℓ_0, the lepton with the smallest ΔR to ℓ_0 is called ℓ_1, the remaining lepton is called ℓ_2;
- *Charge and ΔR with leading b-jet* ordering: the lepton with the charge opposite to the sum of the three lepton charges is called $\hat{\ell}_0$, the lepton with the smallest ΔR with the leading b-jet is called $\hat{\ell}_1$ while the remaining lepton is called $\hat{\ell}_2$.

The jet satisfying the 70% b-tagging requirement and having the highest p_{T} is called leading b-jet. The jet that fails the b-tagging requirement and maximises the invariant mass with the leading b-jet is called spectator jet, j_{s}. Every jet having $|\eta| > 2.5$ is called forward jet, j_{f}. A forward jet is defined as leading if it has the highest p_{T} among all the forward jets. Every jet with $|\eta| < 2.5$ is called central jet. Using the aforementioned leptons and jet definitions, several variables are constructed.

JHEP10(2025)093

Variable	$H \to b\bar{b}$	2ℓ SS				3ℓ			Description
		BDT($t\bar{t}$)	BDT(VV)	BDT($t\bar{t}W$)	BDT(tHq)	BDT(tHq)	BDT($t\bar{t}$)	BDT($t\bar{t}W$)	
$p^*_{\ell_A}$ (b-jet)	—	—	—	—	—	—	—	×	Momentum of lepton with respect to the leading b-jet rest frame.
$p^*_{\ell_B}$ (b-jet)	—	—	—	—	—	×	—	—	
$p^*_{\ell_C}$ (b-jet)	—	—	—	—	—	—	—	×	
$p_{\mathrm{T,min}}$	—	×	—	×	×	—	—	—	p_{T} of softest lepton.
$\Delta R(\ell_A, \ell_B + \ell_C)$	—	—	—	—	—	—	—	×	ΔR between lepton and the system of the other two leptons.
$\Delta R(\ell_B, \ell_A + \ell_C)$	—	—	—	—	—	—	—	×	
$\Delta R(\ell_A, b\text{-jet})$	—	—	—	—	—	×	—	×	ΔR between lepton and leading b-jet.
$\Delta R(\ell_B, b\text{-jet})$	—	—	—	—	—	—	—	×	
$\Delta R(\text{non-}b\text{-jet}, \ell_1)$	—	—	—	—	×	—	—	—	ΔR or $\Delta\eta$ between lepton and its closest b-jet or non-b-jet.
$\Delta R(\text{non-}b\text{-jet}, \ell_2)$	—	—	—	—	×	—	—	—	
$\Delta R(\ell_1, b\text{-jet})$	—	×	×	—	—	—	—	—	
$\Delta R(\ell_2, b\text{-jet})$	—	×	×	—	—	—	—	—	
$\Delta\eta(\ell_1, b\text{-jet})$	—	×	×	—	—	—	—	—	
$\Delta\eta(\ell_2, b\text{-jet})$	—	×	×	—	—	—	—	—	
$m(\ell, \ell)_{\mathrm{SS}}$	—	—	—	—	—	×	×	×	Invariant mass, ΔR, $\Delta\phi$ or $\Delta\eta$ of same-sign leptons.
$\Delta\eta(\ell, \ell)_{\mathrm{SS}}$	—	—	—	—	×	×	—	—	
$\Delta\phi(\ell, \ell)_{\mathrm{SS}}$	—	—	—	×	—	—	—	—	
$\Delta R(\ell, \ell)_{\mathrm{SS}}$	—	×	—	×	—	—	—	—	
$m(\ell_0, \ell_2)$	—	—	—	—	—	×	×	—	Invariant mass and ΔR of leptons, jets and/or leading b-jet. The lepton ordering is charge and ΔR based.
$m(\ell_0, \ell_1)$	—	—	—	—	—	×	×	×	
$m(\ell_1, b\text{-jet})$	—	—	—	—	—	×	—	×	
$m(\ell_2, b\text{-jet})$	—	—	—	—	—	×	×	—	
$\Delta R(\ell_0, \ell_1)$	—	—	—	—	—	—	—	×	
$m(\ell_2, \mathrm{j}_2)$	—	×	×	×	×	—	—	—	
$m(\ell_2, \mathrm{j}_1)$	—	×	×	—	×	—	—	—	
$m(\ell_1, \mathrm{j}_2)$	—	—	—	—	×	—	—	—	
$m(\ell_1 + \ell_2, \mathrm{j}_2)$	—	—	—	×	—	—	—	—	
$m(\ell_1 + \ell_2, \mathrm{j}_1 + \mathrm{j}_2)$	—	—	—	×	×	—	—	—	
$m(\ell_1 + \ell_2, \mathrm{j}_1)$	—	×	—	—	—	—	—	—	
$m(\mathrm{j}_1 + \mathrm{j}_2)$	—	—	×	×	×	—	—	—	
$m(\ell_1 + \ell_2)$	—	×	×	×	×	—	—	—	
$m_H(WW)$	—	×	—	×	×	—	—	—	Mass of a candidate Higgs Boson when decays into a pair of W bosons.
$m(\text{jet}, \text{jet})_W$	—	—	×	×	×	—	—	—	Mass of the best two jet candidates for the W boson.
$m(\text{jet}, \text{jet})_{\mathrm{top}}$	—	×	×	×	×	—	—	—	Mass of the best top-quark candidate from jets.
$m(\hat{\ell}_0, \hat{\ell}_1)$	—	—	—	—	—	—	×	—	Invariant mass of $\hat{\ell}_0$ and $\hat{\ell}_1$.
$m(\hat{\ell}_0, \hat{\ell}_2)$	—	—	—	—	—	×	—	×	Invariant mass and ΔR of $\hat{\ell}_0$ and $\hat{\ell}_2$.
$\Delta R(\hat{\ell}_0, \hat{\ell}_2)$	—	—	—	—	—	—	—	×	
$m(\hat{\ell}_2, b\text{-jet})$	—	—	—	—	—	×	—	×	Invariant mass and ΔR of leading b-jet and $\hat{\ell}_1$ and $\hat{\ell}_2$.
$\Delta R(\hat{\ell}_2, b\text{-jet})$	—	—	—	—	—	—	×	—	
$m(\ell, b\text{-jet})_{\mathrm{top}}$	—	—	—	—	—	—	×	×	Invariant mass of lepton and b-jet giving best top-quark visible mass.
$m(\ell, \ell)_{\mathrm{top}}$	—	—	—	—	—	×	×	—	Invariant mass of two leptons giving best top-quark visible mass.
p_{FW1}	—	—	—	×	—	—	—	—	First Fox-Wolfram moment [136, 137].

JHEP10(2025)093

Variable	$H \to b\bar{b}$	2ℓ SS				3ℓ			Description
		BDT($t\bar{t}$)	BDT(VV)	BDT($t\bar{t}W$)	BDT(tHq)	BDT(tHq)	BDT($t\bar{t}$)	BDT($t\bar{t}W$)	
p_{FW4}	—	×	×	—	—	—	—	×	Fourth Fox-Wolfram moment.
$p_{\mathrm{T,min}}$	—	—	—	—	—	×	×	×	p_{T} of the softest lepton.
$m(j_{\mathrm{s}})$	—	—	—	—	×	—	—	—	Mass of the spectator jet.
$E(j_{\mathrm{s}})$	—	—	—	—	×	—	—	—	Energy of the spectator jet.
$p_{\mathrm{T}}(j_{\mathrm{s}})$	—	—	—	—	×	—	—	—	p_{T} of the spectator jet.
$E_{\mathrm{T}}^{\mathrm{miss}}/H_{\mathrm{T}}$	—	—	×	—	—	—	—	×	Ratio between $E_{\mathrm{T}}^{\mathrm{miss}}$ and H_{T}.
N(jet)	×	—	—	—	—	—	—	—	Number of non-b-tagged jets.
N(non-b-jet)	—	—	—	—	—	—	—	×	Number of non-b-tagged jets.
N(central-jet)	—	—	—	—	—	×	×	×	Number of central jets.
N(b-jet)	—	—	—	—	—	—	×	×	Number of b-tagged jets.
$\Delta m(Z, \ell\ell_{\mathrm{SF}})_{\mathrm{min}}$	—	×	×	×	—	—	×	×	Minimum difference between the reconstructed invariant mass of two leptons with the same flavour and Z-boson mass.
$\Delta m(Z, \ell\ell)_{\mathrm{min}}$	—	—	—	—	—	×	×	×	Minimum difference between the reconstructed invariant mass of two leptons and Z-boson mass.
$E_{\mathrm{T}}^{\mathrm{miss}}$	—	×	×	×	×	×	×	×	$E_{\mathrm{T}}^{\mathrm{miss}}$.
$\Sigma_i \mathrm{charge}(\ell_i)$	—	×	×	×	×	—	—	—	Sum of lepton charges.
$m(b\text{-jet}, j_{\mathrm{s}})$	—	—	—	×	×	×	—	—	Invariant mass, $\Delta\phi$, $\Delta\eta$ and ΔR of leading b-jet and spectator jet.
$\Delta\phi(b\text{-jet}, j_{\mathrm{s}})$	—	—	—	—	—	×	—	—	
$\Delta\eta(b\text{-jet}, j_{\mathrm{s}})$	—	×	—	—	—	—	—	—	
$\Delta R(b\text{-jet}, j_{\mathrm{s}})$	—	—	—	×	×	—	—	×	
$\Delta R(\ell, j_{\mathrm{f}})$	—	×	—	—	—	—	—	—	ΔR and $\Delta\eta$ between the leading forward jet and its closest lepton.
$\Delta\eta(\ell, j_{\mathrm{f}})$	—	—	—	—	×	—	—	—	
$\Sigma_i q(\ell_i)$	—	—	—	—	—	×	×	×	Sum of lepton charges.
Lepton flavours	—	×	—	—	—	—	—	—	Identification of the flavour of the leptons.
$id(\ell_0)$	×	—	—	—	—	—	—	—	identification number of the lepton combining charge and flavour information.
$e\mu$-events	—	×	×	—	—	—	—	—	Identification of the events $e\mu$.
ee-events	—	—	×	×	×	—	—	—	Identification of the events ee.
H_{T}	—	—	×	—	×	×	×	×	H_{T}.
$H_{\mathrm{T}}(\ell)$	—	×	—	×	×	—	—	—	Sum of the transverse momentum of the leptons.
$H_{\mathrm{T}}(\mathrm{jets})$	—	×	—	×	—	—	—	—	Sum of the transverse momentum of the jets.
$\tilde{m}_{lep}$	—	×	×	×	×	×	—	—	$\sqrt{\Sigma_i (E_{\ell_i}^2 + p_{T,\ell_i}^2)}$.
$\Delta R(\ell, \ell)_{\mathrm{min}}$	—	—	—	—	—	—	—	×	Minimum ΔR between two leptons.
$\Delta\phi(\phi_T^{\mathrm{miss}}, \ell_2)$	—	—	—	×	—	—	—	—	$\Delta\phi$ between ϕ_T^{miss} and ℓ_2.
"custom" χ^2	—	×	×	×	—	—	—	—	$\chi^2(m(\ell_i, \ell_j)_{\mathrm{top}})_{\mathrm{min}}$, minimum χ^2 value between the masses of top-quark candidates given by the combination of leptons.
$m(\ell, \ell)_{\mathrm{top}}$	—	×	×	×	—	—	—	—	Invariant mass of two leptons giving best top-quark visible mass.
$\eta(\mathrm{No}\text{-}b\text{-jet})_{\mathrm{max}}$	—	—	—	×	—	—	—	—	Maximum η value among non-b-tagged jets.
$\Delta\eta(\ell_2, \text{non-}b\text{-jet})$	—	—	—	—	—	—	×	—	$\Delta\eta$ between ℓ_2 and closest non-b-tagged jets.
$\Delta\eta(\ell, j_{\mathrm{f}})$	—	—	—	—	—	×	—	—	$\Delta\eta$ between leading forward jet and closest lepton.
N(non-b-jet)	—	—	×	—	×	—	—	—	Number of non b-tagged jets.
N(central-jet)	—	×	×	×	×	—	—	—	Number of central jets.
N(b-jet)	—	×	×	×	—	—	—	—	Number of b-tagged jets.
$b\text{-score}_1$	—	×	×	×	×	×	×	×	Binned DL1r score (calibrated) of leading b-jet.
$b\text{-score}_2$	—	×	×	×	—	—	—	×	Binned DL1r score (calibrated) of second b-jet.

JHEP10(2025)093

Variable	$H \to b\bar{b}$	2ℓ SS				3ℓ			Description
		BDT($t\bar{t}$)	BDT(VV)	BDT($t\bar{t}W$)	BDT(tHq)	BDT(tHq)	BDT($t\bar{t}$)	BDT($t\bar{t}W$)	
b-score$_3$	—	×	×	×	—	—	—	×	Binned DL1r score (calibrated) of third b-jet.
"custom" n_j	×	—	—	—	—	—	—	—	$n_{j,t_{\text{had}}}(\chi^2_{\text{min, ttl}}, \text{PCBT-bin 4})$, number of jets that belong to the hadronic top-quark found from reconstructing $t\bar{t}$ events but allowing only Hypothesis I within the 4^{th} PCBT bin.
"custom" n_j	×	—	—	—	—	—	—	—	$n_{j,t_{\text{had}}}(\chi^2_{\text{min, ttAll}}, \text{PCBT-bin 4})$, number of jets that belong to the hadronic top-quark found from reconstructing $t\bar{t}$ events within the 4^{th} PCBT bin.
"custom" n_j	×	—	—	—	—	—	—	—	$n_{j,t_{\text{had}}}(\chi^2_{\text{min, ttAll}}, \text{PCBT-bin} \in \{1,2,3\})$, number of jets that belong to the hadronic top-quark found from reconstructing $t\bar{t}$ events within the 1^{st}, 2^{nd} or 3^{rd} PCBT bin.
$p_{\text{T}}^{\text{fwd},0}$	×	—	—	—	—	—	—	—	Transverse momentum of the leading forward-jet.
Sphericity	×	—	—	—	—	—	—	—	as defined in ref. [118].
$\chi^2_{\text{min,ttAll}}$	×	—	—	—	—	—	—	—	The minimum χ^2 value found from reconstructing $t\bar{t}$ events.
"custom" n_j	×	—	—	—	—	—	—	—	$n_{j,\text{not-}t_{\text{had}}}(\chi^2_{\text{min, ttl}}, \text{PCBT-bin} \in \{1,2,3\})$, number of jets that do not belong to the hadronic top-quark found from reconstructing $t\bar{t}$ events but allowing only Hypothesis I within the 1^{st}, 2^{nd} or 3^{rd} PCBT bin.
$p_{\text{T}}^{\text{light},1}$	×	—	—	—	—	—	—	—	Transverse momentum of the 2^{nd} leading jet failing to meet the b-tagging requirement.
"custom" χ^2	×	—	—	—	—	—	—	—	$\chi^2_{\text{top-higgs}}(m_H = 111.5, m_t = 168)$, the minimum χ^2 value found from reconstructing $tHq(H \to b\bar{b})$ events, where the leptonic W from the top-quark decay is reconstructed using the neutrino reconstruction technique.
$\chi^2_{\text{min,ttl}}$	×	—	—	—	—	—	—	—	The minimum χ^2 value found from reconstructing $t\bar{t}$ events allowing only Hypothesis I.
$\text{DL1r}_{\text{light},0}$	×	—	—	—	—	—	—	—	Pseudo-continuous b-tagging distribution for the leading jet failing to meet the b-tagging requirement.
$p_{\text{T}}^{\text{light},2}$	×	—	—	—	—	—	—	—	Transverse momentum of the 3^{rd} leading jet failing to meet the b-tagging requirement.
$\eta_{\text{light},0}$	×	—	—	—	—	—	—	—	Pseudo-rapidity of the leading jet failing to meet the b-tagging requirement.
"custom" χ^2	×	—	—	—	—	—	—	—	$\chi^2_{\text{top-higgs}}(m_H = 113, m_t = 165)$, the minimum χ^2 value found from reconstructing $tHq(H \to b\bar{b})$ events, where the leptonic W from the top-quark decay is reconstructed using the neutrino reconstruction technique.
$p_{\text{T}}^{\text{light},0}$	×	—	—	—	—	—	—	—	Transverse momentum of the leading jet failing to meet the b-tagging requirement.
$\Delta\eta_{\text{top-higgs}}$	×	—	—	—	—	—	—	—	The $\Delta\eta$ between the reconstructed top quark and the reconstructed Higgs boson according to the minimum χ^2 method.
"custom" n_j	×	—	—	—	—	—	—	—	$n_{j,t_{\text{had}}}(\chi^2_{\text{min, ttl}}, \text{PCBT-bin 0})$, number of jets that belong to the hadronic top-quark found from reconstructing $t\bar{t}$ events but allowing only Hypothesis I within the 0^{th} PCBT bin.
$m_{t_{\text{had}}}(\chi^2_{\text{min, ttAll}})$	×	—	—	—	—	—	—	—	The mass of the reconstructed hadronic top-quark found from reconstructing $t\bar{t}$ events.

JHEP10(2025)093

Variable	$H \to b\bar{b}$	2ℓ SS				3ℓ			Description
		BDT($t\bar{t}$)	BDT(VV)	BDT($t\bar{t}W$)	BDT(tHq)	BDT(tHq)	BDT($t\bar{t}$)	BDT($t\bar{t}W$)	
$m_{t_{\text{had}}}(\chi^2_{\text{min, ttl}})$	×	—	—	—	—	—	—	—	The mass of the reconstructed hadronic top-quark found from reconstructing $t\bar{t}$ events but allowing only Hypothesis I.
$\eta_{\text{light,2}}$	×	—	—	—	—	—	—	—	Pseudo-rapidity of the 3$^{\text{rd}}$ leading jet failing the b-tagging requirement.
$\Delta R(q_1^W, q_2^W)$	×	—	—	—	—	—	—	—	The minimum ΔR between the two jets assigned to the hadronic W decay from reconstructing $t\bar{t}$ events.
$m(b_{\text{top}}, j_{\text{tag}})$	×	—	—	—	—	—	—	—	The invariant mass of the b-jet from top-quark decay found using a reconstruction of $tHq(H \to b\bar{b})$ events and the light-flavour jet most de-correlated from the top-quark system. The light jet is chosen such that it maximises the invariant mass $m(b_{\text{top}}, j_{\text{tag}})$.
η_{tag}	×	—	—	—	—	—	—	—	The η of the light-flavour jet, η_{tag} most de-correlated from the top-quark system. The light jet is chosen such that it maximises the invariant mass $m(b_{\text{top}}, j_{\text{tag}})$.

Table 6. List of variables considered in the training of the BDTGs in each channel. The × symbol marks in which BDTGs the variable is used. Variables labelled with "custom" are better explained in the description column.

$H \to b\bar{b}$ channel				
	Pre-fit		Post-fit	
Process	SR	CR($t\bar{t}+\geq 1b$)	SR	CR($t\bar{t}+\geq 1b$)
tHq	43 ± 7	9.1 ± 2.0	350 ± 130	72 ± 29
tWH	3.4 ± 2.0	14 ± 8	28 ± 20	110 ± 80
$t\bar{t}+\geq 1b$	6800 ± 1100	20100 ± 2600	8100 ± 1000	25600 ± 1900
$t\bar{t}+\geq 1c$	4000 ± 2400	11000 ± 6000	3900 ± 1500	10200 ± 3300
$t\bar{t}+\geq 0$ light	19300 ± 3300	23100 ± 3500	18500 ± 1100	23300 ± 2100
e/μ_{Fakes}	1700 ± 500	1600 ± 500	1700 ± 500	1600 ± 500
$t\bar{t}W$	20.1 ± 3.0	134 ± 19	20.2 ± 2.9	133 ± 19
$t\bar{t}H$	120 ± 15	683 ± 70	120 ± 15	683 ± 70
$t\bar{t}Z$	68 ± 9	340 ± 40	68 ± 9	340 ± 40
tZq	69 ± 7	20.4 ± 1.9	69 ± 6	20.4 ± 1.9
tWZ	0.20 ± 0.10	0.9 ± 0.5	0.20 ± 0.11	0.9 ± 0.5
Wt channel	970 ± 260	1500 ± 500	970 ± 250	1600 ± 500
t-channel	1070 ± 180	350 ± 120	1060 ± 160	350 ± 120
s-channel	43 ± 8	40 ± 11	42 ± 7	39 ± 10
W + jets	740 ± 310	900 ± 400	750 ± 300	890 ± 350
Z + jets	140 ± 50	100 ± 40	140 ± 50	100 ± 40
VV	48 ± 25	70 ± 40	41 ± 22	63 ± 33
other Higgs	6 ± 5	5.3 ± 2.9	7 ± 5	5.2 ± 2.8
Rare top	0.08 ± 0.04	3.3 ± 1.7	0.08 ± 0.04	3.4 ± 1.7
Total	35000 ± 5000	60000 ± 8000	35870 ± 210	65000 ± 340
Data	35869	65002	35869	65002

Table 7. Pre-fit and post-fit event yields in the SR and CR($t\bar{t}+\geq 1b$) of the $H \to b\bar{b}$ channel. Post-fit yields are after the inclusive fit in all channels. All uncertainties are included, taking into account correlations in the post-fit case.

B Pre-fit and post-fit yields tables

Pre-fit and post-fit yields of the analysis regions are reported in table 7 for the $H \to b\bar{b}$ channel. Tables 8 and 9 show the pre- and post-fit yields for the 2ℓSS channel, respectively. Tables 10 and 11 show the pre- and post-fit yields for the 3ℓ channel, respectively.

JHEP10(2025)093

Pre-fit 2ℓ SS channel					
Process	SR	CR(μ_{HF})	CR(e_{HF})	CR(e_{conv})	CR($t\bar{t}W$)
tHq	3.1 ± 0.5	0.65 ± 0.11	2.5 ± 0.4	0.085 ± 0.024	0.30 ± 0.06
tWH	0.09 ± 0.04	0.20 ± 0.04	0.89 ± 0.13	0.016 ± 0.006	0.39 ± 0.05
μ_{HF}	16 ± 5	59 ± 11	19 ± 4	0.24 ± 0.24	3.0 ± 2.0
e_{HF}	4.9 ± 3.1	-	86 ± 17	1.3 ± 0.8	0.9 ± 0.8
e_{conv}	3.4 ± 2.7	-	80 ± 15	47 ± 15	2.8 ± 1.4
other mis-id leptons	4 ± 4	15 ± 12	41 ± 28	3.0 ± 3.0	3.7 ± 2.6
$e_{\text{ChargeFlip}}$	8.3 ± 1.9	-	220 ± 50	37 ± 11	4.4 ± 1.0
$t\bar{t}W$	14.9 ± 2.1	35 ± 4	160 ± 8	5.0 ± 0.4	131 ± 5
$t\bar{t}Z$	3.7 ± 0.6	8.0 ± 1.4	38 ± 6	1.12 ± 0.21	15.3 ± 2.2
$t\bar{t}H$	2.4 ± 0.4	7.2 ± 1.0	30 ± 4	0.77 ± 0.12	13.5 ± 2.0
tZq	14.2 ± 1.9	3.9 ± 0.5	22.0 ± 2.0	0.68 ± 0.09	1.05 ± 0.18
VV	7.3 ± 3.3	9 ± 5	50 ± 15	1.8 ± 1.5	7.2 ± 3.1
others	0.45 ± 0.13	1.1 ± 0.4	7.9 ± 2.1	0.28 ± 0.10	2.0 ± 0.5
4-tops	0.042 ± 0.014	0.050 ± 0.015	0.54 ± 0.15	0.016 ± 0.007	0.83 ± 0.24
Total	83 ± 10	138 ± 16	760 ± 80	98 ± 21	187 ± 8
Data	101	137	756	110	200

Table 8. Pre-fit event yields in the SR and CRs of the 2ℓ SS channel. The 'others' process includes tWZ, Tri-boson, s-channel, 3-tops and VH processes.

Post-fit 2ℓ SS channel					
Process	SR	CR(μ_{HF})	CR(e_{HF})	CR(e_{conv})	CR($t\bar{t}W$)
tHq	25 ± 9	5.3 ± 2.1	21 ± 8	0.67 ± 0.30	2.4 ± 0.9
tWH	0.7 ± 0.4	1.6 ± 0.7	7.3 ± 3.2	0.13 ± 0.07	3.2 ± 1.4
μ_{HF}	13 ± 6	47 ± 18	15 ± 7	0.22 ± 0.17	2.9 ± 1.9
e_{HF}	2.6 ± 3.4	-	50 ± 60	0.7 ± 0.9	0.5 ± 0.7
e_{conv}	3.8 ± 3.1	-	98 ± 35	58 ± 15	3.4 ± 1.6
other mis-id leptons	4 ± 4	15 ± 11	38 ± 25	3.3 ± 2.8	3.2 ± 2.1
$e_{\text{ChargeFlip}}$	8.0 ± 1.8	-	210 ± 50	36 ± 10	4.2 ± 1.0
$t\bar{t}W$	15.0 ± 2.4	41 ± 5	178 ± 17	5.7 ± 0.6	144 ± 13
$t\bar{t}Z$	3.7 ± 0.6	7.9 ± 1.3	37 ± 6	1.07 ± 0.20	15.1 ± 2.1
$t\bar{t}H$	2.4 ± 0.4	7.3 ± 0.9	30 ± 4	0.78 ± 0.11	13.5 ± 1.9
tZq	14.1 ± 1.9	3.9 ± 0.5	22.1 ± 2.0	0.68 ± 0.09	1.03 ± 0.17
VV	6.0 ± 2.4	7.1 ± 3.5	45 ± 13	2.0 ± 1.6	6.0 ± 2.4
others	0.44 ± 0.13	1.1 ± 0.4	7.9 ± 2.1	0.28 ± 0.11	1.9 ± 0.5
4-tops	0.043 ± 0.014	0.050 ± 0.015	0.55 ± 0.15	0.017 ± 0.007	0.85 ± 0.24
Total	99 ± 8	138 ± 11	762 ± 27	109 ± 10	202 ± 12
Data	101	137	756	110	200

Table 9. Post-fit event yields in the SR and CRs of the 2ℓ SS channel. Post-fit yields are after the inclusive fit in all channels. All uncertainties are included, taking into account correlations in the post-fit case. The 'others' process includes tWZ, Tri-boson, s-channel, 3-tops and VH processes.

JHEP10(2025)093

Pre-fit 3ℓ channel					
Process	SR	CR(μ_{HF})	CR(e_{HF})	CR(e_{conv})	CR($t\bar{t}W$)
tHq	1.45 ± 0.24	0.24 ± 0.06	0.159 ± 0.030	0.025 ± 0.007	0.26 ± 0.06
tWH	0.29 ± 0.04	0.24 ± 0.04	0.150 ± 0.023	0.019 ± 0.004	0.64 ± 0.07
μ_{HF}	9 ± 4	84 ± 11	3.2 ± 1.8	0.08 ± 0.11	10 ± 7
e_{HF}	5.3 ± 2.3	2.7 ± 2.2	47 ± 9	0.16 ± 0.04	6.9 ± 3.0
e_{conv}	4.2 ± 1.8	3.5 ± 3.2	14 ± 6	14 ± 9	11 ± 8
other mis-id leptons	4.9 ± 3.0	14 ± 10	8 ± 5	1.0 ± 1.0	10 ± 8
$t\bar{t}W$	7.9 ± 0.9	13.6 ± 0.6	8.1 ± 0.8	1.97 ± 0.33	118 ± 4
tWZ	0.8 ± 0.5	1.4 ± 0.7	0.8 ± 0.5	0.6 ± 0.4	3.5 ± 1.9
$t\bar{t}Z$	14.3 ± 2.1	15.6 ± 2.4	8.2 ± 1.3	4.9 ± 1.1	37 ± 5
$t\bar{t}H$	7.7 ± 1.0	7.6 ± 1.0	4.7 ± 0.7	0.51 ± 0.16	21.0 ± 2.8
tZq	10.8 ± 1.2	9.2 ± 1.1	4.8 ± 0.6	1.8 ± 0.4	6.0 ± 0.7
tW	1.1 ± 0.7	6 ± 4	3.6 ± 2.5	0.9 ± 0.7	1.6 ± 1.2
VV	12 ± 5	22 ± 7	11.0 ± 3.5	4.8 ± 1.7	13 ± 5
others	0.24 ± 0.08	0.44 ± 0.12	0.16 ± 0.05	0.040 ± 0.012	1.0 ± 0.6
4-tops	0.14 ± 0.04	0.15 ± 0.05	0.085 ± 0.026	0.037 ± 0.013	1.7 ± 0.5
Total	80 ± 11	181 ± 17	113 ± 15	31 ± 10	242 ± 14
Data	90	175	134	26	268

Table 10. Pre-fit event yields in the SR and CRs of the 3ℓ channel. The 'others' process includes gluon-gluon fusion and vector-boson fusion Higgs boson production, Tri-boson, s-channel and t-channel single-top, 3-tops and VH processes.

Post-fit 3ℓ channel					
Process	SR	CR(μ_{HF})	CR(e_{HF})	CR(e_{conv})	CR($t\bar{t}W$)
tHq	12 ± 4	2.0 ± 0.9	1.3 ± 0.5	0.20 ± 0.09	2.2 ± 0.9
tWH	2.3 ± 0.9	2.0 ± 0.9	1.2 ± 0.5	0.15 ± 0.07	5.2 ± 2.2
μ_{HF}	8 ± 4	77 ± 18	3.0 ± 1.5	0.07 ± 0.09	9 ± 6
e_{HF}	8 ± 4	3.8 ± 2.9	68 ± 14	0.22 ± 0.08	10 ± 6
e_{conv}	3.1 ± 2.1	3 ± 4	11 ± 6	11 ± 5	9 ± 11
other mis-id leptons	3.8 ± 2.2	13 ± 8	7 ± 4	1.0 ± 0.9	9 ± 7
$t\bar{t}W$	8.3 ± 1.3	15.0 ± 1.6	9.3 ± 1.2	2.0 ± 0.4	131 ± 12
tWZ	0.9 ± 0.5	1.5 ± 0.7	0.9 ± 0.5	0.62 ± 0.33	3.6 ± 1.9
$t\bar{t}Z$	14.2 ± 2.0	15.5 ± 2.3	8.4 ± 1.3	4.6 ± 0.9	38 ± 5
$t\bar{t}H$	7.7 ± 1.0	7.6 ± 1.0	4.7 ± 0.7	0.48 ± 0.14	21.4 ± 2.8
tZq	10.7 ± 1.2	9.3 ± 1.1	4.9 ± 0.6	1.74 ± 0.32	6.0 ± 0.7
tW	1.1 ± 0.7	5 ± 4	4.0 ± 2.7	0.9 ± 0.7	1.4 ± 1.1
VV	10 ± 4	21 ± 6	10.6 ± 3.4	4.2 ± 1.3	11 ± 4
others	0.23 ± 0.08	0.43 ± 0.12	0.15 ± 0.05	0.037 ± 0.011	0.9 ± 0.4
4-tops	0.14 ± 0.04	0.15 ± 0.05	0.087 ± 0.026	0.035 ± 0.012	1.7 ± 0.5
Total	90 ± 7	177 ± 13	135 ± 11	27 ± 5	260 ± 11
Data	90	175	134	26	268

Table 11. Post-fit event yields in the SR and CRs of the 2ℓSS channel. Post-fit yields are after the inclusive fit in all channels. All uncertainties are included, taking into account correlations in the post-fit case. The 'others' process includes gluon-gluon fusion and vector-boson fusion Higgs boson production, Tri-boson, s-channel and t-channel single-top, 3-tops and VH processes.

Data Availability Statement. This article has no associated data or the data will not be deposited.

JHEP10(2025)093

Code Availability Statement. This article has no associated code or the code will not be deposited.

References

[1] F. Englert and R. Brout, *Broken symmetry and the mass of gauge vector mesons*, *Phys. Rev. Lett.* **13** (1964) 321 [INSPIRE].

[2] P.W. Higgs, *Broken symmetries and the masses of gauge bosons*, *Phys. Rev. Lett.* **13** (1964) 508 [INSPIRE].

[3] ATLAS collaboration, *Observation of a new particle in the search for the Standard Model Higgs boson with the ATLAS detector at the LHC*, *Phys. Lett. B* **716** (2012) 1 [arXiv:1207.7214] [INSPIRE].

[4] CMS collaboration, *Observation of a new boson at a mass of 125 GeV with the CMS experiment at the LHC*, *Phys. Lett. B* **716** (2012) 30 [arXiv:1207.7235] [INSPIRE].

[5] M.E. Peskin and D.V. Schroeder, *An introduction to quantum field theory*, Addison-Wesley, Reading, U.S.A. (1995) [DOI:10.1201/9780429503559] [INSPIRE].

[6] G. Degrassi et al., *Higgs mass and vacuum stability in the Standard Model at NNLO*, *JHEP* **08** (2012) 098 [arXiv:1205.6497] [INSPIRE].

[7] D. Buttazzo et al., *Investigating the near-criticality of the Higgs boson*, *JHEP* **12** (2013) 089 [arXiv:1307.3536] [INSPIRE].

[8] C. Englert et al., *Precision measurements of Higgs couplings: implications for new physics scales*, *J. Phys. G* **41** (2014) 113001 [arXiv:1403.7191] [INSPIRE].

[9] J.F. Gunion and X.-G. He, *Determining the CP nature of a neutral Higgs boson at the LHC*, *Phys. Rev. Lett.* **76** (1996) 4468 [hep-ph/9602226] [INSPIRE].

[10] J. Ellis, D.S. Hwang, K. Sakurai and M. Takeuchi, *Disentangling Higgs-top couplings in associated production*, *JHEP* **04** (2014) 004 [arXiv:1312.5736] [INSPIRE].

[11] X.-G. He, G.-N. Li and Y.-J. Zheng, *Probing Higgs boson CP properties with $t\bar{t}H$ at the LHC and the 100 TeV pp collider*, *Int. J. Mod. Phys. A* **30** (2015) 1550156 [arXiv:1501.00012] [INSPIRE].

[12] ATLAS collaboration, *Observation of Higgs boson production in association with a top quark pair at the LHC with the ATLAS detector*, *Phys. Lett. B* **784** (2018) 173 [arXiv:1806.00425] [INSPIRE].

[13] CMS collaboration, *Observation of $t\bar{t}H$ production*, *Phys. Rev. Lett.* **120** (2018) 231801 [arXiv:1804.02610] [INSPIRE].

[14] T.M.P. Tait and C.-P. Yuan, *Single top quark production as a window to physics beyond the standard model*, *Phys. Rev. D* **63** (2000) 014018 [hep-ph/0007298] [INSPIRE].

[15] V. Barger, M. McCaskey and G. Shaughnessy, *Single top and Higgs associated production at the LHC*, *Phys. Rev. D* **81** (2010) 034020 [arXiv:0911.1556] [INSPIRE].

JHEP10(2025)093

[16] S. Biswas, E. Gabrielli and B. Mele, *Single top and Higgs associated production as a probe of the Htt coupling sign at the LHC*, *JHEP* **01** (2013) 088 [arXiv:1211.0499] [INSPIRE].

[17] M. Farina et al., *Lifting degeneracies in Higgs couplings using single top production in association with a Higgs boson*, *JHEP* **05** (2013) 022 [arXiv:1211.3736] [INSPIRE].

[18] J. Chang, K. Cheung, J.S. Lee and C.-T. Lu, *Probing the top-Yukawa coupling in associated Higgs production with a single top quark*, *JHEP* **05** (2014) 062 [arXiv:1403.2053] [INSPIRE].

[19] ATLAS collaboration, *CP properties of Higgs boson interactions with top quarks in the $t\bar{t}H$ and tH processes using $H \to \gamma\gamma$ with the ATLAS detector*, *Phys. Rev. Lett.* **125** (2020) 061802 [arXiv:2004.04545] [INSPIRE].

[20] CMS collaboration, *Measurements of Higgs boson production cross sections and couplings in the diphoton decay channel at $\sqrt{s} = 13$ TeV*, *JHEP* **07** (2021) 027 [arXiv:2103.06956] [INSPIRE].

[21] ATLAS collaboration, *A detailed map of Higgs boson interactions by the ATLAS experiment ten years after the discovery*, *Nature* **607** (2022) 52 [*Erratum ibid.* **612** (2022) E24] [arXiv:2207.00092] [INSPIRE].

[22] CMS collaboration, *A portrait of the Higgs boson by the CMS experiment ten years after the discovery*, *Nature* **607** (2022) 60 [arXiv:2207.00043] [INSPIRE].

[23] ATLAS and CMS collaborations, *Measurements of the Higgs boson production and decay rates and constraints on its couplings from a combined ATLAS and CMS analysis of the LHC pp collision data at $\sqrt{s} = 7$ and 8 TeV*, *JHEP* **08** (2016) 045 [arXiv:1606.02266] [INSPIRE].

[24] F. Demartin, F. Maltoni, K. Mawatari and M. Zaro, *Higgs production in association with a single top quark at the LHC*, *Eur. Phys. J. C* **75** (2015) 267 [arXiv:1504.00611] [INSPIRE].

[25] F. Demartin et al., *tWH associated production at the LHC*, *Eur. Phys. J. C* **77** (2017) 34 [arXiv:1607.05862] [INSPIRE].

[26] L. Evans and P. Bryant, *LHC machine*, 2008 *JINST* **3** S08001 [INSPIRE].

[27] J.M. Campbell, R. Frederix, F. Maltoni and F. Tramontano, *Next-to-leading-order predictions for t-channel single-top production at hadron colliders*, *Phys. Rev. Lett.* **102** (2009) 182003 [arXiv:0903.0005] [INSPIRE].

[28] F. Maltoni, G. Ridolfi and M. Ubiali, *b-initiated processes at the LHC: a reappraisal*, *JHEP* **04** (2012) 095 [*Erratum ibid.* **04** (2013) 095] [arXiv:1203.6393] [INSPIRE].

[29] E. Bothmann, F. Krauss and M. Schönherr, *Single top-quark production with SHERPA*, *Eur. Phys. J. C* **78** (2018) 220 [arXiv:1711.02568] [INSPIRE].

[30] CMS collaboration, *Search for associated production of a Higgs boson and a single top quark in proton-proton collisions at $\sqrt{s} = 13$ TeV*, *Phys. Rev. D* **99** (2019) 092005 [arXiv:1811.09696] [INSPIRE].

[31] CMS collaboration, *Measurement of the Higgs boson production rate in association with top quarks in final states with electrons, muons, and hadronically decaying tau leptons at $\sqrt{s} = 13$ TeV*, *Eur. Phys. J. C* **81** (2021) 378 [arXiv:2011.03652] [INSPIRE].

[32] CMS collaboration, *Measurement of the $t\bar{t}H$ and tH production rates in the $H \to b\bar{b}$ decay channel using proton-proton collision data at $\sqrt{s} = 13$ TeV*, *JHEP* **02** (2025) 097 [arXiv:2407.10896] [INSPIRE].

[33] M. Aly, T. Dado, A. Held, M. Pinamonti and L. Valery, *Trexfitter*, Zenodo, February (2025).

[34] ATLAS collaboration, *The ATLAS experiment at the CERN Large Hadron Collider*, 2008 *JINST* **3** S08003 [INSPIRE].

JHEP10(2025)093

[35] ATLAS collaboration, *ATLAS Insertable B-Layer technical design report*, CERN-LHCC-2010-013, CERN, Geneva, Switzerland (2010).

[36] ATLAS IBL collaboration, *Production and integration of the ATLAS Insertable B-Layer*, 2018 *JINST* **13** T05008 [arXiv:1803.00844] [INSPIRE].

[37] G. Avoni et al., *The new LUCID-2 detector for luminosity measurement and monitoring in ATLAS*, 2018 *JINST* **13** P07017 [INSPIRE].

[38] ATLAS collaboration, *Performance of the ATLAS trigger system in 2015*, *Eur. Phys. J. C* **77** (2017) 317 [arXiv:1611.09661] [INSPIRE].

[39] ATLAS collaboration, *Software and computing for run 3 of the ATLAS experiment at the LHC*, *Eur. Phys. J. C* **85** (2025) 234 [arXiv:2404.06335] [INSPIRE].

[40] ATLAS collaboration, *ATLAS data quality operations and performance for 2015–2018 data-taking*, 2020 *JINST* **15** P04003 [arXiv:1911.04632] [INSPIRE].

[41] ATLAS collaboration, *Performance of electron and photon triggers in ATLAS during LHC run 2*, *Eur. Phys. J. C* **80** (2020) 47 [arXiv:1909.00761] [INSPIRE].

[42] ATLAS collaboration, *Performance of the ATLAS muon triggers in run 2*, 2020 *JINST* **15** P09015 [arXiv:2004.13447] [INSPIRE].

[43] T. Sjostrand, S. Mrenna and P.Z. Skands, *A brief introduction to PYTHIA 8.1*, *Comput. Phys. Commun.* **178** (2008) 852 [arXiv:0710.3820] [INSPIRE].

[44] T. Sjöstrand et al., *An introduction to PYTHIA 8.2*, *Comput. Phys. Commun.* **191** (2015) 159 [arXiv:1410.3012] [INSPIRE].

[45] R.D. Ball et al., *Parton distributions with LHC data*, *Nucl. Phys. B* **867** (2013) 244 [arXiv:1207.1303] [INSPIRE].

[46] ATLAS collaboration, *The Pythia 8 A3 tune description of ATLAS minimum bias and inelastic measurements incorporating the Donnachie-Landshoff diffractive model*, ATL-PHYS-PUB-2016-017, CERN, Geneva, Switzerland (2016).

[47] Particle Data Group collaboration, *Review of particle physics*, *Phys. Rev. D* **110** (2024) 030001 [INSPIRE].

[48] D.J. Lange, *The EvtGen particle decay simulation package*, *Nucl. Instrum. Meth. A* **462** (2001) 152 [INSPIRE].

[49] J. Alwall et al., *The automated computation of tree-level and next-to-leading order differential cross sections, and their matching to parton shower simulations*, *JHEP* **07** (2014) 079 [arXiv:1405.0301] [INSPIRE].

[50] NNPDF collaboration, *Parton distributions for the LHC run II*, *JHEP* **04** (2015) 040 [arXiv:1410.8849] [INSPIRE].

[51] ATLAS collaboration, *ATLAS Pythia 8 tunes to 7 TeV data*, ATL-PHYS-PUB-2014-021, CERN, Geneva, Switzerland (2014).

[52] LHC Higgs Cross Section Working Group collaboration, *Handbook of LHC Higgs cross sections: 4. Deciphering the nature of the Higgs sector*, *CERN Yellow Rep. Monogr.* **2** (2017) 1 [arXiv:1610.07922] [INSPIRE].

[53] ATLAS collaboration, *SM Higgs production cross sections at* $\sqrt{s} = 13$ *TeV*, https://twiki.cern.ch/twiki/bin/view/LHCPhysics/CERNYellowReportPageAt13TeV (2024).

JHEP10(2025)093

[54] J. Butterworth et al., *PDF4LHC recommendations for LHC run II*, *J. Phys. G* **43** (2016) 023001 [arXiv:1510.03865] [INSPIRE].

[55] S. Frixione et al., *Single-top hadroproduction in association with a W boson*, *JHEP* **07** (2008) 029 [arXiv:0805.3067] [INSPIRE].

[56] ATLAS collaboration, *Studies on top-quark Monte Carlo modelling for Top2016*, ATL-PHYS-PUB-2016-020, CERN, Geneva, Switzerland (2016).

[57] M. Bahr et al., *Herwig++ physics and manual*, *Eur. Phys. J. C* **58** (2008) 639 [arXiv:0803.0883] [INSPIRE].

[58] J. Bellm et al., *Herwig 7.0/Herwig++ 3.0 release note*, *Eur. Phys. J. C* **76** (2016) 196 [arXiv:1512.01178] [INSPIRE].

[59] L.A. Harland-Lang, A.D. Martin, P. Motylinski and R.S. Thorne, *Parton distributions in the LHC era: MMHT 2014 PDFs*, *Eur. Phys. J. C* **75** (2015) 204 [arXiv:1412.3989] [INSPIRE].

[60] S. Frixione, P. Nason and G. Ridolfi, *A positive-weight next-to-leading-order Monte Carlo for heavy flavour hadroproduction*, *JHEP* **09** (2007) 126 [arXiv:0707.3088] [INSPIRE].

[61] P. Nason, *A new method for combining NLO QCD with shower Monte Carlo algorithms*, *JHEP* **11** (2004) 040 [hep-ph/0409146] [INSPIRE].

[62] S. Frixione, P. Nason and C. Oleari, *Matching NLO QCD computations with parton shower simulations: the POWHEG method*, *JHEP* **11** (2007) 070 [arXiv:0709.2092] [INSPIRE].

[63] S. Alioli, P. Nason, C. Oleari and E. Re, *A general framework for implementing NLO calculations in shower Monte Carlo programs: the POWHEG BOX*, *JHEP* **06** (2010) 043 [arXiv:1002.2581] [INSPIRE].

[64] M. Beneke, P. Falgari, S. Klein and C. Schwinn, *Hadronic top-quark pair production with NNLL threshold resummation*, *Nucl. Phys. B* **855** (2012) 695 [arXiv:1109.1536] [INSPIRE].

[65] M. Cacciari et al., *Top-pair production at hadron colliders with next-to-next-to-leading logarithmic soft-gluon resummation*, *Phys. Lett. B* **710** (2012) 612 [arXiv:1111.5869] [INSPIRE].

[66] P. Bärnreuther, M. Czakon and A. Mitov, *Percent level precision physics at the Tevatron: first genuine NNLO QCD corrections to $q\bar{q} \to t\bar{t} + X$*, *Phys. Rev. Lett.* **109** (2012) 132001 [arXiv:1204.5201] [INSPIRE].

[67] M. Czakon and A. Mitov, *NNLO corrections to top-pair production at hadron colliders: the all-fermionic scattering channels*, *JHEP* **12** (2012) 054 [arXiv:1207.0236] [INSPIRE].

[68] M. Czakon and A. Mitov, *NNLO corrections to top pair production at hadron colliders: the quark-gluon reaction*, *JHEP* **01** (2013) 080 [arXiv:1210.6832] [INSPIRE].

[69] M. Czakon, P. Fiedler and A. Mitov, *Total top-quark pair-production cross section at hadron colliders through $O(\alpha_S^4)$*, *Phys. Rev. Lett.* **110** (2013) 252004 [arXiv:1303.6254] [INSPIRE].

[70] M. Czakon and A. Mitov, *Top++: a program for the calculation of the top-pair cross-section at hadron colliders*, *Comput. Phys. Commun.* **185** (2014) 2930 [arXiv:1112.5675] [INSPIRE].

[71] S. Höche et al., *A study of QCD radiation in VBF Higgs production with Vincia and Pythia*, *SciPost Phys.* **12** (2022) 010 [arXiv:2106.10987] [INSPIRE].

[72] F. Buccioni et al., *OpenLoops 2*, *Eur. Phys. J. C* **79** (2019) 866 [arXiv:1907.13071] [INSPIRE].

[73] F. Cascioli, P. Maierhofer and S. Pozzorini, *Scattering amplitudes with OpenLoops*, *Phys. Rev. Lett.* **108** (2012) 111601 [arXiv:1111.5206] [INSPIRE].

JHEP10(2025)093

[74] A. Denner, S. Dittmaier and L. Hofer, *Collier: a fortran-based Complex One-Loop LIbrary in Extended Regularizations*, *Comput. Phys. Commun.* **212** (2017) 220 [arXiv:1604.06792] [INSPIRE].

[75] H.B. Hartanto, B. Jager, L. Reina and D. Wackeroth, *Higgs boson production in association with top quarks in the POWHEG BOX*, *Phys. Rev. D* **91** (2015) 094003 [arXiv:1501.04498] [INSPIRE].

[76] SHERPA collaboration, *Event generation with Sherpa 2.2*, *SciPost Phys.* **7** (2019) 034 [arXiv:1905.09127] [INSPIRE].

[77] R. Frederix and S. Frixione, *Merging meets matching in MC@NLO*, *JHEP* **12** (2012) 061 [arXiv:1209.6215] [INSPIRE].

[78] R. Frederix and I. Tsinikos, *On improving NLO merging for $t\bar{t}W$ production*, *JHEP* **11** (2021) 029 [arXiv:2108.07826] [INSPIRE].

[79] ATLAS collaboration, *Modelling of the $t\bar{t}H$ and $t\bar{t}V$ $(V = W, Z)$ processes for $\sqrt{s} = 13$ TeV ATLAS analyses*, ATL-PHYS-PUB-2016-005, CERN, Geneva, Switzerland (2016).

[80] S. Hoeche, F. Krauss, M. Schonherr and F. Siegert, *QCD matrix elements + parton showers: the NLO case*, *JHEP* **04** (2013) 027 [arXiv:1207.5030] [INSPIRE].

[81] S. Alioli, P. Nason, C. Oleari and E. Re, *NLO single-top production matched with shower in POWHEG: s- and t-channel contributions*, *JHEP* **09** (2009) 111 [*Erratum ibid.* **02** (2010) 011] [arXiv:0907.4076] [INSPIRE].

[82] E. Re, *Single-top Wt-channel production matched with parton showers using the POWHEG method*, *Eur. Phys. J. C* **71** (2011) 1547 [arXiv:1009.2450] [INSPIRE].

[83] T. Gleisberg and S. Hoeche, *Comix, a new matrix element generator*, *JHEP* **12** (2008) 039 [arXiv:0808.3674] [INSPIRE].

[84] C. Anastasiou, L.J. Dixon, K. Melnikov and F. Petriello, *High precision QCD at hadron colliders: electroweak gauge boson rapidity distributions at NNLO*, *Phys. Rev. D* **69** (2004) 094008 [hep-ph/0312266] [INSPIRE].

[85] S. Hoeche, F. Krauss, M. Schonherr and F. Siegert, *A critical appraisal of NLO+PS matching methods*, *JHEP* **09** (2012) 049 [arXiv:1111.1220] [INSPIRE].

[86] S. Catani, F. Krauss, R. Kuhn and B.R. Webber, *QCD matrix elements + parton showers*, *JHEP* **11** (2001) 063 [hep-ph/0109231] [INSPIRE].

[87] S. Hoeche, F. Krauss, S. Schumann and F. Siegert, *QCD matrix elements and truncated showers*, *JHEP* **05** (2009) 053 [arXiv:0903.1219] [INSPIRE].

[88] P. Nason and G. Zanderighi, *W^+W^-, WZ and ZZ production in the POWHEG-BOX-V2*, *Eur. Phys. J. C* **74** (2014) 2702 [arXiv:1311.1365] [INSPIRE].

[89] ATLAS collaboration, *Measurement of the Z/γ^* boson transverse momentum distribution in pp collisions at $\sqrt{s} = 7$ TeV with the ATLAS detector*, *JHEP* **09** (2014) 145 [arXiv:1406.3660] [INSPIRE].

[90] H.-L. Lai et al., *New parton distributions for collider physics*, *Phys. Rev. D* **82** (2010) 074024 [arXiv:1007.2241] [INSPIRE].

[91] J. Pumplin et al., *New generation of parton distributions with uncertainties from global QCD analysis*, *JHEP* **07** (2002) 012 [hep-ph/0201195] [INSPIRE].

[92] S. Alioli, P. Nason, C. Oleari and E. Re, *NLO Higgs boson production via gluon fusion matched with shower in POWHEG*, *JHEP* **04** (2009) 002 [arXiv:0812.0578] [INSPIRE].

JHEP10(2025)093

[93] P. Nason and C. Oleari, *NLO Higgs boson production via vector-boson fusion matched with shower in POWHEG*, *JHEP* **02** (2010) 037 [arXiv:0911.5299] [INSPIRE].

[94] ATLAS collaboration, *The ATLAS simulation infrastructure*, *Eur. Phys. J. C* **70** (2010) 823 [arXiv:1005.4568] [INSPIRE].

[95] GEANT4 collaboration, *GEANT4 — a simulation toolkit*, *Nucl. Instrum. Meth. A* **506** (2003) 250 [INSPIRE].

[96] ATLAS collaboration, *The simulation principle and performance of the ATLAS fast calorimeter simulation FastCaloSim*, ATL-PHYS-PUB-2010-013, CERN, Geneva, Switzerland (2010).

[97] ATLAS collaboration, *Vertex reconstruction performance of the ATLAS detector at* $\sqrt{s} = 13$ *TeV*, ATL-PHYS-PUB-2015-026, CERN, Geneva, Switzerland (2015).

[98] ATLAS collaboration, *Electron and photon performance measurements with the ATLAS detector using the 2015–2017 LHC proton-proton collision data*, 2019 *JINST* **14** P12006 [arXiv:1908.00005] [INSPIRE].

[99] ATLAS collaboration, *Muon reconstruction and identification efficiency in ATLAS using the full run 2 pp collision data set at* $\sqrt{s} = 13$ *TeV*, *Eur. Phys. J. C* **81** (2021) 578 [arXiv:2012.00578] [INSPIRE].

[100] ATLAS collaboration, *Studies of the muon momentum calibration and performance of the ATLAS detector with pp collisions at* $\sqrt{s} = 13$ *TeV*, *Eur. Phys. J. C* **83** (2023) 686 [arXiv:2212.07338] [INSPIRE].

[101] ATLAS collaboration, *Evidence for the associated production of the Higgs boson and a top quark pair with the ATLAS detector*, *Phys. Rev. D* **97** (2018) 072003 [arXiv:1712.08891] [INSPIRE].

[102] ATLAS collaboration, *Electron reconstruction and identification in the ATLAS experiment using the 2015 and 2016 LHC proton-proton collision data at* $\sqrt{s} = 13$ *TeV*, *Eur. Phys. J. C* **79** (2019) 639 [arXiv:1902.04655] [INSPIRE].

[103] ATLAS collaboration, *Jet reconstruction and performance using particle flow with the ATLAS detector*, *Eur. Phys. J. C* **77** (2017) 466 [arXiv:1703.10485] [INSPIRE].

[104] M. Cacciari, G.P. Salam and G. Soyez, *The anti-*k_t *jet clustering algorithm*, *JHEP* **04** (2008) 063 [arXiv:0802.1189] [INSPIRE].

[105] M. Cacciari, G.P. Salam and G. Soyez, *FastJet user manual*, *Eur. Phys. J. C* **72** (2012) 1896 [arXiv:1111.6097] [INSPIRE].

[106] ATLAS collaboration, *Jet energy scale and resolution measured in proton–proton collisions at* $\sqrt{s} = 13$ *TeV with the ATLAS detector*, *Eur. Phys. J. C* **81** (2021) 689 [arXiv:2007.02645] [INSPIRE].

[107] ATLAS collaboration, *Performance of pile-up mitigation techniques for jets in pp collisions at* $\sqrt{s} = 8$ *TeV using the ATLAS detector*, *Eur. Phys. J. C* **76** (2016) 581 [arXiv:1510.03823] [INSPIRE].

[108] ATLAS collaboration, *Identification and rejection of pile-up jets at high pseudorapidity with the ATLAS detector*, *Eur. Phys. J. C* **77** (2017) 580 [*Erratum ibid.* **77** (2017) 712] [arXiv:1705.02211] [INSPIRE].

[109] ATLAS collaboration, *Selection of jets produced in 13 TeV proton-proton collisions with the ATLAS detector*, ATLAS-CONF-2015-029, CERN, Geneva, Switzerland (2015).

JHEP10(2025)093

[110] ATLAS collaboration, *ATLAS flavour-tagging algorithms for the LHC run 2 pp collision dataset*, *Eur. Phys. J. C* **83** (2023) 681 [arXiv:2211.16345] [INSPIRE].

[111] ATLAS collaboration, *Identification of jets containing b-hadrons with recurrent neural networks at the ATLAS experiment*, ATL-PHYS-PUB-2017-003, CERN, Geneva, Switzerland (2017).

[112] ATLAS collaboration, *Reconstruction, energy calibration, and identification of hadronically decaying tau leptons in the ATLAS experiment for run-2 of the LHC*, ATL-PHYS-PUB-2015-045, CERN, Geneva, Switzerland (2015).

[113] ATLAS collaboration, *Measurement of the tau lepton reconstruction and identification performance in the ATLAS experiment using pp collisions at* $\sqrt{s} = 13$ *TeV*, ATLAS-CONF-2017-029, CERN, Geneva, Switzerland (2017).

[114] ATLAS collaboration, *Identification of hadronic tau lepton decays using neural networks in the ATLAS experiment*, ATL-PHYS-PUB-2019-033, CERN, Geneva, Switzerland (2019).

[115] ATLAS collaboration, *Reconstruction, identification, and calibration of hadronically decaying tau leptons with the ATLAS detector for the LHC run 3 and reprocessed run 2 data*, ATL-PHYS-PUB-2022-044, CERN, Geneva, Switzerland (2022).

[116] ATLAS collaboration, *Performance of missing transverse momentum reconstruction with the ATLAS detector using proton-proton collisions at* $\sqrt{s} = 13$ *TeV*, *Eur. Phys. J. C* **78** (2018) 903 [arXiv:1802.08168] [INSPIRE].

[117] T. Chen and C. Guestrin, *XGBoost: a scalable tree boosting system*, in *Proceedings of the 22nd ACM SIGKDD International Conference on Knowledge Discovery and Data Mining, KDD '16, (New York, NY, U.S.A.)*, Association for Computing Machinery, U.S.A. (2016), p. 785 [DOI:10.1145/2939672.2939785] [arXiv:1603.02754] [INSPIRE].

[118] ATLAS collaboration, *Measurement of event shapes at large momentum transfer with the ATLAS detector in pp collisions at* $\sqrt{s} = 7$ *TeV*, *Eur. Phys. J. C* **72** (2012) 2211 [arXiv:1206.2135] [INSPIRE].

[119] ATLAS collaboration, *Tools for estimating fake/non-prompt lepton backgrounds with the ATLAS detector at the LHC*, 2023 *JINST* **18** T11004 [arXiv:2211.16178] [INSPIRE].

[120] ATLAS collaboration, *The performance of missing transverse momentum reconstruction and its significance with the ATLAS detector using 140* fb^{-1} *of* $\sqrt{s} = 13$ *TeV pp collisions*, *Eur. Phys. J. C* **85** (2025) 606 [arXiv:2402.05858] [INSPIRE].

[121] ATLAS collaboration, *ATLAS b-jet identification performance and efficiency measurement with* $t\bar{t}$ *events in pp collisions at* $\sqrt{s} = 13$ *TeV*, *Eur. Phys. J. C* **79** (2019) 970 [arXiv:1907.05120] [INSPIRE].

[122] ATLAS collaboration, *Measurement of the c-jet mistagging efficiency in* $t\bar{t}$ *events using pp collision data at* $\sqrt{s} = 13$ *TeV collected with the ATLAS detector*, *Eur. Phys. J. C* **82** (2022) 95 [arXiv:2109.10627] [INSPIRE].

[123] ATLAS collaboration, *Calibration of the light-flavour jet mistagging efficiency of the b-tagging algorithms with Z+jets events using 139* fb^{-1} *of ATLAS proton–proton collision data at* $\sqrt{s} = 13$ *TeV*, *Eur. Phys. J. C* **83** (2023) 728 [arXiv:2301.06319] [INSPIRE].

[124] ATLAS collaboration, *Luminosity determination in pp collisions at* $\sqrt{s} = 13$ *TeV using the ATLAS detector at the LHC*, *Eur. Phys. J. C* **83** (2023) 982 [arXiv:2212.09379] [INSPIRE].

[125] ATLAS collaboration, *Studies on top-quark Monte Carlo modelling with Sherpa and MG5_aMC@NLO*, ATL-PHYS-PUB-2017-007, CERN, Geneva, Switzerland (2017).

JHEP10(2025)093

[126] E. Bothmann, M. Schönherr and S. Schumann, *Reweighting QCD matrix-element and parton-shower calculations*, *Eur. Phys. J. C* **76** (2016) 590 [arXiv:1606.08753] [INSPIRE].

[127] N. Kidonakis, *Two-loop soft anomalous dimensions for single top quark associated production with a W^- or H^-*, *Phys. Rev. D* **82** (2010) 054018 [arXiv:1005.4451] [INSPIRE].

[128] F.A. Berends, H. Kuijf, B. Tausk and W.T. Giele, *On the production of a W and jets at hadron colliders*, *Nucl. Phys. B* **357** (1991) 32 [INSPIRE].

[129] ATLAS collaboration, *Study of ttbb and ttW background modelling for ttH analyses*, ATL-PHYS-PUB-2022-026, CERN, Geneva, Switzerland (2022) [INSPIRE].

[130] ATLAS collaboration, *Measurement of top-quark pair production in association with charm quarks in proton–proton collisions at $\sqrt{s} = 13$ TeV with the ATLAS detector*, *Phys. Lett. B* **860** (2025) 139177 [arXiv:2409.11305] [INSPIRE].

[131] ROOT collaboration, *HistFactory: a tool for creating statistical models for use with RooFit and RooStats*, CERN-OPEN-2012-016, New York U., New York, NY, U.S.A. (2012) [DOI:10.17181/CERN-OPEN-2012-016].

[132] R.J. Barlow and C. Beeston, *Fitting using finite Monte Carlo samples*, *Comput. Phys. Commun.* **77** (1993) 219 [INSPIRE].

[133] R.D. Cousins, *Generalization of chisquare goodness-offit test for binned data using saturated models, with application to histograms*, https://api.semanticscholar.org/CorpusID:5936965 (2013).

[134] A. Pinto et al., *Uncertainty components in profile likelihood fits*, *Eur. Phys. J. C* **84** (2024) 593 [arXiv:2307.04007] [INSPIRE].

[135] ATLAS collaboration, *ATLAS computing acknowledgements*, ATL-SOFT-PUB-2025-001, CERN, Geneva, Switzerland (2025).

[136] G.C. Fox and S. Wolfram, *Observables for the analysis of event shapes in e^+e^- annihilation and other processes*, *Phys. Rev. Lett.* **41** (1978) 1581 [INSPIRE].

[137] C. Bernaciak, M.S.A. Buschmann, A. Butter and T. Plehn, *Fox-Wolfram moments in Higgs physics*, *Phys. Rev. D* **87** (2013) 073014 [arXiv:1212.4436] [INSPIRE].

JHEP10(2025)093

The ATLAS collaboration

G. Aad[104], E. Aakvaag[17], B. Abbott[123], S. Abdelhameed[119a], K. Abeling[55], N.J. Abicht[49], S.H. Abidi[30], M. Aboelela[45], A. Aboulhorma[36e], H. Abramowicz[157], Y. Abulaiti[120], B.S. Acharya[69a,69b,m], A. Ackermann[63a], C. Adam Bourdarios[4], L. Adamczyk[87a], S.V. Addepalli[149], M.J. Addison[103], J. Adelman[118], A. Adiguzel[22c], T. Adye[137], A.A. Affolder[139], Y. Afik[40], M.N. Agaras[13], A. Aggarwal[102], C. Agheorghiesei[28c], F. Ahmadov[39,ad], S. Ahuja[97], X. Ai[143b], G. Aielli[76a,76b], A. Aikot[169], M. Ait Tamlihat[36e], B. Aitbenchikh[36a], M. Akbiyik[102], T.P.A. Åkesson[100], A.V. Akimov[151], D. Akiyama[174], N.N. Akolkar[25], S. Aktas[172], G.L. Alberghi[24b], J. Albert[171], U. Alberti[20], P. Albicocco[53], G.L. Albouy[60], S. Alderweireldt[52], Z.L. Alegria[124], M. Aleksa[37], I.N. Aleksandrov[39], C. Alexa[28b], T. Alexopoulos[10], F. Alfonsi[24b], M. Algren[56], M. Alhroob[173], B. Ali[135], H.M.J. Ali[93,w], S. Ali[32], S.W. Alibocus[94], M. Aliev[34c], G. Alimonti[71a], W. Alkakhi[55], C. Allaire[66], B.M.M. Allbrooke[152], J.S. Allen[103], J.F. Allen[52], P.P. Allport[21], A. Aloisio[72a,72b], F. Alonso[92], C. Alpigiani[142], Z.M.K. Alsolami[93], A. Alvarez Fernandez[102], M. Alves Cardoso[56], M.G. Alviggi[72a,72b], M. Aly[103], Y. Amaral Coutinho[83b], A. Ambler[106], C. Amelung[37], M. Amerl[103], C.G. Ames[111], T. Amezza[130], D. Amidei[108], B. Amini[54], K. Amirie[161], A. Amirkhanov[39], S.P. Amor Dos Santos[133a], K.R. Amos[169], D. Amperiadou[158], S. An[84], C. Anastopoulos[145], T. Andeen[11], J.K. Anders[94], A.C. Anderson[59], A. Andreazza[71a,71b], S. Angelidakis[9], A. Angerami[42], A.V. Anisenkov[39], A. Annovi[74a], C. Antel[37], E. Antipov[151], M. Antonelli[53], F. Anulli[75a], M. Aoki[84], T. Aoki[159], M.A. Aparo[152], L. Aperio Bella[48], M. Apicella[31], C. Appelt[157], A. Apyan[27], M. Arampatzi[10], S.J. Arbiol Val[88], C. Arcangeletti[53], A.T.H. Arce[51], J-F. Arguin[110], S. Argyropoulos[158], J.-H. Arling[48], O. Arnaez[4], H. Arnold[151], G. Artoni[75a,75b], H. Asada[113], K. Asai[121], S. Asatryan[179], N.A. Asbah[37], R.A. Ashby Pickering[173], A.M. Aslam[97], K. Assamagan[30], R. Astalos[29a], K.S.V. Astrand[100], S. Atashi[165], R.J. Atkin[34a], H. Atmani[36f], P.A. Atmasiddha[131], K. Augsten[135], A.D. Auriol[41], V.A. Austrup[103], A.S. Avad[96], G. Avolio[37], K. Axiotis[56], A. Azzam[13], D. Babal[29b], H. Bachacou[138], K. Bachas[158,q], A. Bachiu[35], E. Bachmann[50], M.J. Backes[63a], A. Badea[40], T.M. Baer[108], P. Bagnaia[75a,75b], M. Bahmani[19], D. Bahner[54], K. Bai[126], J.T. Baines[137], L. Baines[96], O.K. Baker[178], E. Bakos[16], D. Bakshi Gupta[8], L.E. Balabram Filho[83b], V. Balakrishnan[123], R. Balasubramanian[4], E.M. Baldin[38], P. Balek[87a], E. Ballabene[24b,24a], F. Balli[138], L.M. Baltes[63a], W.K. Balunas[33], J. Balz[102], I. Bamwidhi[119b], E. Banas[88], M. Bandieramonte[132], A. Bandyopadhyay[25], S. Bansal[25], L. Barak[157], M. Barakat[48], E.L. Barberio[107], D. Barberis[18b], M. Barbero[104], M.Z. Barel[117], T. Barillari[112], M-S. Barisits[37], T. Barklow[149], P. Baron[136], D.A. Baron Moreno[103], A. Baroncelli[62], A.J. Barr[129], J.D. Barr[98], F. Barreiro[101], J. Barreiro Guimarães da Costa[14], M.G. Barros Teixeira[133a], S. Barsov[38], F. Bartels[63a], R. Bartoldus[149], A.E. Barton[93], P. Bartos[29a], M. Baselga[49], S. Bashiri[88], A. Bassalat[66,b], M.J. Basso[162a], S. Bataju[45], R. Bate[170], R.L. Bates[59], S. Batlamous[101], M. Battaglia[139], D. Battulga[19], M. Bauce[75a,75b], M. Bauer[79], P. Bauer[25], L.T. Bayer[48], L.T. Bazzano Hurrell[31], J.B. Beacham[112], T. Beau[130], J.Y. Beaucamp[92], P.H. Beauchemin[164], P. Bechtle[25], H.P. Beck[20,p], K. Becker[173], A.J. Beddall[82],

JHEP10(2025)093

V.A. Bednyakov[39], C.P. Bee[151], L.J. Beemster[16], M. Begalli[83d], M. Begel[30], J.K. Behr[48], J.F. Beirer[37], F. Beisiegel[25], M. Belfkir[119b], G. Bella[157], L. Bellagamba[24b], A. Bellerive[35], C.D. Bellgraph[68], P. Bellos[21], K. Beloborodov[38], I. Benaoumeur[21], D. Benchekroun[36a], F. Bendebba[36a], Y. Benhammou[157], K.C. Benkendorfer[61], L. Beresford[48], M. Beretta[53], E. Bergeaas Kuutmann[167], N. Berger[4], B. Bergmann[135], J. Beringer[18a], G. Bernardi[5], C. Bernius[149], F.U. Bernlochner[25], A. Berrocal Guardia[13], T. Berry[97], P. Berta[136], A. Berthold[50], A. Berti[133a], R. Bertrand[104], S. Bethke[112], A. Betti[75a,75b], A.J. Bevan[96], L. Bezio[56], N.K. Bhalla[54], S. Bharthuar[112], S. Bhatta[151], P. Bhattarai[149], Z.M. Bhatti[120], K.D. Bhide[54], V.S. Bhopatkar[124], R.M. Bianchi[132], G. Bianco[24b,24a], O. Biebel[111], M. Biglietti[77a], C.S. Billingsley[45], Y. Bimgdi[36f], M. Bindi[55], A. Bingham[177], A. Bingul[22b], C. Bini[75a,75b], G.A. Bird[33], M. Birman[175], M. Biros[136], S. Biryukov[152], T. Bisanz[49], E. Bisceglie[24b,24a], J.P. Biswal[137], D. Biswas[147], I. Bloch[48], A. Blue[59], U. Blumenschein[96], V.S. Bobrovnikov[39], L. Boccardo[57b,57a], M. Boehler[54], B. Boehm[172], D. Bogavac[13], A.G. Bogdanchikov[38], L.S. Boggia[130], V. Boisvert[97], P. Bokan[37], T. Bold[87a], M. Bomben[5], M. Bona[96], M. Boonekamp[138], A.G. Borbély[59], I.S. Bordulev[38], G. Borissov[93], D. Bortoletto[129], D. Boscherini[24b], M. Bosman[13], K. Bouaouda[36a], N. Bouchhar[169], L. Boudet[4], J. Boudreau[132], E.V. Bouhova-Thacker[93], D. Boumediene[41], R. Bouquet[57b,57a], A. Boveia[122], J. Boyd[37], D. Boye[30], I.R. Boyko[39], L. Bozianu[56], J. Bracinik[21], N. Brahimi[4], G. Brandt[177], O. Brandt[33], B. Brau[105], J.E. Brau[126], R. Brener[175], L. Brenner[117], R. Brenner[167], S. Bressler[175], G. Brianti[78a,78b], D. Britton[59], D. Britzger[112], I. Brock[25], R. Brock[109], G. Brooijmans[42], A.J. Brooks[68], E.M. Brooks[162b], E. Brost[30], L.M. Brown[171,162a], L.E. Bruce[61], T.L. Bruckler[129], P.A. Bruckman de Renstrom[88], B. Brüers[48], A. Bruni[24b], G. Bruni[24b], D. Brunner[47a,47b], M. Bruschi[24b], N. Bruscino[75a,75b], T. Buanes[17], Q. Buat[142], D. Buchin[112], A.G. Buckley[59], O. Bulekov[82], B.A. Bullard[149], S. Burdin[94], C.D. Burgard[49], A.M. Burger[91], B. Burghgrave[8], O. Burlayenko[54], J. Burleson[168], J.C. Burzynski[148], E.L. Busch[42], V. Büscher[102], P.J. Bussey[59], J.M. Butler[26], C.M. Buttar[59], J.M. Butterworth[98], W. Buttinger[137], C.J. Buxo Vazquez[109], A.R. Buzykaev[39], S. Cabrera Urbán[169], L. Cadamuro[66], H. Cai[37], Y. Cai[24b,114c,24a], Y. Cai[114a], V.M.M. Cairo[37], O. Cakir[3a], N. Calace[37], P. Calafiura[18a], G. Calderini[130], P. Calfayan[35], L. Calic[100], G. Callea[59], L.P. Caloba[83b], D. Calvet[41], S. Calvet[41], R. Camacho Toro[130], S. Camarda[37], D. Camarero Munoz[27], P. Camarri[76a,76b], C. Camincher[171], M. Campanelli[98], A. Camplani[43], V. Canale[72a,72b], A.C. Canbay[3a], E. Canonero[97], J. Cantero[169], Y. Cao[168], F. Capocasa[27], M. Capua[44b,44a], A. Carbone[71a,71b], R. Cardarelli[76a], J.C.J. Cardenas[8], M.P. Cardiff[27], G. Carducci[44b,44a], T. Carli[37], G. Carlino[72a], J.I. Carlotto[13], B.T. Carlson[132,r], E.M. Carlson[171], J. Carmignani[94], L. Carminati[71a,71b], A. Carnelli[4], M. Carnesale[37], S. Caron[116], E. Carquin[140g], I.B. Carr[107], S. Carrá[73a,73b], G. Carratta[24b,24a], C. Carrion Martinez[169], A.M. Carroll[126], M.P. Casado[13,h], P. Casolaro[72a,72b], M. Caspar[48], W.R. Castiglioni[40], F.L. Castillo[4], L. Castillo Garcia[13], V. Castillo Gimenez[169], N.F. Castro[133a,133e], A. Catinaccio[37], J.R. Catmore[128], T. Cavaliere[4], V. Cavaliere[30], L.J. Caviedes Betancourt[23b], E. Celebi[82], S. Cella[37], V. Cepaitis[56], K. Cerny[125], A.S. Cerqueira[83a], A. Cerri[74a,74b,am], L. Cerrito[76a,76b], F. Cerutti[18a], B. Cervato[71a,71b],

JHEP10(2025)093

A. Cervelli[24b], G. Cesarini[53], S.A. Cetin[82], P.M. Chabrillat[130], R. Chakkappai[66], S. Chakraborty[173], A. Chambers[61], J. Chan[18a], W.Y. Chan[159], J.D. Chapman[33], E. Chapon[138], B. Chargeishvili[155b], D.G. Charlton[21], C. Chauhan[136], Y. Che[114a], S. Chekanov[6], S.V. Chekulaev[162a], G.A. Chelkov[39,a], B. Chen[157], B. Chen[171], H. Chen[114a], H. Chen[30], J. Chen[144a], J. Chen[148], M. Chen[129], S. Chen[89], S.J. Chen[114a], X. Chen[144a], X. Chen[15,ah], Z. Chen[62], C.L. Cheng[176], H.C. Cheng[64a], S. Cheong[149], A. Cheplakov[39], E. Cherepanova[117], R. Cherkaoui El Moursli[36e], E. Cheu[7], K. Cheung[65], L. Chevalier[138], V. Chiarella[53], G. Chiarelli[74a], G. Chiodini[70a], A.S. Chisholm[21], A. Chitan[28b], M. Chitishvili[169], M.V. Chizhov[39,s], K. Choi[11], Y. Chou[142], E.Y.S. Chow[116], K.L. Chu[175], M.C. Chu[64a], X. Chu[14,114c], Z. Chubinidze[53], J. Chudoba[134], J.J. Chwastowski[88], D. Cieri[112], K.M. Ciesla[87a], V. Cindro[95], A. Ciocio[18a], F. Cirotto[72a,72b], Z.H. Citron[175], M. Citterio[71a], D.A. Ciubotaru[28b], A. Clark[56], P.J. Clark[52], N. Clarke Hall[98], C. Clarry[161], S.E. Clawson[48], C. Clement[47a,47b], Y. Coadou[104], M. Cobal[69a,69c], A. Coccaro[57b], R.F. Coelho Barrue[133a], R. Coelho Lopes De Sa[105], S. Coelli[71a], L.S. Colangeli[161], B. Cole[42], P. Collado Soto[101], J. Collot[60], R. Coluccia[70a,70b], P. Conde Muiño[133a,133g], M.P. Connell[34c], S.H. Connell[34c], E.I. Conroy[129], M. Contreras Cossio[11], F. Conventi[72a,aj], A.M. Cooper-Sarkar[129], L. Corazzina[75a,75b], F.A. Corchia[24b,24a], A. Cordeiro Oudot Choi[142], L.D. Corpe[41], M. Corradi[75a,75b], F. Corriveau[106,ab], A. Cortes-Gonzalez[159], M.J. Costa[169], F. Costanza[4], D. Costanzo[145], J. Couthures[4], G. Cowan[97], K. Cranmer[176], L. Cremer[49], D. Cremonini[24b,24a], S. Crépé-Renaudin[60], F. Crescioli[130], T. Cresta[73a,73b], M. Cristinziani[147], M. Cristoforetti[78a,78b], V. Croft[117], G. Crosetti[44b,44a], A. Cueto[101], H. Cui[98], Z. Cui[7], B.M. Cunnett[152], W.R. Cunningham[59], F. Curcio[169], J.R. Curran[52], M.J. Da Cunha Sargedas De Sousa[57b,57a], J.V. Da Fonseca Pinto[83b], C. Da Via[103], W. Dabrowski[87a], T. Dado[37], S. Dahbi[154], T. Dai[108], D. Dal Santo[20], C. Dallapiccola[105], M. Dam[43], G. D'amen[30], V. D'Amico[111], J. Damp[102], J.R. Dandoy[35], M. D'Andrea[57b,57a], D. Dannheim[37], G. D'anniballe[74a,74b], M. Danninger[148], V. Dao[151], G. Darbo[57b], S.J. Das[30], F. Dattola[48], S. D'Auria[71a,71b], A. D'Avanzo[72a,72b], T. Davidek[136], J. Davidson[173], I. Dawson[96], K. De[8], C. De Almeida Rossi[161], R. De Asmundis[72a], N. De Biase[48], S. De Castro[24b,24a], N. De Groot[116], P. de Jong[117], H. De la Torre[118], A. De Maria[114a], A. De Salvo[75a], U. De Sanctis[76a,76b], F. De Santis[70a,70b], A. De Santo[152], J.B. De Vivie De Regie[60], J. Debevc[95], D.V. Dedovich[39], J. Degens[94], A.M. Deiana[45], J. Del Peso[101], L. Delagrange[130], F. Deliot[138], C.M. Delitzsch[49], M. Della Pietra[72a,72b], D. Della Volpe[56], A. Dell'Acqua[37], L. Dell'Asta[71a,71b], M. Delmastro[4], C.C. Delogu[102], P.A. Delsart[60], S. Demers[178], M. Demichev[39], S.P. Denisov[38], H. Denizli[22a,l], L. D'Eramo[41], D. Derendarz[88], F. Derue[130], P. Dervan[94,*], A.M. Desai[1], K. Desch[25], F.A. Di Bello[57b,57a], A. Di Ciaccio[76a,76b], L. Di Ciaccio[4], A. Di Domenico[75a,75b], C. Di Donato[72a,72b], A. Di Girolamo[37], G. Di Gregorio[37], A. Di Luca[78a,78b], B. Di Micco[77a,77b], R. Di Nardo[77a,77b], K.F. Di Petrillo[40], M. Diamantopoulou[35], F.A. Dias[117], M.A. Diaz[140a,140b], A.R. Didenko[39], M. Didenko[169], S.D. Diefenbacher[18a], E.B. Diehl[108], S. Díez Cornell[48], C. Diez Pardos[147], C. Dimitriadi[150], A. Dimitrievska[21], A. Dimri[151], Y. Ding[62], J. Dingfelder[25], T. Dingley[129], I-M. Dinu[28b], S.J. Dittmeier[63b], F. Dittus[37],

JHEP10(2025)093

M. Divisek[136], B. Dixit[94], F. Djama[104], T. Djobava[155b], C. Doglioni[103,100], A. Dohnalova[29a], Z. Dolezal[136], K. Domijan[87a], K.M. Dona[40], M. Donadelli[83d], B. Dong[109], J. Donini[41], A. D'Onofrio[72a,72b], M. D'Onofrio[94], J. Dopke[137], A. Doria[72a], N. Dos Santos Fernandes[133a], I.A. Dos Santos Luz[83e], P. Dougan[103], M.T. Dova[92], A.T. Doyle[59], M.P. Drescher[55], E. Dreyer[175], I. Drivas-koulouris[10], M. Drnevich[120], D. Du[62], T.A. du Pree[117], Z. Duan[114a], M. Dubau[4], F. Dubinin[39], M. Dubovsky[29a], E. Duchovni[175], G. Duckeck[111], P.K. Duckett[98], O.A. Ducu[28b], D. Duda[52], A. Dudarev[37], M.M. Dudek[88], E.R. Duden[27], M. D'uffizi[103], L. Duflot[66], M. Dührssen[37], I. Duminica[28g], A.E. Dumitriu[28b], M. Dunford[63a], K. Dunne[47a,47b], A. Duperrin[104], H. Duran Yildiz[3a], A. Durglishvili[155b], G.I. Dyckes[18a], M. Dyndal[87a], B.S. Dziedzic[37], Z.O. Earnshaw[152], G.H. Eberwein[129], B. Eckerova[29a], S. Eggebrecht[55], E. Egidio Purcino De Souza[83e], G. Eigen[17], K. Einsweiler[18a], T. Ekelof[167], P.A. Ekman[100], S. El Farkh[36b], Y. El Ghazali[62], H. El Jarrari[37], A. El Moussaouy[36a], D. Elitez[37], M. Ellert[167], F. Ellinghaus[177], T.A. Elliot[97], N. Ellis[37], J. Elmsheuser[30], M. Elsawy[119a], M. Elsing[37], D. Emeliyanov[137], Y. Enari[84], S. Epari[110], D. Ernani Martins Neto[88], F. Ernst[37], M. Errenst[177], M. Escalier[66], C. Escobar[169], E. Etzion[157], G. Evans[133a,133b], H. Evans[68], L.S. Evans[48], A. Ezhilov[38], S. Ezzarqtouni[36a], F. Fabbri[24b,24a], L. Fabbri[24b,24a], G. Facini[98], V. Fadeyev[139], R.M. Fakhrutdinov[38], D. Fakoudis[102], S. Falciano[75a], L.F. Falda Ulhoa Coelho[133a], F. Fallavollita[112], G. Falsetti[44b,44a], J. Faltova[136], C. Fan[168], K.Y. Fan[64b], Y. Fan[14], Y. Fang[14,114c], M. Fanti[71a,71b], M. Faraj[69a,69b], Z. Farazpay[99], A. Farbin[8], A. Farilla[77a], K. Farman[154], T. Farooque[109], J.N. Farr[178], S.M. Farrington[137,52], F. Fassi[36e], D. Fassouliotis[9], L. Fayard[66], P. Federic[136], P. Federicova[134], O.L. Fedin[38,a], M. Feickert[176], L. Feligioni[104], D.E. Fellers[18a], C. Feng[143a], Y. Feng[14], Z. Feng[117], M.J. Fenton[165], L. Ferencz[48], B. Fernandez Barbadillo[93], P. Fernandez Martinez[67], M.J.V. Fernoux[104], J. Ferrando[93], A. Ferrari[167], P. Ferrari[117,116], R. Ferrari[73a], D. Ferrere[56], C. Ferretti[108], M.P. Fewell[1], D. Fiacco[75a,75b], F. Fiedler[102], P. Fiedler[135], S. Filimonov[39], M.S. Filip[28b,t], A. Filipčič[95], E.K. Filmer[162a], F. Filthaut[116], M.C.N. Fiolhais[133a,133c,c], L. Fiorini[169], W.C. Fisher[109], T. Fitschen[103], P.M. Fitzhugh[138], I. Fleck[147], P. Fleischmann[108], T. Flick[177], M. Flores[34d,ag], L.R. Flores Castillo[64a], L. Flores Sanz De Acedo[37], F.M. Follega[78a,78b], N. Fomin[33], J.H. Foo[161], A. Formica[138], A.C. Forti[103], E. Fortin[37], A.W. Fortman[18a], L. Foster[18a], L. Fountas[9,i], D. Fournier[66], H. Fox[93], P. Francavilla[74a,74b], S. Francescato[61], S. Franchellucci[56], M. Franchini[24b,24a], S. Franchino[63a], D. Francis[37], L. Franco[116], L. Franconi[48], M. Franklin[61], G. Frattari[27], Y.Y. Frid[157], J. Friend[59], N. Fritzsche[37], A. Froch[56], D. Froidevaux[37], J.A. Frost[129], Y. Fu[109], S. Fuenzalida Garrido[140g], M. Fujimoto[151], K.Y. Fung[64a], E. Furtado De Simas Filho[83e], M. Furukawa[159], J. Fuster[169], A. Gaa[55], A. Gabrielli[24b,24a], A. Gabrielli[161], P. Gadow[37], G. Gagliardi[57b,57a], L.G. Gagnon[18a], S. Gaid[85b], S. Galantzan[157], J. Gallagher[1], E.J. Gallas[129], A.L. Gallen[167], B.J. Gallop[137], K.K. Gan[122], S. Ganguly[159], Y. Gao[52], A. Garabaglu[142], F.M. Garay Walls[140a,140b], C. García[169], A. Garcia Alonso[117], A.G. Garcia Caffaro[178], J.E. García Navarro[169], M.A. Garcia Ruiz[23b], M. Garcia-Sciveres[18a], G.L. Gardner[131], R.W. Gardner[40], N. Garelli[164], R.B. Garg[149], J.M. Gargan[33], C.A. Garner[161], C.M. Garvey[34a],

JHEP10(2025)093

V.K. Gassmann[164], G. Gaudio[73a], V. Gautam[13], P. Gauzzi[75a,75b], J. Gavranovic[95], I.L. Gavrilenko[133a], A. Gavrilyuk[38], C. Gay[170], G. Gaycken[126], E.N. Gazis[10], A. Gekow[122], C. Gemme[57b], M.H. Genest[60], A.D. Gentry[115], S. George[97], T. Geralis[46], A.A. Gerwin[123], P. Gessinger-Befurt[37], M.E. Geyik[177], M. Ghani[173], K. Ghorbanian[96], A. Ghosal[147], A. Ghosh[165], A. Ghosh[7], B. Giacobbe[24b], S. Giagu[75a,75b], T. Giani[117], A. Giannini[62], S.M. Gibson[97], M. Gignac[139], D.T. Gil[87b], A.K. Gilbert[87a], B.J. Gilbert[42], D. Gillberg[35], G. Gilles[117], D.M. Gingrich[2,ai], M.P. Giordani[69a,69c], P.F. Giraud[138], G. Giugliarelli[69a,69c], D. Giugni[71a], F. Giuli[76a,76b], I. Gkialas[9,i], L.K. Gladilin[38], C. Glasman[101], M. Glazewska[20], R.M. Gleason[165], G. Glemža[48], M. Glisic[126], I. Gnesi[44b], Y. Go[30], M. Goblirsch-Kolb[37], B. Gocke[49], D. Godin[110], B. Gokturk[22a], S. Goldfarb[107], T. Golling[56], M.G.D. Gololo[34c], D. Golubkov[38], J.P. Gombas[109], A. Gomes[133a,133b], G. Gomes Da Silva[147], A.J. Gomez Delegido[37], R. Gonçalo[133a], L. Gonella[21], A. Gongadze[155c], F. Gonnella[21], J.L. Gonski[149], R.Y. González Andana[52], S. González de la Hoz[169], M.V. Gonzalez Rodrigues[48], R. Gonzalez Suarez[167], S. Gonzalez-Sevilla[56], L. Goossens[37], B. Gorini[37], E. Gorini[70a,70b], A. Gorišek[95], T.C. Gosart[131], A.T. Goshaw[51], M.I. Gostkin[39], S. Goswami[124], C.A. Gottardo[37], S.A. Gotz[111], M. Gouighri[36b], A.G. Goussiou[142], N. Govender[34c], R.P. Grabarczyk[129], I. Grabowska-Bold[87a], K. Graham[35], E. Gramstad[128], S. Grancagnolo[70a,70b], C.M. Grant[1], P.M. Gravila[28f], F.G. Gravili[70a,70b], H.M. Gray[18a], M. Greco[112], M.J. Green[1], C. Grefe[25], A.S. Grefsrud[17], I.M. Gregor[48], K.T. Greif[165], P. Grenier[149], S.G. Grewe[112], A.A. Grillo[139], K. Grimm[32], S. Grinstein[13,x], J.-F. Grivaz[66], E. Gross[175], J. Grosse-Knetter[55], L. Guan[108], G. Guerrieri[37], R. Guevara[128], R. Gugel[102], J.A.M. Guhit[108], A. Guida[19], E. Guilloton[173], S. Guindon[37], F. Guo[14,114c], J. Guo[144a], L. Guo[48], L. Guo[114b,v], Y. Guo[108], Y. Guo[42], A. Gupta[49], R. Gupta[132], S. Gupta[27], S. Gurbuz[25], S.S. Gurdasani[48], G. Gustavino[75a,75b], P. Gutierrez[123], L.F. Gutierrez Zagazeta[131], M. Gutsche[50], C. Gutschow[98], C. Gwenlan[129], C.B. Gwilliam[94], E.S. Haaland[128], A. Haas[120], M. Habedank[59], C. Haber[18a], H.K. Hadavand[8], A. Haddad[41], A. Hadef[50], A.I. Hagan[93], J.J. Hahn[147], E.H. Haines[98], M. Haleem[172], J. Haley[124], G.D. Hallewell[104], K. Hamano[171], H. Hamdaoui[167], M. Hamer[25], S.E.D. Hammoud[66], E.J. Hampshire[97], J. Han[143a], L. Han[114a], L. Han[62], S. Han[14], K. Hanagaki[84], M. Hance[139], D.A. Hangal[42], H. Hanif[148], M.D. Hank[131], J.B. Hansen[43], P.H. Hansen[43], D. Harada[56], T. Harenberg[177], S. Harkusha[179], M.L. Harris[105], Y.T. Harris[25], J. Harrison[13], N.M. Harrison[122], P.F. Harrison[173], M.L.E. Hart[98], N.M. Hartman[112], N.M. Hartmann[111], R.Z. Hasan[97,137], Y. Hasegawa[146], F. Haslbeck[129], S. Hassan[17], R. Hauser[109], M. Haviernik[136], C.M. Hawkes[21], R.J. Hawkings[37], Y. Hayashi[159], D. Hayden[109], C. Hayes[108], R.L. Hayes[117], C.P. Hays[129], J.M. Hays[96], H.S. Hayward[94], M. He[14,114c], Y. He[48], Y. He[98], N.B. Heatley[96], V. Hedberg[100], C. Heidegger[54], K.K. Heidegger[54], J. Heilman[35], S. Heim[48], T. Heim[18a], J.J. Heinrich[126], L. Heinrich[112], J. Hejbal[134], M. Helbig[50], A. Held[176], S. Hellesund[17], C.M. Helling[170], S. Hellman[47a,47b], A.M. Henriques Correia[37], H. Herde[100], Y. Hernández Jiménez[151], L.M. Herrmann[25], T. Herrmann[50], G. Herten[54], R. Hertenberger[111], L. Hervas[37], M.E. Hesping[102], N.P. Hessey[162a], J. Hessler[112], M. Hidaoui[36b], N. Hidic[136], E. Hill[161], T.S. Hillersoy[17], S.J. Hillier[21], J.R. Hinds[109],

JHEP10(2025)093

F. Hinterkeuser[25], M. Hirose[127], S. Hirose[163], D. Hirschbuehl[177], T.G. Hitchings[103], B. Hiti[95], J. Hobbs[151], R. Hobincu[28e], N. Hod[175], A.M. Hodges[168], M.C. Hodgkinson[145], B.H. Hodkinson[129], A. Hoecker[37], D.D. Hofer[108], J. Hofer[169], J. Hofner[102], M. Holzbock[37], L.B.A.H. Hommels[33], V. Homsak[129], B.P. Honan[103], J.J. Hong[68], T.M. Hong[132], B.H. Hooberman[168], W.H. Hopkins[6], M.C. Hoppesch[168], Y. Horii[113], M.E. Horstmann[112], S. Hou[154], M.R. Housenga[168], J. Howarth[59], J. Hoya[6], M. Hrabovsky[125], T. Hryn'ova[4], P.J. Hsu[65], S.-C. Hsu[142], T. Hsu[66], M. Hu[18a], Q. Hu[62], S. Huang[33], X. Huang[14,114c], Y. Huang[136], Y. Huang[114b], Y. Huang[14], Z. Huang[66], Z. Hubacek[135], F. Huegging[25], T.B. Huffman[129], M. Hufnagel Maranha De Faria[83a], C.A. Hugli[48], M. Huhtinen[37], S.K. Huiberts[17], R. Hulsken[106], C.E. Hultquist[18a], D.L. Humphreys[105], N. Huseynov[12], J. Huston[109], J. Huth[61], L. Huth[48], R. Hyneman[7], G. Iacobucci[56], G. Iakovidis[30], L. Iconomidou-Fayard[66], J.P. Iddon[37], P. Iengo[72a,72b], R. Iguchi[159], Y. Iiyama[159], T. Iizawa[159], Y. Ikegami[84], D. Iliadis[158], N. Ilic[161], H. Imam[36a], G. Inacio Goncalves[83d], S.A. Infante Cabanas[140c], T. Ingebretsen Carlson[47a,47b], J.M. Inglis[96], G. Introzzi[73a,73b], M. Iodice[77a], V. Ippolito[75a,75b], R.K. Irwin[94], M. Ishino[159], W. Islam[176], C. Issever[19], S. Istin[22a,ao], K. Itabashi[84], H. Ito[174], R. Iuppa[78a,78b], A. Ivina[175], V. Izzo[72a], P. Jacka[135], P. Jackson[1], P. Jain[48], K. Jakobs[54], T. Jakoubek[175], J. Jamieson[59], W. Jang[159], S. Jankovych[136], M. Javurkova[105], P. Jawahar[103], L. Jeanty[126], J. Jejelava[155a,ae], P. Jenni[54,f], C.E. Jessiman[35], C. Jia[143a], H. Jia[170], J. Jia[151], X. Jia[112,114c], Z. Jia[114a], C. Jiang[52], Q. Jiang[64b], S. Jiggins[48], M. Jimenez Ortega[169], J. Jimenez Pena[13], S. Jin[114a], A. Jinaru[28b], O. Jinnouchi[141], P. Johansson[145], K.A. Johns[7], J.W. Johnson[139], F.A. Jolly[48], D.M. Jones[152], E. Jones[48], K.S. Jones[8], P. Jones[33], R.W.L. Jones[93], T.J. Jones[94], H.L. Joos[55], R. Joshi[122], J. Jovicevic[16], X. Ju[18a], J.J. Junggeburth[37], T. Junkermann[63a], A. Juste Rozas[13,x], M.K. Juzek[88], S. Kabana[140f], A. Kaczmarska[88], S.A. Kadir[149], M. Kado[112], H. Kagan[122], M. Kagan[149], A. Kahn[131], C. Kahra[102], T. Kaji[159], E. Kajomovitz[156], N. Kakati[175], N. Kakoty[13], I. Kalaitzidou[54], S. Kandel[8], N.J. Kang[139], D. Kar[34h], E. Karentzos[25], K. Karki[8], O. Karkout[117], S.N. Karpov[39], Z.M. Karpova[39], V. Kartvelishvili[93], A.N. Karyukhin[38], E. Kasimi[158], J. Katzy[48], S. Kaur[35], K. Kawade[146], M.P. Kawale[123], C. Kawamoto[89], T. Kawamoto[62], E.F. Kay[37], F.I. Kaya[164], S. Kazakos[109], V.F. Kazanin[38], J.M. Keaveney[34a], R. Keeler[171], G.V. Kehris[61], J.S. Keller[35], J.M. Kelly[171], J.J. Kempster[152], O. Kepka[134], J. Kerr[162b], B.P. Kerridge[137], B.P. Kerševan[95], L. Keszeghova[29a], R.A. Khan[132], A. Khanov[124], A.G. Kharlamov[38], T. Kharlamova[38], E.E. Khoda[142], M. Kholodenko[133a], T.J. Khoo[19], G. Khoriauli[172], Y. Khoulaki[36a], J. Khubua[155b,*], Y.A.R. Khwaira[130], B. Kibirige[34h], D. Kim[6], D.W. Kim[47a,47b], Y.K. Kim[40], N. Kimura[98], M.K. Kingston[55], A. Kirchhoff[55], C. Kirfel[25], F. Kirfel[25], J. Kirk[137], A.E. Kiryunin[112], S. Kita[163], O. Kivernyk[25], M. Klassen[164], C. Klein[35], L. Klein[172], M.H. Klein[45], S.B. Klein[56], U. Klein[94], A. Klimentov[30], T. Klioutchnikova[37], P. Kluit[117], S. Kluth[112], E. Kneringer[79], T.M. Knight[161], A. Knue[49], M. Kobel[50], D. Kobylianskii[175], S.F. Koch[129], M. Kocian[149], P. Kodyš[136], D.M. Koeck[126], T. Koffas[35], O. Kolay[50], I. Koletsou[4], T. Komarek[88], K. Köneke[55], A.X.Y. Kong[1], T. Kono[121], N. Konstantinidis[98], P. Kontaxakis[56], B. Konya[100],

JHEP10(2025)093

R. Kopeliansky[42], S. Koperny[87a], K. Korcyl[88], K. Kordas[158,d], A. Korn[98], S. Korn[55], I. Korolkov[13], N. Korotkova[38], B. Kortman[117], O. Kortner[112], S. Kortner[112], W.H. Kostecka[118], M. Kostov[29a], V.V. Kostyukhin[147], A. Kotsokechagia[37], A. Kotwal[51], A. Koulouris[37], A. Kourkoumeli-Charalampidi[73a,73b], C. Kourkoumelis[9], E. Kourlitis[112], O. Kovanda[126], R. Kowalewski[171], W. Kozanecki[126], A.S. Kozhin[38], V.A. Kramarenko[38], G. Kramberger[95], P. Kramer[25], M.W. Krasny[130], A. Krasznahorkay[105], A.C. Kraus[118], J.W. Kraus[177], J.A. Kremer[48], N.B. Krengel[147], T. Kresse[50], L. Kretschmann[177], J. Kretzschmar[94], P. Krieger[161], K. Krizka[21], K. Kroeninger[49], H. Kroha[112], J. Kroll[134], J. Kroll[131], K.S. Krowpman[109], U. Kruchonak[39], H. Krüger[25], N. Krumnack[81], M.C. Kruse[51], O. Kuchinskaia[39], S. Kuday[3a], S. Kuehn[37], R. Kuesters[54], T. Kuhl[48], V. Kukhtin[39], Y. Kulchitsky[39], S. Kuleshov[140d,140b], J. Kull[1], E.V. Kumar[111], M. Kumar[34h], N. Kumari[48], P. Kumari[162b], A. Kupco[134], A. Kupich[38], O. Kuprash[54], H. Kurashige[86], L.L. Kurchaninov[162a], O. Kurdysh[4], Y.A. Kurochkin[38], A. Kurova[38], M. Kuze[141], A.K. Kvam[105], J. Kvita[125], N.G. Kyriacou[142], C. Lacasta[169], F. Lacava[75a,75b], H. Lacker[19], D. Lacour[130], N.N. Lad[98], E. Ladygin[39], A. Lafarge[41], B. Laforge[130], T. Lagouri[178], F.Z. Lahbabi[36a], S. Lai[55,37], W.S. Lai[98], J.E. Lambert[171], S. Lammers[68], W. Lampl[7], C. Lampoudis[158,d], G. Lamprinoudis[102], A.N. Lancaster[118], E. Lançon[30], U. Landgraf[54], M.P.J. Landon[96], V.S. Lang[54], O.K.B. Langrekken[128], A.J. Lankford[165], F. Lanni[37], K. Lantzsch[25], A. Lanza[73a], M. Lanzac Berrocal[169], J.F. Laporte[138], T. Lari[71a], D. Larsen[17], L. Larson[11], F. Lasagni Manghi[24b], M. Lassnig[37], S.D. Lawlor[145], R. Lazaridou[165], M. Lazzaroni[71a,71b], E.T.T. Le[165], H.D.M. Le[109], E.M. Le Boulicaut[178], L.T. Le Pottier[18a], B. Leban[24b,24a], F. Ledroit-Guillon[60], T.F. Lee[162b], L.L. Leeuw[34c], M. Lefebvre[171], C. Leggett[18a], G. Lehmann Miotto[37], M. Leigh[56], W.A. Leight[105], W. Leinonen[116], A. Leisos[158,u], M.A.L. Leite[83c], C.E. Leitgeb[19], R. Leitner[136], K.J.C. Leney[45], T. Lenz[25], S. Leone[74a], C. Leonidopoulos[52], A. Leopold[150], J.H. Lepage Bourbonnais[35], R. Les[109], C.G. Lester[33], M. Levchenko[38], J. Levêque[4], L.J. Levinson[175], G. Levrini[24b,24a], M.P. Lewicki[88], C. Lewis[142], D.J. Lewis[4], L. Lewitt[145], A. Li[30], B. Li[143a], C. Li[108], C-Q. Li[112], H. Li[143a], H. Li[103], H. Li[15], H. Li[62], H. Li[143a], J. Li[144a], K. Li[14], L. Li[144a], R. Li[178], S. Li[14,114c], S. Li[144b,144a], T. Li[5], X. Li[106], Y. Li[14], Z. Li[159], Z. Li[14,114c], Z. Li[62], S. Liang[14,114c], Z. Liang[14], M. Liberatore[138], B. Liberti[76a], G.B. Libotte[83d], K. Lie[64c], J. Lieber Marin[83e], H. Lien[68], H. Lin[108], S.F. Lin[151], L. Linden[111], R.E. Lindley[7], J.H. Lindon[37], J. Ling[61], E. Lipeles[131], A. Lipniacka[17], A. Lister[170], J.D. Little[68], B. Liu[14], B.X. Liu[114b], D. Liu[144b,144a], D. Liu[139], E.H.L. Liu[21], J.K.K. Liu[120], K. Liu[144b], K. Liu[144b,144a], M. Liu[62], M.Y. Liu[62], P. Liu[14], Q. Liu[144b,142,144a], S. Liu[151], X. Liu[62], X. Liu[143a], Y. Liu[114b,114c], Y. Liu[168], Y.L. Liu[143a], Y.W. Liu[62], Z. Liu[66,k], S.L. Lloyd[96], E.M. Lobodzinska[48], P. Loch[7], E. Lodhi[161], K. Lohwasser[145], E. Loiacono[48], J.D. Lomas[21], J.D. Long[42], I. Longarini[165], R. Longo[168], A. Lopez Solis[13], N.A. Lopez-canelas[7], N. Lorenzo Martinez[4], A.M. Lory[111], M. Losada[119a], G. Löschcke Centeno[4], X. Lou[47a,47b], X. Lou[14,114c], A. Lounis[66], P.A. Love[93], M. Lu[66], S. Lu[131], Y.J. Lu[154], H.J. Lubatti[142], C. Luci[75a,75b], F.L. Lucio Alves[114a], F. Luehring[68], B.S. Lunday[131], O. Lundberg[150], J. Lunde[37], N.A. Luongo[6], M.S. Lutz[37], A.B. Lux[26], D. Lynn[30], R. Lysak[134], V. Lysenko[135], E. Lytken[100], V. Lyubushkin[39],

JHEP10(2025)093

T. Lyubushkina[39], M.M. Lyukova[151], M.Firdaus M. Soberi[52], H. Ma[30], K. Ma[62], L.L. Ma[143a], W. Ma[62], Y. Ma[124], J.C. MacDonald[102], P.C. Machado De Abreu Farias[83e], D. Macina[37], R. Madar[41], T. Madula[98], J. Maeda[86], T. Maeno[30], P.T. Mafa[34c,j], H. Maguire[145], M. Maheshwari[33], V. Maiboroda[66], A. Maio[133a,133b,133d], K. Maj[87a], O. Majersky[48], S. Majewski[126], R. Makhmanazarov[38], N. Makovec[66], V. Maksimovic[16], B. Malaescu[130], J. Malamant[128], Pa. Malecki[88], V.P. Maleev[38], F. Malek[60,o], M. Mali[95], D. Malito[97], U. Mallik[80,*], A. Maloizel[5], S. Maltezos[10], A. Malvezzi Lopes[83d], S. Malyukov[39], J. Mamuzic[95], G. Mancini[53], M.N. Mancini[27], G. Manco[73a,73b], J.P. Mandalia[96], S.S. Mandarry[152], I. Mandić[95], L. Manhaes de Andrade Filho[83a], I.M. Maniatis[175], J. Manjarres Ramos[91], D.C. Mankad[175], A. Mann[111], T. Manoussos[37], M.N. Mantinan[40], S. Manzoni[37], L. Mao[144a], X. Mapekula[34c], A. Marantis[158], R.R. Marcelo Gregorio[96], G. Marchiori[5], C. Marcon[71a], E. Maricic[16], M. Marinescu[48], S. Marium[48], M. Marjanovic[123], A. Markhoos[54], M. Markovitch[66], M.K. Maroun[105], M.C. Marr[148], G.T. Marsden[103], E.J. Marshall[93], Z. Marshall[18a], S. Marti-Garcia[169], J. Martin[98], T.A. Martin[137], V.J. Martin[52], B. Martin dit Latour[17], L. Martinelli[75a,75b], M. Martinez[13,x], P. Martinez Agullo[169], V.I. Martinez Outschoorn[105], P. Martinez Suarez[37], S. Martin-Haugh[137], G. Martinovicova[136], V.S. Martoiu[28b], A.C. Martyniuk[98], A. Marzin[37], D. Mascione[78a,78b], L. Masetti[102], J. Masik[103], A.L. Maslennikov[39], S.L. Mason[42], P. Massarotti[72a,72b], P. Mastrandrea[74a,74b], A. Mastroberardino[44b,44a], T. Masubuchi[127], T.T. Mathew[126], J. Matousek[136], D.M. Mattern[49], J. Maurer[28b], T. Maurin[59], A.J. Maury[66], B. Maček[95], C. Mavungu Tsava[104], D.A. Maximov[38], A.E. May[103], E. Mayer[41], R. Mazini[34h], I. Maznas[118], S.M. Mazza[139], E. Mazzeo[37], J.P. Mc Gowan[171], S.P. Mc Kee[108], C.A. Mc Lean[6], C.C. McCracken[170], E.F. McDonald[107], A.E. McDougall[117], L.F. Mcelhinney[93], J.A. Mcfayden[152], R.P. McGovern[131], R.P. Mckenzie[34h], T.C. Mclachlan[48], D.J. Mclaughlin[98], S.J. McMahon[137], C.M. Mcpartland[94], R.A. McPherson[171,ab], S. Mehlhase[111], A. Mehta[94], D. Melini[169], B.R. Mellado Garcia[34h], A.H. Melo[55], F. Meloni[48], A.M. Mendes Jacques Da Costa[103], L. Meng[93], S. Menke[112], M. Mentink[37], E. Meoni[44b,44a], G. Mercado[118], S. Merianos[158], C. Merlassino[69a,69c], C. Meroni[71a,71b], J. Metcalfe[6], A.S. Mete[6], E. Meuser[102], C. Meyer[68], J-P. Meyer[138], Y. Miao[114a], R.P. Middleton[137], M. Mihovilovic[66], L. Mijović[52], G. Mikenberg[175], M. Mikestikova[134], M. Mikuž[95], H. Mildner[102], A. Milic[37], D.W. Miller[40], E.H. Miller[149], A. Milov[175], D.A. Milstead[47a,47b], T. Min[114a], A.A. Minaenko[38], I.A. Minashvili[155b], A.I. Mincer[120], B. Mindur[87a], M. Mineev[39], Y. Mino[89], L.M. Mir[13], M. Miralles Lopez[59], M. Mironova[18a], M. Missio[41], A. Mitra[173], V.A. Mitsou[169], Y. Mitsumori[113], O. Miu[161], P.S. Miyagawa[96], T. Mkrtchyan[37], M. Mlinarevic[98], T. Mlinarevic[98], M. Mlynarikova[136], L. Mlynarska[87a], C. Mo[144a], S. Mobius[20], M.H. Mohamed Farook[115], S. Mohapatra[42], S. Mohiuddin[124], G. Mokgatitswane[34h], L. Moleri[175], U. Molinatti[129], L.G. Mollier[20], B. Mondal[134], S. Mondal[135], K. Mönig[48], E. Monnier[104], L. Monsonis Romero[169], J. Montejo Berlingen[13], A. Montella[47a,47b], M. Montella[122], F. Montereali[77a,77b], F. Monticelli[92], S. Monzani[69a,69c], A. Morancho Tarda[43], N. Morange[66], A.L. Moreira De Carvalho[48], M. Moreno Llácer[169], C. Moreno Martinez[56], J.M. Moreno Perez[23b], P. Morettini[57b], S. Morgenstern[37], M. Morii[61], M. Morinaga[159],

JHEP10(2025)093

M. Moritsu[90], F. Morodei[75a,75b], P. Moschovakos[37], B. Moser[54], M. Mosidze[155b], T. Moskalets[45], P. Moskvitina[116], J. Moss[32], P. Moszkowicz[87a], A. Moussa[36d], Y. Moyal[175], H. Moyano Gomez[13], E.J.W. Moyse[105], T.G. Mroz[88], O. Mtintsilana[34h], S. Muanza[104], M. Mucha[25], J. Mueller[132], R. Müller[37], G.A. Mullier[167], A.J. Mullin[33], J.J. Mullin[51], A.C. Mullins[45], A.E. Mulski[61], D.P. Mungo[161], D. Munoz Perez[169], F.J. Munoz Sanchez[103], W.J. Murray[173,137], M. Muškinja[95], C. Mwewa[48], A.G. Myagkov[38,a], A.J. Myers[8], G. Myers[108], M. Myska[135], B.P. Nachman[149], K. Nagai[129], K. Nagano[84], R. Nagasaka[159], J.L. Nagle[30,al], E. Nagy[104], A.M. Nairz[37], Y. Nakahama[84], K. Nakamura[84], K. Nakkalil[5], A. Nandi[63b], H. Nanjo[127], E.A. Narayanan[45], Y. Narukawa[159], I. Naryshkin[38], L. Nasella[71a,71b], S. Nasri[119b], C. Nass[25], G. Navarro[23a], A. Nayaz[19], P.Y. Nechaeva[38], S. Nechaeva[24b,24a], F. Nechansky[134], L. Nedic[129], T.J. Neep[21], A. Negri[73a,73b], M. Negrini[24b], C. Nellist[117], C. Nelson[106], K. Nelson[108], S. Nemecek[134], M. Nessi[37,g], M.S. Neubauer[168], J. Newell[94], P.R. Newman[21], Y.W.Y. Ng[168], B. Ngair[119a], H.D.N. Nguyen[110], J.D. Nichols[123], R.B. Nickerson[129], R. Nicolaidou[138], J. Nielsen[139], M. Niemeyer[55], J. Niermann[37], N. Nikiforou[37], V. Nikolaenko[38,a], I. Nikolic-Audit[130], P. Nilsson[30], I. Ninca[48], G. Ninio[157], A. Nisati[75a], R. Nisius[112], N. Nitika[175], J-E. Nitschke[50], E.K. Nkadimeng[34b], T. Nobe[159], D. Noll[18a], T. Nommensen[153], M.B. Norfolk[145], B.J. Norman[35], L.C. Nosler[18a], M. Noury[36a], J. Novak[95], T. Novak[95], R. Novotny[135], L. Nozka[125], K. Ntekas[165], D. Ntounis[149], N.M.J. Nunes De Moura Junior[83b], J. Ocariz[130], I. Ochoa[133a], S. Oerdek[48,y], J.T. Offermann[40], A. Ogrodnik[88], A. Oh[103], C.C. Ohm[150], H. Oide[84], M.L. Ojeda[37], Y. Okumura[159], L.F. Oleiro Seabra[133a], I. Oleksiyuk[56], G. Oliveira Correa[13], D. Oliveira Damazio[30], J.L. Oliver[165], R. Omar[68], Ö.O. Öncel[54], A.P. O'Neill[20], A. Onofre[133a,133e,e], P.U.E. Onyisi[11], M.J. Oreglia[40], D. Orestano[77a,77b], R. Orlandini[77a,77b], R.S. Orr[161], L.M. Osojnak[42], Y. Osumi[113], G. Otero y Garzon[31], H. Otono[90], M. Ouchrif[36d], F. Ould-Saada[128], T. Ovsiannikova[142], M. Owen[59], R.E. Owen[137], V.E. Ozcan[22a], F. Ozturk[88], N. Ozturk[8], S. Ozturk[82], H.A. Pacey[129], K. Pachal[162a], A. Pacheco Pages[13], C. Padilla Aranda[13], G. Padovano[75a,75b], S. Pagan Griso[18a], G. Palacino[68], A. Palazzo[70a,70b], J. Pampel[25], J. Pan[178], T. Pan[64a], D.K. Panchal[11], C.E. Pandini[60], J.G. Panduro Vazquez[137], H.D. Pandya[1], H. Pang[138], P. Pani[48], G. Panizzo[69a,69c], L. Panwar[130], L. Paolozzi[56], S. Parajuli[168], A. Paramonov[6], C. Paraskevopoulos[53], D. Paredes Hernandez[64b], A. Pareti[73a,73b], K.R. Park[42], T.H. Park[112], F. Parodi[57b,57a], J.A. Parsons[42], U. Parzefall[54], B. Pascual Dias[41], L. Pascual Dominguez[101], E. Pasqualucci[75a], S. Passaggio[57b], F. Pastore[97], P. Patel[88], U.M. Patel[51], J.R. Pater[103], T. Pauly[37], F. Pauwels[136], C.I. Pazos[164], M. Pedersen[128], R. Pedro[133a], S.V. Peleganchuk[38], O. Penc[134], S. Peng[15], G.D. Penn[178], K.E. Penski[111], M. Penzin[38], B.S. Peralva[83d], A.P. Pereira Peixoto[142], L. Pereira Sanchez[149], D.V. Perepelitsa[30,al], G. Perera[105], E. Perez Codina[37], M. Perganti[10], H. Pernegger[37], S. Perrella[75a,75b], K. Peters[48], R.F.Y. Peters[103], B.A. Petersen[37], T.C. Petersen[43], E. Petit[104], V. Petousis[135], A.R. Petri[71a,71b], C. Petridou[158,d], T. Petru[136], A. Petrukhin[147], M. Pettee[18a], A. Petukhov[82], K. Petukhova[37], R. Pezoa[140g], L. Pezzotti[24b,24a], G. Pezzullo[178], L. Pfaffenbichler[37], A.J. Pfleger[79], T.M. Pham[176], T. Pham[107], P.W. Phillips[137], G. Piacquadio[151], E. Pianori[18a], F. Piazza[126],

JHEP10(2025)093

R. Piegaia[31], D. Pietreanu[28b], A.D. Pilkington[103], M. Pinamonti[69a,69c], J.L. Pinfold[2], B.C. Pinheiro Pereira[133a], J. Pinol Bel[13], A.E. Pinto Pinoargote[130], L. Pintucci[69a,69c], K.M. Piper[152], A. Pirttikoski[56], D.A. Pizzi[35], L. Pizzimento[64b], A. Plebani[33], M.-A. Pleier[30], V. Pleskot[136], E. Plotnikova[39], G. Poddar[96], R. Poettgen[100], L. Poggioli[130], S. Polacek[136], G. Polesello[73a], A. Poley[148], A. Polini[24b], C.S. Pollard[173], Z.B. Pollock[122], E. Pompa Pacchi[123], N.I. Pond[98], D. Ponomarenko[68], L. Pontecorvo[37], S. Popa[28a], G.A. Popeneciu[28d], A. Poreba[37], D.M. Portillo Quintero[162a], S. Pospisil[135], M.A. Postill[145], P. Postolache[28c], K. Potamianos[173], P.A. Potepa[87a], I.N. Potrap[39], C.J. Potter[33], H. Potti[153], J. Poveda[169], M.E. Pozo Astigarraga[37], R. Pozzi[37], A. Prades Ibanez[76a,76b], S.R. Pradhan[145], J. Pretel[171], D. Price[103], M. Primavera[70a], L. Primomo[69a,69c], M.A. Principe Martin[101], R. Privara[125], T. Procter[87b], M.L. Proffitt[142], N. Proklova[131], K. Prokofiev[64c], G. Proto[112], J. Proudfoot[6], M. Przybycien[87a], W.W. Przygoda[87b], A. Psallidas[46], J.E. Puddefoot[145], D. Pudzha[53], H.I. Purnell[1], D. Pyatiizbyantseva[116], J. Qian[108], R. Qian[109], D. Qichen[129], Y. Qin[13], T. Qiu[52], A. Quadt[55], M. Queitsch-Maitland[103], G. Quetant[56], R.P. Quinn[170], G. Rabanal Bolanos[61], D. Rafanoharana[112], F. Raffaeli[76a,76b], F. Ragusa[71a,71b], J.L. Rainbolt[40], S. Rajagopalan[30], E. Ramakoti[39], L. Rambelli[57b,57a], I.A. Ramirez-Berend[35], K. Ran[48,114c], D.S. Rankin[131], N.P. Rapheeha[34h], H. Rasheed[28b], D.F. Rassloff[63a], A. Rastogi[18a], S. Rave[102], S. Ravera[57b,57a], B. Ravina[37], I. Ravinovich[175], M. Raymond[37], A.L. Read[128], N.P. Readioff[145], D.M. Rebuzzi[73a,73b], A.S. Reed[59], K. Reeves[27], J.A. Reidelsturz[177], D. Reikher[37], A. Rej[49], C. Rembser[37], H. Ren[62], M. Renda[28b], F. Renner[48], A.G. Rennie[59], M. Repik[56], A.L. Rescia[57b,57a], S. Resconi[71a], M. Ressegotti[57b,57a], S. Rettie[117], W.F. Rettie[35], M.M. Revering[33], E. Reynolds[18a], O.L. Rezanova[39], P. Reznicek[136], H. Riani[36d], N. Ribaric[51], B. Ricci[69a,69c], E. Ricci[78a,78b], R. Richter[112], S. Richter[47a,47b], E. Richter-Was[87b], M. Ridel[130], S. Ridouani[36d], P. Rieck[120], P. Riedler[37], E.M. Riefel[47a,47b], J.O. Rieger[117], M. Rijssenbeek[151], M. Rimoldi[37], L. Rinaldi[24b,24a], P. Rincke[167,55], G. Ripellino[167], I. Riu[13], J.C. Rivera Vergara[171], F. Rizatdinova[124], E. Rizvi[96], B.R. Roberts[18a], S.S. Roberts[139], D. Robinson[33], M. Robles Manzano[102], A. Robson[59], A. Rocchi[76a,76b], C. Roda[74a,74b], S. Rodriguez Bosca[37], Y. Rodriguez Garcia[23a], A.M. Rodríguez Vera[118], S. Roe[37], J.T. Roemer[37], O. Røhne[128], R.A. Rojas[37], C.P.A. Roland[130], A. Romaniouk[79], E. Romano[73a,73b], M. Romano[24b], A.C. Romero Hernandez[168], N. Rompotis[94], L. Roos[130], S. Rosati[75a], B.J. Rosser[40], E. Rossi[129], E. Rossi[72a,72b], L.P. Rossi[61], L. Rossini[54], R. Rosten[122], M. Rotaru[28b], B. Rottler[54], D. Rousseau[66], D. Rousso[48], S. Roy-Garand[161], A. Rozanov[104], Z.M.A. Rozario[59], Y. Rozen[156], A. Rubio Jimenez[169], V.H. Ruelas Rivera[19], T.A. Ruggeri[1], A. Ruggiero[129], A. Ruiz-Martinez[169], A. Rummler[37], Z. Rurikova[54], N.A. Rusakovich[39], S. Ruscelli[49], H.L. Russell[171], G. Russo[75a,75b], J.P. Rutherfoord[7], S. Rutherford Colmenares[33], M. Rybar[136], P. Rybczynski[87a], A. Ryzhov[45], J.A. Sabater Iglesias[56], H.F-W. Sadrozinski[139], F. Safai Tehrani[75a], S. Saha[1], M. Sahinsoy[82], B. Sahoo[175], A. Saibel[169], B.T. Saifuddin[123], M. Saimpert[138], G.T. Saito[83c], M. Saito[159], T. Saito[159], A. Sala[71a,71b], A. Salnikov[149], J. Salt[169], A. Salvador Salas[157], F. Salvatore[152], A. Salzburger[37], D. Sammel[54], E. Sampson[93], D. Sampsonidis[158,d], D. Sampsonidou[126], M.A.A. Samy[59], J. Sánchez[169],

JHEP10(2025)093

V. Sanchez Sebastian[169], H. Sandaker[128], C.O. Sander[48], J.A. Sandesara[176], M. Sandhoff[177], C. Sandoval[23b], L. Sanfilippo[63a], D.P.C. Sankey[137], T. Sano[89], A. Sansoni[53], M. Santana Queiroz[18b], L. Santi[37], C. Santoni[41], H. Santos[133a,133b], A. Santra[175], E. Sanzani[24b,24a], K.A. Saoucha[85b], J.G. Saraiva[133a,133d], J. Sardain[7], O. Sasaki[84], K. Sato[163], C. Sauer[37], E. Sauvan[4], P. Savard[161,ai], R. Sawada[159], C. Sawyer[137], L. Sawyer[99], C. Sbarra[24b], A. Sbrizzi[24b,24a], T. Scanlon[98], J. Schaarschmidt[142], U. Schäfer[102], A.C. Schaffer[66,45], D. Schaile[111], R.D. Schamberger[151], C. Scharf[19], M.M. Schefer[20], V.A. Schegelsky[38], D. Scheirich[136], M. Schernau[140f], C. Scheulen[56], C. Schiavi[57b,57a], M. Schioppa[44b,44a], B. Schlag[149], S. Schlenker[37], J. Schmeing[177], E. Schmidt[112], M.A. Schmidt[177], K. Schmieden[25], C. Schmitt[102], N. Schmitt[102], S. Schmitt[48], N.A. Schneider[111], L. Schoeffel[138], A. Schoening[63b], P.G. Scholer[35], E. Schopf[147], M. Schott[25], S. Schramm[56], T. Schroer[56], H-C. Schultz-Coulon[63a], M. Schumacher[54], B.A. Schumm[139], Ph. Schune[138], H.R. Schwartz[7], A. Schwartzman[149], T.A. Schwarz[108], Ph. Schwemling[138], R. Schwienhorst[109], F.G. Sciacca[20], A. Sciandra[30], G. Sciolla[27], F. Scuri[74a], C.D. Sebastiani[37], K. Sedlaczek[118], S.C. Seidel[115], A. Seiden[139], B.D. Seidlitz[42], C. Seitz[48], J.M. Seixas[83b], G. Sekhniaidze[72a], L. Selem[60], N. Semprini-Cesari[24b,24a], A. Semushin[179], D. Sengupta[56], V. Senthilkumar[169], L. Serin[66], M. Sessa[72a,72b], H. Severini[123], F. Sforza[57b,57a], A. Sfyrla[56], Q. Sha[14], E. Shabalina[55], H. Shaddix[118], A.H. Shah[33], R. Shaheen[150], J.D. Shahinian[131], M. Shamim[37], L.Y. Shan[14], M. Shapiro[18a], A. Sharma[37], A.S. Sharma[170], P. Sharma[30], P.B. Shatalov[38], K. Shaw[152], S.M. Shaw[103], Q. Shen[14], D.J. Sheppard[148], P. Sherwood[98], L. Shi[98], X. Shi[14], S. Shimizu[84], C.O. Shimmin[178], I.P.J. Shipsey[129,*], S. Shirabe[90], M. Shiyakova[39,z], M.J. Shochet[40], D.R. Shope[128], B. Shrestha[123], S. Shrestha[122,an], I. Shreyber[39], M.J. Shroff[171], P. Sicho[134], A.M. Sickles[168], E. Sideras Haddad[34h,166], A.C. Sidley[117], A. Sidoti[24b], F. Siegert[50], Dj. Sijacki[16], F. Sili[92], J.M. Silva[52], I. Silva Ferreira[83b], M.V. Silva Oliveira[30], S.B. Silverstein[47a], S. Simion[66], R. Simoniello[37], E.L. Simpson[103], H. Simpson[152], L.R. Simpson[6], S. Simsek[82], S. Sindhu[55], P. Sinervo[161], S.N. Singh[27], S. Singh[30], S. Sinha[48], S. Sinha[103], M. Sioli[24b,24a], K. Sioulas[9], I. Siral[37], E. Sitnikova[48], J. Sjölin[47a,47b], A. Skaf[55], E. Skorda[21], P. Skubic[123], M. Slawinska[88], I. Slazyk[17], I. Sliusar[128], V. Smakhtin[175], B.H. Smart[137], S.Yu. Smirnov[140b], Y. Smirnov[82], L.N. Smirnova[38,a], O. Smirnova[100], A.C. Smith[42], D.R. Smith[165], J.L. Smith[103], M.B. Smith[35], R. Smith[149], H. Smitmanns[102], M. Smizanska[93], K. Smolek[135], P. Smolyanskiy[135], A.A. Snesarev[39], H.L. Snoek[117], S. Snyder[30], R. Sobie[171,ab], A. Soffer[157], C.A. Solans Sanchez[37], E.Yu. Soldatov[39], U. Soldevila[169], A.A. Solodkov[34h], S. Solomon[27], A. Soloshenko[39], K. Solovieva[54], O.V. Solovyanov[41], P. Sommer[50], A. Sonay[13], A. Sopczak[135], A.L. Sopio[52], F. Sopkova[29b], J.D. Sorenson[115], I.R. Sotarriva Alvarez[141], V. Sothilingam[63a], O.J. Soto Sandoval[140c,140b], S. Sottocornola[68], R. Soualah[85a], Z. Soumaimi[36e], D. South[48], N. Soybelman[175], S. Spagnolo[70a,70b], M. Spalla[112], D. Sperlich[54], B. Spisso[72a,72b], D.P. Spiteri[59], L. Splendori[104], M. Spousta[136], E.J. Staats[35], R. Stamen[63a], E. Stanecka[88], W. Stanek-Maslouska[48], M.V. Stange[50], B. Stanislaus[18a], M.M. Stanitzki[48], B. Stapf[48], E.A. Starchenko[38], G.H. Stark[139], J. Stark[91], P. Staroba[134], P. Starovoitov[85b], R. Staszewski[88],

JHEP10(2025)093

C. Stauch[111], G. Stavropoulos[46], A. Stefl[37], A. Stein[102], P. Steinberg[30], B. Stelzer[148,162a], H.J. Stelzer[132], O. Stelzer[162a], H. Stenzel[58], T.J. Stevenson[152], G.A. Stewart[37], J.R. Stewart[124], G. Stoicea[28b], M. Stolarski[133a], S. Stonjek[112], A. Straessner[50], J. Strandberg[150], S. Strandberg[47a,47b], M. Stratmann[177], M. Strauss[123], T. Strebler[104], P. Strizenec[29b], R. Ströhmer[172], D.M. Strom[126], R. Stroynowski[45], A. Strubig[47a,47b], S.A. Stucci[30], B. Stugu[17], J. Stupak[123], N.A. Styles[48], D. Su[149], S. Su[62], X. Su[62], D. Suchy[29a], A.D. Sudhakar Ponnu[55], K. Sugizaki[131], V.V. Sulin[38], D.M.S. Sultan[129], L. Sultanaliyeva[25], S. Sultansoy[3b], S. Sun[176], W. Sun[14], N. Sur[100], M.R. Sutton[152], M. Svatos[134], P.N. Swallow[33], M. Swiatlowski[162a], T. Swirski[172], A. Swoboda[37], I. Sykora[29a], M. Sykora[136], T. Sykora[136], D. Ta[102], K. Tackmann[48,y], A. Taffard[165], R. Tafirout[162a], Y. Takubo[84], M. Talby[104], A.A. Talyshev[38], K.C. Tam[64b], N.M. Tamir[157], A. Tanaka[159], J. Tanaka[159], R. Tanaka[66], M. Tanasini[151], Z. Tao[170], S. Tapia Araya[140g], S. Tapprogge[102], A. Tarek Abouelfadl Mohamed[37], S. Tarem[156], K. Tariq[14], G. Tarna[37], G.F. Tartarelli[71a], M.J. Tartarin[91], P. Tas[136], M. Tasevsky[134], E. Tassi[44b,44a], A.C. Tate[168], Y. Tayalati[36e,aa], G.N. Taylor[107], W. Taylor[162b], R.J. Taylor Vara[169], A.S. Tegetmeier[91], P. Teixeira-Dias[97], J.J. Teoh[161], K. Terashi[159], J. Terron[101], S. Terzo[13], M. Testa[53], R.J. Teuscher[161,ab], A. Thaler[79], O. Theiner[56], T. Theveneaux-Pelzer[104], D.W. Thomas[97], J.P. Thomas[21], E.A. Thompson[18a], P.D. Thompson[21], E. Thomson[131], R.E. Thornberry[45], C. Tian[62], Y. Tian[56], V. Tikhomirov[82], Yu.A. Tikhonov[39], S. Timoshenko[38], D. Timoshyn[136], E.X.L. Ting[1], P. Tipton[178], A. Tishelman-Charny[30], K. Todome[141], S. Todorova-Nova[136], L. Toffolin[69a,69c], M. Togawa[84], J. Tojo[90], S. Tokár[29a], O. Toldaiev[68], G. Tolkachev[104], M. Tomoto[84], L. Tompkins[149,n], E. Torrence[126], H. Torres[91], D.I. Torres Arza[140g], E. Torró Pastor[169], M. Toscani[31], C. Tosciri[40], M. Tost[11], D.R. Tovey[145], T. Trefzger[172], P.M. Tricarico[13], A. Tricoli[30], I.M. Trigger[162a], S. Trincaz-Duvoid[130], D.A. Trischuk[27], A. Tropina[39], L. Truong[34c], M. Trzebinski[88], A. Trzupek[88], F. Tsai[151], M. Tsai[108], A. Tsiamis[158], P.V. Tsiareshka[39], S. Tsigaridas[162a], A. Tsirigotis[158,u], V. Tsiskaridze[155a], E.G. Tskhadadze[155a], Y. Tsujikawa[89], I.I. Tsukerman[38], V. Tsulaia[18a], S. Tsuno[84], K. Tsuri[121], D. Tsybychev[151], Y. Tu[64b], A. Tudorache[28b], V. Tudorache[28b], S.B. Tuncay[129], S. Turchikhin[57b,57a], I. Turk Cakir[3a], R. Turra[71a], T. Turtuvshin[39,ac], P.M. Tuts[42], S. Tzamarias[158,d], Y. Uematsu[84], F. Ukegawa[163], P.A. Ulloa Poblete[140c,140b], E.N. Umaka[30], G. Unal[37], A. Undrus[30], G. Unel[165], J. Urban[29b], P. Urrejola[140e], G. Usai[8], R. Ushioda[160], M. Usman[110], F. Ustuner[52], Z. Uysal[82], V. Vacek[135], B. Vachon[106], T. Vafeiadis[37], A. Vaitkus[98], C. Valderanis[111], E. Valdes Santurio[47a,47b], M. Valente[37], S. Valentinetti[24b,24a], A. Valero[169], E. Valiente Moreno[169], A. Vallier[91], J.A. Valls Ferrer[169], D.R. Van Arneman[117], A. Van Der Graaf[49], H.Z. Van Der Schyf[34h], P. Van Gemmeren[6], M. Van Rijnbach[37], S. Van Stroud[98], I. Van Vulpen[117], P. Vana[136], M. Vanadia[76a,76b], U.M. Vande Voorde[150], W. Vandelli[37], E.R. Vandewall[124], D. Vannicola[157], L. Vannoli[53], R. Vari[75a], M. Varma[178], E.W. Varnes[7], C. Varni[118], D. Varouchas[66], L. Varriale[169], K.E. Varvell[153], M.E. Vasile[28b], L. Vaslin[84], M.D. Vassilev[149], A. Vasyukov[39], L.M. Vaughan[124], R. Vavricka[136], T. Vazquez Schroeder[13], J. Veatch[32], V. Vecchio[103], M.J. Veen[105], I. Veliscek[30], I. Velkovska[95], L.M. Veloce[161], F. Veloso[133a,133c], S. Veneziano[75a], A. Ventura[70a,70b], A. Verbytskyi[112], M. Verducci[74a,74b],

JHEP10(2025)093

C. Vergis[96], M. Verissimo De Araujo[83b], W. Verkerke[117], J.C. Vermeulen[117], C. Vernieri[149], M. Vessella[165], M.C. Vetterli[148,ai], A. Vgenopoulos[102], N. Viaux Maira[140g,af], T. Vickey[145], O.E. Vickey Boeriu[145], G.H.A. Viehhauser[129], L. Vigani[63b], M. Vigl[112], M. Villa[24b,24a], M. Villaplana Perez[169], E.M. Villhauer[40], E. Vilucchi[53], M. Vincent[169], M.G. Vincter[35], A. Visibile[117], A. Visive[117], C. Vittori[37], I. Vivarelli[24b,24a], M.I. Vivas Albornoz[48], E. Voevodina[112], F. Vogel[111], J.C. Voigt[50], P. Vokac[135], Yu. Volkotrub[87b], L. Vomberg[25], E. Von Toerne[25], B. Vormwald[37], K. Vorobev[51], M. Vos[169], K. Voss[147], M. Vozak[37], L. Vozdecky[123], N. Vranjes[16], M. Vranjes Milosavljevic[16], M. Vreeswijk[117], N.K. Vu[144b,144a], R. Vuillermet[37], O. Vujinovic[102], I. Vukotic[40], I.K. Vyas[35], J.F. Wack[33], S. Wada[163], C. Wagner[149], J.M. Wagner[18a], W. Wagner[177], S. Wahdan[177], H. Wahlberg[92], C.H. Waits[123], J. Walder[137], R. Walker[111], K. Walkingshaw Pass[59], W. Walkowiak[147], A. Wall[131], E.J. Wallin[100], T. Wamorkar[18a], K. Wandall-Christensen[169], A. Wang[62], A.Z. Wang[139], C. Wang[102], C. Wang[11], H. Wang[18a], J. Wang[64c], P. Wang[103], P. Wang[98], R. Wang[61], R. Wang[6], S.M. Wang[154], S. Wang[14], T. Wang[116], T. Wang[62], W.T. Wang[129], W. Wang[14], X. Wang[168], X. Wang[144a], X. Wang[48], Y. Wang[114a], Y. Wang[62], Z. Wang[108], Z. Wang[144b], Z. Wang[108], C. Wanotayaroj[84], A. Warburton[106], A.L. Warnerbring[147], S. Waterhouse[97], A.T. Watson[21], H. Watson[52], M.F. Watson[21], E. Watton[37], G. Watts[142], B.M. Waugh[98], J.M. Webb[54], C. Weber[30], H.A. Weber[19], M.S. Weber[20], S.M. Weber[63a], C. Wei[62], Y. Wei[54], A.R. Weidberg[129], E.J. Weik[120], J. Weingarten[49], C. Weiser[54], C.J. Wells[48], T. Wenaus[30], T. Wengler[37], N.S. Wenke[112], N. Wermes[25], M. Wessels[63a], A.M. Wharton[93], A.S. White[61], A. White[8], M.J. White[1], D. Whiteson[165], L. Wickremasinghe[127], W. Wiedenmann[176], M. Wielers[137], R. Wierda[150], C. Wiglesworth[43], H.G. Wilkens[37], J.J.H. Wilkinson[33], D.M. Williams[42], H.H. Williams[131], S. Williams[33], S. Willocq[105], B.J. Wilson[103], D.J. Wilson[103], P.J. Windischhofer[40], F.I. Winkel[31], F. Winklmeier[126], B.T. Winter[54], M. Wittgen[149], M. Wobisch[99], T. Wojtkowski[60], Z. Wolffs[117], J. Wollrath[37], M.W. Wolter[88], H. Wolters[133a,133c], M.C. Wong[139], E.L. Woodward[42], S.D. Worm[48], B.K. Wosiek[88], K.W. Woźniak[88], S. Wozniewski[55], K. Wraight[59], C. Wu[161], C. Wu[21], J. Wu[159], M. Wu[114b], M. Wu[116], S.L. Wu[176], S. Wu[14,ak], X. Wu[62], Y.Q. Wu[161], Y. Wu[62], Z. Wu[4], Z. Wu[114a], J. Wuerzinger[112], T.R. Wyatt[103], B.M. Wynne[52], S. Xella[43], L. Xia[114a], M. Xie[62], A. Xiong[126], D. Xu[14], H. Xu[62], L. Xu[62], R. Xu[131], T. Xu[108], Y. Xu[142], Z. Xu[52], R. Xue[132], B. Yabsley[153], S. Yacoob[34a], Y. Yamaguchi[84], E. Yamashita[159], H. Yamauchi[163], T. Yamazaki[18a], Y. Yamazaki[86], S. Yan[59], Z. Yan[105], H.J. Yang[144a,144b], H.T. Yang[62], S. Yang[62], T. Yang[64c], X. Yang[37], X. Yang[14], Y. Yang[159], Y. Yang[62], W-M. Yao[18a], C.L. Yardley[152], J. Ye[14], S. Ye[30], X. Ye[62], Y. Yeh[98], I. Yeletskikh[39], B. Yeo[18b], M.R. Yexley[98], T.P. Yildirim[129], K. Yorita[174], C.J.S. Young[37], C. Young[149], N.D. Young[126], Y. Yu[62], J. Yuan[14,114c], M. Yuan[108], R. Yuan[144b,144a], L. Yue[98], M. Zaazoua[62], B. Zabinski[88], I. Zahir[36a], A. Zaio[57b,57a], Z.K. Zak[88], T. Zakareishvili[169], S. Zambito[56], J.A. Zamora Saa[140d], J. Zang[159], R. Zanzottera[71a,71b], O. Zaplatilek[135], C. Zeitnitz[177], H. Zeng[14], J.C. Zeng[168], D.T. Zenger Jr[27], O. Zenin[38], T. Ženiš[29a], S. Zenz[96], D. Zerwas[66], M. Zhai[14,114c], D.F. Zhang[145], G. Zhang[14,ak], J. Zhang[143a], J. Zhang[6], K. Zhang[14,114c], L. Zhang[62],

JHEP10(2025)093

L. Zhang[114a], P. Zhang[14,114c], R. Zhang[114a], S. Zhang[91], T. Zhang[159], Y. Zhang[142], Y. Zhang[98], Y. Zhang[62], Y. Zhang[114a], Z. Zhang[18a], Z. Zhang[143a], Z. Zhang[66], H. Zhao[142], T. Zhao[143a], Y. Zhao[35], Z. Zhao[62], Z. Zhao[62], A. Zhemchugov[39], J. Zheng[114a], K. Zheng[168], X. Zheng[62], Z. Zheng[149], D. Zhong[168], B. Zhou[108], H. Zhou[7], N. Zhou[144a], Y. Zhou[15], Y. Zhou[114a], Y. Zhou[7], C.G. Zhu[143a], J. Zhu[108], X. Zhu[144b], Y. Zhu[144a], Y. Zhu[62], X. Zhuang[14], K. Zhukov[68], N.I. Zimine[39], J. Zinsser[63b], M. Ziolkowski[147], L. Živković[16], A. Zoccoli[24b,24a], K. Zoch[61], A. Zografos[37], T.G. Zorbas[145], O. Zormpa[46], L. Zwalinski[37]

[1] *Department of Physics, University of Adelaide, Adelaide; Australia*
[2] *Department of Physics, University of Alberta, Edmonton AB; Canada*
[3] [(a)] *Department of Physics, Ankara University, Ankara;* [(b)] *Division of Physics, TOBB University of Economics and Technology, Ankara; Türkiye*
[4] *LAPP, Université Savoie Mont Blanc, CNRS/IN2P3, Annecy; France*
[5] *APC, Université Paris Cité, CNRS/IN2P3, Paris; France*
[6] *High Energy Physics Division, Argonne National Laboratory, Argonne IL; United States of America*
[7] *Department of Physics, University of Arizona, Tucson AZ; United States of America*
[8] *Department of Physics, University of Texas at Arlington, Arlington TX; United States of America*
[9] *Physics Department, National and Kapodistrian University of Athens, Athens; Greece*
[10] *Physics Department, National Technical University of Athens, Zografou; Greece*
[11] *Department of Physics, University of Texas at Austin, Austin TX; United States of America*
[12] *Institute of Physics, Azerbaijan Academy of Sciences, Baku; Azerbaijan*
[13] *Institut de Física d'Altes Energies (IFAE), Barcelona Institute of Science and Technology, Barcelona; Spain*
[14] *Institute of High Energy Physics, Chinese Academy of Sciences, Beijing; China*
[15] *Physics Department, Tsinghua University, Beijing; China*
[16] *Institute of Physics, University of Belgrade, Belgrade; Serbia*
[17] *Department for Physics and Technology, University of Bergen, Bergen; Norway*
[18] [(a)] *Physics Division, Lawrence Berkeley National Laboratory, Berkeley CA;* [(b)] *University of California, Berkeley CA; United States of America*
[19] *Institut für Physik, Humboldt Universität zu Berlin, Berlin; Germany*
[20] *Albert Einstein Center for Fundamental Physics and Laboratory for High Energy Physics, University of Bern, Bern; Switzerland*
[21] *School of Physics and Astronomy, University of Birmingham, Birmingham; United Kingdom*
[22] [(a)] *Department of Physics, Bogazici University, Istanbul;* [(b)] *Department of Physics Engineering, Gaziantep University, Gaziantep;* [(c)] *Department of Physics, Istanbul University, Istanbul; Türkiye*
[23] [(a)] *Facultad de Ciencias y Centro de Investigaciónes, Universidad Antonio Nariño, Bogotá;* [(b)] *Departamento de Física, Universidad Nacional de Colombia, Bogotá; Colombia*
[24] [(a)] *Dipartimento di Fisica e Astronomia A. Righi, Università di Bologna, Bologna;* [(b)] *INFN Sezione di Bologna; Italy*
[25] *Physikalisches Institut, Universität Bonn, Bonn; Germany*
[26] *Department of Physics, Boston University, Boston MA; United States of America*
[27] *Department of Physics, Brandeis University, Waltham MA; United States of America*
[28] [(a)] *Transilvania University of Brasov, Brasov;* [(b)] *Horia Hulubei National Institute of Physics and Nuclear Engineering, Bucharest;* [(c)] *Department of Physics, Alexandru Ioan Cuza University of Iasi, Iasi;* [(d)] *National Institute for Research and Development of Isotopic and Molecular Technologies, Physics Department, Cluj-Napoca;* [(e)] *National University of Science and Technology Politechnica, Bucharest;* [(f)] *West University in Timisoara, Timisoara;* [(g)] *Faculty of Physics, University of Bucharest, Bucharest; Romania*
[29] [(a)] *Faculty of Mathematics, Physics and Informatics, Comenius University, Bratislava;* [(b)] *Department of Subnuclear Physics, Institute of Experimental Physics of the Slovak Academy of Sciences, Kosice; Slovak Republic*
[30] *Physics Department, Brookhaven National Laboratory, Upton NY; United States of America*

JHEP10(2025)093

[31] Universidad de Buenos Aires, Facultad de Ciencias Exactas y Naturales, Departamento de Física, y CONICET, Instituto de Física de Buenos Aires (IFIBA), Buenos Aires; Argentina
[32] California State University, CA; United States of America
[33] Cavendish Laboratory, University of Cambridge, Cambridge; United Kingdom
[34] [(a)] Department of Physics, University of Cape Town, Cape Town;[(b)] iThemba Labs, Western Cape;[(c)] Department of Mechanical Engineering Science, University of Johannesburg, Johannesburg;[(d)] National Institute of Physics, University of the Philippines Diliman (Philippines);[(e)] Department of Physics, Stellenbosch University, Matieland;[(f)] University of South Africa, Department of Physics, Pretoria;[(g)] University of Zululand, KwaDlangezwa;[(h)] School of Physics, University of the Witwatersrand, Johannesburg; South Africa
[35] Department of Physics, Carleton University, Ottawa ON; Canada
[36] [(a)] Faculté des Sciences Ain Chock, Université Hassan II de Casablanca;[(b)] Faculté des Sciences, Université Ibn-Tofail, Kénitra;[(c)] Faculté des Sciences Semlalia, Université Cadi Ayyad, LPHEA-Marrakech;[(d)] LPMR, Faculté des Sciences, Université Mohamed Premier, Oujda;[(e)] Faculté des sciences, Université Mohammed V, Rabat;[(f)] Institute of Applied Physics, Mohammed VI Polytechnic University, Ben Guerir; Morocco
[37] CERN, Geneva; Switzerland
[38] Affiliated with an institute formerly covered by a cooperation agreement with CERN
[39] Affiliated with an international laboratory covered by a cooperation agreement with CERN
[40] Enrico Fermi Institute, University of Chicago, Chicago IL; United States of America
[41] LPC, Université Clermont Auvergne, CNRS/IN2P3, Clermont-Ferrand; France
[42] Nevis Laboratory, Columbia University, Irvington NY; United States of America
[43] Niels Bohr Institute, University of Copenhagen, Copenhagen; Denmark
[44] [(a)] Dipartimento di Fisica, Università della Calabria, Rende;[(b)] INFN Gruppo Collegato di Cosenza, Laboratori Nazionali di Frascati; Italy
[45] Physics Department, Southern Methodist University, Dallas TX; United States of America
[46] National Centre for Scientific Research "Demokritos", Agia Paraskevi; Greece
[47] [(a)] Department of Physics, Stockholm University;[(b)] Oskar Klein Centre, Stockholm; Sweden
[48] Deutsches Elektronen-Synchrotron DESY, Hamburg and Zeuthen; Germany
[49] Fakultät Physik, Technische Universität Dortmund, Dortmund; Germany
[50] Institut für Kern- und Teilchenphysik, Technische Universität Dresden, Dresden; Germany
[51] Department of Physics, Duke University, Durham NC; United States of America
[52] SUPA — School of Physics and Astronomy, University of Edinburgh, Edinburgh; United Kingdom
[53] INFN e Laboratori Nazionali di Frascati, Frascati; Italy
[54] Physikalisches Institut, Albert-Ludwigs-Universität Freiburg, Freiburg; Germany
[55] II. Physikalisches Institut, Georg-August-Universität Göttingen, Göttingen; Germany
[56] Département de Physique Nucléaire et Corpusculaire, Université de Genève, Genève; Switzerland
[57] [(a)] Dipartimento di Fisica, Università di Genova, Genova;[(b)] INFN Sezione di Genova; Italy
[58] II. Physikalisches Institut, Justus-Liebig-Universität Giessen, Giessen; Germany
[59] SUPA — School of Physics and Astronomy, University of Glasgow, Glasgow; United Kingdom
[60] LPSC, Université Grenoble Alpes, CNRS/IN2P3, Grenoble INP, Grenoble; France
[61] Laboratory for Particle Physics and Cosmology, Harvard University, Cambridge MA; United States of America
[62] Department of Modern Physics and State Key Laboratory of Particle Detection and Electronics, University of Science and Technology of China, Hefei; China
[63] [(a)] Kirchhoff-Institut für Physik, Ruprecht-Karls-Universität Heidelberg, Heidelberg;[(b)] Physikalisches Institut, Ruprecht-Karls-Universität Heidelberg, Heidelberg; Germany
[64] [(a)] Department of Physics, Chinese University of Hong Kong, Shatin, N.T., Hong Kong;[(b)] Department of Physics, University of Hong Kong, Hong Kong;[(c)] Department of Physics and Institute for Advanced Study, Hong Kong University of Science and Technology, Clear Water Bay, Kowloon, Hong Kong; China
[65] Department of Physics, National Tsing Hua University, Hsinchu; Taiwan
[66] IJCLab, Université Paris-Saclay, CNRS/IN2P3, 91405, Orsay; France
[67] Centro Nacional de Microelectrónica (IMB-CNM-CSIC), Barcelona; Spain
[68] Department of Physics, Indiana University, Bloomington IN; United States of America

JHEP10(2025)093

[69] [(a)] INFN Gruppo Collegato di Udine, Sezione di Trieste, Udine; [(b)] ICTP, Trieste; [(c)] Dipartimento Politecnico di Ingegneria e Architettura, Università di Udine, Udine; Italy
[70] [(a)] INFN Sezione di Lecce; [(b)] Dipartimento di Matematica e Fisica, Università del Salento, Lecce; Italy
[71] [(a)] INFN Sezione di Milano; [(b)] Dipartimento di Fisica, Università di Milano, Milano; Italy
[72] [(a)] INFN Sezione di Napoli; [(b)] Dipartimento di Fisica, Università di Napoli, Napoli; Italy
[73] [(a)] INFN Sezione di Pavia; [(b)] Dipartimento di Fisica, Università di Pavia, Pavia; Italy
[74] [(a)] INFN Sezione di Pisa; [(b)] Dipartimento di Fisica E. Fermi, Università di Pisa, Pisa; Italy
[75] [(a)] INFN Sezione di Roma; [(b)] Dipartimento di Fisica, Sapienza Università di Roma, Roma; Italy
[76] [(a)] INFN Sezione di Roma Tor Vergata; [(b)] Dipartimento di Fisica, Università di Roma Tor Vergata, Roma; Italy
[77] [(a)] INFN Sezione di Roma Tre; [(b)] Dipartimento di Matematica e Fisica, Università Roma Tre, Roma; Italy
[78] [(a)] INFN-TIFPA; [(b)] Università degli Studi di Trento, Trento; Italy
[79] Universität Innsbruck, Department of Astro and Particle Physics, Innsbruck; Austria
[80] University of Iowa, Iowa City IA; United States of America
[81] Department of Physics and Astronomy, Iowa State University, Ames IA; United States of America
[82] Istinye University, Sariyer, Istanbul; Türkiye
[83] [(a)] Departamento de Engenharia Elétrica, Universidade Federal de Juiz de Fora (UFJF), Juiz de Fora; [(b)] Universidade Federal do Rio De Janeiro COPPE/EE/IF, Rio de Janeiro; [(c)] Instituto de Física, Universidade de São Paulo, São Paulo; [(d)] Rio de Janeiro State University, Rio de Janeiro; [(e)] Federal University of Bahia, Bahia; Brazil
[84] KEK, High Energy Accelerator Research Organization, Tsukuba; Japan
[85] [(a)] Khalifa University of Science and Technology, Abu Dhabi; [(b)] University of Sharjah, Sharjah; United Arab Emirates
[86] Graduate School of Science, Kobe University, Kobe; Japan
[87] [(a)] AGH University of Krakow, Faculty of Physics and Applied Computer Science, Krakow; [(b)] Marian Smoluchowski Institute of Physics, Jagiellonian University, Krakow; Poland
[88] Institute of Nuclear Physics Polish Academy of Sciences, Krakow; Poland
[89] Faculty of Science, Kyoto University, Kyoto; Japan
[90] Research Center for Advanced Particle Physics and Department of Physics, Kyushu University, Fukuoka; Japan
[91] L2IT, Université de Toulouse, CNRS/IN2P3, UPS, Toulouse; France
[92] Instituto de Física La Plata, Universidad Nacional de La Plata and CONICET, La Plata; Argentina
[93] Physics Department, Lancaster University, Lancaster; United Kingdom
[94] Oliver Lodge Laboratory, University of Liverpool, Liverpool; United Kingdom
[95] Department of Experimental Particle Physics, Jožef Stefan Institute and Department of Physics, University of Ljubljana, Ljubljana; Slovenia
[96] Department of Physics and Astronomy, Queen Mary University of London, London; United Kingdom
[97] Department of Physics, Royal Holloway University of London, Egham; United Kingdom
[98] Department of Physics and Astronomy, University College London, London; United Kingdom
[99] Louisiana Tech University, Ruston LA; United States of America
[100] Fysiska institutionen, Lunds universitet, Lund; Sweden
[101] Departamento de Física Teorica C-15 and CIAFF, Universidad Autónoma de Madrid, Madrid; Spain
[102] Institut für Physik, Universität Mainz, Mainz; Germany
[103] School of Physics and Astronomy, University of Manchester, Manchester; United Kingdom
[104] CPPM, Aix-Marseille Université, CNRS/IN2P3, Marseille; France
[105] Department of Physics, University of Massachusetts, Amherst MA; United States of America
[106] Department of Physics, McGill University, Montreal QC; Canada
[107] School of Physics, University of Melbourne, Victoria; Australia
[108] Department of Physics, University of Michigan, Ann Arbor MI; United States of America
[109] Department of Physics and Astronomy, Michigan State University, East Lansing MI; United States of America
[110] Group of Particle Physics, University of Montreal, Montreal QC; Canada
[111] Fakultät für Physik, Ludwig-Maximilians-Universität München, München; Germany

JHEP10(2025)093

[112] Max-Planck-Institut für Physik (Werner-Heisenberg-Institut), München; Germany
[113] Graduate School of Science and Kobayashi-Maskawa Institute, Nagoya University, Nagoya; Japan
[114] [(a)] Department of Physics, Nanjing University, Nanjing;[(b)] School of Science, Shenzhen Campus of Sun Yat-sen University;[(c)] University of Chinese Academy of Science (UCAS), Beijing; China
[115] Department of Physics and Astronomy, University of New Mexico, Albuquerque NM; United States of America
[116] Institute for Mathematics, Astrophysics and Particle Physics, Radboud University/Nikhef, Nijmegen; Netherlands
[117] Nikhef National Institute for Subatomic Physics and University of Amsterdam, Amsterdam; Netherlands
[118] Department of Physics, Northern Illinois University, DeKalb IL; United States of America
[119] [(a)] New York University Abu Dhabi, Abu Dhabi;[(b)] United Arab Emirates University, Al Ain; United Arab Emirates
[120] Department of Physics, New York University, New York NY; United States of America
[121] Ochanomizu University, Otsuka, Bunkyo-ku, Tokyo; Japan
[122] Ohio State University, Columbus OH; United States of America
[123] Homer L. Dodge Department of Physics and Astronomy, University of Oklahoma, Norman OK; United States of America
[124] Department of Physics, Oklahoma State University, Stillwater OK; United States of America
[125] Palacký University, Joint Laboratory of Optics, Olomouc; Czech Republic
[126] Institute for Fundamental Science, University of Oregon, Eugene, OR; United States of America
[127] Graduate School of Science, University of Osaka, Osaka; Japan
[128] Department of Physics, University of Oslo, Oslo; Norway
[129] Department of Physics, Oxford University, Oxford; United Kingdom
[130] LPNHE, Sorbonne Université, Université Paris Cité, CNRS/IN2P3, Paris; France
[131] Department of Physics, University of Pennsylvania, Philadelphia PA; United States of America
[132] Department of Physics and Astronomy, University of Pittsburgh, Pittsburgh PA; United States of America
[133] [(a)] Laboratório de Instrumentação e Física Experimental de Partículas — LIP, Lisboa;[(b)] Departamento de Física, Faculdade de Ciências, Universidade de Lisboa, Lisboa;[(c)] Departamento de Física, Universidade de Coimbra, Coimbra;[(d)] Centro de Física Nuclear da Universidade de Lisboa, Lisboa;[(e)] Departamento de Física, Escola de Ciências, Universidade do Minho, Braga;[(f)] Departamento de Física Teórica y del Cosmos, Universidad de Granada, Granada (Spain);[(g)] Departamento de Física, Instituto Superior Técnico, Universidade de Lisboa, Lisboa; Portugal
[134] Institute of Physics of the Czech Academy of Sciences, Prague; Czech Republic
[135] Czech Technical University in Prague, Prague; Czech Republic
[136] Charles University, Faculty of Mathematics and Physics, Prague; Czech Republic
[137] Particle Physics Department, Rutherford Appleton Laboratory, Didcot; United Kingdom
[138] IRFU, CEA, Université Paris-Saclay, Gif-sur-Yvette; France
[139] Santa Cruz Institute for Particle Physics, University of California Santa Cruz, Santa Cruz CA; United States of America
[140] [(a)] Departamento de Física, Pontificia Universidad Católica de Chile, Santiago;[(b)] Millennium Institute for Subatomic physics at high energy frontier (SAPHIR), Santiago;[(c)] Instituto de Investigación Multidisciplinario en Ciencia y Tecnología, y Departamento de Física, Universidad de La Serena;[(d)] Universidad Andres Bello, Department of Physics, Santiago;[(e)] Universidad San Sebastian, Recoleta;[(f)] Instituto de Alta Investigación, Universidad de Tarapacá, Arica;[(g)] Departamento de Física, Universidad Técnica Federico Santa María, Valparaíso; Chile
[141] Department of Physics, Institute of Science, Tokyo; Japan
[142] Department of Physics, University of Washington, Seattle WA; United States of America
[143] [(a)] Institute of Frontier and Interdisciplinary Science and Key Laboratory of Particle Physics and Particle Irradiation (MOE), Shandong University, Qingdao;[(b)] School of Physics, Zhengzhou University; China
[144] [(a)] State Key Laboratory of Dark Matter Physics, School of Physics and Astronomy, Shanghai Jiao Tong University, Key Laboratory for Particle Astrophysics and Cosmology (MOE), SKLPPC, Shanghai;[(b)] State Key Laboratory of Dark Matter Physics, Tsung-Dao Lee Institute, Shanghai Jiao Tong University, Shanghai; China

JHEP10(2025)093

[145] Department of Physics and Astronomy, University of Sheffield, Sheffield; United Kingdom
[146] Department of Physics, Shinshu University, Nagano; Japan
[147] Department Physik, Universität Siegen, Siegen; Germany
[148] Department of Physics, Simon Fraser University, Burnaby BC; Canada
[149] SLAC National Accelerator Laboratory, Stanford CA; United States of America
[150] Department of Physics, Royal Institute of Technology, Stockholm; Sweden
[151] Departments of Physics and Astronomy, Stony Brook University, Stony Brook NY; United States of America
[152] Department of Physics and Astronomy, University of Sussex, Brighton; United Kingdom
[153] School of Physics, University of Sydney, Sydney; Australia
[154] Institute of Physics, Academia Sinica, Taipei; Taiwan
[155] [(a)] E. Andronikashvili Institute of Physics, Iv. Javakhishvili Tbilisi State University, Tbilisi;[(b)] High Energy Physics Institute, Tbilisi State University, Tbilisi;[(c)] University of Georgia, Tbilisi; Georgia
[156] Department of Physics, Technion, Israel Institute of Technology, Haifa; Israel
[157] Raymond and Beverly Sackler School of Physics and Astronomy, Tel Aviv University, Tel Aviv; Israel
[158] Department of Physics, Aristotle University of Thessaloniki, Thessaloniki; Greece
[159] International Center for Elementary Particle Physics and Department of Physics, University of Tokyo, Tokyo; Japan
[160] Graduate School of Science and Technology, Tokyo Metropolitan University, Tokyo; Japan
[161] Department of Physics, University of Toronto, Toronto ON; Canada
[162] [(a)] TRIUMF, Vancouver BC;[(b)] Department of Physics and Astronomy, York University, Toronto ON; Canada
[163] Division of Physics and Tomonaga Center for the History of the Universe, Faculty of Pure and Applied Sciences, University of Tsukuba, Tsukuba; Japan
[164] Department of Physics and Astronomy, Tufts University, Medford MA; United States of America
[165] Department of Physics and Astronomy, University of California Irvine, Irvine CA; United States of America
[166] University of West Attica, Athens; Greece
[167] Department of Physics and Astronomy, University of Uppsala, Uppsala; Sweden
[168] Department of Physics, University of Illinois, Urbana IL; United States of America
[169] Instituto de Física Corpuscular (IFIC), Centro Mixto Universidad de Valencia — CSIC, Valencia; Spain
[170] Department of Physics, University of British Columbia, Vancouver BC; Canada
[171] Department of Physics and Astronomy, University of Victoria, Victoria BC; Canada
[172] Fakultät für Physik und Astronomie, Julius-Maximilians-Universität Würzburg, Würzburg; Germany
[173] Department of Physics, University of Warwick, Coventry; United Kingdom
[174] Waseda University, Tokyo; Japan
[175] Department of Particle Physics and Astrophysics, Weizmann Institute of Science, Rehovot; Israel
[176] Department of Physics, University of Wisconsin, Madison WI; United States of America
[177] Fakultät für Mathematik und Naturwissenschaften, Fachgruppe Physik, Bergische Universität Wuppertal, Wuppertal; Germany
[178] Department of Physics, Yale University, New Haven CT; United States of America
[179] Yerevan Physics Institute, Yerevan; Armenia

[a] Also at Affiliated with an institute formerly covered by a cooperation agreement with CERN
[b] Also at An-Najah National University, Nablus; Palestine
[c] Also at Borough of Manhattan Community College, City University of New York, New York NY; United States of America
[d] Also at Center for Interdisciplinary Research and Innovation (CIRI-AUTH), Thessaloniki; Greece
[e] Also at Centre of Physics of the Universities of Minho and Porto (CF-UM-UP); Portugal
[f] Also at CERN, Geneva; Switzerland
[g] Also at Département de Physique Nucléaire et Corpusculaire, Université de Genève, Genève; Switzerland
[h] Also at Departament de Fisica de la Universitat Autonoma de Barcelona, Barcelona; Spain
[i] Also at Department of Financial and Management Engineering, University of the Aegean, Chios; Greece
[j] Also at Department of Mathematical Sciences, University of South Africa, Johannesburg; South Africa

JHEP10(2025)093

[k] Also at Department of Modern Physics and State Key Laboratory of Particle Detection and Electronics, University of Science and Technology of China, Hefei; China
[l] Also at Department of Physics, Bolu Abant Izzet Baysal University, Bolu; Türkiye
[m] Also at Department of Physics, King's College London, London; United Kingdom
[n] Also at Department of Physics, Stanford University, Stanford CA; United States of America
[o] Also at Department of Physics, Stellenbosch University; South Africa
[p] Also at Department of Physics, University of Fribourg, Fribourg; Switzerland
[q] Also at Department of Physics, University of Thessaly; Greece
[r] Also at Department of Physics, Westmont College, Santa Barbara; United States of America
[s] Also at Faculty of Physics, Sofia University, 'St. Kliment Ohridski', Sofia; Bulgaria
[t] Also at Faculty of Physics, University of Bucharest; Romania
[u] Also at Hellenic Open University, Patras; Greece
[v] Also at Henan University; China
[w] Also at Imam Mohammad Ibn Saud Islamic University; Saudi Arabia
[x] Also at Institucio Catalana de Recerca i Estudis Avancats, ICREA, Barcelona; Spain
[y] Also at Institut für Experimentalphysik, Universität Hamburg, Hamburg; Germany
[z] Also at Institute for Nuclear Research and Nuclear Energy (INRNE) of the Bulgarian Academy of Sciences, Sofia; Bulgaria
[aa] Also at Institute of Applied Physics, Mohammed VI Polytechnic University, Ben Guerir; Morocco
[ab] Also at Institute of Particle Physics (IPP); Canada
[ac] Also at Institute of Physics and Technology, Mongolian Academy of Sciences, Ulaanbaatar; Mongolia
[ad] Also at Institute of Physics, Azerbaijan Academy of Sciences, Baku; Azerbaijan
[ae] Also at Institute of Theoretical Physics, Ilia State University, Tbilisi; Georgia
[af] Also at Millennium Institute for Subatomic physics at high energy frontier (SAPHIR), Santiago; Chile
[ag] Also at National Institute of Physics, University of the Philippines Diliman (Philippines); Philippines
[ah] Also at The Collaborative Innovation Center of Quantum Matter (CICQM), Beijing; China
[ai] Also at TRIUMF, Vancouver BC; Canada
[aj] Also at Università di Napoli Parthenope, Napoli; Italy
[ak] Also at University of Chinese Academy of Sciences (UCAS), Beijing; China
[al] Also at University of Colorado Boulder, Department of Physics, Colorado; United States of America
[am] Also at University of Sienna; Italy
[an] Also at Washington College, Chestertown, MD; United States of America
[ao] Also at Yeditepe University, Physics Department, Istanbul; Türkiye
[*] Deceased

JHEP10(2025)093

Phys. Lett. B 860 (2025) 139177

Contents lists available at ScienceDirect

Physics Letters B

journal homepage: www.elsevier.com/locate/physletb

Letter

Measurement of top-quark pair production in association with charm quarks in proton–proton collisions at $\sqrt{s} = 13$ TeV with the ATLAS detector

The ATLAS Collaboration *

ARTICLE INFO

Editor: M. Doser

ABSTRACT

Inclusive cross-sections for top-quark pair production in association with charm quarks are measured with proton–proton collision data at a center-of-mass energy of 13 TeV corresponding to an integrated luminosity of 140 fb^{-1}, collected with the ATLAS experiment at the LHC between 2015 and 2018. The measurements are performed by requiring one or two charged leptons (electrons and muons), two b-tagged jets, and at least one additional jet in the final state. A custom flavor-tagging algorithm is employed for the simultaneous identification of b-jets and c-jets. In a fiducial phase space that replicates the acceptance of the ATLAS detector, the cross-sections for $t\bar{t} + \geq 2c$ and $t\bar{t} + 1c$ production are measured to be $1.28^{+0.27}_{-0.24}$ pb and $6.4^{+1.0}_{-0.9}$ pb, respectively. The measurements are primarily limited by uncertainties in the modeling of inclusive $t\bar{t}$ and $t\bar{t} + b\bar{b}$ production, in the calibration of the flavor-tagging algorithm, and by data statistics. Cross-section predictions from various $t\bar{t}$ simulations are largely consistent with the measured cross-section values, though all underpredict the observed values by 0.5 to 2.0 standard deviations. In a phase-space volume without requirements on the $t\bar{t}$ decay products and the jet multiplicity, the cross-section ratios of $t\bar{t} + \geq 2c$ and $t\bar{t} + 1c$ to total $t\bar{t}$ + jets production are determined to be $(1.23 \pm 0.25)\%$ and $(8.8 \pm 1.3)\%$.

1. Introduction

Due to its pivotal role in the Standard Model (SM) of particle physics and its potential interactions with new physics in various beyond-SM frameworks, the study of the top quark (t) remains a cornerstone of contemporary particle physics research. In particular, the ATLAS [1] and CMS [2] experiments at the Large Hadron Collider (LHC) have directed their attention towards exploring rare final states involving top-quark pairs ($t\bar{t}$), such as associated production of $t\bar{t}$ with Higgs bosons ($t\bar{t}H$) or gauge bosons ($t\bar{t}W$, $t\bar{t}Z$, $t\bar{t}\gamma$), and four-top-quark production ($t\bar{t}t\bar{t}$). Measurements of $t\bar{t}H$ with $H \to b\bar{b}$ decay and $t\bar{t}t\bar{t}$ topologies with single-lepton or dilepton final states [3–7] encounter significant challenges due to substantial, irreducible background contributions stemming from $t\bar{t}$ production in association with heavy-flavor quarks, namely bottom (b) and charm (c) quarks. These heavy-flavor quarks can be produced via radiation of a gluon which then splits into a $b\bar{b}$ or $c\bar{c}$ pair. Depending on the kinematics, the $b\bar{b}$ or $c\bar{c}$ pair can form a jet each ($t\bar{t} + b\bar{b}/c\bar{c}$) or merge into a single jet ($t\bar{t} + 1B/1C$). Single b-quark or c-quark production ($t\bar{t} + 1b/c$) can also occur via a b-quark or c-quark originating from the initial state. Illustrative Feynman diagrams for these three production modes are shown in Fig. 1.

Measurements of $t\bar{t} + b\bar{b}$ and $t\bar{t} + c\bar{c}$ production have been limited by the challenging modeling of these processes. While computations of the $t\bar{t} + b\bar{b}$ production cross-section are available at next-to-leading order (NLO) in quantum chromodynamics (QCD) [8–13], the uncertainties in the choice of the renormalization and factorization scales, denoted by μ_R and μ_F, remain sizable, primarily due to the distinct energy scales associated with the $t\bar{t}$ pair and the $b\bar{b}$ pair. Experimental measurements of $t\bar{t} + b\bar{b}$ production were conducted in proton–proton (pp) collision data at the LHC by the ATLAS and CMS experiments at a center-of-mass energy of $\sqrt{s} = 13$ TeV [14–17]. These measurements, along with those of $t\bar{t}H$ ($H \to b\bar{b}$) and $t\bar{t}t\bar{t}$ production, frequently involve determining the $t\bar{t} + \geq 1c$ normalization *in situ* through a free parameter in the fit, compensating for the limited knowledge of this process. Recent ATLAS measurements of $t\bar{t} + b\bar{b}$ and $t\bar{t}H$ ($H \to b\bar{b}$) [5,17] reported the $t\bar{t} + \geq 1c$ normalization factor to be larger than the value predicted by Monte Carlo (MC) simulations. CMS performed a dedicated $t\bar{t} + c\bar{c}$ measurement in $t\bar{t}$ final states with two charged leptons based on Run 2 data corresponding to 41.5 fb^{-1} [18], but did not explicitly measure the $t\bar{t} + 1c/C$ cross-section. The rates of $t\bar{t} + b\bar{b}$, $t\bar{t} + c\bar{c}$, and $t\bar{t}$ + light jets were found to agree with predictions from MC simulations performed at NLO in the matrix element interfaced with a parton shower (PS) algorithm (NLO+PS) within one to two standard deviations of measurement uncertainties.

Using the complete LHC Run 2 data sample of pp collisions corresponding to an integrated luminosity of 140 fb^{-1}, this Letter presents

* *E-mail address:* atlas.publications@cern.ch.

https://doi.org/10.1016/j.physletb.2024.139177
Received 18 September 2024; Received in revised form 13 November 2024; Accepted 2 December 2024

Available online 4 December 2024

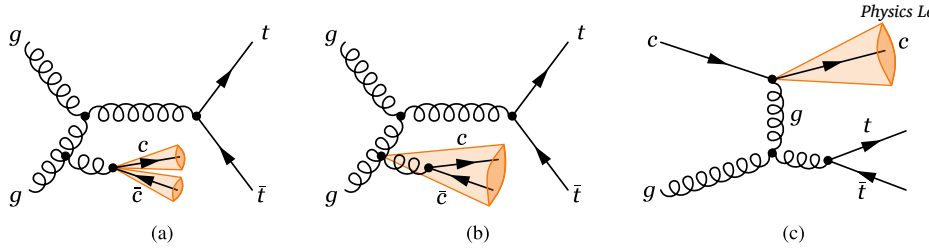

Fig. 1. Illustrative Feynman diagrams for $t\bar{t}+\geq 2c$ and $t\bar{t}+1c$ production: (a) $t\bar{t}+c\bar{c}$ production via initial-state gluon radiation where both c-quarks form a jet each, (b) $t\bar{t}+c\bar{c}$ production via initial-state gluon radiation where the two c-quarks are in the same jet, (c) $t\bar{t}+1c$ production where the c-quark originates from the initial state.

the first ATLAS measurement of $t\bar{t}+\geq 1c$ production. The production rates of $t\bar{t}+\geq 2c$ and $t\bar{t}+1c$ are determined separately to facilitate more detailed comparisons with theoretical predictions, as these processes are expected to be sensitive to different production mechanisms (cf. Fig. 1). The first comprises all final states with two or more c-jets, e.g., $t\bar{t}+c\bar{c}$ production where both c-quarks form separate jets, while the second includes both $t\bar{t}+1c$ production via a c-quark from the initial state and $t\bar{t}+1C$ production. Events with one or two charged leptons in the final state are considered, targeting $t\bar{t}$ topologies where one or both W bosons from the top quarks decay leptonically. While topologies with one charged lepton (single-lepton) offer larger statistics, they introduce additional complexity due to the potential production of extra c-quarks from the hadronically decaying W boson. Conversely, final states with two charged leptons (dilepton) are rarer but expect less background contamination.

The probabilities for $t\bar{t}$ pairs with additional jets initiated by b-quarks, c-quarks, light quarks, and gluons to enter each analysis region are estimated through NLO+PS simulations of inclusive $t\bar{t}$ and of $t\bar{t}+b\bar{b}$ production. This measurement uses a custom flavor tagging algorithm, termed the b/c-tagger, tailored to simultaneous c-jet and b-jet identification, to define analysis regions sensitive to $t\bar{t}+\geq 2c$ and $t\bar{t}+1c$ production. The rates of these processes are then measured in a fiducial phase space designed to replicate the acceptance of the ATLAS detector and in a more inclusive volume. Furthermore, the ratios of $t\bar{t}+\geq 2c$, $t\bar{t}+1c$, and $t\bar{t}+\geq 1b$ to overall $t\bar{t}+$ jets production are extracted and compared with NLO+PS simulations.

2. ATLAS detector

The ATLAS experiment [1] at the LHC is a multipurpose particle detector with a forward–backward symmetric cylindrical geometry and a near 4π coverage in solid angle.[1] It consists of an inner tracking detector (ID) surrounded by a thin superconducting solenoid providing a 2 T axial magnetic field, electromagnetic and hadronic calorimeters, and a muon spectrometer. The ID covers the pseudorapidity range $|\eta| < 2.5$. It consists of silicon pixel, silicon microstrip, and transition radiation tracking detectors. Lead/liquid-argon (LAr) sampling calorimeters provide electromagnetic (EM) energy measurements with high granularity within the region $|\eta| < 3.2$. A steel/scintillator-tile hadronic calorimeter covers the central pseudorapidity range ($|\eta| < 1.7$). The endcap and forward regions are instrumented with LAr calorimeters for EM and hadronic energy measurements up to $|\eta| = 4.9$. The muon spectrometer surrounds the calorimeters and is based on three large superconducting air-core toroidal magnets with eight coils each. The field integral of the toroids ranges between 2.0 and 6.0 T m across most of the detector. The muon spectrometer includes a system of precision tracking chambers up to $|\eta| = 2.7$ and fast detectors for triggering up to $|\eta| = 2.4$. The luminosity is measured mainly by the LUCID–2 [19] detector which is located close to the beampipe. A two-level trigger system is used to select events [20]. The first-level trigger is implemented in hardware and uses a subset of the detector information to accept events at a rate below 100 kHz. This is followed by a software-based trigger that reduces the accepted event rate to 1 kHz on average depending on the data-taking conditions. A software suite [21] is used in data simulation, in the reconstruction and analysis of real and simulated data, in detector operations, and in the trigger and data acquisition systems of the experiment.

3. Simulation of signal and background processes

Samples of simulated events are used to model $t\bar{t}$ + jets production and most background processes. These MC simulated samples were generated employing either the full ATLAS detector simulation [22] based on GEANT4 [23], or a faster simulation where the GEANT4 simulation of the calorimeter response is replaced by a detailed parameterization of the shower shapes [22]. Both simulation methods were found to provide similar modeling for the observables used in this Letter. To account for the effects of multiple interactions in the same and neighboring bunch crossings (pileup), additional interactions were simulated using PYTHIA 8.186 [24] with a set of tuned parameters (*tune*) referred to as A3 [25] and superimposed onto the simulated hard-scatter event. Subsequently, simulated events were reweighted to replicate the pileup conditions observed in the full Run 2 data sample, with a mean number of pp interactions per bunch crossing of 34. All simulated events were processed through the same reconstruction algorithms and analysis chain as the data.

Unless specified otherwise, PYTHIA8 [26] was employed to simulate PS, hadronization, and multi-parton interactions (MPIs). For all samples using PYTHIA8 or HERWIG7 [27–29] for the simulation of the PS, hadronization and MPIs, the decays of b- and c-hadrons were simulated using the EVTGEN program [30]. PYTHIA8 setups use the A14 tune [31] and the NNPDF2.3LO parton distribution function (PDF) set [32]; HERWIG7 setups use the H7UE tune [28] or the default HERWIG tune alongside the MMHT2014LO PDF set [33]. The top-quark mass was set to $m_t = 172.5$ GeV and, unless stated otherwise, the five-flavor scheme (5FS) with massless b-quarks in the matrix element was used for all simulation setups and the corresponding PDF sets.

Inclusive $t\bar{t}$ events were generated with the POWHEG BOX2 [34–37] generator at NLO in QCD employing the NNPDF3.0NLO PDF set [38]. The h_{damp} parameter, which regulates the transverse momentum (p_{T}) of the first additional emission beyond the Born configuration, was set to $1.5\,m_t$ [39]. The hardness scale parameter, which determines the region of phase space vetoed during showering when matched to a PS, was fixed at $p_{\text{T}}^{\text{hard}} = 0$ [40,41]. The scales μ_{R} and μ_{F} were set to the transverse mass of the top quark, $m_{\text{T}}(t) = \sqrt{m_t^2 + p_{\text{T},t}^2}$. In the following, this sample is referred to as $t\bar{t}$ POWHEG+PYTHIA8. To assess uncertainties in the modeling, alternative sets of $t\bar{t}$ events were generated with different configurations: with $p_{\text{T}}^{\text{hard}} = 1$; with $h_{\text{damp}} = 3\,m_t$; and with POWHEG

[1] ATLAS uses a right-handed coordinate system with its origin at the nominal interaction point (IP) in the center of the detector and the z-axis along the beam pipe. The x-axis points from the IP to the center of the LHC ring, and the y-axis points upwards. Polar coordinates (r,ϕ) are used in the transverse plane, ϕ being the azimuthal angle around the z-axis. The pseudorapidity is defined in terms of the polar angle θ as $\eta = -\ln\tan(\theta/2)$ and is equal to the rapidity $y = \frac{1}{2}\ln\left(\frac{E+p_z}{E-p_z}\right)$ in the relativistic limit. Angular distance is measured in units of $\Delta R \equiv \sqrt{(\Delta y)^2 + (\Delta\phi)^2}$.

Box interfaced to Herwig7 instead of Pythia8. To compare the result with another prediction, an additional set was generated with the MadGraph5_aMC@NLO 2.6.0 generator [42] at NLO in QCD, which uses the NNPDF3.0nlo PDF set, MadSpin [43,44] to simulate top-quark decays, and Herwig7 for PS and hadronization [45]. All generated sets of events were reweighted to the predicted cross-section of $\sigma(t\bar{t}) = 832 \pm 51$ pb, as calculated with the Top++2.0 program to next-to-next-to-leading order (NNLO) in QCD, including soft-gluon resummation to next-to-next-to-leading-log order (see Ref. [46] and references therein). The uncertainties include independent variations of μ_{R} and μ_{F}, and variations in the PDF and α_S, following the PDF4LHC prescription with the MSTW2008 68% CL NNLO, CT10 NNLO and NNPDF2.3 5FS PDF sets (see Ref. [47] and references therein, and Refs. [32,48,49]).

The Powheg Box Res [11] generator and OpenLoops [50–52] were used to generate $t\bar{t} + b\bar{b}$ events in the four-flavor scheme (4FS) with massive b-quarks, where the generation of the additional $b\bar{b}$ pair is included in the matrix element, employing the NNPDF3.0nlo 4FS PDF set [38]. The μ_{R} scale was set to $\frac{1}{2}\sqrt[4]{\prod_{i=t,\bar{t},b,\bar{b}} m_{\mathrm{T},i}}$ where $m_{\mathrm{T},i}$ denotes the transverse mass for each parton i. The μ_{F} scale and the h_{damp} parameter were set to $0.5 \times \sum_i m_{\mathrm{T},i}$ with $i \in \{t, \bar{t}, b, \bar{b}, j\}$ and $i \in \{t, \bar{t}, b, \bar{b}\}$, respectively, where j denotes extra partons. The $p_{\mathrm{T}}^{\mathrm{hard}}$ parameter was fixed to 0, and the Born-zero-damp parameter (h_{bzd}), regulating the division between the finite and singular part of the real emission in the NLO calculation, was set to 5. In the following, this sample is referred to as $t\bar{t} + b\bar{b}$ Powheg+Pythia8. To assess uncertainties in the modeling, alternative sets of $t\bar{t} + b\bar{b}$ events were generated with different configurations: with $p_{\mathrm{T}}^{\mathrm{hard}} = 1$; using the dipole recoil scheme instead of the nominal global recoil scheme [11,53]; and interfacing Powheg Box Res with Herwig7 instead of Pythia8. To compare the result with another prediction, alternative sets of $t\bar{t} + b\bar{b}$ events were generated with $h_{\mathrm{bzd}} = 2$. An additional alternative set of events was generated with the Sherpa 2.2.10 generator [54] in the 4FS, for which the virtual corrections for matrix elements at NLO accuracy were provided by Comix [55] and OpenLoops. The Sherpa events were matched with the Sherpa PS algorithm [56] based on Catani–Seymour dipole factorization using the MEPS@NLO prescription [57–60] and a set of tuned parameters developed by the Sherpa authors. All generated sets of events were reweighted to the same prediction cross-section value as computed in Powheg Box Res at NLO in QCD.

A dedicated simulation of $t\bar{t} + c\bar{c}$ production in the three-flavor scheme (3FS) is not available. Hence, $t\bar{t} + c\bar{c}$ contributions are estimated solely using $t\bar{t}$ 5FS simulation, where only the gluon radiation process is simulated in the NLO matrix element, but its splitting into a $c\bar{c}$ pair is done in the PS.

Simulated $t\bar{t}$ and $t\bar{t} + b\bar{b}$ events are sorted into four $t\bar{t}$ + jets categories using particle-level information: $t\bar{t} + \geq 2c$, $t\bar{t} + 1c$, $t\bar{t} + \geq 1b$, and $t\bar{t}$ + light. For the categorization, jets are reconstructed from stable particles[2] following PS and hadronization, using the anti-k_t algorithm [61,62] with a radius parameter $R = 0.4$. They are required to have $p_{\mathrm{T}} > 15$ GeV and $|\eta| < 2.5$. The flavor of a particle-level jet is determined by counting b- and c-hadrons with $p_{\mathrm{T}} > 5$ GeV that are *ghost-associated* [63,64] with the jet. Jets with one or more associated b-hadrons are designated as b-jets, while those with one or more associated c-hadrons but no b-hadron are labeled as c-jets. Events are categorized based on the presence of additional particle-level b-jets and c-jets, excluding jets originating from decays of top quarks and W bosons.[3] Events with one or more b-jets are classified as $t\bar{t} + \geq 1b$, those with two or more c-jets but no b-jet are categorized as $t\bar{t} + \geq 2c$, and events with one c-jet but no b-jet are labeled as $t\bar{t} + 1c$. Any remaining events enter the $t\bar{t}$ + light category.

[2] Particle-level objects are considered stable if $\tau > 3 \times 10^{-11}$ s.

[3] The procedure to exclude these jets is as follows: b-quarks and c-quarks originating directly from the decays of top quarks and W bosons are identified in the MC generator record. Then, the b- and c-hadrons closest in ΔR are flagged. Any jet *ghost-associated* with these hadrons is removed from the categorization.

The $t\bar{t}$ + jets categorization at particle level is used to remove the overlap between the inclusive $t\bar{t}$ 5FS simulation and the $t\bar{t} + b\bar{b}$ 4FS simulation. The latter is expected to provide the more accurate modeling of $t\bar{t} + b\bar{b}$ production and is the preferable setup to simulate $t\bar{t} + \geq 1b$ contributions in this analysis. Thus, events are removed from any of the $t\bar{t}$ 5FS setups if they fall into the $t\bar{t} + \geq 1b$ category at particle level. All other events are retained to estimate contributions in the $t\bar{t} + \geq 2c$, $t\bar{t} + 1c$, and $t\bar{t}$ + light categories. Likewise, events from the $t\bar{t} + b\bar{b}$ 4FS simulation are removed if they fall into the $t\bar{t} + \geq 2c$, $t\bar{t} + 1c$, or $t\bar{t}$ + light categories at particle level. The individual cross-sections assigned to the $t\bar{t}$ and $t\bar{t} + b\bar{b}$ samples are retained, and no rescaling is performed after removing the overlapping events.

Various other processes involving top quarks can mimic $t\bar{t}$ + jets topologies. Single-top-quark t-channel, s-channel, and tW production were simulated using Powheg Box2 at NLO in QCD. For t-channel production, events were generated in the 4FS with the NNPDF3.0nlo 4FS PDF set. For s-channel and tW production, events were generated in the 5FS using the NNPDF3.0nlo 5FS PDF set. The tW simulation employed the diagram-removal scheme [65] to treat interference with $t\bar{t}$ production [39]. Additional sets of tW events were generated in different setups: using the diagram-subtraction scheme [39,65]; using Powheg Box2 interfaced with Herwig 7.04; and using MadGraph5_aMC@NLO 2.6.2 interfaced with Pythia8. Powheg Box2+Herwig7 setups were also generated for t-channel and s-channel production. $t\bar{t}H$ production was simulated with Powheg Box2 at NLO in QCD in the 5FS, using the NNPDF3.0nlo PDF set. Additionally, $t\bar{t}W$, $t\bar{t}Z$, tZq, and tWZ events were generated using the MadGraph5_aMC@NLO 2.3.3 generator at NLO in QCD with the NNPDF3.0nlo PDF set. Secondary sets of $t\bar{t}W$ and $t\bar{t}Z$ events were simulated with Sherpa 2.2.0 at leading order (LO) in QCD. In the following, these processes are collectively referred to as *Other Top*.

W + jets and Z + jets events were simulated using the Sherpa 2.2.1 generator employing NLO matrix elements for up to two partons and LO matrix elements for up to four partons, calculated with the Comix and OpenLoops libraries. Diboson events with semileptonic and fully leptonic decays were simulated using Sherpa 2.2.1 and Sherpa 2.2.2, employing NLO matrix elements for up to one additional parton and LO matrix elements for up to three additional partons. W + jets, Z + jets and diboson events were matched with the Sherpa PS algorithm based on Catani–Seymour dipole factorization using the MEPS@NLO prescription and a set of tuned parameters developed by the Sherpa authors. The NNPDF3.0nnlo PDF set [38] was used, and the cross-sections of the samples were reweighted to NNLO predictions [66]. In the following, W + jets, Z + jets and diboson processes are collectively referred to as *Non-Top*.

The cross-section measurements are conducted within a fiducial volume at particle level, closely resembling the detector-level acceptance, ensuring robustness against variations in acceptance predictions from MC simulations. Events in the single-lepton (dilepton) channel must exhibit five (three) or more jets with $p_{\mathrm{T}} > 25$ GeV and $|\eta| < 2.5$, out of which at least two must be ghost-associated with b-hadrons. No specific requirements are imposed regarding the presence of additional b- or c-jets in the fiducial phase space, but the $t\bar{t}$ + jets categorization is performed as described above. In the single-lepton channel, events must feature exactly one charged lepton ($\ell = e, \mu$), while in the dilepton channel, events must contain exactly two oppositely charged leptons. One lepton must have $p_{\mathrm{T}} > 27$ GeV, any additional lepton must carry $p_{\mathrm{T}} > 10$ GeV, and all are required to be within $|\eta| < 2.5$. Any event featuring a same-flavor lepton pair with an invariant mass below 15 GeV or within the range 83 to 99 GeV is rejected. Leptons are removed if their distance to a jet satisfies $\Delta R < 0.4$. The fiducial phase space accepts approximately 17% of the total number of simulated $t\bar{t} + \geq 1c$ events. The measurements are also performed in a more inclusive phase-space volume without requirements on the $t\bar{t}$ decay products and the jet multiplicity.

4. Event reconstruction and selection

Events are required to have at least one primary vertex with two or more tracks with $p_{\mathrm{T}} > 0.5$ GeV. For events with more than one primary vertex, the hard-scattering primary vertex is selected as the one with the highest sum of squared track p_{T} [67]. A suite of single-electron and single-muon triggers is used to select events with at least one charged lepton [68,69].

Jets are reconstructed using the anti-k_t clustering algorithm with a radius parameter of $R = 0.4$ using particle flow jet constituents that combine measurements from both the ID and the calorimeter [70]. Jet candidates undergo calibration using simulations, with corrections derived from in situ techniques applied to data [71]. They are required to have $p_{\mathrm{T}} > 25$ GeV and $|\eta| < 2.5$, with jets within $|\eta| < 2.4$ and $p_{\mathrm{T}} < 60$ GeV further required to pass the tight working point of the jet vertex tagger [72] to reduce contribution from pileup jets.

Electron candidates are reconstructed from clusters of energy in the EM calorimeter associated with reconstructed tracks from the ID. Their reconstruction, identification, and calibration are detailed in Refs. [73,74]. They must satisfy a set of likelihood-based identification criteria with $p_{\mathrm{T}} > 10$ GeV and $|\eta_{\mathrm{cluster}}| < 2.47$. Electrons in the transition region between the end-caps and barrel region ($1.37 < |\eta_{\mathrm{cluster}}| < 1.52$) are vetoed. Tracks matched to electrons are required to be associated with the primary vertex and satisfy $|z_0 \sin\theta| < 0.5$ mm and $|d_0|/\sigma(d_0) < 5$, where z_0 and d_0 are the longitudinal and transverse impact parameters of the electron track, respectively. For the analysis regions, the identification criteria are tightened, and electrons are required to satisfy a set of variable-radius isolation criteria to reduce contributions from misidentified jets, considering energy depositions in the calorimeter and tracks in the ID [73].

Muons are reconstructed by combining a track from the muon spectrometer with an ID track. Details regarding the reconstruction, identification and calibration of muons are summarized in Refs. [75,76]. The ID tracks must be associated with the primary vertex by passing $|z_0 \sin\theta| < 0.5$ mm and $|d_0|/\sigma(d_0) < 3$. They must fulfill $p_{\mathrm{T}} > 10$ GeV, $|\eta| < 2.5$, and satisfy a set of muon quality criteria. For the analysis regions, the quality criteria are tightened, and muons are required to pass a track-based isolation criterion to reduce contributions from misidentified jets [75].

An overlap removal procedure prevents double counting of energy deposits and improves object resolution and identification efficiencies. Electron candidates sharing tracks with a muon candidate are removed. The nearest jet within $\Delta R < 0.2$ of an electron candidate is removed in favor of the electron. Electrons within $\Delta R < 0.4$ of any jets after this selection are removed in favor of the jet. Muons are removed if they are within $\Delta R < 0.4$ of a jet to reduce contributions from heavy-flavor decays. However, if the jet has fewer than three associated tracks, the muon is kept in favor of the jet.

Jets containing b-hadrons are identified as b-tagged jets using the DL1r algorithm [77], which leverages distinctive b-hadron features like track impact parameters and the presence of displaced vertices in the ID. The algorithm also includes discriminating variables from a recurrent neural network that exploit spatial and kinematic correlations between tracks from the same b-hadron. The DL1r algorithm provides three output scores, p_b, p_c, and p_{light}, and in the standard DL1r calibration, jets are tagged as b-jets using a discriminant $\mathcal{D}_b$ that is built using the Neyman–Pearson lemma [78]:

$$\mathcal{D}_b = \log \frac{p_b}{f_c p_c + (1 - f_c) p_{\mathrm{light}}}.$$

The parameter f_c controls which background contributes more to the decision. To improve the efficiency of selecting jets originating from c-quarks without compromising the b-jet identification performance, the DL1r algorithm was reoptimized as a 2D binned discriminant, the b/c-tagger. This reoptimization was necessary because standard DL1r configurations do not provide calibrated c-tagging working points, requiring a tailored approach to achieve the desired balance between b-jet and c-jet identification. The axes of the discriminant, $\mathcal{D}_c$ and $\mathcal{D}_b$, are calculated from the p_b, p_c, and p_{light} scores following the above formula, with all b- and c-subscripts interchanged for the $\mathcal{D}_c$ discriminant. It was found that $f_b = 0.4$ provides good performance for the b/c-tagger as it leads to a balanced contamination of b-jets and light-flavor jets in the analysis regions; the value of $f_c = 0.018$ was chosen to align the admixture with the standard DL1r calibration.

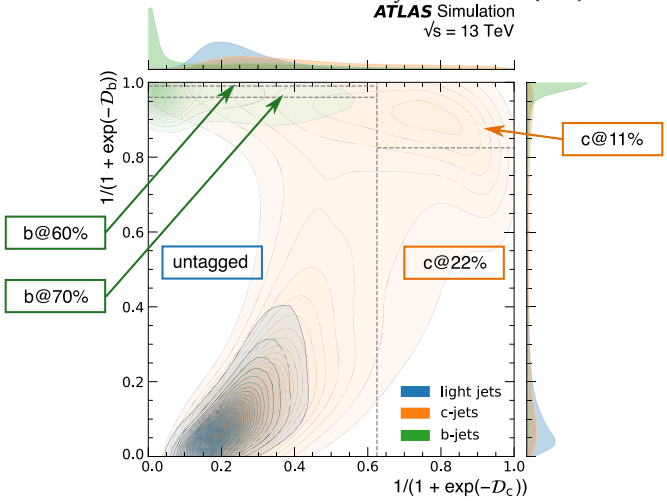

Fig. 2. Distribution of light, c-, and b-jets for the 2D b/c-tagger in simulated $t\bar{t}$ events. Dashed lines correspond to the edges of the working points. For visualization purposes a standard logistic function is applied to both axes of the discriminant. The contours for each jet type are smoothed with a kernel density method to improve readability, with contours corresponding to lines of constant density. The two b-tagging bins comprise the top left corner of the discriminant, with the c-tagging bins to the right of the vertical dashed line. Untagged jets are located in the bottom left corner.

The binning in $\mathcal{D}_c$ and $\mathcal{D}_b$ includes five working points (WPs), two of which are optimized for c-jet identification and two for b-jet identification. The WPs are designed to achieve an approximately constant efficiency for b-jet and c-jet identification across the jet p_{T} and $|\eta|$ range, with $p_{\mathrm{T}} > 20$ GeV. The c-tagging WPs are separated from the others by $\mathcal{D}'_c \geq 0.625$, where the prime indicates that a standard logistic function is applied to the discriminant: $\mathcal{D}'_c = 1/(1 + \exp(-\mathcal{D}_c))$. The tight c-tagging WP includes a tighter cut on $\mathcal{D}'_b$ to increase the light-flavor rejection rate and is designed to achieve an exclusive efficiency of 11% (denoted c@11%).[4] The loose c-tagging WP, which includes c@11%, achieves an inclusive efficiency of 22% (c@22%). The c@11% and c@22% WPs yield b-jet rejection rates of 28.7 and 18.9 and light-flavor rejection rates of 1051 and 104 in simulated $t\bar{t}$ events, respectively. The b-tagging WPs, defined for $\mathcal{D}'_c < 0.625$, use the same $\mathcal{D}'_b$ cuts as the two tightest b-tagging WPs in the standard DL1r calibration. The tighter b-tagging WP is designed to achieve an exclusive efficiency of 60% (b@60%), the looser, which includes b@60%, to achieve an inclusive b-tagging efficiency of 70% (b@70%), with c-jet rejection rates of 37.1 and 12.2 and light-flavor rejection rates of 2320 and 573, respectively. Jets not entering any of the four WP bins are classified as untagged. Consequently, the b/c-tagger comprises a total of five orthogonal bins, with the distribution of light, c- and b-jets illustrated in Fig. 2.

The calibration of the five b/c-tagger WPs follows standard procedures applied to the DL1r algorithm [79–81]. Jets originating from b- and c-quarks are calibrated in data using $t\bar{t}$ events, both selections being orthogonal to the events analyzed in this study by limiting the number

[4] Tightening the cut on $\mathcal{D}'_c$ instead of $\mathcal{D}'_b$ would lead to a more balanced increase in the b-jet and light-flavor rejection rate, but it was found that a focus on higher light-flavor rejection rates yields better $t\bar{t} + \geq 1c$ signal sensitivity.

Table 1
Jet multiplicity and tagging criteria for the signal regions (SRs) and control regions (CRs) in the single-lepton and dilepton channels. All single-lepton regions are defined in the 5-jet-exclusive and 6-jet-inclusive jet selections, all dilepton regions in the 3-jet-exclusive and 4-jet-inclusive jet selections. By construction, $SR^{2\ell}_{tight}$ only exists for the 4-jet-inclusive selection. Identical requirements on inclusive and exclusive working points, e.g., one c@22% and one c@11% in the $CR^{1\ell}_{1}$, indicate a veto of additional tags at the inclusive working point.

	$CR^{1\ell}_{1}$	$CR^{1\ell}_{2}$	$CR^{1\ell}_{3}$	$SR^{1\ell}_{loose}$	$SR^{1\ell}_{tight}$	$CR^{2\ell}_{1}$	$CR^{2\ell}_{2}$	$CR^{2\ell}_{3}$	$SR^{2\ell}_{loose}$	$SR^{2\ell}_{tight}$
N_{jets}	$= 5$ or ≥ 6					$= 3$ or ≥ 4				≥ 4
b@70%	2	–	–	2	2	2	–	≥ 3	2	2
b@60%	–	≥ 3	3	–	–	–	≥ 3	≤ 2	–	–
c@22%	1	0	1	≥ 2	–	0	–	–	1	≥ 2
c@11%	1	–	1	1	≥ 2	–	–	–	–	–

of jets to four (two) in single-lepton (dilepton) final states. All b-tagging calibration scale factors (SFs) are close to unity, with statistical uncertainties dominating the high p_T regime. The c-tagging calibration yields more variation in the SF values. For the b@70% WP, the SFs average around 0.9 and some bins in jet p_T are incompatible with unity within their uncertainties. Light-flavor jet calibration employs the *negative-tag* method [82,83] in conjunction with a *flip-tagger* approach following Ref. [81], and all SFs are compatible with unity within uncertainties. For the b@60% working point, the light-flavor SFs cannot be determined due to the large b-jet contamination and so, following the procedure in Ref. [81], are set to unity with additional uncertainties. The c@11% WP also has large uncertainties due to high contamination of heavy-flavor jets and low statistics. Simulation-to-simulation SFs are derived in bins of jet p_T and $|\eta|$ to account for differences between tagging efficiencies for different PS and hadronization algorithms [84].

A preselection is applied and requires at least one electron or muon with $p_T > 27$ GeV that is matched to the trigger object. The single-lepton channel selects events with exactly one lepton, while the dilepton channel selects those with exactly two oppositely charged leptons. Events must have at least five (three) jets in the single-lepton (dilepton) channel, with at least three (two) b-tagged or c-tagged jets using the b@70% or c@22% working points. For dilepton final states with identical lepton flavors, the same invariant-mass criteria as those applied in the fiducial selection at particle level are imposed. In the single-lepton channel, events are split into those with exactly five jets (5-jet-exclusive) and those with six or more jets (6-jet-inclusive). Similarly, in the dilepton channel, events are categorized as either 3-jet-exclusive or 4-jet-inclusive. Based on the number of identified b- and c-tagged jets, events are further classified into signal regions (SRs) enriched in $t\bar{t}+\geq 2c$ and $t\bar{t}+1c$ events, and control regions (CRs), which determine the normalization of the $t\bar{t}+\geq 1b$ and $t\bar{t}+$ light background. An overview of the seven SRs and 12 CRs is shown in Table 1. Approximately 5.3% of the simulated $t\bar{t}+\geq 1c$ events passing the fiducial selection criteria are reconstructed in the analysis regions.

There are four SRs in the single-lepton channel and three SRs in the dilepton channel with different degrees of purity in $t\bar{t}+\geq 2c$ and $t\bar{t}+1c$ events. The $SR^{1\ell}_{tight}$ and $SR^{2\ell}_{tight}$ regions target $t\bar{t}+\geq 2c$ events, while $SR^{1\ell}_{loose}$ and $SR^{2\ell}_{loose}$ are dominated by $t\bar{t}+1c$. All seven regions require exactly two b-tagged jets at b@70%. In the single-lepton channel, events featuring at least two c-tagged jets at c@22% with exactly one satisfying the c@11% working point enter the $SR^{1\ell}_{loose}$ regions. Events with two or more c-tagged jets at c@11% are classified into $SR^{1\ell}_{tight}$. The expected purity in $t\bar{t}+\geq 2c$ events in the single-lepton SRs ranges between 10% and 28%, while the predicted $t\bar{t}+1c$ contributions are between 29% and 38%. In the dilepton channel, events with exactly one c-tagged jet at c@22% are sorted into $SR^{2\ell}_{loose}$, while events with at least two enter $SR^{2\ell}_{tight}$, which is only defined in the 4-jet-inclusive selection. In the dilepton regions, the expected purity in $t\bar{t}+\geq 2c$ and $t\bar{t}+1c$ events is between 4% and 46%, and between 16% and 38%, respectively.

In the single-lepton channel, three CRs with varying compositions in $t\bar{t}+\geq 1b$ and $t\bar{t}+$ light are defined for each of the two jet multiplicity selections. The $CR^{1\ell}_{1}$ regions select exactly two b-tagged jets at b@70% and exactly one c-tagged jet passing c@22% and c@11%. They are dominated by $t\bar{t}+$ light events. The $CR^{1\ell}_{2}$ regions are characterized by events with three or more b-tagged jets at b@60%, with a veto on c-tagged jets, leading to a mix of $t\bar{t}+\geq 1b$ and $t\bar{t}+$ light. The $CR^{1\ell}_{3}$ regions are pure in $t\bar{t}+\geq 1b$ and select events with exactly three b-tagged jets at b@60% and exactly one c-tagged jet satisfying c@22% and c@11%.

Similarly, the dilepton channel features three CRs for each of the two jet multiplicity selections. The $CR^{2\ell}_{1}$ regions require exactly two b-tagged jets at b@70% and veto c-tagged jets. They are dominated by $t\bar{t}+$ light events. The $CR^{2\ell}_{2}$ regions are pure in $t\bar{t}+\geq 1b$ and select events with three or more b-tagged jets at b@60%. The $CR^{2\ell}_{3}$ regions show a mix of $t\bar{t}+\geq 1b$ and $t\bar{t}+$ light by requiring at least three b-tagged jets at b@70%, with no more than two satisfying the b@60% criteria.

Contributions from processes with non-prompt or misidentified leptons to the single-lepton selection, in the following termed *fake leptons*, were estimated by using the data-driven *matrix method* [85] in dedicated CRs. Prompt-lepton efficiencies were derived in data using a tag-and-probe method in Z-boson decays. Fake-lepton efficiencies were estimated in data in bins of lepton p_T and $|\eta|$ using events with at least three jets, at least two b-tagged jets at the 70% working point of the DL1r tagger, and one lepton fulfilling the looser identification and quality criteria. The isolation requirements were completely dropped. To enrich the selection in fake leptons, only events where the scalar sum of the magnitude of the missing-transverse-momentum vector and the leptonically decaying W-boson mass is no larger than 60 GeV were considered.[5] The fake-lepton contributions to the analysis were then estimated by inverting the efficiency matrix and applying it to the observed event yields in the analysis regions using the looser and the nominal lepton identification and isolation criteria. Fake-lepton contributions to the dilepton selection mainly arise from W + jets and single-lepton $t\bar{t}$ + jets events and were estimated from MC simulation.

5. Systematic uncertainties

The extraction of the $t\bar{t}+\geq 2c$ and $t\bar{t}+1c$ cross-sections is subject to various sources of uncertainties, impacting either the overall event yields in a region, the shape of observable distributions considered in the fit, or both.

Experimental sources of uncertainties include uncertainties in the value of the integrated luminosity of the Run 2 data, the simulation

[5] The magnitude of the missing-transverse-momentum vector, denoted E_T^{miss}, is defined as the negative sum of the transverse momenta of the reconstructed and calibrated physical objects, plus a *soft term* built from all other tracks associated with the primary vertex [86] and not matched to a reconstructed object. The mass of the leptonically decaying W boson is calculated from the kinematics of the lepton and the missing transverse momentum.

of pileup events, and effects related to the reconstruction and identification of physics objects used in the analysis. The uncertainty in the combined 2015–2018 integrated luminosity is 0.83% [87], obtained using the LUCID-2 detector [19] for the primary luminosity measurements, complemented by measurements using the inner detector and calorimeters. Uncertainties in the modeling of pileup are evaluated by varying the pileup reweighting in MC simulations within its associated uncertainties. Furthermore, lepton identification and isolation efficiencies, momentum scale and resolution, and lepton trigger efficiencies are varied within their uncertainties to evaluate their impact on the measurement [73–76]. The uncertainty in the jet energy scale (JES) is derived from a combination of simulations, test-beam data, and in situ measurements [71]. This uncertainty incorporates contributions from various sources such as jet-flavor composition, η-intercalibration, punch-through, single-particle response, calorimeter response to different jet flavors, and pileup. It comprises 30 uncorrelated JES uncertainty subcomponents. Additionally, the jet energy resolution in simulation is varied by its corresponding uncertainty, which is divided into thirteen uncorrelated sources. The uncertainty associated with the jet vertex tagger is determined by varying its efficiency correction factors [72]. Moreover, uncertainties in the calibration of the b/c-tagger are separately determined for b-jets, c-jets, and light-flavor jets, following the procedures detailed in Refs. [79–81]. They are derived as a function of jet p_{T} and separately for each WP, yielding a total of 45 components for b-jets and 20 each for c-jets and light-flavor jets. For jets with p_{T} values above the range covered by the calibration, extrapolation uncertainties derived from MC simulation are applied.

Uncertainties in the modeling of $t\bar{t}+\geq 2c$, $t\bar{t}+1c$, and $t\bar{t}+$light are considered through several alternative inclusive $t\bar{t}$ simulation setups. The alternative set of events with $p_{\mathrm{T}}^{\mathrm{hard}}=1$ is used to assess the uncertainty in the NLO matching between the matrix elements and the PS. The $h_{\mathrm{damp}}=3\,m_t$ sample assesses the uncertainty in the choice of that parameter. The POWHEG+HERWIG7 setup evaluates the uncertainty in the choice of the PS and hadronization algorithm. Additionally, the nominal set of events is reweighted to scenarios where μ_{R} and μ_{F} in the matrix element are halved and doubled independently to assess the uncertainty in the choice of these parameters. To estimate uncertainties in the modeling of initial-state radiation (ISR) and final-state radiation (FSR), the factorized parameter α_S^{ISR} is varied using the *var3c* variation of the A14 tune, and the renormalization scale associated with α_S^{FSR} is varied to 0.625 and 2 relative to its nominal setting. The uncertainty in the PDF set is estimated by using 30 PDF variations of the PDF4LHC prescription.

Uncertainties in the modeling of the $t\bar{t}+\geq 1b$ contributions are considered through a similar suite of alternative $t\bar{t}+b\bar{b}$ simulation setups. The alternative set of events with $p_{\mathrm{T}}^{\mathrm{hard}}=1$ is used to assess the uncertainty in the NLO matching between the matrix elements and the PS. The uncertainty in the choice of the recoil scheme is evaluated with the set of events generated with the alternative dipole recoil scheme. The POWHEG+HERWIG7 setup is used to evaluate the uncertainty in the selection of the PS and hadronization algorithm. Event weight variations identical to those applied in $t\bar{t}$ simulations, including μ_{R}, μ_{F}, ISR, FSR, and the PDF set, are considered for $t\bar{t}+b\bar{b}$.

All uncertainties considered in the modeling of $t\bar{t}$ + jets production are treated as uncorrelated between the $t\bar{t}+\geq 1b$, $t\bar{t}+\geq 1c$, and $t\bar{t}+$light processes. Moreover, the NLO matching and PS uncertainties for $t\bar{t}+\geq 1c$ ($t\bar{t}+\geq 1b$) are parameterized independently for the $t\bar{t}+\geq 2c$ and $t\bar{t}+1c$ ($t\bar{t}+\geq 2b$ and $t\bar{t}+1b$) components as the components are sensitive to different effects. Additionally, the $t\bar{t}+$light PS uncertainty is parameterized separately for the 3-jet-exclusive, 4-jet-inclusive, 5-jet-exclusive, and 6-jet-inclusive regions to avoid strong constraints arising from region-to-region migration effects.

For t-channel, s-channel, and tW single-top-quark production, the POWHEG+HERWIG7 setups are used to assess the uncertainty in the choice of the PS and hadronization algorithm. For tW production, the set of events with the diagram-subtraction scheme is used to gauge the uncertainty in the treatment of the interference with $t\bar{t}$, and the NLO matching uncertainty is evaluated using events generated with MADGRAPH5_AMC@NLO+PYTHIA8. An additional 5% normalization uncertainty is assigned to accommodate the uncertainty in the cross-section value [88]. For the t-channel and s-channel predictions, normalization uncertainties of 50% are assigned to cover NLO matching and cross-section uncertainties. The difference between the sets of $t\bar{t}W$ and $t\bar{t}Z$ events generated with MADGRAPH5_AMC@NLO+PYTHIA8 and SHERPA is used as an uncertainty in the prediction for these processes. Additionally, uncertainties of approximately 13% and 11% are assigned to $t\bar{t}W$ and $t\bar{t}Z$, respectively, to accommodate uncertainties in the assigned cross-section values [89]. Conservative normalization uncertainties of 50% are assigned to each of the remaining top-quark processes considered ($t\bar{t}H$, tWZ, tZq) to cover potential mismodeling of the rates of these processes in the probed fiducial phase space. For the W + jets, Z + jets and diboson background, the assigned uncertainties follow those used in previous ATLAS measurements [90]. Normalization uncertainties of 40% and 35% are considered for W + jets and Z + jets processes, based on variations of the μ_{R} and μ_{F} scales and of the matching parameters in the SHERPA generator. Additional 40% uncertainties are assigned to W + jets events with exactly two heavy-flavor jets and at least three heavy-flavor jets based on the same variations. A 50% uncertainty is assigned to the diboson background, which includes uncertainties in the inclusive cross-section and additional jet production [91–93]. None of the modeling uncertainties of the *Other Top* and *Non-Top* categories have any significant impact on the $t\bar{t}+\geq 2c$ and $t\bar{t}+1c$ cross-section measurements.

The fake-lepton estimate in the single-lepton channel is derived from a data sample with finite statistics, leading to bin-by-bin statistical uncertainties for the fake-electron and fake-muon contributions. In addition, conservative 50% normalization uncertainties are assigned to the data-driven single-lepton and MC-based dilepton estimates.

6. Results

The data from all 19 analysis regions are simultaneously fit using a binned profile likelihood approach using the HistFactory [94] and RooFit [95] toolkits. Systematic uncertainties are incorporated as nuisance parameters in the fit and are constrained by a Gaussian penalty term present in the likelihood function. The statistical uncertainty arising from the limited number of simulated events is included in the likelihood in the form of additional nuisance parameters with Poisson constraint terms. To determine the production cross-sections of the $t\bar{t}+\geq 2c$ and $t\bar{t}+1c$ processes, and to control the $t\bar{t}+\geq 1b$ and $t\bar{t}+$light background processes, normalization factors are defined for all four $t\bar{t}$ + jets categories. These factors, μ_i, serve as unconstrained normalization factors in the profile likelihood fit, and they are applied to both fiducial and non-fiducial $t\bar{t}$ + jets events. The inclusive $t\bar{t}$ + jets normalization factor is computed following

$$\mu(t\bar{t}+\text{jets})=\sum_i \mu_i R_i^{\mathrm{MC}} \quad \text{for } i\in\{t\bar{t}+\geq 1b, t\bar{t}+\geq 2c, t\bar{t}+1c, t\bar{t}+\text{light}\}, \tag{1}$$

where R_i^{MC} is the predicted cross-section ratio of process i to overall $t\bar{t}$ + jets production in MC simulation.

Each of the 12 CRs is represented as a single bin in the fit. $\mathrm{SR}_{\mathrm{loose}}^{1\ell 5\mathrm{j}}$ and $\mathrm{SR}_{\mathrm{tight}}^{1\ell 5\mathrm{j}}$ use the invariant mass between the two geometrically closest c-tagged jets to increase sensitivity to differences between the $t\bar{t}+\geq 2c$, $t\bar{t}+1c$, and $t\bar{t}+$light contributions (only considering c-tagged jets passing $c@11\%$ in $\mathrm{SR}_{\mathrm{tight}}^{1\ell 5\mathrm{j}}$). Due to c-jets originating from the decay of the W boson, the contribution from $t\bar{t}+$light is enhanced around the W-boson mass. $\mathrm{SR}_{\mathrm{loose}}^{2\ell 3\mathrm{j}}$ uses the invariant mass between the c-tagged jet and the geometrically closest b-tagged jet. All three regions use four bins with varying width to maximize sensitivity to the $t\bar{t}+\geq 2c$ and $t\bar{t}+1c$ contributions. In the 4-jet-inclusive and 6-jet-inclusive SRs, the jet multiplicity is used to enhance the separation between $t\bar{t}+\geq 1b$, $t\bar{t}+\geq 2c$,

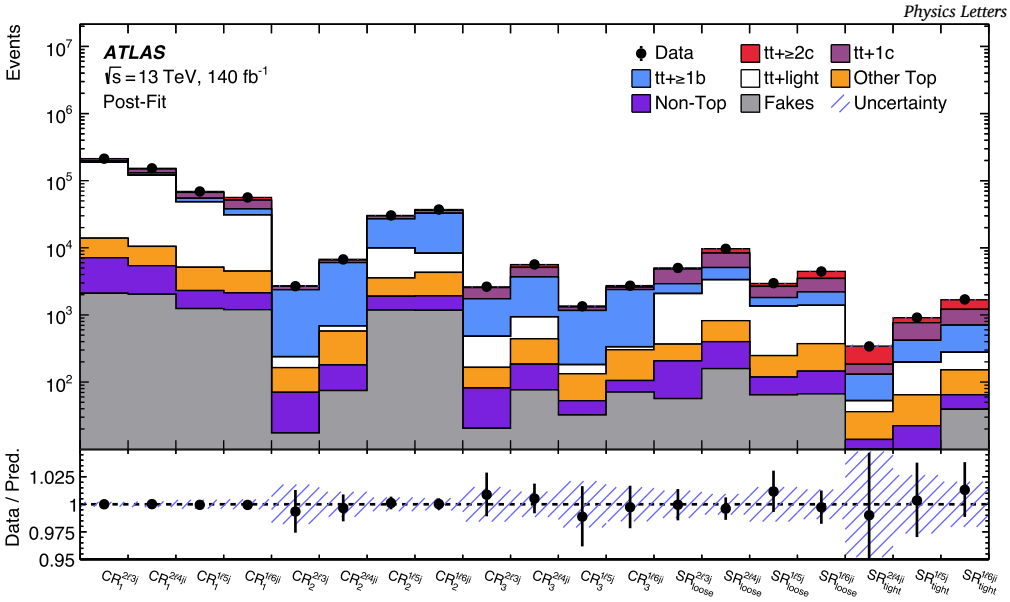

Fig. 3. Post-fit agreement between data and MC simulation in the 12 control regions (CRs) and seven signal regions (SRs). The error bars indicate data statistical uncertainties. The hatched uncertainty bands include all uncertainties and their correlations. *Other Top* includes single-top-quark production and associated production of $t\bar{t}$ and single top quarks with bosons. *Non-Top* includes W + jets, Z + jets, and diboson processes.

$t\bar{t}+1c$, and $t\bar{t}+$ light processes, fitting $6 \leq N_{\text{jets}} \leq 9$ and $4 \leq N_{\text{jets}} \leq 7$ in the single-lepton and dilepton channels, respectively. Overflow events are included in the last bin of each distribution.

Post-fit comparisons between data and simulation for all regions are depicted in Fig. 3. The fitted observable distributions of the SRs are shown in Figs. 4 and 5. Good agreement between data and simulation is observed in all regions and observables with varying relative contributions of the $t\bar{t}$ + jets categories. The goodness of fit was evaluated using a *saturated model* [96] and the compatibility with data was found to be 98%.

The $t\bar{t}+\geq 2c$ and $t\bar{t}+1c$ normalization factors obtained from this fit are used to extract the observed fiducial cross-sections by scaling them with the predicted cross-sections for the fiducial phase space introduced in Section 3. Theoretical uncertainties in the predicted cross-sections owing to the μ_{R} and μ_{F} scale choice and the used PDF set are not propagated to the extracted fiducial cross-section values. The fiducial cross-sections for $t\bar{t}+\geq 2c$ and $t\bar{t}+1c$ processes are determined to be

$$\sigma^{\text{fid}}(t\bar{t}+\geq 2c) = 1.28\,^{+0.16}_{-0.10}\,(\text{stat})\,^{+0.21}_{-0.22}\,(\text{syst})\ \text{pb} = 1.28\,^{+0.27}_{-0.24}\ \text{pb}, \tag{2}$$

$$\sigma^{\text{fid}}(t\bar{t}+1c) = 6.4\,^{+0.5}_{-0.4}\,(\text{stat}) \pm 0.8\,(\text{syst})\ \text{pb} = 6.4\,^{+1.0}_{-0.9}\ \text{pb}. \tag{3}$$

The breakdown into statistical and systematic uncertainties is estimated from the covariance matrix of the profile likelihood fit, following Ref. [97]. The precision of the measured $t\bar{t}+\geq 2c$ and $t\bar{t}+1c$ cross-sections is limited by uncertainties in the modeling of $t\bar{t}+\geq 1c$, $t\bar{t}+\geq 1b$, and $t\bar{t}+$ light, in particular in the NLO matching and the PS, by uncertainties in the b/c-tagger calibration, as well as by data statistics. Table 2 provides a detailed breakdown of the uncertainties that affect the $t\bar{t}+\geq 2c$ and $t\bar{t}+1c$ cross-sections in the fiducial phase space. The uncertainty in the $t\bar{t}+\geq 1b$ and $t\bar{t}+$ light normalization factors on the $t\bar{t}+\geq 2c$ and $t\bar{t}+1c$ cross-sections is included in the data statistics entry. The fit constrains several nuisance parameters that strongly impact the $t\bar{t}+\geq 2c$ and $t\bar{t}+1c$ cross-sections, with none falling below 50% of their prior values. Noteworthy constraints are placed on the $t\bar{t}+\geq 1c$ FSR and $t\bar{t}+1c$ PS nuisance parameters, which arise primarily from discrepancies between the predicted rates of $t\bar{t}+\geq 2c$ and $t\bar{t}+1c$ events in the signal regions. No significant pulls of the nuisance parameters are observed in the fit. The measured $t\bar{t}+\geq 1b$ normalization factor is compatible with those obtained in a dedicated ATLAS $t\bar{t}+b\bar{b}$ measurement performed in a fiducial phase space targeting $e+\mu$ final states [17], reaching a similar level of relative precision.

Table 2
Breakdown of the fiducial $t\bar{t}+\geq 2c$ and $t\bar{t}+1c$ cross-section uncertainties. Systematic uncertainties are grouped into signal and background modeling, instrumental, and MC statistics categories. The table lists the fractional uncertainty in the measured cross-sections in percent and is estimated from the covariance matrix of the profile likelihood fit, following Ref. [97]. Individual groups of uncertainties can be added in quadrature to obtain the total uncertainty. JES and JER denote the jet energy scale and resolution uncertainties, respectively. The fractional uncertainties in the fitted $t\bar{t}+\geq 1b$ and $t\bar{t}+$ light normalization factors are included in the data statistics category. For presentation purposes, all uncertainties are symmetrized.

Uncertainty group	Fractional uncertainty [%] on	
	$\sigma^{\text{fid}}(t\bar{t}+\geq 2c)$	$\sigma^{\text{fid}}(t\bar{t}+1c)$
$t\bar{t}+\geq 1c$ modeling	9	8
Background modeling:		
$t\bar{t}+\geq 1b$	4	4
$t\bar{t}+$ light	6	4
Others	2.5	1.7
Instrumental:		
b-tagging	2.2	1.8
c-tagging	9	4
light mis-tagging	2.2	3.4
JES/JER	6	3.5
Others	1.3	0.9
MC statistics	3.1	2.5
Total systematic uncertainty	17	12
Data statistical uncertainty	11	7
Total	20	14

The measured values for the four processes and the overall $t\bar{t}$ + jets production are depicted in Fig. 6 and listed in Table 3, along with several NLO+PS predictions from different MC simulations. The predictions for $t\bar{t}+\geq 2c$ and $t\bar{t}+1c$ are largely consistent with the measurements, but underpredict the observed cross-sections by 0.5 to 2.0 standard deviations. Considering variations of the μ_{R} and μ_{F} scales and uncertainties in the PDF choice of the predictions, the POWHEG+PYTHIA8 setups agree with the measured $t\bar{t}+\geq 2c$ ($t\bar{t}+1c$) values within 0.5 to 0.8 (0.9 to 1.1) standard deviations of measurement and prediction uncertainties. In contrast, POWHEG+HERWIG7 and MADGRAPH5_AMC@NLO+HERWIG7

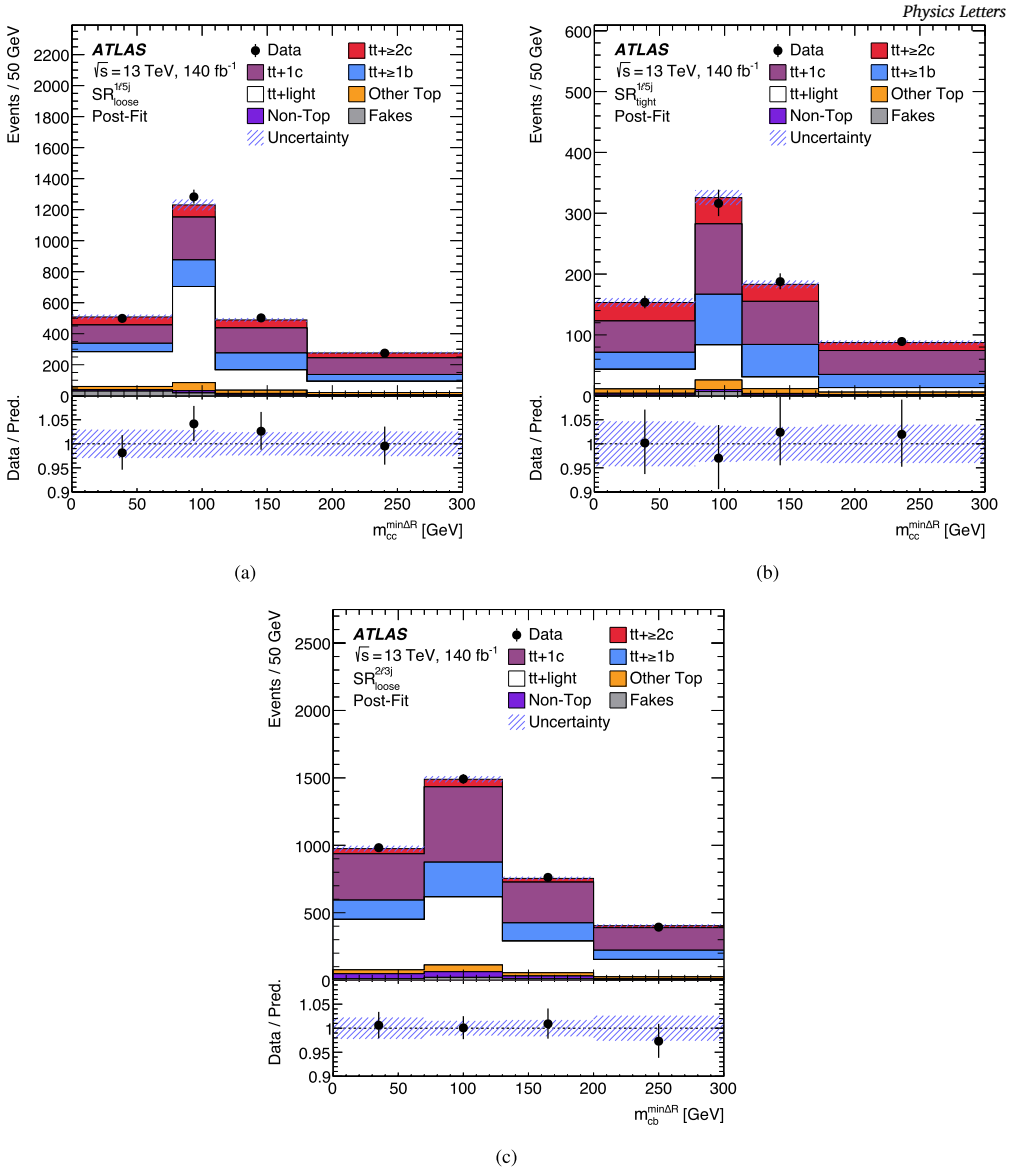

Fig. 4. Post-fit agreement between data and MC prediction for the observables used in the 5-jet-exclusive and 3-jet-exclusive signal regions (SRs): (a) $\mathrm{SR}^{1\ell 5\mathrm{j}}_{\mathrm{loose}}$ and (b) $\mathrm{SR}^{1\ell 5\mathrm{j}}_{\mathrm{tight}}$, both using the invariant mass of the two geometrically closest c-tagged jets, $m_{cc}^{\mathrm{min}\Delta R}$, for the latter only considering c-tagged jets passing $c@11\%$; (c) $\mathrm{SR}^{2\ell 3\mathrm{j}}_{\mathrm{loose}}$ using the invariant mass of the selected c-tagged jet and the geometrically closest b-tagged jet, $m_{cb}^{\mathrm{min}\Delta R}$. The hatched uncertainty bands include all uncertainties and their correlations. The last bins contain overflow events. *Other Top* includes single-top-quark production and associated production of $t\bar{t}$ and single top quarks with bosons. *Non-Top* includes W + jets, Z + jets, and diboson processes.

fall short by 25% to 40%, aligning with the measured values at 1.2 to 2.0 standard deviations. For $t\bar{t}+\geq 1b$, $t\bar{t}+$light, and $t\bar{t}$ + jets, most NLO+PS predictions agree with the measured cross-sections within measurement uncertainties.

To test the compatibility of the two channels, an additional fit was performed where the $t\bar{t}+\geq 2c$ and $t\bar{t}+1c$ normalization factors were parameterized independently in the single-lepton and dilepton regions. The single-lepton channel measures $\sigma^{\mathrm{fid}}(t\bar{t}+\geq 2c) = (1.5 \pm 0.4)$ pb and $\sigma^{\mathrm{fid}}(t\bar{t}+1c) = (6.4 \pm 1.1)$ pb, and the dilepton channel $\sigma^{\mathrm{fid}}(t\bar{t}+\geq 2c) = (1.18 \pm 0.25)$ pb and $\sigma^{\mathrm{fid}}(t\bar{t}+1c) = (6.4 \pm 1.0)$ pb. The results in both channels are consistent with the nominal results within their uncertainties. The compatibility of this fit with the nominal setup was evaluated by performing a χ^2 test on the log-likelihood difference, yielding a compatibility of 58%. In a second test, the $t\bar{t}+\geq 2c$ and $t\bar{t}+1c$ normalization factors were parameterized through one joint parameter of interest, and the NLO matching and PS uncertainties of the two processes were treated as correlated. The resulting cross-section of $\sigma^{\mathrm{fid}}(t\bar{t}+\geq 1c) = (8.2 \pm 0.9)$ pb is consistent with the sum of the $t\bar{t}+\geq 2c$ and $t\bar{t}+1c$ cross-sections in the nominal setup within uncertainties, but shows increased relative precision.

A measurement of the cross-sections in the more inclusive phase space yields $\sigma^{\mathrm{inc}}(t\bar{t}+\geq 2c) = (5.4 \pm 1.1)$ pb and $\sigma^{\mathrm{inc}}(t\bar{t}+1c) = (38 \pm 6)$ pb, showing moderately increased relative uncertainties compared with the fiducial cross-sections.

The normalization factors $\mu(t\bar{t}+\geq 1b)$, $\mu(t\bar{t}+\geq 2c)$, $\mu(t\bar{t}+1c)$, and $\mu(t\bar{t}+\text{light})$ are used to determine the cross-section ratios of these processes to total $t\bar{t}$ + jets production. These measurements benefit from the cancelation of several systematic uncertainties related to detector instrumentation and calibrations, potentially reducing the overall systematic uncertainties. In the more inclusive phase space, the measurement yields ratios of $R^{\mathrm{inc}}_{t\bar{t}+\geq 2c} = (1.23 \pm 0.25)\%$ and $R^{\mathrm{inc}}_{t\bar{t}+1c} = (8.8 \pm 1.3)\%$. In the fiducial phase space, these ratios increase to $R^{\mathrm{fid}}_{t\bar{t}+\geq 2c} = (2.7 \pm 0.5)\%$ and $R^{\mathrm{fid}}_{t\bar{t}+1c} = (13.7 \pm 1.8)\%$. In both phase spaces, the POWHEG+PYTHIA8 simulations underpredict the ratios, but agree with the measured $R^{\mathrm{inc}}_{t\bar{t}+\geq 2c}$ and $R^{\mathrm{inc}}_{t\bar{t}+1c}$ values within 0.9 and 1.1 standard deviations, and in the fidu-

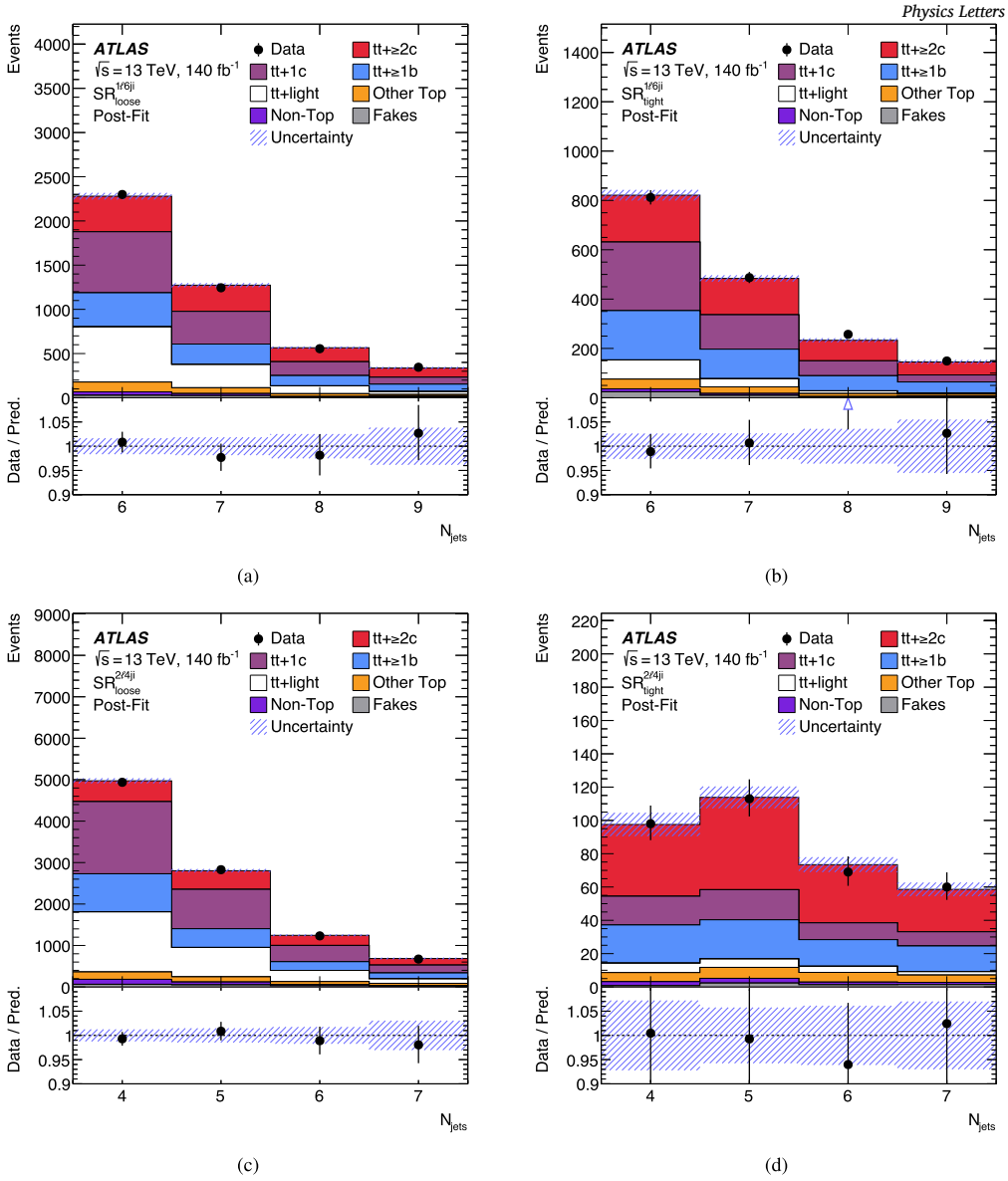

Fig. 5. Post-fit agreement between data and MC prediction for the observables used in the (a) loose 6-jet-inclusive, (b) tight 6-jet-inclusive, (c) loose 4-jet-inclusive, and (d) tight 4-jet-inclusive signal regions (SRs). All regions use the jet multiplicity, N_{jets}, as a fit observable. The hatched uncertainty bands include all uncertainties and their correlations. The last bins contain overflow events. *Other Top* includes single-top-quark production and associated production of $t\bar{t}$ and single top quarks with bosons. *Non-Top* includes W + jets, Z + jets, and diboson processes.

Table 3
Measured fiducial cross-section values in comparison with various NLO+PS predictions. The uncertainties in the predictions include independent and simultaneous variations of the μ_{R} and μ_{F} scales and uncertainties in the choice of the PDF set, but no uncertainties in the parton shower or hadronization. The uncertainties in the measured values include all statistical and systematic uncertainties. For presentation purposes, the quoted measurement and prediction uncertainties are symmetrized.

	$t\bar{t}+\geq 2c$ [pb]	$t\bar{t}+1c$ [pb]	$t\bar{t}+\geq 1b$ [pb]	$t\bar{t}+$ light [pb]	$t\bar{t}+$ jets [pb]
$t\bar{t}$ POWHEG+PYTHIA 8	1.04 ± 0.18	5.1 ± 0.8	3.2 ± 0.5	40 ± 6	50 ± 7
$t\bar{t}$ POWHEG+PYTHIA 8, $h_{\text{damp}} = 3\,m_t$	1.12 ± 0.16	5.4 ± 0.7	3.3 ± 0.5	41 ± 5	51 ± 7
$t\bar{t}$ POWHEG+PYTHIA 8, $p_{\text{T}}^{\text{hard}} = 1$	1.05 ± 0.18	5.2 ± 0.8	3.1 ± 0.5	40 ± 6	50 ± 7
$t\bar{t}$ POWHEG+HERWIG 7	0.94 ± 0.16	4.2 ± 0.7	3.3 ± 0.5	43 ± 6	52 ± 8
$t\bar{t}$ MADGRAPH5_AMC@NLO+HERWIG 7	0.74 ± 0.19	4.0 ± 0.8	2.7 ± 0.6	46 ± 8	53 ± 10
$t\bar{t}+b\bar{b}$ POWHEG+PYTHIA 8	—	—	3.2 ± 1.6	—	—
$t\bar{t}+b\bar{b}$ POWHEG+PYTHIA 8, $p_{\text{T}}^{\text{hard}} = 1$	—	—	2.8 ± 1.3	—	—
$t\bar{t}+b\bar{b}$ POWHEG+PYTHIA 8, $h_{\text{bzd}} = 2$	—	—	3.1 ± 1.5	—	—
$t\bar{t}+b\bar{b}$ POWHEG+PYTHIA 8, dipole recoil	—	—	3.0 ± 1.4	—	—
$t\bar{t}+b\bar{b}$ POWHEG+HERWIG 7	—	—	3.1 ± 1.6	—	—
$t\bar{t}+b\bar{b}$ SHERPA 2.2.10	—	—	3.5 ± 1.0	—	—
Data	1.28 ± 0.25	6.4 ± 0.9	3.46 ± 0.24	36.0 ± 1.8	47.1 ± 2.3

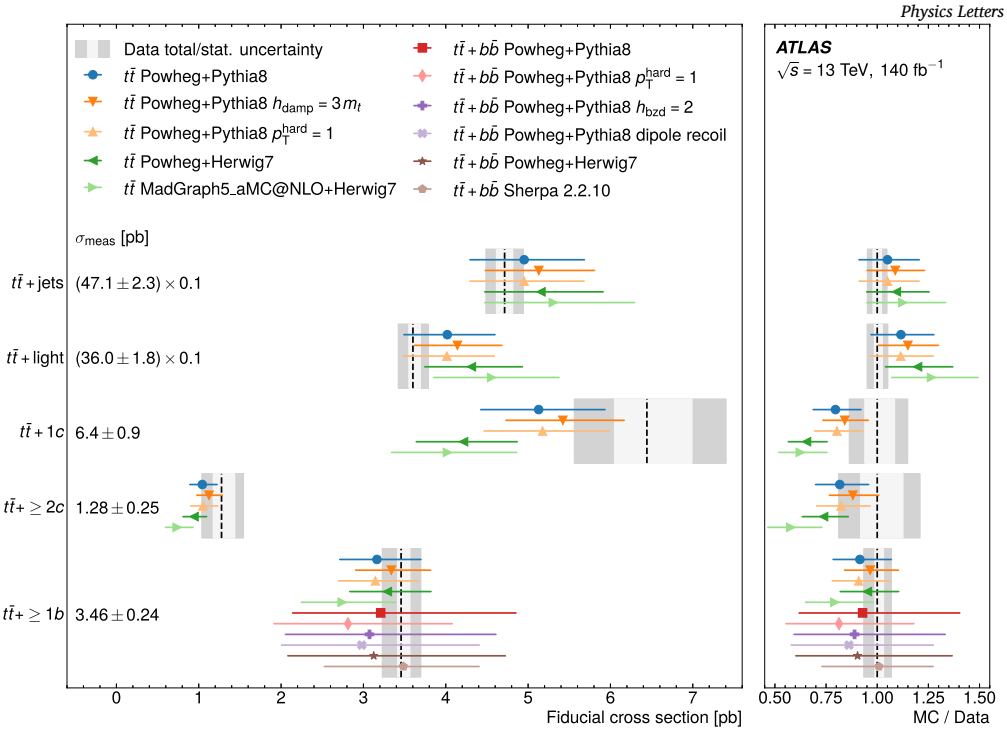

Fig. 6. Measured fiducial cross-section values in comparison with various NLO+PS predictions from inclusive $t\bar{t}$ and $t\bar{t}+b\bar{b}$ simulations. The boxes in the background represent the statistical and total uncertainties of the values extracted from data. The uncertainty bars of the predictions include independent and simultaneous variations of the μ_R and μ_F scales and uncertainties in the choice of the PDF set, but no uncertainties in the parton shower or hadronization. The measured and computed values for $t\bar{t}$ + jets and $t\bar{t}$ + light are scaled by a factor of 0.1 to facilitate visualization. For presentation purposes, the quoted measurement uncertainties are symmetrized.

Table 4
Measured and predicted values for the $t\bar{t}+\geq 1b$, $t\bar{t}+\geq 2c$, and $t\bar{t}+1c$ cross-sections and for the cross-section ratios of these processes to total $t\bar{t}$ + jets production. The quoted uncertainties in the measurements include statistical and systematic uncertainties. The predictions are taken from the nominal setup using inclusive $t\bar{t}$ POWHEG+PYTHIA8 predictions for the $t\bar{t}+\geq 2c$, $t\bar{t}+1c$, and $t\bar{t}$ + light processes, and $t\bar{t}+b\bar{b}$ POWHEG+PYTHIA8 predictions for the $t\bar{t}+\geq 1b$ process. The first use the five-flavor scheme (5FS), the latter the four-flavor scheme (4FS), where the b-quarks are treated as massive particles and are included in the matrix element calculation. The uncertainties in the predictions include independent and simultaneous variations of the μ_R and μ_F scales and uncertainties in the choice of the PDF set.

	Measured	$t\bar{t}$ or $t\bar{t}+b\bar{b}$ POWHEG+PYTHIA8
$\sigma^{fid}(t\bar{t}+\geq 1b)$ [pb]	3.46 ± 0.24	3.2 ± 1.6
$\sigma^{fid}(t\bar{t}+\geq 2c)$ [pb]	1.28 ± 0.25	1.04 ± 0.18
$\sigma^{fid}(t\bar{t}+1c)$ [pb]	6.4 ± 0.9	5.1 ± 0.8
$\sigma^{inc}(t\bar{t}+\geq 1b)$ [pb]	13.0 ± 0.9	12 ± 4
$\sigma^{inc}(t\bar{t}+\geq 2c)$ [pb]	5.4 ± 1.1	4.4 ± 0.7
$\sigma^{inc}(t\bar{t}+1c)$ [pb]	38 ± 6	31 ± 4
$R^{fid}_{t\bar{t}+\geq 1b}$ [%]	7.2 ± 0.4	6.5 ± 3.3
$R^{fid}_{t\bar{t}+\geq 2c}$ [%]	2.7 ± 0.5	2.1 ± 0.4
$R^{fid}_{t\bar{t}+1c}$ [%]	13.7 ± 1.8	10.3 ± 1.6
$R^{inc}_{t\bar{t}+\geq 1b}$ [%]	3.14 ± 0.23	2.6 ± 0.8
$R^{inc}_{t\bar{t}+\geq 2c}$ [%]	1.23 ± 0.25	0.97 ± 0.16
$R^{inc}_{t\bar{t}+1c}$ [%]	8.8 ± 1.3	6.9 ± 1.0

cial phase space within 1.0 and 1.4 standard deviations, respectively. A summary of all results is given in Table 4.

7. Conclusion

The production of $t\bar{t}$ pairs in association with heavy-flavor jets, $t\bar{t}+b\bar{b}$ and $t\bar{t}+c\bar{c}$, is a background in many measurements of rare SM processes and searches for new physics, yet a challenging process to model precisely. This Letter presents a measurement of the production of $t\bar{t}$ with additional jets initiated by charm quarks with the ATLAS experiment at the LHC. The analysis exploits the full ATLAS Run 2 pp collision data sample at a center-of-mass energy of 13 TeV, corresponding to an integrated luminosity of 140 fb^{-1}, and considers events with one or two charged leptons in the final state. A custom flavor tagging algorithm, termed the b/c-tagger, tailored to simultaneously tag c-jets and b-jets, is employed to define analysis regions sensitive to both $t\bar{t}+\geq 2c$ and $t\bar{t}+1c$ production which are determined separately for the first time. Using a profile likelihood fit approach, the cross-sections for $t\bar{t}$ production with two or more additional c-jets and one additional c-jet are found to be $\sigma^{fid}(t\bar{t}+\geq 2c) = 1.28^{+0.27}_{-0.24}$ pb and $\sigma^{fid}(t\bar{t}+1c) = 6.4^{+1.0}_{-0.9}$ pb in a fiducial volume that mimics the acceptance of the ATLAS detector. NLO+PS predictions for $t\bar{t}+\geq 2c$ and $t\bar{t}+1c$ are largely consistent with the measurements, though all underpredict the observed values. POWHEG+PYTHIA8 setups agree with the measured values within 0.5 to 1.1 standard deviations, while POWHEG+HERWIG7 and MADGRAPH5_AMC@NLO+HERWIG7 predict cross-sections up to 40% lower than the measurements, with agreement observed at the level of up to 2.0 standard deviations. The precision of the measured cross-sections is limited by uncertainties in the modeling of $t\bar{t}+\geq 1c$, $t\bar{t}+\geq 1b$, and $t\bar{t}$ + light, and in the b/c-tagger calibration, as well as by data statistics. The cross-section ratios of $t\bar{t}+\geq 2c$ and $t\bar{t}+1c$ to total $t\bar{t}$ + jets production are found to be $R^{inc}_{t\bar{t}+\geq 2c} = (1.23 \pm 0.25)\%$ and $R^{inc}_{t\bar{t}+1c} = (8.8 \pm 1.3)\%$ in a phase-space volume without requirements on the $t\bar{t}$ decay products and the jet multiplicity. These results provide crucial inputs for improving the modeling of $t\bar{t}$ production with additional c-jets, which would benefit from 3FS $t\bar{t}+c\bar{c}$ simulations that incorporate the gluon splitting to a $c\bar{c}$ pair into the matrix element calculation. Understanding $t\bar{t}+\geq 1c$ production is essential for precision measurements of even rarer SM processes and for searches for physics beyond the SM, where $t\bar{t}+\geq 1c$ is an important background.

Declaration of competing interest

The authors declare that they have no known competing financial interests or personal relationships that could have appeared to influence the work reported in this paper.

Acknowledgements

We thank CERN for the very successful operation of the LHC and its injectors, as well as the support staff at CERN and at our institutions worldwide without whom ATLAS could not be operated efficiently.

The crucial computing support from all WLCG partners is acknowledged gratefully, in particular from CERN, the ATLAS Tier-1 facilities at TRIUMF/SFU (Canada), NDGF (Denmark, Norway, Sweden), CC-IN2P3 (France), KIT/GridKA (Germany), INFN-CNAF (Italy), NL-T1 (Netherlands), PIC (Spain), RAL (UK) and BNL (USA), the Tier-2 facilities worldwide and large non-WLCG resource providers. Major contributors of computing resources are listed in Ref. [98].

We gratefully acknowledge the support of ANPCyT, Argentina; YerPhI, Armenia; ARC, Australia; BMWFW and FWF, Austria; ANAS, Azerbaijan; CNPq and FAPESP, Brazil; NSERC, NRC and CFI, Canada; CERN; ANID, Chile; CAS, MOST and NSFC, China; Minciencias, Colombia; MEYS CR, Czech Republic; DNRF and DNSRC, Denmark; IN2P3-CNRS and CEA-DRF/IRFU, France; SRNSFG, Georgia; BMBF, HGF and MPG, Germany; GSRI, Greece; RGC and Hong Kong SAR, China; ISF and Benoziyo Center, Israel; INFN, Italy; MEXT and JSPS, Japan; CNRST, Morocco; NWO, Netherlands; RCN, Norway; MNiSW, Poland; FCT, Portugal; MNE/IFA, Romania; MSTDI, Serbia; MSSR, Slovakia; ARIS and MVZI, Slovenia; DSI/NRF, South Africa; MICIU/AEI, Spain; SRC and Wallenberg Foundation, Sweden; SERI, SNSF and Cantons of Bern and Geneva, Switzerland; NSTC, Taipei; TENMAK, Türkiye; STFC/UKRI, United Kingdom; DOE and NSF, United States of America.

Individual groups and members have received support from BCKDF, Canarie, CRC and DRAC, Canada; CERN-CZ, FORTE and PRIMUS, Czech Republic; COST, ERC, ERDF, Horizon 2020, ICSC-NextGenerationEU and Marie Skłodowska-Curie Actions, European Union; Investissements d'Avenir Labex, Investissements d'Avenir Idex and ANR, France; DFG and AvH Foundation, Germany; Herakleitos, Thales and Aristeia programmes co-financed by EU-ESF and the Greek NSRF, Greece; BSF-NSF and MINERVA, Israel; NCN and NAWA, Poland; La Caixa Banking Foundation, CERCA Programme Generalitat de Catalunya and PROMETEO and GenT Programmes Generalitat Valenciana, Spain; Göran Gustafssons Stiftelse, Sweden; The Royal Society and Leverhulme Trust, United Kingdom.

In addition, individual members wish to acknowledge support from Armenia: Yerevan Physics Institute (FAPERJ); CERN: European Organization for Nuclear Research (CERN PJAS); Chile: Agencia Nacional de Investigación y Desarrollo (FONDECYT 1230812, FONDECYT 1230987, FONDECYT 1240864); China: Chinese Ministry of Science and Technology (MOST-2023YFA1605700), National Natural Science Foundation of China (NSFC - 12175119, NSFC 12275265, NSFC-12075060); Czech Republic: Czech Science Foundation (GACR - 24-11373S), Ministry of Education Youth and Sports (FORTE CZ.02.01.01/00/22_008/0004632), PRIMUS Research Programme (PRIMUS/21/SCI/017); EU: H2020 European Research Council (ERC - 101002463); European Union: European Research Council (ERC - 948254, ERC 101089007), European Union, Future Artificial Intelligence Research (FAIR-NextGenerationEU PE00000013), Italian Center for High Performance Computing, Big Data and Quantum Computing (ICSC, NextGenerationEU); France: Agence Nationale de la Recherche (ANR-20-CE31-0013, ANR-21-CE31-0013, ANR-21-CE31-0022, ANR-22-EDIR-0002); Germany: Baden-Württemberg Stiftung (BW Stiftung-Postdoc Eliteprogramme), Deutsche Forschungsgemeinschaft (DFG - 469666862, DFG - CR 312/5-2); Italy: Istituto Nazionale di Fisica Nucleare (ICSC, NextGenerationEU), Ministero dell'Università e della Ricerca (PRIN - 20223N7F8K - PNRR M4.C2.1.1); Japan: Japan Society for the Promotion of Science (JSPS KAKENHI JP22H01227, JSPS KAKENHI JP22H04944, JSPS KAKENHI JP22KK0227, JSPS KAKENHI JP23KK0245); Netherlands: Netherlands Organisation for Scientific Research (NWO Veni 2020 - VI.Veni.202.179); Norway: Research Council of Norway (RCN-314472); Poland: Ministry of Science and Higher Education (IDUB AGH, POB8, D4 no 9722), Polish National Agency for Academic Exchange (PPN/PPO/2020/1/00002/U/00001), Polish National Science Centre (NCN 2021/42/E/ST2/00350, NCN OPUS 2023/51/B/ST2/02507, NCN OPUS nr 2022/47/B/ST2/03059, NCN UMO-2019/34/E/ST2/00393, NCN & H2020 MSCA 945339, UMO-2020/37/B/ST2/01043, UMO-2021/40/C/ST2/00187, UMO-2022/47/O/ST2/00148, UMO-2023/49/B/ST2/04085, UMO-2023/51/B/ST2/00920); Slovenia: Slovenian Research Agency (ARIS grant J1-3010); Spain: Generalitat Valenciana (Artemisa, FEDER, IDIFEDER/2018/048), Ministry of Science and Innovation (MCIN & NextGenEU PCI2022-135018-2, MICIN & FEDER PID2021-125273NB, RYC2019-028510-I, RYC2020-030254-I, RYC2021-031273-I, RYC2022-038164-I); Sweden: Carl Trygger Foundation (Carl Trygger Foundation CTS 22:2312), Swedish Research Council (Swedish Research Council 2023-04654, VR 2018-00482, VR 2022-03845, VR 2022-04683, VR 2023-03403, VR grant 2021-03651), Knut and Alice Wallenberg Foundation (KAW 2018.0458, KAW 2019.0447, KAW 2022.0358); Switzerland: Swiss National Science Foundation (SNSF - PCEFP2_194658); United Kingdom: Leverhulme Trust (Leverhulme Trust RPG-2020-004), Royal Society (NIF-R1-231091); United States of America: U.S. Department of Energy (ECA DE-AC02-76SF00515), Neubauer Family Foundation.

Data availability

No data was used for the research described in the article.

References

[1] ATLAS Collaboration, The ATLAS experiment at the CERN Large Hadron Collider, J. Instrum. 3 (2008) S08003.

[2] CMS Collaboration, The CMS experiment at the CERN LHC, J. Instrum. 3 (2008) S08004.

[3] CMS Collaboration, Search for $t\bar{t}H$ production in the all-jet final state in proton–proton collisions at $\sqrt{s} = 13$ TeV, J. High Energy Phys. 06 (2018) 101, arXiv:1803.06986 [hep-ex].

[4] CMS Collaboration, Search for $t\bar{t}H$ production in the $H \to b\bar{b}$ decay channel with leptonic $t\bar{t}$ decays in proton–proton collisions at $\sqrt{s} = 13$ TeV, J. High Energy Phys. 03 (2019) 026, arXiv:1804.03682 [hep-ex].

[5] ATLAS Collaboration, Measurement of the associated production of a top-antitop-quark pair and a Higgs boson decaying into a $b\bar{b}$ pair in pp collisions at $\sqrt{s} = 13$ TeV using the ATLAS detector at the LHC, arXiv:2407.10904 [hep-ex], 2024.

[6] ATLAS Collaboration, Measurement of the $t\bar{t}t\bar{t}$ production cross section in pp collisions at $\sqrt{s} = 13$ TeV with the ATLAS detector, J. High Energy Phys. 11 (2021) 118, arXiv:2106.11683 [hep-ex].

[7] CMS Collaboration, Evidence for four-top quark production in proton–proton collisions at $\sqrt{s} = 13$ TeV, Phys. Lett. B 844 (2023) 138076, arXiv:2303.03864 [hep-ex].

[8] A. Bredenstein, A. Denner, S. Dittmaier, S. Pozzorini, NLO QCD corrections to $t\bar{t}b\bar{b}$ production at the LHC: 1. Quark-antiquark annihilation, J. High Energy Phys. 08 (2008) 108, arXiv:0807.1248 [hep-ph].

[9] A. Bredenstein, A. Denner, S. Dittmaier, S. Pozzorini, Next-to-leading order QCD corrections to $pp \to t\bar{t}b\bar{b} + X$ at the LHC, Phys. Rev. Lett. 103 (2009) 012002, arXiv:0905.0110 [hep-ph].

[10] F. Cascioli, P. Maierhöfer, N. Moretti, S. Pozzorini, F. Siegert, NLO matching for $t\bar{t}b\bar{b}$ production with massive b-quarks, Phys. Lett. B 734 (2014) 210, arXiv:1309.5912 [hep-ph].

[11] T. Ježo, J.M. Lindert, N. Moretti, S. Pozzorini, New NLOPS predictions for $t\bar{t} + b$-jet production at the LHC, Eur. Phys. J. C 78 (2018) 502, arXiv:1802.00426 [hep-ph].

[12] F. Buccioni, S. Kallweit, S. Pozzorini, M.F. Zoller, NLO QCD predictions for $t\bar{t}b\bar{b}$ production in association with a light jet at the LHC, J. High Energy Phys. 12 (2019) 015, arXiv:1907.13624 [hep-ph].

[13] G. Bevilacqua, et al., $t\bar{t}b\bar{b}$ at the LHC: on the size of off-shell effects and prompt b-jet identification, Phys. Rev. D 107 (2023) 014028, arXiv:2202.11186 [hep-ph].

[14] ATLAS Collaboration, Measurements of inclusive and differential fiducial cross-sections of $t\bar{t}$ production with additional heavy-flavour jets in proton–proton collisions at $\sqrt{s} = 13$ TeV with the ATLAS detector, J. High Energy Phys. 04 (2019) 046, arXiv:1811.12113 [hep-ex].

[15] CMS Collaboration, Measurement of the $t\bar{t}b\bar{b}$ production cross section in the all-jet final state in pp collisions at $\sqrt{s} = 13$ TeV, Phys. Lett. B 803 (2020) 135285, arXiv:1909.05306 [hep-ex].
[16] CMS Collaboration, Inclusive and differential cross section measurements of $t\bar{t}b\bar{b}$ production in the lepton+jets channel at $\sqrt{s} = 13$ TeV, J. High Energy Phys. 05 (2024) 042, arXiv:2309.14442 [hep-ex].
[17] ATLAS Collaboration, Measurement of $t\bar{t}$ production in association with additional b-jets in the $e\mu$ final state in proton–proton collisions at $\sqrt{s} = 13$ TeV with the ATLAS detector, arXiv:2407.13473 [hep-ex], 2024.
[18] CMS Collaboration, First measurement of the cross section for top quark pair production with additional charm jets using dileptonic final states in pp collisions at $\sqrt{s} = 13$ TeV, Phys. Lett. B 820 (2021) 136565, arXiv:2012.09225 [hep-ex].
[19] G. Avoni, et al., The new LUCID-2 detector for luminosity measurement and monitoring in ATLAS, J. Instrum. 13 (2018) P07017.
[20] ATLAS Collaboration, Performance of the ATLAS trigger system in 2015, Eur. Phys. J. C 77 (2017) 317, arXiv:1611.09661 [hep-ex].
[21] ATLAS Collaboration, Software and computing for Run 3 of the ATLAS experiment at the LHC, arXiv:2404.06335 [hep-ex], 2024.
[22] ATLAS Collaboration, The ATLAS simulation infrastructure, Eur. Phys. J. C 70 (2010) 823, arXiv:1005.4568 [physics.ins-det].
[23] S. Agostinelli, et al., GEANT4 – a simulation toolkit, Nucl. Instrum. Methods A 506 (2003) 250.
[24] T. Sjöstrand, S. Mrenna, P. Skands, A brief introduction to PYTHIA 8.1, Comput. Phys. Commun. 178 (2008) 852, arXiv:0710.3820 [hep-ph].
[25] ATLAS Collaboration, The Pythia 8 A3 tune description of ATLAS minimum bias and inelastic measurements incorporating the Donnachie–Landshoff diffractive model, ATL-PHYS-PUB-2016-017, https://cds.cern.ch/record/2206965, 2016.
[26] T. Sjöstrand, et al., An introduction to PYTHIA 8.2, Comput. Phys. Commun. 191 (2015) 159, arXiv:1410.3012 [hep-ph].
[27] M. Bähr, et al., Herwig++ physics and manual, Eur. Phys. J. C 58 (2008) 639, arXiv:0803.0883 [hep-ph].
[28] J. Bellm, et al., Herwig 7.0/Herwig++ 3.0 release note, Eur. Phys. J. C 76 (2016) 196, arXiv:1512.01178 [hep-ph].
[29] J. Bellm, et al., Herwig 7.1 release note, arXiv:1705.06919 [hep-ph], 2017.
[30] D.J. Lange, The EvtGen particle decay simulation package, Nucl. Instrum. Methods A 462 (2001) 152.
[31] ATLAS Collaboration, ATLAS Pythia 8 tunes to 7 *TeV* data, ATL-PHYS-PUB-2014-021, https://cds.cern.ch/record/1966419, 2014.
[32] NNPDF Collaboration, R.D. Ball, et al., Parton distributions with LHC data, Nucl. Phys. B 867 (2013) 244, arXiv:1207.1303 [hep-ph].
[33] L.A. Harland-Lang, A.D. Martin, P. Motylinski, R.S. Thorne, Parton distributions in the LHC era: MMHT 2014 PDFs, Eur. Phys. J. C 75 (2015) 204, arXiv:1412.3989 [hep-ph].
[34] S. Frixione, G. Ridolfi, P. Nason, A positive-weight next-to-leading-order Monte Carlo for heavy flavour hadroproduction, J. High Energy Phys. 09 (2007) 126, arXiv:0707.3088 [hep-ph].
[35] P. Nason, A new method for combining NLO QCD with shower Monte Carlo algorithms, J. High Energy Phys. 11 (2004) 040, arXiv:hep-ph/0409146.
[36] S. Frixione, P. Nason, C. Oleari, Matching NLO QCD computations with parton shower simulations: the POWHEG method, J. High Energy Phys. 11 (2007) 070, arXiv:0709.2092 [hep-ph].
[37] S. Alioli, P. Nason, C. Oleari, E. Re, A general framework for implementing NLO calculations in shower Monte Carlo programs: the POWHEG BOX, J. High Energy Phys. 06 (2010) 043, arXiv:1002.2581 [hep-ph].
[38] NNPDF Collaboration, R.D. Ball, et al., Parton distributions for the LHC run II, J. High Energy Phys. 04 (2015) 040, arXiv:1410.8849 [hep-ph].
[39] ATLAS Collaboration, Studies on top-quark Monte Carlo modelling for Top2016, ATL-PHYS-PUB-2016-020, https://cds.cern.ch/record/2216168, 2016.
[40] S. Höche, S. Mrenna, S. Payne, C.T. Preuss, P. Skands, A study of QCD radiation in VBF Higgs production with Vincia and Pythia, SciPost Phys. 12 (2022) 010, arXiv:2106.10987 [hep-ph].
[41] ATLAS Collaboration, Studies on the improvement of the matching uncertainty definition in top-quark processes simulated with Powheg+Pythia8, ATL-PHYS-PUB-2023-029, https://cds.cern.ch/record/2872787, 2013.
[42] J. Alwall, et al., The automated computation of tree-level and next-to-leading order differential cross sections, and their matching to parton shower simulations, J. High Energy Phys. 07 (2014) 079, arXiv:1405.0301 [hep-ph].
[43] S. Frixione, E. Laenen, P. Motylinski, B.R. Webber, Angular correlations of lepton pairs from vector boson and top quark decays in Monte Carlo simulations, J. High Energy Phys. 04 (2007) 081, arXiv:hep-ph/0702198.
[44] P. Artoisenet, R. Frederix, O. Mattelaer, R. Rietkerk, Automatic spin-entangled decays of heavy resonances in Monte Carlo simulations, J. High Energy Phys. 03 (2013) 015, arXiv:1212.3460 [hep-ph].
[45] ATLAS Collaboration, Studies on top-quark Monte Carlo modelling with Sherpa and MG5_aMC@NLO, ATL-PHYS-PUB-2017-007, https://cds.cern.ch/record/2261938, 2017.
[46] M. Czakon, A. Mitov, Top++: a program for the calculation of the top-pair cross-section at hadron colliders, Comput. Phys. Commun. 185 (2014) 2930, arXiv:1112.5675 [hep-ph].
[47] J. Butterworth, et al., PDF4LHC recommendations for LHC Run II, J. Phys. G 43 (2016) 023001, arXiv:1510.03865 [hep-ph].
[48] A.D. Martin, W.J. Stirling, R.S. Thorne, G. Watt, Uncertainties on α_S in global PDF analyses and implications for predicted hadronic cross sections, Eur. Phys. J. C 64 (2009) 653, arXiv:0905.3531 [hep-ph].
[49] J. Gao, et al., CT10 next-to-next-to-leading order global analysis of QCD, Phys. Rev. D 89 (2014) 033009, arXiv:1302.6246 [hep-ph].
[50] F. Cascioli, P. Maierhöfer, S. Pozzorini, Scattering amplitudes with open loops, Phys. Rev. Lett. 108 (2012) 111601, arXiv:1111.5206 [hep-ph].
[51] A. Denner, S. Dittmaier, L. Hofer, Collier: a fortran-based complex one-loop library in extended regularizations, Comput. Phys. Commun. 212 (2017) 220, arXiv:1604.06792 [hep-ph].
[52] F. Buccioni, et al., OpenLoops 2, Eur. Phys. J. C 79 (2019) 866, arXiv:1907.13071 [hep-ph].
[53] ATLAS Collaboration, Study of $ttbb$ and ttW background modelling for ttH analyses, ATL-PHYS-PUB-2022-026, https://cds.cern.ch/record/2810864, 2022.
[54] E. Bothmann, et al., Event generation with Sherpa 2.2, SciPost Phys. 7 (2019) 034, arXiv:1905.09127 [hep-ph].
[55] T. Gleisberg, S. Höche, Comix, a new matrix element generator, J. High Energy Phys. 12 (2008) 039, arXiv:0808.3674 [hep-ph].
[56] S. Schumann, F. Krauss, A parton shower algorithm based on Catani–Seymour dipole factorisation, J. High Energy Phys. 03 (2008) 038, arXiv:0709.1027 [hep-ph].
[57] S. Höche, F. Krauss, M. Schönherr, F. Siegert, A critical appraisal of NLO+PS matching methods, J. High Energy Phys. 09 (2012) 049, arXiv:1111.1220 [hep-ph].
[58] S. Höche, F. Krauss, M. Schönherr, F. Siegert, QCD matrix elements + parton showers. The NLO case, J. High Energy Phys. 04 (2013) 027, arXiv:1207.5030 [hep-ph].
[59] S. Catani, F. Krauss, B.R. Webber, R. Kuhn, QCD matrix elements + parton showers, J. High Energy Phys. 11 (2001) 063, arXiv:hep-ph/0109231.
[60] S. Höche, F. Krauss, S. Schumann, F. Siegert, QCD matrix elements and truncated showers, J. High Energy Phys. 05 (2009) 053, arXiv:0903.1219 [hep-ph].
[61] M. Cacciari, G.P. Salam, G. Soyez, The anti-k_t jet clustering algorithm, J. High Energy Phys. 04 (2008) 063, arXiv:0802.1189 [hep-ph].
[62] M. Cacciari, G.P. Salam, G. Soyez, FastJet user manual, Eur. Phys. J. C 72 (2012) 1896, arXiv:1111.6097 [hep-ph].
[63] M. Cacciari, G.P. Salam, Pileup subtraction using jet areas, Phys. Lett. B 659 (2008) 119, arXiv:0707.1378 [hep-ph].
[64] M. Cacciari, G.P. Salam, G. Soyez, The catchment area of jets, J. High Energy Phys. 04 (2008) 005, arXiv:0802.1188 [hep-ph].
[65] S. Frixione, E. Laenen, P. Motylinski, C. White, B.R. Webber, Single-top hadroproduction in association with a W boson, J. High Energy Phys. 07 (2008) 029, arXiv:0805.3067 [hep-ph].
[66] C. Anastasiou, L. Dixon, K. Melnikov, F. Petriello, High-precision QCD at hadron colliders: electroweak gauge boson rapidity distributions at next-to-next-to leading order, Phys. Rev. D 69 (2004) 094008, arXiv:hep-ph/0312266.
[67] ATLAS Collaboration, Vertex reconstruction performance of the ATLAS detector at $\sqrt{s} = 13$ TeV, ATL-PHYS-PUB-2015-026, https://cds.cern.ch/record/2037717, 2015.
[68] ATLAS Collaboration, Performance of electron and photon triggers in ATLAS during LHC Run 2, Eur. Phys. J. C 80 (2020) 47, arXiv:1909.00761 [hep-ex].
[69] ATLAS Collaboration, Performance of the ATLAS muon triggers in Run 2, J. Instrum. 15 (2020) P09015, arXiv:2004.13447 [physics.ins-det].
[70] ATLAS Collaboration, Jet reconstruction and performance using particle flow with the ATLAS Detector, Eur. Phys. J. C 77 (2017) 466, arXiv:1703.10485 [hep-ex].
[71] ATLAS Collaboration, Jet energy scale and resolution measured in proton–proton collisions at $\sqrt{s} = 13$ TeV with the ATLAS detector, Eur. Phys. J. C 81 (2021) 689, arXiv:2007.02645 [hep-ex].
[72] ATLAS Collaboration, Performance of pile-up mitigation techniques for jets in pp collisions at $\sqrt{s} = 8$ TeV using the ATLAS detector, Eur. Phys. J. C 76 (2016) 581, arXiv:1510.03823 [hep-ex].
[73] ATLAS Collaboration, Electron and photon performance measurements with the ATLAS detector using the 2015–2017 LHC proton–proton collision data, J. Instrum. 14 (2019) P12006, arXiv:1908.00005 [hep-ex].
[74] ATLAS Collaboration, Electron and photon efficiencies in LHC Run 2 with the ATLAS experiment, J. High Energy Phys. 05 (2024) 162, arXiv:2308.13362 [hep-ex].
[75] ATLAS Collaboration, Muon reconstruction and identification efficiency in ATLAS using the full Run 2 pp collision data set at $\sqrt{s} = 13$ TeV, Eur. Phys. J. C 81 (2021) 578, arXiv:2012.00578 [hep-ex].
[76] ATLAS Collaboration, Studies of the muon momentum calibration and performance of the ATLAS detector with pp collisions at $\sqrt{s} = 13$ TeV, Eur. Phys. J. C 83 (2023) 686, arXiv:2212.07338 [hep-ex].
[77] ATLAS Collaboration, ATLAS flavour-tagging algorithms for the LHC Run 2 pp collision dataset, Eur. Phys. J. C 83 (2023) 681, arXiv:2211.16345 [physics.data-an].
[78] J. Neyman, E.S. Pearson, On the problem of the most efficient tests of statistical hypotheses, Philos. Trans. R. Soc. A 231 (1933) 289.
[79] ATLAS Collaboration, ATLAS b-jet identification performance and efficiency measurement with $t\bar{t}$ events in pp collisions at $\sqrt{s} = 13$ TeV, Eur. Phys. J. C 79 (2019) 970, arXiv:1907.05120 [hep-ex].
[80] ATLAS Collaboration, Measurement of the c-jet mistagging efficiency in $t\bar{t}$ events using pp collision data at $\sqrt{s} = 13$ TeV collected with the ATLAS detector, Eur. Phys. J. C 82 (2022) 95, arXiv:2109.10627 [hep-ex].
[81] ATLAS Collaboration, Calibration of the light-flavour jet mistagging efficiency of the b-tagging algorithms with Z+jets events using 139 fb^{-1} of ATLAS proton–proton

collision data at $\sqrt{s} = 13$ TeV, Eur. Phys. J. C 83 (2023) 728, arXiv:2301.06319 [hep-ex].

[82] ATLAS Collaboration, Calibration of the performance of b-tagging for c and light-flavour jets in the 2012 ATLAS data, ATLAS-CONF-2014-046, https://cds.cern.ch/record/1741020, 2014.

[83] D0 Collaboration, Measurement of the $t\bar{t}$ production cross section in $p\bar{p}$ collisions at $\sqrt{s} = 1.96$ TeV using secondary vertex b tagging, Phys. Rev. D 74 (2006) 112004, arXiv:hep-ex/0611002.

[84] ATLAS Collaboration, Monte Carlo to Monte Carlo scale factors for flavour tagging efficiency calibration, ATL-PHYS-PUB-2020-009, https://cds.cern.ch/record/2718610, 2020.

[85] ATLAS Collaboration, Tools for estimating fake/non-prompt lepton backgrounds with the ATLAS detector at the LHC, J. Instrum. 18 (2023) T11004, arXiv:2211.16178 [hep-ex].

[86] ATLAS Collaboration, The performance of missing transverse momentum reconstruction and its significance with the ATLAS detector using 140 fb^{-1} of $\sqrt{s} = 13$ TeV pp collisions, arXiv:2402.05858 [hep-ex], 2024.

[87] ATLAS Collaboration, Luminosity determination in pp collisions at $\sqrt{s} = 13$ TeV using the ATLAS detector at the LHC, Eur. Phys. J. C 83 (2023) 982, arXiv:2212.09379 [hep-ex].

[88] N. Kidonakis, N. Yamanaka, Higher-order corrections for tW production at high-energy hadron colliders, J. High Energy Phys. 05 (2021) 278, arXiv:2102.11300 [hep-ph].

[89] D. de Florian, et al., Handbook of LHC Higgs Cross Sections: 4. Deciphering the Nature of the Higgs Sector, arXiv:1610.07922 [hep-ph], 2017.

[90] ATLAS Collaboration, Probing the CP nature of the top-Higgs Yukawa coupling in $t\bar{t}H$ and tH events with $H \to b\bar{b}$ decays using the ATLAS detector at the LHC, Phys. Lett. B 849 (2024) 138469, arXiv:2303.05974 [hep-ex].

[91] M. Grazzini, S. Kallweit, D. Rathlev, M. Wiesemann, $W^{\pm}Z$ production at hadron colliders in NNLO QCD, Phys. Lett. B 761 (2016) 179, arXiv:1604.08576 [hep-ph].

[92] ATLAS Collaboration, Multi-boson simulation for 13 TeV ATLAS analyses, ATL-PHYS-PUB-2016-002, https://cds.cern.ch/record/2119986, 2016.

[93] ATLAS Collaboration, Measurement of $W^{\pm}Z$ production cross sections and gauge boson polarisation in pp collisions at $\sqrt{s} = 13$ TeV with the ATLAS detector, Eur. Phys. J. C 79 (2019) 535, arXiv:1902.05759 [hep-ex].

[94] K. Cranmer, G. Lewis, L. Moneta, A. Shibata, W. Verkerke, HistFactory: a tool for creating statistical models for use with RooFit and RooStats, CERN-OPEN-2012-016, https://cds.cern.ch/record/1456844, 2012.

[95] W. Verkerke, D. Kirkby, The RooFit toolkit for data modeling, arXiv:physics/0306116 [physics.data-an], 2003.

[96] S. Baker, R.D. Cousins, Clarification of the use of CHI-square and likelihood functions in fits to histograms, Nucl. Instrum. Methods Phys. Res. 221 (1984) 437.

[97] A. Pinto, et al., Uncertainty components in profile likelihood fits, Eur. Phys. J. C 84 (2024) 593, arXiv:2307.04007 [physics.data-an].

[98] ATLAS Collaboration, ATLAS computing acknowledgements, ATL-SOFT-PUB-2023-001, https://cds.cern.ch/record/2869272, 2023.

The ATLAS Collaboration

G. Aad [105], E. Aakvaag [17], B. Abbott [124], S. Abdelhameed [120a], K. Abeling [57], N.J. Abicht [51], S.H. Abidi [30], M. Aboelela [46], A. Aboulhorma [36e], H. Abramowicz [156], H. Abreu [155], Y. Abulaiti [121], B.S. Acharya [71a,71b,k], A. Ackermann [65a], C. Adam Bourdarios [4], L. Adamczyk [88a], S.V. Addepalli [148], M.J. Addison [104], J. Adelman [119], A. Adiguzel [22c], T. Adye [138], A.A. Affolder [140], Y. Afik [41], M.N. Agaras [13], A. Aggarwal [103], C. Agheorghiesei [28c], F. Ahmadov [40,y], S. Ahuja [98], X. Ai [64e], G. Aielli [78a,78b], A. Aikot [168], M. Ait Tamlihat [36e], B. Aitbenchikh [36a], M. Akbiyik [103], T.P.A. Åkesson [101], A.V. Akimov [150], D. Akiyama [173], N.N. Akolkar [25], S. Aktas [22a], K. Al Khoury [43], G.L. Alberghi [24b], J. Albert [170], P. Albicocco [55], G.L. Albouy [62], S. Alderweireldt [54], Z.L. Alegria [125], M. Aleksa [37], I.N. Aleksandrov [40], C. Alexa [28b], T. Alexopoulos [10], F. Alfonsi [24b], M. Algren [58], M. Alhroob [172], B. Ali [136], H.M.J. Ali [94,s], S. Ali [32], S.W. Alibocus [95], M. Aliev [34c], G. Alimonti [73a], W. Alkakhi [57], C. Allaire [68], B.M.M. Allbrooke [151], J.S. Allen [104], J.F. Allen [54], C.A. Allendes Flores [141f], P.P. Allport [21], A. Aloisio [74a,74b], F. Alonso [93], C. Alpigiani [143], Z.M.K. Alsolami [94], M. Alvarez Estevez [102], A. Alvarez Fernandez [103], M. Alves Cardoso [58], M.G. Alviggi [74a,74b], M. Aly [104], Y. Amaral Coutinho [85b], A. Ambler [107], C. Amelung [37], M. Amerl [104], C.G. Ames [112], D. Amidei [109], B. Amini [56], K.J. Amirie [159], S.P. Amor Dos Santos [134a], K.R. Amos [168], D. Amperiadou [157], S. An [86], V. Ananiev [129], C. Anastopoulos [144], T. Andeen [11], J.K. Anders [37], A.C. Anderson [61], S.Y. Andrean [49a,49b], A. Andreazza [73a,73b], S. Angelidakis [9], A. Angerami [43], A.V. Anisenkov [39], A. Annovi [76a], C. Antel [58], E. Antipov [150], M. Antonelli [55], F. Anulli [77a], M. Aoki [86], T. Aoki [158], M.A. Aparo [151], L. Aperio Bella [50], C. Appelt [156], A. Apyan [27], S.J. Arbiol Val [89], C. Arcangeletti [55], A.T.H. Arce [53], J-F. Arguin [111], S. Argyropoulos [157], J.-H. Arling [50], O. Arnaez [4], H. Arnold [150], G. Artoni [77a,77b], H. Asada [114], K. Asai [122], S. Asai [158], N.A. Asbah [37], R.A. Ashby Pickering [172], K. Assamagan [30], R. Astalos [29a], K.S.V. Astrand [101], S. Atashi [163], R.J. Atkin [34a], H. Atmani [36f], P.A. Atmasiddha [132], K. Augsten [136], A.D. Auriol [21], V.A. Austrup [104], G. Avolio [37], K. Axiotis [58], G. Azuelos [111,ac], D. Babal [29b], H. Bachacou [139], K. Bachas [157,o], A. Bachiu [35], E. Bachmann [52], A. Badea [41], T.M. Baer [109], P. Bagnaia [77a,77b], M. Bahmani [19], D. Bahner [56], K. Bai [127], J.T. Baines [138], L. Baines [97], O.K. Baker [177], E. Bakos [16], D. Bakshi Gupta [8], L.E. Balabram Filho [85b], V. Balakrishnan [124], R. Balasubramanian [4], E.M. Baldin [39], P. Balek [88a], E. Ballabene [24b,24a], F. Balli [139], L.M. Baltes [65a], W.K. Balunas [33], J. Balz [103], I. Bamwidhi [120b], E. Banas [89], M. Bandieramonte [133], A. Bandyopadhyay [25], S. Bansal [25],

L. Barak [156], M. Barakat [50], E.L. Barberio [108], D. Barberis [59b,59a], M. Barbero [105], M.Z. Barel [118], T. Barillari [113], M-S. Barisits [37], T. Barklow [148], P. Baron [126], D.A. Baron Moreno [104], A. Baroncelli [64a], A.J. Barr [130], J.D. Barr [99], F. Barreiro [102], J. Barreiro Guimarães da Costa [14], M.G. Barros Teixeira [134a], S. Barsov [39], F. Bartels [65a], R. Bartoldus [148], A.E. Barton [94], P. Bartos [29a], A. Basan [103], M. Baselga [51], A. Bassalat [68,b], M.J. Basso [160a], S. Bataju [46], R. Bate [169], R.L. Bates [61], S. Batlamous [102], B. Batool [146], M. Battaglia [140], D. Battulga [19], M. Bauce [77a,77b], M. Bauer [81], P. Bauer [25], L.T. Bazzano Hurrell [31], J.B. Beacham [53], T. Beau [131], J.Y. Beaucamp [93], P.H. Beauchemin [162], P. Bechtle [25], H.P. Beck [20,n], K. Becker [172], A.J. Beddall [84], V.A. Bednyakov [40], C.P. Bee [150], L.J. Beemster [16], T.A. Beermann [37], M. Begalli [85d], M. Begel [30], A. Behera [150], J.K. Behr [50], J.F. Beirer [37], F. Beisiegel [25], M. Belfkir [120b], G. Bella [156], L. Bellagamba [24b], A. Bellerive [35], P. Bellos [21], K. Beloborodov [39], D. Benchekroun [36a], F. Bendebba [36a], Y. Benhammou [156], K.C. Benkendorfer [63], L. Beresford [50], M. Beretta [55], E. Bergeaas Kuutmann [166], N. Berger [4], B. Bergmann [136], J. Beringer [18a], G. Bernardi [5], C. Bernius [148], F.U. Bernlochner [25], F. Bernon [37], A. Berrocal Guardia [13], T. Berry [98], P. Berta [137], A. Berthold [52], S. Bethke [113], A. Betti [77a,77b], A.J. Bevan [97], N.K. Bhalla [56], S. Bhatta [150], D.S. Bhattacharya [171], P. Bhattarai [148], Z.M. Bhatti [121], K.D. Bhide [56], V.S. Bhopatkar [125], R.M. Bianchi [133], G. Bianco [24b,24a], O. Biebel [112], M. Biglietti [79a], C.S. Billingsley [46], Y. Bimgdi [36f], M. Bindi [57], A. Bingham [176], A. Bingul [22b], C. Bini [77a,77b], G.A. Bird [33], M. Birman [174], M. Biros [137], S. Biryukov [151], T. Bisanz [51], E. Bisceglie [45b,45a], J.P. Biswal [138], D. Biswas [146], I. Bloch [50], A. Blue [61], U. Blumenschein [97], J. Blumenthal [103], V.S. Bobrovnikov [39], M. Boehler [56], B. Boehm [171], D. Bogavac [37], A.G. Bogdanchikov [39], L.S. Boggia [131], C. Bohm [49a], V. Boisvert [98], P. Bokan [37], T. Bold [88a], M. Bomben [5], M. Bona [97], M. Boonekamp [139], A.G. Borbély [61], I.S. Bordulev [39], G. Borissov [94], D. Bortoletto [130], D. Boscherini [24b], M. Bosman [13], K. Bouaouda [36a], N. Bouchhar [168], L. Boudet [4], J. Boudreau [133], E.V. Bouhova-Thacker [94], D. Boumediene [42], R. Bouquet [59b,59a], A. Boveia [123], J. Boyd [37], D. Boye [30], I.R. Boyko [40], L. Bozianu [58], J. Bracinik [21], N. Brahimi [4], G. Brandt [176], O. Brandt [33], B. Brau [106], J.E. Brau [127], R. Brener [174], L. Brenner [118], R. Brenner [166], S. Bressler [174], G. Brianti [80a,80b], D. Britton [61], D. Britzger [113], I. Brock [25], R. Brock [110], G. Brooijmans [43], A.J. Brooks [70], E.M. Brooks [160b], E. Brost [30], L.M. Brown [170], L.E. Bruce [63], T.L. Bruckler [130], P.A. Bruckman de Renstrom [89], B. Brüers [50], A. Bruni [24b], G. Bruni [24b], D. Brunner [49a,49b], M. Bruschi [24b], N. Bruscino [77a,77b], T. Buanes [17], Q. Buat [143], D. Buchin [113], A.G. Buckley [61], O. Bulekov [39], B.A. Bullard [148], S. Burdin [95], C.D. Burgard [51], A.M. Burger [37], B. Burghgrave [8], O. Burlayenko [56], J. Burleson [167], J.T.P. Burr [33], J.C. Burzynski [147], E.L. Busch [43], V. Büscher [103], P.J. Bussey [61], J.M. Butler [26], C.M. Buttar [61], J.M. Butterworth [99], W. Buttinger [138], C.J. Buxo Vazquez [110], A.R. Buzykaev [39], S. Cabrera Urbán [168], L. Cadamuro [68], D. Caforio [60], H. Cai [133], Y. Cai [14,115c], Y. Cai [115a], V.M.M. Cairo [37], O. Cakir [3a], N. Calace [37], P. Calafiura [18a], G. Calderini [131], P. Calfayan [35], G. Callea [61], L.P. Caloba [85b], D. Calvet [42], S. Calvet [42], R. Camacho Toro [131], S. Camarda [37], D. Camarero Munoz [27], P. Camarri [78a,78b], M.T. Camerlingo [74a,74b], D. Cameron [37], C. Camincher [170], M. Campanelli [99], A. Camplani [44], V. Canale [74a,74b], A.C. Canbay [3a], E. Canonero [98], J. Cantero [168], Y. Cao [167], F. Capocasa [27], M. Capua [45b,45a], A. Carbone [73a,73b], R. Cardarelli [78a], J.C.J. Cardenas [8], M.P. Cardiff [27], G. Carducci [45b,45a], T. Carli [37], G. Carlino [74a], J.I. Carlotto [13], B.T. Carlson [133,p], E.M. Carlson [170,160a], J. Carmignani [95], L. Carminati [73a,73b], A. Carnelli [139], M. Carnesale [37], S. Caron [117], E. Carquin [141f],

I.B. Carr [108], S. Carrá [73a], G. Carratta [24b,24a], A.M. Carroll [127], M.P. Casado [13,h], M. Caspar [50], F.L. Castillo [4], L. Castillo Garcia [13], V. Castillo Gimenez [168], N.F. Castro [134a,134e], A. Catinaccio [37], J.R. Catmore [129], T. Cavaliere [4], V. Cavaliere [30], L.J. Caviedes Betancourt [23b], Y.C. Cekmecelioglu [50], E. Celebi [84], S. Cella [37], V. Cepaitis [58], K. Cerny [126], A.S. Cerqueira [85a], A. Cerri [151], L. Cerrito [78a,78b], F. Cerutti [18a], B. Cervato [146], A. Cervelli [24b], G. Cesarini [55], S.A. Cetin [84], P.M. Chabrillat [131], D. Chakraborty [119], J. Chan [18a], W.Y. Chan [158], J.D. Chapman [33], E. Chapon [139], B. Chargeishvili [154b], D.G. Charlton [21], M. Chatterjee [20], C. Chauhan [137], Y. Che [115a], S. Chekanov [6], S.V. Chekulaev [160a], G.A. Chelkov [40,a], A. Chen [109], B. Chen [156], B. Chen [170], H. Chen [115a], H. Chen [30], J. Chen [64c], J. Chen [147], M. Chen [130], S. Chen [90], S.J. Chen [115a], X. Chen [64c], X. Chen [15,ab], Y. Chen [64a], C.L. Cheng [175], H.C. Cheng [66a], S. Cheong [148], A. Cheplakov [40], E. Cheremushkina [50], E. Cherepanova [118], R. Cherkaoui El Moursli [36e], E. Cheu [7], K. Cheung [67], L. Chevalier [139], V. Chiarella [55], G. Chiarelli [76a], N. Chiedde [105], G. Chiodini [72a], A.S. Chisholm [21], A. Chitan [28b], M. Chitishvili [168], M.V. Chizhov [40,q], K. Choi [11], Y. Chou [143], E.Y.S. Chow [117], K.L. Chu [174], M.C. Chu [66a], X. Chu [14,115c], Z. Chubinidze [55], J. Chudoba [135], J.J. Chwastowski [89], D. Cieri [113], K.M. Ciesla [88a], V. Cindro [96], A. Ciocio [18a], F. Cirotto [74a,74b], Z.H. Citron [174], M. Citterio [73a], D.A. Ciubotaru [28b], A. Clark [58], P.J. Clark [54], N. Clarke Hall [99], C. Clarry [159], J.M. Clavijo Columbie [50], S.E. Clawson [50], C. Clement [49a,49b], Y. Coadou [105], M. Cobal [71a,71c], A. Coccaro [59b], R.F. Coelho Barrue [134a], R. Coelho Lopes De Sa [106], S. Coelli [73a], L.S. Colangeli [159], B. Cole [43], J. Collot [62], P. Conde Muiño [134a,134g], M.P. Connell [34c], S.H. Connell [34c], E.I. Conroy [130], F. Conventi [74a,ad], H.G. Cooke [21], A.M. Cooper-Sarkar [130], F.A. Corchia [24b,24a], A. Cordeiro Oudot Choi [131], L.D. Corpe [42], M. Corradi [77a,77b], F. Corriveau [107,x], A. Cortes-Gonzalez [19], M.J. Costa [168], F. Costanza [4], D. Costanzo [144], B.M. Cote [123], J. Couthures [4], G. Cowan [98], K. Cranmer [175], L. Cremer [51], D. Cremonini [24b,24a], S. Crépé-Renaudin [62], F. Crescioli [131], M. Cristinziani [146], M. Cristoforetti [80a,80b], V. Croft [118], J.E. Crosby [125], G. Crosetti [45b,45a], A. Cueto [102], H. Cui [99], Z. Cui [7], W.R. Cunningham [61], F. Curcio [168], J.R. Curran [54], P. Czodrowski [37], M.J. Da Cunha Sargedas De Sousa [59b,59a], J.V. Da Fonseca Pinto [85b], C. Da Via [104], W. Dabrowski [88a], T. Dado [37], S. Dahbi [153], T. Dai [109], D. Dal Santo [20], C. Dallapiccola [106], M. Dam [44], G. D'amen [30], V. D'Amico [112], J. Damp [103], J.R. Dandoy [35], D. Dannheim [37], M. Danninger [147], V. Dao [150], G. Darbo [59b], S.J. Das [30], F. Dattola [50], S. D'Auria [73a,73b], A. D'Avanzo [74a,74b], C. David [34a], T. Davidek [137], I. Dawson [97], H.A. Day-hall [136], K. De [8], C. De Almeida Rossi [159], R. De Asmundis [74a], N. De Biase [50], S. De Castro [24b,24a], N. De Groot [117], P. de Jong [118], H. De la Torre [119], A. De Maria [115a], A. De Salvo [77a], U. De Sanctis [78a,78b], F. De Santis [72a,72b], A. De Santo [151], J.B. De Vivie De Regie [62], J. Debevc [96], D.V. Dedovich [40], J. Degens [95], A.M. Deiana [46], F. Del Corso [24b,24a], J. Del Peso [102], L. Delagrange [131], F. Deliot [139], C.M. Delitzsch [51], M. Della Pietra [74a,74b], D. Della Volpe [58], A. Dell'Acqua [37], L. Dell'Asta [73a,73b], M. Delmastro [4], C.C. Delogu [103], P.A. Delsart [62], S. Demers [177], M. Demichev [40], S.P. Denisov [39], L. D'Eramo [42], D. Derendarz [89], F. Derue [131], P. Dervan [95], K. Desch [25], C. Deutsch [25], F.A. Di Bello [59b,59a], A. Di Ciaccio [78a,78b], L. Di Ciaccio [4], A. Di Domenico [77a,77b], C. Di Donato [74a,74b], A. Di Girolamo [37], G. Di Gregorio [37], A. Di Luca [80a,80b], B. Di Micco [79a,79b], R. Di Nardo [79a,79b], K.F. Di Petrillo [41], M. Diamantopoulou [35], F.A. Dias [118], T. Dias Do Vale [147], M.A. Diaz [141a,141b], A.R. Didenko [40], M. Didenko [168], E.B. Diehl [109], S. Díez Cornell [50], C. Diez Pardos [146], C. Dimitriadi [166], A. Dimitrievska [21], J. Dingfelder [25], T. Dingley [130], I-M. Dinu [28b], S.J. Dittmeier [65b], F. Dittus [37], M. Divisek [137], B. Dixit [95], F. Djama [105], T. Djobava [154b],

C. Doglioni [104,101], A. Dohnalova [29a], Z. Dolezal [137], K. Domijan [88a], K.M. Dona [41], M. Donadelli [85d], B. Dong [110], J. Donini [42], A. D'Onofrio [74a,74b], M. D'Onofrio [95], J. Dopke [138], A. Doria [74a], N. Dos Santos Fernandes [134a], P. Dougan [104], M.T. Dova [93], A.T. Doyle [61], M.A. Draguet [130], M.P. Drescher [57], E. Dreyer [174], I. Drivas-koulouris [10], M. Drnevich [121], M. Drozdova [58], D. Du [64a], T.A. du Pree [118], F. Dubinin [39], M. Dubovsky [29a], E. Duchovni [174], G. Duckeck [112], O.A. Ducu [28b], D. Duda [54], A. Dudarev [37], E.R. Duden [27], M. D'uffizi [104], L. Duflot [68], M. Dührssen [37], I. Duminica [28g], A.E. Dumitriu [28b], M. Dunford [65a], S. Dungs [51], K. Dunne [49a,49b], A. Duperrin [105], H. Duran Yildiz [3a], M. Düren [60], A. Durglishvili [154b], B.L. Dwyer [119], G.I. Dyckes [18a], M. Dyndal [88a], B.S. Dziedzic [37], Z.O. Earnshaw [151], G.H. Eberwein [130], B. Eckerova [29a], S. Eggebrecht [57], E. Egidio Purcino De Souza [85e], L.F. Ehrke [58], G. Eigen [17], K. Einsweiler [18a], T. Ekelof [166], P.A. Ekman [101], S. El Farkh [36b], Y. El Ghazali [64a], H. El Jarrari [37], A. El Moussaouy [36a], V. Ellajosyula [166], M. Ellert [166], F. Ellinghaus [176], N. Ellis [37], J. Elmsheuser [30], M. Elsawy [120a], M. Elsing [37], D. Emeliyanov [138], Y. Enari [86], I. Ene [18a], S. Epari [13], P.A. Erland [89], D. Ernani Martins Neto [89], M. Errenst [176], M. Escalier [68], C. Escobar [168], E. Etzion [156], G. Evans [134a], H. Evans [70], L.S. Evans [98], A. Ezhilov [39], S. Ezzarqtouni [36a], F. Fabbri [24b,24a], L. Fabbri [24b,24a], G. Facini [99], V. Fadeyev [140], R.M. Fakhrutdinov [39], D. Fakoudis [103], S. Falciano [77a], L.F. Falda Ulhoa Coelho [134a], F. Fallavollita [113], G. Falsetti [45b,45a], J. Faltova [137], C. Fan [167], K.Y. Fan [66b], Y. Fan [14], Y. Fang [14,115c], M. Fanti [73a,73b], M. Faraj [71a,71b], Z. Farazpay [100], A. Farbin [8], A. Farilla [79a], T. Farooque [110], J.N. Farr [177], S.M. Farrington [138,54], F. Fassi [36e], D. Fassouliotis [9], M. Faucci Giannelli [78a,78b], W.J. Fawcett [33], L. Fayard [68], P. Federic [137], P. Federicova [135], O.L. Fedin [39,a], M. Feickert [175], L. Feligioni [105], D.E. Fellers [127], C. Feng [64b], Z. Feng [118], M.J. Fenton [163], L. Ferencz [50], R.A.M. Ferguson [94], P. Fernandez Martinez [69], M.J.V. Fernoux [105], J. Ferrando [94], A. Ferrari [166], P. Ferrari [118,117], R. Ferrari [75a], D. Ferrere [58], C. Ferretti [109], M.P. Fewell [1], D. Fiacco [77a,77b], F. Fiedler [103], P. Fiedler [136], S. Filimonov [39], A. Filipčič [96], E.K. Filmer [160a], F. Filthaut [117], M.C.N. Fiolhais [134a,134c,c], L. Fiorini [168], W.C. Fisher [110], T. Fitschen [104], P.M. Fitzhugh [139], I. Fleck [146], P. Fleischmann [109], T. Flick [176], M. Flores [34d,z], L.R. Flores Castillo [66a], L. Flores Sanz De Acedo [37], F.M. Follega [80a,80b], N. Fomin [33], J.H. Foo [159], A. Formica [139], A.C. Forti [104], E. Fortin [37], A.W. Fortman [18a], M.G. Foti [18a], L. Fountas [9,i], D. Fournier [68], H. Fox [94], P. Francavilla [76a,76b], S. Francescato [63], S. Franchellucci [58], M. Franchini [24b,24a], S. Franchino [65a], D. Francis [37], L. Franco [117], V. Franco Lima [37], L. Franconi [50], M. Franklin [63], G. Frattari [27], Y.Y. Frid [156], J. Friend [61], N. Fritzsche [37], A. Froch [58], D. Froidevaux [37], J.A. Frost [130], Y. Fu [64a], S. Fuenzalida Garrido [141f], M. Fujimoto [105], K.Y. Fung [66a], E. Furtado De Simas Filho [85e], M. Furukawa [158], J. Fuster [168], A. Gaa [57], A. Gabrielli [24b,24a], A. Gabrielli [159], P. Gadow [37], G. Gagliardi [59b,59a], L.G. Gagnon [18a], S. Gaid [165], S. Galantzan [156], J. Gallagher [1], E.J. Gallas [130], A.L. Gallen [166], B.J. Gallop [138], K.K. Gan [123], S. Ganguly [158], Y. Gao [54], F.M. Garay Walls [141a,141b], B. Garcia [30], C. García [168], A. Garcia Alonso [118], A.G. Garcia Caffaro [177], J.E. García Navarro [168], M. Garcia-Sciveres [18a], G.L. Gardner [132], R.W. Gardner [41], N. Garelli [162], R.B. Garg [148], J.M. Gargan [54], C.A. Garner [159], C.M. Garvey [34a], V.K. Gassmann [162], G. Gaudio [75a], V. Gautam [13], P. Gauzzi [77a,77b], J. Gavranovic [96], I.L. Gavrilenko [39], A. Gavrilyuk [39], C. Gay [169], G. Gaycken [127], E.N. Gazis [10], A.A. Geanta [28b], A. Gekow [123], C. Gemme [59b], M.H. Genest [62], A.D. Gentry [116], S. George [98], W.F. George [21], T. Geralis [48], A.A. Gerwin [124], P. Gessinger-Befurt [37], M.E. Geyik [176], M. Ghani [172], K. Ghorbanian [97],

A. Ghosal [146], A. Ghosh [163], A. Ghosh [7], B. Giacobbe [24b], S. Giagu [77a,77b], T. Giani [118], A. Giannini [64a], S.M. Gibson [98], M. Gignac [140], D.T. Gil [88b], A.K. Gilbert [88a], B.J. Gilbert [43], D. Gillberg [35], G. Gilles [118], L. Ginabat [131], D.M. Gingrich [2,ac], M.P. Giordani [71a,71c], P.F. Giraud [139], G. Giugliarelli [71a,71c], D. Giugni [73a], F. Giuli [78a,78b], I. Gkialas [9,i], L.K. Gladilin [39], C. Glasman [102], G.R. Gledhill [127], G. Glemža [50], M. Glisic [127], I. Gnesi [45b], Y. Go [30], M. Goblirsch-Kolb [37], B. Gocke [51], D. Godin [111], B. Gokturk [22a], S. Goldfarb [108], T. Golling [58], M.G.D. Gololo [34g], D. Golubkov [39], J.P. Gombas [110], A. Gomes [134a,134b], G. Gomes Da Silva [146], A.J. Gomez Delegido [168], R. Gonçalo [134a], L. Gonella [21], A. Gongadze [154c], F. Gonnella [21], J.L. Gonski [148], R.Y. González Andana [54], S. González de la Hoz [168], R. Gonzalez Lopez [95], C. Gonzalez Renteria [18a], M.V. Gonzalez Rodrigues [50], R. Gonzalez Suarez [166], S. Gonzalez-Sevilla [58], L. Goossens [37], B. Gorini [37], E. Gorini [72a,72b], A. Gorišek [96], T.C. Gosart [132], A.T. Goshaw [53], M.I. Gostkin [40], S. Goswami [125], C.A. Gottardo [37], S.A. Gotz [112], M. Gouighri [36b], V. Goumarre [50], A.G. Goussiou [143], N. Govender [34c], R.P. Grabarczyk [130], I. Grabowska-Bold [88a], K. Graham [35], E. Gramstad [129], S. Grancagnolo [72a,72b], C.M. Grant [1,139], P.M. Gravila [28f], F.G. Gravili [72a,72b], H.M. Gray [18a], M. Greco [72a,72b], M.J. Green [1], C. Grefe [25], A.S. Grefsrud [17], I.M. Gregor [50], K.T. Greif [163], P. Grenier [148], S.G. Grewe [113], A.A. Grillo [140], K. Grimm [32], S. Grinstein [13,t], J.-F. Grivaz [68], E. Gross [174], J. Grosse-Knetter [57], L. Guan [109], J.G.R. Guerrero Rojas [168], G. Guerrieri [37], R. Gugel [103], J.A.M. Guhit [109], A. Guida [19], E. Guilloton [172], S. Guindon [37], F. Guo [14,115c], J. Guo [64c], L. Guo [50], L. Guo [14], Y. Guo [109], A. Gupta [51], R. Gupta [133], S. Gurbuz [25], S.S. Gurdasani [56], G. Gustavino [77a,77b], M. Guth [58], P. Gutierrez [124], L.F. Gutierrez Zagazeta [132], M. Gutsche [52], C. Gutschow [99], C. Gwenlan [130], C.B. Gwilliam [95], E.S. Haaland [129], A. Haas [121], M. Habedank [61], C. Haber [18a], H.K. Hadavand [8], A. Hadef [52], A.I. Hagan [94], J.J. Hahn [146], E.H. Haines [99], M. Haleem [171], J. Haley [125], G.D. Hallewell [105], L. Halser [20], K. Hamano [170], M. Hamer [25], E.J. Hampshire [98], J. Han [64b], L. Han [115a], L. Han [64a], S. Han [18a], Y.F. Han [159], K. Hanagaki [86], M. Hance [140], D.A. Hangal [43], H. Hanif [147], M.D. Hank [132], J.B. Hansen [44], P.H. Hansen [44], D. Harada [58], T. Harenberg [176], S. Harkusha [178], M.L. Harris [106], Y.T. Harris [25], J. Harrison [13], N.M. Harrison [123], P.F. Harrison [172], N.M. Hartman [113], N.M. Hartmann [112], R.Z. Hasan [98,138], Y. Hasegawa [145], F. Haslbeck [130], S. Hassan [17], R. Hauser [110], C.M. Hawkes [21], R.J. Hawkings [37], Y. Hayashi [158], D. Hayden [110], C. Hayes [109], R.L. Hayes [118], C.P. Hays [130], J.M. Hays [97], H.S. Hayward [95], F. He [64a], M. He [14,115c], Y. He [50], Y. He [99], N.B. Heatley [97], V. Hedberg [101], A.L. Heggelund [129], N.D. Hehir [97,*], C. Heidegger [56], K.K. Heidegger [56], J. Heilman [35], S. Heim [50], T. Heim [18a], J.G. Heinlein [132], J.J. Heinrich [127], L. Heinrich [113,aa], J. Hejbal [135], A. Held [175], S. Hellesund [17], C.M. Helling [169], S. Hellman [49a,49b], R.C.W. Henderson [94], L. Henkelmann [33], A.M. Henriques Correia [37], H. Herde [101], Y. Hernández Jiménez [150], L.M. Herrmann [25], T. Herrmann [52], G. Herten [56], R. Hertenberger [112], L. Hervas [37], M.E. Hesping [103], N.P. Hessey [160a], J. Hessler [113], M. Hidaoui [36b], N. Hidic [137], E. Hill [159], S.J. Hillier [21], J.R. Hinds [110], F. Hinterkeuser [25], M. Hirose [128], S. Hirose [161], D. Hirschbuehl [176], T.G. Hitchings [104], B. Hiti [96], J. Hobbs [150], R. Hobincu [28e], N. Hod [174], M.C. Hodgkinson [144], B.H. Hodkinson [130], A. Hoecker [37], D.D. Hofer [109], J. Hofer [168], T. Holm [25], M. Holzbock [37], L.B.A.H. Hommels [33], B.P. Honan [104], J.J. Hong [70], J. Hong [64c], T.M. Hong [133], B.H. Hooberman [167], W.H. Hopkins [6], M.C. Hoppesch [167], Y. Horii [114], M.E. Horstmann [113], S. Hou [153], M.R. Housenga [167], A.S. Howard [96], J. Howarth [61], J. Hoya [6], M. Hrabovsky [126],

A. Hrynevich [50], T. Hryn'ova [4], P.J. Hsu [67], S.-C. Hsu [143], T. Hsu [68], M. Hu [18a], Q. Hu [64a], S. Huang [33], X. Huang [14,115c], Y. Huang [144], Y. Huang [103], Y. Huang [14], Z. Huang [104], Z. Hubacek [136], M. Huebner [25], F. Huegging [25], T.B. Huffman [130], M. Hufnagel Maranha De Faria [85a], C.A. Hugli [50], M. Huhtinen [37], S.K. Huiberts [17], R. Hulsken [107], N. Huseynov [12,f], J. Huston [110], J. Huth [63], R. Hyneman [148], G. Iacobucci [58], G. Iakovidis [30], L. Iconomidou-Fayard [68], J.P. Iddon [37], P. Iengo [74a,74b], R. Iguchi [158], Y. Iiyama [158], T. Iizawa [130], Y. Ikegami [86], D. Iliadis [157], N. Ilic [159], H. Imam [85c], G. Inacio Goncalves [85d], T. Ingebretsen Carlson [49a,49b], J.M. Inglis [97], G. Introzzi [75a,75b], M. Iodice [79a], V. Ippolito [77a,77b], R.K. Irwin [95], M. Ishino [158], W. Islam [175], C. Issever [19], S. Istin [22a,ag], H. Ito [173], R. Iuppa [80a,80b], A. Ivina [174], J.M. Izen [47], V. Izzo [74a], P. Jacka [135], P. Jackson [1], C.S. Jagfeld [112], G. Jain [160a], P. Jain [50], K. Jakobs [56], T. Jakoubek [174], J. Jamieson [61], W. Jang [158], M. Javurkova [106], P. Jawahar [104], L. Jeanty [127], J. Jejelava [154a], P. Jenni [56,e], C.E. Jessiman [35], C. Jia [64b], H. Jia [169], J. Jia [150], X. Jia [14,115c], Z. Jia [115a], C. Jiang [54], S. Jiggins [50], J. Jimenez Pena [13], S. Jin [115a], A. Jinaru [28b], O. Jinnouchi [142], P. Johansson [144], K.A. Johns [7], J.W. Johnson [140], F.A. Jolly [50], D.M. Jones [151], E. Jones [50], K.S. Jones [8], P. Jones [33], R.W.L. Jones [94], T.J. Jones [95], H.L. Joos [57,37], R. Joshi [123], J. Jovicevic [16], X. Ju [18a], J.J. Junggeburth [37], T. Junkermann [65a], A. Juste Rozas [13,t], M.K. Juzek [89], S. Kabana [141e], A. Kaczmarska [89], M. Kado [113], H. Kagan [123], M. Kagan [148], A. Kahn [132], C. Kahra [103], T. Kaji [158], E. Kajomovitz [155], N. Kakati [174], I. Kalaitzidou [56], C.W. Kalderon [30], N.J. Kang [140], D. Kar [34g], K. Karava [130], M.J. Kareem [160b], E. Karentzos [25], O. Karkout [118], S.N. Karpov [40], Z.M. Karpova [40], V. Kartvelishvili [94], A.N. Karyukhin [39], E. Kasimi [157], J. Katzy [50], S. Kaur [35], K. Kawade [145], M.P. Kawale [124], C. Kawamoto [90], T. Kawamoto [64a], E.F. Kay [37], F.I. Kaya [162], S. Kazakos [110], V.F. Kazanin [39], Y. Ke [150], J.M. Keaveney [34a], R. Keeler [170], G.V. Kehris [63], J.S. Keller [35], J.J. Kempster [151], O. Kepka [135], J. Kerr [160b], B.P. Kerridge [138], S. Kersten [176], B.P. Kerševan [96], L. Keszeghova [29a], S. Ketabchi Haghighat [159], R.A. Khan [133], A. Khanov [125], A.G. Kharlamov [39], T. Kharlamova [39], E.E. Khoda [143], M. Kholodenko [134a], T.J. Khoo [19], G. Khoriauli [171], J. Khubua [154b,*], Y.A.R. Khwaira [131], B. Kibirige [34g], D. Kim [6], D.W. Kim [49a,49b], Y.K. Kim [41], N. Kimura [99], M.K. Kingston [57], A. Kirchhoff [57], C. Kirfel [25], F. Kirfel [25], J. Kirk [138], A.E. Kiryunin [113], S. Kita [161], C. Kitsaki [10], O. Kivernyk [25], M. Klassen [162], C. Klein [35], L. Klein [171], M.H. Klein [46], S.B. Klein [58], U. Klein [95], A. Klimentov [30], T. Klioutchnikova [37], P. Kluit [118], S. Kluth [113], E. Kneringer [81], T.M. Knight [159], A. Knue [51], D. Kobylianskii [174], S.F. Koch [130], M. Kocian [148], P. Kodyš [137], D.M. Koeck [127], P.T. Koenig [25], T. Koffas [35], O. Kolay [52], I. Koletsou [4], T. Komarek [89], K. Köneke [57], A.X.Y. Kong [1], T. Kono [122], N. Konstantinidis [99], P. Kontaxakis [58], B. Konya [101], R. Kopeliansky [43], S. Koperny [88a], K. Korcyl [89], K. Kordas [157,d], A. Korn [99], S. Korn [57], I. Korolkov [13], N. Korotkova [39], B. Kortman [118], O. Kortner [113], S. Kortner [113], W.H. Kostecka [119], V.V. Kostyukhin [146], A. Kotsokechagia [37], A. Kotwal [53], A. Koulouris [37], A. Kourkoumeli-Charalampidi [75a,75b], C. Kourkoumelis [9], E. Kourlitis [113,aa], O. Kovanda [127], R. Kowalewski [170], W. Kozanecki [127], A.S. Kozhin [39], V.A. Kramarenko [39], G. Kramberger [96], P. Kramer [25], M.W. Krasny [131], A. Krasznahorkay [37], A.C. Kraus [119], J.W. Kraus [176], J.A. Kremer [50], T. Kresse [52], L. Kretschmann [176], J. Kretzschmar [95], K. Kreul [19], P. Krieger [159], K. Krizka [21], K. Kroeninger [51], H. Kroha [113], J. Kroll [135], J. Kroll [132], K.S. Krowpman [110], U. Kruchonak [40], H. Krüger [25], N. Krumnack [83], M.C. Kruse [53], O. Kuchinskaia [39], S. Kuday [3a], S. Kuehn [37], R. Kuesters [56], T. Kuhl [50], V. Kukhtin [40], Y. Kulchitsky [40],

S. Kuleshov [141d,141b], M. Kumar [34g], N. Kumari [50], P. Kumari [160b], A. Kupco [135], T. Kupfer [51], A. Kupich [39], O. Kuprash [56], H. Kurashige [87], L.L. Kurchaninov [160a], O. Kurdysh [68], Y.A. Kurochkin [38], A. Kurova [39], M. Kuze [142], A.K. Kvam [106], J. Kvita [126], T. Kwan [107], N.G. Kyriacou [109], L.A.O. Laatu [105], C. Lacasta [168], F. Lacava [77a,77b], H. Lacker [19], D. Lacour [131], N.N. Lad [99], E. Ladygin [40], A. Lafarge [42], B. Laforge [131], T. Lagouri [177], F.Z. Lahbabi [36a], S. Lai [57], J.E. Lambert [170], S. Lammers [70], W. Lampl [7], C. Lampoudis [157,d], G. Lamprinoudis [103], A.N. Lancaster [119], E. Lançon [30], U. Landgraf [56], M.P.J. Landon [97], V.S. Lang [56], O.K.B. Langrekken [129], A.J. Lankford [163], F. Lanni [37], K. Lantzsch [25], A. Lanza [75a], M. Lanzac Berrocal [168], J.F. Laporte [139], T. Lari [73a], F. Lasagni Manghi [24b], M. Lassnig [37], V. Latonova [135], S.D. Lawlor [144], Z. Lawrence [104], R. Lazaridou [172], M. Lazzaroni [73a,73b], H.D.M. Le [110], E.M. Le Boulicaut [177], L.T. Le Pottier [18a], B. Leban [24b,24a], A. Lebedev [83], M. LeBlanc [104], F. Ledroit-Guillon [62], S.C. Lee [153], S. Lee [49a,49b], T.F. Lee [95], L.L. Leeuw [34c], M. Lefebvre [170], C. Leggett [18a], G. Lehmann Miotto [37], M. Leigh [58], W.A. Leight [106], W. Leinonen [117], A. Leisos [157,r], M.A.L. Leite [85c], C.E. Leitgeb [19], R. Leitner [137], K.J.C. Leney [46], T. Lenz [25], S. Leone [76a], C. Leonidopoulos [54], A. Leopold [149], R. Les [110], C.G. Lester [33], M. Levchenko [39], J. Levêque [4], L.J. Levinson [174], G. Levrini [24b,24a], M.P. Lewicki [89], C. Lewis [143], D.J. Lewis [4], L. Lewitt [144], A. Li [30], B. Li [64b], C. Li [64a], C-Q. Li [113], H. Li [64a], H. Li [64b], H. Li [115a], H. Li [15], H. Li [64b], J. Li [64c], K. Li [14], L. Li [64c], M. Li [14,115c], S. Li [14,115c], S. Li [64d,64c], T. Li [5], X. Li [107], Z. Li [158], Z. Li [14,115c], Z. Li [64a], S. Liang [14,115c], Z. Liang [14], M. Liberatore [139], B. Liberti [78a], K. Lie [66c], J. Lieber Marin [85e], H. Lien [70], H. Lin [109], K. Lin [110], L. Linden [112], R.E. Lindley [7], J.H. Lindon [2], J. Ling [63], E. Lipeles [132], A. Lipniacka [17], A. Lister [169], J.D. Little [70], B. Liu [14], B.X. Liu [115b], D. Liu [64d,64c], E.H.L. Liu [21], J.B. Liu [64a], J.K.K. Liu [33], K. Liu [64d], K. Liu [64d,64c], M. Liu [64a], M.Y. Liu [64a], P. Liu [14], Q. Liu [64d,143,64c], X. Liu [64a], X. Liu [64b], Y. Liu [115b,115c], Y.L. Liu [64b], Y.W. Liu [64a], S.L. Lloyd [97], E.M. Lobodzinska [50], P. Loch [7], E. Lodhi [159], T. Lohse [19], K. Lohwasser [144], E. Loiacono [50], J.D. Lomas [21], J.D. Long [43], I. Longarini [163], R. Longo [167], I. Lopez Paz [69], A. Lopez Solis [50], N.A. Lopez-canelas [7], N. Lorenzo Martinez [4], A.M. Lory [112], M. Losada [120a], G. Löschcke Centeno [151], O. Loseva [39], X. Lou [49a,49b], X. Lou [14,115c], A. Lounis [68], P.A. Love [94], G. Lu [14,115c], M. Lu [68], S. Lu [132], Y.J. Lu [153], H.J. Lubatti [143], C. Luci [77a,77b], F.L. Lucio Alves [115a], F. Luehring [70], O. Lukianchuk [68], B.S. Lunday [132], O. Lundberg [149], B. Lund-Jensen [149,*], N.A. Luongo [6], M.S. Lutz [37], A.B. Lux [26], D. Lynn [30], R. Lysak [135], E. Lytken [101], V. Lyubushkin [40], T. Lyubushkina [40], M.M. Lyukova [150], M. Firdaus M. Soberi [54], H. Ma [30], K. Ma [64a], L.L. Ma [64b], W. Ma [64a], Y. Ma [125], J.C. MacDonald [103], P.C. Machado De Abreu Farias [85e], R. Madar [42], T. Madula [99], J. Maeda [87], T. Maeno [30], P.T. Mafa [34c], H. Maguire [144], V. Maiboroda [139], A. Maio [134a,134b,134d], K. Maj [88a], O. Majersky [50], S. Majewski [127], N. Makovec [68], V. Maksimovic [16], B. Malaescu [131], Pa. Malecki [89], V.P. Maleev [39], F. Malek [62,m], M. Mali [96], D. Malito [98], U. Mallik [82,*], S. Maltezos [10], S. Malyukov [40], J. Mamuzic [13], G. Mancini [55], M.N. Mancini [27], G. Manco [75a,75b], J.P. Mandalia [97], S.S. Mandarry [151], I. Mandić [96], L. Manhaes de Andrade Filho [85a], I.M. Maniatis [174], J. Manjarres Ramos [92], D.C. Mankad [174], A. Mann [112], S. Manzoni [37], L. Mao [64c], X. Mapekula [34c], A. Marantis [157,r], G. Marchiori [5], M. Marcisovsky [135], C. Marcon [73a], M. Marinescu [21], S. Marium [50], M. Marjanovic [124], A. Markhoos [56], M. Markovitch [68], M.K. Maroun [106], E.J. Marshall [94], Z. Marshall [18a], S. Marti-Garcia [168], J. Martin [99], T.A. Martin [138], V.J. Martin [54], B. Martin dit Latour [17], L. Martinelli [77a,77b], M. Martinez [13,t], P. Martinez Agullo [168], V.I. Martinez Outschoorn [106],

P. Martinez Suarez [13], S. Martin-Haugh [138], G. Martinovicova [137], V.S. Martoiu [28b], A.C. Martyniuk [99], A. Marzin [37], D. Mascione [80a,80b], L. Masetti [103], J. Masik [104], A.L. Maslennikov [39], S.L. Mason [43], P. Massarotti [74a,74b], P. Mastrandrea [76a,76b], A. Mastroberardino [45b,45a], T. Masubuchi [128], T.T. Mathew [127], T. Mathisen [166], J. Matousek [137], D.M. Mattern [51], J. Maurer [28b], T. Maurin [61], A.J. Maury [68], B. Maček [96], D.A. Maximov [39], A.E. May [104], R. Mazini [34g], I. Maznas [119], M. Mazza [110], S.M. Mazza [140], E. Mazzeo [73a,73b], J.P. Mc Gowan [170], S.P. Mc Kee [109], C.A. Mc Lean [6], C.C. McCracken [169], E.F. McDonald [108], A.E. McDougall [118], L.F. Mcelhinney [94], J.A. Mcfayden [151], R.P. McGovern [132], R.P. Mckenzie [34g], T.C. Mclachlan [50], D.J. Mclaughlin [99], S.J. McMahon [138], C.M. Mcpartland [95], R.A. McPherson [170,x], S. Mehlhase [112], A. Mehta [95], D. Melini [168], B.R. Mellado Garcia [34g], A.H. Melo [57], F. Meloni [50], A.M. Mendes Jacques Da Costa [104], H.Y. Meng [159], L. Meng [94], S. Menke [113], M. Mentink [37], E. Meoni [45b,45a], G. Mercado [119], S. Merianos [157], C. Merlassino [71a,71c], L. Merola [74a,74b], C. Meroni [73a,73b], J. Metcalfe [6], A.S. Mete [6], E. Meuser [103], C. Meyer [70], J-P. Meyer [139], R.P. Middleton [138], L. Mijović [54], G. Mikenberg [174], M. Mikestikova [135], M. Mikuž [96], H. Mildner [103], A. Milic [37], D.W. Miller [41], E.H. Miller [148], L.S. Miller [35], A. Milov [174], D.A. Milstead [49a,49b], T. Min [115a], A.A. Minaenko [39], I.A. Minashvili [154b], A.I. Mincer [121], B. Mindur [88a], M. Mineev [40], Y. Mino [90], L.M. Mir [13], M. Miralles Lopez [61], M. Mironova [18a], M.C. Missio [117], A. Mitra [172], V.A. Mitsou [168], Y. Mitsumori [114], O. Miu [159], P.S. Miyagawa [97], T. Mkrtchyan [65a], M. Mlinarevic [99], T. Mlinarevic [99], M. Mlynarikova [37], S. Mobius [20], P. Mogg [112], M.H. Mohamed Farook [116], A.F. Mohammed [14,115c], S. Mohapatra [43], G. Mokgatitswane [34g], L. Moleri [174], B. Mondal [146], S. Mondal [136], K. Mönig [50], E. Monnier [105], L. Monsonis Romero [168], J. Montejo Berlingen [13], A. Montella [49a,49b], M. Montella [123], F. Montereali [79a,79b], F. Monticelli [93], S. Monzani [71a,71c], A. Morancho Tarda [44], N. Morange [68], A.L. Moreira De Carvalho [50], M. Moreno Llácer [168], C. Moreno Martinez [58], J.M. Moreno Perez [23b], P. Morettini [59b], S. Morgenstern [37], M. Morii [63], M. Morinaga [158], M. Moritsu [91], F. Morodei [77a,77b], P. Moschovakos [37], B. Moser [130], M. Mosidze [154b], T. Moskalets [46], P. Moskvitina [117], J. Moss [32,j], P. Moszkowicz [88a], A. Moussa [36d], Y. Moyal [174], E.J.W. Moyse [106], O. Mtintsilana [34g], S. Muanza [105], J. Mueller [133], D. Muenstermann [94], R. Müller [37], G.A. Mullier [166], A.J. Mullin [33], J.J. Mullin [132], A.E. Mulski [63], D.P. Mungo [159], D. Munoz Perez [168], F.J. Munoz Sanchez [104], M. Murin [104], W.J. Murray [172,138], M. Muškinja [96], C. Mwewa [30], A.G. Myagkov [39,a], A.J. Myers [8], G. Myers [109], M. Myska [136], B.P. Nachman [18a], K. Nagai [130], K. Nagano [86], R. Nagasaka [158], J.L. Nagle [30,ae], E. Nagy [105], A.M. Nairz [37], Y. Nakahama [86], K. Nakamura [86], K. Nakkalil [5], H. Nanjo [128], E.A. Narayanan [46], Y. Narukawa [158], I. Naryshkin [39], L. Nasella [73a,73b], S. Nasri [120b], C. Nass [25], G. Navarro [23a], J. Navarro-Gonzalez [168], A. Nayaz [19], P.Y. Nechaeva [39], S. Nechaeva [24b,24a], F. Nechansky [135], L. Nedic [130], T.J. Neep [21], A. Negri [75a,75b], M. Negrini [24b], C. Nellist [118], C. Nelson [107], K. Nelson [109], S. Nemecek [135], M. Nessi [37,g], M.S. Neubauer [167], F. Neuhaus [103], J. Neundorf [50], J. Newell [95], P.R. Newman [21], C.W. Ng [133], Y.W.Y. Ng [50], B. Ngair [120a], H.D.N. Nguyen [111], R.B. Nickerson [130], R. Nicolaidou [139], J. Nielsen [140], M. Niemeyer [57], J. Niermann [37], N. Nikiforou [37], V. Nikolaenko [39,a], I. Nikolic-Audit [131], K. Nikolopoulos [21], P. Nilsson [30], I. Ninca [50], G. Ninio [156], A. Nisati [77a], N. Nishu [2], R. Nisius [113], N. Nitika [71a,71c], J-E. Nitschke [52], E.K. Nkadimeng [34g], T. Nobe [158], T. Nommensen [152], M.B. Norfolk [144], B.J. Norman [35], M. Noury [36a], J. Novak [96], T. Novak [96], L. Novotny [136], R. Novotny [116], L. Nozka [126], K. Ntekas [163], N.M.J. Nunes De Moura Junior [85b], J. Ocariz [131], A. Ochi [87], I. Ochoa [134a], S. Oerdek [50,u], J.T. Offermann [41], A. Ogrodnik [137], A. Oh [104], C.C. Ohm [149],

H. Oide [86], R. Oishi [158], M.L. Ojeda [37], Y. Okumura [158], L.F. Oleiro Seabra [134a], I. Oleksiyuk [58], S.A. Olivares Pino [141d], G. Oliveira Correa [13], D. Oliveira Damazio [30], J.L. Oliver [163], Ö.O. Öncel [56], A.P. O'Neill [20], A. Onofre [134a,134e], P.U.E. Onyisi [11], M.J. Oreglia [41], D. Orestano [79a,79b], N. Orlando [13], R.S. Orr [159], L.M. Osojnak [132], Y. Osumi [114], G. Otero y Garzon [31], H. Otono [91], P.S. Ott [65a], G.J. Ottino [18a], M. Ouchrif [36d], F. Ould-Saada [129], T. Ovsiannikova [143], M. Owen [61], R.E. Owen [138], V.E. Ozcan [22a], F. Ozturk [89], N. Ozturk [8], S. Ozturk [84], H.A. Pacey [130], A. Pacheco Pages [13], C. Padilla Aranda [13], G. Padovano [77a,77b], S. Pagan Griso [18a], G. Palacino [70], A. Palazzo [72a,72b], J. Pampel [25], J. Pan [177], T. Pan [66a], D.K. Panchal [11], C.E. Pandini [118], J.G. Panduro Vazquez [138], H.D. Pandya [1], H. Pang [15], P. Pani [50], G. Panizzo [71a,71c], L. Panwar [131], L. Paolozzi [58], S. Parajuli [167], A. Paramonov [6], C. Paraskevopoulos [55], D. Paredes Hernandez [66b], A. Pareti [75a,75b], K.R. Park [43], T.H. Park [159], M.A. Parker [33], F. Parodi [59b,59a], V.A. Parrish [54], J.A. Parsons [43], U. Parzefall [56], B. Pascual Dias [111], L. Pascual Dominguez [102], E. Pasqualucci [77a], S. Passaggio [59b], F. Pastore [98], P. Patel [89], U.M. Patel [53], J.R. Pater [104], T. Pauly [37], F. Pauwels [137], C.I. Pazos [162], M. Pedersen [129], R. Pedro [134a], S.V. Peleganchuk [39], O. Penc [37], E.A. Pender [54], S. Peng [15], G.D. Penn [177], K.E. Penski [112], M. Penzin [39], B.S. Peralva [85d], A.P. Pereira Peixoto [143], L. Pereira Sanchez [148], D.V. Perepelitsa [30,ae], G. Perera [106], E. Perez Codina [160a], M. Perganti [10], H. Pernegger [37], S. Perrella [77a,77b], O. Perrin [42], K. Peters [50], R.F.Y. Peters [104], B.A. Petersen [37], T.C. Petersen [44], E. Petit [105], V. Petousis [136], C. Petridou [157,d], T. Petru [137], A. Petrukhin [146], M. Pettee [18a], A. Petukhov [84], K. Petukhova [37], R. Pezoa [141f], L. Pezzotti [37], G. Pezzullo [177], A.J. Pfleger [37], T.M. Pham [175], T. Pham [108], P.W. Phillips [138], G. Piacquadio [150], E. Pianori [18a], F. Piazza [127], R. Piegaia [31], D. Pietreanu [28b], A.D. Pilkington [104], M. Pinamonti [71a,71c], J.L. Pinfold [2], B.C. Pinheiro Pereira [134a], J. Pinol Bel [13], A.E. Pinto Pinoargote [139], L. Pintucci [71a,71c], K.M. Piper [151], A. Pirttikoski [58], D.A. Pizzi [35], L. Pizzimento [66b], A. Pizzini [118], M.-A. Pleier [30], V. Pleskot [137], E. Plotnikova [40], G. Poddar [97], R. Poettgen [101], L. Poggioli [131], S. Polacek [137], G. Polesello [75a], A. Poley [147,160a], A. Polini [24b], C.S. Pollard [172], Z.B. Pollock [123], E. Pompa Pacchi [124], N.I. Pond [99], D. Ponomarenko [70], L. Pontecorvo [37], S. Popa [28a], G.A. Popeneciu [28d], A. Poreba [37], D.M. Portillo Quintero [160a], S. Pospisil [136], M.A. Postill [144], P. Postolache [28c], K. Potamianos [172], P.A. Potepa [88a], I.N. Potrap [40], C.J. Potter [33], H. Potti [152], J. Poveda [168], M.E. Pozo Astigarraga [37], A. Prades Ibanez [78a,78b], J. Pretel [170], D. Price [104], M. Primavera [72a], L. Primomo [71a,71c], M.A. Principe Martin [102], R. Privara [126], T. Procter [61], M.L. Proffitt [143], N. Proklova [132], K. Prokofiev [66c], G. Proto [113], J. Proudfoot [6], M. Przybycien [88a], W.W. Przygoda [88b], A. Psallidas [48], J.E. Puddefoot [144], D. Pudzha [56], D. Pyatiizbyantseva [39], J. Qian [109], R. Qian [110], D. Qichen [104], Y. Qin [13], T. Qiu [54], A. Quadt [57], M. Queitsch-Maitland [104], G. Quetant [58], R.P. Quinn [169], G. Rabanal Bolanos [63], D. Rafanoharana [56], F. Raffaeli [78a,78b], F. Ragusa [73a,73b], J.L. Rainbolt [41], J.A. Raine [58], S. Rajagopalan [30], E. Ramakoti [39], L. Rambelli [59b,59a], I.A. Ramirez-Berend [35], K. Ran [50,115c], D.S. Rankin [132], N.P. Rapheeha [34g], H. Rasheed [28b], V. Raskina [131], D.F. Rassloff [65a], A. Rastogi [18a], S. Rave [103], S. Ravera [59b,59a], B. Ravina [57], I. Ravinovich [174], M. Raymond [37], A.L. Read [129], N.P. Readioff [144], D.M. Rebuzzi [75a,75b], G. Redlinger [30], A.S. Reed [113], K. Reeves [27], J.A. Reidelsturz [176], D. Reikher [127], A. Rej [51], C. Rembser [37], M. Renda [28b], F. Renner [50], A.G. Rennie [163], A.L. Rescia [50], S. Resconi [73a], M. Ressegotti [59b,59a], S. Rettie [37], J.G. Reyes Rivera [110], E. Reynolds [18a], O.L. Rezanova [39], P. Reznicek [137], H. Riani [36d], N. Ribaric [53], E. Ricci [80a,80b], R. Richter [113], S. Richter [49a,49b], E. Richter-Was [88b], M. Ridel [131], S. Ridouani [36d],

P. Rieck [121], P. Riedler [37], E.M. Riefel [49a,49b], J.O. Rieger [118], M. Rijssenbeek [150], M. Rimoldi [37], L. Rinaldi [24b,24a], P. Rincke [57,166], T.T. Rinn [30], M.P. Rinnagel [112], G. Ripellino [166], I. Riu [13], J.C. Rivera Vergara [170], F. Rizatdinova [125], E. Rizvi [97], B.R. Roberts [18a], S.S. Roberts [140], S.H. Robertson [107,x], D. Robinson [33], M. Robles Manzano [103], A. Robson [61], A. Rocchi [78a,78b], C. Roda [76a,76b], S. Rodriguez Bosca [37], Y. Rodriguez Garcia [23a], A.M. Rodríguez Vera [119], S. Roe [37], J.T. Roemer [37], O. Røhne [129], R.A. Rojas [106], C.P.A. Roland [131], J. Roloff [30], A. Romaniouk [81], E. Romano [75a,75b], M. Romano [24b], A.C. Romero Hernandez [167], N. Rompotis [95], L. Roos [131], S. Rosati [77a], B.J. Rosser [41], E. Rossi [130], E. Rossi [74a,74b], L.P. Rossi [63], L. Rossini [56], R. Rosten [123], M. Rotaru [28b], B. Rottler [56], C. Rougier [92], D. Rousseau [68], D. Rousso [50], A. Roy [167], S. Roy-Garand [159], A. Rozanov [105], Z.M.A. Rozario [61], Y. Rozen [155], A. Rubio Jimenez [168], V.H. Ruelas Rivera [19], T.A. Ruggeri [1], A. Ruggiero [130], A. Ruiz-Martinez [168], A. Rummler [37], Z. Rurikova [56], N.A. Rusakovich [40], H.L. Russell [170], G. Russo [77a,77b], J.P. Rutherfoord [7], S. Rutherford Colmenares [33], M. Rybar [137], E.B. Rye [129], A. Ryzhov [46], J.A. Sabater Iglesias [58], H.F-W. Sadrozinski [140], F. Safai Tehrani [77a], B. Safarzadeh Samani [138], S. Saha [1], M. Sahinsoy [84], A. Saibel [168], M. Saimpert [139], M. Saito [158], T. Saito [158], A. Sala [73a,73b], D. Salamani [37], A. Salnikov [148], J. Salt [168], A. Salvador Salas [156], D. Salvatore [45b,45a], F. Salvatore [151], A. Salzburger [37], D. Sammel [56], E. Sampson [94], D. Sampsonidis [157,d], D. Sampsonidou [127], J. Sánchez [168], V. Sanchez Sebastian [168], H. Sandaker [129], C.O. Sander [50], J.A. Sandesara [106], M. Sandhoff [176], C. Sandoval [23b], L. Sanfilippo [65a], D.P.C. Sankey [138], T. Sano [90], A. Sansoni [55], L. Santi [37,77b], C. Santoni [42], H. Santos [134a,134b], A. Santra [174], E. Sanzani [24b,24a], K.A. Saoucha [165], J.G. Saraiva [134a,134d], J. Sardain [7], O. Sasaki [86], K. Sato [161], C. Sauer [37], E. Sauvan [4], P. Savard [159,ac], R. Sawada [158], C. Sawyer [138], L. Sawyer [100], C. Sbarra [24b], A. Sbrizzi [24b,24a], T. Scanlon [99], J. Schaarschmidt [143], U. Schäfer [103], A.C. Schaffer [68,46], D. Schaile [112], R.D. Schamberger [150], C. Scharf [19], M.M. Schefer [20], V.A. Schegelsky [39], D. Scheirich [137], M. Schernau [141e], C. Scheulen [58], C. Schiavi [59b,59a], M. Schioppa [45b,45a], B. Schlag [148], S. Schlenker [37], J. Schmeing [176], M.A. Schmidt [176], K. Schmieden [103], C. Schmitt [103], N. Schmitt [103], S. Schmitt [50], L. Schoeffel [139], A. Schoening [65b], P.G. Scholer [35], E. Schopf [130], M. Schott [25], J. Schovancova [37], S. Schramm [58], T. Schroer [58], H-C. Schultz-Coulon [65a], M. Schumacher [56], B.A. Schumm [140], Ph. Schune [139], A.J. Schuy [143], H.R. Schwartz [140], A. Schwartzman [148], T.A. Schwarz [109], Ph. Schwemling [139], R. Schwienhorst [110], F.G. Sciacca [20], A. Sciandra [30], G. Sciolla [27], F. Scuri [76a], C.D. Sebastiani [95], K. Sedlaczek [119], S.C. Seidel [116], A. Seiden [140], B.D. Seidlitz [43], C. Seitz [50], J.M. Seixas [85b], G. Sekhniaidze [74a], L. Selem [62], N. Semprini-Cesari [24b,24a], A. Semushin [178,39], D. Sengupta [58], V. Senthilkumar [168], L. Serin [68], M. Sessa [78a,78b], H. Severini [124], F. Sforza [59b,59a], A. Sfyrla [58], Q. Sha [14], E. Shabalina [57], A.H. Shah [33], R. Shaheen [149], J.D. Shahinian [132], D. Shaked Renous [174], L.Y. Shan [14], M. Shapiro [18a], A. Sharma [37], A.S. Sharma [169], P. Sharma [30], P.B. Shatalov [39], K. Shaw [151], S.M. Shaw [104], Q. Shen [64c], D.J. Sheppard [147], P. Sherwood [99], L. Shi [99], X. Shi [14], S. Shimizu [86], C.O. Shimmin [177], I.P.J. Shipsey [130,*], S. Shirabe [91], M. Shiyakova [40,v], M.J. Shochet [41], D.R. Shope [129], B. Shrestha [124], S. Shrestha [123,af], I. Shreyber [39], M.J. Shroff [170], P. Sicho [135], A.M. Sickles [167], E. Sideras Haddad [34g,164], A.C. Sidley [118], A. Sidoti [24b], F. Siegert [52], Dj. Sijacki [16], F. Sili [93], J.M. Silva [54], I. Silva Ferreira [85b], M.V. Silva Oliveira [30], S.B. Silverstein [49a], S. Simion [68], R. Simoniello [37], E.L. Simpson [104], H. Simpson [151], L.R. Simpson [109], S. Simsek [84], S. Sindhu [57], P. Sinervo [159], S. Singh [30], S. Sinha [50], S. Sinha [104], M. Sioli [24b,24a], I. Siral [37],

E. Sitnikova [50], J. Sjölin [49a,49b], A. Skaf [57], E. Skorda [21], P. Skubic [124], M. Slawinska [89], I. Slazyk [17], V. Smakhtin [174], B.H. Smart [138], S.Yu. Smirnov [39], Y. Smirnov [39], L.N. Smirnova [39,a], O. Smirnova [101], A.C. Smith [43], D.R. Smith [163], E.A. Smith [41], J.L. Smith [104], R. Smith [148], H. Smitmanns [103], M. Smizanska [94], K. Smolek [136], A.A. Snesarev [39], H.L. Snoek [118], S. Snyder [30], R. Sobie [170,x], A. Soffer [156], C.A. Solans Sanchez [37], E.Yu. Soldatov [39], U. Soldevila [168], A.A. Solodkov [39], S. Solomon [27], A. Soloshenko [40], K. Solovieva [56], O.V. Solovyanov [42], P. Sommer [52], A. Sonay [13], W.Y. Song [160b], A. Sopczak [136], A.L. Sopio [54], F. Sopkova [29b], J.D. Sorenson [116], I.R. Sotarriva Alvarez [142], V. Sothilingam [65a], O.J. Soto Sandoval [141c,141b], S. Sottocornola [70], R. Soualah [165], Z. Soumaimi [36e], D. South [50], N. Soybelman [174], S. Spagnolo [72a,72b], M. Spalla [113], D. Sperlich [56], G. Spigo [37], B. Spisso [74a,74b], D.P. Spiteri [61], M. Spousta [137], E.J. Staats [35], R. Stamen [65a], A. Stampekis [21], E. Stanecka [89], W. Stanek-Maslouska [50], M.V. Stange [52], B. Stanislaus [18a], M.M. Stanitzki [50], B. Stapf [50], E.A. Starchenko [39], G.H. Stark [140], J. Stark [92], P. Staroba [135], P. Starovoitov [65a], S. Stärz [107], R. Staszewski [89], G. Stavropoulos [48], A. Stefl [37], P. Steinberg [30], B. Stelzer [147,160a], H.J. Stelzer [133], O. Stelzer-Chilton [160a], H. Stenzel [60], T.J. Stevenson [151], G.A. Stewart [37], J.R. Stewart [125], M.C. Stockton [37], G. Stoicea [28b], M. Stolarski [134a], S. Stonjek [113], A. Straessner [52], J. Strandberg [149], S. Strandberg [49a,49b], M. Stratmann [176], M. Strauss [124], T. Strebler [105], P. Strizenec [29b], R. Ströhmer [171], D.M. Strom [127], R. Stroynowski [46], A. Strubig [49a,49b], S.A. Stucci [30], B. Stugu [17], J. Stupak [124], N.A. Styles [50], D. Su [148], S. Su [64a], W. Su [64d], X. Su [64a], D. Suchy [29a], K. Sugizaki [158], V.V. Sulin [39], M.J. Sullivan [95], D.M.S. Sultan [130], L. Sultanaliyeva [39], S. Sultansoy [3b], T. Sumida [90], S. Sun [175], W. Sun [14], O. Sunneborn Gudnadottir [166], N. Sur [105], M.R. Sutton [151], H. Suzuki [161], M. Svatos [135], M. Swiatlowski [160a], T. Swirski [171], I. Sykora [29a], M. Sykora [137], T. Sykora [137], D. Ta [103], K. Tackmann [50,u], A. Taffard [163], R. Tafirout [160a], J.S. Tafoya Vargas [68], Y. Takubo [86], M. Talby [105], A.A. Talyshev [39], K.C. Tam [66b], N.M. Tamir [156], A. Tanaka [158], J. Tanaka [158], R. Tanaka [68], M. Tanasini [150], Z. Tao [169], S. Tapia Araya [141f], S. Tapprogge [103], A. Tarek Abouelfadl Mohamed [110], S. Tarem [155], K. Tariq [14], G. Tarna [28b], G.F. Tartarelli [73a], M.J. Tartarin [92], P. Tas [137], M. Tasevsky [135], E. Tassi [45b,45a], A.C. Tate [167], G. Tateno [158], Y. Tayalati [36e,w], G.N. Taylor [108], W. Taylor [160b], P. Teixeira-Dias [98], J.J. Teoh [159], K. Terashi [158], J. Terron [102], S. Terzo [13], M. Testa [55], R.J. Teuscher [159,x], A. Thaler [81], O. Theiner [58], T. Theveneaux-Pelzer [105], O. Thielmann [176], D.W. Thomas [98], J.P. Thomas [21], E.A. Thompson [18a], P.D. Thompson [21], E. Thomson [132], R.E. Thornberry [46], C. Tian [64a], Y. Tian [58], V. Tikhomirov [39,a], Yu.A. Tikhonov [39], S. Timoshenko [39], D. Timoshyn [137], E.X.L. Ting [1], P. Tipton [177], A. Tishelman-Charny [30], S.H. Tlou [34g], K. Todome [142], S. Todorova-Nova [137], S. Todt [52], L. Toffolin [71a,71c], M. Togawa [86], J. Tojo [91], S. Tokár [29a], K. Tokushuku [86], O. Toldaiev [70], G. Tolkachev [105], M. Tomoto [86,114], L. Tompkins [148,l], E. Torrence [127], H. Torres [92], E. Torró Pastor [168], M. Toscani [31], C. Tosciri [41], M. Tost [11], D.R. Tovey [144], I.S. Trandafir [28b], T. Trefzger [171], A. Tricoli [30], I.M. Trigger [160a], S. Trincaz-Duvoid [131], D.A. Trischuk [27], B. Trocmé [62], A. Tropina [40], L. Truong [34c], M. Trzebinski [89], A. Trzupek [89], F. Tsai [150], M. Tsai [109], A. Tsiamis [157], P.V. Tsiareshka [40], S. Tsigaridas [160a], A. Tsirigotis [157,r], V. Tsiskaridze [159], E.G. Tskhadadze [154a], M. Tsopoulou [157], Y. Tsujikawa [90], I.I. Tsukerman [39], V. Tsulaia [18a], S. Tsuno [86], K. Tsuri [122], D. Tsybychev [150], Y. Tu [66b], A. Tudorache [28b], V. Tudorache [28b], A.N. Tuna [63], S. Turchikhin [59b,59a], I. Turk Cakir [3a], R. Turra [73a], T. Turtuvshin [40], P.M. Tuts [43], S. Tzamarias [157,d], E. Tzovara [103],

F. Ukegawa [161], P.A. Ulloa Poblete [141c,141b], E.N. Umaka [30], G. Unal [37], A. Undrus [30], G. Unel [163], J. Urban [29b], P. Urrejola [141a], G. Usai [8], R. Ushioda [142], M. Usman [111], F. Ustuner [54], Z. Uysal [84], V. Vacek [136], B. Vachon [107], T. Vafeiadis [37], A. Vaitkus [99], C. Valderanis [112], E. Valdes Santurio [49a,49b], M. Valente [160a], S. Valentinetti [24b,24a], A. Valero [168], E. Valiente Moreno [168], A. Vallier [92], J.A. Valls Ferrer [168], D.R. Van Arneman [118], T.R. Van Daalen [143], A. Van Der Graaf [51], P. Van Gemmeren [6], M. Van Rijnbach [37], S. Van Stroud [99], I. Van Vulpen [118], P. Vana [137], M. Vanadia [78a,78b], U.M. Vande Voorde [149], W. Vandelli [37], E.R. Vandewall [125], D. Vannicola [156], L. Vannoli [55], R. Vari [77a], E.W. Varnes [7], C. Varni [18b], D. Varouchas [68], L. Varriale [168], K.E. Varvell [152], M.E. Vasile [28b], L. Vaslin [86], A. Vasyukov [40], L.M. Vaughan [125], R. Vavricka [103], T. Vazquez Schroeder [37], J. Veatch [32], V. Vecchio [104], M.J. Veen [106], I. Veliscek [30], L.M. Veloce [159], F. Veloso [134a,134c], S. Veneziano [77a], A. Ventura [72a,72b], S. Ventura Gonzalez [139], A. Verbytskyi [113], M. Verducci [76a,76b], C. Vergis [97], M. Verissimo De Araujo [85b], W. Verkerke [118], J.C. Vermeulen [118], C. Vernieri [148], M. Vessella [163], M.C. Vetterli [147,ac], A. Vgenopoulos [103], N. Viaux Maira [141f], T. Vickey [144], O.E. Vickey Boeriu [144], G.H.A. Viehhauser [130], L. Vigani [65b], M. Vigl [113], M. Villa [24b,24a], M. Villaplana Perez [168], E.M. Villhauer [54], E. Vilucchi [55], M.G. Vincter [35], A. Visibile [118], C. Vittori [37], I. Vivarelli [24b,24a], E. Voevodina [113], F. Vogel [112], J.C. Voigt [52], P. Vokac [136], Yu. Volkotrub [88b], E. Von Toerne [25], B. Vormwald [37], V. Vorobel [137], K. Vorobev [39], M. Vos [168], K. Voss [146], M. Vozak [118], L. Vozdecky [124], N. Vranjes [16], M. Vranjes Milosavljevic [16], M. Vreeswijk [118], N.K. Vu [64d], R. Vuillermet [37], O. Vujinovic [103], I. Vukotic [41], I.K. Vyas [35], S. Wada [161], C. Wagner [148], J.M. Wagner [18a], W. Wagner [176], S. Wahdan [176], H. Wahlberg [93], C.H. Waits [124], J. Walder [138], R. Walker [112], W. Walkowiak [146], A. Wall [132], E.J. Wallin [101], T. Wamorkar [6], A.Z. Wang [140], C. Wang [103], C. Wang [11], H. Wang [18a], J. Wang [66c], P. Wang [104], P. Wang [99], R. Wang [63], R. Wang [6], S.M. Wang [153], S. Wang [14], T. Wang [64a], W.T. Wang [82], W. Wang [14], X. Wang [167], X. Wang [64c], Y. Wang [64d], Y. Wang [115a], Y. Wang [64a], Z. Wang [109], Z. Wang [64d,53,64c], Z. Wang [109], A. Warburton [107], R.J. Ward [21], N. Warrack [61], S. Waterhouse [98], A.T. Watson [21], H. Watson [54], M.F. Watson [21], E. Watton [61,138], G. Watts [143], B.M. Waugh [99], J.M. Webb [56], C. Weber [30], H.A. Weber [19], M.S. Weber [20], S.M. Weber [65a], C. Wei [64a], Y. Wei [56], A.R. Weidberg [130], E.J. Weik [121], J. Weingarten [51], C. Weiser [56], C.J. Wells [50], T. Wenaus [30], B. Wendland [51], T. Wengler [37], N.S. Wenke [113], N. Wermes [25], M. Wessels [65a], A.M. Wharton [94], A.S. White [63], A. White [8], M.J. White [1], D. Whiteson [163], L. Wickremasinghe [128], W. Wiedenmann [175], M. Wielers [138], C. Wiglesworth [44], D.J. Wilbern [124], H.G. Wilkens [37], J.J.H. Wilkinson [33], D.M. Williams [43], H.H. Williams [132], S. Williams [33], S. Willocq [106], B.J. Wilson [104], D.J. Wilson [104], P.J. Windischhofer [41], F.I. Winkel [31], F. Winklmeier [127], B.T. Winter [56], J.K. Winter [104], M. Wittgen [148], M. Wobisch [100], T. Wojtkowski [62], Z. Wolffs [118], J. Wollrath [37], M.W. Wolter [89], H. Wolters [134a,134c], M.C. Wong [140], E.L. Woodward [43], S.D. Worm [50], B.K. Wosiek [89], K.W. Woźniak [89], S. Wozniewski [57], K. Wraight [61], C. Wu [21], M. Wu [115b], M. Wu [117], S.L. Wu [175], X. Wu [58], X. Wu [64a], Y. Wu [64a], Z. Wu [4], J. Wuerzinger [113,aa], T.R. Wyatt [104], B.M. Wynne [54], S. Xella [44], L. Xia [115a], M. Xia [15], M. Xie [64a], A. Xiong [127], J. Xiong [18a], D. Xu [14], H. Xu [64a], L. Xu [64a], R. Xu [132], T. Xu [109], Y. Xu [143], Z. Xu [54], Z. Xu [115a], B. Yabsley [152], S. Yacoob [34a], Y. Yamaguchi [86], E. Yamashita [158], H. Yamauchi [161], T. Yamazaki [18a], Y. Yamazaki [87], S. Yan [61], Z. Yan [106], H.J. Yang [64c,64d], H.T. Yang [64a], S. Yang [64a], T. Yang [66c], X. Yang [37], X. Yang [14], Y. Yang [46], Y. Yang [64a], W-M. Yao [18a], H. Ye [57], J. Ye [14], S. Ye [30],

X. Ye [64a], Y. Yeh [99], I. Yeletskikh [40], B. Yeo [18b], M.R. Yexley [99], T.P. Yildirim [130], P. Yin [43], K. Yorita [173], S. Younas [28b], C.J.S. Young [37], C. Young [148], C. Yu [14,115c], Y. Yu [64a], J. Yuan [14,115c], M. Yuan [109], R. Yuan [64d,64c], L. Yue [99], M. Zaazoua [64a], B. Zabinski [89], I. Zahir [36a], E. Zaid [54], Z.K. Zak [89], T. Zakareishvili [168], S. Zambito [58], J.A. Zamora Saa [141d,141b], J. Zang [158], D. Zanzi [56], R. Zanzottera [73a,73b], O. Zaplatilek [136], C. Zeitnitz [176], H. Zeng [14], J.C. Zeng [167], D.T. Zenger Jr [27], O. Zenin [39], T. Ženiš [29a], S. Zenz [97], S. Zerradi [36a], D. Zerwas [68], M. Zhai [14,115c], D.F. Zhang [144], J. Zhang [64b], J. Zhang [6], K. Zhang [14,115c], L. Zhang [64a], L. Zhang [115a], P. Zhang [14,115c], R. Zhang [175], S. Zhang [109], S. Zhang [92], T. Zhang [158], X. Zhang [64c], Y. Zhang [143], Y. Zhang [99], Y. Zhang [115a], Z. Zhang [18a], Z. Zhang [64b], Z. Zhang [68], H. Zhao [143], T. Zhao [64b], Y. Zhao [140], Z. Zhao [64a], Z. Zhao [64a], A. Zhemchugov [40], J. Zheng [115a], K. Zheng [167], X. Zheng [64a], Z. Zheng [148], D. Zhong [167], B. Zhou [109], H. Zhou [7], N. Zhou [64c], Y. Zhou [15], Y. Zhou [115a], Y. Zhou [7], C.G. Zhu [64b], J. Zhu [109], X. Zhu [64d], Y. Zhu [64c], Y. Zhu [64a], X. Zhuang [14], K. Zhukov [70], N.I. Zimine [40], J. Zinsser [65b], M. Ziolkowski [146], L. Živković [16], A. Zoccoli [24b,24a], K. Zoch [63], T.G. Zorbas [144], O. Zormpa [48], W. Zou [43], L. Zwalinski [37]

[1] *Department of Physics, University of Adelaide, Adelaide; Australia*
[2] *Department of Physics, University of Alberta, Edmonton AB; Canada*
[3] [(a)] *Department of Physics, Ankara University, Ankara;* [(b)] *Division of Physics, TOBB University of Economics and Technology, Ankara; Türkiye*
[4] *LAPP, Université Savoie Mont Blanc, CNRS/IN2P3, Annecy; France*
[5] *APC, Université Paris Cité, CNRS/IN2P3, Paris; France*
[6] *High Energy Physics Division, Argonne National Laboratory, Argonne IL; United States of America*
[7] *Department of Physics, University of Arizona, Tucson AZ; United States of America*
[8] *Department of Physics, University of Texas at Arlington, Arlington TX; United States of America*
[9] *Physics Department, National and Kapodistrian University of Athens, Athens; Greece*
[10] *Physics Department, National Technical University of Athens, Zografou; Greece*
[11] *Department of Physics, University of Texas at Austin, Austin TX; United States of America*
[12] *Institute of Physics, Azerbaijan Academy of Sciences, Baku; Azerbaijan*
[13] *Institut de Física d'Altes Energies (IFAE), Barcelona Institute of Science and Technology, Barcelona; Spain*
[14] *Institute of High Energy Physics, Chinese Academy of Sciences, Beijing; China*
[15] *Physics Department, Tsinghua University, Beijing; China*
[16] *Institute of Physics, University of Belgrade, Belgrade; Serbia*
[17] *Department for Physics and Technology, University of Bergen, Bergen; Norway*
[18] [(a)] *Physics Division, Lawrence Berkeley National Laboratory, Berkeley CA;* [(b)] *University of California, Berkeley CA; United States of America*
[19] *Institut für Physik, Humboldt Universität zu Berlin, Berlin; Germany*
[20] *Albert Einstein Center for Fundamental Physics and Laboratory for High Energy Physics, University of Bern, Bern; Switzerland*
[21] *School of Physics and Astronomy, University of Birmingham, Birmingham; United Kingdom*
[22] [(a)] *Department of Physics, Bogazici University, Istanbul;* [(b)] *Department of Physics Engineering, Gaziantep University, Gaziantep;* [(c)] *Department of Physics, Istanbul University, Istanbul; Türkiye*
[23] [(a)] *Facultad de Ciencias y Centro de Investigaciónes, Universidad Antonio Nariño, Bogotá;* [(b)] *Departamento de Física, Universidad Nacional de Colombia, Bogotá; Colombia*
[24] [(a)] *Dipartimento di Fisica e Astronomia A. Righi, Università di Bologna, Bologna;* [(b)] *INFN Sezione di Bologna; Italy*
[25] *Physikalisches Institut, Universität Bonn, Bonn; Germany*
[26] *Department of Physics, Boston University, Boston MA; United States of America*
[27] *Department of Physics, Brandeis University, Waltham MA; United States of America*
[28] [(a)] *Transilvania University of Brasov, Brasov;* [(b)] *Horia Hulubei National Institute of Physics and Nuclear Engineering, Bucharest;* [(c)] *Department of Physics, Alexandru Ioan Cuza University of Iasi, Iasi;* [(d)] *National Institute for Research and Development of Isotopic and Molecular Technologies, Physics Department, Cluj-Napoca;* [(e)] *National University of Science and Technology Politechnica, Bucharest;* [(f)] *West University in Timisoara, Timisoara;* [(g)] *Faculty of Physics, University of Bucharest, Bucharest; Romania*
[29] [(a)] *Faculty of Mathematics, Physics and Informatics, Comenius University, Bratislava;* [(b)] *Department of Subnuclear Physics, Institute of Experimental Physics of the Slovak Academy of Sciences, Kosice; Slovak Republic*
[30] *Physics Department, Brookhaven National Laboratory, Upton NY; United States of America*
[31] *Universidad de Buenos Aires, Facultad de Ciencias Exactas y Naturales, Departamento de Física, y CONICET, Instituto de Física de Buenos Aires (IFIBA), Buenos Aires; Argentina*
[32] *California State University, CA; United States of America*
[33] *Cavendish Laboratory, University of Cambridge, Cambridge; United Kingdom*
[34] [(a)] *Department of Physics, University of Cape Town, Cape Town;* [(b)] *iThemba Labs, Western Cape;* [(c)] *Department of Mechanical Engineering Science, University of Johannesburg, Johannesburg;* [(d)] *National Institute of Physics, University of the Philippines Diliman (Philippines);* [(e)] *University of South Africa, Department of Physics, Pretoria;* [(f)] *University of Zululand, KwaDlangezwa;* [(g)] *School of Physics, University of the Witwatersrand, Johannesburg; South Africa*
[35] *Department of Physics, Carleton University, Ottawa ON; Canada*
[36] [(a)] *Faculté des Sciences Ain Chock, Université Hassan II de Casablanca;* [(b)] *Faculté des Sciences, Université Ibn-Tofail, Kénitra;* [(c)] *Faculté des Sciences Semlalia, Université Cadi Ayyad, LPHEA-Marrakech;* [(d)] *LPMR, Faculté des Sciences, Université Mohamed Premier, Oujda;* [(e)] *Faculté des sciences, Université Mohammed V, Rabat;* [(f)] *Institute of Applied Physics, Mohammed VI Polytechnic University, Ben Guerir; Morocco*
[37] *CERN, Geneva; Switzerland*
[38] *Affiliated with an institute formerly covered by a cooperation agreement with CERN*
[39] *Affiliated with an institute covered by a cooperation agreement with CERN*
[40] *Affiliated with an international laboratory covered by a cooperation agreement with CERN*
[41] *Enrico Fermi Institute, University of Chicago, Chicago IL; United States of America*
[42] *LPC, Université Clermont Auvergne, CNRS/IN2P3, Clermont-Ferrand; France*
[43] *Nevis Laboratory, Columbia University, Irvington NY; United States of America*
[44] *Niels Bohr Institute, University of Copenhagen, Copenhagen; Denmark*
[45] [(a)] *Dipartimento di Fisica, Università della Calabria, Rende;* [(b)] *INFN Gruppo Collegato di Cosenza, Laboratori Nazionali di Frascati; Italy*
[46] *Physics Department, Southern Methodist University, Dallas TX; United States of America*

[47] Physics Department, University of Texas at Dallas, Richardson TX; United States of America
[48] National Centre for Scientific Research "Demokritos", Agia Paraskevi; Greece
[49] [(a)] Department of Physics, Stockholm University; [(b)] Oskar Klein Centre, Stockholm; Sweden
[50] Deutsches Elektronen-Synchrotron DESY, Hamburg and Zeuthen; Germany
[51] Fakultät Physik, Technische Universität Dortmund, Dortmund; Germany
[52] Institut für Kern- und Teilchenphysik, Technische Universität Dresden, Dresden; Germany
[53] Department of Physics, Duke University, Durham NC; United States of America
[54] SUPA - School of Physics and Astronomy, University of Edinburgh, Edinburgh; United Kingdom
[55] INFN e Laboratori Nazionali di Frascati, Frascati; Italy
[56] Physikalisches Institut, Albert-Ludwigs-Universität Freiburg, Freiburg; Germany
[57] II. Physikalisches Institut, Georg-August-Universität Göttingen, Göttingen; Germany
[58] Département de Physique Nucléaire et Corpusculaire, Université de Genève, Genève; Switzerland
[59] [(a)] Dipartimento di Fisica, Università di Genova, Genova; [(b)] INFN Sezione di Genova; Italy
[60] II. Physikalisches Institut, Justus-Liebig-Universität Giessen, Giessen; Germany
[61] SUPA - School of Physics and Astronomy, University of Glasgow, Glasgow; United Kingdom
[62] LPSC, Université Grenoble Alpes, CNRS/IN2P3, Grenoble INP, Grenoble; France
[63] Laboratory for Particle Physics and Cosmology, Harvard University, Cambridge MA; United States of America
[64] [(a)] Department of Modern Physics and State Key Laboratory of Particle Detection and Electronics, University of Science and Technology of China, Hefei; [(b)] Institute of Frontier and Interdisciplinary Science and Key Laboratory of Particle Physics and Particle Irradiation (MOE), Shandong University, Qingdao; [(c)] School of Physics and Astronomy, Shanghai Jiao Tong University, Key Laboratory for Particle Astrophysics and Cosmology (MOE), SKLPPC, Shanghai; [(d)] Tsung-Dao Lee Institute, Shanghai; [(e)] School of Physics, Zhengzhou University; China
[65] [(a)] Kirchhoff-Institut für Physik, Ruprecht-Karls-Universität Heidelberg, Heidelberg; [(b)] Physikalisches Institut, Ruprecht-Karls-Universität Heidelberg, Heidelberg; Germany
[66] [(a)] Department of Physics, Chinese University of Hong Kong, Shatin, N.T., Hong Kong; [(b)] Department of Physics, University of Hong Kong, Hong Kong; [(c)] Department of Physics and Institute for Advanced Study, Hong Kong University of Science and Technology, Clear Water Bay, Kowloon, Hong Kong; China
[67] Department of Physics, National Tsing Hua University, Hsinchu; Taiwan
[68] IJCLab, Université Paris-Saclay, CNRS/IN2P3, 91405, Orsay; France
[69] Centro Nacional de Microelectrónica (IMB-CNM-CSIC), Barcelona; Spain
[70] Department of Physics, Indiana University, Bloomington IN; United States of America
[71] [(a)] INFN Gruppo Collegato di Udine, Sezione di Trieste, Udine; [(b)] ICTP, Trieste; [(c)] Dipartimento Politecnico di Ingegneria e Architettura, Università di Udine, Udine; Italy
[72] [(a)] INFN Sezione di Lecce; [(b)] Dipartimento di Matematica e Fisica, Università del Salento, Lecce; Italy
[73] [(a)] INFN Sezione di Milano; [(b)] Dipartimento di Fisica, Università di Milano, Milano; Italy
[74] [(a)] INFN Sezione di Napoli; [(b)] Dipartimento di Fisica, Università di Napoli, Napoli; Italy
[75] [(a)] INFN Sezione di Pavia; [(b)] Dipartimento di Fisica, Università di Pavia, Pavia; Italy
[76] [(a)] INFN Sezione di Pisa; [(b)] Dipartimento di Fisica E. Fermi, Università di Pisa, Pisa; Italy
[77] [(a)] INFN Sezione di Roma; [(b)] Dipartimento di Fisica, Sapienza Università di Roma, Roma; Italy
[78] [(a)] INFN Sezione di Roma Tor Vergata; [(b)] Dipartimento di Fisica, Università di Roma Tor Vergata, Roma; Italy
[79] [(a)] INFN Sezione di Roma Tre; [(b)] Dipartimento di Matematica e Fisica, Università Roma Tre, Roma; Italy
[80] [(a)] INFN-TIFPA; [(b)] Università degli Studi di Trento, Trento; Italy
[81] Universität Innsbruck, Department of Astro and Particle Physics, Innsbruck; Austria
[82] University of Iowa, Iowa City IA; United States of America
[83] Department of Physics and Astronomy, Iowa State University, Ames IA; United States of America
[84] Istinye University, Sariyer, Istanbul; Türkiye
[85] [(a)] Departamento de Engenharia Elétrica, Universidade Federal de Juiz de Fora (UFJF), Juiz de Fora; [(b)] Universidade Federal do Rio De Janeiro COPPE/EE/IF, Rio de Janeiro; [(c)] Instituto de Física, Universidade de São Paulo, São Paulo; [(d)] Rio de Janeiro State University, Rio de Janeiro; [(e)] Federal University of Bahia, Bahia; Brazil
[86] KEK, High Energy Accelerator Research Organization, Tsukuba; Japan
[87] Graduate School of Science, Kobe University, Kobe; Japan
[88] [(a)] AGH University of Krakow, Faculty of Physics and Applied Computer Science, Krakow; [(b)] Marian Smoluchowski Institute of Physics, Jagiellonian University, Krakow; Poland
[89] Institute of Nuclear Physics Polish Academy of Sciences, Krakow; Poland
[90] Faculty of Science, Kyoto University, Kyoto; Japan
[91] Research Center for Advanced Particle Physics and Department of Physics, Kyushu University, Fukuoka; Japan
[92] L2IT, Université de Toulouse, CNRS/IN2P3, UPS, Toulouse; France
[93] Instituto de Física La Plata, Universidad Nacional de La Plata and CONICET, La Plata; Argentina
[94] Physics Department, Lancaster University, Lancaster; United Kingdom
[95] Oliver Lodge Laboratory, University of Liverpool, Liverpool; United Kingdom
[96] Department of Experimental Particle Physics, Jožef Stefan Institute and Department of Physics, University of Ljubljana, Ljubljana; Slovenia
[97] School of Physics and Astronomy, Queen Mary University of London, London; United Kingdom
[98] Department of Physics, Royal Holloway University of London, Egham; United Kingdom
[99] Department of Physics and Astronomy, University College London, London; United Kingdom
[100] Louisiana Tech University, Ruston LA; United States of America
[101] Fysiska institutionen, Lunds universitet, Lund; Sweden
[102] Departamento de Física Teorica C-15 and CIAFF, Universidad Autónoma de Madrid, Madrid; Spain
[103] Institut für Physik, Universität Mainz, Mainz; Germany
[104] School of Physics and Astronomy, University of Manchester, Manchester; United Kingdom
[105] CPPM, Aix-Marseille Université, CNRS/IN2P3, Marseille; France
[106] Department of Physics, University of Massachusetts, Amherst MA; United States of America
[107] Department of Physics, McGill University, Montreal QC; Canada
[108] School of Physics, University of Melbourne, Victoria; Australia
[109] Department of Physics, University of Michigan, Ann Arbor MI; United States of America
[110] Department of Physics and Astronomy, Michigan State University, East Lansing MI; United States of America
[111] Group of Particle Physics, University of Montreal, Montreal QC; Canada
[112] Fakultät für Physik, Ludwig-Maximilians-Universität München, München; Germany
[113] Max-Planck-Institut für Physik (Werner-Heisenberg-Institut), München; Germany
[114] Graduate School of Science and Kobayashi-Maskawa Institute, Nagoya University, Nagoya; Japan
[115] [(a)] Department of Physics, Nanjing University, Nanjing; [(b)] School of Science, Shenzhen Campus of Sun Yat-sen University; [(c)] University of Chinese Academy of Science (UCAS), Beijing; China
[116] Department of Physics and Astronomy, University of New Mexico, Albuquerque NM; United States of America
[117] Institute for Mathematics, Astrophysics and Particle Physics, Radboud University/Nikhef, Nijmegen; Netherlands
[118] Nikhef National Institute for Subatomic Physics and University of Amsterdam, Amsterdam; Netherlands
[119] Department of Physics, Northern Illinois University, DeKalb IL; United States of America
[120] [(a)] New York University Abu Dhabi, Abu Dhabi; [(b)] United Arab Emirates University, Al Ain; United Arab Emirates
[121] Department of Physics, New York University, New York NY; United States of America
[122] Ochanomizu University, Otsuka, Bunkyo-ku, Tokyo; Japan

[123] Ohio State University, Columbus OH; United States of America
[124] Homer L. Dodge Department of Physics and Astronomy, University of Oklahoma, Norman OK; United States of America
[125] Department of Physics, Oklahoma State University, Stillwater OK; United States of America
[126] Palacký University, Joint Laboratory of Optics, Olomouc; Czech Republic
[127] Institute for Fundamental Science, University of Oregon, Eugene, OR; United States of America
[128] Graduate School of Science, Osaka University, Osaka; Japan
[129] Department of Physics, University of Oslo, Oslo; Norway
[130] Department of Physics, Oxford University, Oxford; United Kingdom
[131] LPNHE, Sorbonne Université, Université Paris Cité, CNRS/IN2P3, Paris; France
[132] Department of Physics, University of Pennsylvania, Philadelphia PA; United States of America
[133] Department of Physics and Astronomy, University of Pittsburgh, Pittsburgh PA; United States of America
[134] [(a)] Laboratório de Instrumentação e Física Experimental de Partículas - LIP, Lisboa; [(b)] Departamento de Física, Faculdade de Ciências, Universidade de Lisboa, Lisboa; [(c)] Departamento de Física, Universidade de Coimbra, Coimbra; [(d)] Centro de Física Nuclear da Universidade de Lisboa, Lisboa; [(e)] Departamento de Física, Universidade do Minho, Braga; [(f)] Departamento de Física Teórica y del Cosmos, Universidad de Granada, Granada (Spain); [(g)] Departamento de Física, Instituto Superior Técnico, Universidade de Lisboa, Lisboa; Portugal
[135] Institute of Physics of the Czech Academy of Sciences, Prague; Czech Republic
[136] Czech Technical University in Prague, Prague; Czech Republic
[137] Charles University, Faculty of Mathematics and Physics, Prague; Czech Republic
[138] Particle Physics Department, Rutherford Appleton Laboratory, Didcot; United Kingdom
[139] IRFU, CEA, Université Paris-Saclay, Gif-sur-Yvette; France
[140] Santa Cruz Institute for Particle Physics, University of California Santa Cruz, Santa Cruz CA; United States of America
[141] [(a)] Departamento de Física, Pontificia Universidad Católica de Chile, Santiago; [(b)] Millennium Institute for Subatomic physics at high energy frontier (SAPHIR), Santiago; [(c)] Instituto de Investigación Multidisciplinario en Ciencia y Tecnología, y Departamento de Física, Universidad de La Serena; [(d)] Universidad Andres Bello, Department of Physics, Santiago; [(e)] Instituto de Alta Investigación, Universidad de Tarapacá, Arica; [(f)] Departamento de Física, Universidad Técnica Federico Santa María, Valparaíso; Chile
[142] Department of Physics, Institute of Science, Tokyo; Japan
[143] Department of Physics, University of Washington, Seattle WA; United States of America
[144] Department of Physics and Astronomy, University of Sheffield, Sheffield; United Kingdom
[145] Department of Physics, Shinshu University, Nagano; Japan
[146] Department Physik, Universität Siegen, Siegen; Germany
[147] Department of Physics, Simon Fraser University, Burnaby BC; Canada
[148] SLAC National Accelerator Laboratory, Stanford CA; United States of America
[149] Department of Physics, Royal Institute of Technology, Stockholm; Sweden
[150] Departments of Physics and Astronomy, Stony Brook University, Stony Brook NY; United States of America
[151] Department of Physics and Astronomy, University of Sussex, Brighton; United Kingdom
[152] School of Physics, University of Sydney, Sydney; Australia
[153] Institute of Physics, Academia Sinica, Taipei; Taiwan
[154] [(a)] E. Andronikashvili Institute of Physics, Iv. Javakhishvili Tbilisi State University, Tbilisi; [(b)] High Energy Physics Institute, Tbilisi State University, Tbilisi; [(c)] University of Georgia, Tbilisi; Georgia
[155] Department of Physics, Technion, Israel Institute of Technology, Haifa; Israel
[156] Raymond and Beverly Sackler School of Physics and Astronomy, Tel Aviv University, Tel Aviv; Israel
[157] Department of Physics, Aristotle University of Thessaloniki, Thessaloniki; Greece
[158] International Center for Elementary Particle Physics and Department of Physics, University of Tokyo, Tokyo; Japan
[159] Department of Physics, University of Toronto, Toronto ON; Canada
[160] [(a)] TRIUMF, Vancouver BC; [(b)] Department of Physics and Astronomy, York University, Toronto ON; Canada
[161] Division of Physics and Tomonaga Center for the History of the Universe, Faculty of Pure and Applied Sciences, University of Tsukuba, Tsukuba; Japan
[162] Department of Physics and Astronomy, Tufts University, Medford MA; United States of America
[163] Department of Physics and Astronomy, University of California Irvine, Irvine CA; United States of America
[164] University of West Attica, Athens; Greece
[165] University of Sharjah, Sharjah; United Arab Emirates
[166] Department of Physics and Astronomy, University of Uppsala, Uppsala; Sweden
[167] Department of Physics, University of Illinois, Urbana IL; United States of America
[168] Instituto de Física Corpuscular (IFIC), Centro Mixto Universidad de Valencia - CSIC, Valencia; Spain
[169] Department of Physics, University of British Columbia, Vancouver BC; Canada
[170] Department of Physics and Astronomy, University of Victoria, Victoria BC; Canada
[171] Fakultät für Physik und Astronomie, Julius-Maximilians-Universität Würzburg, Würzburg; Germany
[172] Department of Physics, University of Warwick, Coventry; United Kingdom
[173] Waseda University, Tokyo; Japan
[174] Department of Particle Physics and Astrophysics, Weizmann Institute of Science, Rehovot; Israel
[175] Department of Physics, University of Wisconsin, Madison WI; United States of America
[176] Fakultät für Mathematik und Naturwissenschaften, Fachgruppe Physik, Bergische Universität Wuppertal, Wuppertal; Germany
[177] Department of Physics, Yale University, New Haven CT; United States of America
[178] Yerevan Physics Institute, Yerevan; Armenia

[a] Also Affiliated with an institute covered by a cooperation agreement with CERN.
[b] Also at An-Najah National University, Nablus; Palestine.
[c] Also at Borough of Manhattan Community College, City University of New York, New York NY; United States of America.
[d] Also at Center for Interdisciplinary Research and Innovation (CIRI-AUTH), Thessaloniki; Greece.
[e] Also at CERN, Geneva; Switzerland.
[f] Also at CMD-AC UNEC Research Center, Azerbaijan State University of Economics (UNEC); Azerbaijan.
[g] Also at Département de Physique Nucléaire et Corpusculaire, Université de Genève, Genève; Switzerland.
[h] Also at Departament de Fisica de la Universitat Autonoma de Barcelona, Barcelona; Spain.
[i] Also at Department of Financial and Management Engineering, University of the Aegean, Chios; Greece.
[j] Also at Department of Physics, California State University, Sacramento; United States of America.
[k] Also at Department of Physics, King's College London, London; United Kingdom.
[l] Also at Department of Physics, Stanford University, Stanford CA; United States of America.
[m] Also at Department of Physics, Stellenbosch University; South Africa.
[n] Also at Department of Physics, University of Fribourg, Fribourg; Switzerland.
[o] Also at Department of Physics, University of Thessaly; Greece.
[p] Also at Department of Physics, Westmont College, Santa Barbara; United States of America.
[q] Also at Faculty of Physics, Sofia University, 'St. Kliment Ohridski', Sofia; Bulgaria.
[r] Also at Hellenic Open University, Patras; Greece.

[s] Also at Imam Mohammad Ibn Saud Islamic University; Saudi Arabia.
[t] Also at Institucio Catalana de Recerca i Estudis Avancats, ICREA, Barcelona; Spain.
[u] Also at Institut für Experimentalphysik, Universität Hamburg, Hamburg; Germany.
[v] Also at Institute for Nuclear Research and Nuclear Energy (INRNE) of the Bulgarian Academy of Sciences, Sofia; Bulgaria.
[w] Also at Institute of Applied Physics, Mohammed VI Polytechnic University, Ben Guerir; Morocco.
[x] Also at Institute of Particle Physics (IPP); Canada.
[y] Also at Institute of Physics, Azerbaijan Academy of Sciences, Baku; Azerbaijan.
[z] Also at National Institute of Physics, University of the Philippines Diliman (Philippines); Philippines.
[aa] Also at Technical University of Munich, Munich; Germany.
[ab] Also at The Collaborative Innovation Center of Quantum Matter (CICQM), Beijing; China.
[ac] Also at TRIUMF, Vancouver BC; Canada.
[ad] Also at Università di Napoli Parthenope, Napoli; Italy.
[ae] Also at University of Colorado Boulder, Department of Physics, Colorado; United States of America.
[af] Also at Washington College, Chestertown, MD; United States of America.
[ag] Also at Yeditepe University, Physics Department, Istanbul; Türkiye.
[*] Deceased.

Eur. Phys. J. C (2025) 85:886
https://doi.org/10.1140/epjc/s10052-025-14507-0

THE EUROPEAN PHYSICAL JOURNAL C

Regular Article - Experimental Physics

Search for a new pseudoscalar decaying into a pair of bottom and antibottom quarks in top-associated production in $\sqrt{s} = 13$ TeV proton–proton collisions with the ATLAS detector

ATLAS Collaboration[⋆]

CERN, 1211 Geneva 23, Switzerland

Received: 24 March 2025 / Accepted: 10 July 2025

Abstract A search for a pseudoscalar a produced in association with a top-quark pair, or in association with a single top quark plus a W boson, with the pseudoscalar decaying into b-quarks ($a \to b\bar{b}$), is performed using the full Run 2 data sample using a dileptonic decay mode signature. The search covers pseudoscalar boson masses between 12 and 100 GeV and involves both the kinematic regime where the decay products of the pseudoscalar are reconstructed as two standard b-tagged small-radius jets, or merged into a large-radius jet due to its Lorentz boost. No significant excess relative to expectations is observed. Assuming a branching ratio BR($a \to b\bar{b}$) = 100%, the range of pseudoscalar masses between 50 and 80 GeV is excluded at 95% confidence level for a coupling of the pseudoscalar to the top quark of 0.5, while a coupling of 1.0 is excluded at 95% confidence level for the masses considered, with the coupling defined as the strength modifier of the Standard Model Yukawa coupling.

Contents

1 Introduction

Since the discovery of the Higgs boson [1,2], there is an ongoing effort at the Large Hadron Collider (LHC) [3] to measure its properties and search for new physics. The Higgs boson was discovered by observing few decay modes [1,2] consistent with the Standard Model (SM) predictions. Part of the interest is about the nature of the discovered particle and whether it is the single boson predicted by the SM or, alternatively, part of an extended Higgs sector as suggested by models such as the two-Higgs-doublet model (2HDM) [4,5], which can be embedded into supersymmetric models [6–11]. It predicts a total of five bosons: a light (h) and a heavy (H) CP-even Higgs boson, with the light one corresponding to the observed Higgs boson; two charged Higgs bosons (H^+ and H^-); and a CP-odd particle (a), also referred to as pseudoscalar. The additional scalar/pseudoscalar states of these models may also provide a portal into dark matter, serving as a mediator between the SM and dark matter sector [12,13]. A pseudoscalar a is also be predicted in axion models [14].

This analysis performs a search for a light pseudoscalar with a mass smaller than the SM Higgs boson, produced in association either with a top-quark pair or a single top quark and a W boson, where the pseudoscalar decays into a bottom-antibottom quark pair, as proposed in [15]. It is based on a simplified model with the following Yukawa lagrangian:

$$\mathcal{L} = -\frac{g_t y_t}{\sqrt{2}} a\bar{t}(i\gamma^5)t - \frac{g_b y_b}{\sqrt{2}} a\bar{b}(i\gamma^5)b,$$

⋆ e-mail: atlas.publications@cern.ch

Published online: 19 August 2025

where $y_j/\sqrt{2} = m_j/v$ is the SM Yukawa coupling of particle j to the pseudoscalar a and g_j is the coupling modifier, with $j = t$ or b. Figure 1 shows two example Feynman diagrams for this process. This decay channel is favoured by many models for the range of explored pseudoscalar masses, $m_a < m_h$, although the branching ratios of the pseudoscalar depend on the specific model parameters. This is the first search for this process, exploring the couplings of the pseudoscalar to bottom quarks. Previously, the ATLAS and CMS Collaborations performed similar searches of $t\bar{t}a$ associated production exploiting leptonic decays of the pseudoscalar. The CMS Collaboration studied the decay of a pseudoscalar to the three families of leptons [16], while the ATLAS Collaboration studied the pseudoscalar coupling to muons [17]. None of these searches found significant excesses, but these decay channels are typically disfavoured compared with the $b\bar{b}$ decays when assuming a Yukawa coupling.

The search is performed in the dileptonic decay channel, with both top and antitop quarks (or both W bosons) decaying leptonically. Despite the reduced branching ratio of this decay channel, the reduced jet multiplicity of the final state and the precisely measured kinematics of the two leptons allow for a more efficient identification of the b-jets originating from the top and antitop quark decays than its semileptonic (with only one W boson from either the top or antitop quarks decaying leptonically) or fully hadronic (with the two W bosons decaying hadronically) counterparts.

For masses of the pseudoscalar below ∼30 GeV, the $b\bar{b}$ pair has a large Lorentz-boost and is thus reconstructed as a single large-radius jet. On the other hand, for higher masses, the jets are well separated at detector level. The analysis is designed to exploit both kinematic regimes to have good signal sensitivity, making use of multiple signal regions, reconstructed objects, and machine learning techniques.

2 ATLAS detector

The ATLAS detector [18] at the LHC covers nearly the entire solid angle around the collision point.[1] It consists of an inner tracking detector surrounded by a thin superconducting solenoid, electromagnetic and hadronic calorimeters, and a muon spectrometer incorporating three large superconducting air-core toroidal magnetic systems.

The inner-detector system (ID) is immersed in a 2 T axial magnetic field and provides charged-particle tracking in the range of $|\eta| < 2.5$. The high-granularity silicon pixel detector covers the vertex region and typically provides four measurements per track, the first hit generally being in the insertable B-layer installed before Run 2 [19,20]. It is followed by the SemiConductor Tracker, which usually provides eight measurements per track. These silicon detectors are complemented by the transition radiation tracker (TRT), which enables radially extended track reconstruction up to $|\eta| = 2.0$. The TRT also provides electron identification information based on the fraction of hits (typically 30 in total) above a higher energy-deposit threshold corresponding to transition radiation.

The calorimeter system covers the pseudorapidity range $|\eta| < 4.9$. Within the region $|\eta| < 3.2$, electromagnetic calorimetry is provided by barrel and endcap high-granularity lead/liquid-argon (LAr) calorimeters, with an additional thin LAr presampler covering $|\eta| < 1.8$ to correct for energy loss in material upstream of the calorimeters. Hadronic calorimetry is provided by the steel/scintillator-tile calorimeter, segmented into three barrel structures within $|\eta| < 1.7$, and two copper/LAr hadronic endcap calorimeters. The solid angle coverage is completed with forward copper/LAr and tungsten/LAr calorimeter modules optimised for electromagnetic and hadronic energy measurements respectively.

The muon spectrometer comprises separate trigger and high-precision tracking chambers measuring the deflection of muons in a magnetic field generated by the superconducting air-core toroidal magnets. The field integral of the toroids ranges between 2.0 and 6.0 Tm across most of the detector. Three layers of precision chambers, each consisting of layers of monitored drift tubes, cover the region $|\eta| < 2.7$, complemented by cathode-strip chambers in the forward region, where the background is highest. The muon trigger system covers the range $|\eta| < 2.4$ with resistive-plate chambers in the barrel, and thin-gap chambers in the endcap regions.

The luminosity is measured mainly by the LUCID-2 [21] detector that records Cherenkov light produced in the quartz windows of photomultipliers located close to the beampipe.

Events are selected by the first-level trigger system implemented in custom hardware, followed by selections made by algorithms implemented in software in the high-level trigger [22]. The first-level trigger accepts events from the 40 MHz bunch crossings at a rate below 100 kHz, which the high-level trigger further reduces to record complete events to disk at about 1 kHz.

A software suite [23] is used in data simulation, in the reconstruction and analysis of real and simulated data, in detector operations, and in the trigger and data acquisition systems of the experiment.

[1] ATLAS uses a right-handed coordinate system with its origin at the nominal interaction point (IP) in the centre of the detector and the z-axis along the beam pipe. The x-axis points from the IP to the centre of the LHC ring, and the y-axis points upwards. Polar coordinates (r, ϕ) are used in the transverse plane, ϕ being the azimuthal angle around the z-axis. The pseudorapidity is defined in terms of the polar angle θ as $\eta = -\ln\tan(\theta/2)$ and is equal to the rapidity $y = \frac{1}{2}\ln\left(\frac{E+p_z c}{E-p_z c}\right)$ in the relativistic limit. Angular distance is measured in units of $\Delta R \equiv \sqrt{(\Delta y)^2 + (\Delta\phi)^2}$.

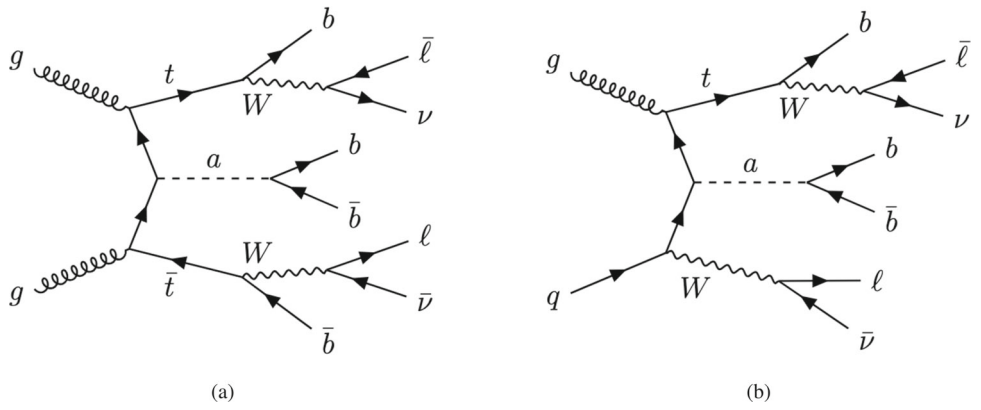

Fig. 1 Feynman diagrams for (**a**) $t\bar{t}$- and (**b**) tW-associated production of a pseudoscalar particle a that decays into a pair of b-quarks

3 Data and simulated event samples

This search is based on proton–proton (pp) collision data at a centre-of-mass energy of 13 TeV collected with the ATLAS detector at the LHC from 2015 to 2018, referred to as the Run 2 data sample in the following. After applying the data quality requirements that ensure that all subdetectors were operational, the integrated luminosity of the data sample is 140.1 ± 1.2 fb^{-1} [24].

The signal consists in the production of a light pseudoscalar a in association with a top-quark pair, $t\bar{t}a$, or in association with a single top quark and a W boson, tWa. The main background in this search is $t\bar{t}$ production in association with jets, followed by smaller contributions from single top quark, $t\bar{t}H$, $t\bar{t}V$, V+jets, diboson and other rare processes involving the production of a top quark. The analysis only considers the decay of the pseudoscalar to a $b\bar{b}$ pair. Decays of the pseudoscalar to other final states like a $\tau\bar{\tau}$ pair or a $c\bar{c}$ pair are not considered, as these are suppressed both by the Yukawa coupling for the masses considered (roughly a factor 5 and 20, respectively) and by the large b-jet multiplicity required in the analysis signal regions.

All signal and background samples are simulated using various Monte Carlo (MC) matrix-element (ME) generators interfaced with different algorithms for the parton shower, hadronisation, and underlying event. The effect from multiple pp interactions originating from the same or neighbouring bunch crossings, usually referred to as pile-up, is simulated by overlaying the simulated hard-scattering event with inelastic pp collisions simulated using Pythia 8.1 [25] and the A3 set of tuned parameters (tune) [26]. A reweighting is applied to the simulated samples such that they match the pile-up conditions in data. For the detector simulation two different approaches are used. The full ATLAS detector simulation (FS) is based on Geant 4 [27], while the "fast" detector simulation (AF2) uses a parameterisation of the calorimeter response [28]. Most background samples are produced with FS while signal samples are produced with AF2. Both MC and data are processed using the same reconstruction and analysis software.

The $t\bar{t}a$ signal samples are simulated with MadGraph5_aMC@NLO 2.3.3 [29] generator at next-to-leading order (NLO) in the strong coupling constant α_s. A simplified model based on the decoupling limit of the 2HDM+a type II is used. Additionally, the subdominant tWa signal samples are simulated with the same generator at leading-order (LO). For notational simplicity, in the following $t\bar{t}a$ refers to the production of the pseudoscalar a in association with either a top-quark pair or a single top quark and a W boson. Samples are simulated for the following values of the pseudoscalar mass m_a: 12, 16, 20, 25, 30, 40, 50, 60, 80 and 100 GeV. Additional $t\bar{t}a$ signal samples for 20 and 60 GeV are also simulated with FS to check that no significant differences between the two detector simulations are observed.

The production of top-quark pairs with additional jets represents the main background source, especially the production of $t\bar{t}$ plus heavy flavour ($t\bar{t}$ +HF): $t\bar{t}+b$-jets and $t\bar{t}+c$-jets. For the modelling of $t\bar{t}+b$-jets events, four flavour-scheme samples (4FS), with massive b-quarks, are simulated using the PowhegBox-Res framework at NLO [30] and the NNPDF3.1nnlo parton distribution function (PDF) set is used. For the modelling of $t\bar{t}+c$-jets and $t\bar{t}$+light-jets events, five flavour-scheme (5FS) samples with massless b-quarks are simulated using PowhegBox-v2 [31–34], also at NLO. To avoid double-counting of events, neither the $t\bar{t}+b$-jets events from the 5FS samples nor the $t\bar{t}+c$-jets nor the $t\bar{t}$+light-jets events from the 4FS samples are used. The simulated $t\bar{t}$ events are categorised based on the number of additional jets matched to b- or c-hadrons with transverse momentum p_T larger than 5 GeV within $\Delta R < 0.3$ of the jet axis.

To model the production of single-top-quark events, which mostly contribute through the tW-channel, and the produc-

tion of $t\bar{t}H$, the same POWHEGBOX-v2 [31–34] settings, as used in the $t\bar{t}$+light/c-jets production, are used. The production of $t\bar{t}Z$ and $t\bar{t}W$ events is modelled using the MADGRAPH5_aMC@NLO 2.3.3 [29] generator at NLO. For all samples listed above, the NNPDF 3.0nlo [35] PDF sets are used and a top-quark mass of $m_{\text{top}} = 172.5$ GeV is set. The events are interfaced with PYTHIA8.230 [36] using the A14 tune [37] and the NNPDF 2.3lo set of PDFs [38] for the parton shower and hadronisation modelling.

The production of tZq and tWZ events is performed using MADGRAPH5_aMC@NLO v2.3.3, at LO and NLO in QCD respectively, in the 4FS with the `CTEQ6L1` PDF set [39] and using PYTHIA 8.212 for the parton shower.

Finally, the production of V+jets and diboson samples (VV) is simulated with different versions of the SHERPA [40] generator and the simulated events are matched with the SHERPA parton shower [41] using the MEPS@NLO prescription [42–45] with the set of tuned parameters developed by the SHERPA authors. All samples and their basic generation parameters are summarised in Table 1.

For all samples, except those generated with SHERPA, the decays of b- and c-hadrons are simulated using the EVTGEN programme [46].

4 Object definition

In this section, the reconstruction and definition of the physics objects are described, together with the additional corrections applied to each.

4.1 Physics objects

Electron candidates are reconstructed from energy deposits (clusters) in the electromagnetic calorimeter associated with reconstructed tracks in the inner detector. Candidates are selected with $p_{\text{T}} > 10$ GeV and $|\eta| < 2.47$, excluding the calorimeter transition region $1.37 < |\eta| < 1.52$. Electrons satisfy the `TightLH` [58] likelihood-based identification criterion and are required to match the PromptLeptonTagger working point `PLVLoose` [59]. They are further required to have $|z_0 \sin\theta| < 0.5$ mm and a d_0 significance $|\frac{d_0}{\sigma(d_0)}| < 5$, where the transverse impact parameter (d_0) is calculated relative to the beamline, and the longitudinal impact parameter (z_0) as the longitudinal distance between the primary vertex and the point where d_0 is measured.

Muon candidates are reconstructed from track segments in the various layers of the muon spectrometer and matched with tracks from the inner detector. The final muon candidates are refitted using the complete track information from both detector systems and must have $p_{\text{T}} > 10$ GeV and $|\eta| < 2.5$. Muons are required to satisfy the `Medium` quality requirements and match the PromptLeptonTagger working point `PLVLoose` [60]. Further requirements are $|\frac{d_0}{\sigma(d_0)}| < 3$, and $|z_0 \sin\theta| < 0.5$ mm.

Small-R jet candidates are reconstructed by clustering particle flow objects [61] using the anti-k_t algorithm [62,63] with a radius parameter of $R = 0.4$ and a four-momentum recombination scheme. The energy of the jet is corrected to the particle level by the application of a jet energy scale calibration derived from $\sqrt{s} = 13$ TeV data and simulation [64]. Baseline jets are required to have $p_{\text{T}} > 20$ GeV and $|\eta| < 2.5$. For pile-up rejection, jets with $p_{\text{T}} \in [20, 60]$ GeV and $|\eta| < 2.4$ are required to have a jet vertex tagger weight [65] larger than 0.5.

The b-tagging is the identification of jets that originate from the decay of b-hadrons using dedicated algorithms. A deep neural-network, called DL1r [66–69] is used. Small-R jets with a DL1r score above a certain threshold are defined as b-tagged jets. The pseudo-continuous (PC) b-tagging working point is used: each jet is classified with an integer from one to five depending on how many calibrated b-tagging working points (WP) the jet fulfils. The four calibrated DL1r WPs are 85%, 77%, 70% and 60%, each corresponding to the approximate average b-tagging efficiency in an inclusive $t\bar{t}$ MC sample. Jets not satisfying any WP are assigned a value of one, and this value is increased by one for every WP that they fulfil. The sum of the PC b-tagging over all jets in an event is defined as `sumPCBTag`. Jets satisfying the 70% WP are referred to as b-jets, while jets satisfying the 85% WP, but not the 70% WP, are classified as loose-b-jets.

Large-R jet candidates are formed by reclustering the small-R jets and tracks with a larger radius parameter of $R = 0.8$ using the anti-k_t algorithm [62,63]. The larger radius for track association allows more tracks from the targeted double b-hadron decays to be associated with the reclustered jet. The tracks in and around the small-R jet associated with the reclustered jet through ghost association [70,71] are selected with a loose track selection [72]. In this procedure, the p_{T} of the tracks is set to infinitesimal values, such that the "ghost" tracks can then be reclustered with the constituents of the reclustered jets with the appropriate radius parameter. Since the p_{T} of the tracks is infinitesimally small, they do not influence the reconstruction of the jet, allowing the use of additional tracks that leak outside the small-R jets.

To resolve the substructure within a large-R jet originating from a boosted $X \to b\bar{b}$ decay, which the small-R jet reconstruction fails to completely capture, additional information is extracted from the large-R jet by reconstructing track-subjets inside the large-R jet. The track-subjets are derived using the tracks that are ghost associated to each large-R jet as inputs to the exclusive-k_T method [73]. The selected tracks for a given jet are clustered using the k_T algorithm with a radius parameter of $R = 0.8$. The clustering stops when there are exactly two track clusters left.

Table 1 Nominal simulated signal and background event samples. The matrix element generator, PDF set, parton-shower (PS) generator and calculation accuracy of the cross section in QCD and EW used for normalisation are shown. MADGRAPH is abbreviated to MG

Process	Matrix element generator	PDF set	PS generator	Normalisation
$t\bar{t}a, a \to b\bar{b}$	MG_aMC@NLO v2.3.3	NNPDF3.0 NLO	PYTHIA 8.230	–
$tWa, a \to b\bar{b}$				
$t\bar{t}$ + jets	POWHEGBOX-v2	NNPDF3.0 NLO	PYTHIA 8.230	$(\text{NLO+NNLL})_{\text{QCD}}$ [47–53]
$t\bar{t} + b\bar{b}$	POWHEGBOX-Res	NNPDF3.1 NNLO	PYTHIA 8.244	–
Single-top	POWHEGBOX-v2	NNPDF3.0 NLO	PYTHIA 8.230	$(\text{NLO+NNLL})_{\text{QCD}}$ [54,55]
$t\bar{t}H$	POWHEGBOX-v2	NNPDF3.0 NLO	PYTHIA 8.230	$\text{NLO}_{\text{QCD+EW}}$ [56]
$t\bar{t}Z$	MG5_aMC@NLO v2.3.3	NNPDF3.0 NLO	PYTHIA 8.210	$\text{NLO}_{\text{QCD+EW}}$ [56]
$t\bar{t}W$	MG5_aMC@NLO v2.3.3	NNPDF3.0 NLO	PYTHIA 8.210	$\text{NLO}_{\text{QCD+EW}}$ [56]
tZq, tWZ	MG5_aMC@NLO v2.3.3	CTEQ6L1	PYTHIA 8.212	–
		NNPDF3.0 NLO		
Z/W + jets	SHERPA 2.2.11	NNPDF3.1 NNLO	SHERPA	NNLO_{QCD} [57]
Diboson	SHERPA 2.2.1	NNPDF3.1 NNLO	SHERPA	–
	SHERPA 2.2.2			

These clusters are used as the track-subjets associated with a given jet. For signal events, each track-subjet should originate from the decay of one b-hadron ideally. The associated large-R jet is required to satisfy $|\eta| < 2.0$ to account for their extended radius and the acceptance of the ID. Furthermore, each track-subjet is required to satisfy $p_{\text{T}} > 5\,\text{GeV}$ where the track-subjet p_{T} is estimated from the sum of its constituent tracks' four-momenta. The four-momentum of the large-R jet is defined as the sum of the four-momenta of its track-subjets.

In addition, secondary vertices (SV) inside the large-R jets are reconstructed to help the identification of b-hadrons. For this purpose, an algorithm that combines the track-cluster-based low-p_{T} vertex tagger (TC-LVT) [74] and the multiple-secondary-vertex finder algorithms (MSVF) [75] is used. The TC-LVT algorithm was developed for soft b-hadron tagging and optimised to reconstruct low-p_{T} b-hadron decays. The clustering algorithm from TC-LVT is used to identify displaced tracks not originating from the primary vertex. The MSVF algorithm is used to identify multiple SVs in the track cluster. The algorithm builds all two-track proto-vertices consistent with displaced tracks that are not compatible with a hadronic material interaction, a photon conversion, or the decay of long-lived light-flavoured hadrons. All displaced tracks reconstructed in the ID are used to build proto-vertices. Proto-vertices define track-to-track relations, since a single track can be associated with more than one proto-vertex. Each set of tracks that are mutually connected to each other forms a secondary vertex. After secondary vertices are formed, tracks not compatible with the vertex are removed, and the ambiguity caused by distant vertices sharing common tracks is resolved. Nearby vertices are also merged by the MSVF algorithm. Finally, reconstructed SVs are required to be ΔR-matched to a large-R jet. Further details and studies about the large-R jets can be found in Ref. [76].

In contrast to b-tagging, the B-tagging is the identification of pairs of b-jets that are too close to be resolved and identified individually. For this purpose the DeXTer tagger is used. It is a double b-tagger based on a deep sets neural network (NN) architecture designed to do flavour tagging of merged reconstructed jets [77] and uses information of the SVs and jet kinematics. This is done in two transverse momentum ranges: a low p_{T} range between 20 and 200 GeV and a high p_{T} one, above 200 GeV. Two working points are defined: the 0–40% tagging interval is referred to as `Tight` WP, and the `Loose` WP is defined by the inclusive 40–60% tagging interval. A sample of Z+jets and $t\bar{t}$ events is used to measure the DeXTer efficiency in data, and to derive B-tagging and b-mistagging rate correction factors for the simulated events. Large-R jets satisfying the `Tight` WP are referred to as B-jets.

The missing transverse momentum $E_{\text{T}}^{\text{miss}}$ measures the event momentum imbalance in the transverse plane of the detector. It is defined as the magnitude of the negative vector sum of p_{T} for all selected and calibrated physics objects in the event, with an extra term added to account for soft energy that is not associated with any of the selected objects. This soft term is calculated from inner detector tracks matched to the primary vertex to make it more resilient to pile-up contamination [78]. The $E_{\text{T}}^{\text{miss}}$ computation is based on the momenta of the objects defined previously, and after applying the overlap removal procedure defined in the next section.

4.2 Corrections to physics objects

The overlap removal is the procedure followed to prevent double-counting of objects. First, electrons that share a track with a muon are removed. To prevent double-counting of electron energy deposits as jets, the closest small-R jet within $\Delta R < 0.2$ of a selected electron is removed. If the nearest jet surviving that selection is within $\Delta R = 0.4$ of the electron, the electron is discarded. To reduce the background from muons from heavy-flavour decays inside jets, muon candidates are required to be separated by $\Delta R > 0.4$ from the nearest small-R jet, removing the muon if the jet has at least three associated tracks, and removing the jet otherwise. This avoids an inefficiency for high-energy muons undergoing significant energy loss in the calorimeter.

To avoid double-counting of jets, the jet overlap removal is done as follows. First, every small-R jet is tested to see if it is eligible to be DeXTer-tagged. This requires the small-R jet to have $p_{\mathrm{T}} > 20$ GeV and be isolated, meaning it is the only constituent of its reclustered jet [79] with the anti-k_t algorithm and radius parameter $R = 0.8$. These jets are then tested by the DeXTer tagger: if a small-R jet passes the `Loose` working point selection, it is defined as a B-tagged large-R jet and removed from the small-R jet list. Otherwise, it is kept as a small-R jet. Thus, this first step gives two jet lists: the DeXTer-tagged large-R jets and the small-R jets, which are either not eligible for DeXTer tagging or fail the tagger. Finally, the jet overlap removal procedure with leptons is repeated for large-R jets using $\Delta R = 0.8$.

The μ-in-jet p_{T} correction is the procedure of adding the muons reconstructed inside of a b-jet to the four-momentum of the respective b-jet. Around 20% of all b-hadron decays produce a low-momentum or soft muon inside of the resulting jet, but those soft muons are removed in the overlap removal as described above. This correction recovers the original energy of those b-jets and reduces biases from the invariant masses calculated with them. The soft muons used are required to have $p_{\mathrm{T}} > 4$ GeV and $|\eta| < 2.5$, and fulfil the `Medium` soft muon quality requirement.

In the case of the DeXTer-tagged jet, the μ-in-jet p_{T} correction is carried out as follows. First, the soft muons are matched to track-subjets within an angular distance of $\Delta R < 0.3$. At most the two highest p_{T} soft muons are taken into account for each track-subjet, and any muon is only matched once to the closest subjet. At last, the matched muons are added to the four-momentum of the track-subjet.

5 Event selection

Only events recorded with a single-electron [80] or single-muon trigger [81] under stable beam conditions and for which all detector subsystems were operational are considered [82]. Single-lepton triggers with p_{T} thresholds varying from 20 to 140 GeV, depending on the year, lepton flavour, isolation requirement and luminosity, are combined in a logical OR to increase the overall efficiency. The triggers with the lower p_{T} thresholds include isolation requirements on the lepton candidate, resulting in inefficiencies at high p_{T} that are recovered by the triggers with higher p_{T} thresholds.

5.1 Preselection

Events are required to have exactly two leptons (electrons, muons, or both) with opposite charge, satisfying the criteria defined in Sect. 4. Since single-lepton triggers are used, at least one of the two reconstructed leptons is required to have a $p_{\mathrm{T}} > 27$ GeV and match a lepton with the same flavour reconstructed by the trigger algorithm within ΔR of 0.15. The chosen p_{T} threshold ensures a fully efficient trigger for the whole Run 2 period. In the ee and $\mu\mu$ channels, the dilepton invariant mass must be above 15 GeV and outside the Z boson mass window 83–99 GeV. Further suppression of the background is achieved by requiring at least three jets (either large-R or small-R) with at least one of which being b-tagged using the DL1r 85% WP. The fraction of signal events in the preselection region is negligible for all masses.

5.2 Signal and control regions

After preselection, the data sample is dominated by background from $t\bar{t}$ events. To take advantage of the high jet and b-object multiplicities of the $t\bar{t}a$ signal process, events are classified into non-overlapping regions based on the total number of B-jets and b-jets. Some of the regions also require the presence of at least one loose (and not tight) b-jet (small-R jets tagged with the DL1r 85% WP but failing to meet the 70% WP). The name of every signal region (SR) or control region (CR) includes the number of B-jets followed by "B" and of b-jets followed by "b". The names of those regions requiring at least an extra loose b-jet indicate it in their name with "+1bL". Due to the high b-jet multiplicity of the signal, only regions with at least three b-objects are considered as signal regions (B-jets count as two b-objects). To maximise the signal sensitivity, signal events are classified into two boosted regions (SR 1B1b+1bL and SR 1B2b) and two resolved regions (SR 0B3b and SR 0B4b). The loose b-tagged jet in one of the signal regions is required to suppress $t\bar{t}$+light events. The complementarity between boosted and resolved regions is illustrated in Fig. 2, which shows the invariant mass of the B-jet in SR 1B2b and the invariant mass of the pair of b-jets with the largest p_T in SR 0B4b for different values of the pseudoscalar mass. Regions containing one B-jet are particularly relevant in the boosted regime ($m_a < 30$ GeV). Regions with no B-jets and a high b-jet multiplicity are more powerful in the resolved regime ($m_a > 30$ GeV).

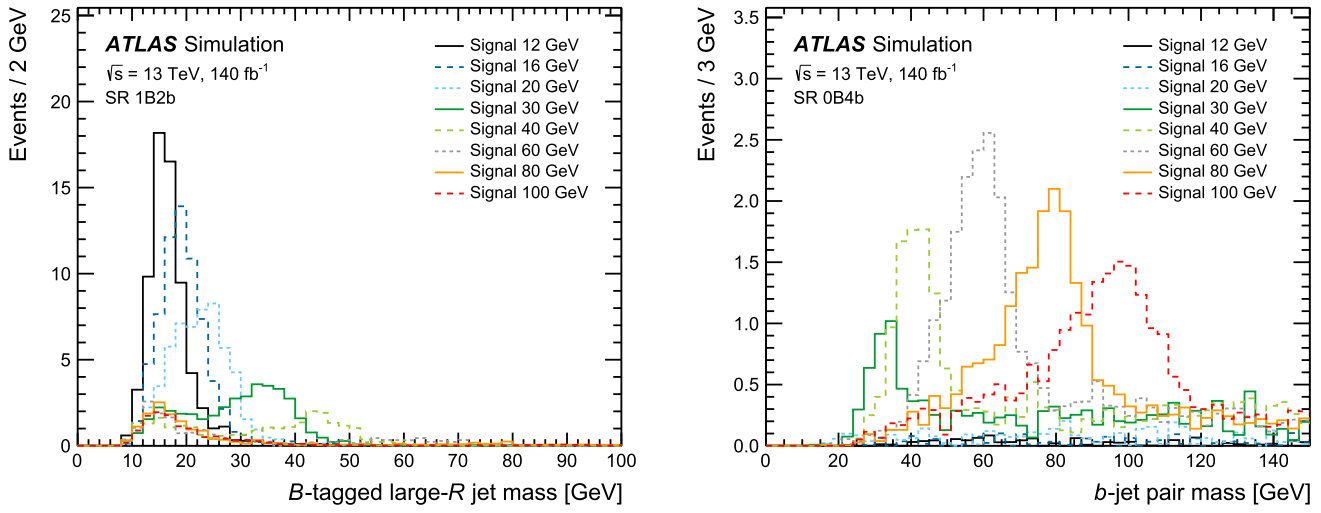

(a) (b)

Fig. 2 Invariant mass of the (**a**) B-jet in SR 1B2b and of the (**b**) pair of b-jets with the largest p_{T} in SR 0B4b for various values of m_a. The distributions are normalised according to the predicted m_a-dependent theoretical cross sections with a Yukawa coupling of the a-boson to the top quark of 0.5

Table 2 Overview of the jet multiplicities considered per region in the fit

Region	Large-R jets	Small-R jets	B-jets	b-jets	Loose b-jets
SR 0B4b	≥ 0	≥ 4	$= 0$	≥ 4	–
SR 0B3b	≥ 0	≥ 3	$= 0$	$= 3$	–
SR 1B2b	≥ 1	≥ 2	$= 1$	≥ 2	–
SR 1B1b+1bL	≥ 1	≥ 2	$= 1$	$= 1$	≥ 1
CR 0B2b+1bL	≥ 0	≥ 3	$= 0$	$= 2$	≥ 1

In addition to the four signal regions described above, a control region is included in the fit to improve the $t\bar{t}$+$\geq$1c normalisation (Sect. 8). The control region (CR 0B2b+1bL), orthogonal to all four signal regions, is composed of events with no B-jets and exactly two b-jets, as well as at least one additional loose (and non-tight) b-jet. Similarly to the SR, the loose b-tagged jet is required to suppress $t\bar{t}$+light events that would otherwise dominate the control region. Finally, events entering the CR are required to have a sum of the pseudo-continuous b-tagging scores between 12 and 15. The number of b-jets in the 0B3b, 1B1b+1bL and 0B2b+1bL regions is exclusive, while it is inclusive in the 0B4b and 1B2b regions. Table 2 summarises the selections for each region, which are applied in addition to the previously mentioned preselection requirements.

6 Background estimate

Data-driven corrections are derived for the $t\bar{t}$ Monte Carlo simulation, the main background process in this search. These corrections are derived to improve the description of the rates of $t\bar{t}$ plus heavy flavour jets and the transverse momenta of lepton and jets observed in data, using a method similar to the one developed for other ATLAS searches [83–85]. The corrections are derived in very inclusive control regions where the contamination of signal is predicted to be below 1% for all considered pseudoscalar mass hypotheses. The region of choice satisfies the preselection requirements described in Sect. 5.1, with an extra requirement of at least two b-jets and no B-jets. Additionally, to suppress the Z+jets contribution, only the different lepton flavour ($e\mu$) region is considered.

The first correction targets the production rate of heavy-flavour jets: c-jets and b-jets. It was observed in previous ATLAS and CMS analyses [86–88] that the rate of $t\bar{t}$+HF events is underestimated in MC simulation. Due to the high b-object multiplicity of the $t\bar{t}a$ signal, these HF events represent a large fraction of the $t\bar{t}$+jets background in the signal regions, and therefore the MC simulation must be corrected. To have a more accurate flavour composition, an event reweighting procedure is applied based on the `sumPCBTag` distribution. Figure 3a shows how the $t\bar{t}$+light production is dominant at low values of `sumPCBTag`, while the $t\bar{t}$+HF

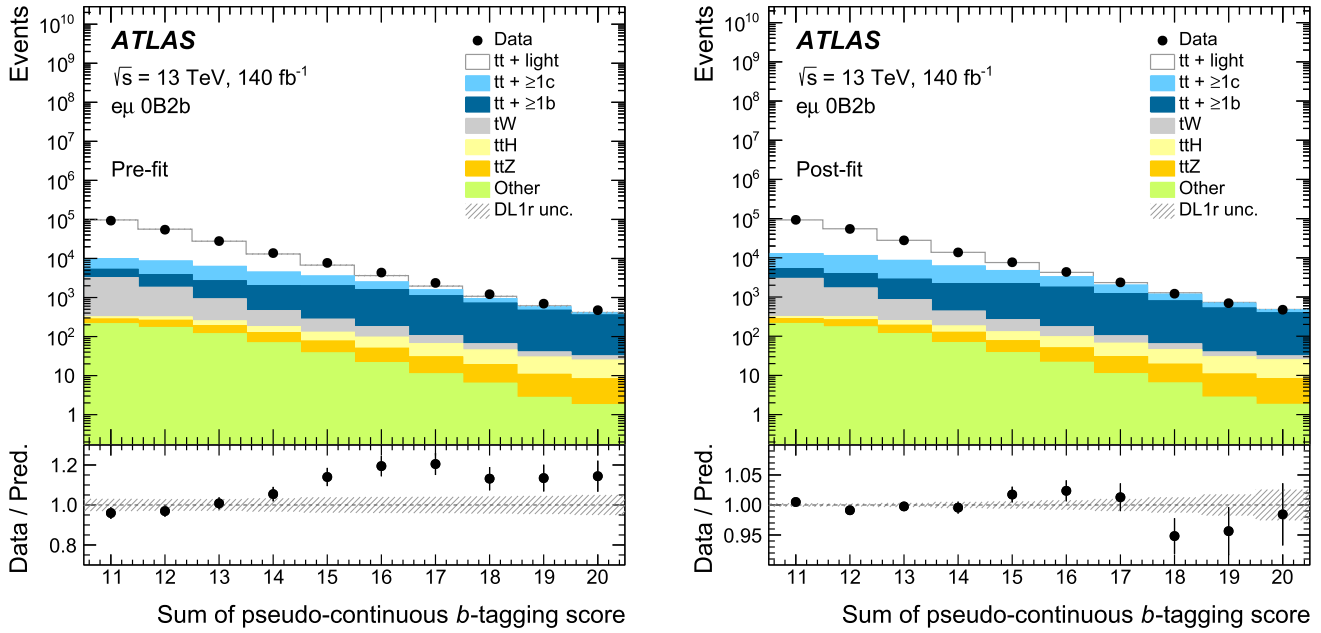

Fig. 3 Comparison of the data versus MC distribution of the sum of the pseudo-continuous b-tagging score of all the jets per event (**a**) before and (**b**) after applying the normalisation factors extracted from the heavy-flavour correction fit

Table 3 Normalisation factors for the three $t\bar{t}$+jets HF categories resulting from the likelihood fit performed using the `sumPCBTag` distribution

HF category	Norm. factor
$t\bar{t}+$ light, tW	0.91 ± 0.03
$t\bar{t}+\geq 1c$	1.58 ± 0.14
$t\bar{t}+\geq 1b$	1.13 ± 0.07

production populates the tail of the distribution. The correction procedure consists in deriving three normalisation factors: one for each component, using a likelihood fit to the `sumPCBTag` MC distributions compared with data. In this fit, DL1r b-tagging systematic uncertainties (detailed in Sect. 9) are included. Figure 3b shows the improved agreement after the fit. The normalisation factors and their corresponding uncertainties are shown in Table 3.

This procedure also corrects the distribution of the number of jets (inclusive of all jet types) per event, N_{jets}, which was also observed to be mismodelled in the simulation. Figure 4 shows the corresponding distribution, before and after applying the normalisation factors from Table 3. In the following, in all Figures and Tables, the category "Other" includes the following minor background processes: Z+jets, $t\bar{t}W$, tq, tZ, tWZ, WW, ZZ, WZ and W+jets.

The second correction targets the transverse momenta of the jets and leptons originating from the decay of top quark/antiquark, a quantity that was also observed to be mismodelled by current $t\bar{t}$ 5FS MC generators. The disagreement between data and MC persists even after applying the $t\bar{t}$+HF correction. To improve the agreement between data and MC for these variables, a kinematic reweighting factor for the $t\bar{t}+\geq 1c$, $t\bar{t}$+light, and tW components is derived from the data/MC ratio, after subtracting other background components from the data. These mismodellings are assumed to be independent of the flavour of the extra radiation, and applied equally to $t\bar{t}$+light, $t\bar{t}+\geq 1c$, and tW.

The event hardness or H_{T}, which is defined as the scalar sum of the p_{T} of all the jets and leptons in the event, is largely correlated with the total number of jets in the event, as every additional jet in the event shifts H_{T} to larger values. Performing the kinematic reweighting directly with H_{T} would therefore spoil the data/MC agreement achieved after the HF correction to the number of jets distribution shown in Fig. 4. To reduce the N_{jets} dependency, a new variable, $H_{\text{T}}^{\text{red}}(n)$, is defined:

$$H_{\text{T}}^{\text{red}}(n) = H_{\text{T}} - (n-3)\Delta H_{\text{T}}(n),$$

where n is the number of jets (small-R and large-R jets, with a minimum of three jets) and $\Delta H_{\text{T}}(n)$ is the average offset in H_{T} caused by the addition of each extra jet to the event. Correction factors are derived over a binned $H_{\text{T}}^{\text{red}}$ distribution, and the results are fitted using a continuous hyperbolic function which is later used for the MC reweighting. Figure 5 shows the H_{T} distribution before and after applying the

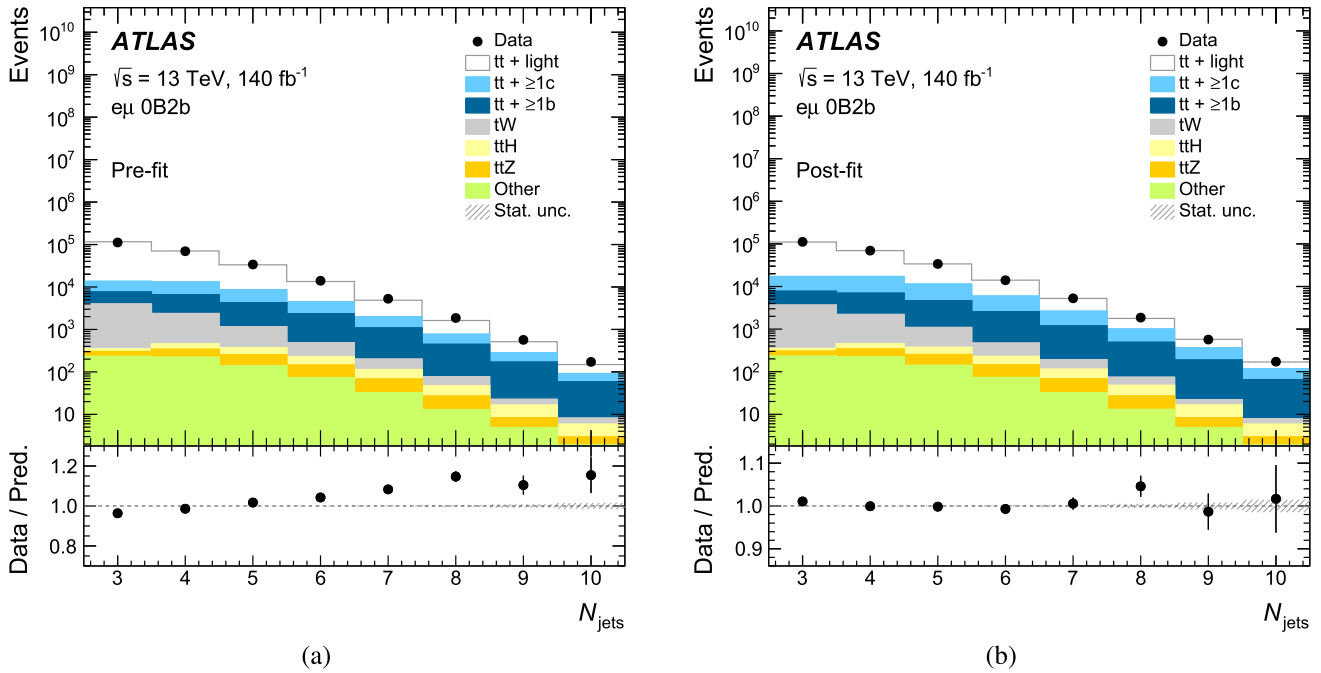

Fig. 4 Comparison of the data versus MC N_{jets} distribution (**a**) before and (**b**) after applying the $t\bar{t}$+jets normalisation factors extracted from the heavy flavour correction fit. Only statistical uncertainties are shown

correction. Similar improvements are observed for individual leptons and jets. No significant changes in the number of jets distribution are observed after the kinematic corrections are applied. Following the same procedure, dedicated kinematic reweighting corrections are derived for the alternative $t\bar{t}$+light, $t\bar{t}$+$\geq$1c, and tW samples employed in the evaluation of systematic uncertainties described in Sect. 9. Residual differences between data and the MC are taken into account in the analysis fit by including free-floating individual normalisations for the various $t\bar{t}$+jets background contributions.

7 Analysis strategy

The analysis uses various machine learning (ML) algorithms to improve the sensitivity to the target signal. First, two different boosted decision trees (BDTs) are trained to identify the jets originating from the decay of the top quark and antiquark and the jets originating from the pseudoscalar decay. Second, a mass-parameterised NN is trained for signal/background discrimination in each of the SRs described in Sect. 5.2. The final fit uses the NN output score distribution in each of the four SRs and the `sumPCBTag` distribution in the CR. In addition to the signal strength μ, three normalisation factors, corresponding to the main background contributions, are left to freely float in the fit. Figure 6 shows a diagram summarising the ML approach followed in the analysis as well as the CR and SRs used in the final fit. Further details on each step are given in the following.

7.1 Event reconstruction BDTs

Two different BDTs are trained to do partial event reconstruction. One targets the identification of the lepton-jet pairs associated with the top quark/antiquark decays, while the other identifies the pair of jets from the pseudoscalar decay. The two BDTs use the five leading small-R jets, together with the two charged leptons in the case of the top quark/antiquark BDT, and in each case select the pair of jets or the lepton/jet pair most likely to correspond to the pseudoscalar or the top quark/antiquark, respectively. Both BDTs were designed to reconstruct resolved topologies, thus they do not use large-R track-jets. Also, no attempt to reconstruct the two neutrinos from the top quark/antiquark decay is made. The two BDTs are trained using all signal samples inclusively, such that they are generic and valid for all considered masses. During the BDT training process, target labels for each jet are assigned based on a one-to-one matching between reconstructed jets at the detector level and parton-level b-quarks/leptons. Consequently, a reconstructed jet/lepton is assigned as originating from a (anti-)top quark, or pseudoscalar decay candidate based on the aforementioned generator information.

The BDT targeting the top quark/antiquark decay attempts to pair each lepton with its corresponding b-jet, considering each lepton in turn. For this, the BDT receives as input several kinematic variables that depend on the tag lepton/jet pair (jl-pair), such as its invariant mass or transverse momentum, or the separation angle between the lepton and the jet. It also uses information about the lepton and jet candidates them-

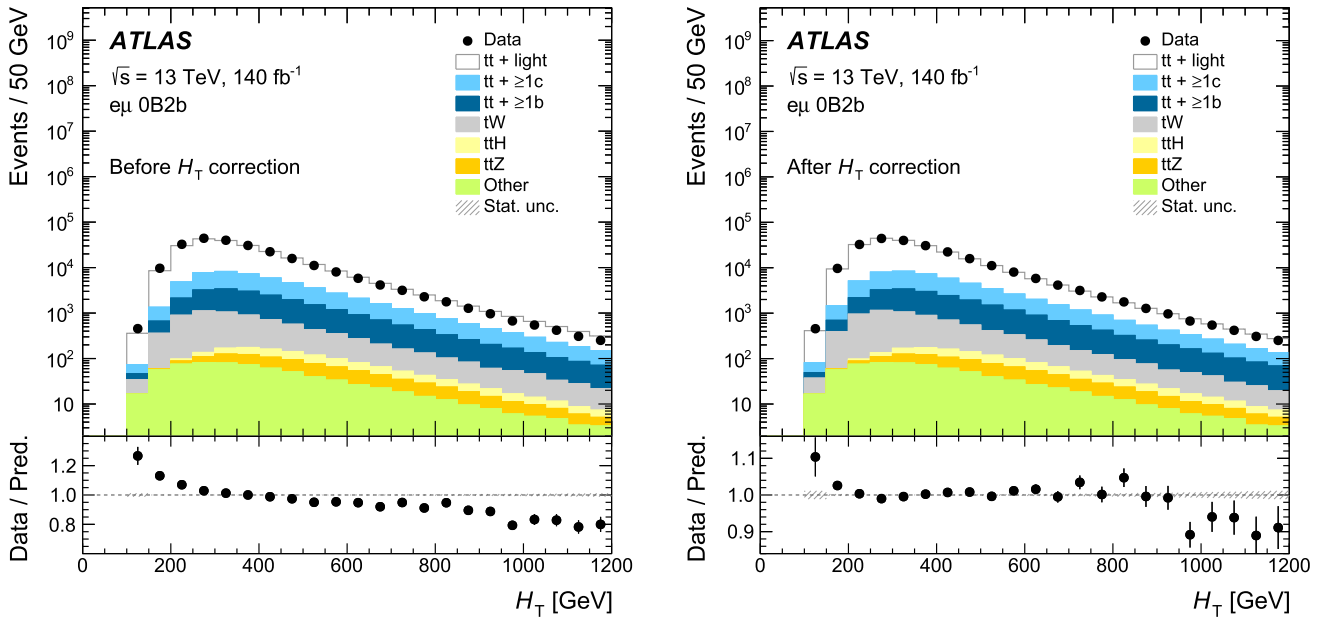

(a) (b)

Fig. 5 Comparison between data and MC of the H_T distribution (**a**) before and (**b**) after correcting it using H_T^{red}. Only statistical uncertainties are shown

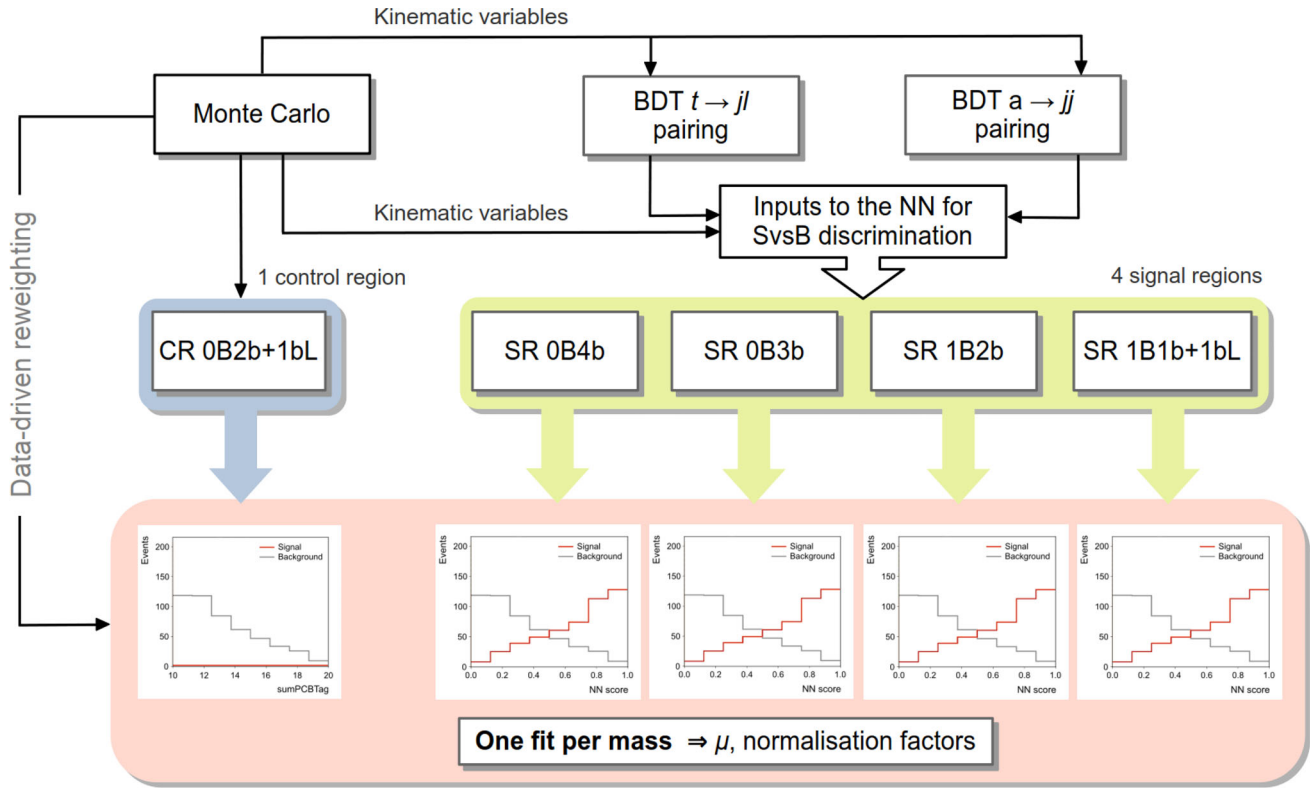

Fig. 6 Diagram of the analysis strategy, illustrating the data-driven corrections, jet/lepton and dijet pairings by two BDTs and the NN for signal versus background discrimination. The CR and SRs are used in the final fits to extract the signal strength (μ) as well as normalisation factors for the main backgrounds

selves, such as their pseudorapidity and transverse momenta, or the jet index indicating in decreasing order the hardness of the jets. In addition, the BDT uses information from the auxiliary jl-pair built with the lepton that is not being evaluated, together with information from the top/antitop system formed by the tag and auxiliary jl-pairs, and variables that refer to the full event. In a similar way, the BDT targeting the pseudoscalar decay receives various kinematic variables connected to the pair of two jets, jj-pair, as its mass or transverse momentum, together with information about the jets themselves or about the overall event. The full list of variables used by each BDT is shown in Table 4.

For the training of both BDTs, generator information is used to define the targets (b-quarks and leptons from the decays of the top quark, top antiquark and pseudoscalar a) and to identify the correct permutations at detector level, which are used as signal (or target) during the training, while all wrong permutations are used as background. A mix of signal and $t\bar{t}$ samples is used during the training of both BDTs. In both cases, two sets of BDTs are trained using k-2 fold training to avoid biases. The BDT trained with odd events is applied to even events and vice versa. The training is performed with the TMVA package of ROOT [89].

Following the training of both BDTs, they are applied to data and MC as follows. For the top quark/antiquark BDT, the lepton/jet permutation with the highest BDT score is identified for each lepton as the most likely jl-pair and the selected jet is assigned to the top quark or antitop quark decay depending on the lepton charge. If both leptons are initially assigned to the same jet, only the one with the highest BDT score keeps the assignment, while the other lepton is reassigned to the second most likely jet in terms of BDT score. In a similar way, for the pseudoscalar BDT, the permutation of two jets with the highest BDT score is selected and the two corresponding jets are assigned to the pseudoscalar decay. The selected jl- and jj-pairs are used to define related variables, such as the top-quark or pseudoscalar reconstructed invariant mass or separation angles, that are later used as input by the signal-versus-background discrimination neural networks. Figure 7 shows the prefit data/MC comparison of the reconstructed mass of the lb-pair selected by the top-quark BDT and of the jj-pair selected by the pseudoscalar BDT in SR 0B3b, the signal region with the largest statistics.

7.2 Signal-versus-background discriminating neural networks

As described in Sect. 5.2, events are divided into four signal regions according to their B- and b-jet multiplicity to better separate signal from background. The four signal regions used in the final fit are SR 0B4b, SR 0B3b, SR 1B2b and SR 1B1b+1bL. Independent NNs are trained individually per region to separate signal from background.

To make better use of the MC samples in the training, five different trainings are performed independently per region, where 80% of the events in the region constitute the training sample and the remaining 20% are used as the validation sample. An appropriate distribution of events in the various samples guarantees that no event is used both in the training and the evaluation of the NNs.

Each NN contains two hidden layers with twice as many nodes as the input layer, connected by Rectified Linear Unit (ReLU) activation functions. The final layer is a single node, normalised by a sigmoid function. The dropout for every layer is set to 0.3. To avoid overtraining, early stopping is implemented when the validation loss function does not improve during the last four epochs. The training is done using PyTorch 1.13.1 [90], and each of the NNs combines basic four-momentum information with high-level variables, such as invariant masses or angular distances, as well as relevant variables from the BDTs described in Sect. 7.1. The full list of input variables depends slightly on the region, given the slightly different signal topologies per region. Table 5 shows the overall list of input variables used by the NNs. Some of the most important variables in the NNs are $H_{\mathrm{T}}^{\mathrm{jets}}$, the invariant mass of two small-R jets or the mass and p_{T} of the large-R jet, among others.

All NNs are mass-parameterised, meaning that they receive the mass hypothesis as input during the evaluation. For the training, background MC samples are randomly assigned a mass from the grid of generated signal samples, while appropriate mass values are assigned to the signal events. Once the NNs are trained, the data scores are evaluated for each value of m_a considered in the analysis. In each SR, the resulting NN score is the distribution used in the profile likelihood fit, as discussed in the next section. Figure 8 shows the prefit distributions of the four NN scores corresponding to the 30 GeV mass hypothesis.

8 Statistical treatment

To test for the presence of a $t\bar{t}a$ signal, for each mass hypothesis, a binned maximum-likelihood fit to the data is performed simultaneously in all SRs and the CR (Sect. 5.2). In each SR, the input to the fit is the corresponding NN distribution described in Sect. 7.2, evaluated at the appropriate mass hypothesis. In the CR, the input to the fit is the `sumPCBTag` distribution. The parameter of interest is the signal strength, μ, a multiplicative factor to the cross section of the signal process. In addition to the signal strength μ, the fit includes three additional free parameters that work as scale factors to the normalisation for the three main background components: $k(t\bar{t}+\text{light}, tW)$, $k(t\bar{t}+\geq 1c)$, and $k(t\bar{t}+\geq 1b)$. To estimate the signal strength, a binned likelihood function $\mathcal{L}(\mu, \theta)$ is used,

Table 4 Input variables used in the (a) top quark/antiquark reconstruction BDT and (b) pseudoscalar reconstruction BDT

(a)

Top quark/antiquark reconstruction BDT

Object	Variables
Full event	N_{jets}, $N_{b\text{-jets}}$
Lepton (tag, aux.)	p_{T}, η
Jet (tag, aux.)	p_{T}, η, PC b-tag, jet index
jl pair (tag, aux.)	m, p_{T}, η, ΔR
$t\bar{t}$ pair	m, p_{T}, η, ΔR, $\Delta\phi$
jj pair	ΔR

(b)

Pseudoscalar reconstruction BDT

Object	Variables
Full event	N_{jets}, $N_{b\text{-jets}}$, `sumPCBTag`
Jet (1st, 2nd)	p_{T}, η, PC b-tag, jet index
jj pair	m, p_{T}, η, E, ϕ, ΔR

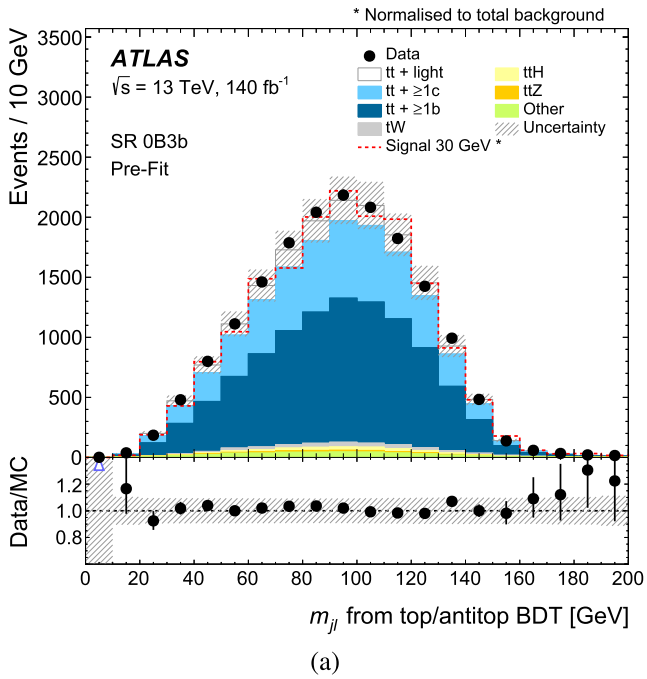

(a)

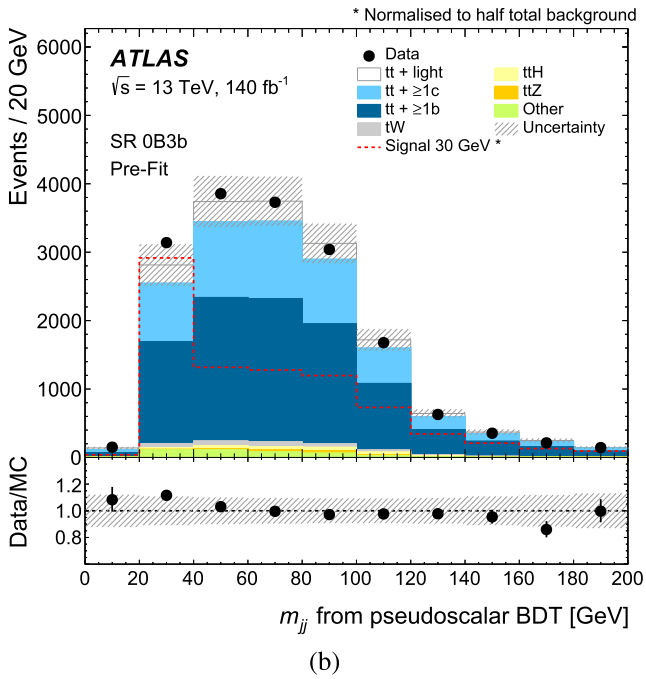

(b)

Fig. 7 Distribution (**a**) of the antitop-quark m_{jl} and (**b**) pseudoscalar m_{jj} selected by the top quark and pseudoscalar BDTs, respectively in SR 0B3b before the fit. The dashed line shows the distribution of the 30 GeV signal normalised to the total or half the total number of events in the region. The band displays the total pre-fit uncertainty

Table 5 List of input variables of the signal-versus-background discrimination NN. The distributions corresponding to both the pair with the maximum p_{T} and minimum ΔR are included for bb variables. Angular variables with one b or one B use the pair with the minimum ΔR. The m_{bbbb} and m_{bbb} variables correspond to the combination with the maximum scalar sum of p_{T}

Object	Variables
Full event	N_{jets}, $H_{\text{T}}^{\text{jets}}$, $E_{\text{T}}^{\text{miss}}$
BDT $t \to jl$	Score, p_{T}^{jl}, ΔR_{jl}, $\Delta\eta_{jl}$, $\Delta\phi_{jl}$, jet index
BDT $a \to jj$	Score, p_{T}^{jj}, η_{jj}, m_{jj}, ΔR_{jj}, $\Delta\eta_{jj}$, $\Delta\phi_{jj}$, jet index
Leptons	ΔR_{ll}, $\Delta\eta_{ll}$, $\Delta\phi_{ll}$, $\Delta\phi_{E_{\text{T}}^{\text{miss}},l}$, $\Delta R_{ll,bb}$, $\Delta R_{ll,B}$, $\Delta R_{ll,b}$
Large-R jets	p_{T}, η, m, ΔR_{Bb}, $\Delta\phi_{E_{\text{T}}^{\text{miss}},B}$
Small-R jets	p_{T}^{bb}, m_{bb}, m_{bbb}, m_{bbbb}, ΔR_{bb}, $\Delta\eta_{bb}$, $\Delta\phi_{bb}$, $\Delta\phi_{E_{\text{T}}^{\text{miss}},b}$
	p_{T}, η, PC b-tag

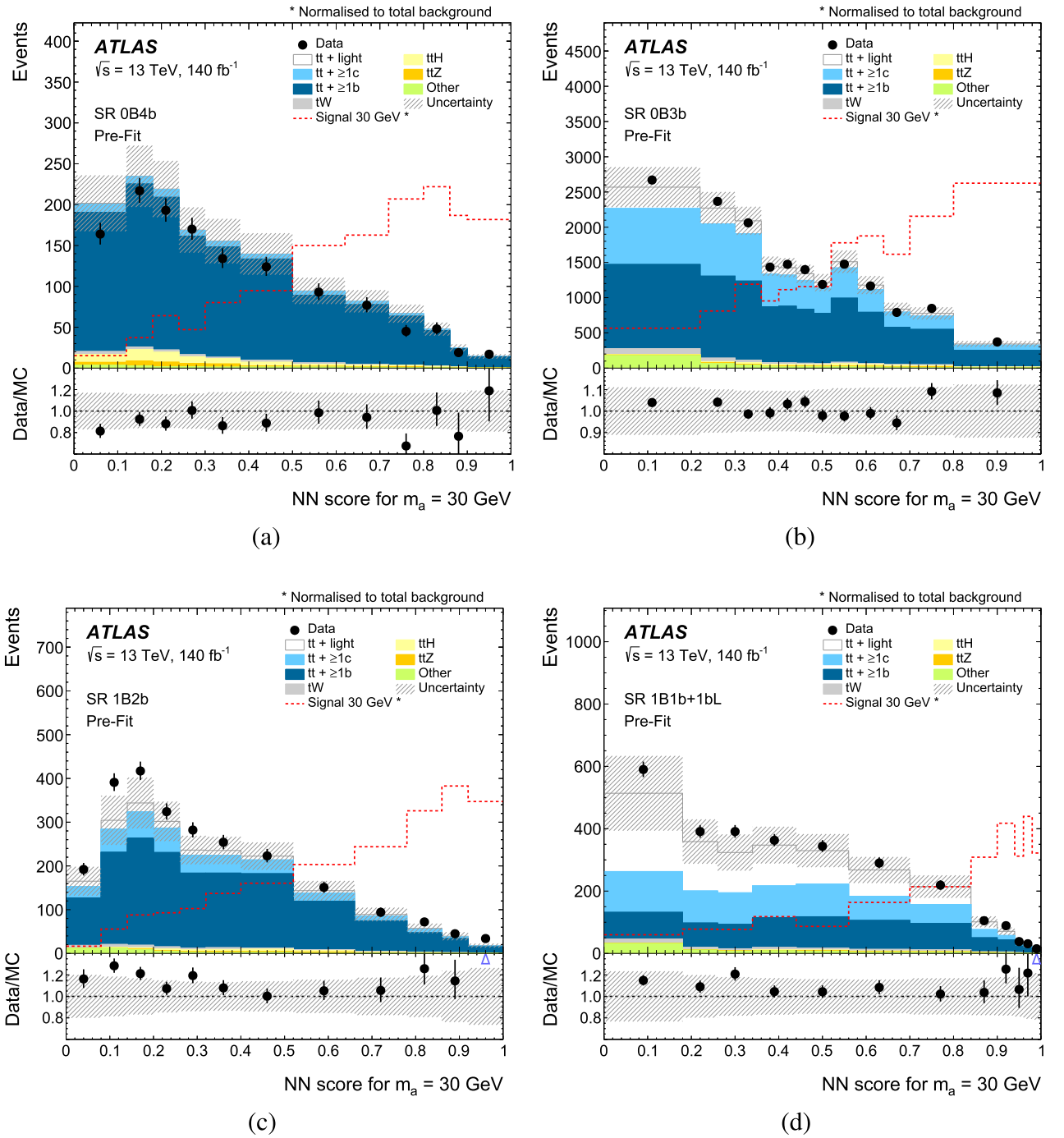

Fig. 8 Pre-fit distributions corresponding to the NN output score of (**a**) SR 0B4b, (**b**) SR 0B3b, (**c**) SR 1B2b and (**d**) SR 1B1b+1bL for the 30 GeV mass hypothesis fit. The dashed line shows the distribution of signal normalised to the total number of events in each region. The band displays the total pre-fit uncertainty. Arrows appearing in the bottom panels indicate the ratio being outside the displayed range

$$\mathcal{L}(\mu,\theta) = \prod_{i}^{N} \frac{(E[n_i(\mu,\theta)])^{n_i}}{n_i!} e^{-E[n_i(\mu,\theta)]} \prod_{\theta_j \in \theta} \rho(\theta_j|\tilde{\theta}_j).$$

The function is constructed as a product of Poisson probability terms with one Poisson term included for every bin i of the NN distribution in the analysis regions. The binning of the NN distributions for each signal is chosen to provide a good separation of signal and background while maintaining a stable performance of the fit. The expected number of events, $E[n_i(\mu,\theta)]$, in each bin, n_i, is a function of μ,

and a set of nuisance parameters, θ. The nuisance parameters encode effects from the normalisation of backgrounds, including the systematic uncertainties and one parameter per bin to model statistical uncertainties in the simulated samples. Unlike the free-floating parameters, all nuisance parameters are constrained by prior distributions, $\rho(\theta|\tilde{\theta})$, which follow Gaussian, log-normal, or Poisson distributions centred around their nominal values, $\tilde{\theta}$. This procedure allows the reduction of the impact of the uncertainties by taking advantage of the separated populations of signal and background. The best-fit value of the signal strength is obtained by performing a fit to the data under the signal-plus-background hypothesis, maximising $\mathcal{L}(\mu, \theta)$ over μ and θ. To set upper limits on μ, the following test statistic is used:

$$\tilde{q}_\mu = \begin{cases} -2\ln \dfrac{\mathcal{L}\left(\mu, \hat{\hat{\theta}}(\mu)\right)}{\mathcal{L}\left(0, \hat{\hat{\theta}}(0)\right)} & \hat{\mu} < 0, \\ -2\ln \dfrac{\mathcal{L}\left(\mu, \hat{\hat{\theta}}(\mu)\right)}{\mathcal{L}\left(\hat{\mu}, \hat{\theta}\right)} & 0 \le \hat{\mu} \le \mu, \\ 0 & \hat{\mu} > \mu. \end{cases}$$

The values of the signal strength and nuisance parameters that maximise the likelihood function are represented by $\hat{\mu}$ and $\hat{\theta}$, respectively. For a given value of μ, the values of the nuisance parameters that maximise the likelihood function are represented by $\hat{\hat{\theta}}(\mu)$. This test statistic measures the compatibility of the observed data with the background-only hypothesis ($\mu = 0$), represented by the p-value, and is estimated by integrating the distribution of $\tilde{q}_0$ based on the asymptotic formula in Ref. [91]. The test statistic is set to zero for $\hat{\mu} > \mu$, as this case indicates that the μ hypothesis is compatible with the observed data and cannot be rejected. Upper limits on μ are derived by using $\tilde{q}_\mu$ in the $\mathrm{CL_s}$ method [92,93].

The systematic uncertainties, including those derived from MC samples, can show fluctuations due to generator weights or statistical variations. To ensure the quality of the templates and the stability of the fit, smoothing algorithms are applied to the histograms before the fit. In addition, systematic uncertainties are pruned to reduce computing time. Only uncertainties with an effect greater than 1% are included in the fit. This is done separately for shape and normalisation effects.

9 Systematic uncertainties

Various sources of systematic uncertainties are considered. Each systematic uncertainty is introduced as a nuisance parameter (NP) in the statistical analysis described in Sect. 8. Section 9.1 describes all experimental uncertainties, related to the luminosity and pile-up or the reconstruction and identification of jets and leptons. They are applied to all MC samples equally and their effects are treated in a correlated way across all four SRs and the CR in the final fit. The signal and background modelling uncertainties are detailed in Sect. 9.2, and can be different depending on the process. They are implemented as decorrelated between regions, given their different coverage of phase spaces, and decorrelated between signal and background samples in the fit.

9.1 Experimental uncertainties

Luminosity and pile-up modelling. The uncertainty in the integrated luminosity for the full Run 2 data sample is 0.83% [24], obtained using the LUCID-2 detector [21] for the primary luminosity measurements. A variation in the pile-up reweighting of simulated events is included to cover the uncertainty in the ratio of the simulated and measured distribution of inelastic cross sections.

Leptons. Uncertainties associated with leptons are related to the trigger, reconstruction, identification and isolation, as well as the lepton energy or momentum scale and resolution. The reconstruction, identification, and isolation efficiency of electrons and muons, as well as the efficiency of the trigger used to record the events, differ slightly between data and simulation, and is corrected by dedicated scale factors. Efficiency scale factors are measured using tag-and-probe techniques on $Z \to ll$ data and simulated samples [58,60], and are applied to the simulation to correct for differences. Additional sources of uncertainty originate from the corrections applied to adjust the lepton momentum scale and resolution in the simulation to match those in data, measured using $Z \to ll$ and $J/\psi \to ll$ events [58,60].

Jets. Uncertainties associated with jets arise from the efficiency of pile-up rejection by the jet vertex tagger (JVT), from the jet energy scale (JES) and resolution (JER), and from the different flavour-tagging algorithms used, DL1r and DeXTer. Scale factors are applied to correct for discrepancies between data and MC for JVT efficiencies, and are estimated by using $Z \to \mu\mu$ with tag-and-probe techniques [65]. The jet energy scale and its uncertainty are derived by combining information from test-beam data, LHC collision data and simulation [64]. The jet energy resolution is measured in Run 2 data and simulation as a function of jet p_{T} and rapidity using dijet events.

To correct flavour-tagging efficiencies in simulated samples to match those measured in data, scale factors are derived. They are calculated as a function of p_{T} for b-jets, c-jets, and light jets separately in dedicated calibration analyses. For b-jet efficiencies, $t\bar{t}$ events in the dilepton topology are used, exploiting the very pure sample of b-jets arising from the decay of the top quarks [67]. For c-jet mistag rates, $t\bar{t}$ events in the single-lepton topology are used, exploiting c-jets from the hadronically decaying W boson [68].

The negative-tag method is used in Z+jets events [69] for light-jets mistag rates. The use of DeXTer introduces additional scale factors to correct for the differences in efficiency between simulated samples and data. The scale factors for DeXTer are derived as a function of p_{T} for B- and b-jets. The calibration measurements with data are performed using both $t\bar{t}$ and Z+jets events simultaneously to measure B-jet tagging and b-jet mistagging efficiency in data. Nevertheless, the DeXTer uncertainties are provided with conservative error bands, leaving the calibration to be performed in situ in the final fit of the analysis. Further details on the methodology can be found in Refs. [77,77].

Missing transverse momentum. All the described uncertainties in energy scales or resolutions of the reconstructed objects (hard components) are propagated to the missing transverse momentum. Additional uncertainties in the scale and resolution of the soft term are considered, to account for the disagreement between data and MC for the p_{T} balance between the hard and soft components [78].

Tracks. Systematic uncertainties related to the track selection efficiency are determined by changing the amount of tracker material and the physical models in the GEANT4 simulation [94,95]. Dedicated uncertainties are considered for the track parameters, including the transverse and longitudinal impact parameters and the track sagitta.

Large- R jet mass scale correction. To correct for the mismodelling in the large-R jet mass, additional mass scale corrections are estimated. The large-R jet mass scale is varied by ±5% and compared with the nominal results.

9.2 Modelling uncertainties

Renormalisation (μ_{r}) *and factorisation* (μ_{f}) *scales.* Variations in the renormalisation and factorisation scales are used to estimate the uncertainty due to missing higher order corrections. The uncertainties are combined by taking an envelope of all the variations.

Initial-state radiation and final-state radiation modelling. For the ISR, the amount of radiation is increased (decreased) using the `Var3cUp` (`Var3cDown`) variation of the A14 tune [37]. For the FSR, the amount of radiation is increased (decreased) varying the coupling of the QCD emission in the final state by a factor of 0.5 (2).

PDF uncertainties. The PDF uncertainties follow the PDF4LHC recommendations [96]. The α_{s} uncertainty is derived using the same PDF set evaluated with two different α_{s} values. The uncertainties from the PDF and α_{s} are added in quadrature.

Parton shower. The uncertainty associated with hadronisation and parton shower is evaluated by comparing samples with different parton shower models. The nominal $t\bar{t}a$ samples simulated using POWHEG+PYTHIA 8 are compared with samples simulated using MADGRAPH5_AMC@NLO +HERWIG 7 [97]. The comparison is done after normalising both $t\bar{t}a$ samples. The nominal $t\bar{t}$ (4FS and 5FS) POWHEG+PYTHIA 8 samples are compared with samples simulated using POWHEG+HERWIG 7. The tW and $t\bar{t}H$ MADGRAPH5_AMC@NLO+PYTHIA 8 samples are compared with MADGRAPH5_AMC@NLO+HERWIG 7 samples.

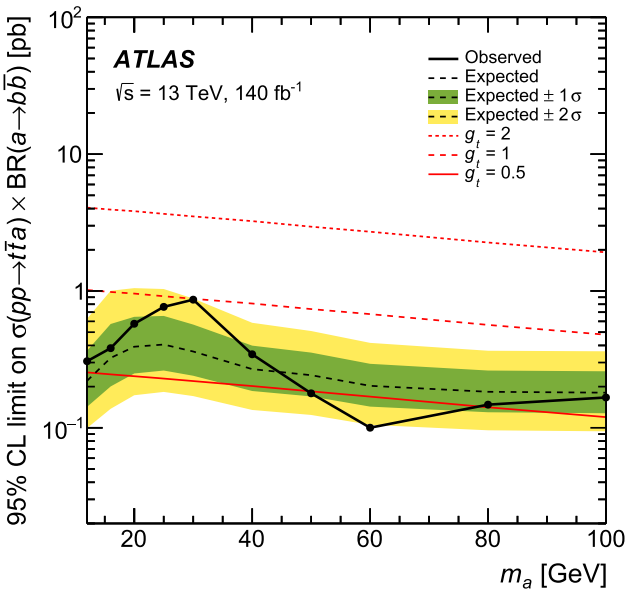

Fig. 9 Expected and observed 95% CL upper limits of $\sigma(t\bar{t}a) \times \mathrm{BR}(a \to b\bar{b})$ as a function of the a-boson mass. The lines correspond to the signal cross sections calculated using different coupling strengths of the a boson to the top quark assuming a $\mathrm{BR}(a \to b\bar{b}) = 100\%$

Matrix element uncertainties. For the 5FS and 4FS $t\bar{t}$ samples, the uncertainty associated with the matching between the Matrix element calculations and the parton shower is calculated by comparing the nominal POWHEG+PYTHIA 8 sample with an alternative set of samples simulated also in POWHEG+PYTHIA 8 but using the `pThard=1` setting. For tW and $t\bar{t}H$, the matrix element uncertainty is evaluated by comparing the nominal POWHEG+PYTHIA 8 samples to those simulated with MADGRAPH5_AMC@NLO+PYTHIA 8. For $t\bar{t}Z$, the nominal samples are compared with an alternative sample simulated using SHERPA 2.2.0, which accounts both for the matrix element and parton shower uncertainties.

POWHEG *damping function.* In the $t\bar{t}b\bar{b}$ (4FS) samples, the effect of the choice of a damping scale h_{bzd} that controls the resummation of infrared divergences is evaluated by comparing the nominal sample ($h_{\mathrm{bzd}} = 5$) with an alternative sample in which the scale is set to 2 [30].

Initial-state shower recoil. The uncertainty due to the recoil choice of ISR emissions is evaluated by comparing the nominal sample, in which the whole final state recoils the ISR emission, with an alternative one, in which only one final-state parton recoils against the ISR emission [30].

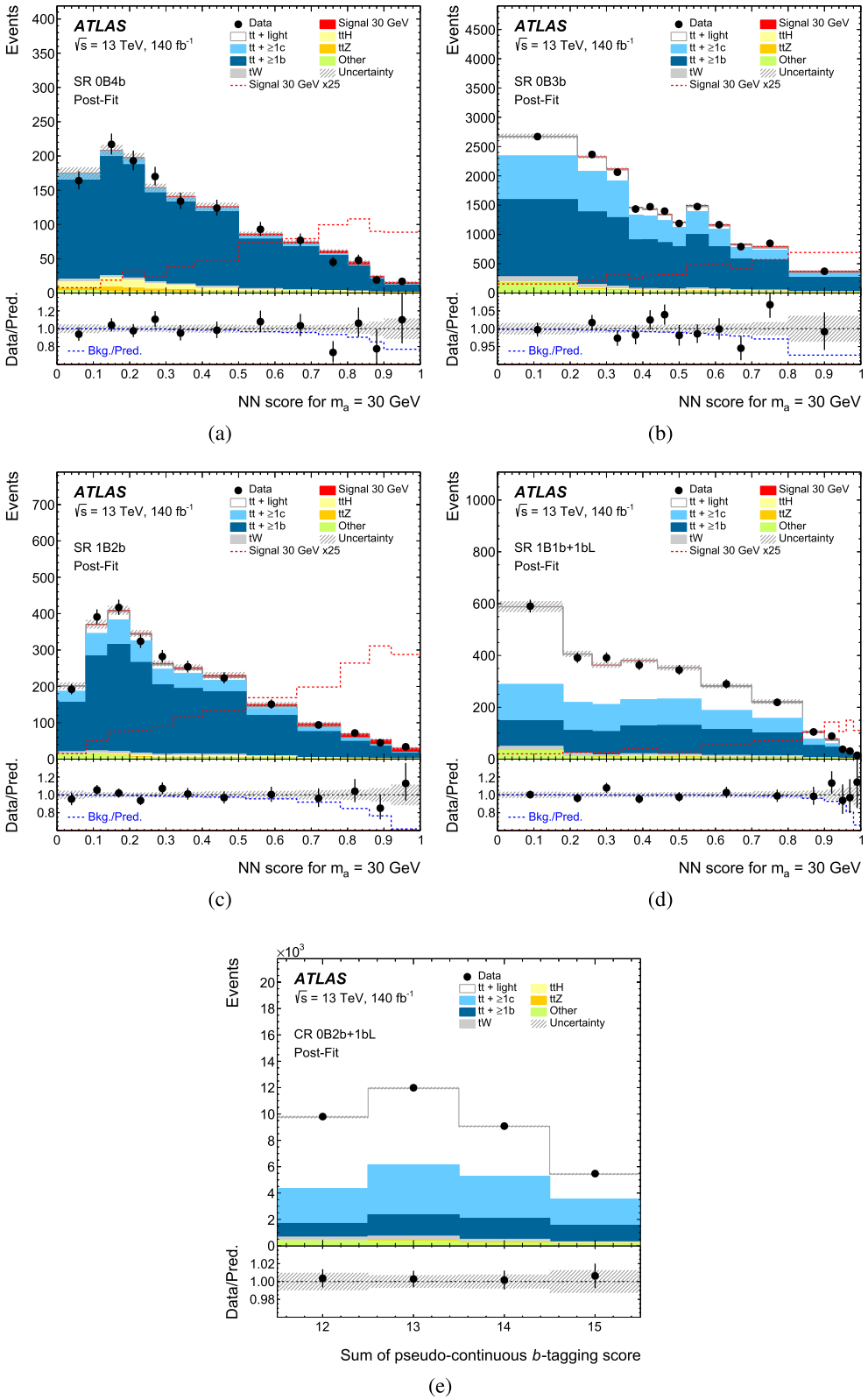

Fig. 10 Post-fit distributions corresponding to the NN output score of (**a**) SR 0B4b, (**b**) SR 0B3b, (**c**) SR 1B2b and (**d**) SR 1B1b+1bL and to the sum of the pseudo-continuous *b*-tagging score of (**e**) CR 0B2b+1bL for the 30 GeV mass hypothesis fit. The dashed lines in the top and ratio panels show the post-fit distribution of the signal scaled by a factor of 25 and the post-fit ratio of the background over the total prediction, respectively. The band displays the total post-fit uncertainty

Table 6 Post-fit background and signal yields in the four signal regions and in the control region for the $m_a = 30$ GeV hypothesis. The uncertainties in each yield are the total uncertainties of each component after the fit

Sample	SR 0B4b	SR 0B3b	SR 1B2b	SR 1B1b+1bL	CR 0B2b+1bL
Signal 30 GeV	28 ± 14	180 ± 98	71 ± 31	35 ± 16	110 ± 63
$t\bar{t}$+light	5 ± 2	1400 ± 320	130 ± 24	1100 ± 180	17,000 ± 3000
$t\bar{t}$+≥1c	58 ± 21	4700 ± 1200	380 ± 140	740 ± 230	12,000 ± 3500
$t\bar{t}$+≥1b	1093 ± 47	9820 ± 700	1758 ± 97	815 ± 70	5510 ± 650
tW	22 ± 12	360 ± 140	46 ± 20	64 ± 17	830 ± 220
$t\bar{t}H$	62 ± 9	222 ± 22	31 ± 4	14 ± 12	136 ± 13
$t\bar{t}Z$	27 ± 6	120 ± 22	15 ± 3	11 ± 2	128 ± 25
Other	14 ± 2	394 ± 35	47 ± 4	78 ± 10	1060 ± 120
Total pred.	1300 ± 35	17,000 ± 130	2500 ± 50	2900 ± 53	36,000 ± 190
Data	1301	17,242	2479	2866	36,350

Table 7 Table of the impact of each group of uncertainties in the fitted cross section for the hypothesis masses of 12, 30 and 80 GeV. The values shown are the average of up and down uncertainties. The fitted cross section values include the BR($t\bar{t} \to WbWb$) × BR($W \to l\nu$) × BR($W \to l\nu$) in addition to the BR($a \to b\bar{b}$)

Fitted cross section [fb]	$m_a = 12$ GeV $\hat{\sigma} = 9$	$m_a = 30$ GeV $\hat{\sigma} = 46$	$m_a = 80$ GeV $\hat{\sigma} = -6.1$
Uncertainty source	$\Delta\hat{\sigma}$	$\Delta\hat{\sigma}$	$\Delta\hat{\sigma}$
Data statistics	6.1	11.0	6.0
MC statistics	2.4	4.2	1.8
Luminosity & pile-up	0.1	0.4	0.1
Jet reconstruction	0.5	4.9	1.2
Lepton reconstruction	<0.1	<0.1	<0.1
$E_{\mathrm{T}}^{\mathrm{miss}}$ reconstruction	<0.1	0.3	<0.1
Track reconstruction	4.1	1.5	0.1
DL1r	0.4	3.5	1.4
DeXTer	4.2	18	1.1
Modelling signal	1.7	7.5	1.3
Modelling $t\bar{t} + b$	2.7	13	5.5
Modelling $t\bar{t} + c$	0.9	1.8	1.4
Modelling $t\bar{t}$+light	0.8	2.0	2.2
Modelling tW	0.3	0.7	0.6
Modelling ttH	0.1	0.3	0.2
Modelling ttZ	0.1	0.2	1.0
Norm factors	0.7	6.7	4.7
Reweighting	<0.1	<0.1	<0.1
Total systematic uncertainty	8.0	22	7.8
Total uncertainty	10	24	9.7

Interference between $t\bar{t}$ and tW. To account for uncertainties in the interference between $t\bar{t}$+jets and tW, the nominal tW sample simulated using diagram removal (DR) is compared with another sample simulated using diagram subtraction (DS).

Reweighting uncertainties. To account for the systematic uncertainties associated with the reweighting functions described in Sect. 6, several uncertainties are determined by the variations of $t\bar{t}$+light + tW, $t\bar{t}$+≥1c and $t\bar{t}$+ ≥1b normalisation factors and the variations of the parameters of the $H_{\mathrm{T}}^{\mathrm{red}}$ hyperbolic fit. The uncertainties are evaluated after diagonalising the fit correlation matrix and propagating the diagonal variations in a correlated way.

10 Results

The expected and observed upper limits on the inclusive $\sigma(t\bar{t}a) \times \mathrm{BR}(a \to b\bar{b})$ are shown in Fig. 9 as a function of the a-boson mass, which ranges from 12 to 100 GeV. This result is compared with the predicted cross sections for the signal corresponding to three different values of the coupling of the a-boson to the top quark, defined as a strength modifier to the SM Yukawa coupling. No significant excess is observed: the largest excess corresponds to the 30 GeV mass hypothesis, with a local significance of 2.0 standard deviations. Assuming $\mathrm{BR}(a \to b\bar{b}) = 100\%$, the mass region between 50 and 80 GeV is excluded for a coupling of the pseudoscalar to the top quark of 0.5, while a coupling of 1.0 is excluded for all masses. Post-fit distributions of the NN output score corresponding to this mass in each of the four signal regions and of the sum of the pseudo-continuous b-tagging score of all jets in the control region are shown in Fig. 10. Table 6 shows the post-fit event yields per signal and background component in each of the signal and control regions for the same mass hypothesis.

Table 7 summarises the impact of the different sources of uncertainties in the fitted signal strength for three different mass hypotheses: 12, 30 and 80 GeV, which are representative of the low, medium and high mass ranges, respectively. Fits to low-mass hypotheses are limited by data statistics, track reconstruction and DeXTer-related uncertainties. Fits to medium-mass hypotheses are dominated by DeXTer-related uncertainties, followed by the modelling of the $t\bar{t}$+$\geq$1b process and data statistics. Finally, fits to high-mass hypotheses are limited mainly by data statistics, the modelling of the $t\bar{t}$+$\geq$1b process and the normalisation of $t\bar{t}$+HF. In all cases, the uncertainties in the modelling of the signal are subdominant compared with that of $t\bar{t}$+$\geq$1b. No large pulls are observed in any of the fits. Including the pre-fit reweighting corrections detailed in Table 3, the final normalisation factors extracted in the fit corresponding to the 30 GeV mass hypothesis are 1.0 ± 0.3 for $t\bar{t}$+light and tW, 1.5 ± 0.5 for $t\bar{t}$+$\geq$1c and 1.2 ± 0.2 for $t\bar{t}$+$\geq$1b. These results are compatible with the latest ATLAS $t\bar{t}H$ Run 2 analysis [98].

11 Conclusions

A search for a pseudoscalar a produced in association with either a pair of top quarks or a single top and a W boson in the dilepton decay channel is performed using the full Run 2 pp data sample collected by the ATLAS detector at the LHC. The search targets the dominant decay channel of the pseudoscalar mass probed in this analysis: $a \to b\bar{b}$. The search covers the pseudoscalar boson mass between 12 and 100 GeV, involving both the kinematic regime where the decay products of the pseudoscalar merge into large B-jets and the regime where the b-tagged jets are resolved. Limits on the signal production cross section times the branching ratio of the decay into a pair of bottom quarks are extracted. Assuming $\mathrm{BR}(a \to b\bar{b}) = 100\%$, the mass region between 50 and 80 GeV is excluded for a coupling of the pseudoscalar to the top quark of 0.5, while a coupling of 1.0 is excluded for all masses. These model independent results are the first limits of their kind and complement previous searches by ATLAS [17] and CMS [16] exploring leptonic decays of the pseudoscalar.

Acknowledgements We thank CERN for the very successful operation of the LHC and its injectors, as well as the support staff at CERN and at our institutions worldwide without whom ATLAS could not be operated efficiently. The crucial computing support from all WLCG partners is acknowledged gratefully, in particular from CERN, the ATLAS Tier-1 facilities at TRIUMF/SFU (Canada), NDGF (Denmark, Norway, Sweden), CC-IN2P3 (France), KIT/GridKA (Germany), INFN-CNAF (Italy), NL-T1 (Netherlands), PIC (Spain), RAL (UK) and BNL (USA), the Tier-2 facilities worldwide and large non-WLCG resource providers. Major contributors of computing resources are listed in Ref. [99]. We gratefully acknowledge the support of ANPCyT, Argentina; YerPhI, Armenia; ARC, Australia; BMWFW and FWF, Austria; ANAS, Azerbaijan; CNPq and FAPESP, Brazil; NSERC, NRC and CFI, Canada; CERN; ANID, Chile; CAS, MOST and NSFC, China; Minciencias, Colombia; MEYS CR, Czech Republic; DNRF and DNSRC, Denmark; IN2P3-CNRS and CEA-DRF/IRFU, France; SRNSFG, Georgia; BMBF, HGF and MPG, Germany; GSRI, Greece; RGC and Hong Kong SAR, China; ICHEP and Academy of Sciences and Humanities, Israel; INFN, Italy; MEXT and JSPS, Japan; CNRST, Morocco; NWO, Netherlands; RCN, Norway; MNiSW, Poland; FCT, Portugal; MNE/IFA, Romania; MSTDI, Serbia; MSSR, Slovakia; ARIS and MVZI, Slovenia; DSI/NRF, South Africa; MICIU/AEI, Spain; SRC and Wallenberg Foundation, Sweden; SERI, SNSF and Cantons of Bern and Geneva, Switzerland; NSTC, Taipei; TENMAK, Türkiye; STFC/UKRI, United Kingdom; DOE and NSF, United States of America. Individual groups and members have received support from BCKDF, CANARIE, CRC and DRAC, Canada; CERN-CZ, FORTE and PRIMUS, Czech Republic; COST, ERC, ERDF, Horizon 2020, ICSC-NextGenerationEU and Marie Skłodowska-Curie Actions, European Union; Investissements d'Avenir Labex, Investissements d'Avenir Idex and ANR, France; DFG and AvH Foundation, Germany; Herakleitos, Thales and Aristeia programmes co-financed by EU-ESF and the Greek NSRF, Greece; BSF-NSF and MINERVA, Israel; NCN and NAWA, Poland; La Caixa Banking Foundation, CERCA Programme Generalitat de Catalunya and PROMETEO and GenT Programmes Generalitat Valenciana, Spain; Göran Gustafssons Stiftelse, Sweden; The Royal Society and Leverhulme Trust, United Kingdom. In addition, individual members wish to acknowledge support from Armenia: Yerevan Physics Institute (FAPERJ); CERN: European Organization for Nuclear Research (CERN DOCT); Chile: Agencia Nacional de Investigación y Desarrollo (FONDECYT 1230812, FONDECYT 1230987, FONDECYT 1240864); China: Chinese Ministry of Science and Technology (MOST-2023YFA1605700, MOST-2023YFA1609300), National Natural Science Foundation of China (NSFC - 12175119, NSFC 12275265); Czech Republic: Czech Science Foundation (GACR - 24-11373S), Ministry of Education Youth and Sports (ERC-CZ-LL2327, FORTE CZ.02.01.01/00/22_008/0004632), PRIMUS Research Programme (PRIMUS/21/SCI/017); EU: H2020 European Research Council (ERC - 101002463); European Union: European Research Council (ERC - 948254, ERC 101089007, ERC, BARD, 101116429), European Regional Development Fund (SMASH COFUND 101081355, SLO ERDF), Horizon 2020 Framework Programme (MUCCA -

CHIST-ERA-19-XAI-00), European Union, Future Artificial Intelligence Research (FAIR-NextGenerationEU PE00000013), Horizon 2020 (EuroHPC - EHPC-DEV-2024D11-051), Italian Center for High Performance Computing, Big Data and Quantum Computing (ICSC, NextGenerationEU); France: Agence Nationale de la Recherche (ANR-21-CE31-0022, ANR-22-EDIR-0002); Germany: Baden-Württemberg Stiftung (BW Stiftung-Postdoc Eliteprogramme), Deutsche Forschungsgemeinschaft (DFG - 469666862, DFG - CR 312/5-2); China: Research Grants Council (GRF); Italy: Istituto Nazionale di Fisica Nucleare (ICSC, NextGenerationEU), Ministero dell'Università e della Ricerca (NextGenEU I53D23000820006 M4C2.1.1); Japan: Japan Society for the Promotion of Science (JSPS KAKENHI JP22H01227, JSPS KAKENHI JP22H04944, JSPS KAKENHI JP22KK0227, JSPS KAKENHI JP23KK0245, JSPS KAKENHI JP24K23939); Norway: Research Council of Norway (RCN-314472); Poland: Ministry of Science and Higher Education (IDUB AGH, POB8, D4 no 9722), Polish National Science Centre (NCN 2021/42/E/ST2/00350, NCN OPUS 2023/51/B/ST2/02507, NCN OPUS nr 2022/47/B/ST2/03059, NCN UMO-2019/34/E/ST2/00393, UMO-2022/47/O/ST2/00148, UMO-2023/49/B/ST2/04085, UMO-2023/51/B/ST2/00920, UMO-2024/53/N/ST2/00869); Portugal: Foundation for Science and Technology (FCT); Spain: Generalitat Valenciana (Artemisa, FEDER, IDIFEDER/2018/048), Ministry of Science and Innovation (MCIN & NextGenEU PCI2022-135018-2, MICIN & FEDER PID2021-125273NB, RYC2019-028510-I, RYC2020-030254-I, RYC2021-031273-I, RYC2022-038164-I); Sweden: Carl Trygger Foundation (Carl Trygger Foundation CTS 22:2312), Swedish Research Council (Swedish Research Council 2023-04654, VR 2021-03651, VR 2022-03845, VR 2022-04683, VR 2023-03403, VR 2024-05451), Knut and Alice Wallenberg Foundation (KAW 2018.0458, KAW 2022.0358, KAW 2023.0366); Switzerland: Swiss National Science Foundation (SNSF- PCEFP2_194658); United Kingdom: Leverhulme Trust (Leverhulme Trust RPG-2020-004), Royal Society (NIF-R1-231091); United States of America: U.S. Department of Energy (ECA DE-AC02-76SF00515), Neubauer Family Foundation.

Funded by SCOAP[3].

References

1. ATLAS Collaboration, Observation of a new particle in the search for the Standard Model Higgs boson with the ATLAS detector at the LHC. Phys. Lett. B **716**, 1 (2012). https://doi.org/10.1016/j.physletb.2012.08.020. arXiv:1207.7214 [hep-ex]
2. C.M.S. Collaboration, Observation of a new boson at a mass of 125 GeV with the CMS experiment at the LHC. Phys. Lett. B **716**, 30 (2012). https://doi.org/10.1016/j.physletb.2012.08.021. arXiv:1207.7235 [hep-ex]
3. L. Evans, P. Bryant, L.H.C. Machine, JINST **3**, S08001 (2008). https://doi.org/10.1088/1748-0221/3/08/S08001
4. G.C. Branco et al., Theory and phenomenology of two-Higgs-doublet models. Phys. Rep. **516**, 1 (2012). https://doi.org/10.1016/j.physrep.2012.02.002. arXiv:1106.0034 [hep-ph]
5. M. Aoki, S. Kanemura, K. Tsumura, K. Yagyu, Models of Yukawa interaction in the two Higgs doublet model, and their collider phenomenology. Phys. Rev. D **80**, 015017 (2009). https://doi.org/10.1103/PhysRevD.80.015017. arXiv:0902.4665 [hep-ph]
6. Y.A. Golfand, E.P. Likhtman, Extension of the algebra of Poincare group generators and violation of p invariance. JETP Lett. **13**, 323 (1971). https://doi.org/10.1142/9789814542340_0001
7. D.V. Volkov, V.P. Akulov, Is the neutrino a goldstone particle? Phys. Lett. B **46**, 109 (1973). https://doi.org/10.1016/0370-2693(73)90490-5
8. J. Wess, B. Zumino, Supergauge transformations in four dimensions. Nucl. Phys. B **70**, 39 (1974). https://doi.org/10.1016/0550-3213(74)90355-1
9. J. Wess, B. Zumino, Supergauge invariant extension of quantum electrodynamics. Nucl. Phys. B **78**, 1 (1974). https://doi.org/10.1016/0550-3213(74)90112-6
10. S. Ferrara, B. Zumino, Supergauge invariant Yang–Mills theories. Nucl. Phys. B **79**, 413 (1974). https://doi.org/10.1016/0550-3213(74)90559-8
11. A. Salam, J. Strathdee, Super-symmetry and non-Abelian gauges. Phys. Lett. B **51**, 353 (1974). https://doi.org/10.1016/0370-2693(74)90226-3
12. M.R. Buckley, D. Feld, D. Gonçalves, Scalar simplified models for dark matter. Phys. Rev. D **91** (2015). https://doi.org/10.1103/physrevd.91.015017. arXiv:1410.6497 [hep-ph]
13. M. Bauer, U. Haisch, F. Kahlhoefer, Simplified dark matter models with two Higgs doublets: I. Pseudoscalar mediators. JHEP **05**, 138 (2017). https://doi.org/10.1007/jhep05(2017)138. arXiv:1701.07427 [hep-ph]
14. J.E. Kim, Light pseudoscalars, particle physics and cosmology. Phys. Rep. **150**, 1 (1987). https://doi.org/10.1016/0370-1573(87)90017-2
15. M. Casolino, T. Farooque, A. Juste, T. Liu, M. Spannowsky, Probing a light CP-odd scalar in di-top-associated production at the LHC. Eur. Phys. J. C **75**, 498 (2015). https://doi.org/10.1140/epjc/s10052-015-3708-y. arXiv:1507.07004 [hep-ph]
16. CMS Collaboration, Search for a scalar or pseudoscalar dilepton resonance produced in association with a massive vector boson or top quark-antiquark pair in multilepton events at $\sqrt{s} =$ 13 TeV. Phys. Rev. D **110**, 012013 (2024). https://doi.org/10.1103/PhysRevD.110.012013. arXiv:2402.11098 [hep-ex]
17. ATLAS Collaboration, Search for a new pseudoscalar decaying into a pair of muons in events with a top-quark pair at $\sqrt{s} = 13$ TeV TeV with the ATLAS detector. Phys. Rev. D **108**, 092007 (2023). https://doi.org/10.1103/PhysRevD.108.092007. arXiv:2304.14247 [hep-ex]
18. ATLAS Collaboration, The ATLAS Experiment at the CERN Large Hadron Collider. JINST **3**, S08003 (2008). https://doi.org/10.1088/1748-0221/3/08/S08003
19. ATLAS Collaboration, ATLAS Insertable B-Layer: Technical Design Report, ATLAS-TDR-19; CERN-LHCC-2010-013 (2010). https://cds.cern.ch/record/1291633. Addendum: ATLAS-TDR-19-ADD-1; CERN-LHCC-2012-009 (2012). https://cds.cern.ch/record/1451888
20. B. Abbott et al., Production and integration of the ATLAS Insertable B-Layer. JINST **13**, T05008 (2018). https://doi.org/10.1088/1748-0221/13/05/T05008. arXiv:1803.00844 [physics.ins-det]
21. G. Avoni et al., The new LUCID-2 detector for luminosity measurement and monitoring in ATLAS. JINST **13**, P07017 (2018). https://doi.org/10.1088/1748-0221/13/07/P07017

22. ATLAS Collaboration, Performance of the ATLAS trigger system in 2015. Eur. Phys. J. C **77**, 317 (2017). https://doi.org/10.1140/epjc/s10052-017-4852-3. arXiv:1611.09661 [hep-ex]
23. ATLAS Collaboration, Software and computing for Run 3 of the ATLAS experiment at the LHC. Eur. Phys. J. C **85**, 234 (2025). https://doi.org/10.1140/epjc/s10052-024-13701-w. arXiv:2404.06335 [hep-ex]
24. ATLAS Collaboration, Luminosity determination in pp collisions at $\sqrt{s} = 13$ TeV using the ATLAS detector at the LHC. Eur. Phys. J. C **83**, 982 (2023). https://doi.org/10.1140/epjc/s10052-023-11747-w. arXiv:2212.09379 [hep-ex]
25. T. Sjöstrand, S. Mrenna, P. Skands, A brief introduction to PYTHIA 8.1. Comput. Phys. Commun. **178**, 852 (2008). https://doi.org/10.1016/j.cpc.2008.01.036. arXiv:0710.3820 [hep-ph]
26. ATLAS Collaboration, The Pythia 8 A3 tune description of ATLAS minimum bias and inelastic measurements incorporating the Donnachie–Landshoff diffractive model, ATL-PHYS-PUB-2016-017 (2016). https://cds.cern.ch/record/2206965
27. S. Agostinelli et al., Geant4—a simulation toolkit. Nucl. Instrum. Methods A **506**, 250 (2003). https://doi.org/10.1016/S0168-9002(03)01368-8
28. ATLAS Collaboration, The ATLAS simulation infrastructure. Eur. Phys. J. C **70**, 823 (2010). https://doi.org/10.1140/epjc/s10052-010-1429-9. arXiv:1005.4568 [physics.ins-det]
29. J. Alwall et al., The automated computation of tree-level and next-to-leading order differential cross sections, and their matching to parton shower simulations. JHEP **07**, 079 (2014). https://doi.org/10.1007/JHEP07(2014)079. arXiv:1405.0301 [hep-ph]
30. ATLAS Collaboration, Studies of Monte Carlo predictions for the $t\bar{t}b\bar{b}$ process, ATL-PHYS-PUB-2022-006 (2022). https://cds.cern.ch/record/2802806
31. S. Frixione, G. Ridolfi, P. Nason, A positive-weight next-to-leading-order Monte Carlo for heavy flavour hadroproduction. JHEP **09**, 126 (2007). https://doi.org/10.1088/1126-6708/2007/09/126. arXiv:0707.3088 [hep-ph]
32. P. Nason, A new method for combining NLO QCD with shower Monte Carlo algorithms. JHEP **11**, 040 (2004). https://doi.org/10.1088/1126-6708/2004/11/040. arXiv:hep-ph/0409146
33. S. Frixione, P. Nason, C. Oleari, Matching NLO QCD computations with parton shower simulations: the POWHEG method. JHEP **11**, 070 (2007). https://doi.org/10.1088/1126-6708/2007/11/070. arXiv:0709.2092 [hep-ph]
34. S. Alioli, P. Nason, C. Oleari, E. Re, A general framework for implementing NLO calculations in shower Monte Carlo programs: the POWHEG BOX. JHEP **06**, 043 (2010). https://doi.org/10.1007/JHEP06(2010)043. arXiv:1002.2581 [hep-ph]
35. NNPDF Collaboration, R.D. Ball et al., Parton distributions for the LHC run II. JHEP **04**, 040 (2015). https://doi.org/10.1007/JHEP04(2015)040. arXiv:1410.8849 [hep-ph]
36. T. Sjöstrand et al., An introduction to PYTHIA 8.2. Comput. Phys. Commun. **191**, 159 (2015). https://doi.org/10.1016/j.cpc.2015.01.024. arXiv:1410.3012 [hep-ph]
37. ATLAS Collaboration, ATLAS Pythia 8 tunes to 7 TeV data, ATL-PHYS-PUB-2014-021 (2014). https://cds.cern.ch/record/1966419
38. NNPDF Collaboration, R.D. Ball et al., Parton distributions with LHC data. Nucl. Phys. B **867**, 244 (2013). https://doi.org/10.1016/j.nuclphysb.2012.10.003. arXiv:1207.1303 [hep-ph]
39. J. Pumplin et al., New generation of parton distributions with uncertainties from global QCD analysis. JHEP **07**, 012 (2002). https://doi.org/10.1088/1126-6708/2002/07/012. arXiv:hep-ph/0201195
40. E. Bothmann et al., Event generation with Sherpa 2.2. SciPost Phys. **7**, 034 (2019). https://doi.org/10.21468/SciPostPhys.7.3.034. arXiv:1905.09127 [hep-ph]
41. S. Schumann, F. Krauss, A parton shower algorithm based on Catani–Seymour dipole factorisation. JHEP **03**, 038 (2008). https://doi.org/10.1088/1126-6708/2008/03/038. arXiv:0709.1027 [hep-ph]
42. S. Höche, F. Krauss, M. Schönherr, F. Siegert, A critical appraisal of NLO+PS matching methods. JHEP **09**, 049 (2012). https://doi.org/10.1007/JHEP09(2012)049. arXiv:1111.1220 [hep-ph]
43. S. Höche, F. Krauss, M. Schönherr, F. Siegert, QCD matrix elements + parton showers. The NLO case. JHEP **04**, 027 (2013). https://doi.org/10.1007/JHEP04(2013)027. arXiv:1207.5030 [hep-ph]
44. S. Catani, F. Krauss, B.R. Webber, R. Kuhn, QCD matrix elements + parton showers. JHEP **11**, 063 (2001). https://doi.org/10.1088/1126-6708/2001/11/063. arXiv:hep-ph/0109231
45. S. Höche, F. Krauss, S. Schumann, F. Siegert, QCD matrix elements and truncated showers. JHEP **05**, 053 (2009). https://doi.org/10.1088/1126-6708/2009/05/053. arXiv:0903.1219 [hep-ph]
46. D.J. Lange, The EvtGen particle decay simulation package. Nucl. Instrum. Methods A **462**, 152 (2001). https://doi.org/10.1016/S0168-9002(01)00089-4
47. M. Beneke, P. Falgari, S. Klein, C. Schwinn, Hadronic top-quark pair production with NNLL threshold resummation. Nucl. Phys. B **855**, 695 (2012). https://doi.org/10.1016/j.nuclphysb.2011.10.021. arXiv:1109.1536 [hep-ph]
48. M. Cacciari, M. Czakon, M. Mangano, A. Mitov, P. Nason, Top-pair production at hadron colliders with next-to-next-to-leading logarithmic soft-gluon resummation. Phys. Lett. B **710**, 612 (2012). https://doi.org/10.1016/j.physletb.2012.03.013. arXiv:1111.5869 [hep-ph]
49. P. Bärnreuther, M. Czakon, A. Mitov, Percent-level-precision physics at the tevatron: next-to-next-to-leading order QCD corrections to $q\bar{q} \to t\bar{t} + X$. Phys. Rev. Lett. **109**, 132001 (2012). https://doi.org/10.1103/PhysRevLett.109.132001. arXiv:1204.5201 [hep-ph]
50. M. Czakon, A. Mitov, NNLO corrections to top-pair production at hadron colliders: the all-fermionic scattering channels. JHEP **12**, 054 (2012). https://doi.org/10.1007/JHEP12(2012)054. arXiv:1207.0236 [hep-ph]
51. M. Czakon, A. Mitov, NNLO corrections to top pair production at hadron colliders: the quark-gluon reaction. JHEP **01**, 080 (2013). https://doi.org/10.1007/JHEP01(2013)080. arXiv:1210.6832 [hep-ph]
52. M. Czakon, P. Fiedler, A. Mitov, Total top-quark pair-production cross section at hadron colliders through $\mathcal{O}(\alpha_S^4)$. Phys. Rev. Lett. **110**, 252004 (2013). https://doi.org/10.1103/PhysRevLett.110.252004. arXiv:1303.6254 [hep-ph]
53. M. Czakon, A. Mitov, Top++: a program for the calculation of the top-pair cross-section at hadron colliders. Comput. Phys. Commun. **185**, 2930 (2014). https://doi.org/10.1016/j.cpc.2014.06.021. arXiv:1112.5675 [hep-ph]
54. N. Kidonakis, Two-loop soft anomalous dimensions for single top quark associated production with a W^- or H^-. Phys. Rev. D **82**, 054018 (2010). https://doi.org/10.1103/PhysRevD.82.054018. arXiv:1005.4451 [hep-ph]
55. N. Kidonakis, 'Top Quark Production', in *Proceedings, Helmholtz International Summer School on Physics of Heavy Quarks and Hadrons (HQ2013) (JINR, Dubna, Russia, 15th–28th July 2013)*, p. 139. https://doi.org/10.3204/DESY-PROC-2013-03/Kidonakis. arXiv:1311.0283 [hep-ph]
56. D. de Florian et al., Handbook of LHC Higgs Cross Sections: 4. Deciphering the Nature of the Higgs Sector (2017). https://doi.org/10.23731/CYRM-2017-002. arXiv:1610.07922 [hep-ph]
57. C. Anastasiou, L. Dixon, K. Melnikov, F. Petriello, High-precision QCD at hadron colliders: electroweak gauge boson rapidity distributions at next-to-next-to leading order. Phys. Rev. D **69**, 094008 (2004). https://doi.org/10.1103/PhysRevD.69.094008. arXiv:hep-ph/0312266

58. ATLAS Collaboration, Electron and photon performance measurements with the ATLAS detector using the 2015-2017 LHC proton-proton collision data. JINST **14**, P12006 (2019). https://doi.org/10.1088/1748-0221/14/12/P12006. arXiv:1908.00005 [hep-ex]
59. ATLAS Collaboration, Evidence for the associated production of the Higgs boson and a top quark pair with the ATLAS detector. Phys. Rev. D **97**, 072003 (2018). https://doi.org/10.1103/PhysRevD.97.072003. arXiv:1712.08891 [hep-ex]
60. ATLAS Collaboration, Muon reconstruction and identification efficiency in ATLAS using the full Run 2 pp collision data set at $\sqrt{s} = 13$ TeV. Eur. Phys. J. C **81**, 578 (2021). https://doi.org/10.1140/epjc/s10052-021-09233-2. arXiv:2012.00578 [hep-ex]
61. ATLAS Collaboration, Jet reconstruction and performance using particle flow with the ATLAS detector. Eur. Phys. J. C **77**, 466 (2017). https://doi.org/10.1140/epjc/s10052-017-5031-2. arXiv:1703.10485 [hep-ex]
62. M. Cacciari, G.P. Salam, G. Soyez, The anti-k_t jet clustering algorithm. JHEP **04**, 063 (2008). https://doi.org/10.1088/1126-6708/2008/04/063. arXiv:0802.1189 [hep-ph]
63. M. Cacciari, G.P. Salam, G. Soyez, FastJet user manual. Eur. Phys. J. C **72**, 1896 (2012). https://doi.org/10.1140/epjc/s10052-012-1896-2. arXiv:1111.6097 [hep-ph]
64. ATLAS Collaboration, Jet energy scale and resolution measured in proton–proton collisions at $\sqrt{s} = 13$ TeV with the ATLAS detector. Eur. Phys. J. C **81**, 689 (2021). https://doi.org/10.1140/epjc/s10052-021-09402-3. arXiv:2007.02645 [hep-ex]
65. ATLAS Collaboration, Performance of pile-up mitigation techniques for jets in pp collisions at $\sqrt{s} = 8$ TeV using the ATLAS detector. Eur. Phys. J. C **76**, 581 (2016). https://doi.org/10.1140/epjc/s10052-016-4395-z. arXiv:1510.03823 [hep-ex]
66. ATLAS Collaboration, ATLAS flavour-tagging algorithms for the LHC Run 2 pp collision dataset. Eur. Phys. J. C **83**, 681 (2023). https://doi.org/10.1140/epjc/s10052-023-11699-1. arXiv:2211.16345 [physics.data-an]
67. ATLAS Collaboration, ATLAS b-jet identification performance and efficiency measurement with $t\bar{t}$ events in pp collisions at $\sqrt{s} = 13$ TeV. Eur. Phys. J. C **79**, 970 (2019). https://doi.org/10.1140/epjc/s10052-019-7450-8. arXiv:1907.05120 [hep-ex]
68. ATLAS Collaboration, Measurement of the c-jet mistagging efficiency in $t\bar{t}$ events using pp collision data at $\sqrt{s} = 13$ TeV collected with the ATLAS detector. Eur. Phys. J. C **82**, 95 (2022). https://doi.org/10.1140/epjc/s10052-021-09843-w. arXiv:2109.10627 [hep-ex]
69. ATLAS Collaboration, Calibration of the light-flavour jet mistagging efficiency of the b-tagging algorithms with Z+jets events using 139 fb^{-1} of ATLAS proton–proton collision data at $\sqrt{s} = 13$ TeV. Eur. Phys. J. C **83**, 728 (2023). https://doi.org/10.1140/epjc/s10052-023-11736-z. arXiv:2301.06319 [hep-ex]
70. M. Cacciari, G.P. Salam, Pileup subtraction using jet areas. Phys. Lett. B **659**, 119 (2008). https://doi.org/10.1016/j.physletb.2007.09.077. arXiv:0707.1378 [hep-ph]
71. M. Cacciari, G.P. Salam, G. Soyez, The catchment area of jets. JHEP **04**, 005 (2008). https://doi.org/10.1088/1126-6708/2008/04/005. arXiv:0802.1188 [hep-ph]
72. ATLAS Collaboration, Deep Sets based Neural Networks for Impact Parameter Flavour Tagging in ATLAS, ATL-PHYS-PUB-2020-014 (2020). https://cds.cern.ch/record/2718948
73. ATLAS Collaboration, Variable Radius, Exclusive-k_T, and Center-of-Mass Subjet Reconstruction for Higgs($\to b\bar{b}$) Tagging in ATLAS, ATL-PHYS-PUB-2017-010 (2017). https://cds.cern.ch/record/2268678
74. ATLAS Collaboration, Calibration of a soft secondary vertex tagger using proton–proton collisions at $\sqrt{s} = 13$ TeV with the ATLAS detector. Phys. Rev. D **110**, 032015 (2024). https://doi.org/10.1103/PhysRevD.110.032015. arXiv:2405.03253 [hep-ex]
75. V. Kostyukhin, Secondary vertex based b-tagging, tech. rep. ATL-PHYS-2003-033, revised version number 1 submitted on 2003-09-22 11:21:01: CERN (2003). https://cds.cern.ch/record/685550
76. ATLAS Collaboration, Performance of the reconstruction of large impact parameter tracks in the inner detector of ATLAS. Eur. Phys. J. C **83**, 1081 (2023). https://doi.org/10.1140/epjc/s10052-023-12024-6. arXiv:2304.12867 [hep-ex]
77. ATLAS Collaboration, DeXTer: Deep Sets based Neural Networks for Low-p_T $X \to b\bar{b}$ Identification in ATLAS, ATL-PHYS-PUB-2022-042 (2022). https://cds.cern.ch/record/2825434
78. ATLAS Collaboration, The performance of missing transverse momentum reconstruction and its significance with the ATLAS detector using 140 fb^{-1} of $\sqrt{s} = 13$ TeV pp collisions (2024). arXiv:2402.05858 [hep-ex]
79. B. Nachman, P. Nef, A. Schwartzman, M. Swiatlowski, C. Wanotayaroj, Jets from Jets: re-clustering as a tool for large radius jet reconstruction and grooming at the LHC. JHEP **02**, 075 (2015). https://doi.org/10.1007/JHEP02(2015)075. arXiv:1407.2922 [hep-ph]
80. ATLAS Collaboration, Performance of electron and photon triggers in ATLAS during LHC Run 2. Eur. Phys. J. C **80**, 47 (2020). https://doi.org/10.1140/epjc/s10052-019-7500-2. arXiv:1909.00761 [hep-ex]
81. ATLAS Collaboration, Performance of the ATLAS muon triggers in Run 2. JINST **15**, P09015 (2020). https://doi.org/10.1088/1748-0221/15/09/p09015. arXiv:2004.13447 [physics.ins-det]
82. ATLAS Collaboration, ATLAS data quality operations and performance for 2015–2018 data-taking. JINST **15**, P04003 (2020). https://doi.org/10.1088/1748-0221/15/04/P04003. arXiv:1911.04632 [physics.ins-det]
83. ATLAS Collaboration, Search for charged Higgs bosons decaying into a top quark and a bottom quark at $\sqrt{s} = 13$ TeV with the ATLAS detector. JHEP **06**, 145 (2021). https://doi.org/10.1007/JHEP06(2021)145. arXiv:2102.10076 [hep-ex]
84. ATLAS Collaboration, Measurement of the $t\bar{t}t\bar{t}$ production cross section in pp collisions at $\sqrt{s} = 13$ TeV with the ATLAS detector. JHEP **11**, 118 (2021). https://doi.org/10.1007/JHEP11(2021)118. arXiv:2106.11683 [hep-ex]
85. ATLAS Collaboration, Search for a new scalar resonance in flavour-changing neutral-current top-quark decays $t \to qX$ ($q = u, c$), with $X \to b\bar{b}$, in proton–proton collisions at $\sqrt{s} = 13$ TeV with the ATLAS detector. JHEP **07**, 199 (2023). https://doi.org/10.1007/JHEP07(2023)199. arXiv:2301.03902 [hep-ex]
86. CMS Collaboration, Measurement of the $t\bar{t}$ production cross section in the all-jet final state in pp collisions at $\sqrt{s} = 7$ TeV. JHEP **05**, 065 (2013). https://doi.org/10.1007/JHEP05(2013)065. arXiv:1302.0508 [hep-ex]
87. CMS Collaboration, Measurement of the cross section for $t\bar{t}$ production with additional jets and b jets in pp collisions at $\sqrt{s} = 13$ TeV. JHEP **07**, 125 (2020). https://doi.org/10.1007/JHEP07(2020)125. arXiv:2003.06467 [hep-ex]
88. ATLAS Collaboration, Measurements of inclusive and differential fiducial cross-sections of $t\bar{t}$ production with additional heavy-flavour jets in proton–proton collisions at $\sqrt{s} = 13$ TeV with the ATLAS detector. JHEP **04**, 046 (2019). https://doi.org/10.1007/JHEP04(2019)046. arXiv:1811.12113 [hep-ex]
89. A. Hoecker et al., TMVA—Toolkit for Multivariate Data Analysis (2009). arXiv:physics/0703039 [physics.data-an]
90. A. Paszke et al., PyTorch: an imperative style, high-performance deep learning library (2019). https://doi.org/10.48550/arXiv.1912.01703. arXiv:1912.01703 [cs.LG]
91. G. Cowan, K. Cranmer, E. Gross, O. Vitells, Asymptotic formulae for likelihood-based tests of new physics. Eur. Phys. J. C **71**, 1554 (2011). https://doi.org/10.1140/epjc/s10052-011-1554-0. arXiv:1007.1727 [physics.data-an]. Erratum: Eur. Phys. J. C **73**, 2501 (2013)

98. ATLAS Collaboration, Measurement of the associated production of a top-antitop-quark pair and a Higgs boson decaying into a $b\bar{b}$ pair in pp collisions at $\sqrt{s} = 13$ TeV using the ATLAS detector at the LHC. Eur. Phys. J. C **85**, 210 (2025). https://doi.org/10.1140/epjc/s10052-025-13740-x. arXiv:2407.10904 [hep-ex]

99. ATLAS Collaboration, ATLAS Computing Acknowledgements, ATL-SOFT-PUB-2025-001 (2025). https://cds.cern.ch/record/2922210

ATLAS Collaboration*

G. Aad[104], E. Aakvaag[17], B. Abbott[123], S. Abdelhameed[119a], K. Abeling[55], N.J. Abicht[49], S. H. Abidi[30], M. Aboelela[45], A. Aboulhorma[36e], H. Abramowicz[157], Y. Abulaiti[120], B. S. Acharya[69a,69b,n], A. Ackermann[63a], C. Adam Bourdarios[4], L. Adamczyk[86a], S. V. Addepalli[149], M. J. Addison[103], J. Adelman[118], A. Adiguzel[22c], T. Adye[137], A. A. Affolder[139], Y. Afik[40], M. N. Agaras[13], A. Aggarwal[102], C. Agheorghiesei[28c], F. Ahmadov[39,ae], S. Ahuja[97], X. Ai[143b], G. Aielli[76a,76b], A. Aikot[169], M. Ait Tamlihat[36e], B. Aitbenchikh[36a], M. Akbiyik[102], T. P. A. Åkesson[100], A. V. Akimov[151], D. Akiyama[174], N. N. Akolkar[25], S. Aktas[22a], G. L. Alberghi[24b], J. Albert[171], P. Albicocco[53], G. L. Albouy[60], S. Alderweireldt[52], Z. L. Alegria[124], M. Aleksa[37], I. N. Aleksandrov[39], C. Alexa[28b], T. Alexopoulos[10], F. Alfonsi[24b], M. Algren[56], M. Alhroob[173], B. Ali[135], H. M. J. Ali[93,x], S. Ali[32], S. W. Alibocus[94], M. Aliev[34c], G. Alimonti[71a], W. Alkakhi[55], C. Allaire[66], B. M. M. Allbrooke[152], J. S. Allen[103], J. F. Allen[52], P. P. Allport[21], A. Aloisio[72a,72b], F. Alonso[92], C. Alpigiani[142], Z. M. K. Alsolami[93], A. Alvarez Fernandez[102], M. Alves Cardoso[56], M. G. Alviggi[72a,72b], M. Aly[103], Y. Amaral Coutinho[83b], A. Ambler[106], C. Amelung[37], M. Amerl[103], C. G. Ames[111], T. Amezza[130], D. Amidei[108], B. Amini[54], K. Amirie[161], A. Amirkhanov[39], S. P. Amor Dos Santos[133a], K. R. Amos[169], D. Amperiadou[158], S. An[84], C. Anastopoulos[145], T. Andeen[11], J. K. Anders[94], A. C. Anderson[59], A. Andreazza[71a,71b], S. Angelidakis[9], A. Angerami[42], A. V. Anisenkov[39], A. Annovi[74a], C. Antel[56], E. Antipov[151], M. Antonelli[53], F. Anulli[75a], M. Aoki[84], T. Aoki[159], M. A. Aparo[152], L. Aperio Bella[48], M. Apicella[31], C. Appelt[157], A. Apyan[27], S. J. Arbiol Val[87], C. Arcangeletti[53], A. T. H. Arce[51], J-F. Arguin[110], S. Argyropoulos[158], J.-H. Arling[48], O. Arnaez[4], H. Arnold[151], G. Artoni[75a,75b], H. Asada[113], K. Asai[121], S. Asai[159], S. Asatryan[179], N. A. Asbah[37], R. A. Ashby Pickering[173], A. M. Aslam[97], K. Assamagan[30], R. Astalos[29a], K. S. V. Astrand[100], S. Atashi[165], R. J. Atkin[34a], H. Atmani[36f], P. A. Atmasiddha[131], K. Augsten[135], A. D. Auriol[41], V. A. Austrup[103], G. Avolio[37], K. Axiotis[56], G. Azuelos[110,ai], D. Babal[29b], H. Bachacou[138], K. Bachas[158,r], A. Bachiu[35], E. Bachmann[50], M. J. Backes[63a], A. Badea[40], T. M. Baer[108], P. Bagnaia[75a,75b], M. Bahmani[19], D. Bahner[54], K. Bai[126], J. T. Baines[137], L. Baines[96], O. K. Baker[178], E. Bakos[16], D. Bakshi Gupta[8], L. E. Balabram Filho[83b], V. Balakrishnan[123], R. Balasubramanian[4], E. M. Baldin[38], P. Balek[86a], E. Ballabene[24a,24b], F. Balli[138], L. M. Baltes[63a], W. K. Balunas[33], J. Balz[102], I. Bamwidhi[119b], E. Banas[87], M. Bandieramonte[132], A. Bandyopadhyay[25], S. Bansal[25], L. Barak[157], M. Barakat[48], E. L. Barberio[107], D. Barberis[18b], M. Barbero[104], M. Z. Barel[117], T. Barillari[112], M-S. Barisits[37], T. Barklow[149], P. Baron[136], D. A. Baron Moreno[103], A. Baroncelli[62], A. J. Barr[129], J. D. Barr[98], F. Barreiro[101], J. Barreiro Guimarães da Costa[14], M. G. Barros Teixeira[133a], S. Barsov[38], F. Bartels[63a], R. Bartoldus[149], A. E. Barton[93], P. Bartos[29a], A. Basan[102], M. Baselga[49], S. Bashiri[87], A. Bassalat[66,b], M. J. Basso[162a], S. Bataju[45], R. Bate[170], R. L. Bates[59], S. Batlamous[101], M. Battaglia[139], D. Battulga[19], M. Bauce[75a,75b], M. Bauer[79], P. Bauer[25], L. T. Bayer[48], L. T. Bazzano Hurrell[31], J. B. Beacham[112], T. Beau[130], J. Y. Beaucamp[92], P. H. Beauchemin[164], P. Bechtle[25], H. P. Beck[20,q], K. Becker[173], A. J. Beddall[82], V. A. Bednyakov[39], C. P. Bee[151], L. J. Beemster[16], M. Begalli[83d], M. Begel[30], J. K. Behr[48], J. F. Beirer[37], F. Beisiegel[25], M. Belfkir[119b], G. Bella[157], L. Bellagamba[24b], A. Bellerive[35], C. D. Bellgraph[68], P. Bellos[21], K. Beloborodov[38], D. Benchekroun[36a], F. Bendebba[36a], Y. Benhammou[157], K. C. Benkendorfer[61], L. Beresford[48], M. Beretta[53], E. Bergeaas Kuutmann[167], N. Berger[4], B. Bergmann[135], J. Beringer[18a], G. Bernardi[5], C. Bernius[149], F. U. Bernlochner[25], F. Bernon[37], A. Berrocal Guardia[13], T. Berry[97], P. Berta[136], A. Berthold[50], A. Berti[133a], R. Bertrand[104], S. Bethke[112], A. Betti[75a,75b], A. J. Bevan[96], L. Bezio[56], N. K. Bhalla[54], S. Bharthuar[112], S. Bhatta[151], P. Bhattarai[149], Z. M. Bhatti[120], K. D. Bhide[54], V. S. Bhopatkar[124], R. M. Bianchi[132], G. Bianco[24b,24a], O. Biebel[111], M. Biglietti[77a], C. S. Billingsley[45], Y. Bimgdi[36f], M. Bindi[55], A. Bingham[177], A. Bingul[22b], C. Bini[75a,75b], G. A. Bird[33], M. Birman[175], M. Biros[136], S. Biryukov[152], T. Bisanz[49], E. Bisceglie[24b,24a], J. P. Biswal[137], D. Biswas[147],

I. Bloch[48], A. Blue[59], U. Blumenschein[96], J. Blumenthal[102], V. S. Bobrovnikov[39], M. Boehler[54], B. Boehm[172], D. Bogavac[13], A. G. Bogdanchikov[38], L. S. Boggia[130], V. Boisvert[97], P. Bokan[37], T. Bold[86a], M. Bomben[5], M. Bona[96], M. Boonekamp[138], A. G. Borbély[59], I. S. Bordulev[38], G. Borissov[93], D. Bortoletto[129], D. Boscherini[24b], M. Bosman[13], K. Bouaouda[36a], N. Bouchhar[169], L. Boudet[4], J. Boudreau[132], E. V. Bouhova-Thacker[93], D. Boumediene[41], R. Bouquet[57b,57a], A. Boveia[122], J. Boyd[37], D. Boye[30], I. R. Boyko[39], L. Bozianu[56], J. Bracinik[21], N. Brahimi[4], G. Brandt[177], O. Brandt[33], B. Brau[105], J. E. Brau[126], R. Brener[175], L. Brenner[117], R. Brenner[167], S. Bressler[175], G. Brianti[78a,78b], D. Britton[59], D. Britzger[112], I. Brock[25], R. Brock[109], G. Brooijmans[42], A. J. Brooks[68], E. M. Brooks[162b], E. Brost[30], L. M. Brown[171,162a], L. E. Bruce[61], T. L. Bruckler[129], P. A. Bruckman de Renstrom[87], B. Brüers[48], A. Bruni[24b], G. Bruni[24b], D. Brunner[47a,47b], M. Bruschi[24b], N. Bruscino[75a,75b], T. Buanes[17], Q. Buat[142], D. Buchin[112], A. G. Buckley[59], O. Bulekov[82], B. A. Bullard[149], S. Burdin[94], C. D. Burgard[49], A. M. Burger[91], B. Burghgrave[8], O. Burlayenko[54], J. Burleson[168], J. C. Burzynski[148], E. L. Busch[42], V. Büscher[102], P. J. Bussey[59], J. M. Butler[26], C. M. Buttar[59], J. M. Butterworth[98], W. Buttinger[137], C. J. Buxo Vazquez[109], A. R. Buzykaev[39], S. Cabrera Urbán[169], L. Cadamuro[66], D. Caforio[58], H. Cai[132], Y. Cai[24b,114c,24a], Y. Cai[114a], V. M. M. Cairo[37], O. Cakir[3a], N. Calace[37], P. Calafiura[18a], G. Calderini[130], P. Calfayan[35], G. Callea[59], L. P. Caloba[83b], D. Calvet[41], S. Calvet[41], R. Camacho Toro[130], S. Camarda[37], D. Camarero Munoz[27], P. Camarri[76a,76b], C. Camincher[171], M. Campanelli[98], A. Camplani[43], V. Canale[72a,72b], A. C. Canbay[3a], E. Canonero[97], J. Cantero[169], Y. Cao[168], F. Capocasa[27], M. Capua[44b,44a], A. Carbone[71a,71b], R. Cardarelli[76a], J. C. J. Cardenas[8], M. P. Cardiff[27], G. Carducci[44b,44a], T. Carli[37], G. Carlino[72a], J. I. Carlotto[13], B. T. Carlson[132,s], E. M. Carlson[171], J. Carmignani[94], L. Carminati[71a,71b], A. Carnelli[4], M. Carnesale[37], S. Caron[116], E. Carquin[140f], I. B. Carr[107], S. Carrá[73a,73b], G. Carratta[24b,24a], A. M. Carroll[126], M. P. Casado[13,i], M. Caspar[48], F. L. Castillo[4], L. Castillo Garcia[13], V. Castillo Gimenez[169], N. F. Castro[133a,133e], A. Catinaccio[37], J. R. Catmore[128], T. Cavaliere[4], V. Cavaliere[30], L. J. Caviedes Betancourt[23b], E. Celebi[82], S. Cella[37], V. Cepaitis[56], K. Cerny[125], A. S. Cerqueira[83a], A. Cerri[74a,74b,al], L. Cerrito[76a,76b], F. Cerutti[18a], B. Cervato[71a,71b], A. Cervelli[24b], G. Cesarini[53], S. A. Cetin[82], P. M. Chabrillat[130], S. Chakraborty[173], J. Chan[18a], W. Y. Chan[159], J. D. Chapman[33], E. Chapon[138], B. Chargeishvili[155b], D. G. Charlton[21], C. Chauhan[136], Y. Che[114a], S. Chekanov[6], S. V. Chekulaev[162a], G. A. Chelkov[39,a], B. Chen[157], B. Chen[171], H. Chen[114a], H. Chen[30], J. Chen[144a], J. Chen[148], M. Chen[129], S. Chen[89], S. J. Chen[114a], X. Chen[144a], X. Chen[15,ah], Z. Chen[62], C. L. Cheng[176], H. C. Cheng[64a], S. Cheong[149], A. Cheplakov[39], E. Cherepanova[117], R. Cherkaoui El Moursli[36e], E. Cheu[7], K. Cheung[65], L. Chevalier[138], V. Chiarella[53], G. Chiarelli[74a], G. Chiodini[70a], A. S. Chisholm[21], A. Chitan[28b], M. Chitishvili[169], M. V. Chizhov[39,t], K. Choi[11], Y. Chou[142], E. Y. S. Chow[116], K. L. Chu[175], M. C. Chu[64a], X. Chu[14,114c], Z. Chubinidze[53], J. Chudoba[134], J. J. Chwastowski[87], D. Cieri[112], K. M. Ciesla[86a], V. Cindro[95], A. Ciocio[18a], F. Cirotto[72a,72b], Z. H. Citron[175], M. Citterio[71a], D. A. Ciubotaru[28b], A. Clark[56], P. J. Clark[52], N. Clarke Hall[98], C. Clarry[161], S. E. Clawson[48], C. Clement[47a,47b], Y. Coadou[104], M. Cobal[69a,69c], A. Coccaro[57b], R. F. Coelho Barrue[133a], R. Coelho Lopes De Sa[105], S. Coelli[71a], L. S. Colangeli[161], B. Cole[42], P. Collado Soto[101], J. Collot[60], R. Coluccia[70a,70b], P. Conde Muiño[133a,133g], M. P. Connell[34c], S. H. Connell[34c], E. I. Conroy[129], F. Conventi[72a,aj], H. G. Cooke[21], A. M. Cooper-Sarkar[129], L. Corazzina[75a,75b], F. A. Corchia[24b,24a], A. Cordeiro Oudot Choi[142], L. D. Corpe[41], M. Corradi[75a,75b], F. Corriveau[106,ac], A. Cortes-Gonzalez[159], M. J. Costa[169], F. Costanza[4], D. Costanzo[145], B. M. Cote[122], J. Couthures[4], G. Cowan[97], K. Cranmer[176], L. Cremer[49], D. Cremonini[24b,24a], S. Crépé-Renaudin[60], F. Crescioli[130], T. Cresta[73a,73b], M. Cristinziani[147], M. Cristoforetti[78a,78b], V. Croft[117], J. E. Crosby[124], G. Crosetti[44b,44a], A. Cueto[101], H. Cui[98], Z. Cui[7], W. R. Cunningham[59], F. Curcio[169], J. R. Curran[52], M. J. Da Cunha Sargedas De Sousa[57b,57a], J. V. Da Fonseca Pinto[83b], C. Da Via[103], W. Dabrowski[86a], T. Dado[37], S. Dahbi[154], T. Dai[108], D. Dal Santo[20], C. Dallapiccola[105], M. Dam[43], G. D'amen[30], V. D'Amico[111], J. Damp[102], J. R. Dandoy[35], D. Dannheim[37], G. D'anniballe[74a,74b], M. Danninger[148], V. Dao[151], G. Darbo[57b], S. J. Das[30], F. Dattola[48], S. D'Auria[71a,71b], A. D'Avanzo[72a,72b], T. Davidek[136], J. Davidson[173], I. Dawson[96], K. De[8], C. De Almeida Rossi[161], R. De Asmundis[72a], N. De Biase[48], S. De Castro[24b,24a], N. De Groot[116], P. de Jong[117], H. De la Torre[118], A. De Maria[114a], A. De Salvo[75a], U. De Sanctis[76a,76b], F. De Santis[70a,70b], A. De Santo[152], J. B. De Vivie De Regie[60], J. Debevc[95], D. V. Dedovich[39], J. Degens[94], A. M. Deiana[45], J. Del Peso[101], L. Delagrange[130], F. Deliot[138], C. M. Delitzsch[49], M. Della Pietra[72a,72b], D. Della Volpe[56], A. Dell'Acqua[37], L. Dell'Asta[71a,71b], M. Delmastro[4], C. C. Delogu[102], P. A. Delsart[60],

S. Demers[178], M. Demichev[39], S. P. Denisov[38], H. Denizli[22a,m], L. D'Eramo[41], D. Derendarz[87], F. Derue[130], P. Dervan[94], K. Desch[25], F. A. Di Bello[57b,57a], A. Di Ciaccio[76a,76b], L. Di Ciaccio[4], A. Di Domenico[75a,75b], C. Di Donato[72a,72b], A. Di Girolamo[37], G. Di Gregorio[37], A. Di Luca[78a,78b], B. Di Micco[77a,77b], R. Di Nardo[77a,77b], K. F. Di Petrillo[40], M. Diamantopoulou[35], F. A. Dias[117], M. A. Diaz[140a,140b], A. R. Didenko[39], M. Didenko[169], S. D. Diefenbacher[18a], E. B. Diehl[108], S. Díez Cornell[48], C. Diez Pardos[147], C. Dimitriadi[150], A. Dimitrievska[21], A. Dimri[151], J. Dingfelder[25], T. Dingley[129], I-M. Dinu[28b], S. J. Dittmeier[63b], F. Dittus[37], M. Divisek[136], B. Dixit[94], F. Djama[104], T. Djobava[155b], C. Doglioni[103,100], A. Dohnalova[29a], Z. Dolezal[136], K. Domijan[86a], K. M. Dona[40], M. Donadelli[83d], B. Dong[109], J. Donini[41], A. D'Onofrio[72a,72b], M. D'Onofrio[94], J. Dopke[137], A. Doria[72a], N. Dos Santos Fernandes[133a], P. Dougan[103], M. T. Dova[92], A. T. Doyle[59], M. A. Draguet[129], M. P. Drescher[55], E. Dreyer[175], I. Drivas-koulouris[10], M. Drnevich[120], M. Drozdova[56], D. Du[62], T. A. du Pree[117], Z. Duan[114a], F. Dubinin[39], M. Dubovsky[29a], E. Duchovni[175], G. Duckeck[111], P. K. Duckett[98], O. A. Ducu[28b], D. Duda[52], A. Dudarev[37], E. R. Duden[27], M. D'uffizi[103], L. Duflot[66], M. Dührssen[37], I. Duminica[28g], A. E. Dumitriu[28b], M. Dunford[63a], S. Dungs[49], K. Dunne[47a,47b], A. Duperrin[104], H. Duran Yildiz[3a], M. Düren[58], A. Durglishvili[155b], D. Duvnjak[35], B. L. Dwyer[118], G. I. Dyckes[18a], M. Dyndal[86a], B. S. Dziedzic[37], Z. O. Earnshaw[152], G. H. Eberwein[129], B. Eckerova[29a], S. Eggebrecht[55], E. Egidio Purcino De Souza[83e], G. Eigen[17], K. Einsweiler[18a], T. Ekelof[167], P. A. Ekman[100], S. El Farkh[36b], Y. El Ghazali[62], H. El Jarrari[37], A. El Moussaouy[36a], V. Ellajosyula[167], M. Ellert[167], F. Ellinghaus[177], N. Ellis[37], J. Elmsheuser[30], M. Elsawy[119a], M. Elsing[37], D. Emeliyanov[137], Y. Enari[84], I. Ene[18a], S. Epari[110], D. Ernani Martins Neto[87], F. Ernst[37], M. Errenst[177], M. Escalier[66], C. Escobar[169], E. Etzion[157], G. Evans[133a,133b], H. Evans[68], L. S. Evans[97], A. Ezhilov[38], S. Ezzarqtouni[36a], F. Fabbri[24b,24a], L. Fabbri[24b,24a], G. Facini[98], V. Fadeyev[139], R. M. Fakhrutdinov[38], D. Fakoudis[102], S. Falciano[75a], L. F. Falda Ulhoa Coelho[133a], F. Fallavollita[112], G. Falsetti[44b,44a], J. Faltova[136], C. Fan[168], K. Y. Fan[64b], Y. Fan[14], Y. Fang[14,114c], M. Fanti[71a,71b], M. Faraj[69a,69b], Z. Farazpay[99], A. Farbin[8], A. Farilla[77a], T. Farooque[109], J. N. Farr[178], S. M. Farrington[137,52], F. Fassi[36e], D. Fassouliotis[9], L. Fayard[66], P. Federic[136], P. Federicova[134], O. L. Fedin[38,a], M. Feickert[176], L. Feligioni[104], D. E. Fellers[18a], C. Feng[143a], Z. Feng[117], M. J. Fenton[165], L. Ferencz[48], B. Fernandez Barbadillo[93], P. Fernandez Martinez[67], M. J. V. Fernoux[104], J. Ferrando[93], A. Ferrari[167], P. Ferrari[117,116], R. Ferrari[73a], D. Ferrere[56], C. Ferretti[108], M. P. Fewell[1], D. Fiacco[75a,75b], F. Fiedler[102], P. Fiedler[135], S. Filimonov[39], M. S. Filip[28b,u], A. Filipčič[95], E. K. Filmer[162a], F. Filthaut[116], M. C. N. Fiolhais[133a,133c,c], L. Fiorini[169], W. C. Fisher[109], T. Fitschen[103], P. M. Fitzhugh[138], I. Fleck[147], P. Fleischmann[108], T. Flick[177], M. Flores[34d,ag], L. R. Flores Castillo[64a], L. Flores Sanz De Acedo[37], F. M. Follega[78a,78b], N. Fomin[33], J. H. Foo[161], A. Formica[138], A. C. Forti[103], E. Fortin[37], A. W. Fortman[18a], L. Foster[18a], L. Fountas[9,j], D. Fournier[66], H. Fox[93], P. Francavilla[74a,74b], S. Francescato[61], S. Franchellucci[56], M. Franchini[24b,24a], S. Franchino[63a], D. Francis[37], L. Franco[116], V. Franco Lima[37], L. Franconi[48], M. Franklin[61], G. Frattari[27], Y. Y. Frid[157], J. Friend[59], N. Fritzsche[37], A. Froch[56], D. Froidevaux[37], J. A. Frost[129], Y. Fu[109], S. Fuenzalida Garrido[140f], M. Fujimoto[104], K. Y. Fung[64a], E. Furtado De Simas Filho[83e], M. Furukawa[159], J. Fuster[169], A. Gaa[55], A. Gabrielli[24b,24a], A. Gabrielli[161], P. Gadow[37], G. Gagliardi[57b,57a], L. G. Gagnon[18a], S. Gaid[88b], S. Galantzan[157], J. Gallagher[1], E. J. Gallas[129], A. L. Gallen[167], B. J. Gallop[137], K. K. Gan[122], S. Ganguly[159], Y. Gao[52], A. Garabaglu[142], F. M. Garay Walls[140a,140b], C. García[169], A. Garcia Alonso[117], A. G. Garcia Caffaro[178], J. E. García Navarro[169], M. Garcia-Sciveres[18a], G. L. Gardner[131], R. W. Gardner[40], N. Garelli[164], R. B. Garg[149], J. M. Gargan[52], C. A. Garner[161], C. M. Garvey[34a], V. K. Gassmann[164], G. Gaudio[73a], V. Gautam[13], P. Gauzzi[75a,75b], J. Gavranovic[95], I. L. Gavrilenko[133a], A. Gavrilyuk[38], C. Gay[170], G. Gaycken[126], E. N. Gazis[10], A. Gekow[122], C. Gemme[57b], M. H. Genest[60], A. D. Gentry[115], S. George[97], T. Geralis[46], A. A. Gerwin[123], P. Gessinger-Befurt[37], M. E. Geyik[177], M. Ghani[173], K. Ghorbanian[96], A. Ghosal[147], A. Ghosh[165], A. Ghosh[7], B. Giacobbe[24b], S. Giagu[75a,75b], T. Giani[117], A. Giannini[62], S. M. Gibson[97], M. Gignac[139], D. T. Gil[86b], A. K. Gilbert[86a], B. J. Gilbert[42], D. Gillberg[35], G. Gilles[117], D. M. Gingrich[2,ai], M. P. Giordani[69a,69c], P. F. Giraud[138], G. Giugliarelli[69a,69c], D. Giugni[71a], F. Giuli[76a,76b], I. Gkialas[9,j], L. K. Gladilin[38], C. Glasman[101], M. Glazewska[20], R. M. Gleason[165], G. Glemža[48], M. Glisic[126], I. Gnesi[44b], Y. Go[30], M. Goblirsch-Kolb[37], B. Gocke[49], D. Godin[110], B. Gokturk[22a], S. Goldfarb[107], T. Golling[56], M. G. D. Gololo[34c], D. Golubkov[38], J. P. Gombas[109], A. Gomes[133a,133b], G. Gomes Da Silva[147], A. J. Gomez Delegido[169], R. Gonçalo[133a], L. Gonella[21], A. Gongadze[155c], F. Gonnella[21], J. L. Gonski[149], R. Y. González Andana[52], S. González de la Hoz[169], M. V. Gonzalez Rodrigues[48], R. Gonzalez Suarez[167], S. Gonzalez-Sevilla[56], L. Goossens[37], B. Gorini[37],

E. Gorini[70a,70b], A. Gorišek[95], T. C. Gosart[131], A. T. Goshaw[51], M. I. Gostkin[39], S. Goswami[124], C. A. Gottardo[37], S. A. Gotz[111], M. Gouighri[36b], A. G. Goussiou[142], N. Govender[34c], R. P. Grabarczyk[129], I. Grabowska-Bold[86a], K. Graham[35], E. Gramstad[128], S. Grancagnolo[70a,70b], C. M. Grant[1], P. M. Gravila[28f], F. G. Gravili[70a,70b], H. M. Gray[18a], M. Greco[112], M. J. Green[1], C. Grefe[25], A. S. Grefsrud[17], I. M. Gregor[48], K. T. Greif[165], P. Grenier[149], S. G. Grewe[112], A. A. Grillo[139], K. Grimm[32], S. Grinstein[13,y], J.-F. Grivaz[66], E. Gross[175], J. Grosse-Knetter[55], L. Guan[108], G. Guerrieri[37], R. Guevara[128], R. Gugel[102], J. A. M. Guhit[108], A. Guida[19], E. Guilloton[173], S. Guindon[37], F. Guo[14,114c], J. Guo[144a], L. Guo[48], L. Guo[114b,w], Y. Guo[108], A. Gupta[49], R. Gupta[132], S. Gupta[27], S. Gurbuz[25], S. S. Gurdasani[48], G. Gustavino[75a,75b], P. Gutierrez[123], L. F. Gutierrez Zagazeta[131], M. Gutsche[50], C. Gutschow[98], C. Gwenlan[129], C. B. Gwilliam[94], E. S. Haaland[128], A. Haas[120], M. Habedank[59], C. Haber[18a], H. K. Hadavand[8], A. Haddad[41], A. Hadef[50], A. I. Hagan[93], J. J. Hahn[147], E. H. Haines[98], M. Haleem[172], J. Haley[124], G. D. Hallewell[104], L. Halser[20], K. Hamano[171], M. Hamer[25], S. E. D. Hammoud[66], E. J. Hampshire[97], J. Han[143a], L. Han[114a], L. Han[62], S. Han[18a], K. Hanagaki[84], M. Hance[139], D. A. Hangal[42], H. Hanif[148], M. D. Hank[131], J. B. Hansen[43], P. H. Hansen[43], D. Harada[56], T. Harenberg[177], S. Harkusha[179], M. L. Harris[105], Y. T. Harris[25], J. Harrison[13], N. M. Harrison[122], P. F. Harrison[173], M. L. E. Hart[98], N. M. Hartman[112], N. M. Hartmann[111], R. Z. Hasan[97,137], Y. Hasegawa[146], F. Haslbeck[129], S. Hassan[17], R. Hauser[109], M. Haviernik[136], C. M. Hawkes[21], R. J. Hawkings[37], Y. Hayashi[159], D. Hayden[109], C. Hayes[108], R. L. Hayes[117], C. P. Hays[129], J. M. Hays[96], H. S. Hayward[94], M. He[14,114c], Y. He[48], Y. He[98], N. B. Heatley[96], V. Hedberg[100], C. Heidegger[54], K. K. Heidegger[54], J. Heilman[35], S. Heim[48], T. Heim[18a], J. G. Heinlein[131], J. J. Heinrich[126], L. Heinrich[112], J. Hejbal[134], M. Helbig[50], A. Held[176], S. Hellesund[17], C. M. Helling[170], S. Hellman[47a,47b], A. M. Henriques Correia[37], H. Herde[100], Y. Hernández Jiménez[151], L. M. Herrmann[25], T. Herrmann[50], G. Herten[54], R. Hertenberger[111], L. Hervas[37], M. E. Hesping[102], N. P. Hessey[162a], J. Hessler[112], M. Hidaoui[36b], N. Hidic[136], E. Hill[161], T. S. Hillersoy[17], S. J. Hillier[21], J. R. Hinds[109], F. Hinterkeuser[25], M. Hirose[127], S. Hirose[163], D. Hirschbuehl[177], T. G. Hitchings[103], B. Hiti[95], J. Hobbs[151], R. Hobincu[28e], N. Hod[175], A. M. Hodges[168], M. C. Hodgkinson[145], B. H. Hodkinson[129], A. Hoecker[37], D. D. Hofer[108], J. Hofer[169], M. Holzbock[37], L. B. A. H. Hommels[33], V. Homsak[129], B. P. Honan[103], J. J. Hong[68], T. M. Hong[132], B. H. Hooberman[168], W. H. Hopkins[6], M. C. Hoppesch[168], Y. Horii[113], M. E. Horstmann[112], S. Hou[154], M. R. Housenga[168], A. S. Howard[95], J. Howarth[59], J. Hoya[6], M. Hrabovsky[125], T. Hryn'ova[4], P. J. Hsu[65], S.-C. Hsu[142], T. Hsu[66], M. Hu[18a], Q. Hu[62], S. Huang[33], X. Huang[14,114c], Y. Huang[136], Y. Huang[114b], Y. Huang[102], Y. Huang[14], Z. Huang[66], Z. Hubacek[135], M. Huebner[25], F. Huegging[25], T. B. Huffman[129], M. Hufnagel Maranha De Faria[83a], C. A. Hugli[48], M. Huhtinen[37], S. K. Huiberts[17], R. Hulsken[106], C. E. Hultquist[18a], N. Huseynov[12,g], J. Huston[109], J. Huth[61], R. Hyneman[7], G. Iacobucci[56], G. Iakovidis[30], L. Iconomidou-Fayard[66], J. P. Iddon[37], P. Iengo[72a,72b], R. Iguchi[159], Y. Iiyama[159], T. Iizawa[159], Y. Ikegami[84], D. Iliadis[158], N. Ilic[161], H. Imam[36a], G. Inacio Goncalves[83d], S. A. Infante Cabanas[140c], T. Ingebretsen Carlson[47a,47b], J. M. Inglis[96], G. Introzzi[73a,73b], M. Iodice[77a], V. Ippolito[75a,75b], R. K. Irwin[94], M. Ishino[159], W. Islam[176], C. Issever[19], S. Istin[22a,an], K. Itabashi[84], H. Ito[174], R. Iuppa[78a,78b], A. Ivina[175], V. Izzo[72a], P. Jacka[134], P. Jackson[1], P. Jain[48], K. Jakobs[54], T. Jakoubek[175], J. Jamieson[59], W. Jang[159], S. Jankovych[136], M. Javurkova[105], P. Jawahar[103], L. Jeanty[126], J. Jejelava[155a,af], P. Jenni[54,f], C. E. Jessiman[35], C. Jia[143a], H. Jia[170], J. Jia[151], X. Jia[14,114c], Z. Jia[114a], C. Jiang[52], Q. Jiang[64b], S. Jiggins[48], M. Jimenez Ortega[169], J. Jimenez Pena[13], S. Jin[114a], A. Jinaru[28b], O. Jinnouchi[141], P. Johansson[145], K. A. Johns[7], J. W. Johnson[139], F. A. Jolly[48], D. M. Jones[152], E. Jones[48], K. S. Jones[8], P. Jones[33], R. W. L. Jones[93], T. J. Jones[94], H. L. Joos[55,37], R. Joshi[122], J. Jovicevic[16], X. Ju[18a], J. J. Junggeburth[37], T. Junkermann[63a], A. Juste Rozas[13,y], M. K. Juzek[87], S. Kabana[140e], A. Kaczmarska[87], M. Kado[112], H. Kagan[122], M. Kagan[149], A. Kahn[131], C. Kahra[102], T. Kaji[159], E. Kajomovitz[156], N. Kakati[175], N. Kakoty[13], I. Kalaitzidou[54], S. Kandel[8], N. J. Kang[139], D. Kar[34g], K. Karava[129], E. Karentzos[25], O. Karkout[117], S. N. Karpov[39], Z. M. Karpova[39], V. Kartvelishvili[93], A. N. Karyukhin[38], E. Kasimi[158], J. Katzy[48], S. Kaur[35], K. Kawade[146], M. P. Kawale[123], C. Kawamoto[89], T. Kawamoto[62], E. F. Kay[37], F. I. Kaya[164], S. Kazakos[109], V. F. Kazanin[38], J. M. Keaveney[34a], R. Keeler[171], G. V. Kehris[61], J. S. Keller[35], J. J. Kempster[152], O. Kepka[134], J. Kerr[162b], B. P. Kerridge[137], B. P. Kerševan[95], L. Keszeghova[29a], R. A. Khan[132], A. Khanov[124], A. G. Kharlamov[38], T. Kharlamova[38], E. E. Khoda[142], M. Kholodenko[133a], T. J. Khoo[19], G. Khoriauli[172], Y. Khoulaki[36a], J. Khubua[155b,*], Y. A. R. Khwaira[130], B. Kibirige[34g], D. Kim[6], D. W. Kim[47a,47b], Y. K. Kim[40], N. Kimura[98], M. K. Kingston[55], A. Kirchhoff[55], C. Kirfel[25], F. Kirfel[25],

J. Kirk[137], A. E. Kiryunin[112], S. Kita[163], O. Kivernyk[25], M. Klassen[164], C. Klein[35], L. Klein[172], M. H. Klein[45], S. B. Klein[56], U. Klein[94], A. Klimentov[30], T. Klioutchnikova[37], P. Kluit[117], S. Kluth[112], E. Kneringer[79], T. M. Knight[161], A. Knue[49], M. Kobel[50], D. Kobylianskii[175], S. F. Koch[129], M. Kocian[149], P. Kodyš[136], D. M. Koeck[126], T. Koffas[35], O. Kolay[50], I. Koletsou[4], T. Komarek[87], K. Köneke[55], A. X. Y. Kong[1], T. Kono[121], N. Konstantinidis[98], P. Kontaxakis[56], B. Konya[100], R. Kopeliansky[42], S. Koperny[86a], K. Korcyl[87], K. Kordas[158,d], A. Korn[98], S. Korn[55], I. Korolkov[13], N. Korotkova[38], B. Kortman[117], O. Kortner[112], S. Kortner[112], W. H. Kostecka[118], M. Kostov[29a], V. V. Kostyukhin[147], A. Kotsokechagia[37], A. Kotwal[51], A. Koulouris[37], A. Kourkoumeli-Charalampidi[73a,73b], C. Kourkoumelis[9], E. Kourlitis[112], O. Kovanda[126], R. Kowalewski[171], W. Kozanecki[126], A. S. Kozhin[38], V. A. Kramarenko[38], G. Kramberger[95], P. Kramer[25], M. W. Krasny[130], A. Krasznahorkay[105], A. C. Kraus[118], J. W. Kraus[177], J. A. Kremer[48], N. B. Krengel[147], T. Kresse[50], L. Kretschmann[177], J. Kretzschmar[94], K. Kreul[19], P. Krieger[161], K. Krizka[21], K. Kroeninger[49], H. Kroha[112], J. Kroll[134], J. Kroll[131], K. S. Krowpman[109], U. Kruchonak[39], H. Krüger[25], N. Krumnack[81], M. C. Kruse[51], O. Kuchinskaia[39], S. Kuday[3a], S. Kuehn[37], R. Kuesters[54], T. Kuhl[48], V. Kukhtin[39], Y. Kulchitsky[39], S. Kuleshov[140d,140b], J. Kull[1], M. Kumar[34g], N. Kumari[48], P. Kumari[162b], A. Kupco[134], T. Kupfer[49], A. Kupich[38], O. Kuprash[54], H. Kurashige[85], L. L. Kurchaninov[162a], O. Kurdysh[4], Y. A. Kurochkin[38], A. Kurova[38], M. Kuze[141], A. K. Kvam[105], J. Kvita[125], N. G. Kyriacou[108], C. Lacasta[169], F. Lacava[75a,75b], H. Lacker[19], D. Lacour[130], N. N. Lad[98], E. Ladygin[39], A. Lafarge[41], B. Laforge[130], T. Lagouri[178], F. Z. Lahbabi[36a], S. Lai[55], J. E. Lambert[171], S. Lammers[68], W. Lampl[7], C. Lampoudis[158,d], G. Lamprinoudis[102], A. N. Lancaster[118], E. Lançon[30], U. Landgraf[54], M. P. J. Landon[96], V. S. Lang[54], O. K. B. Langrekken[128], A. J. Lankford[165], F. Lanni[37], K. Lantzsch[25], A. Lanza[73a], M. Lanzac Berrocal[169], J. F. Laporte[138], T. Lari[71a], D. Larsen[17], L. Larson[11], F. Lasagni Manghi[24b], M. Lassnig[37], S. D. Lawlor[145], R. Lazaridou[173], M. Lazzaroni[71a,71b], H. D. M. Le[109], E. M. Le Boulicaut[178], L. T. Le Pottier[18a], B. Leban[24b,24a], F. Ledroit-Guillon[60], T. F. Lee[162b], L. L. Leeuw[34c], M. Lefebvre[171], C. Leggett[18a], G. Lehmann Miotto[37], M. Leigh[56], W. A. Leight[105], W. Leinonen[116], A. Leisos[158,v], M. A. L. Leite[83c], C. E. Leitgeb[19], R. Leitner[136], K. J. C. Leney[45], T. Lenz[25], S. Leone[74a], C. Leonidopoulos[52], A. Leopold[150], J. H. Lepage Bourbonnais[35], R. Les[109], C. G. Lester[33], M. Levchenko[38], J. Levêque[4], L. J. Levinson[175], G. Levrini[24b,24a], M. P. Lewicki[87], C. Lewis[142], D. J. Lewis[4], L. Lewitt[145], A. Li[30], B. Li[143a], C. Li[108], C-Q. Li[112], H. Li[143a], H. Li[103], H. Li[15], H. Li[62], H. Li[143a], J. Li[144a], K. Li[14], L. Li[144a], R. Li[178], S. Li[14,114c], S. Li[144b,144a], T. Li[5], X. Li[106], Z. Li[159], Z. Li[14,114c], Z. Li[62], S. Liang[14,114c], Z. Liang[14], M. Liberatore[138], B. Liberti[76a], K. Lie[64c], J. Lieber Marin[83e], H. Lien[68], H. Lin[108], S. F. Lin[151], L. Linden[111], R. E. Lindley[7], J. H. Lindon[37], J. Ling[61], E. Lipeles[131], A. Lipniacka[17], A. Lister[170], J. D. Little[68], B. Liu[14], B. X. Liu[114b], D. Liu[144b,144a], D. Liu[139], E. H. L. Liu[21], J. K. K. Liu[120], K. Liu[144b], K. Liu[144b,144a], M. Liu[62], M. Y. Liu[62], P. Liu[14], Q. Liu[144b,142,144a], X. Liu[62], X. Liu[143a], Y. Liu[114b,114c], Y. L. Liu[143a], Y. W. Liu[62], Z. Liu[66,l], S. L. Lloyd[96], E. M. Lobodzinska[48], P. Loch[7], E. Lodhi[161], T. Lohse[19], K. Lohwasser[145], E. Loiacono[48], J. D. Lomas[21], J. D. Long[42], I. Longarini[165], R. Longo[168], A. Lopez Solis[13], N. A. Lopez-canelas[7], N. Lorenzo Martinez[4], A. M. Lory[111], M. Losada[119a], G. Löschcke Centeno[152], X. Lou[47a,47b], X. Lou[14,114c], A. Lounis[66], P. A. Love[93], M. Lu[66], S. Lu[131], Y. J. Lu[154], H. J. Lubatti[142], C. Luci[75a,75b], F. L. Lucio Alves[114a], F. Luehring[68], B. S. Lunday[131], O. Lundberg[150], J. Lunde[37], N. A. Luongo[6], M. S. Lutz[37], A. B. Lux[26], D. Lynn[30], R. Lysak[134], V. Lysenko[135], E. Lytken[100], V. Lyubushkin[39], T. Lyubushkina[39], M. M. Lyukova[151], M. Firdaus M. Soberi[52], H. Ma[30], K. Ma[62], L. L. Ma[143a], W. Ma[62], Y. Ma[124], J. C. MacDonald[102], P. C. Machado De Abreu Farias[83e], R. Madar[41], T. Madula[98], J. Maeda[85], T. Maeno[30], P. T. Mafa[34c,k], H. Maguire[145], V. Maiboroda[66], A. Maio[133a,133b,133d], K. Maj[86a], O. Majersky[48], S. Majewski[126], R. Makhmanazarov[38], N. Makovec[66], V. Maksimovic[16], B. Malaescu[130], J. Malamant[128], Pa. Malecki[87], V. P. Maleev[38], F. Malek[60,p], M. Mali[95], D. Malito[97], U. Mallik[80,*], A. Maloizel[5], S. Maltezos[10], A. Malvezzi Lopes[83d], S. Malyukov[39], J. Mamuzic[13], G. Mancini[53], M. N. Mancini[27], G. Manco[73a,73b], J. P. Mandalia[96], S. S. Mandarry[152], I. Mandić[95], L. Manhaes de Andrade Filho[83a], I. M. Maniatis[175], J. Manjarres Ramos[91], D. C. Mankad[175], A. Mann[111], T. Manoussos[37], M. N. Mantinan[40], S. Manzoni[37], L. Mao[144a], X. Mapekula[34c], A. Marantis[158], R. R. Marcelo Gregorio[96], G. Marchiori[5], M. Marcisovsky[134], C. Marcon[71a], E. Maricic[16], M. Marinescu[48], S. Marium[48], M. Marjanovic[123], A. Markhoos[54], M. Markovitch[66], M. K. Maroun[105], G. T. Marsden[103], E. J. Marshall[93], Z. Marshall[18a], S. Marti-Garcia[169], J. Martin[98], T. A. Martin[137], V. J. Martin[52], B. Martin dit Latour[17], L. Martinelli[75a,75b], M. Martinez[13,y], P. Martinez Agullo[169],

V. I. Martinez Outschoorn[105], P. Martinez Suarez[13], S. Martin-Haugh[137], G. Martinovicova[136], V. S. Martoiu[28b], A. C. Martyniuk[98], A. Marzin[37], D. Mascione[78a,78b], L. Masetti[102], J. Masik[103], A. L. Maslennikov[39], S. L. Mason[42], P. Massarotti[72a,72b], P. Mastrandrea[74a,74b], A. Mastroberardino[44b,44a], T. Masubuchi[127], T. T. Mathew[126], J. Matousek[136], D. M. Mattern[49], J. Maurer[28b], T. Maurin[59], A. J. Maury[66], B. Maček[95], C. Mavungu Tsava[104], D. A. Maximov[38], A. E. May[103], E. Mayer[41], R. Mazini[34g], I. Maznas[118], S. M. Mazza[139], E. Mazzeo[37], J. P. Mc Gowan[171], S. P. Mc Kee[108], C. A. Mc Lean[6], C. C. McCracken[170], E. F. McDonald[107], A. E. McDougall[117], L. F. Mcelhinney[93], J. A. Mcfayden[152], R. P. McGovern[131], R. P. Mckenzie[34g], T. C. Mclachlan[48], D. J. Mclaughlin[98], S. J. McMahon[137], C. M. Mcpartland[94], R. A. McPherson[171,ac], S. Mehlhase[111], A. Mehta[94], D. Melini[169], B. R. Mellado Garcia[34g], A. H. Melo[55], F. Meloni[48], A. M. Mendes Jacques Da Costa[103], L. Meng[93], S. Menke[112], M. Mentink[37], E. Meoni[44b,44a], G. Mercado[118], S. Merianos[158], C. Merlassino[69a,69c], C. Meroni[71a,71b], J. Metcalfe[6], A. S. Mete[6], E. Meuser[102], C. Meyer[68], J-P. Meyer[138], Y. Miao[114a], R. P. Middleton[137], M. Mihovilovic[66], L. Mijović[52], G. Mikenberg[175], M. Mikestikova[134], M. Mikuž[95], H. Mildner[102], A. Milic[37], D. W. Miller[40], E. H. Miller[149], L. S. Miller[35], A. Milov[175], D. A. Milstead[47a,47b], T. Min[114a], A. A. Minaenko[38], I. A. Minashvili[155b], A. I. Mincer[120], B. Mindur[86a], M. Mineev[39], Y. Mino[89], L. M. Mir[13], M. Miralles Lopez[59], M. Mironova[18a], M. C. Missio[116], A. Mitra[173], V. A. Mitsou[169], Y. Mitsumori[113], O. Miu[161], P. S. Miyagawa[96], T. Mkrtchyan[63a], M. Mlinarevic[98], T. Mlinarevic[98], M. Mlynarikova[37], S. Mobius[20], M. H. Mohamed Farook[115], S. Mohapatra[42], S. Mohiuddin[124], G. Mokgatitswane[34g], L. Moleri[175], U. Molinatti[129], L. G. Mollier[20], B. Mondal[147], S. Mondal[135], K. Mönig[48], E. Monnier[104], L. Monsonis Romero[169], J. Montejo Berlingen[13], A. Montella[47a,47b], M. Montella[122], F. Montereali[77a,77b], F. Monticelli[92], S. Monzani[69a,69c], A. Morancho Tarda[43], N. Morange[66], A. L. Moreira De Carvalho[48], M. Moreno Llácer[169], C. Moreno Martinez[56], J. M. Moreno Perez[23b], P. Morettini[57b], S. Morgenstern[37], M. Morii[61], M. Morinaga[159], M. Moritsu[90], F. Morodei[75a,75b], P. Moschovakos[37], B. Moser[54], M. Mosidze[155b], T. Moskalets[45], P. Moskvitina[116], J. Moss[32], P. Moszkowicz[86a], A. Moussa[36d], Y. Moyal[175], H. Moyano Gomez[13], E. J. W. Moyse[105], O. Mtintsilana[34g], S. Muanza[104], M. Mucha[25], J. Mueller[132], R. Müller[37], G. A. Mullier[167], A. J. Mullin[33], J. J. Mullin[51], A. C. Mullins[45], A. E. Mulski[61], D. P. Mungo[161], D. Munoz Perez[169], F. J. Munoz Sanchez[103], W. J. Murray[173,137], M. Muškinja[95], C. Mwewa[48], A. G. Myagkov[38,a], A. J. Myers[8], G. Myers[108], M. Myska[135], B. P. Nachman[18a], K. Nagai[129], K. Nagano[84], R. Nagasaka[159], J. L. Nagle[30,ak], E. Nagy[104], A. M. Nairz[37], Y. Nakahama[84], K. Nakamura[84], K. Nakkalil[5], A. Nandi[63b], H. Nanjo[127], E. A. Narayanan[45], Y. Narukawa[159], I. Naryshkin[38], L. Nasella[71a,71b], S. Nasri[119b], C. Nass[25], G. Navarro[23a], J. Navarro-Gonzalez[169], A. Nayaz[19], P. Y. Nechaeva[38], S. Nechaeva[24b,24a], F. Nechansky[134], L. Nedic[129], T. J. Neep[21], A. Negri[73a,73b], M. Negrini[24b], C. Nellist[117], C. Nelson[106], K. Nelson[108], S. Nemecek[134], M. Nessi[37,h], M. S. Neubauer[168], J. Newell[94], P. R. Newman[21], Y. W. Y. Ng[168], B. Ngair[119a], H. D. N. Nguyen[110], J. D. Nichols[123], R. B. Nickerson[129], R. Nicolaidou[138], J. Nielsen[139], M. Niemeyer[55], J. Niermann[37], N. Nikiforou[37], V. Nikolaenko[38,a], I. Nikolic-Audit[130], P. Nilsson[30], I. Ninca[48], G. Ninio[157], A. Nisati[75a], N. Nishu[2], R. Nisius[112], N. Nitika[69a,69c], J-E. Nitschke[50], E. K. Nkadimeng[34b], T. Nobe[159], T. Nommensen[153], M. B. Norfolk[145], B. J. Norman[35], M. Noury[36a], J. Novak[95], T. Novak[95], R. Novotny[135], L. Nozka[125], K. Ntekas[165], N. M. J. Nunes De Moura Junior[83b], J. Ocariz[130], A. Ochi[85], I. Ochoa[133a], S. Oerdek[48,z], J. T. Offermann[40], A. Ogrodnik[136], A. Oh[103], C. C. Ohm[150], H. Oide[84], M. L. Ojeda[37], Y. Okumura[159], L. F. Oleiro Seabra[133a], I. Oleksiyuk[56], G. Oliveira Correa[13], D. Oliveira Damazio[30], J. L. Oliver[165], Ö. O. Öncel[54], A. P. O'Neill[20], A. Onofre[133a,133e,e], P. U. E. Onyisi[11], M. J. Oreglia[40], D. Orestano[77a,77b], R. Orlandini[77a,77b], R. S. Orr[161], L. M. Osojnak[131], Y. Osumi[113], G. Otero y Garzon[31], H. Otono[90], G. J. Ottino[18a], M. Ouchrif[36d], F. Ould-Saada[128], T. Ovsiannikova[142], M. Owen[59], R. E. Owen[137], V. E. Ozcan[22a], F. Ozturk[87], N. Ozturk[8], S. Ozturk[82], H. A. Pacey[129], K. Pachal[162a], A. Pacheco Pages[13], C. Padilla Aranda[13], G. Padovano[75a,75b], S. Pagan Griso[18a], G. Palacino[68], A. Palazzo[70a,70b], J. Pampel[25], J. Pan[178], T. Pan[64a], D. K. Panchal[11], C. E. Pandini[60], J. G. Panduro Vazquez[137], H. D. Pandya[1], H. Pang[138], P. Pani[48], G. Panizzo[69a,69c], L. Panwar[130], L. Paolozzi[56], S. Parajuli[168], A. Paramonov[6], C. Paraskevopoulos[53], D. Paredes Hernandez[64b], A. Pareti[73a,73b], K. R. Park[42], T. H. Park[112], F. Parodi[57b,57a], J. A. Parsons[42], U. Parzefall[54], B. Pascual Dias[41], L. Pascual Dominguez[101], E. Pasqualucci[75a], S. Passaggio[57b], F. Pastore[97], P. Patel[87], U. M. Patel[51], J. R. Pater[103], T. Pauly[37], F. Pauwels[136], C. I. Pazos[164], M. Pedersen[128], R. Pedro[133a], S. V. Peleganchuk[38], O. Penc[37], E. A. Pender[52], S. Peng[15], G. D. Penn[178], K. E. Penski[111], M. Penzin[38], B. S. Peralva[83d], A. P. Pereira Peixoto[142], L. Pereira Sanchez[149],

D. V. Perepelitsa[30,ak], G. Perera[105], E. Perez Codina[37], M. Perganti[10], H. Pernegger[37], S. Perrella[75a,75b], O. Perrin[41], K. Peters[48], R. F. Y. Peters[103], B. A. Petersen[37], T. C. Petersen[43], E. Petit[104], V. Petousis[135], A. R. Petri[71a,71b], C. Petridou[158,d], T. Petru[136], A. Petrukhin[147], M. Pettee[18a], A. Petukhov[82], K. Petukhova[37], R. Pezoa[140f], L. Pezzotti[24b,24a], G. Pezzullo[178], L. Pfaffenbichler[37], A. J. Pfleger[37], T. M. Pham[176], T. Pham[107], P. W. Phillips[137], G. Piacquadio[151], E. Pianori[18a], F. Piazza[126], R. Piegaia[31], D. Pietreanu[28b], A. D. Pilkington[103], M. Pinamonti[69a,69c], J. L. Pinfold[2], B. C. Pinheiro Pereira[133a], J. Pinol Bel[13], A. E. Pinto Pinoargote[130], L. Pintucci[69a,69c], K. M. Piper[152], A. Pirttikoski[56], D. A. Pizzi[35], L. Pizzimento[64b], A. Plebani[33], M.-A. Pleier[30], V. Pleskot[136], E. Plotnikova[39], G. Poddar[96], R. Poettgen[100], L. Poggioli[130], S. Polacek[136], G. Polesello[73a], A. Poley[148], A. Polini[24b], C. S. Pollard[173], Z. B. Pollock[122], E. Pompa Pacchi[123], N. I. Pond[98], D. Ponomarenko[68], L. Pontecorvo[37], S. Popa[28a], G. A. Popeneciu[28d], A. Poreba[37], D. M. Portillo Quintero[162a], S. Pospisil[135], M. A. Postill[145], P. Postolache[28c], K. Potamianos[173], P. A. Potepa[86a], I. N. Potrap[39], C. J. Potter[33], H. Potti[153], J. Poveda[169], M. E. Pozo Astigarraga[37], R. Pozzi[37], A. Prades Ibanez[76a,76b], J. Pretel[171], D. Price[103], M. Primavera[70a], L. Primomo[69a,69c], M. A. Principe Martin[101], R. Privara[125], T. Procter[86b], M. L. Proffitt[142], N. Proklova[131], K. Prokofiev[64c], G. Proto[112], J. Proudfoot[6], M. Przybycien[86a], W. W. Przygoda[86b], A. Psallidas[46], J. E. Puddefoot[145], D. Pudzha[53], D. Pyatiizbyantseva[116], J. Qian[108], R. Qian[109], D. Qichen[103], Y. Qin[13], T. Qiu[52], A. Quadt[55], M. Queitsch-Maitland[103], G. Quetant[56], R. P. Quinn[170], G. Rabanal Bolanos[61], D. Rafanoharana[112], F. Raffaeli[76a,76b], F. Ragusa[71a,71b], J. L. Rainbolt[40], J. A. Raine[56], S. Rajagopalan[30], E. Ramakoti[39], L. Rambelli[57b,57a], I. A. Ramirez-Berend[35], K. Ran[48,114c], D. S. Rankin[131], N. P. Rapheeha[34g], H. Rasheed[28b], D. F. Rassloff[63a], A. Rastogi[18a], S. Rave[102], S. Ravera[57b,57a], B. Ravina[37], I. Ravinovich[175], M. Raymond[37], A. L. Read[128], N. P. Readioff[145], D. M. Rebuzzi[73a,73b], A. S. Reed[112], K. Reeves[27], J. A. Reidelsturz[177], D. Reikher[126], A. Rej[49], C. Rembser[37], H. Ren[62], M. Renda[28b], F. Renner[48], A. G. Rennie[59], A. L. Rescia[48], S. Resconi[71a], M. Ressegotti[57b,57a], S. Rettie[37], W. F. Rettie[35], E. Reynolds[18a], O. L. Rezanova[39], P. Reznicek[136], H. Riani[36d], N. Ribaric[51], E. Ricci[78a,78b], R. Richter[112], S. Richter[47a,47b], E. Richter-Was[86b], M. Ridel[130], S. Ridouani[36d], P. Rieck[120], P. Riedler[37], E. M. Riefel[47a,47b], J. O. Rieger[117], M. Rijssenbeek[151], M. Rimoldi[37], L. Rinaldi[24b,24a], P. Rincke[167,55], G. Ripellino[167], I. Riu[13], J. C. Rivera Vergara[171], F. Rizatdinova[124], E. Rizvi[96], B. R. Roberts[18a], S. S. Roberts[139], D. Robinson[33], M. Robles Manzano[102], A. Robson[59], A. Rocchi[76a,76b], C. Roda[74a,74b], S. Rodriguez Bosca[37], Y. Rodriguez Garcia[23a], A. M. Rodríguez Vera[118], S. Roe[37], J. T. Roemer[37], O. Røhne[128], R. A. Rojas[37], C. P. A. Roland[130], A. Romaniouk[79], E. Romano[73a,73b], M. Romano[24b], A. C. Romero Hernandez[168], N. Rompotis[94], L. Roos[130], S. Rosati[75a], B. J. Rosser[40], E. Rossi[129], E. Rossi[72a,72b], L. P. Rossi[61], L. Rossini[54], R. Rosten[122], M. Rotaru[28b], B. Rottler[54], D. Rousseau[66], D. Rousso[48], S. Roy-Garand[161], A. Rozanov[104], Z. M. A. Rozario[59], Y. Rozen[156], A. Rubio Jimenez[169], V. H. Ruelas Rivera[19], T. A. Ruggeri[1], A. Ruggiero[129], A. Ruiz-Martinez[169], A. Rummler[37], Z. Rurikova[54], N. A. Rusakovich[39], H. L. Russell[171], G. Russo[75a,75b], J. P. Rutherfoord[7], S. Rutherford Colmenares[33], M. Rybar[136], P. Rybczynski[86a], A. Ryzhov[45], J. A. Sabater Iglesias[56], H.F-W. Sadrozinski[139], F. Safai Tehrani[75a], S. Saha[1], M. Sahinsoy[82], B. Sahoo[175], A. Saibel[169], B. T. Saifuddin[123], M. Saimpert[138], G. T. Saito[83c], M. Saito[159], T. Saito[159], A. Sala[71a,71b], A. Salnikov[149], J. Salt[169], A. Salvador Salas[157], F. Salvatore[152], A. Salzburger[37], D. Sammel[54], E. Sampson[93], D. Sampsonidis[158,d], D. Sampsonidou[126], J. Sánchez[169], V. Sanchez Sebastian[169], H. Sandaker[128], C. O. Sander[48], J. A. Sandesara[176], M. Sandhoff[177], C. Sandoval[23b], L. Sanfilippo[63a], D. P. C. Sankey[137], T. Sano[89], A. Sansoni[53], L. Santi[37], C. Santoni[41], H. Santos[133a,133b], A. Santra[175], E. Sanzani[24b,24a], K. A. Saoucha[88b], J. G. Saraiva[133a,133d], J. Sardain[7], O. Sasaki[84], K. Sato[163], C. Sauer[37], E. Sauvan[4], P. Savard[161,ai], R. Sawada[159], C. Sawyer[137], L. Sawyer[99], C. Sbarra[24b], A. Sbrizzi[24b,24a], T. Scanlon[98], J. Schaarschmidt[142], U. Schäfer[102], A. C. Schaffer[66,45], D. Schaile[111], R. D. Schamberger[151], C. Scharf[19], M. M. Schefer[20], V. A. Schegelsky[38], D. Scheirich[136], M. Schernau[140e], C. Scheulen[56], C. Schiavi[57b,57a], M. Schioppa[44b,44a], B. Schlag[149], S. Schlenker[37], J. Schmeing[177], E. Schmidt[112], M. A. Schmidt[177], K. Schmieden[102], C. Schmitt[102], N. Schmitt[102], S. Schmitt[48], L. Schoeffel[138], A. Schoening[63b], P. G. Scholer[35], E. Schopf[147], M. Schott[25], S. Schramm[56], T. Schroer[56], H-C. Schultz-Coulon[63a], M. Schumacher[54], B. A. Schumm[139], Ph. Schune[138], H. R. Schwartz[139], A. Schwartzman[149], T. A. Schwarz[108], Ph. Schwemling[138], R. Schwienhorst[109], F. G. Sciacca[20], A. Sciandra[30], G. Sciolla[27], F. Scuri[74a], C. D. Sebastiani[37], K. Sedlaczek[118], S. C. Seidel[115], A. Seiden[139], B. D. Seidlitz[42], C. Seitz[48], J. M. Seixas[83b], G. Sekhniaidze[72a], L. Selem[60], N. Semprini-Cesari[24b,24a], A. Semushin[179], D. Sengupta[56], V. Senthilkumar[169], L. Serin[66], M. Sessa[72a,72b], H. Severini[123],

F. Sforza[57b,57a], A. Sfyrla[56], Q. Sha[14], E. Shabalina[55], H. Shaddix[118], A. H. Shah[33], R. Shaheen[150], J. D. Shahinian[131], M. Shamim[37], L. Y. Shan[14], M. Shapiro[18a], A. Sharma[37], A. S. Sharma[170], P. Sharma[30], P. B. Shatalov[38], K. Shaw[152], S. M. Shaw[103], Q. Shen[144a], D. J. Sheppard[148], P. Sherwood[98], L. Shi[98], X. Shi[14], S. Shimizu[84], C. O. Shimmin[178], I. P. J. Shipsey[129,*], S. Shirabe[90], M. Shiyakova[39,aa], M. J. Shochet[40], D. R. Shope[128], B. Shrestha[123], S. Shrestha[122,am], I. Shreyber[39], M. J. Shroff[171], P. Sicho[134], A. M. Sickles[168], E. Sideras Haddad[34g,166], A. C. Sidley[117], A. Sidoti[24b], F. Siegert[50], Dj. Sijacki[16], F. Sili[92], J. M. Silva[52], I. Silva Ferreira[83b], M. V. Silva Oliveira[30], S. B. Silverstein[47a], S. Simion[66], R. Simoniello[37], E. L. Simpson[103], H. Simpson[152], L. R. Simpson[6], S. Simsek[82], S. Sindhu[55], P. Sinervo[161], S. N. Singh[27], S. Singh[30], S. Sinha[48], S. Sinha[103], M. Sioli[24b,24a], K. Sioulas[9], I. Siral[37], E. Sitnikova[48], J. Sjölin[47a,47b], A. Skaf[55], E. Skorda[21], P. Skubic[123], M. Slawinska[87], I. Slazyk[17], I. Sliusar[128], V. Smakhtin[175], B. H. Smart[137], S. Yu. Smirnov[140b], Y. Smirnov[82], L. N. Smirnova[38,a], O. Smirnova[100], A. C. Smith[42], D. R. Smith[165], J. L. Smith[103], M. B. Smith[35], R. Smith[149], H. Smitmanns[102], M. Smizanska[93], K. Smolek[135], P. Smolyanskiy[135], A. A. Snesarev[39], H. L. Snoek[117], S. Snyder[30], R. Sobie[171,ac], A. Soffer[157], C. A. Solans Sanchez[37], E. Yu. Soldatov[39], U. Soldevila[169], A. A. Solodkov[34g], S. Solomon[27], A. Soloshenko[39], K. Solovieva[54], O. V. Solovyanov[41], P. Sommer[50], A. Sonay[13], A. Sopczak[135], A. L. Sopio[52], F. Sopkova[29b], J. D. Sorenson[115], I. R. Sotarriva Alvarez[141], V. Sothilingam[63a], O. J. Soto Sandoval[140c,140b], S. Sottocornola[68], R. Soualah[88a], Z. Soumaimi[36e], D. South[48], N. Soybelman[175], S. Spagnolo[70a,70b], M. Spalla[112], D. Sperlich[54], B. Spisso[72a,72b], D. P. Spiteri[59], L. Splendori[104], M. Spousta[136], E. J. Staats[35], R. Stamen[63a], E. Stanecka[87], W. Stanek-Maslouska[48], M. V. Stange[50], B. Stanislaus[18a], M. M. Stanitzki[48], B. Stapf[48], E. A. Starchenko[38], G. H. Stark[139], J. Stark[91], P. Staroba[134], P. Starovoitov[88b], R. Staszewski[87], G. Stavropoulos[46], A. Stefl[37], P. Steinberg[30], B. Stelzer[148,162a], H. J. Stelzer[132], O. Stelzer-Chilton[162a], H. Stenzel[58], T. J. Stevenson[152], G. A. Stewart[37], J. R. Stewart[124], M. C. Stockton[37], G. Stoicea[28b], M. Stolarski[133a], S. Stonjek[112], A. Straessner[50], J. Strandberg[150], S. Strandberg[47a,47b], M. Stratmann[177], M. Strauss[123], T. Strebler[104], P. Strizenec[29b], R. Ströhmer[172], D. M. Strom[126], R. Stroynowski[45], A. Strubig[47a,47b], S. A. Stucci[30], B. Stugu[17], J. Stupak[123], N. A. Styles[48], D. Su[149], S. Su[62], X. Su[62], D. Suchy[29a], K. Sugizaki[131], V. V. Sulin[38], M.J. Sullivan[94], D. M. S. Sultan[129], L. Sultanaliyeva[38], S. Sultansoy[3b], S. Sun[176], W. Sun[14], O. Sunneborn Gudnadottir[167], N. Sur[100], M. R. Sutton[152], H. Suzuki[163], M. Svatos[134], P. N. Swallow[33], M. Swiatlowski[162a], T. Swirski[172], I. Sykora[29a], M. Sykora[136], T. Sykora[136], D. Ta[102], K. Tackmann[48,z], A. Taffard[165], R. Tafirout[162a], Y. Takubo[84], M. Talby[104], A. A. Talyshev[38], K. C. Tam[64b], N. M. Tamir[157], A. Tanaka[159], J. Tanaka[159], R. Tanaka[66], M. Tanasini[151], Z. Tao[170], S. Tapia Araya[140f], S. Tapprogge[102], A. Tarek Abouelfadl Mohamed[109], S. Tarem[156], K. Tariq[14], G. Tarna[28b], G. F. Tartarelli[71a], M. J. Tartarin[91], P. Tas[136], M. Tasevsky[134], E. Tassi[44b,44a], A. C. Tate[168], G. Tateno[159], Y. Tayalati[36e,ab], G. N. Taylor[107], W. Taylor[162b], A. S. Tegetmeier[91], P. Teixeira-Dias[97], J. J. Teoh[161], K. Terashi[159], J. Terron[101], S. Terzo[13], M. Testa[53], R. J. Teuscher[161,ac], A. Thaler[79], O. Theiner[56], T. Theveneaux-Pelzer[104], D. W. Thomas[97], J. P. Thomas[21], E. A. Thompson[18a], P. D. Thompson[21], E. Thomson[131], R. E. Thornberry[45], C. Tian[62], Y. Tian[56], V. Tikhomirov[82], Yu. A. Tikhonov[39], S. Timoshenko[38], D. Timoshyn[136], E. X. L. Ting[1], P. Tipton[178], A. Tishelman-Charny[30], K. Todome[141], S. Todorova-Nova[136], S. Todt[50], L. Toffolin[69a,69c], M. Togawa[84], J. Tojo[90], S. Tokár[29a], O. Toldaiev[68], G. Tolkachev[104], M. Tomoto[84,113], L. Tompkins[149,o], E. Torrence[126], H. Torres[91], E. Torró Pastor[169], M. Toscani[31], C. Tosciri[40], M. Tost[11], D. R. Tovey[145], T. Trefzger[172], P. M. Tricarico[13], A. Tricoli[30], I. M. Trigger[162a], S. Trincaz-Duvoid[130], D. A. Trischuk[27], A. Tropina[39], L. Truong[34c], M. Trzebinski[87], A. Trzupek[87], F. Tsai[151], M. Tsai[108], A. Tsiamis[158], P. V. Tsiareshka[39], S. Tsigaridas[162a], A. Tsirigotis[158,v], V. Tsiskaridze[161], E. G. Tskhadadze[155a], M. Tsopoulou[158], Y. Tsujikawa[89], I. I. Tsukerman[38], V. Tsulaia[18a], S. Tsuno[84], K. Tsuri[121], D. Tsybychev[151], Y. Tu[64b], A. Tudorache[28b], V. Tudorache[28b], S. B. Tuncay[129], S. Turchikhin[57b,57a], I. Turk Cakir[3a], R. Turra[71a], T. Turtuvshin[39,ad], P. M. Tuts[42], S. Tzamarias[158,d], E. Tzovara[102], Y. Uematsu[84], F. Ukegawa[163], P. A. Ulloa Poblete[140c,140b], E. N. Umaka[30], G. Unal[37], A. Undrus[30], G. Unel[165], J. Urban[29b], P. Urrejola[140a], G. Usai[8], R. Ushioda[160], M. Usman[110], F. Ustuner[52], Z. Uysal[82], V. Vacek[135], B. Vachon[106], T. Vafeiadis[37], A. Vaitkus[98], C. Valderanis[111], E. Valdes Santurio[47a,47b], M. Valente[37], S. Valentinetti[24b,24a], A. Valero[169], E. Valiente Moreno[169], A. Vallier[91], J. A. Valls Ferrer[169], D. R. Van Arneman[117], T. R. Van Daalen[142], A. Van Der Graaf[49], H. Z. Van Der Schyf[34g], P. Van Gemmeren[6], M. Van Rijnbach[37], S. Van Stroud[98], I. Van Vulpen[117], P. Vana[136], M. Vanadia[76a,76b], U. M. Vande Voorde[150], W. Vandelli[37], E. R. Vandewall[124], D. Vannicola[157], L. Vannoli[53], R. Vari[75a], M. Varma[178],

E. W. Varnes[7], C. Varni[18b], D. Varouchas[66], L. Varriale[169], K. E. Varvell[153], M. E. Vasile[28b], L. Vaslin[84], M. D. Vassilev[149], A. Vasyukov[39], L. M. Vaughan[124], R. Vavricka[136], T. VazquezSchroeder[13], J. Veatch[32], V. Vecchio[103], M. J. Veen[105], I. Veliscek[30], I. Velkovska[95], L. M. Veloce[161], F. Veloso[133a,133c], S. Veneziano[75a], A. Ventura[70a,70b], S. Ventura Gonzalez[138], A. Verbytskyi[112], M. Verducci[74a,74b], C. Vergis[96], M. Verissimo De Araujo[83b], W. Verkerke[117], J. C. Vermeulen[117], C. Vernieri[149], M. Vessella[165], M. C. Vetterli[148,ai], A. Vgenopoulos[102], N. Viaux Maira[140f], T. Vickey[145], O. E. Vickey Boeriu[145], G. H. A. Viehhauser[129], L. Vigani[63b], M. Vigl[112], M. Villa[24b,24a], M. Villaplana Perez[169], E. M. Villhauer[40], E. Vilucchi[53], M. Vincent[169], M. G. Vincter[35], A. Visibile[117], C. Vittori[37], I. Vivarelli[24b,24a], E. Voevodina[112], F. Vogel[111], J. C. Voigt[50], P. Vokac[135], Yu. Volkotrub[86b], E. Von Toerne[25], B. Vormwald[37], K. Vorobev[51], M. Vos[169], K. Voss[147], M. Vozak[37], L. Vozdecky[123], N. Vranjes[16], M. Vranjes Milosavljevic[16], M. Vreeswijk[117], N. K. Vu[144b,144a], R. Vuillermet[37], O. Vujinovic[102], I. Vukotic[40], I. K. Vyas[35], J. F. Wack[33], S. Wada[163], C. Wagner[149], J. M. Wagner[18a], W. Wagner[177], S. Wahdan[177], H. Wahlberg[92], C. H. Waits[123], J. Walder[137], R. Walker[111], K. Walkingshaw Pass[59], W. Walkowiak[147], A. Wall[131], E. J. Wallin[100], T. Wamorkar[18a], A. Wang[62], A. Z. Wang[139], C. Wang[102], C. Wang[11], H. Wang[18a], J. Wang[64c], P. Wang[103], P. Wang[98], R. Wang[61], R. Wang[6], S. M. Wang[154], S. Wang[14], T. Wang[62], T. Wang[62], W. T. Wang[80], W. Wang[14], X. Wang[168], X. Wang[144a], X. Wang[48], Y. Wang[114a], Y. Wang[62], Z. Wang[108], Z. Wang[144b], Z. Wang[108], C. Wanotayaroj[84], A. Warburton[106], A. L. Warnerbring[147], N. Warrack[59], S. Waterhouse[97], A. T. Watson[21], H. Watson[52], M. F. Watson[21], E. Watton[59], G. Watts[142], B. M. Waugh[98], J. M. Webb[54], C. Weber[30], H. A. Weber[19], M. S. Weber[20], S. M. Weber[63a], C. Wei[62], Y. Wei[54], A. R. Weidberg[129], E. J. Weik[120], J. Weingarten[49], C. Weiser[54], C. J. Wells[48], T. Wenaus[30], B. Wendland[49], T. Wengler[37], N. S. Wenke[112], N. Wermes[25], M. Wessels[63a], A. M. Wharton[93], A. S. White[61], A. White[8], M. J. White[1], D. Whiteson[165], L. Wickremasinghe[127], W. Wiedenmann[176], M. Wielers[137], R. Wierda[150], C. Wiglesworth[43], H. G. Wilkens[37], J. J. H. Wilkinson[33], D. M. Williams[42], H. H. Williams[131], S. Williams[33], S. Willocq[105], B. J. Wilson[103], D. J. Wilson[103], P. J. Windischhofer[40], F. I. Winkel[31], F. Winklmeier[126], B. T. Winter[54], M. Wittgen[149], M. Wobisch[99], T. Wojtkowski[60], Z. Wolffs[117], J. Wollrath[37], M. W. Wolter[87], H. Wolters[133a,133c], M. C. Wong[139], E. L. Woodward[42], S. D. Worm[48], B. K. Wosiek[87], K. W. Woźniak[87], S. Wozniewski[55], K. Wraight[59], C. Wu[161], C. Wu[21], J. Wu[159], M. Wu[114b], M. Wu[116], S. L. Wu[176], S. Wu[14], X. Wu[62], Y. Wu[62], Z. Wu[4], J. Wuerzinger[112], T. R. Wyatt[103], B. M. Wynne[52], S. Xella[43], L. Xia[114a], M. Xia[15], M. Xie[62], A. Xiong[126], J. Xiong[18a], D. Xu[14], H. Xu[62], L. Xu[62], R. Xu[131], T. Xu[108], Y. Xu[142], Z. Xu[52], Z. Xu[114a], B. Yabsley[153], S. Yacoob[34a], Y. Yamaguchi[84], E. Yamashita[159], H. Yamauchi[163], T. Yamazaki[18a], Y. Yamazaki[85], S. Yan[59], Z. Yan[105], H. J. Yang[144a,144b], H. T. Yang[62], S. Yang[62], T. Yang[64c], X. Yang[37], X. Yang[14], Y. Yang[159], Y. Yang[62], W-M. Yao[18a], C. L. Yardley[152], J. Ye[14], S. Ye[30], X. Ye[62], Y. Yeh[98], I. Yeletskikh[39], B. Yeo[18b], M. R. Yexley[98], T. P. Yildirim[129], P. Yin[42], K. Yorita[174], C. J. S. Young[37], C. Young[149], N. D. Young[126], Y. Yu[62], J. Yuan[14,114c], M. Yuan[108], R. Yuan[144b,144a], L. Yue[98], M. Zaazoua[62], B. Zabinski[87], I. Zahir[36a], A. Zaio[57b,57a], Z. K. Zak[87], T. Zakareishvili[169], S. Zambito[56], J. A. Zamora Saa[140d], J. Zang[159], R. Zanzottera[71a,71b], O. Zaplatilek[135], C. Zeitnitz[177], H. Zeng[14], J. C. Zeng[168], D. T. Zenger Jr[27], O. Zenin[38], T. Ženiš[29a], S. Zenz[96], D. Zerwas[66], M. Zhai[14,114c], D. F. Zhang[145], G. Zhang[14], J. Zhang[143a], J. Zhang[6], K. Zhang[14,114c], L. Zhang[62], L. Zhang[114a], P. Zhang[14,114c], R. Zhang[114a], S. Zhang[91], T. Zhang[159], Y. Zhang[142], Y. Zhang[98], Y. Zhang[62], Y. Zhang[114a], Z. Zhang[143a], Z. Zhang[66], H. Zhao[142], T. Zhao[143a], Y. Zhao[35], Z. Zhao[62], Z. Zhao[62], A. Zhemchugov[39], J. Zheng[114a], K. Zheng[168], X. Zheng[62], Z. Zheng[149], D. Zhong[168], B. Zhou[108], H. Zhou[7], N. Zhou[144a], Y. Zhou[15], Y. Zhou[114a], Y. Zhou[7], C. G. Zhu[143a], J. Zhu[108], X. Zhu[144b], Y. Zhu[144a], Y. Zhu[62], X. Zhuang[14], K. Zhukov[68], N. I. Zimine[39], J. Zinsser[63b], M. Ziolkowski[147], L. Živković[16], A. Zoccoli[24b,24a], K. Zoch[61], A. Zografos[37], T. G. Zorbas[145], O. Zormpa[46], L. Zwalinski[37]

[1] Department of Physics, University of Adelaide, Adelaide, Australia
[2] Department of Physics, University of Alberta, Edmonton, AB, Canada
[3] [(a)]Department of Physics, Ankara University, Ankara, Türkiye; [(b)]Division of Physics, TOBB University of Economics and Technology, Ankara, Türkiye
[4] LAPP, CNRS/IN2P3, Université Savoie Mont Blanc, Annecy, France
[5] APC, Université Paris Cité, CNRS/IN2P3, Paris, France
[6] High Energy Physics Division, Argonne National Laboratory, Argonne, IL, USA

[7] Department of Physics, University of Arizona, Tucson, AZ, USA
[8] Department of Physics, University of Texas at Arlington, Arlington, TX, USA
[9] Physics Department, National and Kapodistrian University of Athens, Athens, Greece
[10] Physics Department, National Technical University of Athens, Zografou, Greece
[11] Department of Physics, University of Texas at Austin, Austin, TX, USA
[12] Institute of Physics, Azerbaijan Academy of Sciences, Baku, Azerbaijan
[13] Institut de Física d'Altes Energies (IFAE), Barcelona Institute of Science and Technology, Barcelona, Spain
[14] Institute of High Energy Physics, Chinese Academy of Sciences, Beijing, China
[15] Physics Department, Tsinghua University, Beijing, China
[16] Institute of Physics, University of Belgrade, Belgrade, Serbia
[17] Department for Physics and Technology, University of Bergen, Bergen, Norway
[18] [(a)]Physics Division, Lawrence Berkeley National Laboratory, Berkeley, CA, USA; [(b)]University of California, Berkeley, CA, USA
[19] Institut für Physik, Humboldt Universität zu Berlin, Berlin, Germany
[20] Albert Einstein Center for Fundamental Physics and Laboratory for High Energy Physics, University of Bern, Bern, Switzerland
[21] School of Physics and Astronomy, University of Birmingham, Birmingham, UK
[22] [(a)]Department of Physics, Bogazici University, Istanbul, Türkiye; [(b)]Department of Physics Engineering, Gaziantep University, Gaziantep, Türkiye; [(c)]Department of Physics, Istanbul University, Istanbul, Türkiye
[23] [(a)]Facultad de Ciencias y Centro de Investigaciónes, Universidad Antonio Nariño, Bogotá, Colombia; [(b)]Departamento de Física, Universidad Nacional de Colombia, Bogotá, Colombia
[24] [(a)]Dipartimento di Fisica e Astronomia A. Righi, Università di Bologna, Bologna, Italy; [(b)]INFN Sezione di Bologna, Bologna, Italy
[25] Physikalisches Institut, Universität Bonn, Bonn, Germany
[26] Department of Physics, Boston University, Boston, MA, USA
[27] Department of Physics, Brandeis University, Waltham, MA, USA
[28] [(a)]Transilvania University of Brasov, Brasov, Romania; [(b)]Horia Hulubei National Institute of Physics and Nuclear Engineering, Bucharest, Romania; [(c)]Department of Physics, Alexandru Ioan Cuza University of Iasi, Iasi, Romania; [(d)]National Institute for Research and Development of Isotopic and Molecular Technologies, Physics Department, Cluj-Napoca, Romania; [(e)]National University of Science and Technology Politechnica, Bucharest, Romania; [(f)]West University in Timisoara, Timisoara, Romania; [(g)]Faculty of Physics, University of Bucharest, Bucharest, Romania
[29] [(a)]Faculty of Mathematics, Physics and Informatics, Comenius University, Bratislava, Slovak Republic; [(b)]Department of Subnuclear Physics, Institute of Experimental Physics of the Slovak Academy of Sciences, Kosice, Slovak Republic
[30] Physics Department, Brookhaven National Laboratory, Upton, NY, USA
[31] Facultad de Ciencias Exactas y Naturales, Departamento de Física, y CONICET, Instituto de Física de Buenos Aires (IFIBA), Universidad de Buenos Aires, Buenos Aires, Argentina
[32] California State University, Long Beach, CA, USA
[33] Cavendish Laboratory, University of Cambridge, Cambridge, UK
[34] [(a)]Department of Physics, University of Cape Town, Cape Town, South Africa; [(b)]iThemba Labs, Western Cape, South Africa; [(c)]Department of Mechanical Engineering Science, University of Johannesburg, Johannesburg, South Africa; [(d)]National Institute of Physics, University of the Philippines Diliman (Philippines), Quezon City, Philippines; [(e)]University of South Africa, Department of Physics, Pretoria, South Africa; [(f)]University of Zululand, KwaDlangezwa, South Africa; [(g)]School of Physics, University of the Witwatersrand, Johannesburg, South Africa
[35] Department of Physics, Carleton University, Ottawa, ON, Canada
[36] [(a)]Faculté des Sciences Ain Chock, Université Hassan II de Casablanca, Casablanca, Morocco; [(b)]Faculté des Sciences, Université Ibn-Tofail, Kénitra, Morocco; [(c)]Faculté des Sciences Semlalia, LPHEA-Marrakech, Université Cadi Ayyad, Marrakech, Morocco; [(d)]LPMR, Faculté des Sciences, Université Mohamed Premier, Oujda, Morocco; [(e)]Faculté des sciences, Université Mohammed V, Rabat, Morocco; [(f)]Institute of Applied Physics, Mohammed VI Polytechnic University, Ben Guerir, Morocco
[37] CERN, Geneva, Switzerland
[38] Affiliated with an Institute Formerly Covered by a Cooperation Agreement with CERN, Geneva, Switzerland
[39] Affiliated with an International Laboratory Covered by a Cooperation Agreement with CERN, Geneva, Switzerland

[40] Enrico Fermi Institute, University of Chicago, Chicago, IL, USA
[41] LPC, CNRS/IN2P3, Université Clermont Auvergne, Clermont-Ferrand, France
[42] Nevis Laboratory, Columbia University, Irvington, NY, USA
[43] Niels Bohr Institute, University of Copenhagen, Copenhagen, Denmark
[44] [(a)]Dipartimento di Fisica, Università della Calabria, Rende, Italy; [(b)]Laboratori Nazionali di Frascati, INFN Gruppo Collegato di Cosenza, Cosenza, Italy
[45] Physics Department, Southern Methodist University, Dallas, TX, USA
[46] National Centre for Scientific Research "Demokritos", Agia Paraskevi, Greece
[47] [(a)]Department of Physics, Stockholm University, Stockholm, Sweden; [(b)]Oskar Klein Centre, Stockholm, Sweden
[48] Deutsches Elektronen-Synchrotron DESY, Hamburg and Zeuthen, Germany
[49] Fakultät Physik , Technische Universität Dortmund, Dortmund, Germany
[50] Institut für Kern- und Teilchenphysik, Technische Universität Dresden, Dresden, Germany
[51] Department of Physics, Duke University, Durham, NC, USA
[52] SUPA-School of Physics and Astronomy, University of Edinburgh, Edinburgh, UK
[53] INFN e Laboratori Nazionali di Frascati, Frascati, Italy
[54] Physikalisches Institut, Albert-Ludwigs-Universität Freiburg, Freiburg, Germany
[55] II. Physikalisches Institut, Georg-August-Universität Göttingen, Göttingen, Germany
[56] Département de Physique Nucléaire et Corpusculaire, Université de Genève, Geneva, Switzerland
[57] [(a)]Dipartimento di Fisica, Università di Genova, Genoa, Italy; [(b)]INFN Sezione di Genova, Genoa, Italy
[58] II. Physikalisches Institut, Justus-Liebig-Universität Giessen, Giessen, Germany
[59] SUPA-School of Physics and Astronomy, University of Glasgow, Glasgow, UK
[60] LPSC, Université Grenoble Alpes, CNRS/IN2P3, Grenoble INP, Grenoble, France
[61] Laboratory for Particle Physics and Cosmology, Harvard University, Cambridge, MA, USA
[62] Department of Modern Physics and State Key Laboratory of Particle Detection and Electronics, University of Science and Technology of China, Hefei, China
[63] [(a)]Kirchhoff-Institut für Physik, Ruprecht-Karls-Universität Heidelberg, Heidelberg, Germany; [(b)]Physikalisches Institut, Ruprecht-Karls-Universität Heidelberg, Heidelberg, Germany
[64] [(a)]Department of Physics, Chinese University of Hong Kong, Shatin, N.T., Hong Kong, China; [(b)]Department of Physics, University of Hong Kong, Hong Kong, China; [(c)]Department of Physics and Institute for Advanced Study, Hong Kong University of Science and Technology, Clear Water Bay, Kowloon, Hong Kong, China
[65] Department of Physics, National Tsing Hua University, Hsinchu, Taiwan
[66] IJCLab, CNRS/IN2P3, Université Paris-Saclay, 91405 Orsay, France
[67] Centro Nacional de Microelectrónica (IMB-CNM-CSIC), Barcelona, Spain
[68] Department of Physics, Indiana University, Bloomington, IN, USA
[69] [(a)]INFN Gruppo Collegato di Udine, Sezione di Trieste, Udine, Italy; [(b)]ICTP, Trieste, Italy; [(c)]Dipartimento Politecnico di Ingegneria e Architettura, Università di Udine, Udine, Italy
[70] [(a)]INFN Sezione di Lecce, Lecce, Italy; [(b)]Dipartimento di Matematica e Fisica, Università del Salento, Lecce, Italy
[71] [(a)]INFN Sezione di Milano, Milan, Italy; [(b)]Dipartimento di Fisica, Università di Milano, Milan, Italy
[72] [(a)]INFN Sezione di Napoli, Naples, Italy; [(b)]Dipartimento di Fisica, Università di Napoli, Naples, Italy
[73] [(a)]INFN Sezione di Pavia, Pavia, Italy; [(b)]Dipartimento di Fisica, Università di Pavia, Pavia, Italy
[74] [(a)]INFN Sezione di Pisa, Pisa, Italy; [(b)]Dipartimento di Fisica E. Fermi, Università di Pisa, Pisa, Italy
[75] [(a)]INFN Sezione di Roma, Rome, Italy; [(b)]Dipartimento di Fisica, Sapienza Università di Roma, Rome, Italy
[76] [(a)]INFN Sezione di Roma Tor Vergata, Rome, Italy; [(b)]Dipartimento di Fisica, Università di Roma Tor Vergata, Rome, Italy
[77] [(a)]INFN Sezione di Roma Tre, Rome, Italy; [(b)]Dipartimento di Matematica e Fisica, Università Roma Tre, Rome, Italy
[78] [(a)]INFN-TIFPA, Povo, Italy; [(b)]Università degli Studi di Trento, Trento, Italy
[79] Universität Innsbruck, Department of Astro and Particle Physics, Innsbruck, Austria
[80] University of Iowa, Iowa City, IA, USA
[81] Department of Physics and Astronomy, Iowa State University, Ames, IA, USA
[82] Istinye University, Sariyer, Istanbul, Türkiye
[83] [(a)]Departamento de Engenharia Elétrica, Universidade Federal de Juiz de Fora (UFJF), Juiz de Fora, Brazil; [(b)]Universidade Federal do Rio De Janeiro COPPE/EE/IF, Rio de Janeiro, Brazil; [(c)]Instituto de Física,

Universidade de São Paulo, São Paulo, Brazil; [(d)]Rio de Janeiro State University, Rio de Janeiro, Brazil; [(e)]Federal University of Bahia, Bahia, Brazil
[84] KEK, High Energy Accelerator Research Organization, Tsukuba, Japan
[85] Graduate School of Science, Kobe University, Kobe, Japan
[86] [(a)]AGH University of Krakow, Faculty of Physics and Applied Computer Science, Kraków, Poland; [(b)]Marian Smoluchowski Institute of Physics, Jagiellonian University, Kraków, Poland
[87] Institute of Nuclear Physics Polish Academy of Sciences, Kraków, Poland
[88] [(a)]Khalifa University of Science and Technology, Abu Dhabi, United Arab Emirates; [(b)]University of Sharjah, Sharjah, United Arab Emirates
[89] Faculty of Science, Kyoto University, Kyoto, Japan
[90] Research Center for Advanced Particle Physics and Department of Physics, Kyushu University, Fukuoka , Japan
[91] L2IT, CNRS/IN2P3, UPS, Université de Toulouse, Toulouse, France
[92] Instituto de Física La Plata, Universidad Nacional de La Plata and CONICET, La Plata, Argentina
[93] Physics Department, Lancaster University, Lancaster, UK
[94] Oliver Lodge Laboratory, University of Liverpool, Liverpool, UK
[95] Department of Experimental Particle Physics, Jožef Stefan Institute and Department of Physics, University of Ljubljana, Ljubljana, Slovenia
[96] Department of Physics and Astronomy, Queen Mary University of London, London, UK
[97] Department of Physics, Royal Holloway University of London, Egham, UK
[98] Department of Physics and Astronomy, University College London, London, UK
[99] Louisiana Tech University, Ruston, LA, USA
[100] Fysiska institutionen, Lunds universitet, Lund, Sweden
[101] Departamento de Física Teorica C-15 and CIAFF, Universidad Autónoma de Madrid, Madrid, Spain
[102] Institut für Physik, Universität Mainz, Mainz, Germany
[103] School of Physics and Astronomy, University of Manchester, Manchester, UK
[104] CPPM, CNRS/IN2P3, Aix-Marseille Université, Marseille, France
[105] Department of Physics, University of Massachusetts, Amherst, MA, USA
[106] Department of Physics, McGill University, Montreal, QC, Canada
[107] School of Physics, University of Melbourne, Victoria, Australia
[108] Department of Physics, University of Michigan, Ann Arbor, MI, USA
[109] Department of Physics and Astronomy, Michigan State University, East Lansing, MI, USA
[110] Group of Particle Physics, University of Montreal, Montreal, QC, Canada
[111] Fakultät für Physik, Ludwig-Maximilians-Universität München, Munich, Germany
[112] Max-Planck-Institut für Physik (Werner-Heisenberg-Institut), Munich, Germany
[113] Graduate School of Science and Kobayashi-Maskawa Institute, Nagoya University, Nagoya, Japan
[114] [(a)]Department of Physics, Nanjing University, Nanjing, China; [(b)]School of Science, Shenzhen Campus of Sun Yat-sen University, Guangzhou, China; [(c)]University of Chinese Academy of Science (UCAS), Beijing, China
[115] Department of Physics and Astronomy, University of New Mexico, Albuquerque, NM, USA
[116] Institute for Mathematics, Astrophysics and Particle Physics, Radboud University/Nikhef, Nijmegen, Netherlands
[117] Nikhef National Institute for Subatomic Physics and University of Amsterdam, Amsterdam, Netherlands
[118] Department of Physics, Northern Illinois University, DeKalb, IL, USA
[119] [(a)]New York University Abu Dhabi, Abu Dhabi, United Arab Emirates; [(b)]United Arab Emirates University, Al Ain, United Arab Emirates
[120] Department of Physics, New York University, New York, NY, USA
[121] Ochanomizu University, Otsuka, Bunkyo-ku, Tokyo, Japan
[122] Ohio State University, Columbus, OH, USA
[123] Homer L. Dodge Department of Physics and Astronomy, University of Oklahoma, Norman, OK, USA
[124] Department of Physics, Oklahoma State University, Stillwater, OK, USA
[125] Palacký University, Joint Laboratory of Optics, Olomouc, Czech Republic
[126] Institute for Fundamental Science, University of Oregon, Eugene, OR, USA
[127] Graduate School of Science, University of Osaka, Osaka, Japan
[128] Department of Physics, University of Oslo, Oslo, Norway
[129] Department of Physics, Oxford University, Oxford, UK

[130] LPNHE, CNRS/IN2P3, Sorbonne Université, Université Paris Cité, Paris, France
[131] Department of Physics, University of Pennsylvania, Philadelphia, PA, USA
[132] Department of Physics and Astronomy, University of Pittsburgh, Pittsburgh, PA, USA
[133] [(a)]Laboratório de Instrumentação e Física Experimental de Partículas - LIP, Lisbon, Portugal; [(b)]Departamento de Física, Faculdade de Ciências, Universidade de Lisboa, Lisbon, Portugal; [(c)]Departamento de Física, Universidade de Coimbra, Coimbra, Portugal; [(d)]Centro de Física Nuclear da Universidade de Lisboa, Lisbon, Portugal; [(e)]Departamento de Física, Escola de Ciências, Universidade do Minho, Braga, Portugal; [(f)]Departamento de Física Teórica y del Cosmos, Universidad de Granada, Granada, Spain; [(g)]Departamento de Física, Instituto Superior Técnico, Universidade de Lisboa, Lisbon, Portugal
[134] Institute of Physics of the Czech Academy of Sciences, Prague, Czech Republic
[135] Czech Technical University in Prague, Prague, Czech Republic
[136] Faculty of Mathematics and Physics, Charles University, Prague, Czech Republic
[137] Particle Physics Department, Rutherford Appleton Laboratory, Didcot, UK
[138] IRFU, CEA, Université Paris-Saclay, Gif-sur-Yvette, France
[139] Santa Cruz Institute for Particle Physics, University of California Santa Cruz, Santa Cruz, CA, USA
[140] [(a)]Departamento de Física, Pontificia Universidad Católica de Chile, Santiago, Chile; [(b)]Millennium Institute for Subatomic Physics at High Energy Frontier (SAPHIR), Santiago, Chile; [(c)]Instituto de Investigación Multidisciplinario en Ciencia y Tecnología y Departamento de Física, Universidad de La Serena, La Serena, Chile; [(d)]Universidad Andres Bello, Department of Physics, Santiago, Chile; [(e)]Instituto de Alta Investigación, Universidad de Tarapacá, Arica, Chile; [(f)]Departamento de Física, Universidad Técnica Federico Santa María, Valparaíso, Chile
[141] Department of Physics, Institute of Science, Tokyo, Japan
[142] Department of Physics, University of Washington, Seattle, WA, USA
[143] [(a)]Institute of Frontier and Interdisciplinary Science and Key Laboratory of Particle Physics and Particle Irradiation (MOE), Shandong University, Qingdao, China; [(b)]School of Physics, Zhengzhou University, Zhengzhou, China
[144] [(a)]State Key Laboratory of Dark Matter Physics, School of Physics and Astronomy, Shanghai Jiao Tong University, Key Laboratory for Particle Astrophysics and Cosmology (MOE), SKLPPC, Shanghai, China; [(b)]State Key Laboratory of Dark Matter Physics, Tsung-Dao Lee Institute, Shanghai Jiao Tong University, Shanghai, China
[145] Department of Physics and Astronomy, University of Sheffield, Sheffield, UK
[146] Department of Physics, Shinshu University, Nagano, Japan
[147] Department Physik, Universität Siegen, Siegen, Germany
[148] Department of Physics, Simon Fraser University, Burnaby, BC, Canada
[149] SLAC National Accelerator Laboratory, Stanford, CA, USA
[150] Department of Physics, Royal Institute of Technology, Stockholm, Sweden
[151] Departments of Physics and Astronomy, Stony Brook University, Stony Brook, NY, USA
[152] Department of Physics and Astronomy, University of Sussex, Brighton, UK
[153] School of Physics, University of Sydney, Sydney, Australia
[154] Institute of Physics, Academia Sinica, Taipei, Taiwan
[155] [(a)]E. Andronikashvili Institute of Physics, Iv. Javakhishvili Tbilisi State University, Tbilisi, Georgia; [(b)]High Energy Physics Institute, Tbilisi State University, Tbilisi, Georgia; [(c)]University of Georgia, Tbilisi, Georgia
[156] Department of Physics, Technion, Israel Institute of Technology, Haifa, Israel
[157] Raymond and Beverly Sackler School of Physics and Astronomy, Tel Aviv University, Tel Aviv, Israel
[158] Department of Physics, Aristotle University of Thessaloniki, Thessaloníki, Greece
[159] International Center for Elementary Particle Physics and Department of Physics, University of Tokyo, Tokyo, Japan
[160] Graduate School of Science and Technology, Tokyo Metropolitan University, Tokyo, Japan
[161] Department of Physics, University of Toronto, Toronto, ON, Canada
[162] [(a)]TRIUMF, Vancouver, BC, Canada; [(b)]Department of Physics and Astronomy, York University, Toronto, ON, Canada
[163] Division of Physics and Tomonaga Center for the History of the Universe, Faculty of Pure and Applied Sciences, University of Tsukuba, Tsukuba, Japan
[164] Department of Physics and Astronomy, Tufts University, Medford, MA, USA
[165] Department of Physics and Astronomy, University of California Irvine, Irvine, CA, USA
[166] University of West Attica, Athens, Greece
[167] Department of Physics and Astronomy, University of Uppsala, Uppsala, Sweden
[168] Department of Physics, University of Illinois, Urbana, IL, USA

[169] Instituto de Física Corpuscular (IFIC), Centro Mixto Universidad de Valencia - CSIC, Valencia, Spain
[170] Department of Physics, University of British Columbia, Vancouver, BC, Canada
[171] Department of Physics and Astronomy, University of Victoria, Victoria, BC, Canada
[172] Fakultät für Physik und Astronomie, Julius-Maximilians-Universität Würzburg, Würzburg, Germany
[173] Department of Physics, University of Warwick, Coventry, UK
[174] Waseda University, Tokyo, Japan
[175] Department of Particle Physics and Astrophysics, Weizmann Institute of Science, Rehovot, Israel
[176] Department of Physics, University of Wisconsin, Madison, WI, USA
[177] Fakultät für Mathematik und Naturwissenschaften, Fachgruppe Physik, Bergische Universität Wuppertal, Wuppertal, Germany
[178] Department of Physics, Yale University, New Haven, CT, USA
[179] Yerevan Physics Institute, Yerevan, Armenia

[a] Also at Affiliated with an Institute Formerly Covered by a Cooperation Agreement with CERN, Geneva, Switzerland
[b] Also at An-Najah National University, Nablus, Palestine
[c] Also at Borough of Manhattan Community College, City University of New York, New York, NY, USA
[d] Also at Center for Interdisciplinary Research and Innovation (CIRI-AUTH), Thessaloníki, Greece
[e] Also at Centre of Physics of the Universities of Minho and Porto (CF-UM-UP), Porto, Portugal
[f] Also at CERN, Geneva, Switzerland
[g] Also at CMD-AC UNEC Research Center, Azerbaijan State University of Economics (UNEC), Baku, Azerbaijan
[h] Also at Département de Physique Nucléaire et Corpusculaire, Université de Genève, Geneva, Switzerland
[i] Also at Departament de Fisica de la Universitat Autonoma de Barcelona, Barcelona, Spain
[j] Also at Department of Financial and Management Engineering, University of the Aegean, Chios, Greece
[k] Also at Department of Mathematical Sciences, University of South Africa, Johannesburg, South Africa
[l] Also at Department of Modern Physics and State Key Laboratory of Particle Detection and Electronics, University of Science and Technology of China, Hefei, China
[m] Also at Department of Physics, Bolu Abant Izzet Baysal University, Bolu, Türkiye
[n] Also at Department of Physics, King's College London, London, UK
[o] Also at Department of Physics, Stanford University, Stanford, CA, USA
[p] Also at Department of Physics, Stellenbosch University, South Africa
[q] Also at Department of Physics, University of Fribourg, Fribourg, Switzerland
[r] Also at Department of Physics, University of Thessaly, Volos, Greece
[s] Also at Department of Physics, Westmont College, Santa Barbara, USA
[t] Also at Faculty of Physics, Sofia University 'St. Kliment Ohridski', Sofia, Bulgaria
[u] Also at Faculty of Physics, University of Bucharest, Bucharest, Romania
[v] Also at Hellenic Open University, Patras, Greece
[w] Also at Henan University, Henan, China
[x] Also at Imam Mohammad Ibn Saud Islamic University, Riyadh, Saudi Arabia
[y] Also at Institucio Catalana de Recerca i Estudis Avancats, ICREA, Barcelona, Spain
[z] Also at Institut für Experimentalphysik, Universität Hamburg, Hamburg, Germany
[aa] Also at Institute for Nuclear Research and Nuclear Energy (INRNE) of the Bulgarian Academy of Sciences, Sofia, Bulgaria
[ab] Also at Institute of Applied Physics, Mohammed VI Polytechnic University, Ben Guerir, Morocco
[ac] Also at Institute of Particle Physics (IPP), Toronto, Canada
[ad] Also at Institute of Physics and Technology, Mongolian Academy of Sciences, Ulaanbaatar, Mongolia
[ae] Also at Institute of Physics, Azerbaijan Academy of Sciences, Baku, Azerbaijan
[af] Also at Institute of Theoretical Physics, Ilia State University, Tbilisi, Georgia
[ag] Also at National Institute of Physics, University of the Philippines Diliman (Philippines), Quezon City, Philippines
[ah] Also at The Collaborative Innovation Center of Quantum Matter (CICQM), Beijing, China
[ai] Also at TRIUMF, Vancouver, BC, Canada
[aj] Also at Università di Napoli Parthenope, Naples, Italy
[ak] Also at Department of Physics, University of Colorado Boulder, Colorado, USA
[al] Also at University of Sienna, Siena, Italy

[am] Also at Washington College, Chestertown, MD, USA
[an] Also at Physics Department, Yeditepe University, Istanbul, Türkiye
* Deceased

[138] Department of Physics and Astronomy, University of Sheffield, Sheffield; United Kingdom
[139] Department of Physics, Shinshu University, Nagano; Japan
[140] Department Physik, Universität Siegen, Siegen; Germany
[141] Department of Physics, Simon Fraser University, Burnaby BC; Canada
[142] SLAC National Accelerator Laboratory, Stanford CA; United States of America
[143] Department of Physics, Royal Institute of Technology, Stockholm; Sweden
[144] Departments of Physics and Astronomy, Stony Brook University, Stony Brook NY; United States of America
[145] Department of Physics and Astronomy, University of Sussex, Brighton; United Kingdom
[146] School of Physics, University of Sydney, Sydney; Australia
[147] Institute of Physics, Academia Sinica, Taipei; Taiwan
[148] [(a)] E. Andronikashvili Institute of Physics, Iv. Javakhishvili Tbilisi State University, Tbilisi; [(b)] High Energy Physics Institute, Tbilisi State University, Tbilisi; [(c)] University of Georgia, Tbilisi; Georgia
[149] Department of Physics, Technion, Israel Institute of Technology, Haifa; Israel
[150] Raymond and Beverly Sackler School of Physics and Astronomy, Tel Aviv University, Tel Aviv; Israel
[151] Department of Physics, Aristotle University of Thessaloniki, Thessaloniki; Greece
[152] International Center for Elementary Particle Physics and Department of Physics, University of Tokyo, Tokyo; Japan
[153] Department of Physics, Tokyo Institute of Technology, Tokyo; Japan
[154] Department of Physics, University of Toronto, Toronto ON; Canada
[155] [(a)] TRIUMF, Vancouver BC; [(b)] Department of Physics and Astronomy, York University, Toronto ON; Canada
[156] Division of Physics and Tomonaga Center for the History of the Universe, Faculty of Pure and Applied Sciences, University of Tsukuba, Tsukuba; Japan
[157] Department of Physics and Astronomy, Tufts University, Medford MA; United States of America
[158] United Arab Emirates University, Al Ain; United Arab Emirates
[159] Department of Physics and Astronomy, University of California Irvine, Irvine CA; United States of America
[160] Department of Physics and Astronomy, University of Uppsala, Uppsala; Sweden
[161] Department of Physics, University of Illinois, Urbana IL; United States of America
[162] Instituto de Física Corpuscular (IFIC), Centro Mixto Universidad de Valencia – CSIC, Valencia; Spain
[163] Department of Physics, University of British Columbia, Vancouver BC; Canada
[164] Department of Physics and Astronomy, University of Victoria, Victoria BC; Canada
[165] Fakultät für Physik und Astronomie, Julius-Maximilians-Universität Würzburg, Würzburg; Germany
[166] Department of Physics, University of Warwick, Coventry; United Kingdom
[167] Waseda University, Tokyo; Japan
[168] Department of Particle Physics and Astrophysics, Weizmann Institute of Science, Rehovot; Israel
[169] Department of Physics, University of Wisconsin, Madison WI; United States of America
[170] Fakultät für Mathematik und Naturwissenschaften, Fachgruppe Physik, Bergische Universität Wuppertal, Wuppertal; Germany
[171] Department of Physics, Yale University, New Haven CT; United States of America

[a] Also Affiliated with an institute covered by a cooperation agreement with CERN.
[b] Also at An-Najah National University, Nablus; Palestine.
[c] Also at Borough of Manhattan Community College, City University of New York, New York NY; United States of America.
[d] Also at Bruno Kessler Foundation, Trento; Italy.
[e] Also at Center for High Energy Physics, Peking University; China.
[f] Also at Centro Studi e Ricerche Enrico Fermi; Italy.
[g] Also at CERN, Geneva; Switzerland.
[h] Also at Département de Physique Nucléaire et Corpusculaire, Université de Genève, Genève; Switzerland.
[i] Also at Departament de Fisica de la Universitat Autonoma de Barcelona, Barcelona; Spain.
[j] Also at Department of Financial and Management Engineering, University of the Aegean, Chios; Greece.
[k] Also at Department of Physics and Astronomy, Michigan State University, East Lansing MI; United States of America.
[l] Also at Department of Physics and Astronomy, University of Louisville, Louisville, KY; United States of America.
[m] Also at Department of Physics, Ben Gurion University of the Negev, Beer Sheva; Israel.
[n] Also at Department of Physics, California State University, East Bay; United States of America.
[o] Also at Department of Physics, California State University, Sacramento; United States of America.
[p] Also at Department of Physics, King's College London, London; United Kingdom.
[q] Also at Department of Physics, Stanford University, Stanford CA; United States of America.
[r] Also at Department of Physics, University of Fribourg, Fribourg; Switzerland.
[s] Also at Department of Physics, University of Thessaly; Greece.
[t] Also at Department of Physics, Westmont College, Santa Barbara; United States of America.
[u] Also at Hellenic Open University, Patras; Greece.
[v] Also at Institucio Catalana de Recerca i Estudis Avancats, ICREA, Barcelona; Spain.
[w] Also at Institut für Experimentalphysik, Universität Hamburg, Hamburg; Germany.
[x] Also at Institute for Nuclear Research and Nuclear Energy (INRNE) of the Bulgarian Academy of Sciences, Sofia; Bulgaria.
[y] Also at Institute of Particle Physics (IPP); Canada.
[z] Also at Institute of Physics, Azerbaijan Academy of Sciences, Baku; Azerbaijan.
[aa] Also at Institute of Theoretical Physics, Ilia State University, Tbilisi; Georgia.
[ab] Also at L2IT, Université de Toulouse, CNRS/IN2P3, UPS, Toulouse; France.
[ac] Also at Lawrence Livermore National Laboratory, Livermore; United States of America.
[ad] Also at National Institute of Physics, University of the Philippines Diliman (Philippines); Philippines.
[ae] Also at The City College of New York, New York NY; United States of America.
[af] Also at The Collaborative Innovation Center of Quantum Matter (CICQM), Beijing; China.
[ag] Also at TRIUMF, Vancouver BC; Canada.
[ah] Also at Università di Napoli Parthenope, Napoli; Italy.
[ai] Also at University of Chinese Academy of Sciences (UCAS), Beijing; China.
[aj] Also at University of Colorado Boulder, Department of Physics, Colorado; United States of America.
[ak] Also at Yeditepe University, Physics Department, Istanbul; Türkiye.
[*] Deceased.